AD-A118 921 BEDFORD RESEARCH ASSOCIATES MA F/G 4/1
LOW ENERGY ELECTRON AND PHOTON CROSS SECTIONS FOR O, N2, AND O2--ETC(U)
JAN 82 H T WADZINSKI, J R JASPERSE F19628-80-C-0216
UNCLASSIFIED AFGL-TR-82-0008 NL

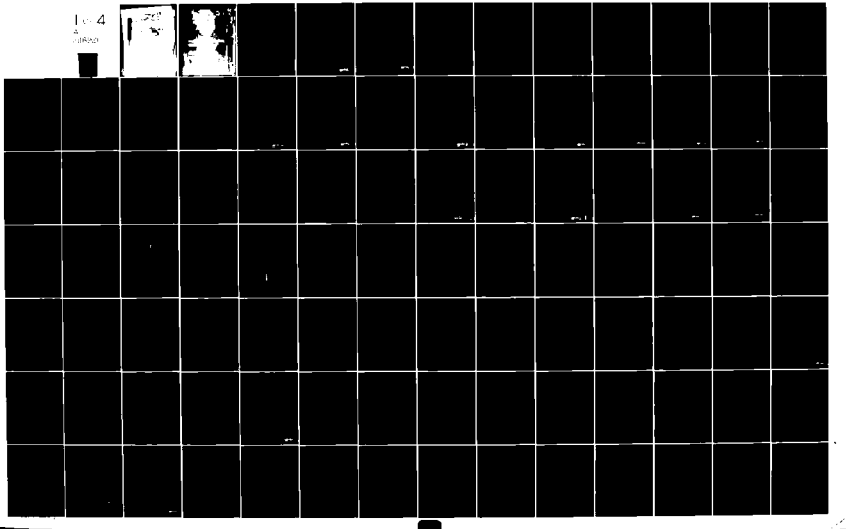

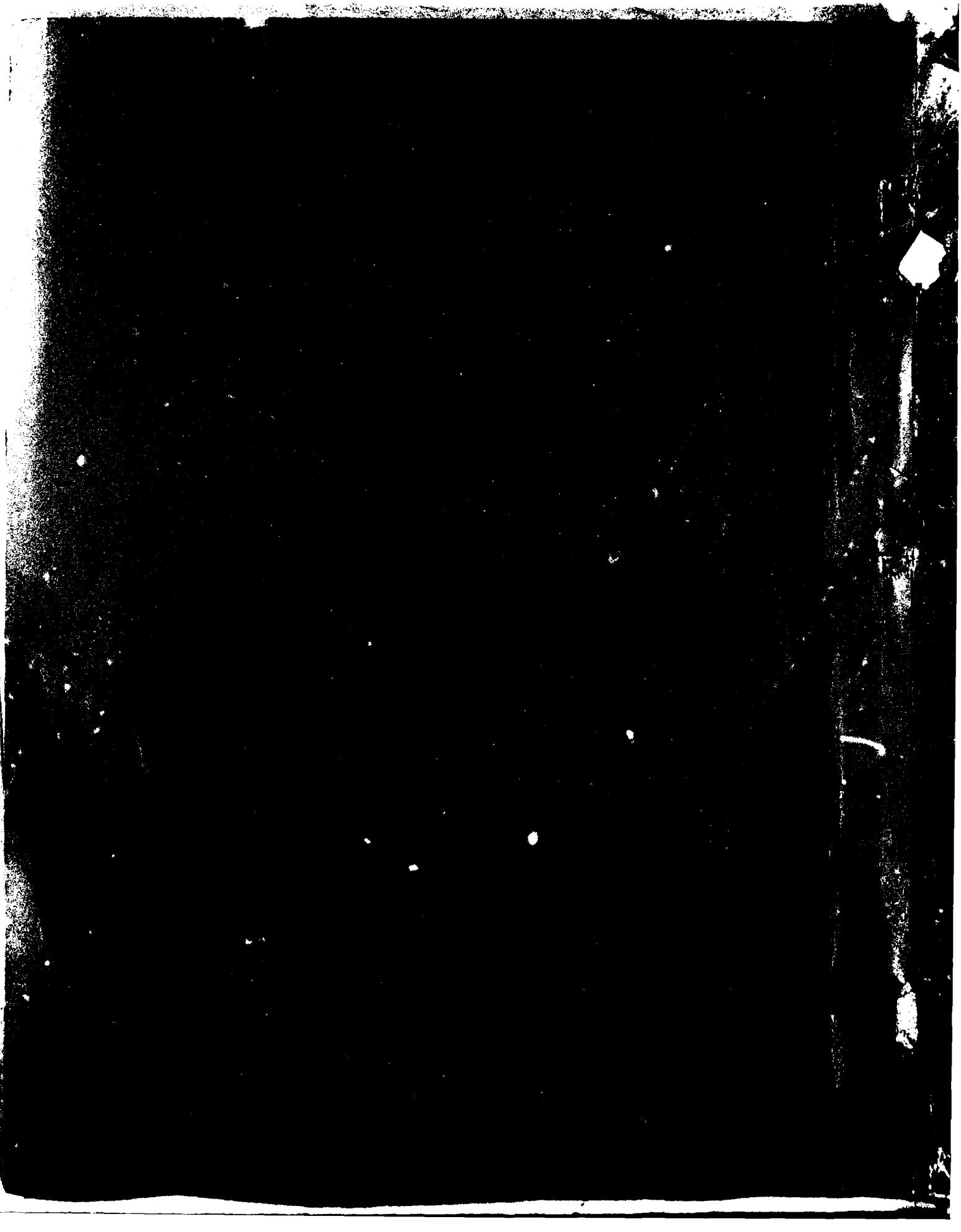

Unclassified
SECURITY CLASSIFICATION OF THIS PAGE (When Data Entered)

| REPORT DOCUMENTATION PAGE | READ INSTRUCTIONS BEFORE COMPLETING FORM |
|---|---|
| 1. REPORT NUMBER: AFGL-TR-82-0008 | 2. GOVT ACCESSION NO.: AD-A118921 |
| 3. RECIPIENT'S CATALOG NUMBER | |
| 4. TITLE (and Subtitle): LOW ENERGY ELECTRON AND PHOTON CROSS SECTIONS FOR O, $N_2$, AND $O_2$, AND RELATED DATA | 5. TYPE OF REPORT & PERIOD COVERED: Scientific. Interim. |
| | 6. PERFORMING ORG. REPORT NUMBER: ERP, No. 762 |
| 7. AUTHOR(s): H. T. Wadzinski*<br>J. R. Jasperse | 8. CONTRACT OR GRANT NUMBER(s) |
| 9. PERFORMING ORGANIZATION NAME AND ADDRESS: Air Force Geophysics Laboratory (PHY)<br>Hanscom AFB<br>Massachusetts 01731 | 10. PROGRAM ELEMENT, PROJECT, TASK AREA & WORK UNIT NUMBERS: 62101F<br>46430612 |
| 11. CONTROLLING OFFICE NAME AND ADDRESS: Air Force Geophysics Laboratory (PHY)<br>Hanscom AFB<br>Massachusetts 01731 | 12. REPORT DATE: 4 January 1982<br>13. NUMBER OF PAGES: 332 |
| 14. MONITORING AGENCY NAME & ADDRESS(if different from Controlling Office) | 15. SECURITY CLASS. (of this report): Unclassified<br>15a. DECLASSIFICATION/DOWNGRADING SCHEDULE |

16. DISTRIBUTION STATEMENT (of this Report)

Approved for public release; distribution unlimited.

17. DISTRIBUTION STATEMENT (of the abstract entered in Block 20, if different from Report)

18. SUPPLEMENTARY NOTES

*Bedford Research Associates
2 DeAngelo Drive
Bedford, MA 01730

This research was partially supported by Bedford Research Associates under contract F19628-80-C-0216.

19. KEY WORDS (Continue on reverse side if necessary and identify by block number)

Cross sections
Atmospheric modelling

20. ABSTRACT (Continue on reverse side if necessary and identify by block number)

This report provides a set of low energy (0-300 eV) cross sections for use in calculating the photoelectron flux in the terrestrial daytime ionosphere.

DD FORM 1 JAN 73 1473

Unclassified
SECURITY CLASSIFICATION OF THIS PAGE (When Data Entered)

## Preface

The authors wish to thank many people who helped in the understanding of this data, especially G. Victor, A. Phelps, W. Hoegy, K. Kirby, and D. Torr. These people as well as B. Schneider, A. Temkin, and C. Jackman Provided their most recent results. Data published in graphical form was digitized by the JILA Information Center and obtained through J. Galligher. The programming for the plotting and use of the data was done by N. Grossbard, D. Dechichio, and K. Hoxie.

## Contents

## Illustrations

## Illustrations



## Tables

# Low Energy Electron and Photon Cross Sections for O, $N_2$, and $O_2$, and Related Data

## 1. INTRODUCTION

The purpose of this report is to provide a set of low energy (0-300 eV) cross sections for use in calculating the photoelectron flux in the terrestrial daytime ionosphere. ~~We also give~~ data on the neutral particle composition of the upper atmosphere and ionizing electromagnetic radiation from the sun.

Section 2 gives some useful values for neutral, ion, and electron densities and the associated temperatures found in the mid-latitude daytime ionosphere.

Details on the atomic and molecular structure of atmosphere constituents are often required. Section 3 contains tables of the energy levels of the main species in the upper atmosphere.

In calculating the photoelectron flux the cross sections that describe the electron neutral particle collisions must be known. Section 4 contains the cross sections for electron collisions with neutrals, including momentum transfer cross sections and cross sections for collisions that excite the neutral species. These collisions remove energy from the electrons. Section 5 discusses deexcitation collisions that give energy to the electrons and are important at low energies. Section 6 contains electron impact ionization cross sections for the neutral species. Data for electron-ion recombination are given in Section 7.

(Received for publication 30 December 1981)

Electromagnetic radiation from the sun photoionizes the neutral particle gas. The data needed to model these processes are given in the last two chapters.

There are two sets of appendices. The first contains supportive material. Appendix B contains graphs of many of the data sets discussed in this work.

## 2. COMPOSITION OF THE UPPER ATMOSPHERE

The upper atmosphere is composed of atoms, simple molecules, and their ions. When the sun is relatively quiet, the atmosphere is often approximated as being in the steady state.

One basic parameter used is the exospheric temperature, the limiting temperature of the neutrals several hundred kilometers above the earth. This can vary from about 700°K to possibly 2000°K, depending on solar conditions. The solar energy output is frequently referenced by the intensity of 10.7-cm radiation.

The variations in the atmospheric structure are due to many causes that are discussed by Jacchia (1977).[1] Some are as follows: the exospheric temperature is 20 percent or more cooler at night; solar activity as determined by the 10.7-cm radiation can raise the exospheric temperature by 500°K; other solar activity that is manifested through the geomagnetic Kp index can add 1000°K to the temperature near the poles. Thus, there is a large range of possible exospheric temperatures. In addition, the change in photon and particulate radiation will change the ionic composition of the upper atmosphere as shown by Johnson (1969).[2] Keneshea et al (1970)[3] calculate the concentrations of electrons, $NO^+$, and $O_2^+$, through a night showing changes in these constituents up to an altitude of 140 km. Oppenheimer et al (1977a,[4] 1977b[5]) present satellite data for $NO^+$, $O_2^+$, $O^+$, and $N_2^+$ densities covering 160 to 400 km showing variations that are less amenable to interpretation due to the satellite motion.

---

1. Jacchia, L.G. (1977) Thermospheric Temperature, Density and Composition: New Models, Smithsonian Astrophysical Observatory Special Report 375.
2. Johnson, C.Y. (1969) Annals of the IQSY 5:197, (Stickland, A.C., ed.) MIT Press, Cambridge, Mass.
3. Keneshea, T.J., Narcisi, R.S., and Swider, W., Jr. (1970) J. Geophys. Res. 75:845, AFCRL-70-0172, AD A0703050.
4. Oppenheimer, M., Dalgarno, A., Trebino, F.P., Brace, L.H., Brinton, H.C., and Hoffman, J.H. (1977) J. Geophys. Res. 82:191.
5. Oppenheimer, M., Constantinides, F.R., Kirby-Docken, K., Victor, G.A., Dalgarno, A., and Hoffman, J.H. (1977) J. Geophys. Res. 82:5485.

These variations can also be seen in the satellite measurements reported and modelled by Brace et al (1976),[6] Brace and Theis (1978),[7] and Hoegy and Brace (1978)[8] and in the radar measurements by Evans (1967,[9] 1970[10]).

Figures 1 through 6 show the major neutral species from the neutral model of Jacchia (1977)[1] with 1000°K exospheric temperature that matches the data of Reber and Nicholet (1965)[11] and Johnson (1969).[2] The ionic densities come from Istomin (1966)[12] and Johnson (1966,[13] 1969[2]). The electron density corresponding to these ion densities is given as well as the density range measured by Brace and Theis (1978).[7] These data were for daytime midlatitude conditions.

The electron temperatures below 450 km are from Sagalyn and Wand (1971).[14] The extension to higher altitudes is estimated from Evans (1970).[10] The range data is from Brace and Theis (1978).[7] The neutral temperature is from the Jacchia model (1977)[1] with an exospheric temperature of 1000°K. The corresponding range is estimated to correspond to exospheric temperatures of 600°K and 1800°K. The ion temperatures below 450 km are primarily from Sagalyn and Wand (1971).[14] Below 170 km this data was modified to agree with the neutral temperature from the Jacchia model used. The extension to higher altitudes was estimated from Evans (1967).[9]

All of this data, with the exception of that of Sagalyn and Wand, was taken during quiet solar conditions with an average 10.7-cm intensity below 95. The data of Sagalyn and Wand[14] were taken when the average 10.7-cm intensity was near 145. These values come from the articles involved or from Jacchia (1977).[1]

## 3. ENERGY LEVELS OF MAJOR CONSTITUENTS

Tables 1 through 4 list the states of interest of the major atmosphere constituents. The data for atomic oxygen were obtained from Moore (1949)[15] and the

6. Brace, L.H., Hoegy, W.R., Mayr, H.G., Victor, G.A., Hanson, W.B., Reber, C.A., and Hinteregger, H.E. (1976) J. Geophys. Res. 81:5421.
7. Brace, L.H., and Theis, R.F. (1978) Geophys. Res. Lett. 5:275.
8. Hoegy, W.R., and Brace, L.H. (1978) Geophys. Res. Lett. 5:269.
9. Evans, J.V. (1967) Planet Space Sci. 15:1557.
10. Evans, J.V. (1970) Planet Space Sci. 18:1225.
11. Reber, C.A., and Nicholet, M. (1965) Planet Space Sci. 13:617.
12. Istomin, V.G. (1966) Annls. Geophys. 22:255.
13. Johnson, C.Y. (1966) J. Geophys. Res. 71:330.
14. Sagalyn, R.C., and Wand, R.H. (1971) J. Geophys. Res. 76:3783, AFCRL-71-0495, AD A0731424.
15. Moore, C.E. (1949) Atomic Energy Levels Volume 1, U.S. Govt. Printing Office, Washington, D.C.

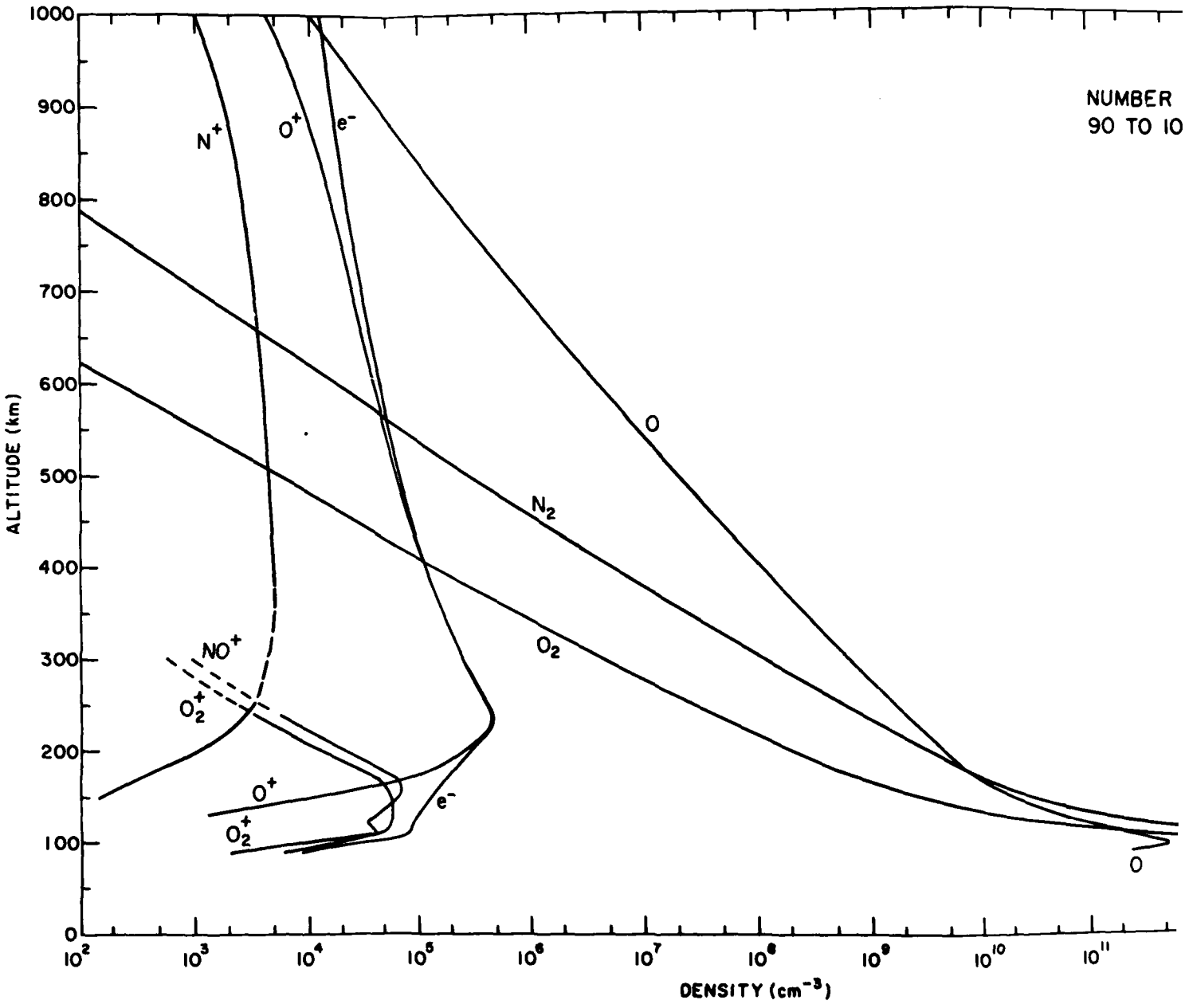


**Figure 1.** Number Densities from 90 to 1000 km. T
Johnson (1969)[2] that are rocket measurements below
ments above 400. The neutral densities are from th
for an exospheric temperature 1000°K. These are c
C. Y. Johnson. The solar intensity at 10.7 cm was
were measured. These data were for daytime midla

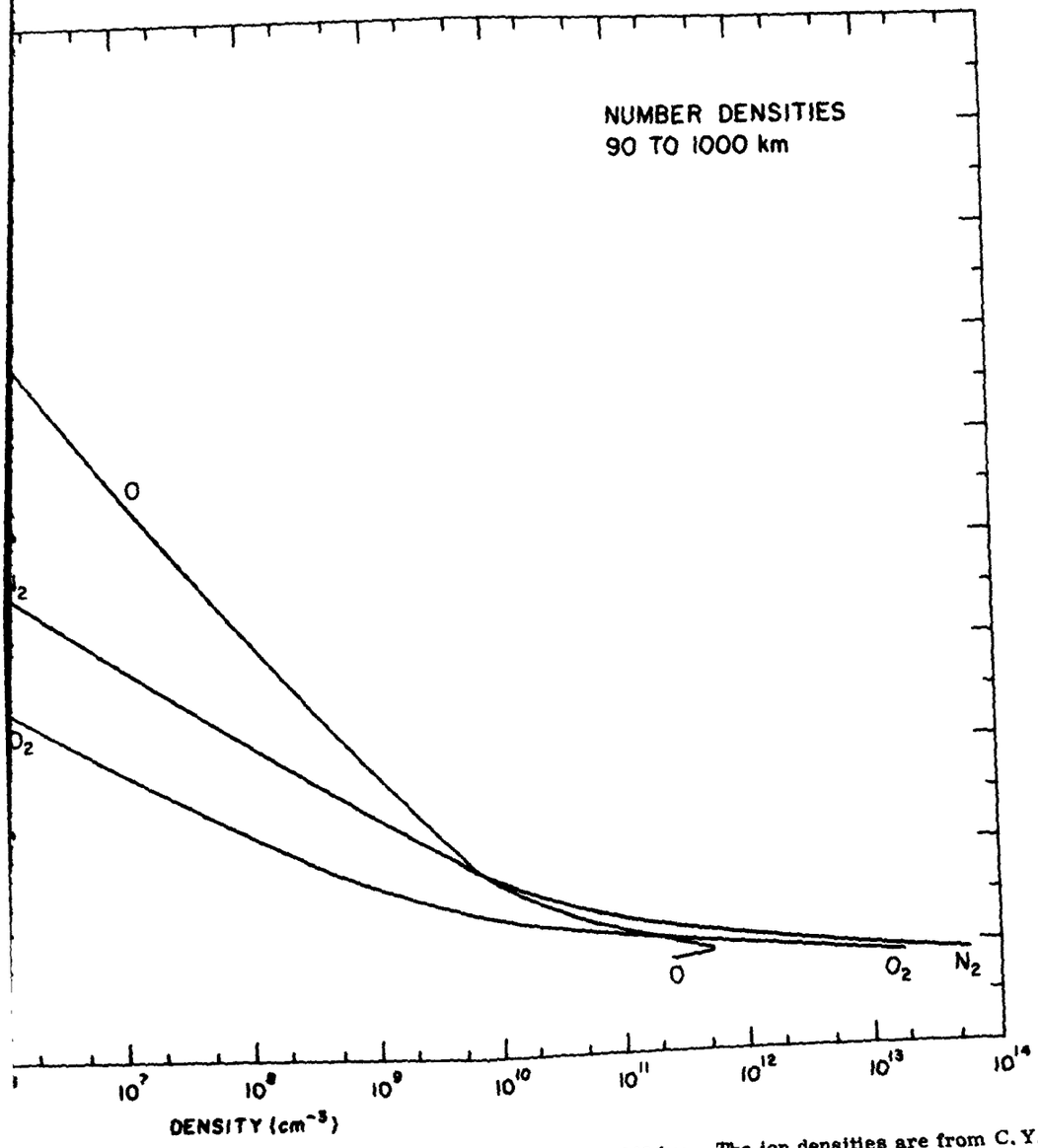


Figure 1. Number Densities from 90 to 1000 km. The ion densities are from C. Y. Johnson (1969)[2] that are rocket measurements below 240 km and satellite measurements above 400. The neutral densities are from the model of L. Jacchia (1977)[1] for an exospheric temperature 1000°K. These are close to the values used by C. Y. Johnson. The so'ar intensity at 10.7 cm was about 80 when the ion densities were measured. These data were for daytime midlatitude conditions



2

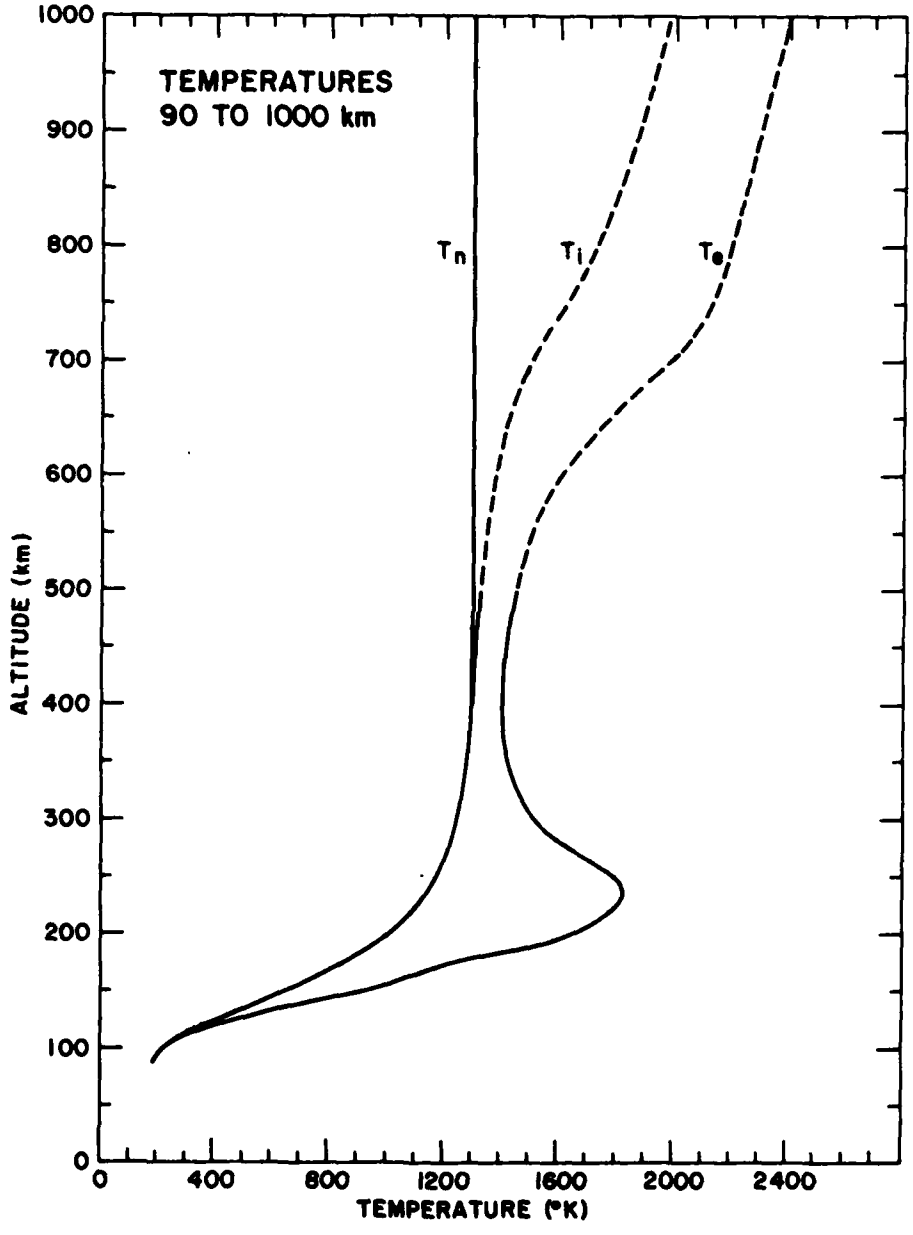


Figure 2. Temperatures from 90 to 1000 km. The electron and the ion temperatures below 500 km are from Sagalyn and Wand (1971).[14] The values above 500 km are extrapolations based on the data of Evans (1970).[10] The neutral temperatures are from the Jacchia model for an exospheric temperature 1300°K. The solar 10.7-cm intensity was about 146 when the measurements were made. These data were for daytime midlatitude conditions

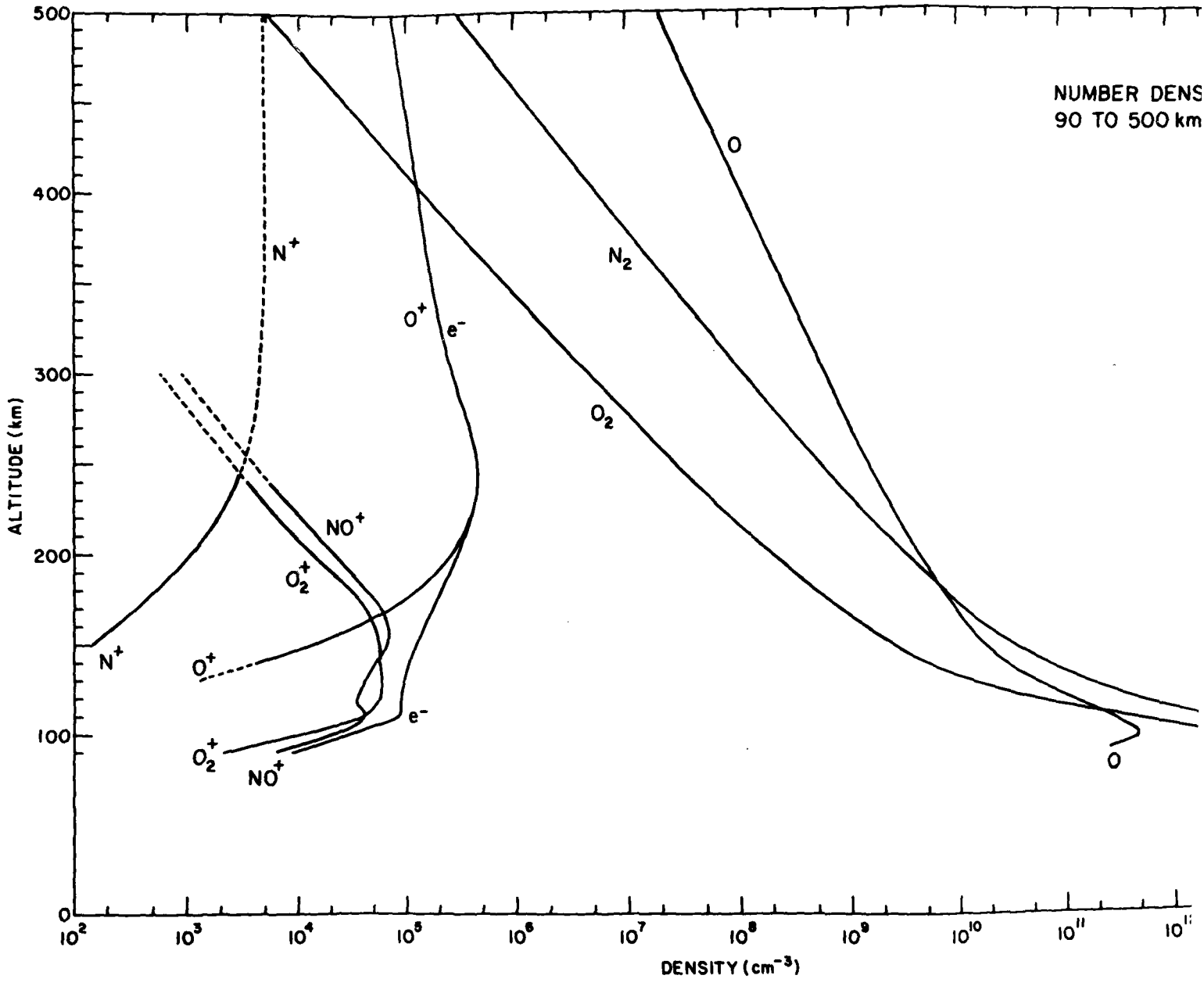


Figure 3. Number Densities from 90 to 500 km. The ion C. Y. Johnson (1969)[2] that are rocket measurements belo measurements above 400. The neutral densities are fro (1977)[1] for an exospheric temperature 1000°K. These a by C. Y. Johnson. The solar intensity at 10.7 cm was at sities were measured. These data were for daytime mic

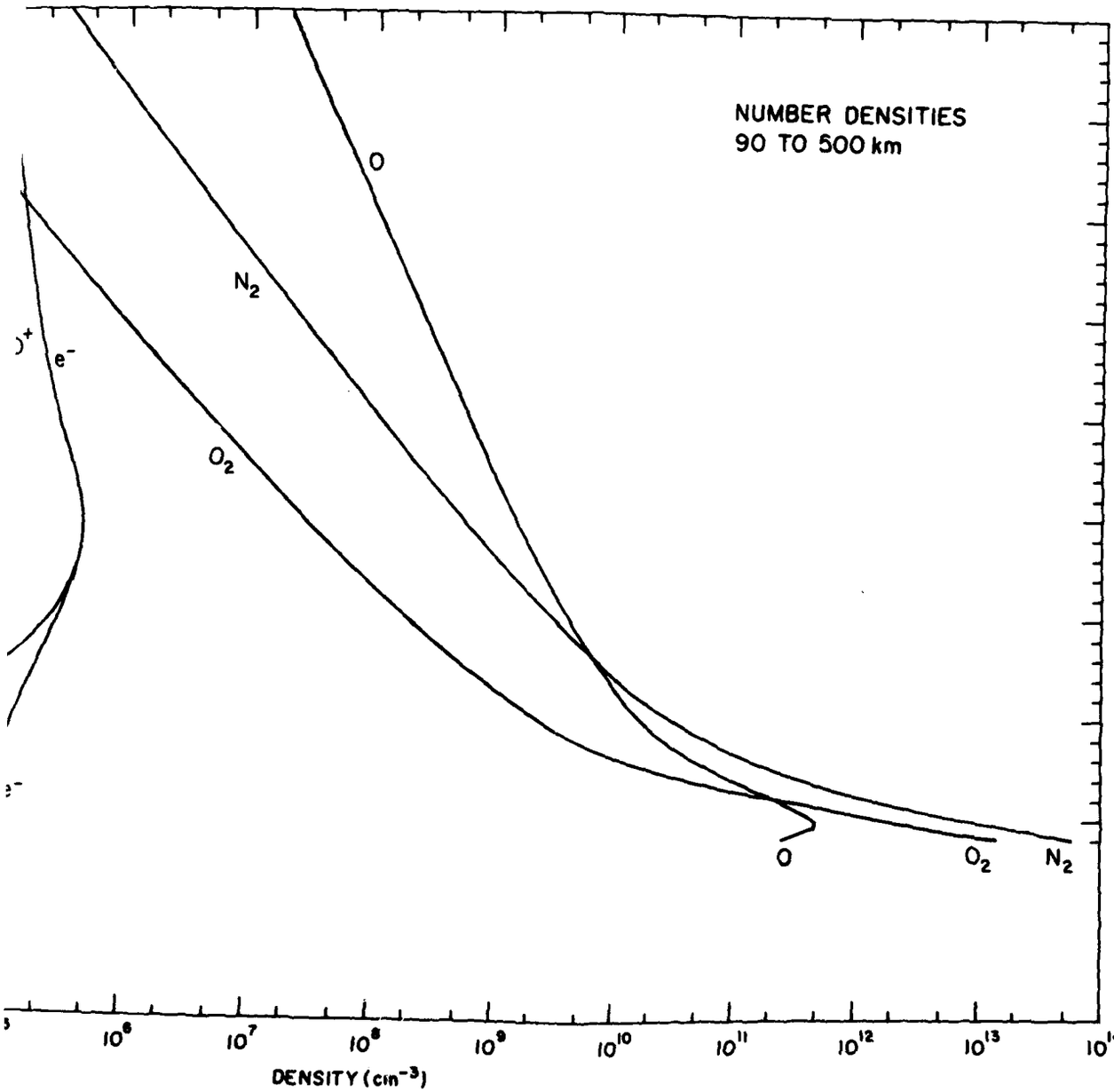


Figure 3. Number Densities from 90 to 500 km. The ion densities are from C. Y. Johnson (1969)[2] that are rocket measurements below 240 km and satellite measurements above 400. The neutral densities are from the model of L. Jacchia (1977)[1] for an exospheric temperature 1000°K. These are close to the values used by C. Y. Johnson. The solar intensity at 10.7 cm was about 80 when the ion densities were measured. These data were for daytime midlatitude conditions

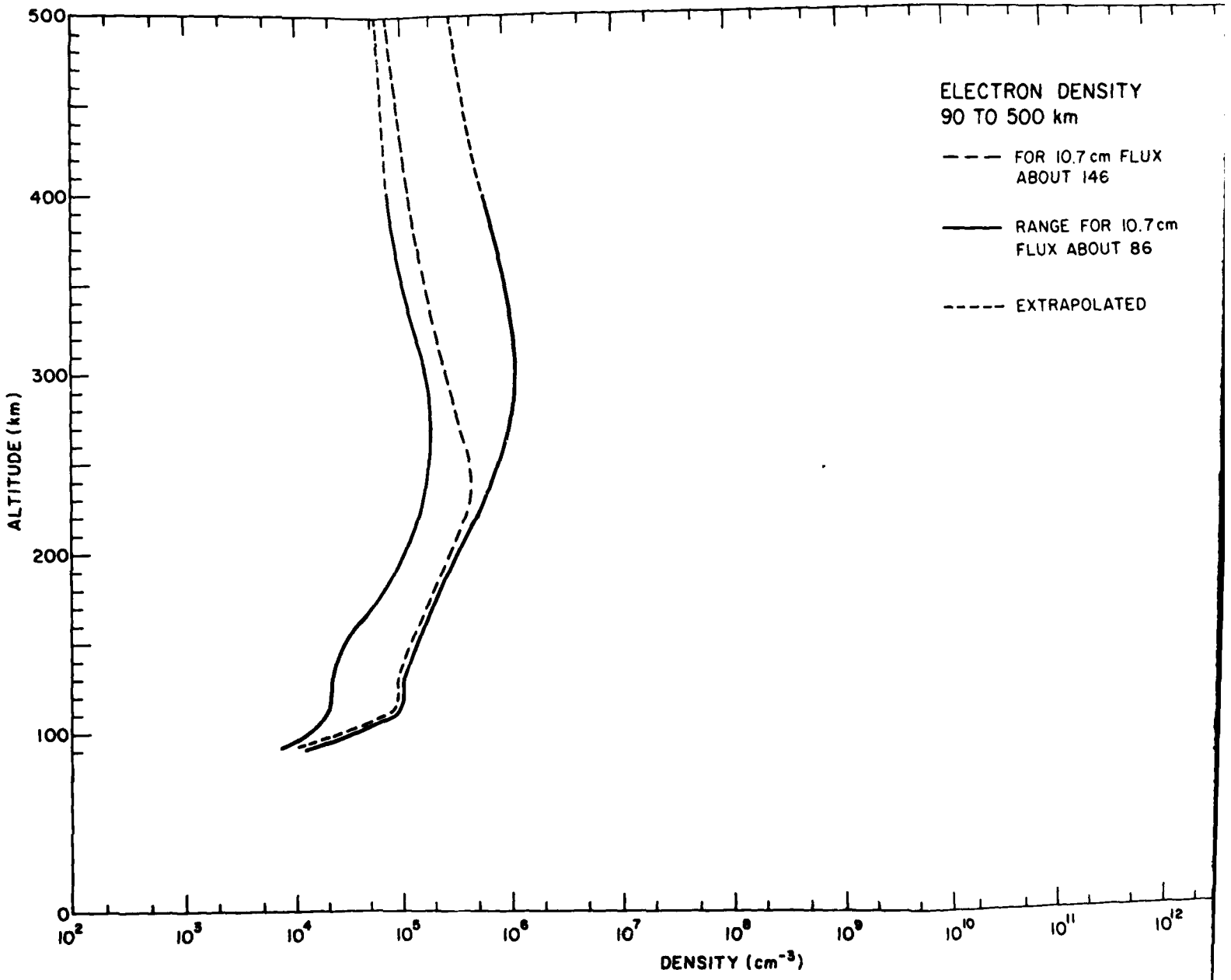


**Figure 4. Electron Densities** from 90 to 500 km. The middl
density measured by Sagalyn and Wand (1971)[14] with the sola
about 146. The bracketing curves are the electron density ra
by Brace and Theis (1978)[7] with the solar 10.7 cm-intensity
data were for daytime midlatitude conditions

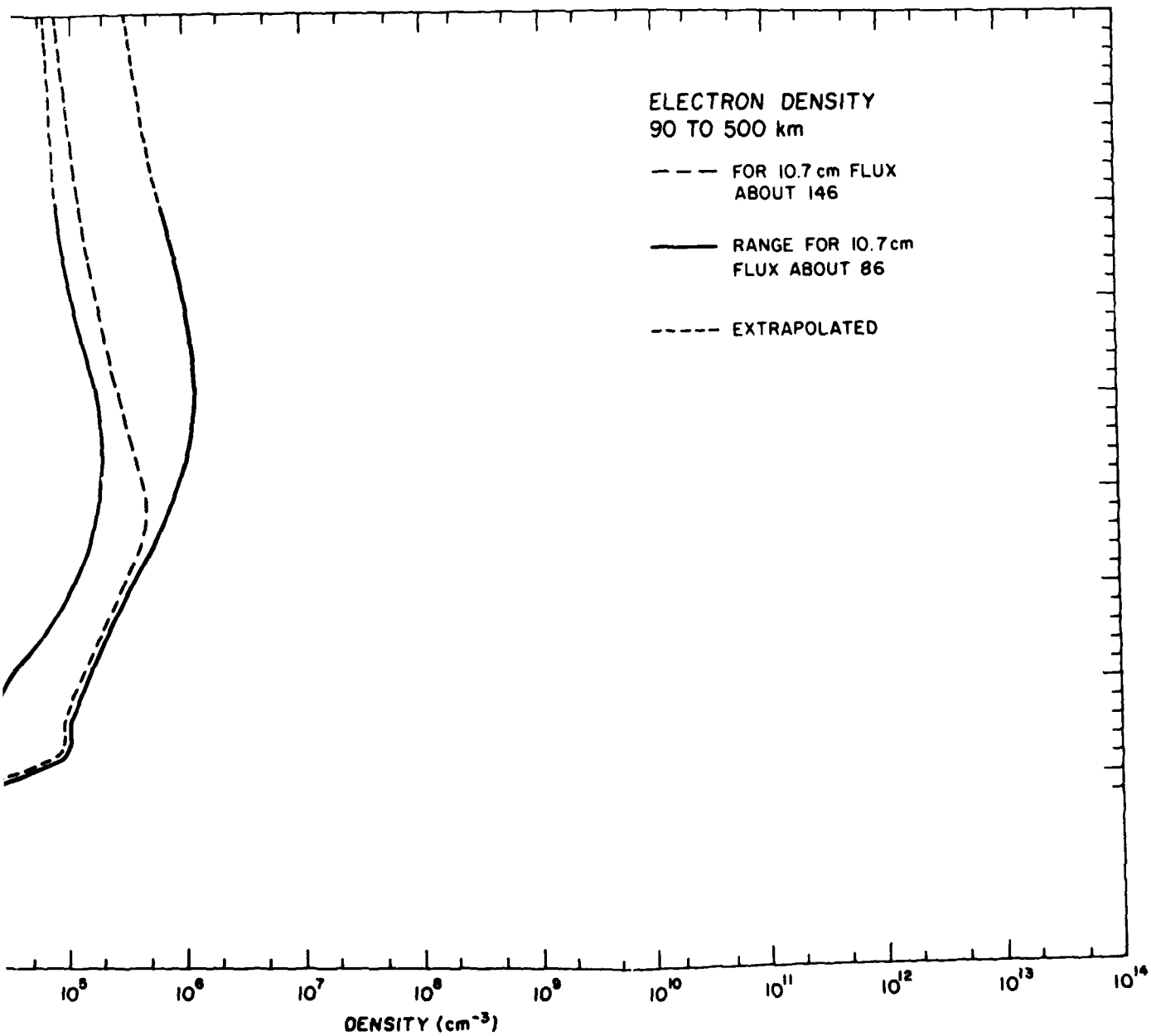


**Figure 4.** Electron Densities from 90 to 500 km. The middle curve is the electron density measured by Sagalyn and Wand (1971)[14] with the solar 10.7-cm intensity about 146. The bracketing curves are the electron density range limits measured by Brace and Theis (1978)[7] with the solar 10.7 cm-intensity about 86. These data were for daytime midlatitude conditions



2

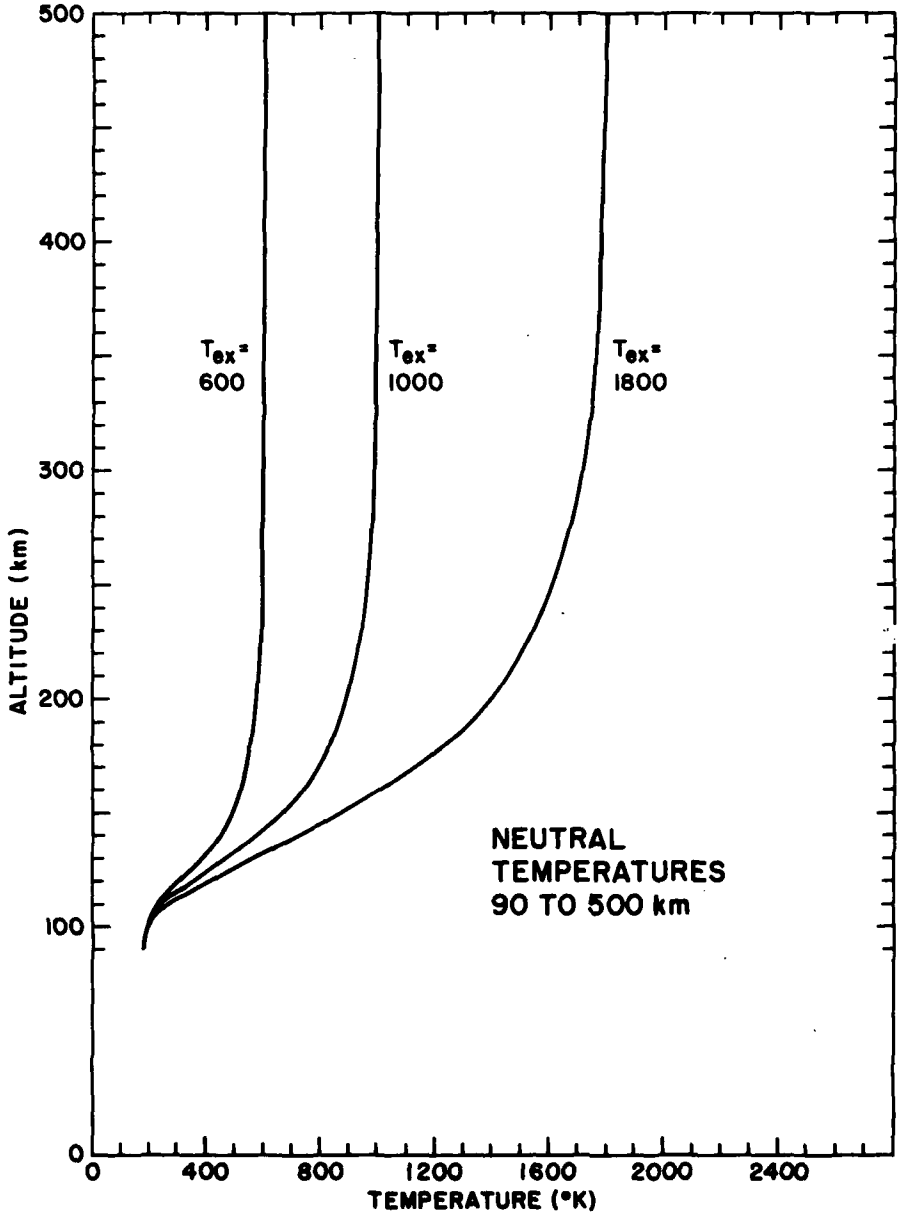


Figure 5. Neutral Temperatures from 90 to 500 km. The data are from Jacchia 1977 model.[1] The central curve is for an exospheric temperature 1000°K. The range estimates of 600°K and 1800°K are based on the electron data of Brace and Theis (1978)[7]. These data were for daytime midlatitude conditions

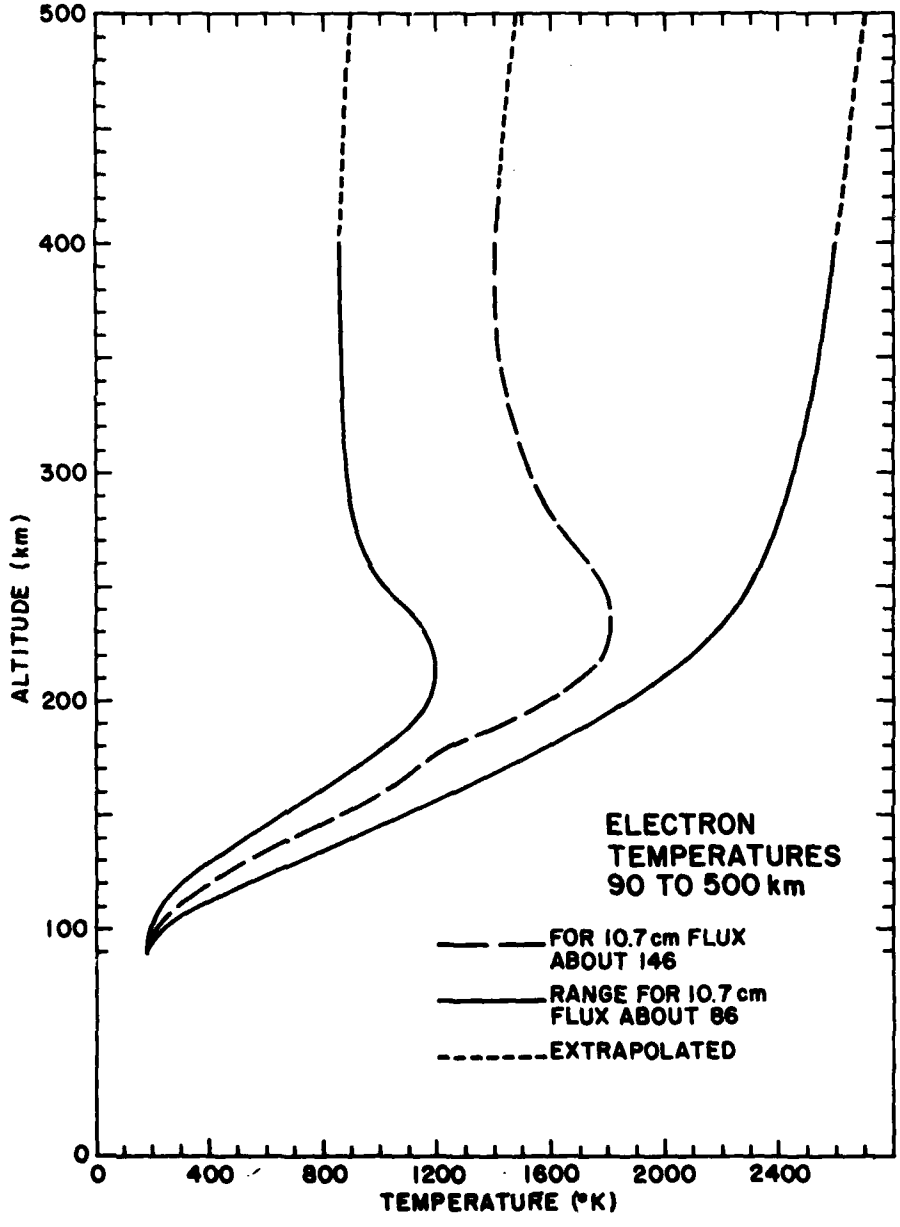


**Figure 6. Electron Temperatures from 90 to 500 km. The central curve is the electron temperature from Sagalyn and Wand (1971)[14] measured when the solar 10.7-cm flux was about 146. The bracketing curves are the range limits measured by Brace and Theis (1978)[7] with the solar 10.7-cm flux about 86. These data were for daytime midlatitude conditions**

Table 1. Atomic Oxygen Energy Levels

| Use Index | Energy (eV) | O | $O^-$ | $O^+$ |
|---|---|---|---|---|
| | 37. | | | $3s\ ^{4,2}P$ |
| | 34.20 | | | $2p^4\ ^2D$ |
| | 28.50 | | | $2p^4\ ^4P$ |
| Q | 18.64 | | | $2p^3\ ^2P^o$ |
| Q | 16.94 | | | $2p^3\ ^2D^o$ |
| Q | 13.62 | | | $2p^3\ ^4S^o$ |
| | . | | | |
| | . | | | |
| | . | | | |
| R | 12.75 | $4d\ ^{5,3}D^o$ | | |
| Q | 12.73 | $3s'\ ^1D^o$ | | |
| R | 12.70 | $5s\ ^3S^o$ | | |
| R | 12.66 | $5s\ ^5S^o$ | | |
| Q | 12.54 | $3s'\ ^3D$ | | |
| R | 12.38 | $4p\ ^3P$ | | |
| R | 12.29 | $4p\ ^5P$ | | |
| Q,R | 12.08 | $3d\ ^{5,3}D$ | | |
| R | 11.93 | $4s\ ^3S^o$ | | |
| R | 11.84 | $4s\ ^5S$ | | |
| Q | 10.99 | $3p\ ^3P$ | | |
| Q | 10.74 | $3p\ ^5P$ | | |
| R | 9.52 | $3s\ ^3S^o$ | | |
| Q | 9.15 | $3s\ ^5S^o$ | | |
| Q | 4.17 | $2p^4\ ^1S$ | | |
| Q | 1.97 | $2p^4\ ^1D$ | | |
| Q | 0.0292 | $2p^4\ {}^3P_0$ | | |
| Q | 0.0195 | $2p^4\ {}^3P_1$ | | |
| | 0.00 | $2p^4\ {}^3P_2$ | | |
| | -1.47 | | $2p^5\ ^2P$ | |

Table 2. Molecular Nitrogen Energy Levels

| Use Index | Vibrational Spacing | Energy (eV) | $N_2$ | $N_2^-$ | $N_2^+$ | N+N | $N+N^+$ |
|---|---|---|---|---|---|---|---|
| (Q, R) | | 38. | | | $G\ ^2\Sigma_g^+$ | | |
| | | . | | | | | |
| | | . | | | | | |
| | | . | | | | | |
| | | 24.29 | | | | | $^4S^o+^3P$ |
| Q, R | | 23.59 | | | $C\ ^2\Sigma_u^+$ | | |
| Q, R | | 22.07 | | | $D\ ^2\Pi_g$ | | |
| | | 21. | | | | $^4S^o+2s^22p^23s$ | |
| | | 20.69 | | | | $^4S^o+2s2p^4$ | |
| Q, R | | 18.75 | | | $B\ ^2\Sigma_u^+$ | | |
| Q, R | | 16.70 | | | $A\ ^2\Pi_{u\frac{1}{2}}$ | | |
| Q, R | | 15.58 | | | $X\ ^2\Sigma_g^+$ | | |
| | | . | | | | | |
| | | . | | | | | |
| | | . | | | | | |
| | | 14.53 | | | | $^2D^o+^2D^o$ | |
| | | . | | | | | |
| | | . | | | | | |
| | | . | | | | | |
| | 0.24 | 14.07 | $x\ ^1\Sigma_g^-$ | | | | |
| | | 13.33 | | | | $^4S^o+^2P^o$ | |
| | 0.25 | 13.33 | $o_3\ ^1\Pi_u$ | | | | |
| | 0.12 | 13.11 | $H\ ^3\Phi_u$ | | | | |
| | 0.27 | 12.96 | $c_4'\ ^1\Sigma_u^+$ | | | | |
| | 0.27 | 12.95 | $c_3\ ^1\Pi_u$ | | | | |
| Q | 0.09 | 12.96 | $b'\ ^1\Sigma_u^+$ | | | | |
| | | [12.99] | $D\ ^3\Sigma_u^+$ | | | | |
| Q | 0.08 | 12.50 | $b\ ^1\Pi_u$ | | | | |
| Q | | [12.25] | $a''\ ^1\Sigma_g^+$ | | | | |
| | 0.10 | 12.19 | $C'\ ^3\Pi_u$ | | | | |
| | | 12.14 | | | | $^4S^o+^2D^o$ | |

Table 2. Molecular Nitrogen Energy Levels (Cont)

| Use Index | Vibrational Spacing | Energy (eV) | $N_2$ | $N_2^-$ | $N_2^+$ | N+N | $N+N^+$ |
|---|---|---|---|---|---|---|---|
| Q | 0.37 | 11.88 | $E\ ^3\Sigma_g$ | | | | |
| | 0.27 | 11.47 | | $E\ ^2\Sigma_g^+$ | | | |
| | | 11.2 | | ⎡ | | | |
| Q | 0.25 | 11.03 | $C\ ^3\Pi_u$ | Shape resonances decaying to $B\ ^3\Pi_g$ | | | |
| | | 9.76 | | | | $^4S^o+^4S^o$ | |
| | | 9.6 | | ⎡ | | | |
| | | 9 | | ⎢ | | | |
| Q | 0.19 | 8.94 | $w\ ^1\Delta_u$ | ⎢ | | | |
| Q | 0.21 | 8.59 | $a\ ^1\Pi_g$ | ⎢ Shape resonances decaying to $A\ ^3\Sigma_b^+$ | | | |
| Q | 0.19 | 8.45 | $a'\ ^1\Sigma_u^-$ | ⎢ | | | |
| Q | 0.19 | 8.22 | $B'\ ^3\Sigma_u^-$ | ⎢ | | | |
| | | 8.2 | | ⎣ | | | |
| Q | 0.19 | 7.42 | $W\ ^3\Delta_u$ | | | | |
| Q | 0.21 | 7.39 | $B\ ^3\Pi_g$ | | | | |
| Q | 0.18 | 6.22 | $A\ ^3\Sigma_u^+$ | | | | |
| | 0.24 | 1.90 | | $X\ ^2\Pi_g$ | | | |
| Q | 0.29 | 0.0 | $X\ ^1\Sigma_g^+$ | | | | |

Table 3. Molecular Oxygen Energy Levels

| Use Index | Vibrational Spacing | Energy (eV) | $O_2$ | $O_2^-$ | $O_2^+$ | O + O | $O^-$ + O |
|---|---|---|---|---|---|---|---|
| | | (41.6) | | | $(^2\Sigma_g^-)$ | | |
| (Q,R) | | (39.6) | | | $(^4\Sigma_g^-)$ | | |
| | | 27.9 | | | $(^2\Sigma_u^-)$ | | |
| Q,R | | (24.58) | | | $c\ ^4\Sigma_u^-$ | | |
| | | 23.23 | | | $(^2\Pi_u)$ | | |
| Q,R | 0.14 | 20.34 | | | $B\ ^2\Sigma_g^-$ | | |
| | 0.15 | 19.85 | | | $D(^2\Delta_g)$ | | |
| | | 18.73 | | | | $O + O^+$ | |
| Q,R | 0.15 | 18.22 | | | $b\ ^4\Sigma_g^-$ | | |
| Q,R | 0.11 | 17.11 | | | $A\ ^2\Pi_u$ | | |
| Q,R | 0.13 | 16.16 | | | $a\ ^4\Pi_u$ | | |
| Q,R | 0.24 | 12.07 | | | $X\ ^2\Pi_g$ | | |
| | | . | | | | | |
| | | . | | | | | |
| | | . | | | | | |
| | | 11. | | | | | |
| | 0.24 | 9.43 | $f\ ^1\Sigma_u^+$ | Resonances | | | |
| | | 9.30 | | | | $^3P+^1S$ | |
| | | 9.06 | | | | $^1D+^1D$ | |
| | | 8. | | | | | |
| | | 7.85 | | | | | $^2P+^1S$ |
| | | 7.09 | | | | $^3P+^1D$ | |
| Q | 0.09 | 6.17 | $B\ ^3\Sigma_u^-$ | | | | |

Table 3. Molecular Oxygen Energy Levels (Continued)

| Use Index | Vibrational Spacing | Energy (eV) | $O_2$ | $O_2^-$ | $O_2^+$ | O + O | $O^-$ + O |
|---|---|---|---|---|---|---|---|
| | | 5.62 | | | | | $^2P+^1D$ |
| | | 5.12 | | | | $^3P+^3P$ | |
| Q | 0.10 | 4.39 | $A\ ^3\Sigma_u^+$ | | | | |
| | 0.11 | 4.30 | $A'\ ^3\Delta_u$ | | | | |
| | 0.10 | 4.10 | $c\ ^1\Sigma_u^-$ | | | | |
| Q | | 3.65 | | | | | $^2P+^3P$ |
| | 0.07 | 2.70 | | $A\ ^2\Pi_u$ | | | |
| Q | 0.18 | 1.64 | $b\ ^1\Sigma_g^+$ | | | | |
| Q | 0.18 | 0.98 | $a\ ^1\Delta_g$ | | | | |
| Q | 0.20 | 0.00 | $X\ ^3\Sigma_g^-$ | | | | |
| | 0.14 | -0.44 | | $X\ ^2\Pi_g$ | | | |

Table 4. Nitric Oxide Energy Levels

| Vibrational Spacing | Energy (eV) | NO | $NO^-$ | $NO^+$ | N+O | $N+O^-$ |
|---|---|---|---|---|---|---|
| 0.16 | 17.89 | Grandchild Resonances | | $A'\ ^1\Sigma^+$ | | |
| 0.16 | 17.66 | | | $b'\ ^3\Sigma^-$ | | |
| 0.16 | 16.94 | | | $w\ ^3\Delta$ | | |
| 0.21 | 16.61 | | | $b\ ^3\Pi$ | | |
| 0.16 | 15.73 | | | $a\ ^3\Sigma^+$ | | |
| | 12. | | Resonances | | | |
| | 10.67 | | | | $^4S^o+^1S$ | |
| | 10.07 | | | | $^2P^o+^3P$ | |
| 0.30 | 9.26 | | | $X\ ^1\Sigma^+$ | | |
| | 8.88 | | | | $^2D^o+^3P$ | |
| | 8.47 | | | | $^4S^o+^1D$ | |
| 0.30 | 7.52 | $E\ ^2\Sigma^+$ | | | | |
| 0.15 | 7.48 | $B'\ ^2\Delta_i$ | | | | |
| | 7.00 | | | | | |
| 0.29 | 6.58 | $D\ ^2\Sigma^+$ | | | | |
| | 6.50 | | | | $^4S^o+^3P$ | |
| 0.30 | 6.46 | $C\ ^2\Pi_r$ | | | | |
| 0.15 | (6.04) | $b(^4\Sigma^-)$ | | | | |
| 0.13 | 5.69 | $B\ ^2\Pi_r$ | | | | |
| 0.29 | 5.45 | $A\ ^2\Sigma^+$ | | | | |
| | 5.03 | | | | | $^4S^o+^2P$ |
| 0.13 | (4.77) | $a\ (^4\Pi_i)$ | | | | |
| | (1.13) | | $b'\ \Sigma^+$ | | | |
| 0.18 | 0.724 | | $a\ ^1\Delta$ | | | |
| 0.24 | 0.00 | $X\ ^2\Pi_r$ | | | | |
| 0.17 | -0.02 | | $X\ ^3\Sigma^-$ | | | |

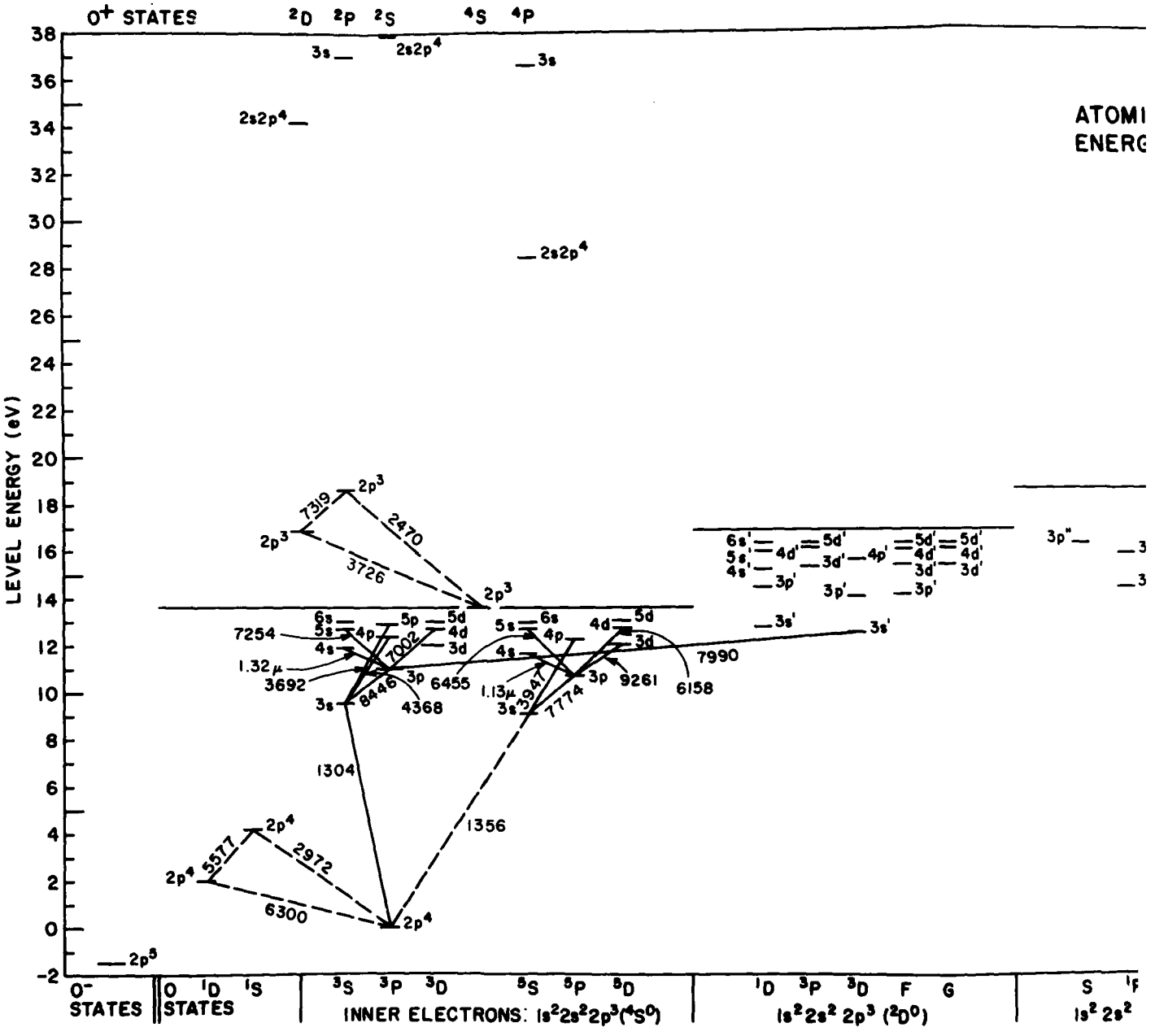


Figure 7. Atom
from Moore (194

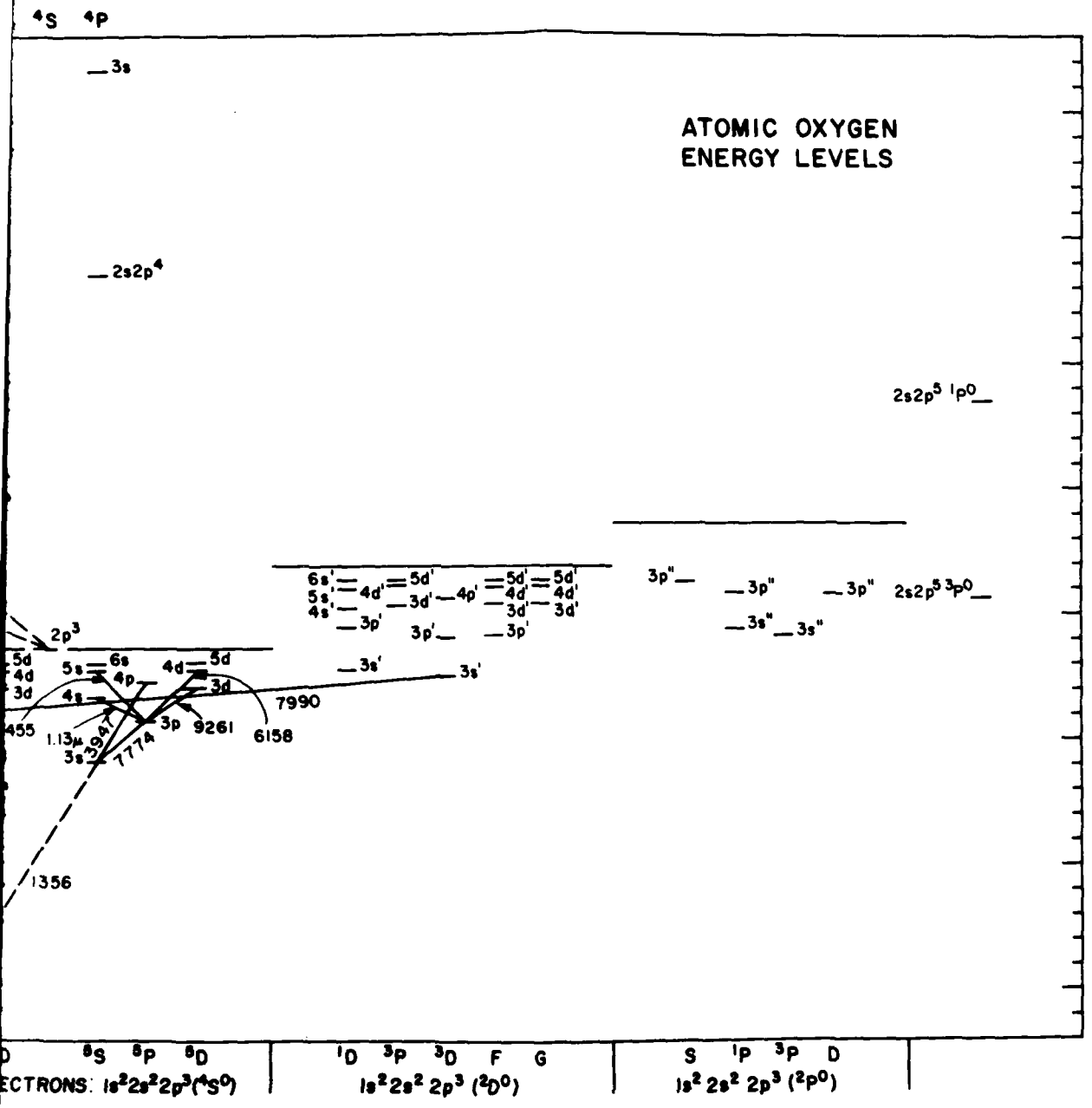


Figure 7. Atomic Oxygen States. The data are from Moore (1949)[15]



2

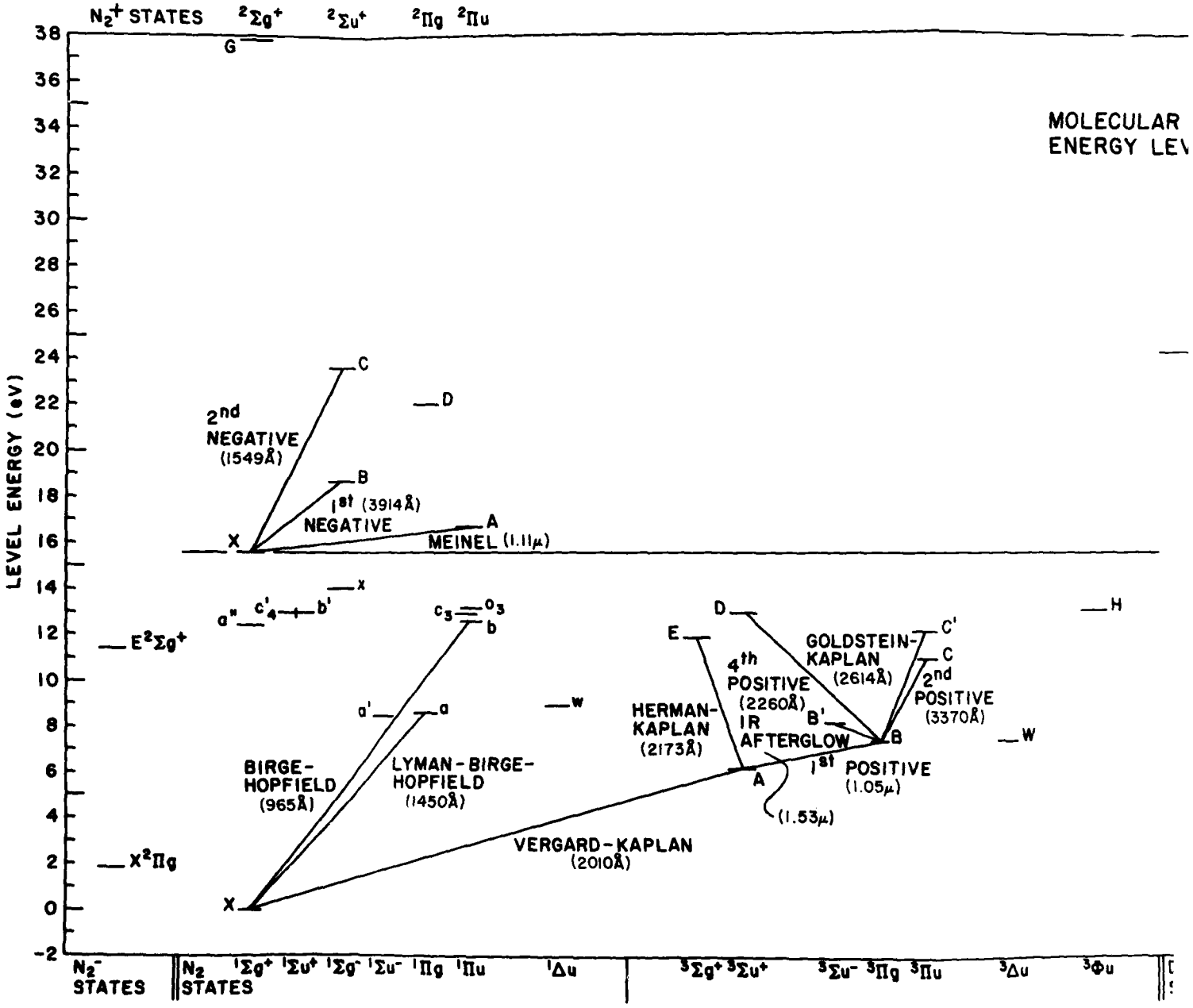


Figure 8. Molecular Ni
are from Huber and Her
and Krupenie (1977)[17]

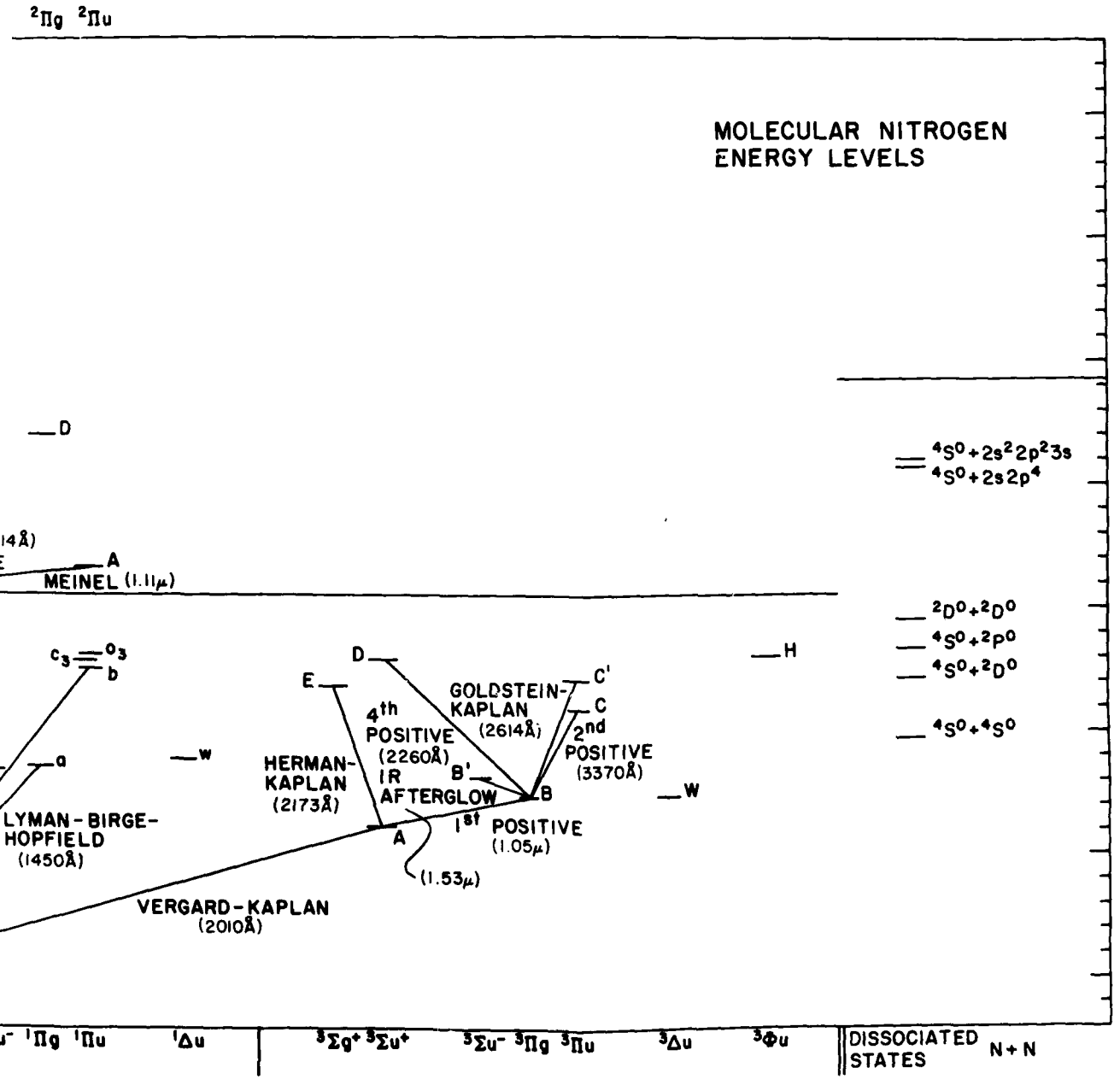


Figure 8. Molecular Nitrogen States. The data are from Huber and Herzberg (1979)[16] and Lofthus and Krupenie (1977)[17]



2

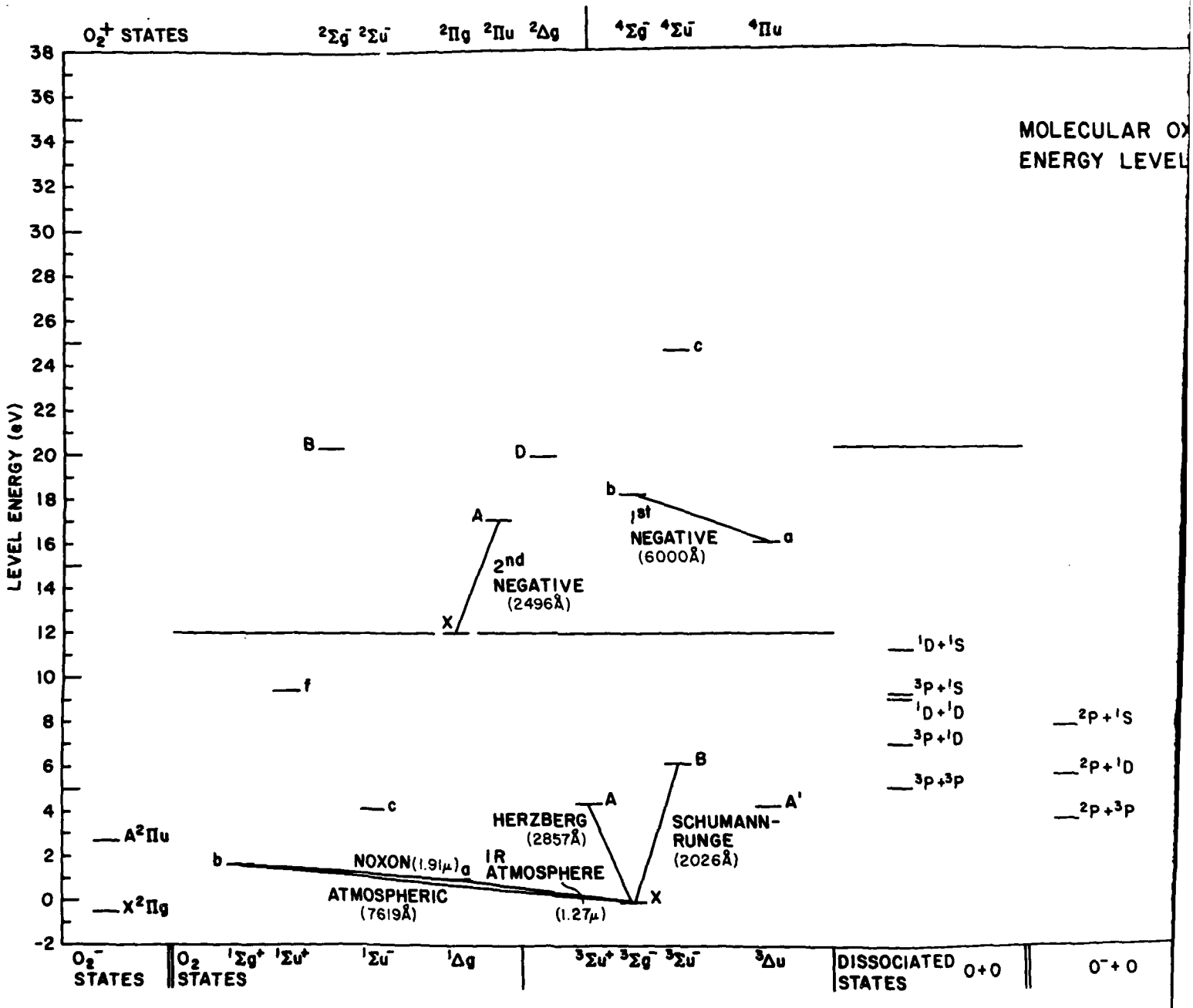


Figure 9. Molecular Oxyge
from Huber and Herzberg (
(1972)[18]

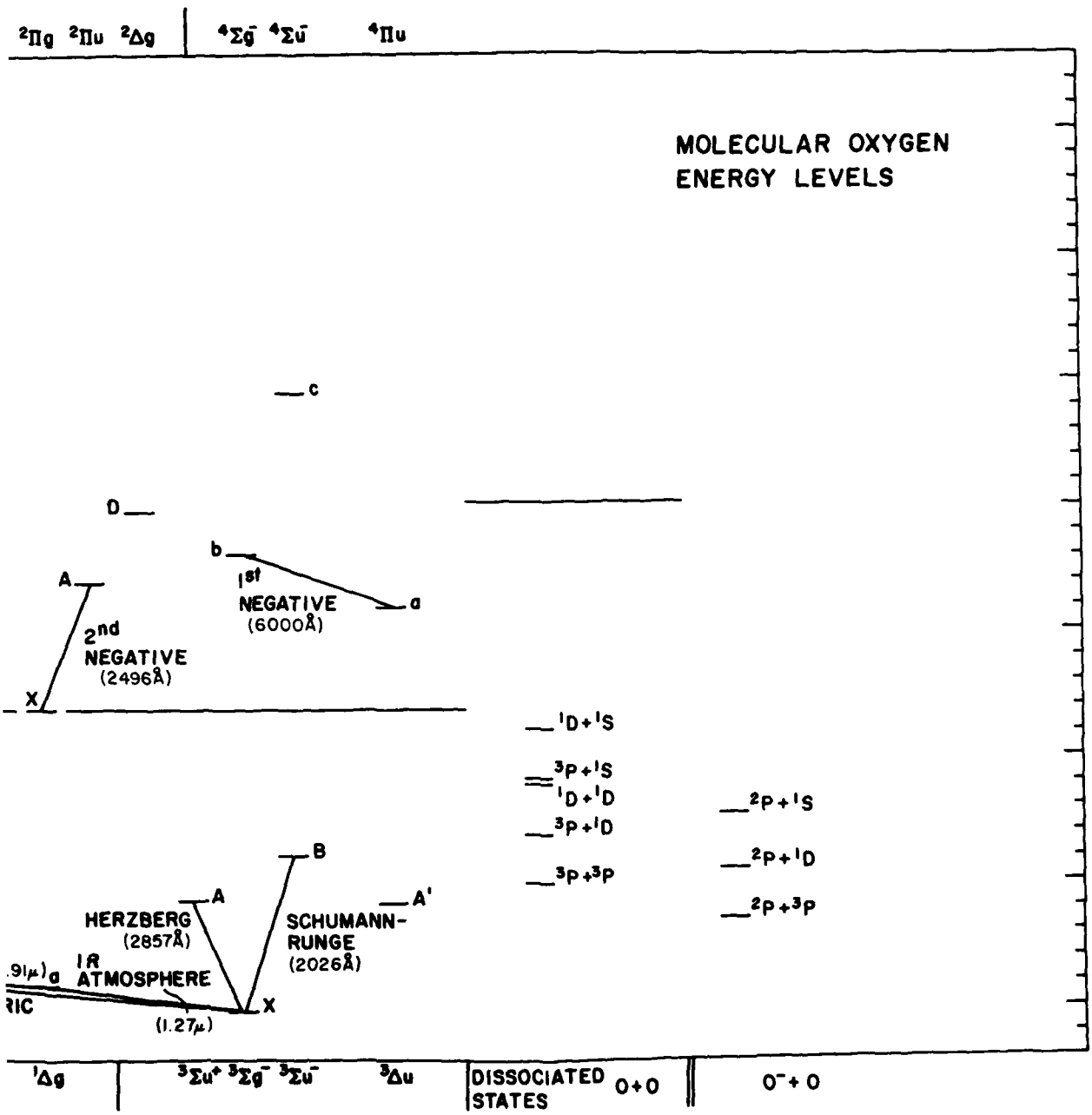


Figure 9. Molecular Oxygen States. The data are from Huber and Herzberg (1979)[16] and Krupenie (1972)[18]



2

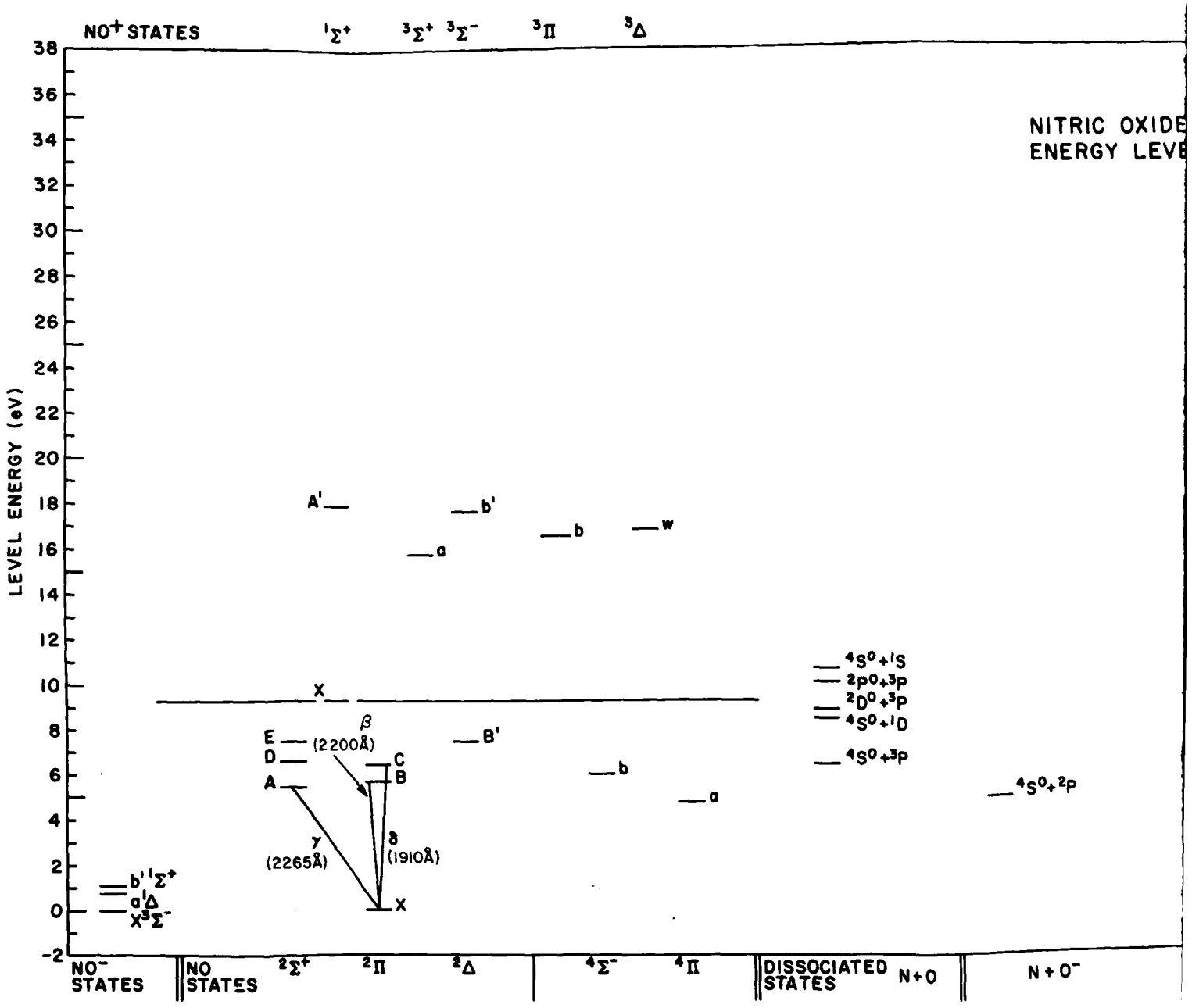


Figure 10. Nitric Oxide S
Huber and Herzberg (1979

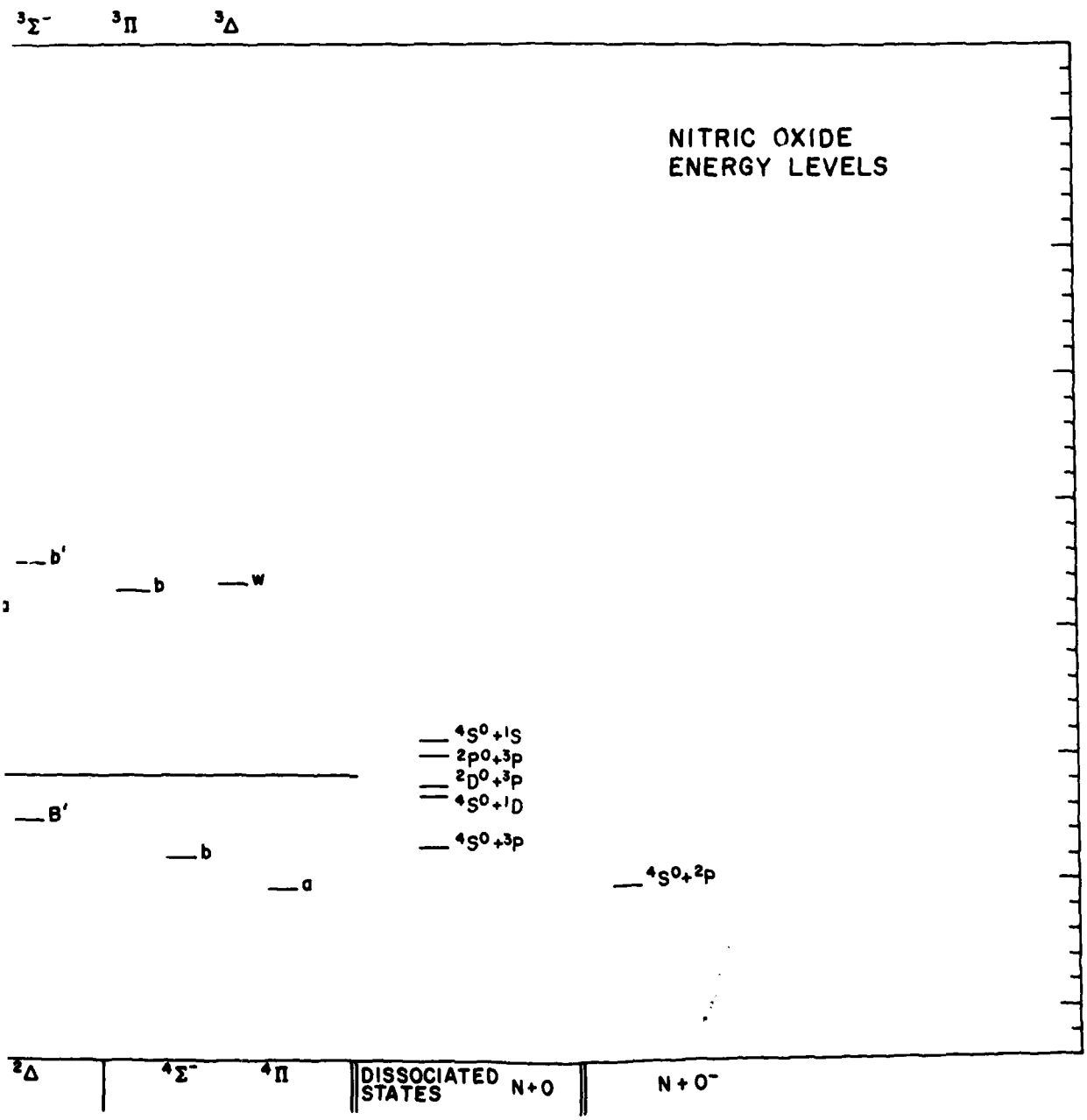


Figure 10. Nitric Oxide States. The data are from Huber and Herzberg (1979)[16]



2

molecular data primarily from Huber and Herzberg (1979).[16] Additional tabulations and discussions of the data for $N_2$ and $O_2$ may be found in Lofthus and Krupenie (1977)[17] and Krupenie (1972),[18] respectively.

The well-known electronic states are listed through the most energetic for which the electron excitation cross section is given in section 4; similarly for the ionic states. The states that are not well-known in Huber and Herzberg[16] have the poorly-determined quantities enclosed in parentheses. The states that do not correspond to those in Huber and Herzberg[16] are enclosed by angular brackets. The radiative bands and lines-of-interest in atmospheric work are shown in the figures following the tables.

For atomic oxygen, the fine structure of the excited states is not given since it is less than ten percent that of the ground state. The rotational level spacing is not given for the molecules. For the ground states, the initial rotational level spacing is 0.00050 eV for $N_2$ and 0.00036 eV for $O_2$.

The tables do not contain all of the states whose excitation cross sections are given in this report. Conversely, cross sections are not given for all of the states in the tables. The column headed "Use Index" contains a Q or R if a specific cross section is given for that level or if the cross section is included in a sum over the cross sections of related Rydberg states.

Graphical presentations of states of O, $N_2$, $O_2$, and NO may be found in Figures 7, 8, 9, and 10, respectively. These graphs do not contain all of the states.

## 4. ELECTRON-NEUTRAL PARTICLE CROSS SECTIONS

The electron-neutral particle cross sections must be known in order to calculate the electron distribution function for the earth's ionosphere (Ashihara and Takayanagi, 1974;[19] Jasperse, 1975,[20] 1976,[21] 1977;[22] Victor et al, 1976;[23] Jasperse and Smith, 1978;[24] and Oran and Strickland 1979.[25]

The variety of states and cascading processes make experimental identification of the many cross sections difficult, especially for the higher lying states. As the energy increases many states may be summed over: rotational states for vibrational excitation; vibrational (and rotational) states for electronic excitation; rotational (and possibly vibrational) virtual states for resonances. At energies high enough to allow the excitation of several different levels, the total cross section must be broken down into the sum of the separate cross sections. This is a difficult task and may cause ambiguities in the final result (Lawton and Phelps, 1978, Appendix C[26]).

---

Because of the large number of references cited above, they will not be listed here. See References, page 69.

At the very low energies, measurements of the cross sections are difficult and much data comes from calculations. Due to the complexity of multi-electron molecules, approximations in the calculations must be used.

The differential cross sections have been measured for a number of the scattering interactions at specific energies. Since few different energy values were taken, in general, this report will not consider the angular dependence of cross sections except the implied dependence in the momentum-transfer cross sections. The angular behavior of photoproduction is discussed in Appendix A.4.

Figures 11 through 13 show the main cross sections for O, $N_2$, and $O_2$.

For greater accessibility the figures showing the cross sections in detail have all been placed in Appendix B. Figures B1 through B14 contain an overview of the electron cross sections. Figures B1 through B3 show the momentum-transfer cross sections for elastic scattering of electrons from O, $N_2$, and $O_2$. Figures B4 through B14 show sums over various types of excitational cross sections: rotational excitation of $N_2$ and $O_2$, atomic oxygen fine structure excitation, $N_2$ and $O_2$ vibrational excitation, electronic state excitation of O, $N_2$, and $O_2$, and ionization of O, $N_2$, and $O_2$.

#### 4.1 Momentum-transfer Cross Sections

The momentum-transfer (or diffusion) cross section is one of the series of integral cross sections that are weighed by a function of the scattering angle $\theta$ : $(1 - \cos^{\ell}\theta)\, dQ$. These arise in an angular decomposition of the Boltzmann collision integral. (Shkarovsky et al, 1966;[27] Ferzinger and Kaper, 1972[28]). The total cross section is

$$Q_T = \int dQ .$$

For $\ell = 1$ the cross section is the momentum-transfer cross section:

$$Q_M = \int (1 - \cos\theta)\, dQ ,$$

which is the cross-section integral weighted by the fraction of the forward momentum lost in the collision. Given the masses of the projectile and target, the

27. Shkarofsky, I.P., Johnson, T.W., and Bachynski, M.P. (1966) The Particle Kinetics of Plasma, Addison-Wesley, Reading, Massachusetts.

28. Ferzinger, J.H., and Kaper, H.G. (1972) Mathematical Theory of Transport Processes in Gasses, N. Holland Publishing Co., Amsterdam, Holland.

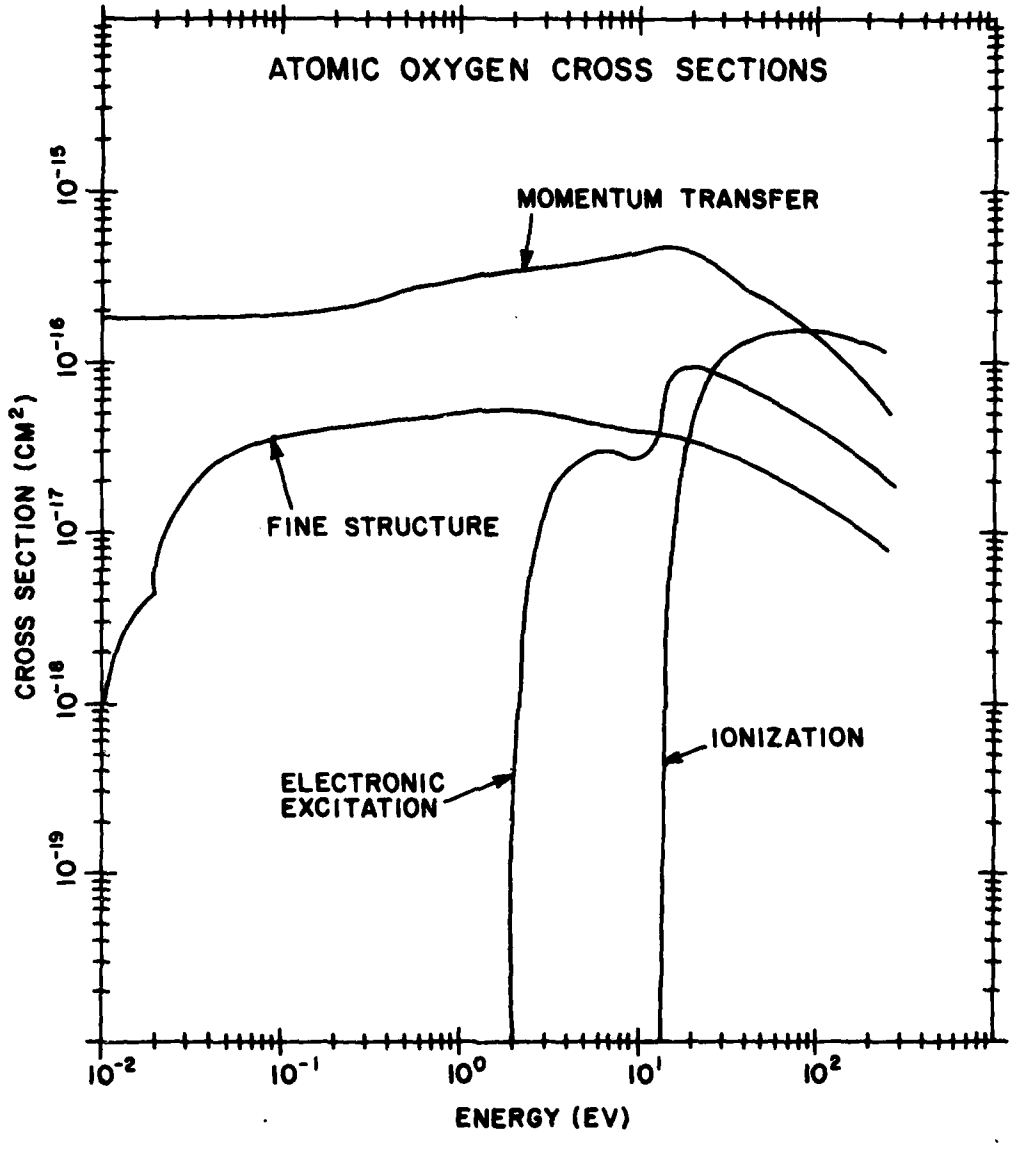


Figure 11. Summed Cross Sections for Electron Scattering from Atomic Oxygen. Refer to Appendix B for details

cross-section integral weighted by the fraction of projectile energy lost is $(2m/M)Q_M$ to order $(m/M)^2$. (If dQ does not depend on $\theta$, $Q_M$ equals $Q_T$.)

The momentum transfer cross section can be obtained by a weighted integral of the differential cross section obtained from experiment or theory. Some experiments obtain the momentum-transfer cross section directly, for example, swarm experiments (Lane, 1980;[29] Schultz, 1973a,[30] 1973b[31]). Porter and Jump (1978)[32] review the total and differential elastic cross-sections for atmospheric species. Their data can be used to calculate the momentum transfer cross sections.

The experimental data for the elastic cross section of O (Sunshine et al, 1967[33]) has error bars in the vicinity of 20 percent. The calculations by Thomas and Nesbet (1975)[34] gives both the elastic and the momentum transfer cross sections up to 11 eV. This curve is close to that of Henry (1967)[35] for the elastic cross section. Both of these curves are near the lower limit of the error spread of Sunshine et al [33] although an earlier experiment by Neynaber et al (1961)[36] does lie lower. The calculations of Rountree et al (1974)[37] are towards the top of the error range between 2 and 6 eV, while Henry (1967)[35] and Saraph (1973)[38] are more central. In view of the errors in the data, an argument could be made for any of these. The data needed to go to the momentum transfer cross section is lacking except for Thomas and Nesbet (1975)[34] who tabulate both cross sections. Above 11 eV, the momentum-transfer cross section of Thomas and Nesbet can be extended using 0.7 of the calculated elastic cross section of Smith et al (1967).[39] The factor is chosen for a smooth fit. Beyond 54.4 eV the curve must be extrapolated. This is generally within 20 percent of the data points of Porter and Jump (1978).[32]


29. Lane, N.F. (1980) Rev. Mod. Phys. 52:29.
30. Schulz, G.J. (1973a) Rev. Mod. Phys. 45:378.
31. Schulz, G.J. (1973b) Rev. Mod. Phys. 45:423.
32. Porter, H.S., and Jump, F.W. (1978) Computer Sciences Corporation, TM-78/6017.
33. Sunshine, G., Aubrey, B.B., and Bederson, B. (1967) Phys. Rev. 154:1.
34. Thomas, L.D., and Nesbet, R.K. (1975) Phys. Rev. A11:170; addendum, Phys. Rev. A12:1279.
35. Henry, R.J.W. (1967) Planet Space Sci. 15:1747.
36. Neynaber, R.H., Marino, L.L., Rothe, E.W., and Trujillo, S.M. (1961) Phys. Rev. 123:148.
37. Rountree, S.P., Smith, E.R., and Henry, R.J.W. (1974) J. Phys. B7:L167.
38. Saraph, H.E. (1973) J. Phys. B6:2243.
39. Smith, K., Henry, R.J.W., and Burke, P.G. (1967) Phys. Rev. 157:51.

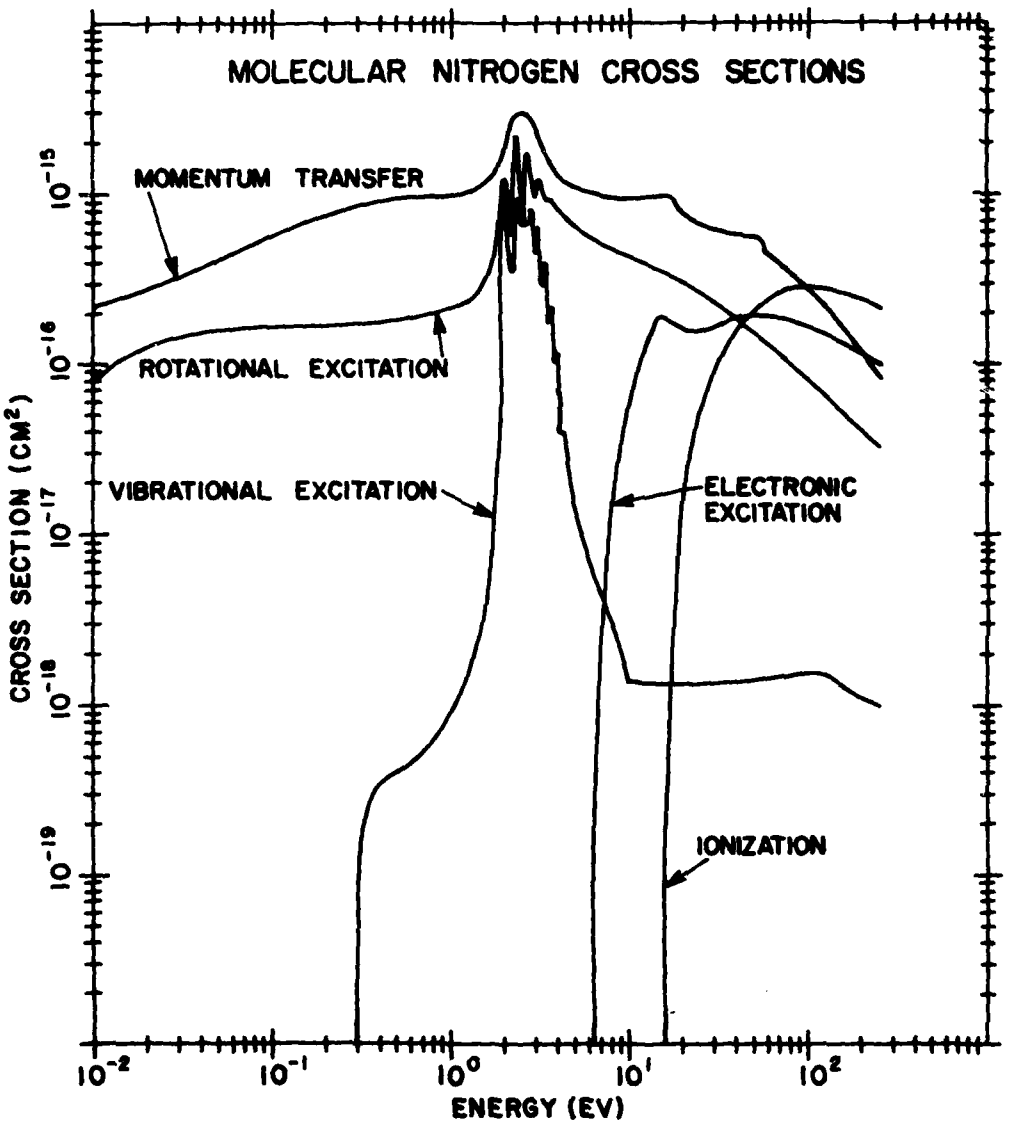


**Figure 12. Summed Cross Sections for Electron Scattering from Molecular Nitrogen. Refer to Appendix B for details**

The momentum-transfer cross section of $N_2$ was initially determined by Frost and Phelps (1962)[40] and by Englehardt, Phelps, and Risk (1964).[41] The calculation by Morrison and Collins (1978)[42] agrees with experiment in the range 3 to 30 eV. Below 1.4 eV the calculation is about 20 percent higher than experiment. For a complete review of the calculational techniques see Lane (1980).[29] Above 18 eV more recent experiments and calculations agree with each other to within 20 percent. (Srivastava et al, 1976;[43] Choi et al, 1979[44]). The momentum-transfer cross section measured by Shyn and Carignan (1980)[45] agrees with the others generally within 20 percent, but it does not show the resonant structure between 2 and 4 eV.

Hake and Phelps (1967)[46] determined the $O_2$ momentum-transfer cross section. Drift velocity data obtained by Nelson and Davis (1972)[47] indicates a lower cross section below 1 eV, which is also indicated by earlier microwave experiments. Trajmar, Cartwright, and Williams (1971)[48] measure the total cross sections and the differential cross sections at certain energies. At energies above 10 eV momentum-transfer cross sections obtained from their differential cross sections are below the values of Hake and Phelps dropping to approximately one-eighth at 45 eV. The fitted values from the survey of Porter and Jump (1978)[32] are used.

These cross sections are shown in Figures B1 through B3.

#### 4.2 Rotational Excitation Total Cross Sections

The order of magnitude of the energy separation between the rotational levels of a diatomic molecule can be estimated semiclassically by assuming an angular momentum of $\hbar$ and an average separation of two Bohr radii yielding a rotational inertia of $(M_1 + M_2)\, a_0^2$. The estimated energy is

$$\frac{\hbar^2}{2(M_1 + M_2)\, a_0^2} = \left( \frac{1}{2} \alpha^2 \, mc^2 \right) \left( \frac{m}{M_1 + M_2} \right)$$

40. Frost, L.S., and Phelps, A.V. (1962) Phys. Rev. 127:1621.
41. Englehardt, A.G., Phelps, A.V., and Risk, C.G. (1964) Phys. Rev. 135:A1566.
42. Morrison, M.A., and Collins, L.A. (1978) Phys. Rev. A17:918.
43. Srivastava, S.K., Chutjian, A., and Trajmar, S. (1976) J. Chem. Phys. 64:1340.
44. Choi, B.H., Poe, R.T., Sun, J.G., and Shan, Y. (1979) Phys. Rev. A19:116.
45. Shyn, T.W., and Carignan, G.R. (1980) Phys. Rev. A22:923.
46. Hake, R.D., and Phelps, A.V. (1967) Phys. Rev. 158:70.
47. Nelson, D.R., and Davis, F.J. (1972) J. Chem. Phys. 57:4079.
48. Trajmar, S., Cartwright, D.C., and Williams, W. (1971) Phys. Rev. A4:1462.

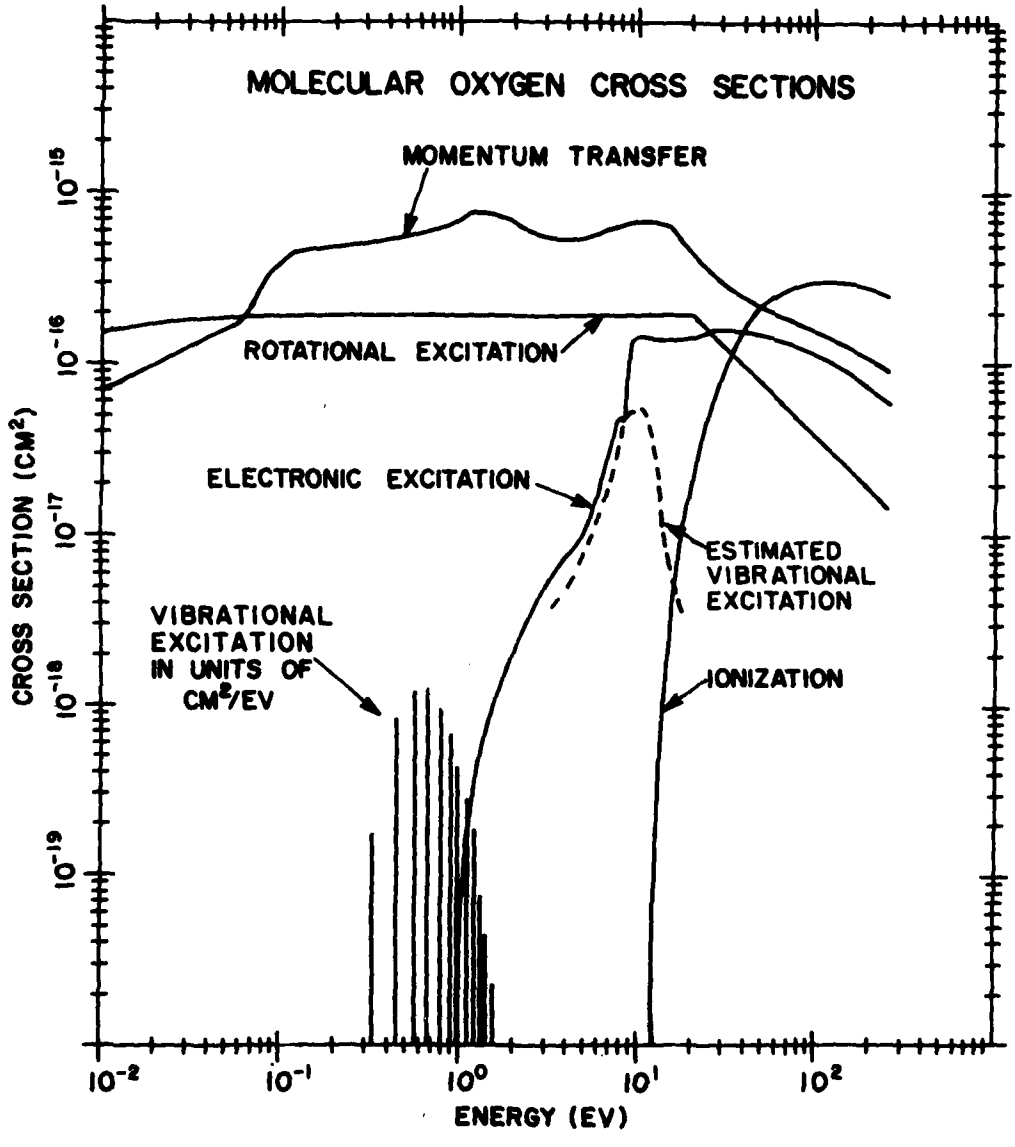


**Figure 13. Summed Cross Sections for Electron Scattering from Molecular Oxygen. Refer to Appendix B for details. Note the "low energy" vibrational excitational cross sections are, in effect, delta functions and, as such, have units of $cm^2/eV$.**

The electron mass is m, $\alpha$ is the fine structure constant, and $\frac{1}{2}\alpha^2 mc^2$ is a Rydberg of energy, 13.6 eV. For $N_2$ and $O_2$ this separation is about 0.0002 eV, and the equivalent temperature about 2°K; the rotational levels are well populated in the Earth's ionosphere.

The cross sections for transfers between such low-lying states are hard to determine either experimentally or theoretically. "Beam experiments do not have the resolution necessary for a study of rotational excitation or for distinguishing rotational levels in vibrational transitions. Thus, in the case of $N_2$ or in fact for all molecules except $H_2$ one has to rely on theory." (Schulz, 1973b).[31] "At present there are still no reliable theoretical estimates of the rotational excitation cross sections for $N_2$ below the resonance [near 2 eV], or for $O_2$ at any energy." (Lane, 1980).[29]

An early determination of the rotational excitation cross section for $N_2$ was done theoretically by Gerjuoy and Stein (1955);[49] nonspherical effects were considered by Dalgarno and Moffett (1963).[50] Takayanagi and Geltman (1965,[51] 1966[52]) used a distorted wave and additional long- and short-range interactions. With only long-range interactions the cross section shows the quadrupole-polarization cancellation and remains below the Gerjuoy-Stein result. When the short range effects are included, the calculation of the peak of the cross section violates unitarity. Chen (1966a,[53] 1966b[54]) has calculated the cross section semiempirically using the $N_2$ resonant states. Chandra and Temkin (1976)[55] used their hybrid theory with an adiabatic nuclear rotation approximation. The results of Chandra and Temkin are much larger and exhibit the J = 0 to J = 4 enhancement in the resonance region (Burke and Chandra, 1972[56]). The elastic cross section of Chandra and Temkin is substantially larger than the experiment of Golden (1966).[57] The better cross section is probably that of Chen (1966a,[53] 1966b[54]) scaled up nearly to that of Chandra and Temkin (1976).[55] This would have the empirically correct resonance positions and a better overall magnitude.

The Gerjuoy-Stein (1955)[49] formula is used for the rotational excitation cross sections of $O_2$. Sampson and Mjolsness (1966)[58] attempted to refine the calculation

49. Gerjuoy, E., and Stein, S. (1955) Phys. Rev. 97:1671.
50. Dalgarno, A., and Moffett, R.J. (1963) Proc. Nat'l. Acad. Sci., India A33:511.
51. Takayanagi, K., and Geltman, S. (1965) Phys. Rev. A138:1003.
52. Geltman, S., and Takayanagi, K. (1966) Phys. Rev. 143:25.
53. Chen, J.C.Y. (1966a) Phys. Rev. 146:61.
54. Chen, J.C.Y. (1966b) J. Chem. Phys. 45:2710.
55. Chandra, N., and Temkin, A. (1976) Phys. Rev. A13:188.
56. Burke, P.G., and Chandra, N. (1972) J. Phys. B5:1969.
57. Golden, D.E. (1966) Phys. Rev. Lett. 17:847.
58. Sampson, D.H., and Mjolsness, R.C. (1966) Phys. Rev. 144:116.

using the distorted wave approximation with a quadrupolar pseudopotential; however, for an electron energy in the vicinity of 0.15 eV their cross section is two orders of magnitude too small to account for energy loss observations. Geltman and Takayanagi (1966)[52] use short range interactions as well that produce a larger low energy cross section but lead to nonunitarity at larger energies. This does provide an estimate of the cross section below 1.5 eV, which may be too high (Lawton and Phelps, 1978[26]).

The lowest rotational excitation cross sections for $N_2$, from Chandra and Temkin, are shown in Figures B15 through B19. Higher rotational cross sections for $N_2$ and rotational cross sections for $O_2$ from the Gerjuoy-Stein formula with a cutoff at 20 eV are shown in Figures B20 through B36.

The cross sections shown are integrated over solid angle. Chandra and Temkin (1976)[55] and Ehrhardt and Willmann (1967)[59] have data on the differential cross sections.

#### 4.3 Fine-structure Excitation Total Cross Sections

The ground state of oxygen has a fine structure of three levels being at energies of 0, 0.019, and 0.029 eV or of 0°, 156°, and 235°K. The initial calculation of the fine-structure cross section was by Breig and Lin (1966).[60] More recent calculations are by Saraph (1973),[38] Tambe and Henry (1974,[61] 1976[62]), and LeDourneuf and Nesbet (1976).[53] The last two calculations agree within ten percent where they overlap and probably form the best set. A comparison of the calculations with an application to ionospheric electron cooling may be found in Hoegy (1976).[64]

These cross sections are found in Figures B27 through B39. Thomas and Nesbet (1975)[34] consider the differential cross sections.

#### 4.4 Vibrational Excitation Total Cross Sections

The separation of successive vibrational energy levels is usually in the vicinity of 0.2 eV or 2000°K. In the ionosphere this is high enough so that the excited levels are relatively depopulated but low enough so that excitation by energetic

59. Ehrhardt, H., and Willmann, K. (1967) Z. Phys. 204:462.
60. Breig, G.L., and Lin, C.C. (1966) Phys Rev. 151:67.
61. Tambe, B.R., and Henry, R.J.W. (1974) Phys. Rev. A10:2097.
62. Tambe, B.R., and Henry, R.J.W. (1976) Phys. Rev. A13:224.
63. LeDourneuf, M., and Nesbet, R.K. (1976) J. Phys. B9:L241.
64. Hoegy, W.R. (1976) Geophys. Res. Lett. 3:541.

electrons provides a sink for the electron energy, especially in the case of $N_2$. The vibrational excitation cross sections are reviewed by Schulz (1976).[65]

For the $N_2$ vibrational excitation cross sections, the first experimental work was by Schulz (1962),[66] which was given in arbitrary units. The measurement of the total cross section by Golden (1966)[57] is the main work in absolute units. There is a series of resonances between 2 and 5 eV which can be identified with the vibrational states of $N_2^-$ $X\,^2\Pi_g$. Although the states have a width which is sufficiently narrow to produce well defined resonances, the lifetimes are short enough so that the energy of the state is dependent on the initial and final states (Birtwistle and Herzenberg, 1971,[67] Dubé and Herzenberg, 1979[68]).

There have been many calculations of the separate vibrational excitation cross sections; for a review see Lane (1980).[29] The calculation by Schneider, LeDourneuf, and Vo Ky Lan (1979)[69] agrees well with the experimental general structure of the separate cross sections and is about ten percent larger than the measured absolute total cross section.

The low energy cross sections with the target not in the ground vibrational state have been calculated by Chen (1964a,[70] 1964b[71]) and Dubé and Herzenberg (1979).[68] There is no experimental data for confirmation.

The $N_2^-$ state $E\,^2\Sigma_g^+$ is related to Feshbach resonances near 11.5 eV in the vibrational excitation cross section (Schulz, 1973a,[30] 1973b[31]). Schulz (1976)[65] illustrates the behavior of the differential cross section for excitation to the first vibrational state and 90° scattering; this shows the resonance sequence below 4 eV, the broad resonances near 8, 13.5, and 20 eV and the sharp Feshbach resonances near 11.5 eV. The general magnitude agrees with work by Truhlar et al, (1972,[72] 1976,[73] 1977[74]) who measure the cross section up to 75 eV. The calculations of Choi et al (1979)[44] covering the range up to 500 eV are higher than experiments

---


65. Schulz, G.J. (1976) in Principles of Laser Plasmas (G. Bekefi, ed.) John Wiley and Sons, New York, New York.

66. Schulz, G.J. (1962) Phys. Rev. 125:229.

67. Birtwistle, D.T., and Herzenberg, A. (1971) J. Phys. B4:53.

68. Dubé, L., and Herzenberg, A. (1979) Phys. Rev. A20:194.

69. Schneider, B., LeDourneuf, M., and Vo Ky Lan (1979) Phys. Rev. Lett. 43:1426.

70. Chen, J.C.Y. (1964a) J. Chem. Phys. 40:3507.

71. Chen, J.C.Y. (1964b) J. Chem. Phys. 40:3513, errata (1964) J. Chem. Phys. 41:3263.

72. Truhlar, D.G., Trajmar, S., and Williams, W. (1972) J. Chem. Phys. 37:3250.

73. Truhlar, D.G., Brandt, M.A., Chutjian, A., Srivastava, S.K., and Trajmar, S. (1976) J. Chem. Phys. 65:2962.

74. Truhlar, D.G., Brandt, M.A., Srivastava, S.K., Trajmar, S., and Chutjian, A. (1977) J. Chem. Phys. 66:655.

where comparison is possible. They provide cross sections for excitation to the second vibrational state at high energies where no experimental data exists.

The total vibrational excitation cross section is approximately half of the total cross section as indicated by the experiment of Shyn and Carignan (1980).[45]

The total cross section to the first vibrational state, shown in Figure B40, comes from Chen (1966a,[53] 1966b[54]) below 1.5 eV, from Schneider (1980)[75] to 6.6 eV, from Truhlar et al,[72,73,74] between 10 and 50 eV, and from Choi et al,[44] above 75 eV. The cross section for exciting the second vibrational state shown in Figure B41 uses Schneider (1980)[75] below 6.6 eV and Choi, et al,[44] above 50 eV. The other $N_2$ vibrational cross sections, Figures B42 through B52, use the data of Schneider (1980).[75]

Below 2 eV, the $O_2$ vibrational excitation cross sections are dominated by resonances belonging to the vibrational states of $O_2^-$ ($X\ ^2\Pi_g$). This produces a set of peaks in the cross section that can be individually identified with vibrational states of the resonance. The most complete set of energies and total cross sections for each peak are those measured by Linder and Schmidt (1971).[76] Lawton and Phelps (1978)[26] mention that either the cross sections should be increased by a factor of 2 to match experimental values of transport coefficients or there are other effects which have not been accounted for, for example, larger than expected rotational excitation cross sections. The resonance widths are assumed equal by Linder and Schmidt[76] and estimated at 0.5 meV; Koike and Watanabe (1973)[77] determine the individual widths.

A broad peak is found in the differential cross sections for vibrational excitation by Wong, Boness, and Schulz (1973)[78] and is attributed to $O_2^-\ ^4\Sigma_u^-$. The published data is for a scattering angle of 25°. The total cross section may be eliminated by integrating over an assumed angular distribution. If the angular dependence for $N_2$ calculated by Chandra and Temkin (1976)[55] is used, the integrated cross section is 7 times the differential cross section at 25° for the lowest four vibrational states.

The low energy resonances of the vibrational cross sections for $O_2$ are so narrow that they have been treated as delta functions in Figures B53 through B56.

Differential vibrational cross sections are discussed in Chen (1966a,[53] 1966b[54]) Trajmar et al (1972),[79] Wong et al (1973),[78] Chandra and Temkin (1976,[55] Truhlar (1976,[73] 1977[74]), and Schulz (1976).[66]

---

75. Schneider, B.I. (1980) Private communication.
76. Linder, F., and Schmidt, H. (1971) Z Naturforsch. 26:1617.
77. Koike, F., and Watanabe, T. (1973) J. Phys. Soc. Japan 34:1022.
78. Wong, S.F., Boness, M.J.W., and Schulz, G.S. (1973) Phys. Rev. Lett. 31:699.
79. Trajmar, S., Williams, W., and Kupperman, A. (1972) J. Chem. Phys. 56:3759.

### 4.5 Electron Excitation Total Cross Sections

The electronic states of the atmospheric species start at an energy of a few electron volts. These states are not thermally excited. They do form a sink for the energy of the photoelectrons through excitation by the electrons and subsequent radiative decay.

It is at these energies that the separation of the effects from different states becomes difficult. As a result, the determination of a particular cross section at a particular electron energy depends on knowing the others or on having a method of separating them. Comparing sets of cross sections with other data which can be connected with them (for example, electron transport coefficients) allows determination of a set which is self-consistent in a given context. If the cross sections are to be used to model a similar situation, such a set should give good results if it is sufficiently complete. Such sets were determined using electron transport coefficients for $O_2$ (Lawton and Phelps, 1978)[26] and $N_2$ (Phelps, Levron, and Tachibana, 1979;[80] Phelps, 1980[81]).

Atomic oxygen is difficult to handle experimentally because it is so reactive. The theoretical approach is also difficult due to the need to properly represent the open shell configuration of the atom, its interactions with the incoming electron including exchange and polarization, and the effects of low-lying states of the atom and its negative ion, that is, excitation and resonances.

The cross sections for excitation to the other states of the ground configuration, $^1D$ and $^1S$, have been calculated using different approaches (Smith et al 1967;[39] Vo Ky Lan et al 1972;[82] Thomas and Nesbet 1975 [34]). The results are within 20 percent of each other; those of Smith et al and Vo Ky Lan et al are within ten percent. The total elastic cross section obtained by Vo Ky Lan et al in the same series of calculations is in good agreement with the data of Sunshine et al (1967).[33] The set chosen here is that of Vo Ky Lan et al extended to higher energies by the calculation of Smith et al.

The higher states have one electron excited to higher orbital states. The lowest-lying of these states, $3s\ ^3S^o$ and $3s\ ^5S^o$, have the experimental measurements of Stone and Zipf (1974)[83] with relatively large errors for the $^5S$ state. One problem is properly accounting for fast cascade transitions. For $^3S$ close-coupling

80. Phelps, A.V., Levron, D., and Tachibana, K. (1979) Abstracts of contributed papers, XIth International Conference on the Physics of Electronic and Atomic Collisions, Kyoto, Japan, 1979.

81. Phelps, A.V. (1980) Private communication.

82. Vo Ky Lan, Feautrier, N., LeDourneuf, M., and Van Regemorter, H. (1972) J. Phys. B5:1506

83. Stone, E.J. and Zipf, E.C. (1974) J. Chem. Phys. 60:4237.

calculations of Rountree and Henry (1972)[84] and Smith (1976)[85] agree with each other. The distorted wave calculation of Sawada and Ganas (1973)[86] is higher and the *measurements of Stone and Zipf*[83] are higher by roughly a factor of 6. Smith[85] includes theoretical cross sections to the higher states 3d $^3D^o$, 4s $^3S^o$, and 3p $^3P$, calculates transition rates, and determines a total cross section to 3s $^3S^o$, including cascading. This value is smaller than the measured value by a factor of 2.5 at 5 Ry. However, both have a very large error base, 50 percent and 40 percent, which allow them to be compatible. In view of the difficulty in performing the measurement and the agreement in the calculations, the cross section for excitation to 3s $^3S^o$ chosen is that calculated by Smith (1976)[85] with five states near threshold and a two-configuration ground state representation for higher energies. This cross section can be continued to higher energies using the calculations by Rountree and Henry (1972),[84] whose low energy region has a structure that may be due to an improperly positioned resonance (Smith, 1976[85]).

The other cross section measured by Stone and Zipf,[83] 3s $^5S^o$, has the same difficulties. The distorted wave calculation of Sawada and Ganas (1973)[86] and the close-coupling calculation of Smith (1976)[85] agree but are a factor of 6 to 8 below the measurement. *Since the amount of cascading is unknown,* the theoretical cross sections are chosen.

Both of the theoretical cross sections, to $^3S^o$ and $^5S^o$, might be scaled upward by a factor of 2 to achieve a smaller difference with the measured value.

The higher states are treated theoretically by distorted wave (Sawada and Ganas, 1973[86]), 3p $^5P$, 3p $^3P$, 4p $^5P$, and 4p $^3P$, or by close-coupling (Smith, 1976[85]), 3p $^3P$, 4s $^3S^o$, and 3d $^3D^o$. For the only case which appears in both sets, 3p $^3P$, the cross sections agree to within ten percent above 2 Ry for the three-configuration calculation by Smith. Below 2 Ry, the structure in the Smith calculation seems to be due to the non-use of exchange. For this choice of cross sections for 3p $^3P$ that by Sawada and Ganas seems best. Smith checks his basis states by calculating the dipole oscillator strengths and comparing them with those obtained by other methods. The errors are estimated at 50 percent.

Dalgarno and LeJeune (1971)[87] use oscillator strengths and general theoretical arguments to obtain parameters for the formula of Green and Dutta (1967)[88] applied to oxygen excitation cross sections where the final state has one n = 3 electron.


84. Rountree, S.P., and Henry, R.J.W. (1972) Phys. Rev. A6:2106.

85. Smith, E.R. (1976) Phys. Rev. A13:65.

86. Sawada, T., and Ganas, P.S. (1973) Phys. Rev. A7:617.

87. Dalgarno, A., and LeJeune, G. (1971) Planet Space Sci. 19:1963.

88. Green, A.E.S., and Dutta, S.K. (1967) J. Geophys. Res. 72:3933.

89. Jackman, C.H., Garvey, R.H., and Green, A.E.S. (1977) J. Geophys. Res. 82:5801.

Jackman et al (1977,[89] 1980 [90]) have collected a number of oxygen excitation cross sections. We will use their set of cross sections except as follows: the cross section to $2p^4\ ^1D$ is the major one below 9 eV; increasing the parameter F to 0.011 will align the cross section with that of Vo Ky Lan et al, (1972).[82] The cross sections to ($^4S^o$) 3s $^3S^o$ are taken from Smith (1976)[85] and Rountree and Henry (1972).[84] The cross section to ($^4S^o$) 3d $^3D^o$ can be adjusted to agree with the calculation of Smith by decreasing the parameter F to 0.009. Finally, the cross sections to ($^4S^o$) 4s $^3S^o$, ($^4S^o$) 4p $^3P$, and ($^4S^o$) 4p $^5P$ do not agree with the calculations of Smith (1976)[85] and Sawada and Ganas (1973)[86] over the entire energy range. Since the total contribution of these cross sections is less than eight percent of the total cross section and since the magnitudes are close, the Jackman et al cross sections are used without change.

There is some disparity between various determinations of the cross section for electron excitation of $N_2$ to the first excited state, A $^3\Sigma_u^+$. Most have a sharp peak near 10 eV which might be due to a series of shape resonances. The results of Cartwright et al (1977)[91] have a broad peak at 16.5 eV and are ascribed to better identification, elimination of other excited states which may cascade to A $^3\Sigma_u^+$, and eliminating the need for the resonance at 11 eV (Borst, 1972 [92]). The theoretical calculation of Chung and Lin (1972)[93] is above the experimental data by at least a factor of 2. The fit of Porter et al (1976)[94] resembles the experimental cross section of Brinkmann and Trajmar (1970)[95] which is smaller than the others.

The experimental values of Cartwright et al (1977)[91] and the theoretical values of Chung and Lin (1972)[93] for excitation to B $^3\Pi_g$ agree. Other results including those by Porter et al (1976)[94] tend to climb more rapidly to a peak near 10 eV and drop below the Cartwright et al results. These peaks can be explained by shape resonances originally positioned in the range of 9 to 11.2 eV.

There are a few determinations of the cross section for $N_2$ excitation to W $^3\Delta_u$. The experimental work of Cartwright et al (1977)[91] is much larger and does not have the same shape as the theoretical work of Chung and Lin (1972).[93]

Cartwright et al (1977)[91] have measured the cross section for electron excitation of $N_2$ to B' $^3\Sigma_u^-$ and a' $^1\Sigma_u^-$.

---


90. Jackman, C.H. Garvey, R.H., and Green, A.E.S. (1980) Private communication.

91. Cartwright, D.C., Trajmar, S., Chutjian, A., and Williams, W. (1977) Phys. Rev. A16:1041.

92. Borst, W.L. (1972) Phys. Rev. A5:648.

93. Chung, E.S., and Lin, C.C. (1972) Phys. Rev. A6:988.

94. Porter, H.S., Jackman, C.H., and Green, A.E.S. (1976) J. Chem. Phys. 76:154.

95. Brinkmann, R.T., and Trajmar, S. (1970) Ann. Geophys. 26:201.

The $N_2$ state a $^1\Pi_g$ is the head of the Lyman-Birge-Hopfield band and the cross section has been measured by a number of people. The results of Cartwright et al (1977)[91] are near the bottom of the range, a result attributed to better screening of scattering effects due to other states. The data fit by Jackman et al (1980)[82] is close to the theoretical curve of Chung and Lin, which is higher than the Cartwright et al data except at the peak near 18 eV.

Comments on the data for W $^1\Delta_u$ are identical to those for W $^3\Delta_u$.

The cross section for electron excitation on $N_2$ to the C $^3\Pi_u$ state shows generally good agreement (see Cartwright et al, 1977 [91]). The calculation by Chung and Lin (1972)[93] is higher by as much as a factor of 2 at higher energies. The data fit by Porter et al[94] matches the experimental data. The unnormalized data of Finn et al (1972)[96] and Kisker (1972)[97] show a more gradual rise near threshold followed by a steeper climb to the peak.

The enhanced scattering seen by Borst et al (1972)[98] in studying the excitation of $N_2$ to the E $^3\Sigma_g^+$ state may be close to $N_2^-$ E $^2\Sigma_g^+$ which is about 0.4 eV lower in energy. Other experiments, Brinkmann and Trajmar (1970)[95] and Cartwright et al (1977),[91] examine the non-resonant part. The data of Cartwright et al is more than a factor of 2 lower than that of Brinkmann and Trajmar or the calculation of Chung and Lin (1972).[93] The data fit of Jackman et al is close to the experimental data of Brinkmann and Trajmar.

The cross section for excitation of a" $^1\Sigma_g^+$ below 50 eV is determined by Cartwright et al (1977)[91] using 5 points. The values roughly agree with those measured by Brinkmann and Trajmar (1970),[95] and calculated by Chung and Lin (1972)[93] from 12 to 20 eV. At higher energies the values of Cartwright et al are below the others.

Phelps et al (1979)[80] used the cross sections of Cartwright et al in his comparison of measured and fitted electron transport coefficients. Those for C $^3\Pi_u$ and E $^3\Sigma_g^+$ were used as measured while those for A $^3\Sigma_u^+$, B $^3\Pi_g$, W $^3\Delta_u$, B' $^3\Sigma_u^-$, a' $^1\Sigma_u^-$, a $^1\Pi_g$, W $^1\Delta_u$, and a" $^1\Sigma_g^+$, were scaled down by a factor of 0.7.

The excitation of higher states of $N_2$ has not been thoroughly studied. Chutjian et al (1977)[99] give cross sections at 40 and 60 eV and fit these two points and the thresholds for excitation to b' $^1\Pi_u$, b' $^1\Sigma_u^+$, C $^1\Pi_u$, C' $^1\Sigma_u^+$, and o $^1\Pi_u$ and to F and G triplet states which do not correspond to known states. The cross sections for excitation to b' $^1\Sigma_u^+$ and b $^1\Pi_u$ were also calculated by Chung and Lin (1972)[93]

96. Finn, T.G., Aarts, J.F.M., and Doering, J.P. (1972) J. Chem. Phys. 56:5632.
97. Kisker, E. (1972) Z. Physik 257:51.
98. Borst, W.L., Wells, W.C., and Zipf, E.C. (1972) Phys. Rev. A5:1744.
99. Chutjian, A., Cartwright, D.C., and Trajmar, S. (1977) Phys. Rev. A16:1052.

but these results are larger up to a factor of 80. Zipf and McLaughlin (1978)[100] list cross sections at 200 eV, including b' $^1\Sigma_u^+$ and b $^1\Pi_u$. These values for the lowest vibrational state are consistent with values of Chutjian et al. If the vibrational states are summed over then the total cross section is 40 to over 400 times that of Chutjian et al.

In view of the above considerations, the data chosen includes the cross sections measured by Cartwright et al (1977):[91] those to the excited states A $^3\Sigma_g^+$, B $^3\Pi_g$, W $^3\Sigma_u$, B' $^3\Sigma_u^-$, a' $^1\Sigma_u^-$, a $^1\Pi_g$, w $^1\Sigma_u$, C $^3\Pi_g$, E $^3\Sigma_g^+$, and a'' $^1\Sigma_g^+$. These are extrapolated beyond 50 eV as outlined in Appendix A1. The parameterized cross sections of Jackman et al (1980)[90] are used for other excited states: b $^1\Pi_u$, b' $^1\Sigma_u$, and the sums of the Rydberg series associated with the ion states X $^2\Sigma_g$, A $^2\Pi_u$, B $^2\Sigma_u$, D $^2\Pi_g$, C $^2\Sigma_u$, and a state at 40 eV.

The cross sections for electron excitation of $O_2$ to the states a $^1\Delta_g$ and b $^1\Sigma_g^+$ were studied by Linder and Schmidt (1971)[76] and Trajmar et al (1971).[48] Their cross sections agree where comparison is possible.

At higher energies, the cross sections become difficult to determine. Among the complications are dissociative attachment starting at 3.65 eV, the states C $^1\Sigma_g^-$, A' $^3\Delta_u$, and A $^3\Sigma_u^+$ at 4.1, 4.3, and 4.4 eV with vibrational spacings near 0.1 eV, non-associative detachment from 5.12 eV, the B $^3\Sigma_u^-$ state at 6.2 eV with its vibrational levels, and a series of states and resonances above 8 eV. Lawton and Phelps (1978) have calculated the electron transport coefficients from adjusted cross sections and have compared them with experiment. The electronic excitation cross sections for a $^1\Delta_g$ and b $^1\Sigma_g^+$ were those of Trajmar et al (1971).[48] The cross sections for excitation to higher energy states were approximated by cross sections corresponding to average electron energy losses of 4.5, 6.0, and 8.4 eV. Through direct use of the Franck-Condon principle, the third loss can be conceptually related to the excitation of upper vibrational levels of B $^3\Sigma_u^-$; the first to upper levels of C $^1\Sigma_u^-$ and A $^3\Sigma_u^+$. The 6.0 eV loss cross section is related to dissociation to 2 O(3P): the B $^3\Sigma_u^-$ state is related to the state O(3P) + O(3D). The first two cross sections were fitted heuristically (Lawton and Phelps, 1978, Appendix C, Section 8). Above 15 eV the 8.4 loss cross section was considered dominant and it alone was adjusted slightly higher than measured values.

The data chosen for $O_2$ excitation cross sections are those of Linder and Schmidt (1971)[76] and Trajmar et al (1971)[48] for the states of a $^1\Delta_g$ and b $^1\Sigma_g^+$ which were extrapolated to higher energies. The cross sections of Lawton and Phelps (1978) for energy losses of 4.5 and 6.0 eV, roughly corresponding to a set of states including A $^3\Sigma_u^+$ and to dissociation. The 8.4 eV loss cross section of Phelps was modified by subtracting the cross sections to the Rydberg states used separately.

---

100. Zipf, E.C., and McLaughlin, R.W. (1978) Planet Space Sci. 26:449.

These three cross sections were extrapolated to higher energies. The sums of the Rydberg series associated with the ion states $X\ ^2\Pi_g$, $a\ ^4\Pi$, $A\ ^2\Pi_u$, $b\ ^4\Sigma$, $B\ ^2\Sigma_g$, $c\ ^4\Sigma$, and a state at 37 eV are used as tabulated by Jackman et al (1980).[90]

Excitation cross sections for individual states of atomic oxygen are shown in Figures B57 through B70. Figures B71 through B88 contain sums of cross sections to Rydberg states. The cross sections in each sum are weighted by the fraction of excitations which are non-ionizing (Porter et al, 1976[94]).

Excitation cross sections for $N_2$ and $O_2$ are handled similarly. Figures B89 through B100 show cross sections for the excitation of individual $N_2$ levels and B101 through B106 show weighted sums over Rydberg levels. Individual cross sections for excited $O_2$ levels are in Figures B107 through B111 and weighted sums over Rydberg levels are in Figures B112 through B118.

Discussions of differential excitation cross sections may be found in Henry et al (1969),[101] Trajmar et al (1971,[48] 1972[79]), Sawada and Ganas (1973),[87] Hall and Trajmar (1975),[102] Cartwright et al (1977),[91] and Chutjian et al (1977).[99]

#### 4.6 Molecular Dissociation Total Cross Sections

Molecular dissociation by electron impact can be considered as a single complex process. The total cross section does not determine the electron energy in the three particle final states and more structure must be included either experimentally or theoretically. It is natural to divide the process so that the significant parameters are excitation cross sections for the different molecular states and branching ratios. Below the lowest dissociation energy the states cannot dissociate; above it dissociation may be probable or not depending on the relative accessability of dissociated and nondissociated states. The survey of Porter et al (1976)[94] lists the branching ratios for states considered lying below the ionization threshold. Rydberg states, which could not ionize, were considered to dissociate; as were all of the $O_2$ states for which dissociation was energetically possible. Dissociation branching ratios less than unity were given for the $N_2$ states: $a\ ^1\Pi_g$, $b\ ^1\Pi_u$, $b'\ ^1\Sigma_u^+$, and $C\ ^3\Pi_u$.

Zipf and McLaughlin (1978)[100] reviewed the dissociation data for $N_2$. The total dissociation cross section used for comparison was that of Winters (1966)[103] which was also used by Porter et al.[94] The cross sections were grouped by families (for example, $^1\Pi_u$ states) or by characteristics (for example, states leading to the production of excited N atoms that radiate at EUV wavelengths) making cross-comparison difficult.

---

101. Henry, R.J.W., Burke, P.G., and Sinfailem, A. (1969) Phys. Rev. 178:218.
102. Hall, R.A., and Trajmar, S. (1975) J. Phys. B8:L293.
103. Winters, H.F. (1966) J. Chem. Phys. 44:1472.

## 5. ELECTRON DEEXCITATION TOTAL CROSS SECTIONS

The cross sections considered in the last sections described the collision of an electron and an atom or molecule in which the electron loses some of its energy. The opposite process, in which the electron gains energy through deexcitation of the atom or molecule, can be related to the first.

Let two states be considered, labeled 1 and 2, each with a momentum P and other quantum numbers defining the channel C. The differential cross section can be written in terms of the S-matrix:

$$\frac{d\sigma}{d\Omega}\ (2 \leftarrow 1) = \frac{h^2}{P_1^2}\ |\langle C_2\ |S-1|\ C_1\rangle\ |^2\ .$$

From the symmetry properties of S (Messiah, 1963,[104] p. 866; Goldberger and Watson, 1964,[105] p. 351)

$$\frac{d\sigma\ (1 \leftarrow 2)}{d\Omega} = \frac{P_1^2}{P_2^2}\ \frac{d\sigma\ (2 \leftarrow 1)}{d\Omega}$$

Usually it is the total cross section that is of interest having been averaged over initial spin states and summed over final spin states. If g is the number of spin states,

$$\sigma\ (1 \leftarrow 2) = \frac{g_1}{g_2}\ \frac{P_1^2}{P_2^2}\ \sigma\ (2 \leftarrow 1)\ .$$

A detailed derivation of this result may be found in section 7.3 of Goldberger and Watson (1964).[105]

This result is also found in terms of the collision strength, $\Omega_{12} = \Omega_{21}$:

$$\sigma\ (2 \leftarrow 1) = \frac{\pi}{g_1}\left(\frac{\hbar}{P_1}\right)^2\ \Omega_{21}\ .$$

---

104. Messiah, A. (1963) Quantum Mechanics, N. Holland Publishing Co., Amsterdam, The Netherlands.

105. Goldberger, M. L., and Watson, K. M. (1964) Collision Theory, John Wiley and Sons, Inc., New York, New York.

The collision strength can be given in terms of reduced matrix elements:

$$\Omega_{21} = \sum_{\ell_1 \ell_2 J} (2J+1) \left| \langle C_2\, \ell_2\, S_2\, J \,||\, S - 1 \,||\, C_1\, \ell_1\, S_1 J \rangle \right|^2 .$$

From these relations between cross sections, the cross sections for deexcitation to the ground state can be related to the known excitation cross sections.

## 6. ELECTRON IONIZATION TOTAL CROSS SECTIONS

The experimental total cross sections for ionization of O, $N_2$, $O_2$, NO, and other atoms and molecules were reviewed by Kieffer and Dunn (1966).[106] The different data of interest agree fairly well except for O where the values of Boksenberg (1961)[107] are above those of Fite and Brackmann (1958)[108] and Rothe et al (1962)[109] by up to 50 percent. For $N_2$, $O_2$, and NO, the values of Rapp and Englander-Golden (1965)[110] can be used. Tate and Smith (1932)[111] provide values which are higher at the peaks. Opal et al (1972)[112] measured the cross sections of $N_2$, $O_2$, NO, and other molecules as a function of the energy of the secondary electron, the one with the lesser energy. The observations were very well described by

$$Q(E_{in}, E_s) = C(E_{in})/(1 + (E_s/\bar{E})^{2.1})$$

where $E_{in}$ and $E_s$ are the energies of the incoming and secondary electrons and $\bar{E}$ is a fitted parameter. A good approximation to this formula which is easily integrable over the secondary energy is to replace the 2.1 exponent by 2.0. The total cross sections agree with those compiled by Kieffer and Dunn.[106] The energy of the other electron is undetermined since the ionic state and its excitation energy are unknown.

Opal et al (1971)[113] showed that the dependence on the energy of the secondary electron smoothly followed a simple function to within 20 percent with the main

106. Kieffer, L.J., and Dunn, G.H. (1966) Rev. Mod. Phys. 38:1.
107. Boksenberg, A. (1961) Thesis, University of London.
108. Fite, W.L., and Brackmann, R.T. (1958) Phys. Rev. 112:1141.
109. Rothe, E.W., Marino, L.L., Neynaber, P.H., and Trujillo, S.M. (1962) Phys. Rev. 125:582.
110. Rapp, D., and Englander-Golden, P. (1965) J. Chem. Phys. 43:1464.
111. Tate, J.T., and Smith, P.T. (1932) Phys. Rev. 39:270.
112. Opal, C.B., Beaty, E.C., and Peterson, W.K. (1972) Atomic Data 4:209.
113. Opal, C.B., Peterson, W.K., and Beaty, E.C. (1970) J. Chem. Phys. 55:4100.

exceptions being the noble gases. The cross section structure in the rest does not allow a simple decomposition of the cross section without additional data. For $N_2$, there is additional data: cross sections to the specific ionic states of $A\ ^2\Pi_u$ (Holland and Maier, 1972 [114]) and $B\ ^2\Sigma_u^+$ (0, 0) (Borst and Zipf, 1970 [115]). These comprise half of the total ionization cross section above their thresholds. Not considering the vibrational levels, the remaining part of the total cross section below 22 eV can be ascribed to the ground state of $N_2^+$.

Green and Sawada (1972)[116] fitted the data of Opal et al (1971)[113] and that compiled by Kieffer and Dunn (1966)[106] allowing the cross sections to be used as analytic functions. Porter et al (1976)[94] separated the cross section into cross sections for separate states of the ions using a semiempirical formula. The separation was affected using many criteria, for example, the total cross section, the thresholds for the states, ionization cross sections, dissociative ionization cross sections, branching ratios, and others. Green and Sawada (1972)[116] and Jackman et al (1977)[90] did the same with a simple non-relativistic formula. In both cases, the main curve to be fit was the total cross section. Since the total cross sections used were those of Kieffer and Dunn (1966)[106] for $N_2$ and $O_2$ and Fite and Brackmann (1958)[108] and Rothe et al (1962)[109] for O, the parameter set by Jackman et al will be used instead. This set has the further advantage of providing an estimate of the excitation energy and the energy of the other electron.

In the case of $N_2$, where the cross sections to specific ionic states have been measured, a comparison may be made. Below 150 eV, curves of Jackman et al are about 50 percent below the data of Holland and Maier (1972)[114] for $A\ ^2\Pi_u$ and 50 percent above the data of Borst and Zipf (1970)[115] for $B\ ^2\Sigma_u$ (0, 0). In the second comparison, the agreement may be closer when all vibrational levels are included in the measurement.

Figures B119 through B132 contain cross sections for electron impact ionization of oxygen. Figures B119 through B125 use states of neutral oxygen which can decay by ejecting an electron; B126 through B129 do the same for sums of Rydberg states; B130 through B132 show the cross sections leading directly to states of $O^+$. Figures B133 through B143 and B144 through B156 show ionization cross sections for $N_2$ and $O_2$ respectively; in both cases the sums of cross sections to Rydberg states are given first, then the cross sections to individual states of the ion.


114. Holland, R.F., and Maier, W.B. (1972) J. Chem. Phys. 56:5229.

115. Borst, W.L., and Zipf, E.C. (1970) Phys. Rev. A1:834.

116. Green, A.E.S., and Sawada, T. (1972) J. Atmos. Terr. Phys. 34:1719.

## 7. ELECTRON-ION RECOMBINATION

Initially, recombination was considered to be radiative; the electron energy was carried away by a photon when the electron became bound. The resulting recombination rate was four orders of magnitude lower than observed in the lower ionosphere. (Bates and Massey, 1947;[117] Bardsley and Biondi, 1970[118]). The rapid rate is due to dissociative recombination. That this is the dominant rate is borne out by the comparison by Dalgarno (1979)[119] and by Torr (1979)[120] of recombination rates from different experiments and obtained from an analysis of data from Atmospheric Explorer satellites.

The recombination rates of atmospheric species are measured directly in laboratory experiments or determined from measured cross sections. The analysis of atmospheric data provides a check on the rates and assumptions involved (Dalgarno, 1979;[119] Torr, 1979;[120] Oppenheimer et al 1976a,[121] 1976b,[122] 1977[4]). The recombination rates which seem suited for atmospheric work are given in Table 5. The accompanying cross sections are those which would yield the rates listed given a Maxwell energy distribution for the electrons. The theoretical relations are given in Appendix A3.

The cross sections are discussed below. Figures 14 through 17 show the main cross section as a heavy line. The cross sections calculated from the recombination rates given in Table 5 are shown as dotted lines.

The cross sections for dissociative recombination are well behaved near 0.1 eV. Using this as the main part of the cross sections allows the rates to be calculated. These rates and the cross sections from which they are derived are given in Table 6.

The recombination cross section for $NO^+$ was measured by Walls and Dunn (1974),[123] Huang et al (1975),[124] and Mul and McGowan (1979)[125] and calculated

117. Bates, D.R., and Massey, H.S.W. (1947) Proc. Roy. Soc. A192:1.

118. Bardsley, J.N., and Biondi, M.A. (1970) Adv. in Atomic and Molecular Phys. 6:1, (Bates, D.R., and Esterman, I., eds.) Academic Press, New York.

119. Dalgarno, A. (1979) Adv. in Atomic and Molecular Phys. 15:37, (Bates, D.R., and Bederson, B., eds.) Academic Press, New York.

120. Torr, D.G. (1979) Rev. Geophys. and Space Phys. 17:510.

121 Oppenheimer, M., Dalgarno, A., and Brinton, H.C. (1976a) J. Geophys. Res. 81:3762.

122. Oppenheimer, M., Dalgarno, A., and Brinton, H.C. (1976b) J. Geophys. Res. 81:4678.

123. Walls, F.L., and Dunn, G.H. (1974) J. Geophys. Res. 79:1911.

124. Huang, C.M., Biondi, M.A., and Johnson, R. (1975) Phys. Rev. A11:901.

125. Mul, P.M., and McGowan, J.W. (1979) J. Phys. B12:1591.

by Michaels (1975,[126] 1980[127]). The results, especially the experimental, are in agreement. The data of Walls and Dunn show more structure and go to a higher energy, 4 eV. Differences in the extrapolation beyond 4 eV influence the

Table 5. Electron Recombination Rates and Calculated Cross Sections

| Process | Rate Coefficient ($cm^3/s$) | Calculated Cross Section ($cm^2$) | Reference for Rate Coefficient |
|---|---|---|---|
| $e^- + O \rightarrow h\nu + O$ | $1.68\times10^{-12}\left(\frac{1000^oK}{T_e}\right)^{0.69}$ | $6.2\times10^{-20}\left(\frac{0.1\,eV}{E}\right)^{1.19}$ | Tinsley et al (1973)[128] |
| $e^- + N_2^+ \rightarrow N + N$ | $1.13\times10^{-7}\left(\frac{1000^oK}{T_e}\right)^{0.39}$ | $5.3\times10^{-15}\left(\frac{0.1\,eV}{E}\right)^{0.89}$ | Oppenheimer et al (1976a,[121] 1976b[122]) |
| $e^- + O_2^+ \rightarrow O + O$ | $0.84\times10^{-7}\left(\frac{1000^oK}{T_e}\right)^{0.70}$ | $3.1\times10^{-15}\left(\frac{0.1\,eV}{E}\right)^{1.20}$ | Oppenheimer et al (1976a,[121] 1976b[122]) |
| $e^- + NO^+ \rightarrow N + O$ | $1.58\times10^{-7}\left(\frac{1000^oK}{T_e}\right)^{0.83}$ | $4.9\times10^{-15}\left(\frac{0.1\,eV}{E}\right)^{1.33}$ | Torr (1979)[120] |

Table 6. Electron Recombination Cross Sections and Calculated Rates

| Process | Calculated Rate Coefficients ($cm^3/s$) | Low Energy Cross Section ($cm^2$) | Reference for Cross Section |
|---|---|---|---|
| $e^- + O \rightarrow h\nu + O$ | $1.4\times10^{-12}\left(\frac{1000^oK}{T_e}\right)^{0.65}$ | $5.4\times10^{-20}\left(\frac{0.1\,eV}{E}\right)^{1.15}$ | Appendix A5 |
| $e^- + N_2^+ \rightarrow N + N$ | $2.2\times10^{-7}\left(\frac{1000^oK}{T_e}\right)^{0.50}$ | $9.5\times10^{-15}\left(\frac{0.1\,eV}{E}\right)^{1.00}$ | Mul and McGowan (1979)[125] |
| $e^- + O_2^+ \rightarrow O + O$ | $0.88\times10^{-7}\left(\frac{1000^oK}{T_e}\right)^{0.65}$ | $3.4\times10^{-15}\left(\frac{0.1\,eV}{E}\right)^{1.15}$ | Walls and Dunn (1974)[123] |
| $e^- + NO^+ \rightarrow N + O$ | $1.38\times10^{-7}\left(\frac{1000^oK}{T_e}\right)^{0.95}$ | $3.5\times10^{-15}\left(\frac{0.1\,eV}{E}\right)^{1.45}$ | Walls and Dunn (1974)[123] |

126. Michaels, H.H. (1975) Theoretical Study of Dissociative Recombination of $e + NO^+$, AFCRL-TR-75-0509, ADA024309.

127. Michaels, H.H. (1980) Theoretical Research Investigation Upon Reaction Rates to the Nitric Oxide (Positive) Ion, AFGL-TR-80-0072, AD A104303.

128. Tinsley, B.A., Christensen, A.B., Bittencourt, J., Gouveia, H., Angreji, P.D., and Takahasi, K. (1973) J. Geophys. Res. 78:1174.

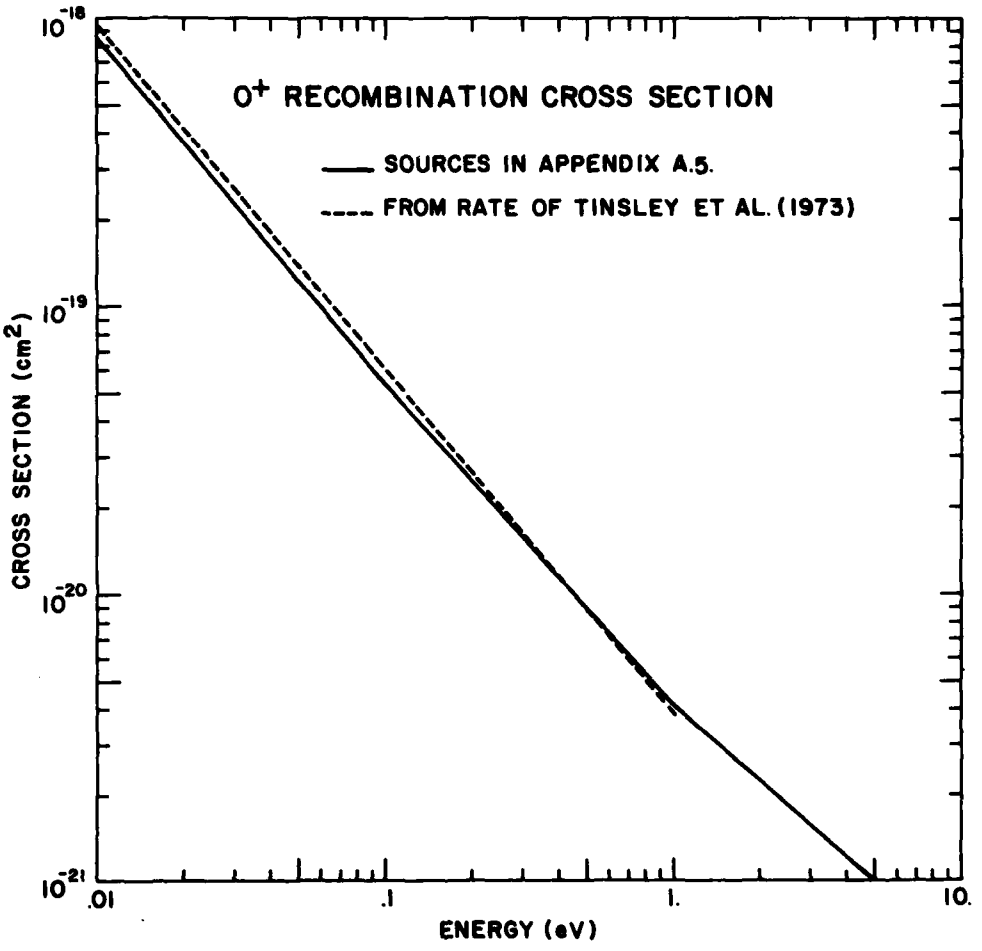


**Figure 14.** $O^+$ **Recombination Cross Section. The solid line represents the data from the sources in Appendix A5. The dashed line is the cross section from the rate of Tinsley et al (1973)[128]**

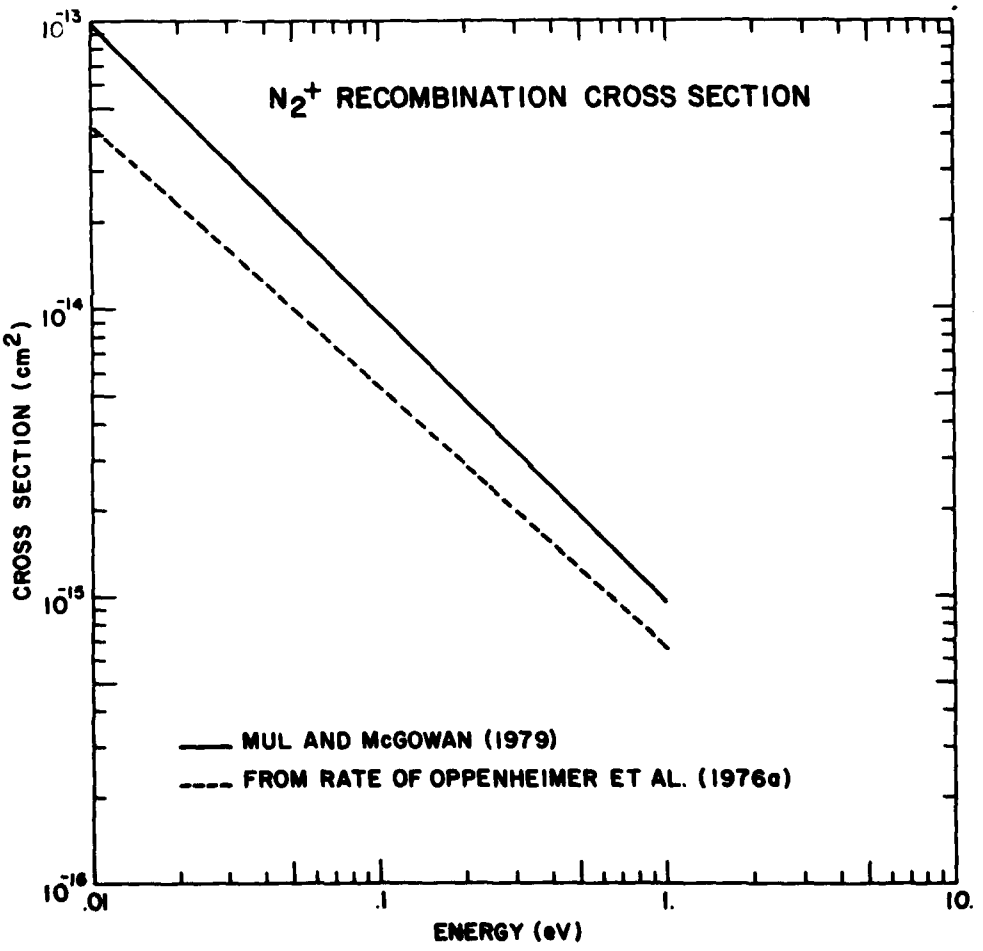


**Figure 15.** $N_2^+$ Recombination Cross Section. The solid line represents the data of Mul and McGowan (1979).[125] The dashed line is the cross section from the rate of Oppenheimer et al (1976a)[121]

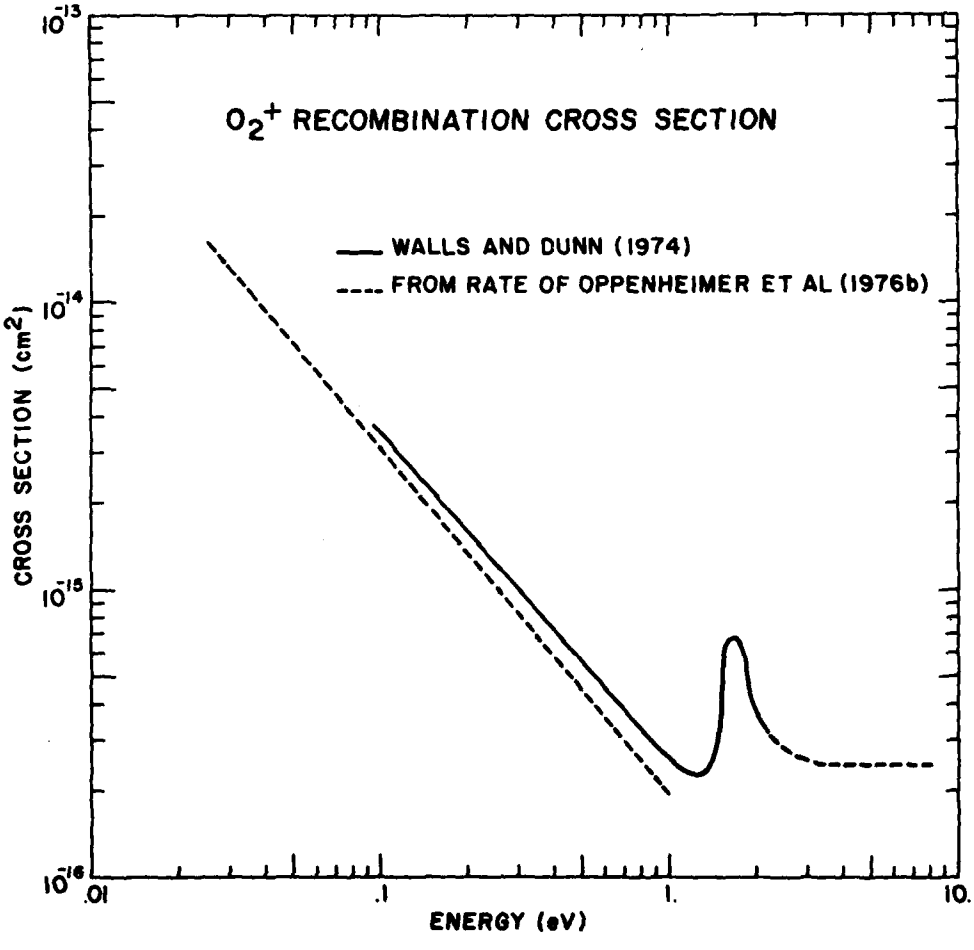


Figure 16. $O_2^+$ Recombination Cross Section. The solid line represents the data of Walls and Dunn (1974).[123] The dashed line is the cross section from the rate of Oppenheimer et al (1976b)[122]

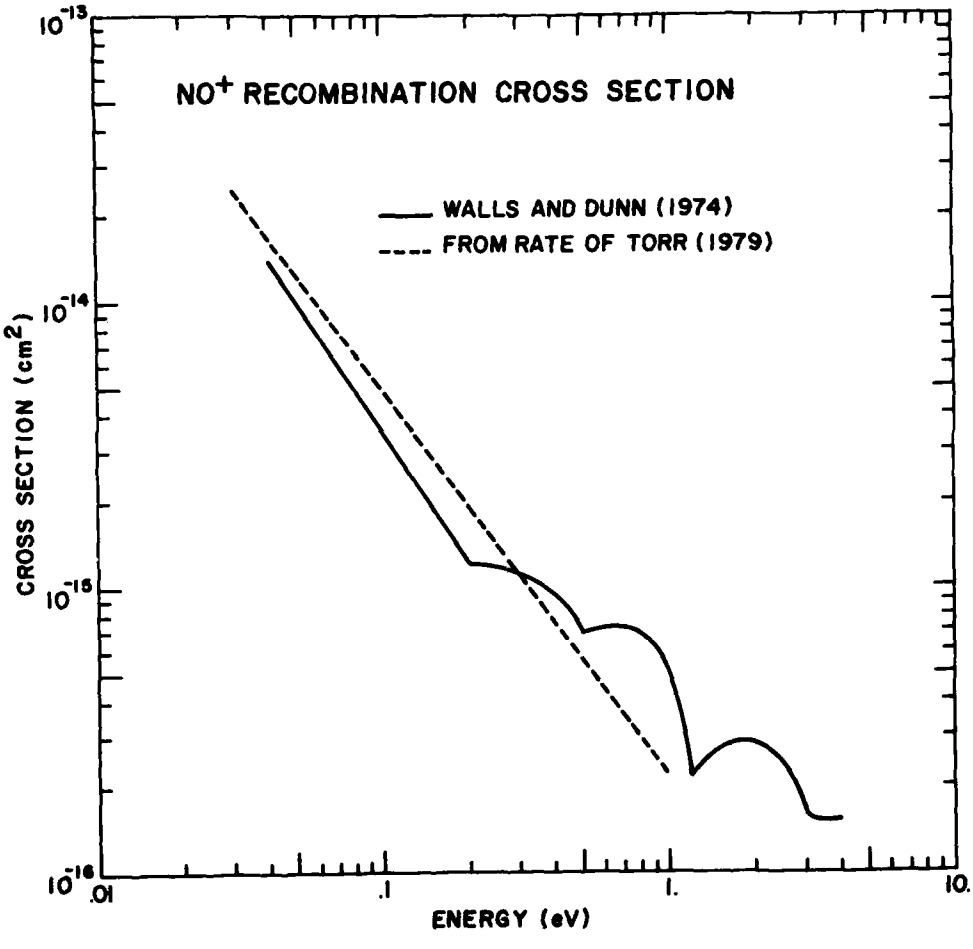


**Figure 17.** $NO^+$ Recombination Cross Section. The solid line represents the data of Walls and Dunn (1974).[123] The dashed line is the cross section from the rate of Torr (1979)[120]

rate coefficient, calculated for Maxwellian electron velocity distribution, only for temperatures beyond $10^4$ °K. Thus, there is no experimental data of any sort beyond 4 eV. The results of Walls and Dunn (1974)[123] were in better agreement with atmospheric data in the atmosphere and in the Walls and Dunn experiment the ions are in the ground state. There are considerations, such as additional reactions, which weaken this conclusion. (Dalgarno, 1979 [119]).

The reaction, $N(^2D) + O \rightarrow NO^+ + e$, suggested by Zipf (1978)[129] and Dalgarno (1979)[119] was investigated by Torr (1982)[130] and found to have only minor effects.

For $O_2^+$, the results from the satellite and from the experiments of Mehr and Biondi (1969)[131] and Walls and Dunn (1974)[123] agree, implying that the cross section is relatively independent of the initial vibrational state (Dalgarno, 1979 [119]). The recombination cross sections of Walls and Dunn (1974)[123] and Mul and McGowan (1979)[125] are parallel in the region of overlap with Mul and McGowan being about 50 percent higher. Again, Walls and Dunn[123] extend to a higher energy, 10 eV, with much scatter and/or structure above a peak at 1.5 eV. Due to this uncertainty, the graph is shown with a dashed line above 2 eV.

The $N_2^+$ recombination cross section has been measured by Mul and McGowan (1979)[125] up to 1 eV with no structure and an energy dependence of $E^{-1}$. The derived rate coefficient is above that of Mehr and Biondi (1969).[132] Other considerations, including comparison with Atmospheric Explorer data, have left the situation unresolved (Dalgarno, 1979 [119]).

For atomic oxygen the rate is calculated and the published details can be used to estimate specific parts of the total cross section. This is carried out in Appendix A5. In treating the cross section as a sum, each component having its own energy dependence, the cross section at high energies is modified. The low energy cross section is not greatly changed. The calculated rates have a temperature dependence of $T^{-0.7}$ near 1000°K (Massey and Bates, 1942;[132] Biondi, 1969;[133] Tinsley et al, 1973 [128]).

## 8. PHOTON NEUTRAL PARTICLE CROSS SECTIONS

The ionospheric density is low enough that simple photoabsorption results in reemission and the total process resembles elastic scattering. The main interest is in the energetic electrons produced through photoionization. In the energy range

129. Zipf, E.C. (1978) Trans. Am. Geophys. Union 59:336.
130. Torr, D.G. (1982) Private communication.
131. Mehr, F.J., and Biondi, M.A. (1969) Phys. Rev. 181:264.
132. Massey, H.S.W., and Bates, D.R. (1942) Rep. Prog. Phys. 9:62.
133. Biondi, M.A. (1969) Can. J. Chem. 47:1711.

in which photoionization is possible, absorption must also be considered. Kirby et al (1979)[134] have compiled the photoionization and the photoabsorption cross sections for O, $N_2$, and $O_2$ from 34 to 1030Å. The wavelengths were chosen to match those in the detailed spectrum of Heroux and Hinteregger (1978).[135]

The branching ratios to different ionic states are included. In particular, the states $^4S^o$, $^2D^o$, $^2P^o$, $^4P^e$, $^2P^e$ are given for $O^+$; the bound states $X\ ^2\Pi_g$, $a\ ^4\Pi_u + A\ ^2\Pi_u$, and $b\ ^4\Sigma_g^-$; the dissociating states $B\ ^2\Sigma_g^-$, $^2\Pi_u$, $c\ ^4\Sigma_u^-$, $^2\Sigma_u^-$, and $^{2,4}\Sigma_g^-$ and a general dissociating state are given for $O_2^+$; a general dissociating state and the bound states $X\ ^2\Sigma_g^+$, $A\ ^2\Pi_u$, $B\ ^2\Sigma_u^+$, $F\ ^2\Sigma_u$, and $^2\Sigma_g^+$ are given for $N_2^+$.

The process of molecular dissociative ionization has a three particle final state with the kinetic energy divided among the three particles. This is described by a differential cross section per unit electron energy. The dissociative ionization cross sections given are integrated over the electron energy. The one for $N_2$ given by Kirby et al, (1979)[134] includes cross sections for dissociative ionic states not included in the list of specific states (Wight et al, 1976[136]). The data of Gardner and Samson (1975)[137] for 40.8 eV photons ionizing $N_2$ shows that the structure in the dissociative ionization cross section as a function of the electron energy is due to the presence of specific states.

The differential ionization cross section can be shown to be (see Appendix A4),

$$\frac{d\sigma}{d\Omega} = \frac{\sigma}{4\pi}\left(1 - \frac{1}{2}\beta P_2(\cos\theta)\right).$$

The odd Legendre polynomials are eliminated by parity conservation. The higher even polynomials are dependent on higher multipoles and are suppressed.

For atomic oxygen Smith (1976)[86] calculates $\sigma$ and $\beta$ using close coupling with up to five states for the $^4S^o$, $^2D^o$, $^2P^o$, and $^4P^e$ states of $O^+$.

The photoionization cross sections obtained from Kirby et al (1979)[134] are shown in Figures B157 through B176. The photoionization cross sections for atomic oxygen are given in Figures B157 through B161, for $N_2$ in B162 through B167, and for $O_2$ in B168 through B176. Total photoabsorption cross sections for the three species are given in Figures B177 through B179.

---

134. Kirby, K., Constantinides, E.R., Babeu, S., Oppenheimer, M., and Victor, G.A. (1979) Atomic Data and Nuclear Data Tables 23:63.

135. Heroux, L., and Hinteregger, H.E. (1978) J. Geophys. Res. 83:6305.

136. Wight, G.R., Van der Weil, M.J., and Brian, G.E. (1976) J. Phys. B9:675.

137. Gardner, J.L., and Samson, J.A.R. (1975) J. Chem. Phys. 62:1447.

## 9. IONIZING SOLAR RADIATION

The thermal part of the solar spectrum roughly corresponds to that of a black body near 6000°, and the photon number density is attenuated by expanding from the radius of the sun to that of the Earth's orbit. In the ionosphere, this part of the spectrum has small effect since what little is absorbed only excites the atom or molecule and the energy is then remitted. The photoionization and photodissociation of the atmosphere species are the means of putting additional energy into the upper atmosphere. This is done by the extreme ultraviolet (EUV) region of the spectrum.

The EUV spectrum is composed primarily of lines and is highly structured if examined in great detail. It must be measured above the atmosphere of the earth.

The solar output does vary, particularly in the extreme ultraviolet (Hinteregger, 1980[138]). Torr et al (1979)[139] have listed the solar flux values from 50 to 1050Å (248 to 11.8 eV) for five days of low or high solar activity. The data consist of the main lines and the total fluxes in 50Å intervals with the main lines excluded.

More detailed data, more lines, and narrower intervals are provided by Heroux et al (1974)[140] for 23 August 1972, a day of moderate solar activity having F10.7 of $120 \times 10^{-22}$ $W/m^2Hz^2$. Data for 23 April 1974, a day with F10.7 near $70 \times 10^{-22}$ $W/M^2Hz^2$, are found in Manson (1976a,[141] 1976b[142]) and Heroux and Hinteregger (1978).[134]

The solar flux data for F10.7 of 120 are shown in Figure B180 and for F10.7 of 70 in B181. The energy range has been divided into intervals and for each interval an average flux is shown.

---

138. Hinteregger, H.E. (1980) XXIII Cospar, preprint.

139. Torr, M.A., Torr, D.G., Ong, R.A., and Hinteregger, H.E. (1979) Geophys. Res. Lett. 6:771, AFGL-TR-80-0284, AD A090081.

140. Heroux, L., Cohen, M., and Higgins, J.E. (1974) J. Geophys. Res. 79:5237, AFGL-TR-76-0297, AD A062634.

141. Manson, J.E. (1976a) Satellite Measurements of Solar UV During 1974, AFCRL-TR-76-0006, AD A021490.

142. Manson, J.E. (1976b) J. Geophys. Res. 81:1629, AFGL-TR-76-0103, AD A024617.

## References


1. Jacchia, L.G. (1977) Thermospheric Temperature, Density and Composition: New Models, Smithsonian Astrophysical Observatory Special Report 375.
2. Johnson, C.Y. (1969) Annals of the IQSY 5:197, (Stickland, A. C., ed) MIT Press, Cambridge, Mass.
3. Keneshea, T.J., Narcisi, R.S., and Swider, W. Jr. (1970) J. Geophys. Res. 75:845, AFCRL-70-0172, AD A0703350.
4. Oppenheimer, M., Dalgarno, A., Trebino, F.P., Brace, L.H., Brinton, H.C., and Hoffman, J.H. (1977) J. Geophys. Res. 82:191.
5. Oppenheimer, M. Constantinides, F.R., Kirby-Docken, K., Victor, G.A., Dalgarno, A., and Hoffman, J.H. (1977) J. Geophys. Res. 82:5485.
6. Brace, L.H., Hoegy, W.R., Mayr, H.G., Victor, G.A., Hanson, W.B., Reber, C.A., and Hinteregger, H.E. (1976) J. Geophys. Res. 81:5421.
7. Brace, L.H., and Theis, R.F. (1978) Geophys. Res. Lett. 5:275.
8. Hoegy, W.R., and Brace, L.H. (1978) Geophys. Res. Lett. 5:269.
9. Evans, J.V. (1967) Planet Space Sci. 15:1557.
10. Evans, J.V. (1970) Planet Space Sci. 18:1225.
11. Reber, C.A., and Nicholet, M. (1965) Planet Space Sci. 13:617.
12. Istomin, V.G. (1966) Annls. Géophys. 22:255.
13. Johnson, C.Y. (1966) J. Geophys. Res. 71:330.
14. Sagalyn, R.C., and Wand, R.H. (1971) J. Geophys. Res. 76:3783, AFCRL-71-0495, AD A0731424.
15. Moore, C.E. (1949) Atomic Energy Levels, Volume 1, U.S. Govt. Printing Office, Washington, D.C.
16. Huber, K., and Herzberg, G. (1979) Molecular Spectra and Molecular Structure; Part IV: Constants of Diatomic Molecules, Van Nostrand Reinhold Co., New York.
17. Lofthus, A., and Krupenie, P.H. (1977) J. Phys. Chem. Ref. Data 6:113.

18. Krupenie, P.H. (1972) J. Phys. Chem. Ref. Data 1:423.

19. Ashihara, O., and Takayangi, K. (1974) Planet Space Sci. 22:1201.

20. Jasperse, J. (1975) Electron Distribution Function in a Nonuniform Magnetized; Weakly Photoionized Gas Application; Model Ionosphere AFCRL-TR-75-20266, AD 147 77.

21. Jasperse, J. (1976) Planet Space Sci. 24:33, AFCRL-TR-76-0047, AD4 020 765.

22. Jasperse, J. (1977) Planet Space Sci. 25:743.

23. Victor, G.A., Kirby-Docken, K., and Dalgarno, A. (1976) Planet Space Sci. 24:679.

24. Jasperse, J., and Smith, E.R. (1978) Geophys. Res. Lett. 5:843, AFGL-TR-78-0287, AD A062310.

25. Oran, E.S., and Strickland, D.J. (1979) Planet Space Sci. 26:1161.

26. Lawton, S.A., and Phelps, A.V. (1978) J. Chem. Phys. 69:1055.

27. Shkarofsky, I.P., Johnson, T.W., and Bachynski, M.P. (1966) The Particle Kinetics of Plasma, Addison-Wesley, Reading, Massachusetts.

28. Ferzinger, J.H., and Kaper, H.G. (1972) Mathematical Theory of Transport Processes in Gasses, N. Holland Publishing Co., Amsterdam, Netherlands.

29. Lane, N.F. (1980) Rev. Mod. Phys. 52:29.

30. Schulz, G.J. (1973a) Rev. Mod. Phys. 45:378.

31. Schulz, G.J. (1973b) Rev. Mod. Phys. 45:423.

32. Porter, H.S., and Jump, F.W. (1978) Computer Sciences Corporation, TM-78/6017.

33. Sunshine, G., Aubrey, B.B., and Bederson, B. (1967) Phys. Rev. 154:1.

34. Thomas, L.D., and Nesbet, R.K. (1975) Phys. Rev. A11:170; addendum, Phys. Rev. A12:1279.

35. Henry, R.J.W. (1967) Planet Space Sci. 15:1747.

36. Neynaber, R.H., Marino, L.L., Rothe, E.W., and Trujillo, S.M. (1961) Phys. Rev. 123:148.

37. Rountree, S.P., Smith, E.R., and Henry, R.J.W. (1974) J. Phys. B7:L167.

38. Saraph, H.E. (1973) J. Phys. B6:2243.

39. Smith, K., Henry, R.J.W., and Burke, P.G. (1967) Phys. Rev. 157:51.

40. Frost, L.S., and Phelps, A.V. (1962) Phys. Rev. 127:1621.

41. Englehardt, A.G., Phelps, A.V., and Risk, C.G. (1964) Phys. Rev. 135:A1566.

42. Morrison, M.A., and Collins, L.A. (1978) Phys. Rev. A17:918.

43. Srivastava, S.K., Chutjian, A., and Trajmar, S. (1976) J. Chem. Phys. 64:1340.

44. Choi, B.H., Poe, R.T., Sun, J.G., and Shan, Y. (1979) Phys. Rev. A19:116.

45. Shyn, T.W., and Carignan, G.R. (1980) Phys. Rev. A22:923.

46. Hake, R.D., and Phelps, A.V. (1967) Phys. Rev. 158:70.

47. Nelson, D.R., and Davis, F.J. (1972) J. Chem. Phys. 57:4079.

48. Trajmar, S., Cartwright, D.C., and Williams, W. (1971) Phys. Rev. A4:1462.

49. Gerjuoy, E., and Stein, S. (1955) Phys. Rev. 97:1671.

50. Dalgarno, A., and Moffett, R.J. (1963) Proc. Nat'l. Acad. Sci., India A33:511.
51. Takayanagi, K., and Geltman, S. (1965) Phys. Rev. A138:1003.
52. Geltman, S., and Takayanagi, K. (1966) Phys. Rev. 143:25.
53. Chen, J.C.Y. (1966a) Phys. Rev. 146:61.
54. Chen, J.C.Y. (1966b) J. Chem. Phys. 45:2710.
55. Chandra, N., and Temkin, A. (1976) Phys. Rev. A13:188.
56. Burke, P.G., and Chandra, N. (1972) J. Phys. B5:1969.
57. Golden, D.E. (1966) Phys. Rev. Lett. 17:847.
58. Sampson, D.H., and Mjolsness, R.C. (1966) Phys. Rev. 144:116.
59. Ehrhardt, H., and Willmann, K. (1967) Z. Phys. 204:462.
60. Breig, G.L., and Lin, C.C. (1966) Phys. Rev. 151:67.
61. Tambe, B.R., and Henry, R.J.W. (1974) Phys. Rev. A10:2097.
62. Tambe, B.R., and Henry, R.J.W. (1976) Phys. Rev. A13:224.
63. LeDourneuf M, and Nesbet, R.K. (1976) Z. Phys. B9:L241.
64. Hoegy, W.R. (1976) Geophys. Res. Lett. 3:541.
65. Schulz, G.J. (1976) in Principles of Laser Plasmas (G. Bekefi, ed.) John Wiley and Sons, New York.
66. Schulz, G.J. (1962) Phys. Rev. 125:229.
67. Birtwistle, D.T., and Herzenberg, A. (1971) J. Phys. B4:53.
68. Dube, L., and Herzenberg, A. (1979) Phys. Rev. A20:194.
69. Schneider, B., LeDourneuf, M., and Vo Ky Lan (1979) Phys. Rev. Lett. 43:1426.
70. Chen, J.C.Y. (1964a) J. Chem. Phys. 40:3507.
71. Chen, J.C.Y. (1964b) J. Chem. Phys. 40:3513, errata (1964) J. Chem. Phys. 41:3263.
72. Truhlar, D.G., Trajmar, S., and Williams, W. (1972) J. Chem. Phys. 37:3250.
73. Truhlar, D.G., Brandt, M.A., Chutjian, A., Srivastava, S.K., and Trajmar, S. (1976) J. Chem. Phys. 65:2962.
74. Truhlar, D.G., Brandt, M.A., Srivastava, S.K., Trajmar, S., and Chutjian, A. (1977) J. Chem. Phys. 66:655.
75. Schneider, B.I. (1980) Private communication.
76. Linder, F., and Schmidt, H. (1971) Z. Naturforsch. 26:1617.
77. Koike, F., and Watanabe, T. (1973) J. Phys. Soc. Japan 34:1022.
78. Wong, S.F., Boness, M.J.W., and Schulz, G.S. (1973) Phys. Rev. Lett. 31:696.
79. Trajmar, S., Williams, W., and Kupperman, A. (1972) J. Chem. Phys. 56:3759.
80. Phelps, A.V., Levron, D., and Tachibana, K. (1979) Abstracts of contributed papers, XIth International Conference on the Physics of Electronic and Atomic Collisions.
81. Phelps, A.V. (1980) Private communication.
82. Vo Ky Lan, Feautrier, N., LeDourneuf, M., and Van Regemorter, H. (1972) J. Phys. B5:1506

83. Stone, E.J., and Zipf, E.C. (1974) J. Chem. Phys. 60:4237.
84. Rountree, S.P., and Henry, R.J.W. (1972) Phys. Rev. A6:2106.
85. Smith, E.R. (1976) Phys. Rev. A13:65.
86. Sawada, T., and Ganas, P.S. (1973) Phys. Rev. A7:617.
87. Dalgarno, A., and LeJeune, G. (1971) Planet Space Sci. 19:1963.
88. Green, A.E.S., and Dutta, S.K. (1967) J. Geophys. Res. 72:3933.
89. Jackman, C.H., Garvey, R.H., and Green, A.E.S. (1977) J. Geophys. Res. 82:5801.
90. Jackman, C.H., Garvey, R.H., and Green, A.E.S. (1980) Private communication.
91. Cartwright, D.C., Trajmar, S., Chutjian, A., and Williams, W. (1977) Phys. Rev. A16:1041.
92. Borst, W.L. (1972) Phys. Rev. A5:648.
93. Chung, E.S., and Lin, C.C. (1972) Phys. Rev. A6:988.
94. Porter, H.S., Jackman, C.H., and Green, A.E.S. (1976) J. Chem. Phys. 76:154.
95. Brinkmann, R.T., and Trajmar, S. (1970) Ann. Geophys. 26:201.
96. Finn, T.G., Aarts, J.F.M., and Doering, J.P. (1972) J. Chem. Phys. 56:5632.
97. Kisker, E. (1972) Z. Physik 257:51.
98. Borst, W.L., Wells, W.C., and Zipf, E.C. (1972) Phys. Rev. A5:1744.
99. Chutjian, A., Cartwright, D.C., and Trajmar, S. (1977) Phys. Rev. A16:1052.
100. Zipf, E.C., and McLaughlin, R.W. (1978) Planet Space Sci. 26:449.
101. Henry, R.J.W., Burke, P.G., and Sinfailem, A. (1969) Phys. Rev. 178:218.
102. Hall, R.A., and Trajmar, S. (1975) J. Phys. B8:L293.
103. Winters, H.F. (1966) J. Chem. Phys. 44:1472.
104. Messiah, A. (1963) Quantum Mechanics, N. Holland Publishing Co., Amsterdam, Netherlands.
105. Goldberger, M.L., and Watson, K.M. (1964) Collision Theory, John Wiley and Sons, Inc., New York, New York.
106. Keiffer, L.J., and Dunn, G.H. (1966) Rev. Mod. Phys. 38:1.
107. Boksenberg, A. (1961) Thesis, University of London.
108. Fite, W.L., and Brackmann, R.T. (1958) Phys. Rev. 112:1141.
109. Rothe, E.W., Marino, L.L., Neynaber, P.H., and Trujillo, S.M. (1962) Phys. Rev. 125:582.
110. Rapp, D., and Englander-Golden, P. (1965) J. Chem. Phys. 43:1464.
111. Tate, J.T., and Smith, P.T. (1932) Phys. Rev. 39:270.
112. Opal, C.B., Beaty, E.C., and Peterson, W.K. (1972) Atomic Data 4:209.
113. Opal, C.B., Peterson, W.K., and Beaty, E.C. (1970) J. Chem. Phys. 55:4100.
114. Holland, R.F., and Maier, W.B. (1972) J. Chem. Phys. 56:5229.
115. Borst, W.L., and Zipf, E.C. (1970) Phys. Rev. A1:834.
116. Green, A.E.S., and Sawada, T. (1972) J. Atmos. Terr. Phys. 34:1719.

117. Bates, D.R., and Massey, H.S.W. (1947) Proc. Roy. Soc. A192:1.

118. Bardsley, J.N., and Biondi, M.A. (1970) Adv. in Atomic and Molecular Phys. 6:1, (Bates, D.R., and Esterman, I., eds.) Academic Press, New York.

119. Dalgarno, A. (1979) Adv. in Atomic and Molecular Phys. 15:37, (Bates, D.R., and Bederson, B., eds.) Academic Press, New York.

120. Torr, D.G. (1979) Rev. Geophys. and Space Phys. 17:510.

121. Oppenheimer, M., Dalgarno, A., and Brinton, H.C. (1976a) J. Geophys. Res. 81:3762.

122. Oppenheimer, M., Dalgarno, A., and Brinton, H.C. (1976b) J. Geophys. Res. 81:4678.

123. Walls, F.L., and Dunn, G.H. (1974) J. Geophys. Res. 79:1911.

124. Huang, C.M., Biondi, M.A., and Johnson, R. (1975) Phys. Rev. A11:901.

125. Mul, P.M., and McGowan, J.W. (1979) J. Phys. B12:1591.

126. Michaels, H.H. (1975) Theoretical Study of Dissociative Recombination of $e + NO^+$, AFCRL-TR-75-0509, AD A024309.

127. Michaels, H.H. (1980) Theoretical Research Investigation Upon Reaction Rates to the Nitric Oxide (Positive) Ion, AFGL-TR-80-0072, AD A104303.

128. Tinsley, B.A., Christensen, A.B., Bittencourt, J., Gouveia, H., Angreji, P.D., and Takahasi, K. (1973) J. Geophys. Res. 78:1174.

129. Zipf, E.C. (1978) Trans. Am. Geophys. Union 59:336.

130. Torr, D.G. (1982) Private communication.

131. Mehr, F.J., and Biondi, M.A. (1969) Phys. Rev. 181:264.

132. Massey, H.S.W., and Bates, D.R. (1942) Rep. Prog. Phys. 9:62.

133. Biondi, M.A. (1969) Can. J. Chem. 47:1711.

134. Kirby, K., Constantinides, E.R., Babeu, S., Oppenheimer, M., and Victor, G.A. (1979) Atomic Data and Nuclear Data Tables 23:63.

135. Heroux, L., and Hinteregger, H.E. (1978) J. Geophys. Res. 83:5305.

136. Wight, G.R., Van der Weil, M.J., and Brian, C.E. (1976) J. Phys. B9:675.

137. Gardner, J.L., and Samson, J.A.R. (1975) J. Chem. Phys. 62:1447.

138. Hinteregger, H.E. (1980) XXIII Cospar, preprint.

139. Torr, M.A., Torr, D.G., Ong, R.A., and Hinteregger, H.E. (1979) Geophys. Res. Lett. 6:771, AFGL-TR-80-0284, AD A090081.

140. Heroux, L., Cohen, M., and Higgins, J.E. (1974) J. Geophys. Res. 79:5237, AFGL-TR-76-0031, AD A020775.

141. Manson, J.E. (1976a) Satellite Measurements of Solar UV During 1974, AFCRL-TR-76-0006, AD A021490.

142. Manson, J.E. (1976b) J. Geophys. Res. 81:1629, AFGL-TR-76-0103, AD A024617.

# Appendix A

## A1. BEHAVIOR OF CROSS SECTIONS AT HIGH ENERGIES

For many of the cross sections the measured or calculated cross sections end at an energy that is below the maximum energy of interest. The Born approximation, which is often good at high energies, implies a $E^{-1}$ dependence. A parallel argument can be advanced based on the decreasing size of the solid angle of the scattering cone (Landau and Lifshitz, 1976;[A1] Messiah, 1963[A2]). Similarly if the interaction can be defined relative to a specific orbital angular momentum $l$, the cross section from state a to state b is

$$Q_{ab} = \frac{(2l+1)\pi}{k_a^2} \left| 1_{ab} - S_{ab} \right|^2 ;$$

again resulting in a $E^{-1}$ dependence. This shows that discrete states are being considered. Summing over the orbital angular momenta can cause cancellation of the $E^{-1}$ factor if the scattering matrix is independent of $l$ for allowed angular momenta. This leads to classical results. The Coulomb interaction, which mediates electron scattering, is long range and involves many orbital angular momenta. The Born approximation adjusted for this yields a $E^{-1}$ ln E behavior for the excitation cross section where the upper state can decay via an allowed dipole transition,

A1. Landau, L. D., and Lifshitz, E. M. (1965) Quantum Mechanics, Non-Relativistic Theory, Addison Wesley, Reading, Massachusetts.

A2. Messiah, A. (1963) Quantum Mechanics, N. Holland Publishing Co., Amsterdam, Netherlands.

$E^{-1}$ behavior where the decay is a forbidden transition (that is, does not occur by an electric dipole interaction), and $E^{-3}$ behavior where the decay transition is spin forbidden (Henry et al, 1969[A3]). The angular factor in the momentum-transfer cross section for allowed dipole transitions causes a $E^{-2}$ dependence at high energies.

To extend a cross section to energies not considered in the experiment or calculation providing the data, the high energy dependencies were used. To allow the derivative as well as the magnitude to be roughly fitted a constant was added to the energy in the denominator. The following formulae in Table A1 were pegged to two data points at the end of the data and used to extend the cross section to higher energies.

Table A1. Cross Section Dependence at High Energies

| | |
|---|---|
| Momentum transfer for allowed dipole transitions | $\frac{A}{(E - E_o)^2}$ |
| Electric dipole decay allowed | $\frac{A \ln E}{E - E_o}$ |
| Electric dipole decay forbidden | $\frac{A}{E - E_o}$ |
| Spin change | $\frac{A}{(E - E_o)^3}$ |

Using the restriction that $|S_{ab}| \leq 1$, limits can be imposed on the cross sections. For the case where the initial and final states are different and all of the angular momentum states are known, the maximum cross section is

$$\frac{\pi(2\ell + 1)}{K^2} ,$$

which can also be obtained by requiring flux conservation. Similarly for elastic scattering the maximum total cross section for a resonance having a spin of J is

$$\frac{4\pi(2J + 1)}{K^2 (2S_1 + 1)(2S_2 + 1)} ,$$

A3. Henry, R.J.W., Burke, P.F., and Sinfailem, A.L. (1969) Phys. Rev. 178:218.

where the spins have been appropriately summed and averaged over and $S_1$ and $S_2$ are the spins of the target and projectile (Goldberger and Watson, 1964[A4]).

## A2. EMPIRICAL CURVE FITTING

The empirical forms for cross sections to discrete states as given by Jackman et al (1977)[A5] can be put in the following forms with X equal to $E/\bar{W}$ where $\bar{W}$ is the energy of the state:

$$\sigma = G[1 - X^{-\alpha}]^{\beta} X^{-\Omega}$$

$$\sigma = G[1 - X^{-\alpha}]^{\beta} X^{-1} \ln(KX + e) .$$

The two forms are for states whose decay to the ground state, by the emission of photons, is forbidden or allowed. The term in square brackets causes the drop to zero at threshold and can be adjusted to the position and magnitude at the peak. It becomes negligible at high energies. Taking two points well beyond the peak of a smooth curve and assuming that $[1 - X^{-\alpha}]^{\beta} \simeq 1$, fit the points with the parameters G and either $\Omega$ or K. At the maximum $X = X_M$ and $\sigma = \sigma_M$ the two parameters $\alpha$ and $\beta$ may be determined by solving by iteration:

$$A = \left(1 + \frac{\beta}{H}\right)^{H} ,$$

$$B = \left(1 + \frac{H}{\beta}\right)^{\beta} \quad \text{for H and } \beta .$$

For the forbidden case we have

$$A = X_M^{\Omega} ,$$

$$B = \frac{G}{X_M^{\Omega} \sigma_M} ,$$

$$H = \frac{\Omega}{\alpha} .$$

---


A4. Goldberger, M. L., and Watson, K. M. (1964) Collision Theory, John Wiley and Sons, New York, New York.

A5. Jackman, C. H., Garvey, R. H., and Green, A. E. S. (1977) J. Geophys. Res. 82:5801.

For the allowed case we have

$$L \equiv 1 - \frac{K X_M}{(KX_M + e) \ln (KX_M + e)} ,$$

$$A = X_M^L$$

$$B = \frac{G \ln (KX_M + e)}{X_M \sigma_M} ,$$

$$H = \frac{L}{\alpha} .$$

The curves can also be fitted to the data by requiring a minimum of the squares of the deviations. The significance of the data depends on its relative magnitude; suggesting that the logarithm of the cross section be fitted. The error bars shown by Cartwright et al (1977)[A6] indicate that the logarithmic error is roughly constant reinforcing this approach. When this was tried, parameters were obtained which reasonably matched the data; however, the same data set might be fit by very different parameters resulting in a similar curve. For example, the data for the cross section for excitation of $N_2$ to a $^1\Pi_g$ could be fit in the energy range 10-50 eV by:

| G | $\alpha$ | $\beta$ | $\Omega$ |
|---|---|---|---|
| 8.0 | 0.09 | 1.5 | 12.0 |
| 1.0 | 0.3 | 1.5 | 2.0 |

In both of these cases the estimated errors in G and $\alpha$ were at least an order of magnitude higher than the estimated values.

## A3. RECOMBINATION RATE CALCULATIONS

For recombination collisions between electrons and ions, only the motion of the electron need to be considered to first approximation. Let the electron distribution be a linear combination of a normalized Maxwell distribution, $f_M$, and a rough approximation to the continuous slowing down distribution, $f_D$.

A6. Cartwright, D.C., Trajmar, S., Chutjian, A., and Williams, W. (1977) Phys. Rev. A16:1041.

$$f_M = \left(\frac{4E}{\pi T^3}\right)^{1/2} e^{-E/T}$$

$$f_D = \frac{1}{D} e^{-E/D}$$

$$f = \frac{1}{1+A} (f_M + A f_D) .$$

Approximating the cross section by

$$\sigma = S (E_o/E)^a$$

yields the rate

$$\alpha = \int \sigma \left(\frac{2E}{m}\right)^{1/2} f \, dE$$

$$= S\left(\frac{T}{E_o}\right)^{+(1/2)-a} \Gamma(2-a)\left(\frac{8E_o}{\pi m}\right)^{1/2} x$$

$$\frac{1}{1+A}\left(1+A\frac{1}{2}\left(\frac{T}{D}\right)^{a-1/2} \frac{\sqrt{\pi}\,\Gamma(3/2-a)}{\Gamma(2-a)}\right),$$

"a" must be in the range $[0, 3/2\rangle$ with the largest contribution from $f_D$ occurring for "a" equal to 0 if D is greater than T. From Jasperse (1977)[A7] T/D can be estimated at 0.04 or less and A is $10^{-4}$ or less. Thus, the contribution to $\alpha$ from the nonMaxwellian part of the distribution is on the order of 0.04 percent of the contribution from the Maxwellian part.

The assumed cross section is incorrect at very low energies. However, if the assumed cross section has no major errors above the energy peak of $f_M$ at 1/2 T, there should be no change in the above conclusion. For cross sections with higher thresholds or structures at higher energies, individual calculations must be done. For a temperature of 1000°K, the maximum is at 0.043 eV. Thus, the rates can be calculated based on the Maxwell distributions.

A7. Jasperse, J. (1977) Planet Space Sci. 25:743.

## A4. ANGULAR BEHAVIOR OF PHOTOPRODUCTION

The purpose of this section is to give the derivation of the form of the differential photoionization cross section.

Let the initial state, I, with spin projection M be represented by $|I\,M>$. Let $|F'\,M',\ \vec{p}\,\mu>$ be the final state of the ion in state F' with spin projection M' and an electron with $\vec{p}$ and spin projection $\mu$. The interaction with a photon of momentum $\vec{\kappa}$ and polarization $\hat{\varepsilon}$ is

$$\mathcal{O} = \vec{A}\cdot\vec{p} + \frac{1}{2}g\,\vec{H}\cdot\vec{s}$$

where

$$\vec{A} = \hat{\varepsilon}\,e^{i\vec{\kappa}\cdot\vec{r}}$$

$$\vec{H} = \vec{\nabla}\times\vec{A} = i\kappa\,\hat{\eta}\;e^{i\vec{\kappa}\cdot\vec{r}}$$

and

$$\hat{\eta} = \hat{\kappa}\times\hat{e}\ .$$

The cross section is

$$d\sigma = \frac{1}{2I+1}\sum_{M}\sum_{M'\mu} d\sigma_{M\,M'\mu} \propto \frac{1}{2I+1}\sum_{MM'\mu}\left|\langle F'\,M',\ \vec{p}\,\mu\,|\,\mathcal{O}\,|\,I\,M\rangle\right|^2$$

Using the relations from Brink and Satchler, (1968)[A8] page 151:

$$\delta^3(\vec{p}-\vec{p}') = \frac{1}{4\pi p^2}\,\delta(p-p')\sum_{\ell m} C_m^{\ell}(\hat{p}')\;C_m^{\ell}(\hat{p})^*$$

$$e^{i\vec{\kappa}\cdot\vec{r}} = \sum_{k}(-i)^k(2k+1)^{\frac{3}{2}}\,j_k(\kappa r)\,(C^k(\hat{\kappa})\,C^k(\hat{r}))^0\ ,$$

---

A8. Brink, D.M., and Satchler, G.R. (1968) Angular Momentum, Oxford University Press, London, England.

where

$$\left(C^k(\hat{\kappa})\, C^k(\hat{r})\right)^0 = \sum_{M M'} C^k_m(\hat{\kappa})\, C^k_{m'}(\hat{r}) \langle\, \mathrm{km\ km'} \,|00\rangle \ .$$

The final states and the interaction operator can be expanded:

$$|\, F' M',\, \vec{p}\mu\,\rangle = \sum_{F \ell m} |F' M'\, p\, \ell m\, \tfrac{1}{2}\mu;\, F\, M\rangle\, A^{F\ell}(p)\, (\hat{p})^{\ell *}_m \ ,$$

$$\mathcal{O} = \sum_k \left[ \left( \mathcal{O}^k_E \left( (\hat{\kappa})^{k-1}\, \hat{\varepsilon} \right)^k \right)^0 + \left( \mathcal{O}^k_M \left( (\hat{\kappa})^{k-1}\, \hat{\eta} \right)^k \right)^0 \right] \ ,$$

where

$$(\hat{p})^\ell_m = \frac{2^\ell\, \ell!\, \ell!}{(2\ell)!}\ C^\ell_m(\hat{p})$$

is a symmetric traceless tensor formed from the vector $\hat{p}$ and $\mathcal{O}^k_E$ and $\mathcal{O}^k_M$ are the properly normalized electric and magnetic $2^k$ -pole operators.

Using the reduced matrix elements the sums over the projections can be carried out:

$$d\sigma = \Sigma(\mathrm{factors}_1) \left( (\hat{p})^\ell \left( (\hat{\kappa})^{k-1} \hat{\pi} \right)^k\ (\hat{p})^{\ell'} \left( (\hat{\kappa})^{k'-1} \hat{\pi}' \right)^{k'} \right)^0 \ ,$$

where $\hat{\pi}$ and $\hat{\pi}'$ are $\hat{\varepsilon}$ and/or $\hat{\eta}$. The summations can be rearranged via 6-j and 9-j symbols:

$$d\sigma = \Sigma(\mathrm{factors}_2) \left( \left( (\hat{p})^\ell\, (\hat{p})^{\ell'} \right)^{\overline{\ell}} \left( \left( (\hat{\kappa})^{k-1} \hat{\pi} \right)^k\ \left( (\hat{\kappa})^{k'-1} \hat{\pi}' \right)^{k'} \right)^{\overline{\ell}} \right)^0$$

$$= \Sigma(\mathrm{factors}_3) \left( (\hat{p})^{\overline{\ell}} \left( \left( (\hat{\kappa})^{k-1}\, (\hat{\kappa})^{k'-1} \right)^{\overline{k}}\ (\hat{\pi}\, \hat{\pi}')^{\overline{\pi}} \right)^{\overline{\ell}} \right)^0 \ .$$

Summing over the photon polarization directions

$$\Sigma\, (\hat{\pi}\, \hat{\pi})^{\overline{\pi}} \propto (\hat{\kappa})^{\overline{\pi}} \ ,$$

since $\hat{\kappa}$ is the only remaining direction. Thus

$$d\sigma = \Sigma \text{ (factors}_4\text{)} \left( (\hat{p})^{\overline{\ell}} \left( (\hat{\kappa})^{\overline{k}} (\hat{\kappa})^{\overline{\pi}} \right)^{\overline{\ell}} \right)^0$$

$$= \Sigma \text{ (factors}_5\text{)} \left( (\hat{p})^{\overline{\ell}} (\hat{\kappa})^{\overline{\ell}} \right)^0$$

$$= \Sigma \text{ (factors)} \; P_{\overline{\ell}} \; (\cos \theta) ,$$

where

$$\cos \theta = \hat{p} \cdot \hat{\kappa} .$$

If the highest multipole considered is $2^{k\,max}$, since $\overline{I} = k \times k'$ ,

$$\overline{I}_{max} = 2\, k_{max} .$$

Parity is conserved and the states have well-determined parity. The non-zero operators must all have a definite parity. Therefore, all terms

$$\left( (\hat{\kappa})^{k-1} \hat{\pi} \right)^k$$

of interest must have the same parity and

$$\left( \left( (\hat{\kappa})^{k-1} \hat{\pi} \right)^k \left( (\hat{\kappa})^{k'-1} \hat{\pi}' \right)^{k'} \right)^{\overline{\ell}}$$

must have positive parity. This is reduced to $(\hat{\kappa})^{\overline{\ell}}$ which has parity $(-1)^{\overline{\ell}}$. Thus, $\overline{\ell}$ must be even. A detailed reduction leads to the same result.

To estimate the relative magnitudes of the different terms, $j_k$ $(\kappa r)$ is expanded in powers of $\kappa r$ starting with $(\kappa r)^k$. The expectation value of $r^k$ is about $a^k$ where "a" is a typical distance for the system in question; for example, the Bohr radius for hydrogenic atoms. In general units $\kappa$ is the inverse of the photon wavelength, $\Delta E/\hbar c$, where $\Delta E$ is the energy gained by the atom or molecule. The electron energy of a single electron is of the order of $-Z_{eff}\, e^2/a$ where $Z_{eff}$ is the effective charge binding the electron. Using this ionization energy to estimate the energy transferred,

$$\kappa = \frac{\Delta E}{\hbar c} \simeq \frac{Z_{eff}\, e^2}{\hbar c a} = \frac{Z_{eff}\, \alpha}{a}$$

where

$\alpha = \frac{1}{137}$ , the estimated expectation value of $(Kr)^k$ is

$$\langle (\kappa r)^k \rangle \simeq \langle \kappa^k \rangle \langle r^k \rangle \simeq \left( \frac{Z_{eff}\, \alpha}{a} \right)^k a^k = (Z_{eff}\, \alpha)^k \ .$$

For the outer electrons with $Z_{eff}$ about unity, the effects of each higher multipole can be expected to be suppressed by two orders of magnitude. The strongest interaction, electric dipole, leads to the isotropic ($\overline{l} = 0$) term and to the $\overline{l} = 2$ term.

In summary, the differential ionization cross section can be expanded as a series of even Legendre polynomials dependent on the cosine of the angle between the incoming photon and the outgoing electron. Successive multipoles are suppressed resulting in the dominance of the dipole interaction and yielding the standard formula for atoms and molecules:

$$\frac{d\sigma}{d\Omega} = \frac{\sigma}{4\pi} \left( 1 - \frac{1}{2} \beta P_2 \right) .$$

## A5. OXYGEN RADIATIVE RECOMBINATION

Oxygen radiative recombination may proceed via different intermediate states having different cross sections and energy dependencies. The purpose of this section is to find general expressions for the recombination rate and cross sections and, in the process, note the areas of difficulty.

Rate coefficients for two particle reactions are determined by integrating the product of the cross section and the relative velocity over the energy or momentum distributions of the two kinds of incoming particles. When one of the particles is an electron and the other is an atom or molecule, with a Maxwellian distribution, the difference in mass reduces the non-electron distribution to a near delta function sensitive to changes in the cross section occurring on a scale less than

$$kT \left( \frac{m_e}{M} \right)^{1/2} .$$

The rates to be used with upper atmosphere data do not depend significantly on energies above 1 eV. (Walls and Dunn, 1974[A9]). However, the higher energies are of interest in modelling the high energy tail of the electron distribution.

As an example of the problems that may arise by modelling the cross section on the rate coefficient, let us consider $O^+$ radiative recombination. Using the expressions in Section A3 for a pure Maxwellian distribution, we can relate the rate with a given power dependence on the temperature to a cross section with a related dependence on the energy. An early theoretical set of values for the recombination rate is that presented by Massey and Bates (1943).[A10] A recent calculation using scaled Thomas-Fermi methods was reported by Tinsley et al, (1973).[A11]

The recombination to the 0 levels n = 3, 4, 5, 6 was done by other techniques by Julienne et al, (1974)[A12] and the coefficients reported for 1160°K. Pradhan (1978)[A13] calculated the photoionization cross section from O ($^3$P) to $O^+$ ($^4$S) which is related to the radiative recombination cross section, as outlined in Section 5. Table A2 presents the total radiative recombination cross section at different energies with the following contributions: to level 2 from Pradhan (1978);[A13] to levels 3, 4, 5 and 6 from the recombination rates of Julienne et al, (1974)[A12] with the temperature dependence of Tinsley et al, (1973);[A11] to levels 7 and higher from the recombination rate of Tinsley et al, (1973).[A11] The sum of the above cross sections is given as is a total cross section obtained from the total rate fitted to a power law dependence on the temperature.

The last line in the table is an approximate combined cross section obtained from

$$\sigma = \left\{ 4.7 \left( \frac{0.1\,\text{eV}}{E} \right)^{1.26} + 0.44 \left( \frac{0.1\,\text{eV}}{E} \right)^{0.5} \right\} \times 10^{-20}\ \text{cm}^2 \ .$$

The object of this exercise is to show that the total cross sections obtained from different fits to the rates are in reasonable agreement at low energies. However, at high energies where the dependence of the cross section on the rate is lessened by the reduced values of the distribution and of the cross section itself, the cross section determined by the rate may not include those parts having a slower decline as a function of energy than the main low energy part.


A9. Walls, F.L., and Dunn, G.H. (1974) J. Geophys. Res. 79:1911.

A10. Massey, H.S.W., and Bates, D.R. (1942) Rep. Prog. Phys. 9:62.

A11. Tinsley, B.A., Christensen, A.B., Bittencourt, J., Gouveia, H., Angreji, P.D., and Takahasi, K. (1973) J. Geophys. Res. 78:1174.

A12. Julienne, P.S., Davis, S., and Oran, E. (1974) J. Geophys. Res. 71:2540.

A13. Pradhan, A.K. (1978) J. Phys. B11:L729.

Table A2. $O^+(^4S)$ Radiative Recombination Cross Sections

| To Level | From Calculation Of | $-\frac{\ln Q}{\ln E}$ | Energy (eV) 0.01 | 0.1 | 1.0 | 10.2 | 20.4 |
|---|---|---|---|---|---|---|---|
| 2 | Photoionization Q | 0.5 | 16.3 | 1.65 | 0.188 | 0.043 | 0.031 |
| 3,4,5,6 | Recombination rate | 1.1 | 21.4 | 1.70 | 0.135 | 0.010 | 0.005 |
| 7 - ∞ | Recombination rate | 1.4 | 49.8 | 1.98 | 0.079 | 0.003 | 0.001 |
| Total cross section | | | 87.6 | 5.34 | 0.402 | 0.056 | 0.037 |
| Approximate cross sections | | 1.2 | 87.4 | 5.52 | 0.348 | 0.021 | 0.009 |
| | | 1.15 | 76.3 | 5.40 | 0.382 | 0.026 | 0.012 |
| Approximate combined cross sections | | 1.26<br>.5 | 87.6 | 5.17 | 0.400 | 0.058 | 0.037 |
| Units: $10^{-20}$ cm$^2$ = $10^{-2}$ Mb. | | | | | | | |

## References


A1. Landau, L.D., and Lifshitz, E.M. (1965) Quantum Mechanics, Non-Relativistic Theory, Addison Wesley, Reading, Massachusetts.

A2. Messiah, A. (1963) Quantum Mechanics, N. Holland Publishing Co., Amsterdam, Netherlands.

A3. Henry, R.J.W., Burke, P.G., and Sinfailem, A.L. (1969) Phys. Rev. 178:218.

A4. Goldberger, M.L., and Watson, K.M. (1964) Collision Theory, John Wiley and Sons, Inc., New York, New York.

A5. Jackman, C.H., Garvey, R.H., and Green, A.E.S. (1977) J. Geophys. Res. 82:5801.

A6. Cartwright, D.C., Trajmar, S., Chutjian, A., and Williams, W. (1977) Phys. Rev. A16:1041.

A7. Jasperse, J. (1977) Planet Space Sci. 25:743.

A8. Brink, D.M., and Satchler, G.R. (1968) Angular Momentum, Oxford University Press, London, England.

A9. Walls, F.L., and Dunn, G.H. (1974) J. Geophys. Res. 79:1911.

A10. Massey, H.S.W., and Bates, D.R. (1942) Rep. Prog. Phys. 9:62.

A11. Tinsley, B.A., Christensen, A.B., Bittencourt, J., Gouveia, H., Angreji, P.D., and Takahasi, K. (1973) J. Geophys. Res. 78:1174.

A12. Julienne, P.S., Davis, S., and Oran, E. (1974) J. Geophys. Res. 71:2540.

A13. Pradhan, A.K. (1978) J. Phys. B11:L729.

# Appendix B

## Graphs

This appendix contains graphical presentations of the data. The initial graphs show the momentum-transfer cross sections and summations over the cross sections of each different type and species. The individual electron cross sections are next. Graphs of the photon cross sections and of the solar flux are the last.

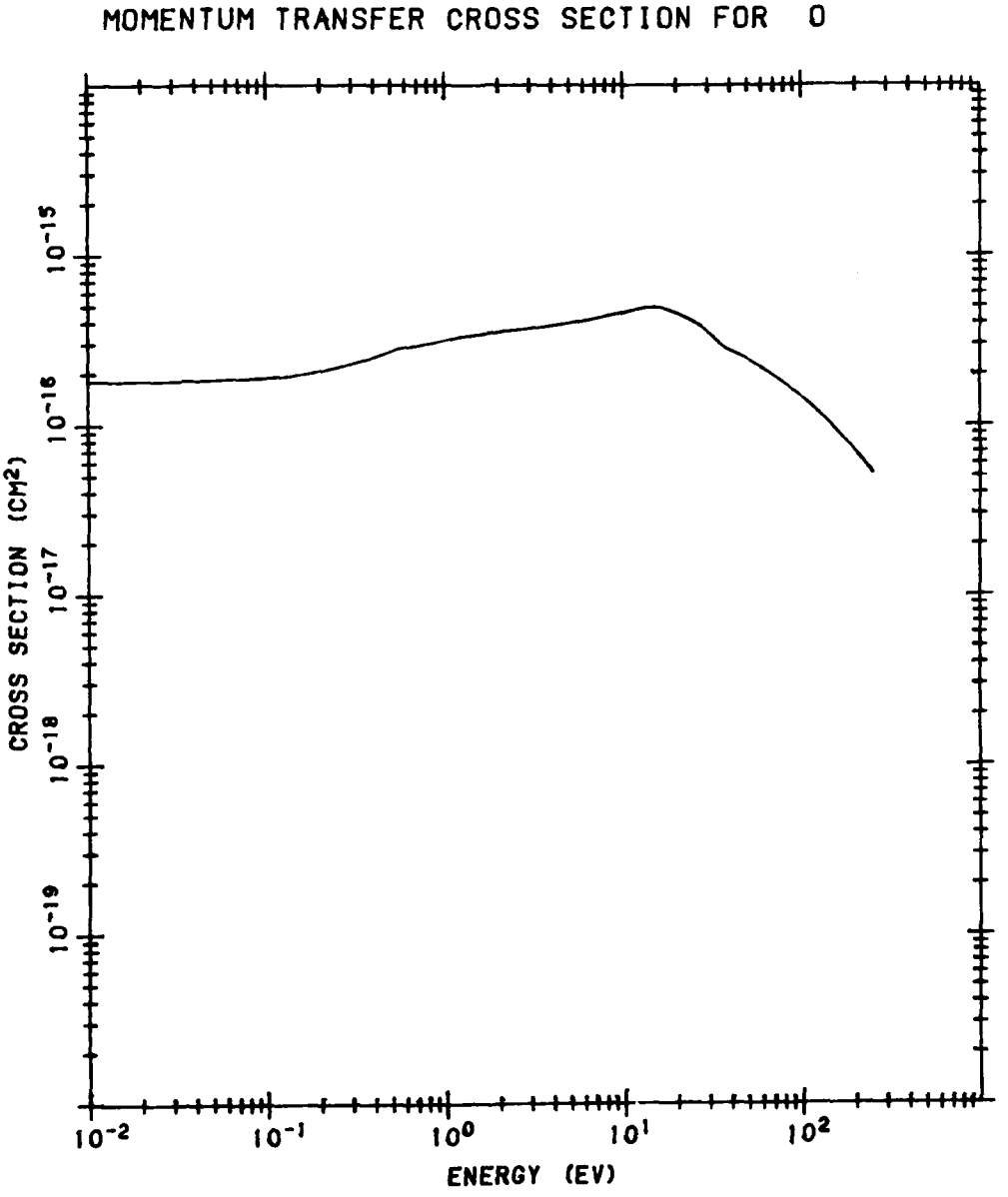


Figure B1. Momentum Transfer Cross Section for O. The data from 0.136 eV to 11 eV are from Thomas and Nesbet (1975).[B1] This is continued to 0 eV. The data from 11 eV to 54 eV are 0.7 of the elastic cross section of Smith et al (1967).[B2] Above 54 eV a $1/E^2$ extrapolation is used

B1. Thomas, L.D., and Nesbet, R.K. (1975) Phys. Rev. A11:170; addendum, Phys. Rev. A12:1279.

B2. Smith, K., Henry, R.J.W., and Burke, P.G. (1967) Phys. Rev. 157:51.

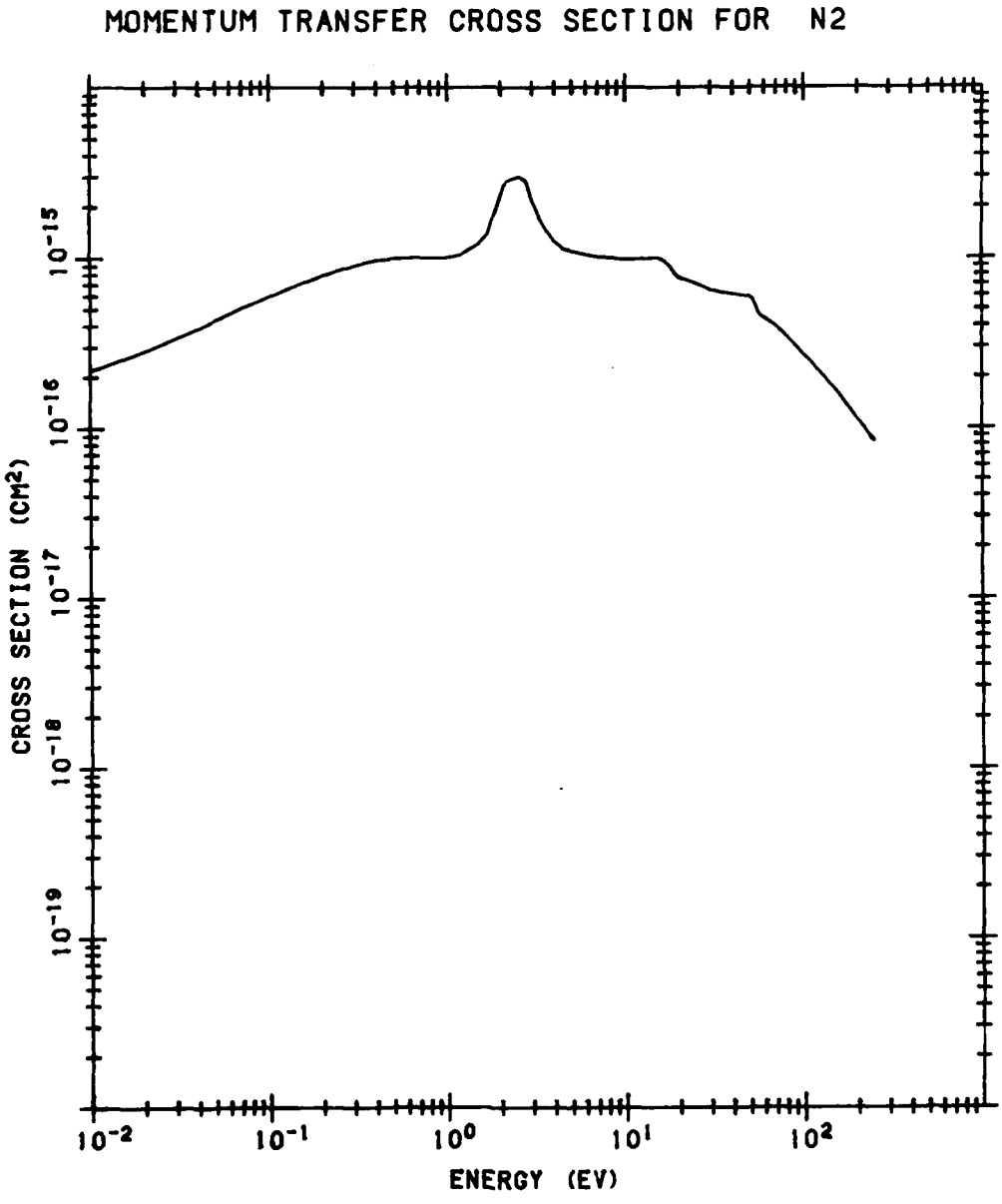


Figure B2. Momentum Transfer Cross Section for $N_2$. The data between 0 eV and 8 eV are from Englehardt et al (1964);[B3] between 10 eV and 75 eV from Srivastava et al (1976);[B4] between 100 eV and 250 eV from Choi et al (1979)[B5]

B3. Englehardt, A.G., Phelps, A.V., and Risk, C.G. (1964) Phys. Rev. 135:A1566.

B4. Srivastava, S.K., Chutjian, A., and Trajmar, S. (1976) J. Chem. Phys. 64:1340.

B5. Choi, B.H., Poe, R.T., Sun, J.G., and Shan, Y. (1979) Phys. Rev. A19:116.

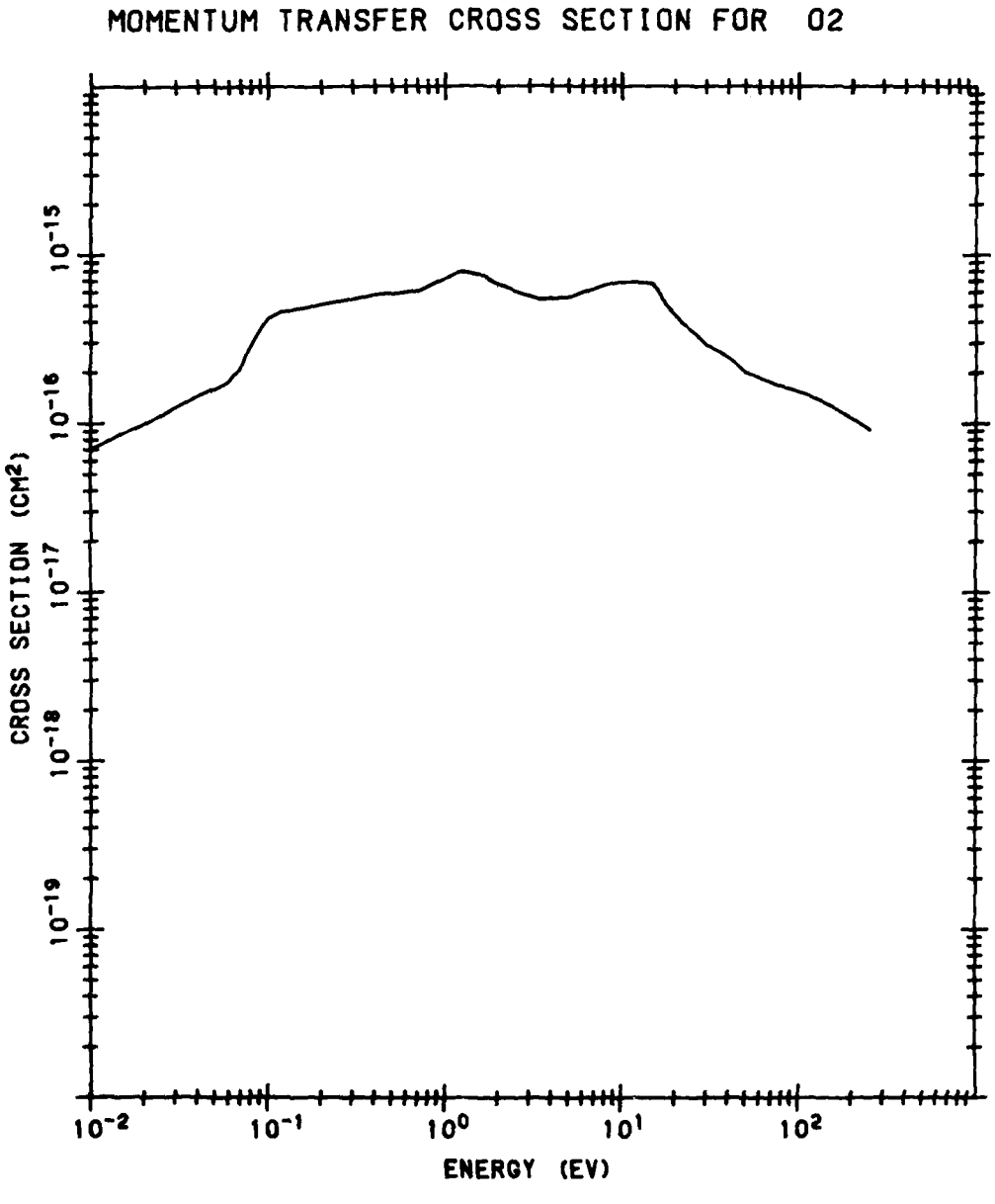


Figure B3. Momentum Transfer Cross Section for $O_2$. The data below 8 eV are from Lawton and Phelps (1979).[B6] The higher energies are from Porter and Jump (1978)[B7]

B6. Lawton, S.A., and Phelps, A.V. (1978) J. Chem. Phys. 69:1055.

B7. Porter, H.S., and Jump, F.W. (1978) Computer Sciences Corporation/TM-78/6017.

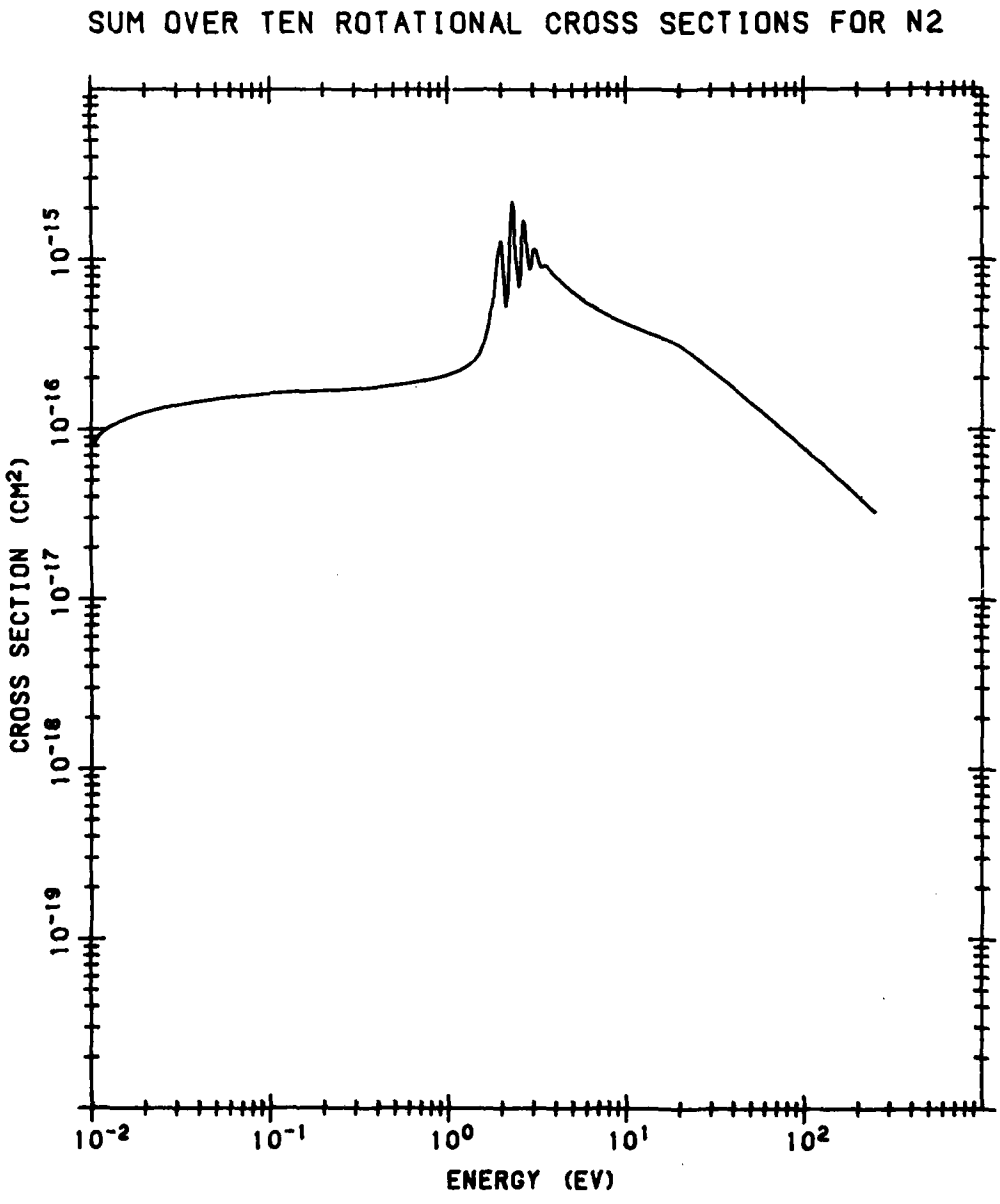


**Figure B4. Sum of $N_2$ Rotational Excitation Cross Sections**

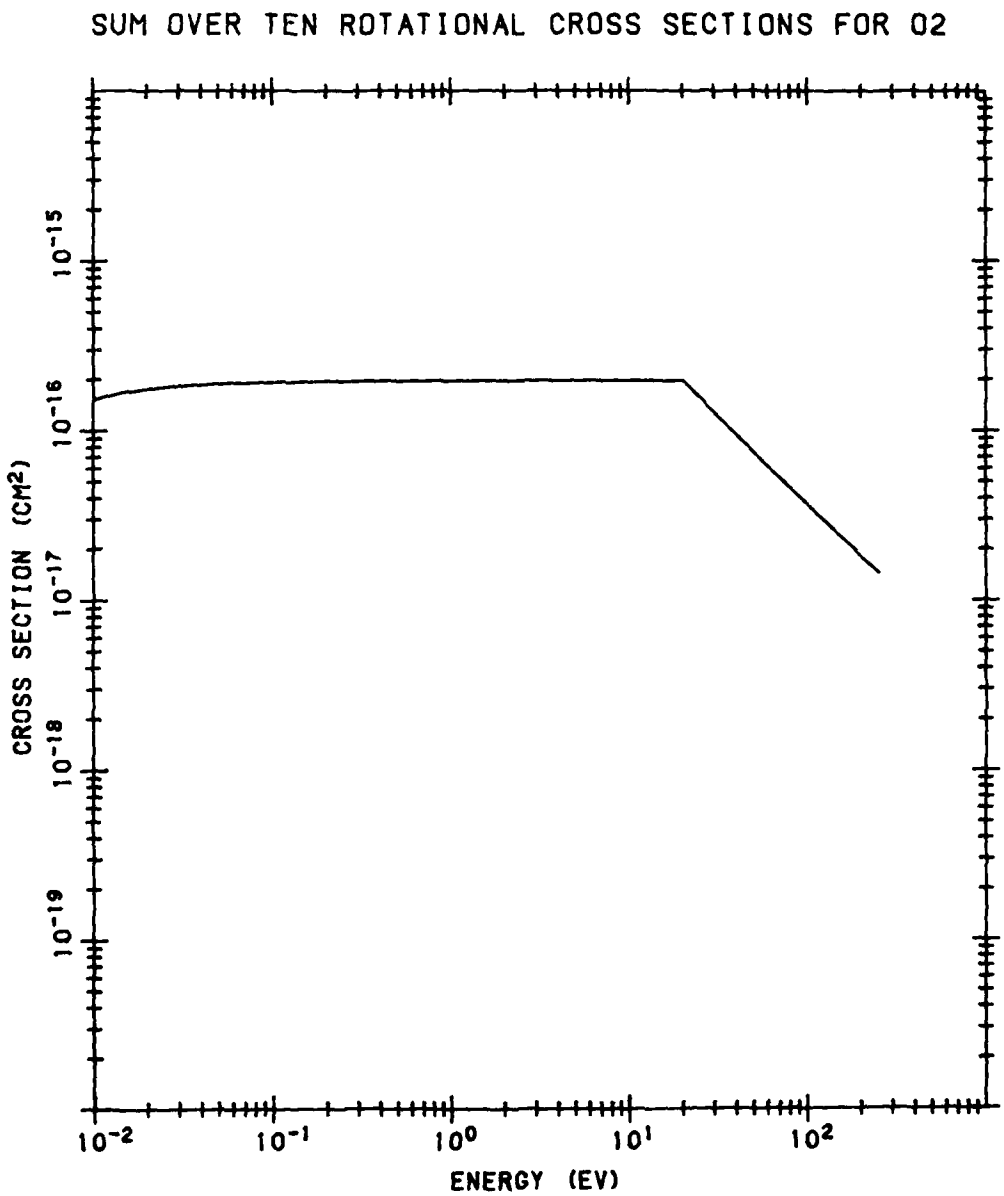


Figure B5. Sum of $O_2$ Rotational Excitation Cross Sections

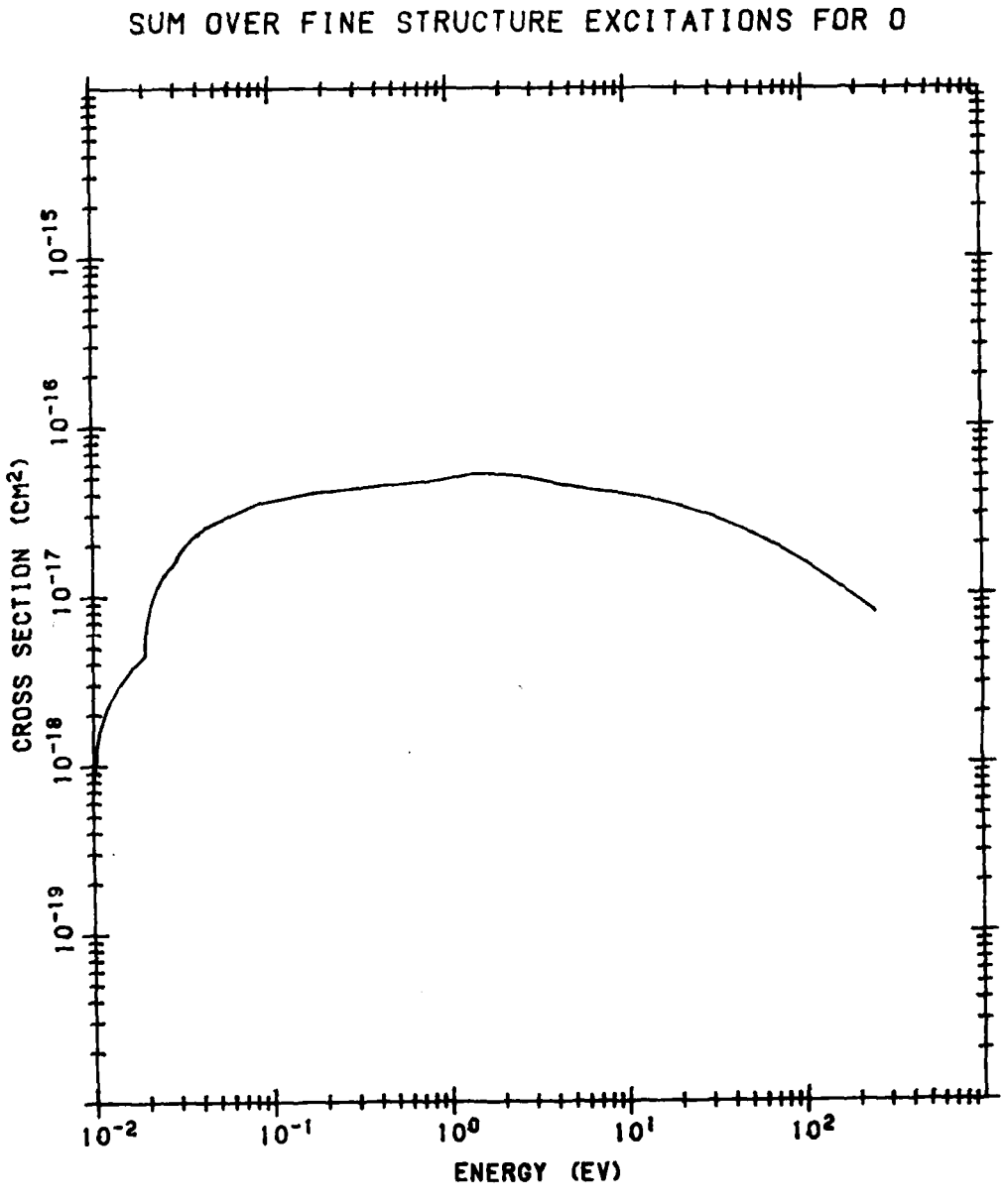


Figure B6. Sum of O Fine Structure Cross Sections

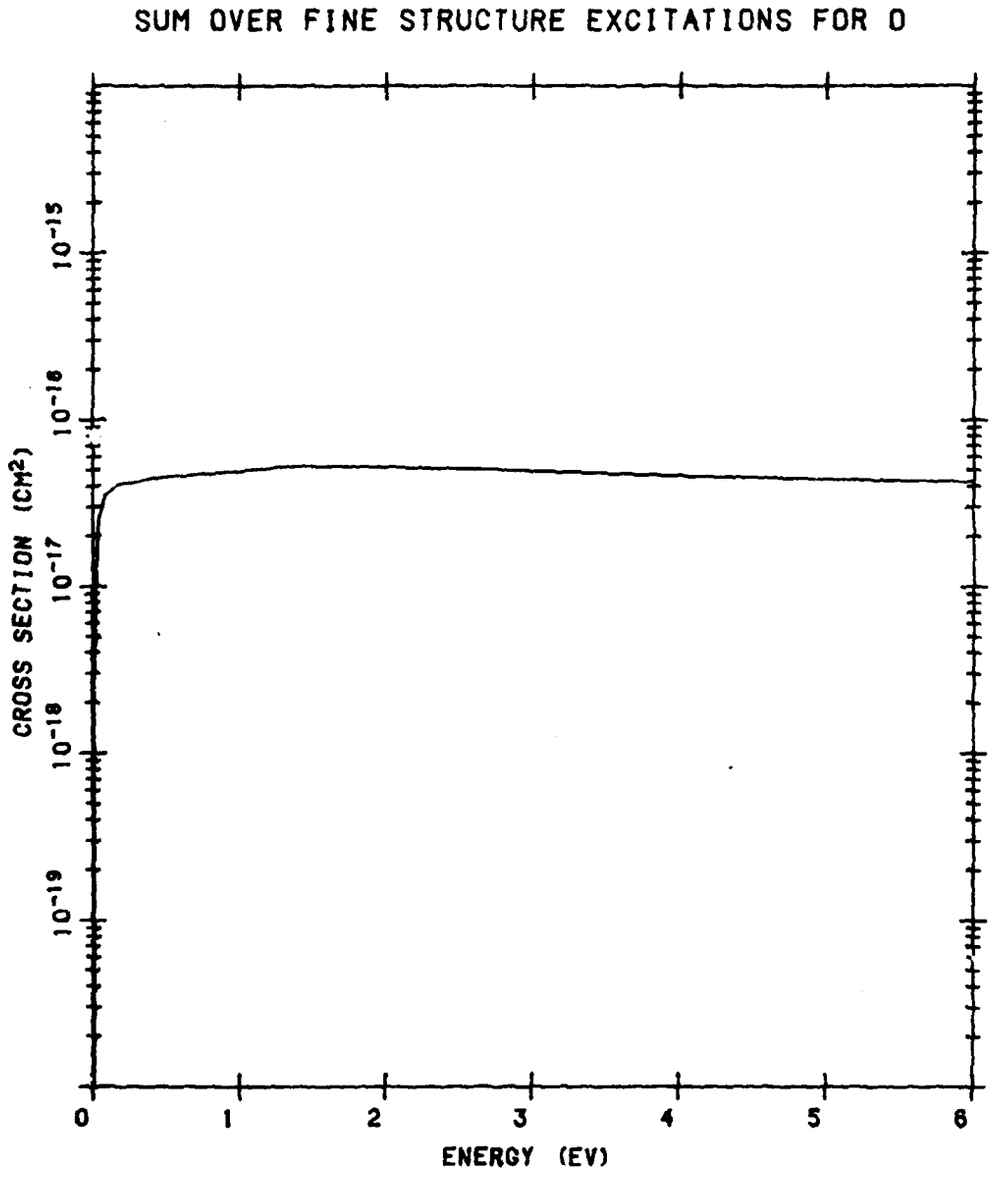


**Figure B6. Sum of O Fine Structure Cross Sections (Cont.)**

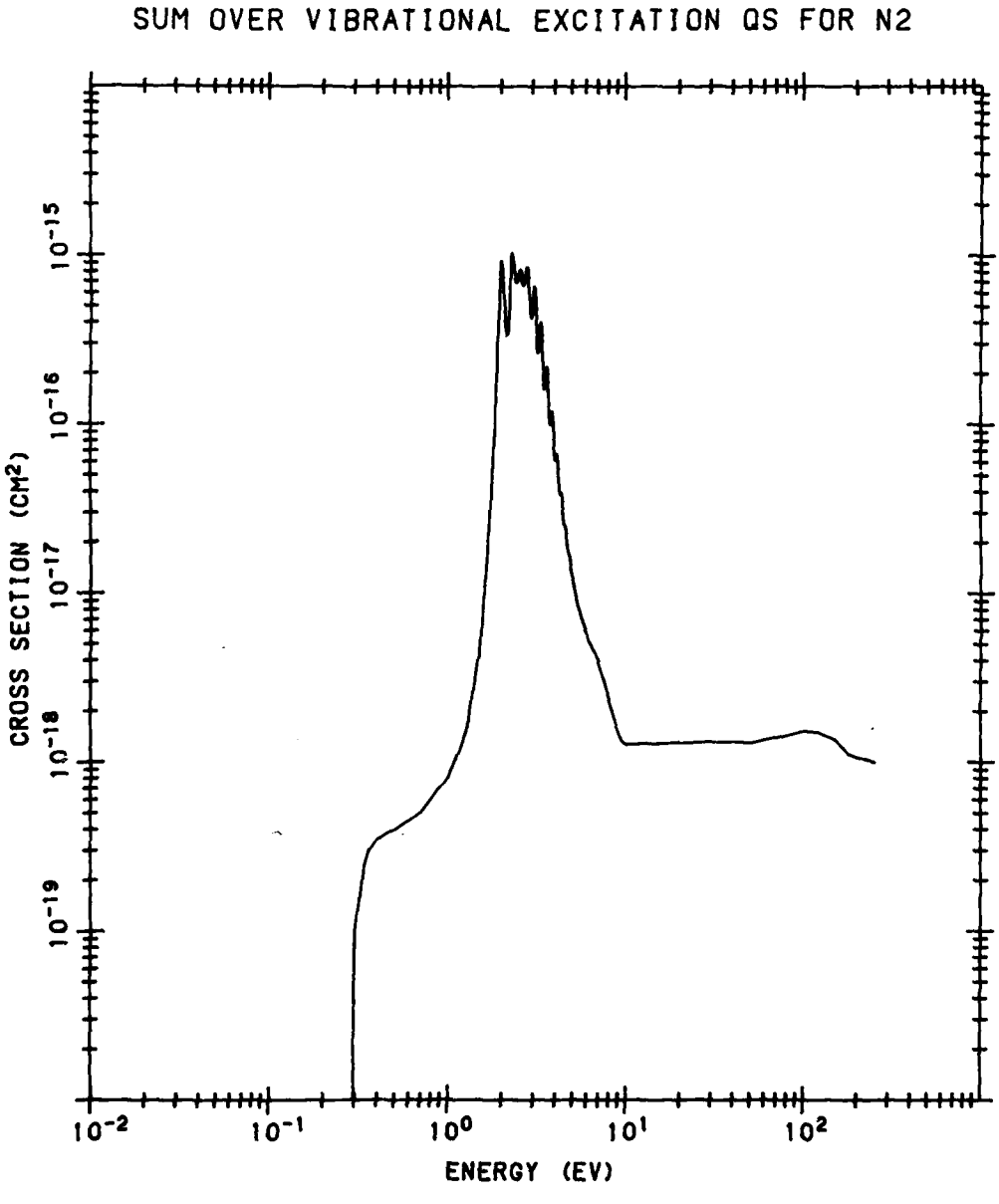


Figure B7. Sum of $N_2$ Vibrational Excitation Cross Sections

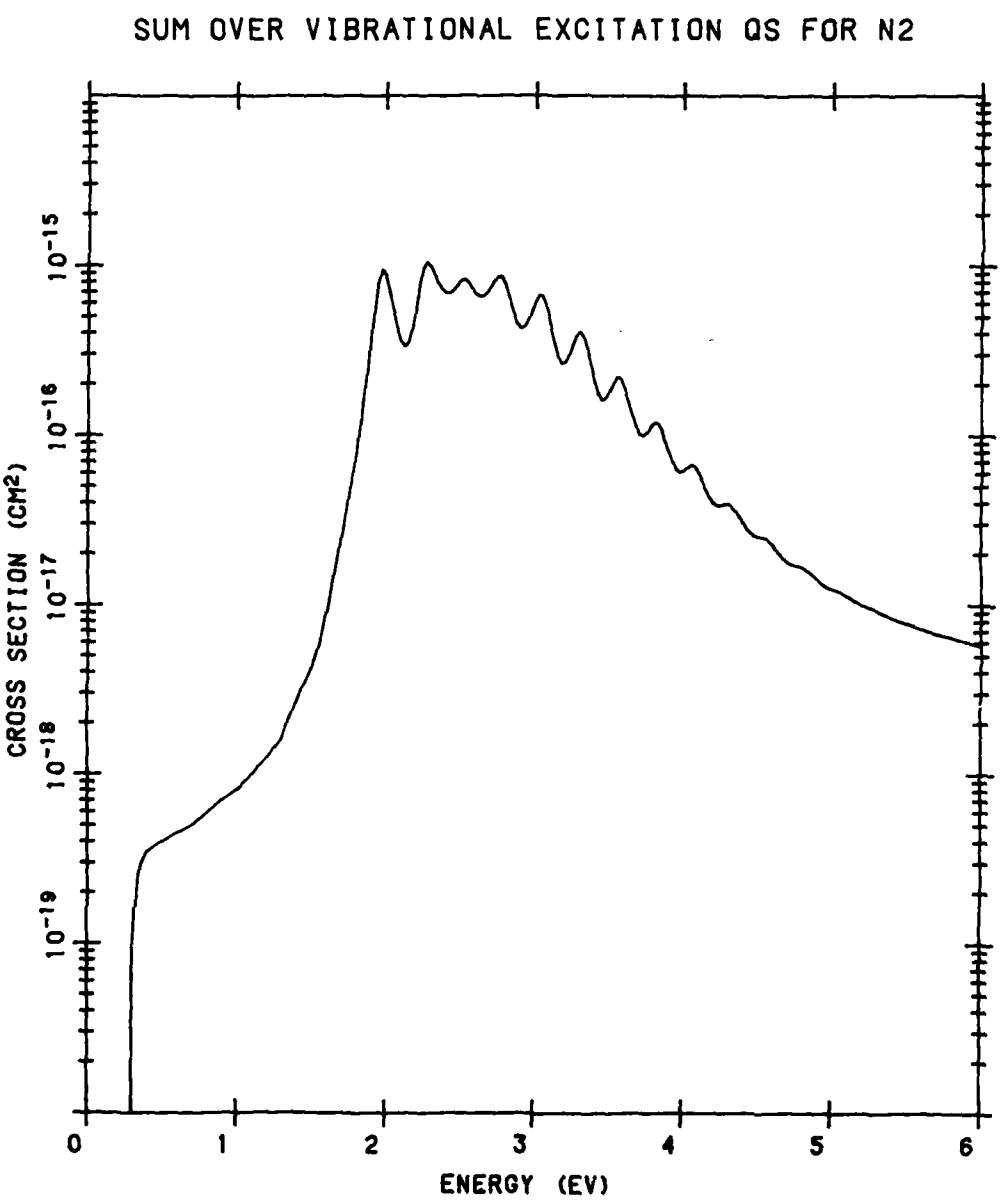


**Figure B7. S n of $N_2$ Vibrational Excitation Cross Sections (Cont.)**

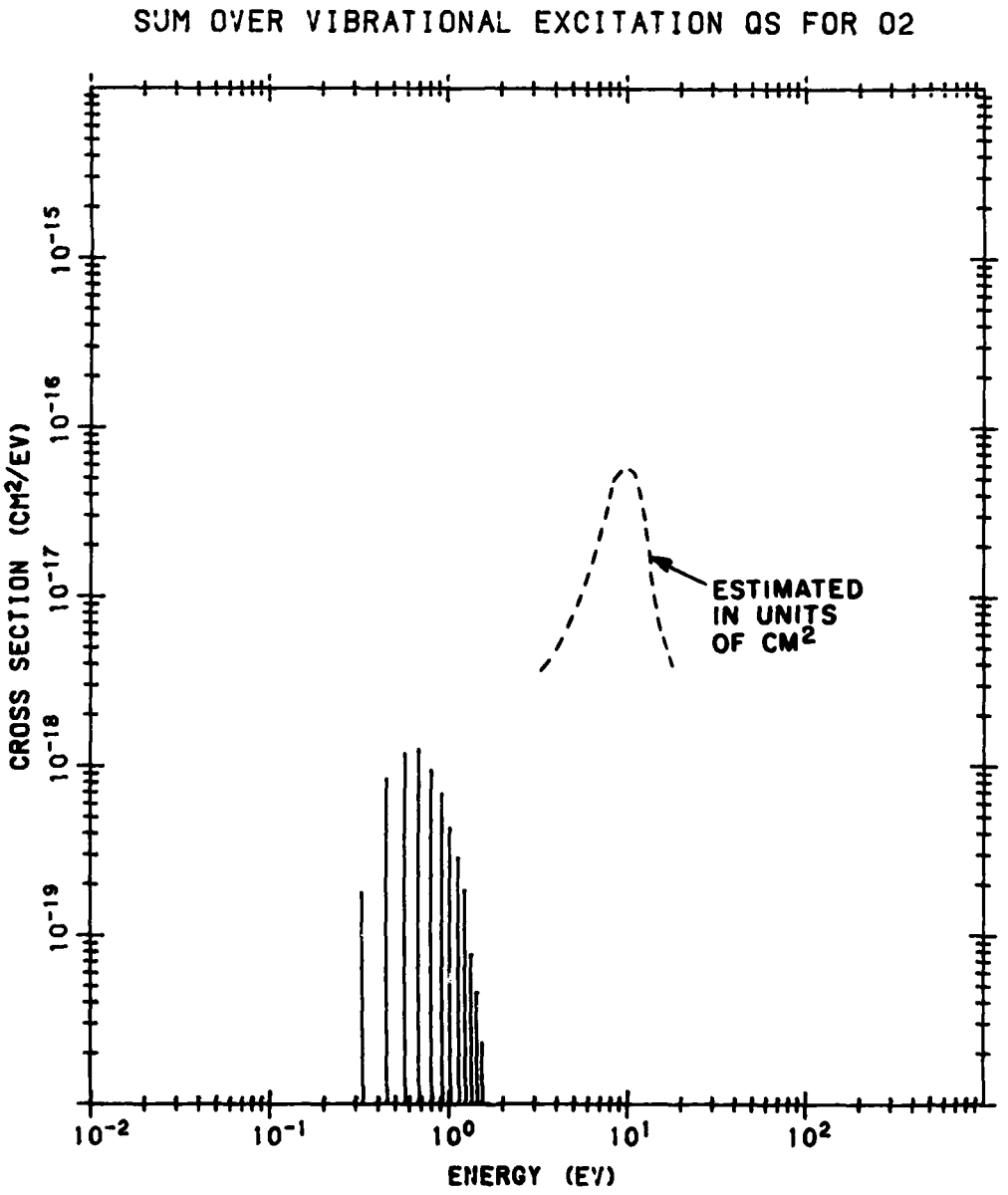


**Figure B8. Sum of $O_2$ Vibrational Excitation Cross Sections**

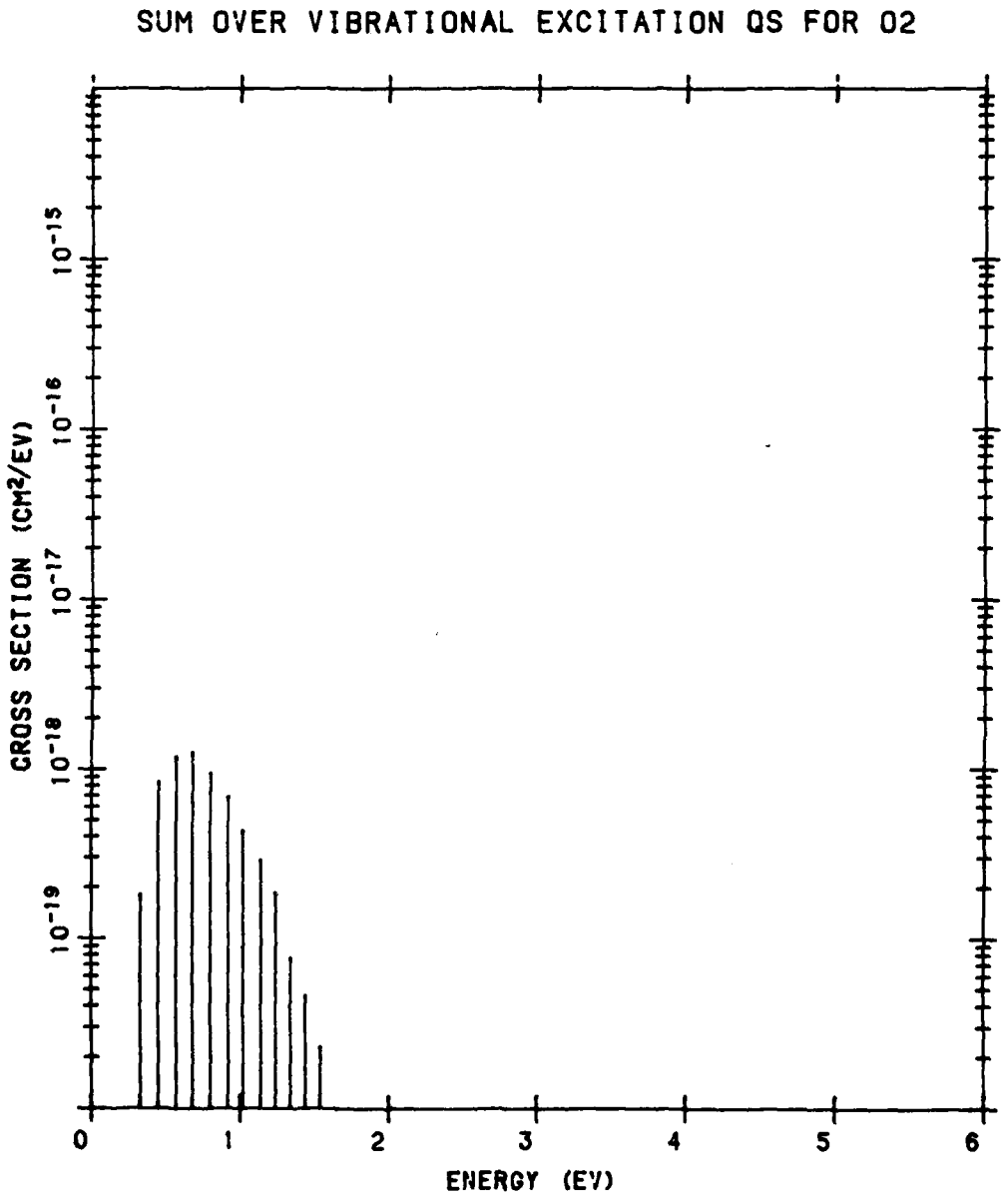


**Figure B8. Sum of $O_2$ Vibrational Excitation Cross Sections (Cont.)**

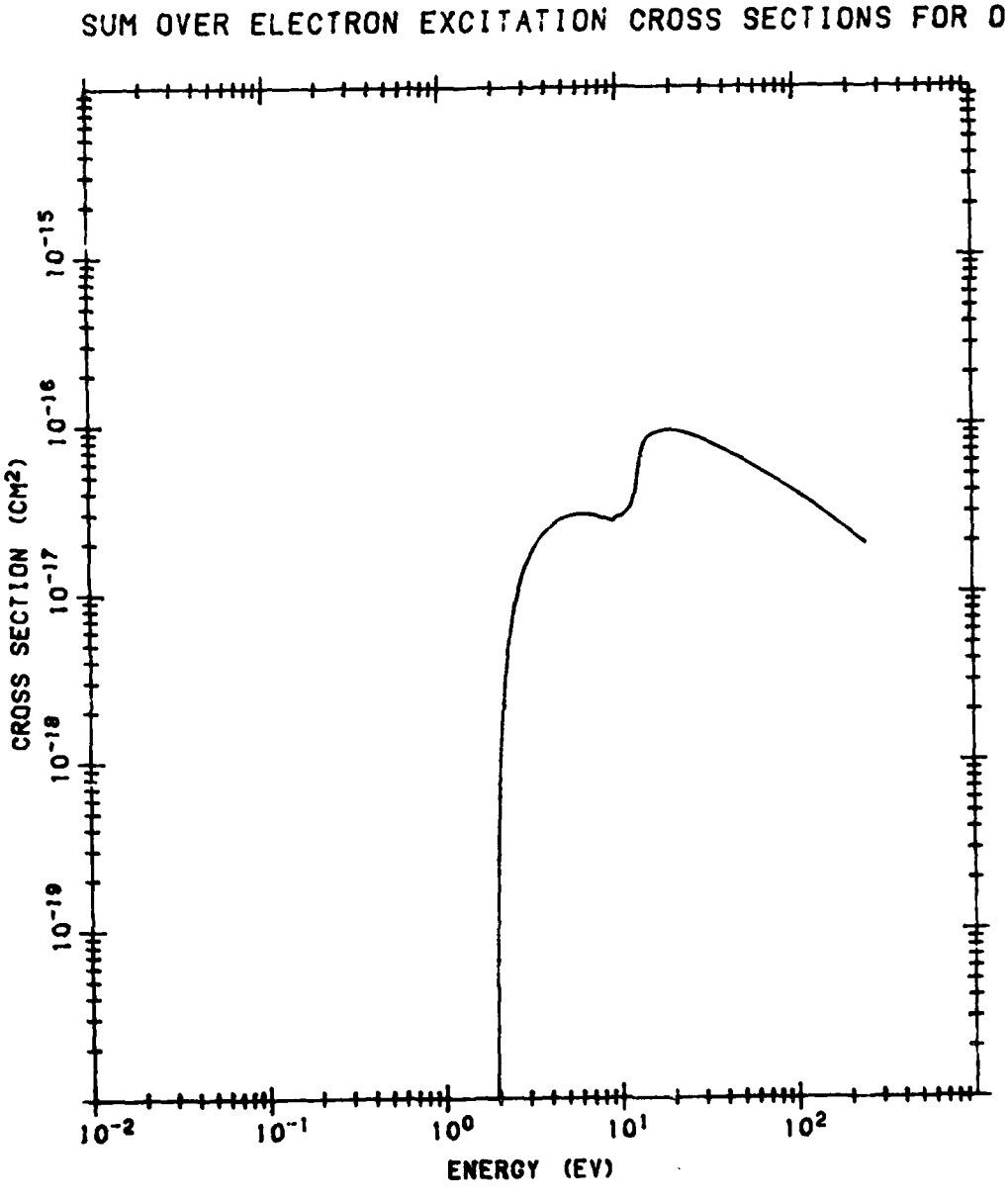


**Figure B9. Sum of O Electron Excitation Cross Sections**

AD-A118 921 BEDFORD RESEARCH ASSOCIATES MA F/G 4/1
LOW ENERGY ELECTRON AND PHOTON CROSS SECTIONS FOR O, N2, AND O2--ETC(U)
JAN 82 H T WADZINSKI, J R JASPERSE F19628-80-C-0216
UNCLASSIFIED AFGL-TR-82-0008 NL

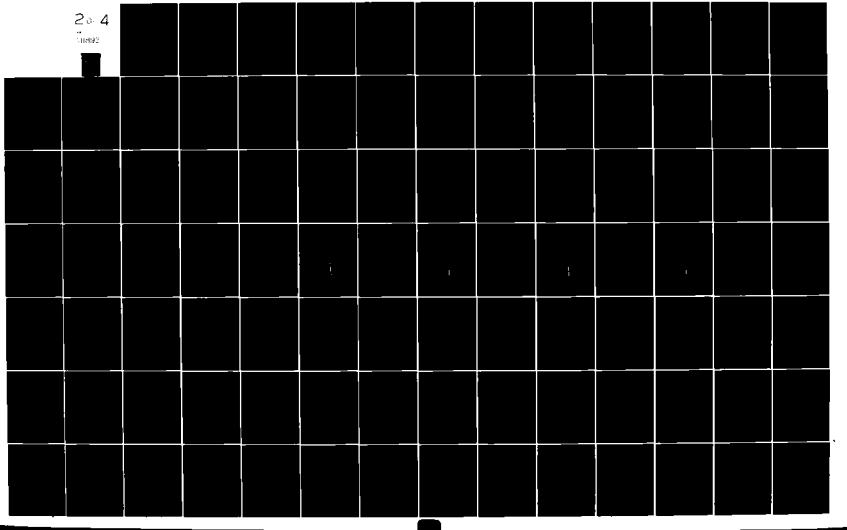

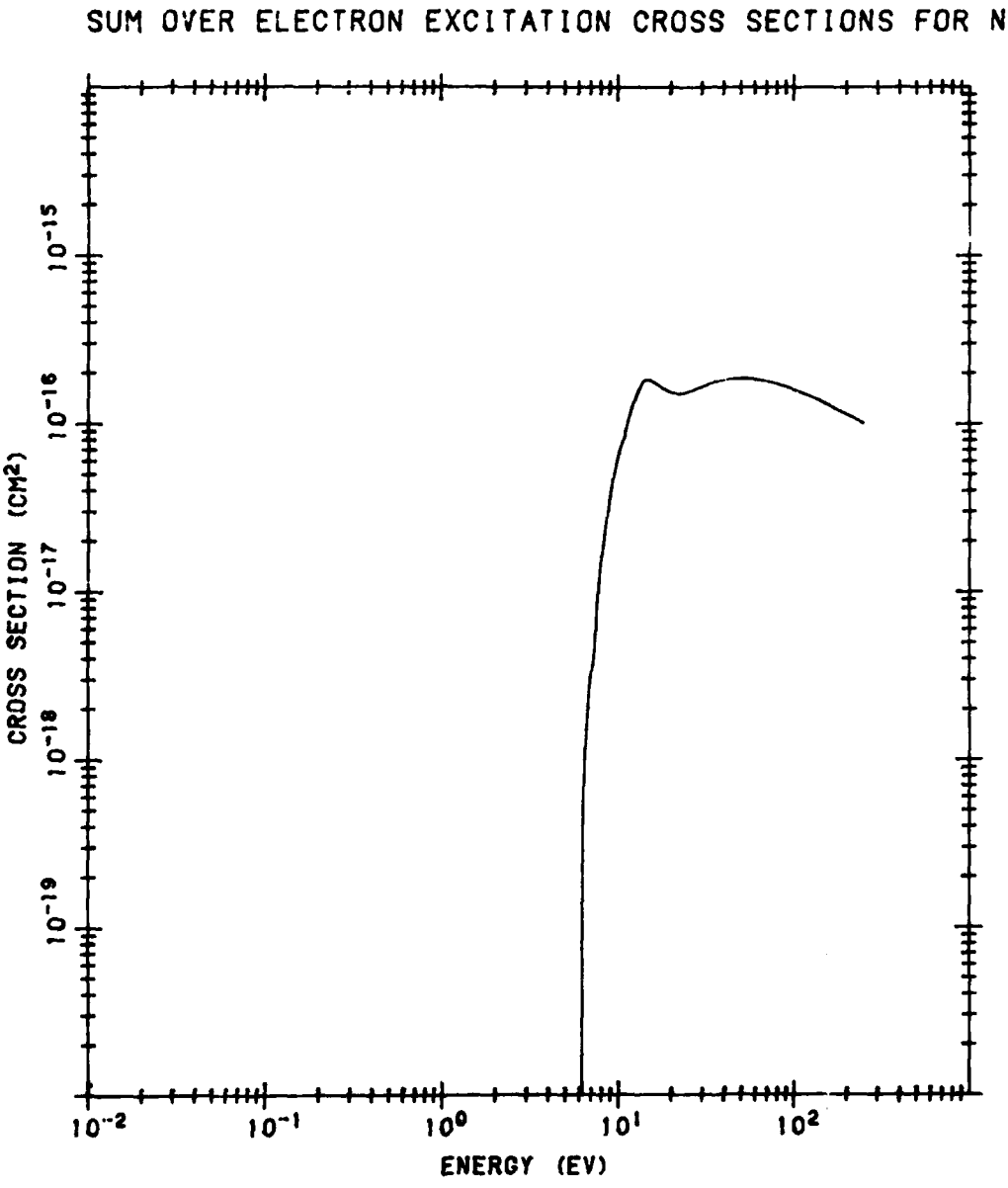


**Figure B10. Sum of $N_2$ Electron Excitation Cross Sections**

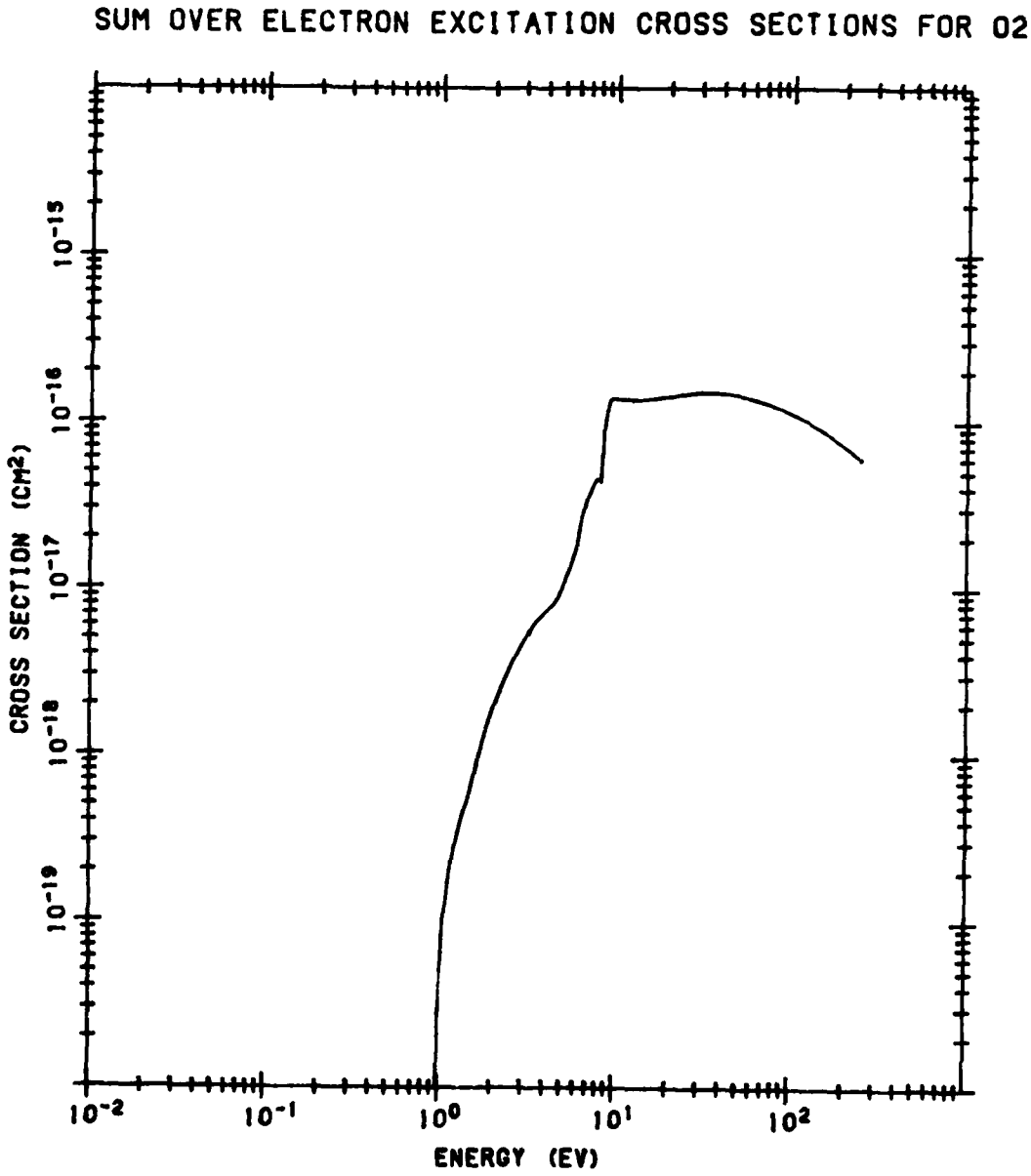


**Figure B11. Sum of $O_2$ Electron Excitation Cross Sections**

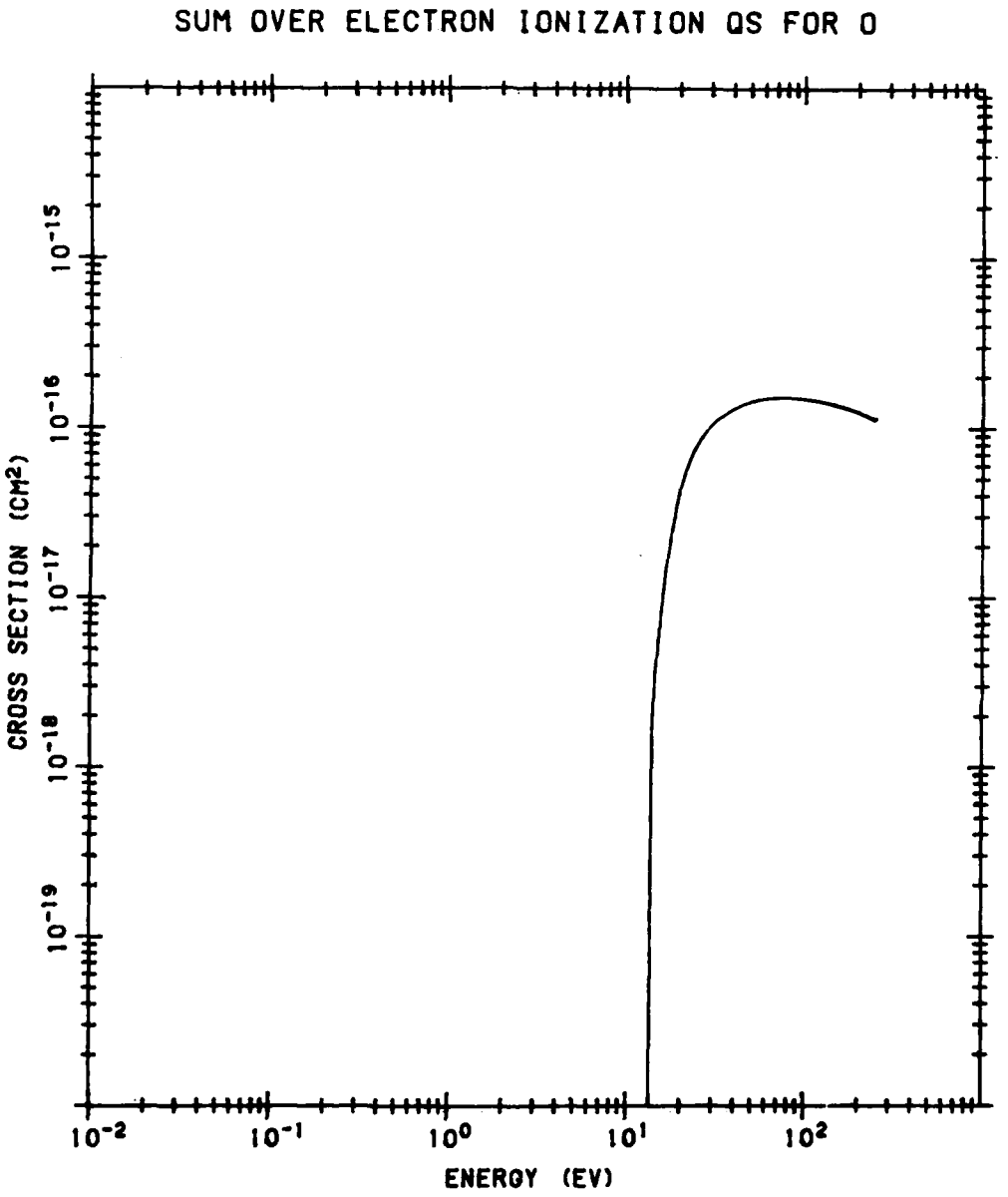


**Figure B12. Sum of O Ionization Cross Sections**

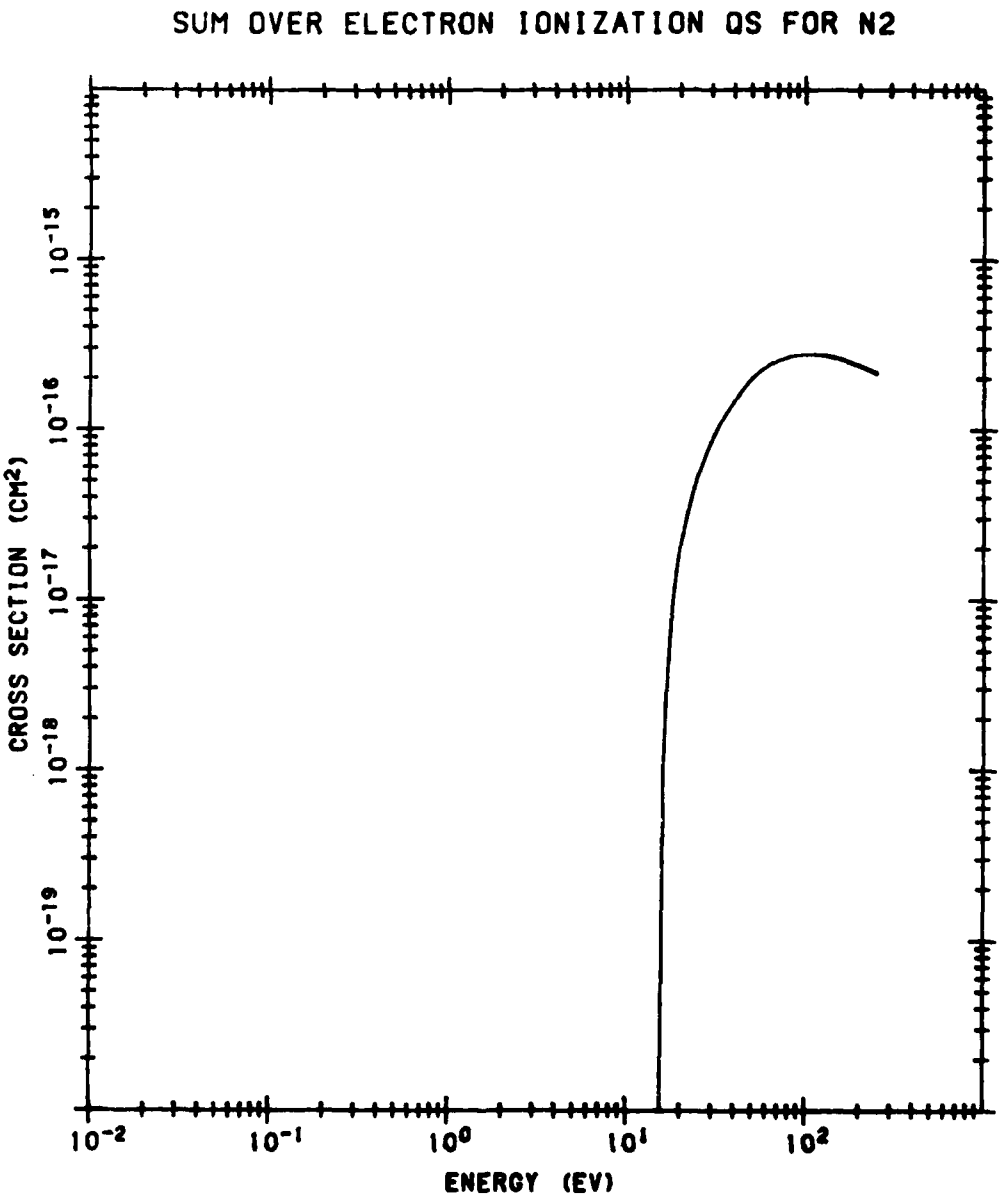


**Figure B13. Sum of $N_2$ Ionization Cross Sections**

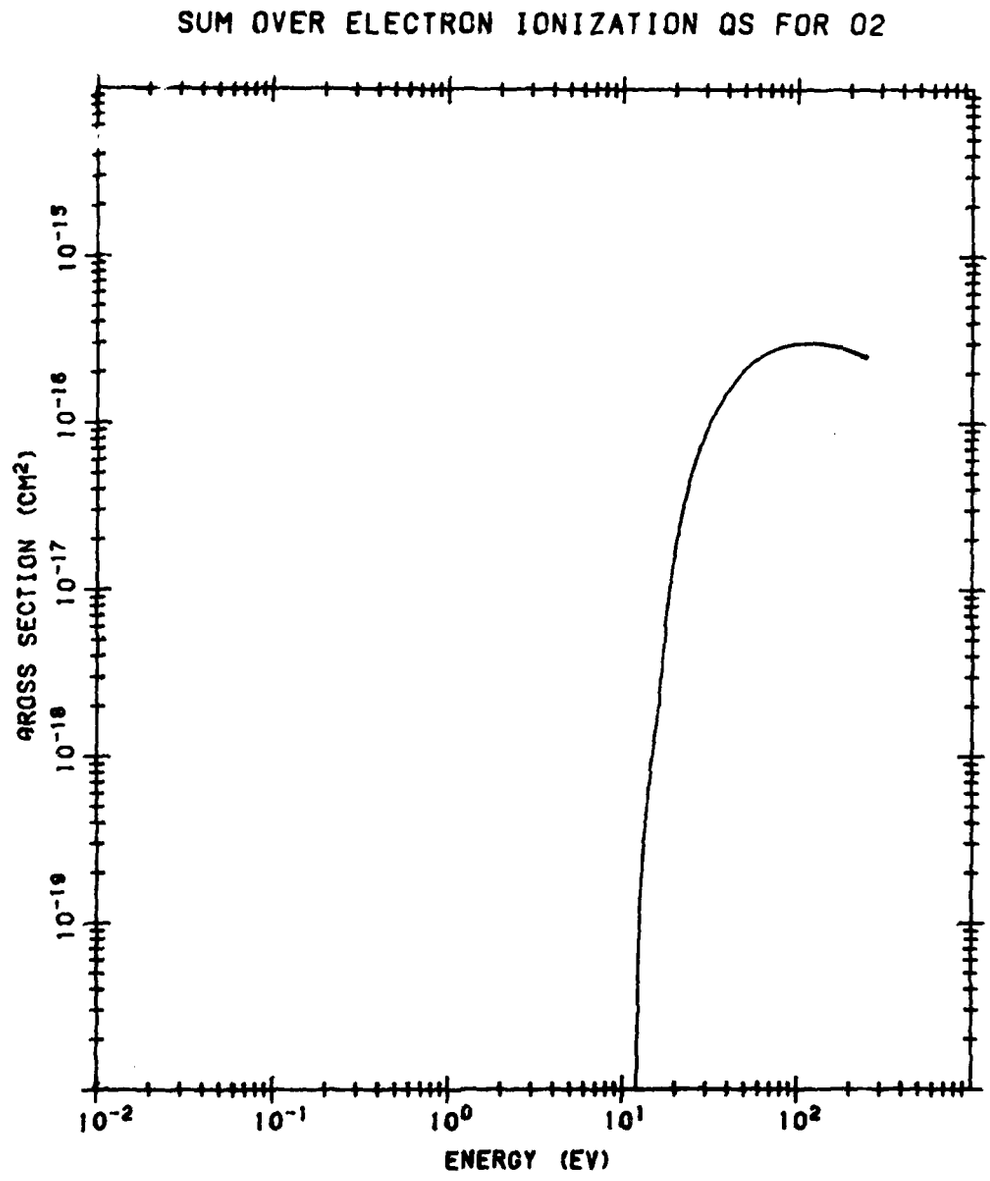


**Figure B14. Sum of $O_2$ Ionization Cross Sections**

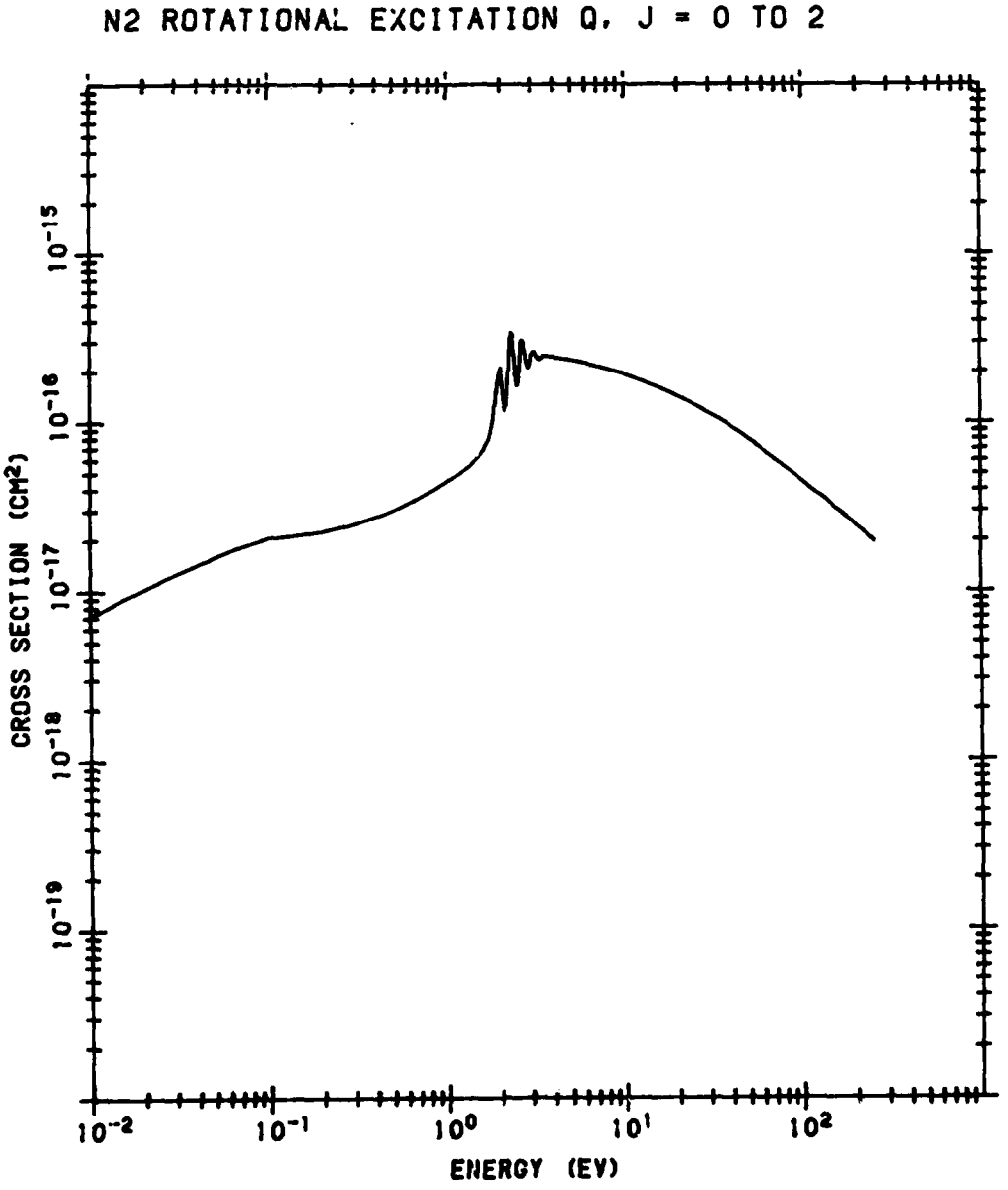


Figure B15. $N_2$ Rotational Excitation Cross Section from J of 0 to 2. The data are from Chandra and Temkin (1976)[B8] below 3.8 eV. Higher energies are extrapolated as 1/E

B8. Chandra, N., and Temkin, A. (1976) Phys. Rev. A13:188.

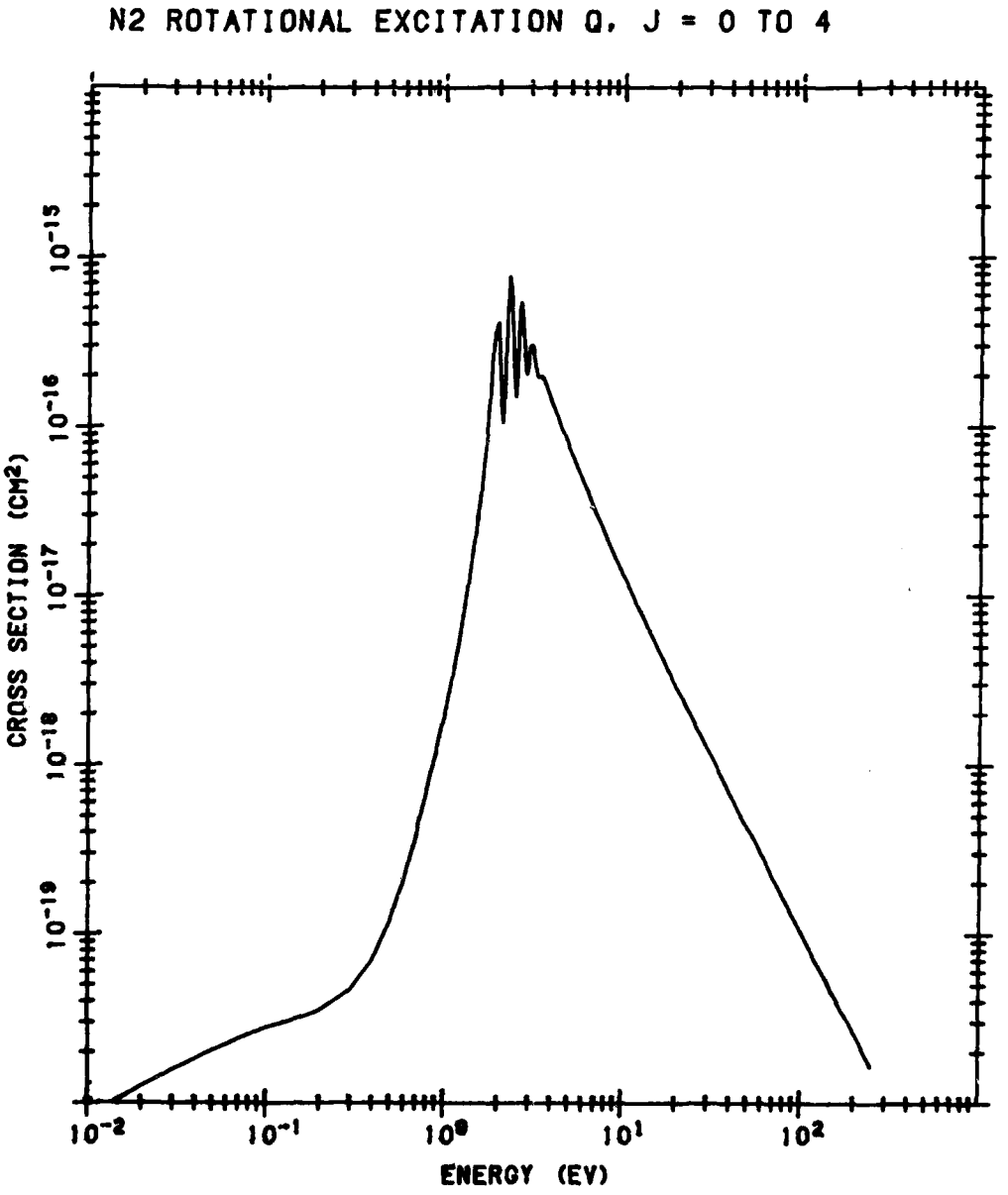


**Figure B16. $N_2$ Rotational Excitation Cross Section from J of 0 to 4. The data are from Chandra and Temkin (1976)[B8] below 3.8 eV. Higher energies are extrapolated as $1/E^2$**

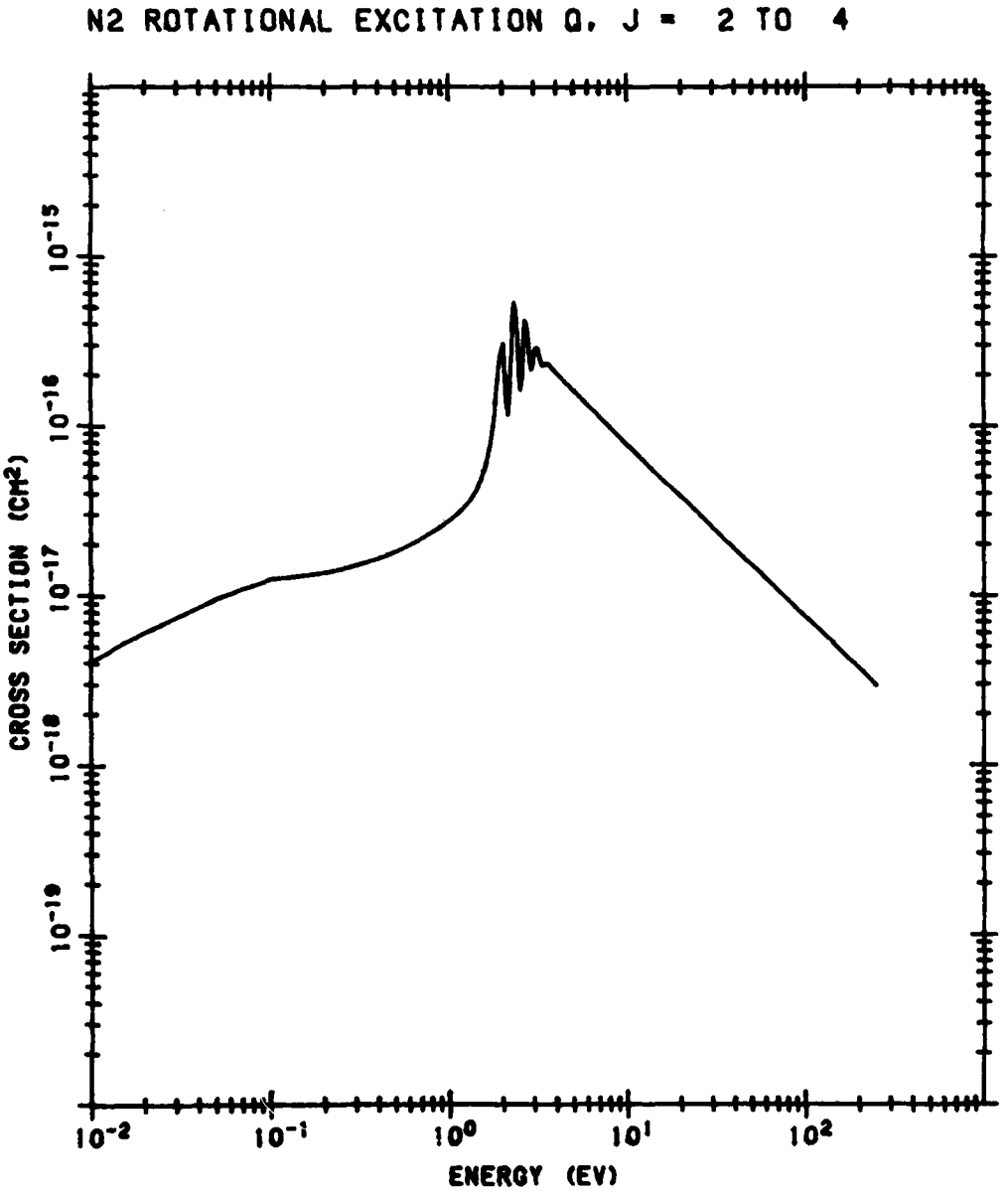


**Figure B17.** $N_2$ Rotational Excitation Cross Section from J of 1 to 3. The source of the data is the same as that of Figure B15

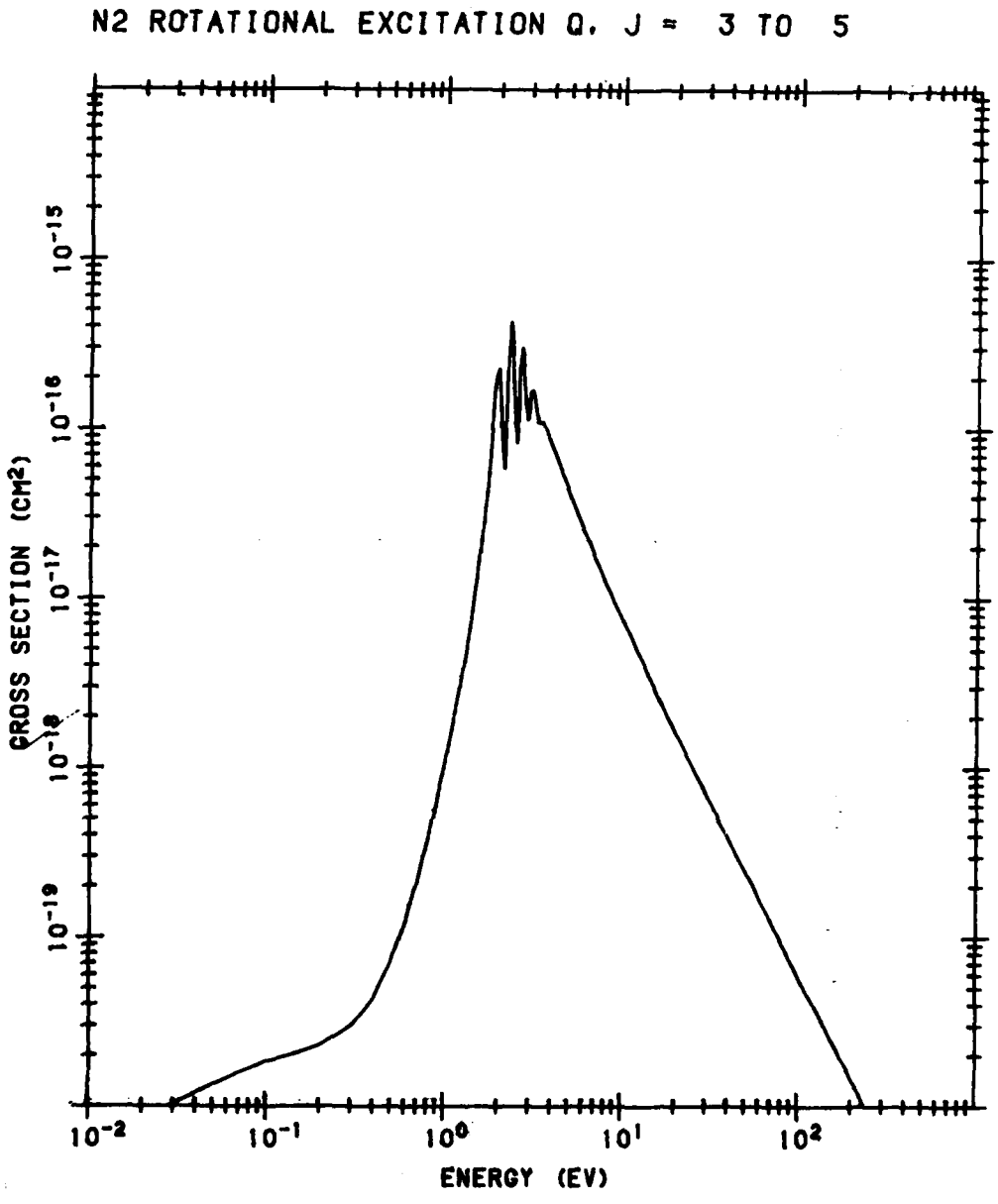


Figure B18. $N_2$ Rotational Excitation Cross Section from J of 1 to 5. The source of the data is the same as that of Figure B16

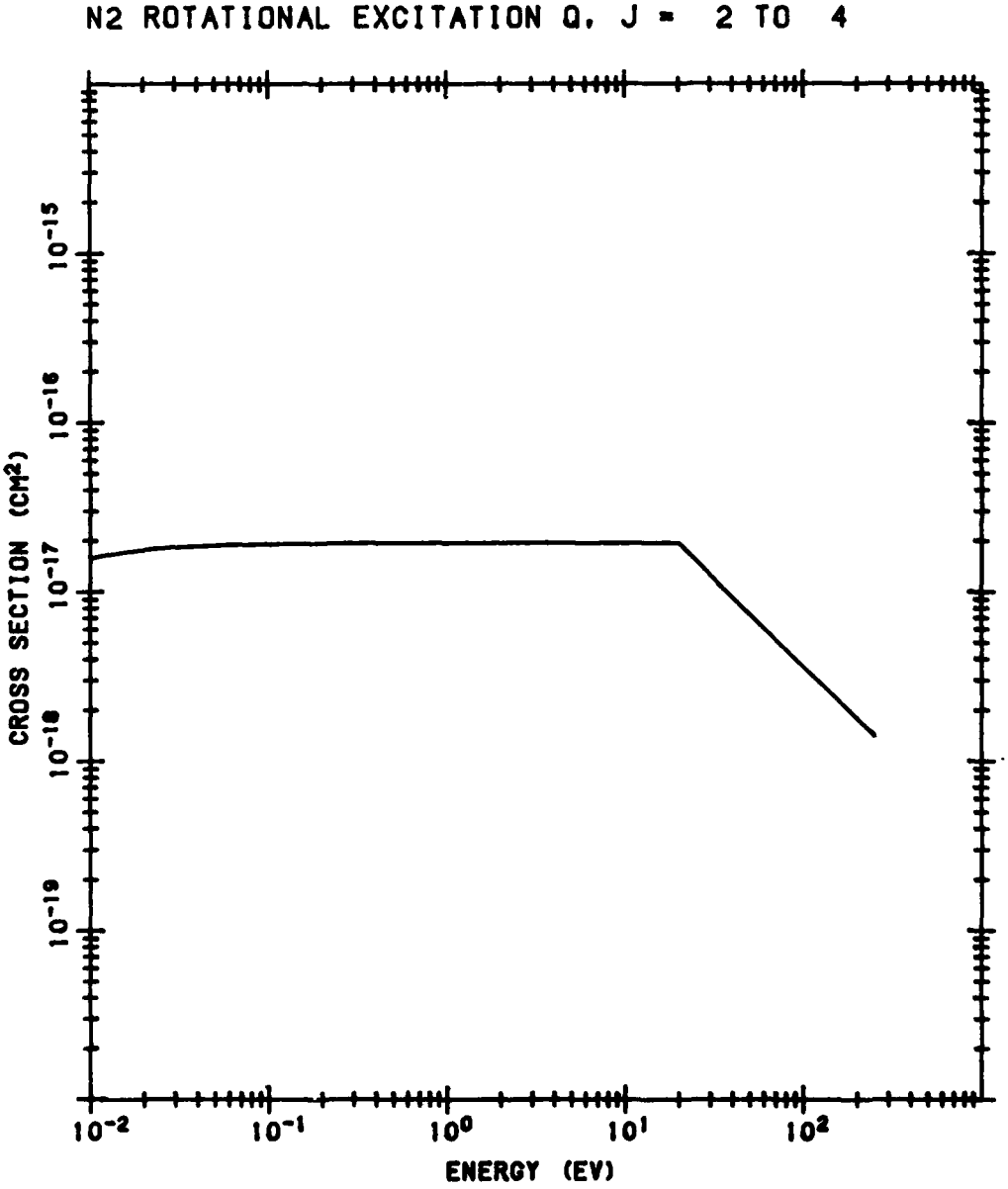


Figure B19. $N_2$ Rotational Excitation Cross Section from J of 2 to 4. The data are from the formula of Gerjuoy and Stein (1955)[B9] below 20 eV using a quadrupole moment of -1.1 (Lane, 1980 [B10]). The higher energies follow a 1/E extrapolation

B9. Gerjuoy, E., and Stein, S. (1955) Phys. Rev. 97:1671.

B10. Lane, N.F. (1980) Rev. Mod. Phys. 52:29.

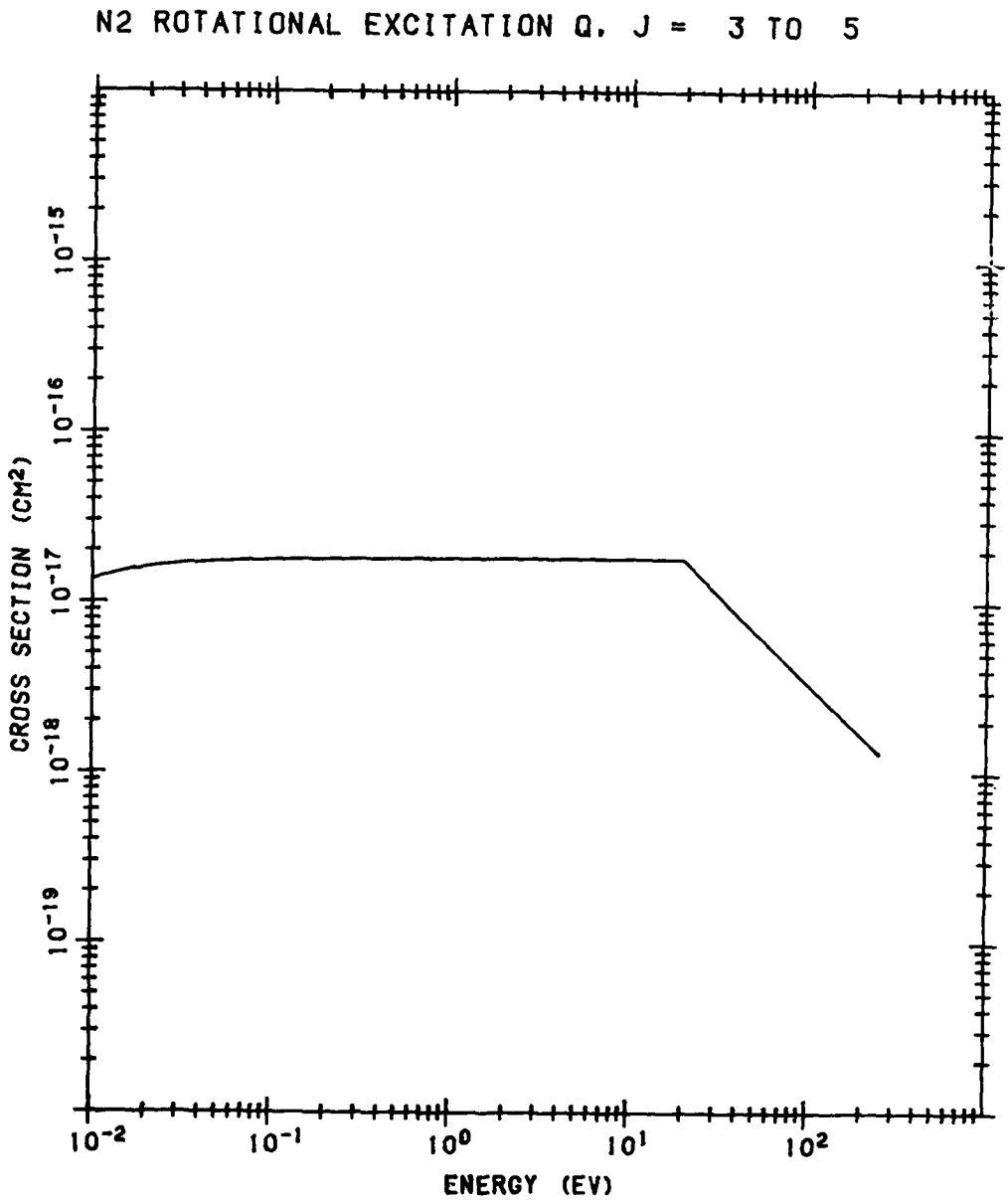


Figure B20. $N_2$ Rotational Excitation Cross Section from J of 3 to 5. The source of the data is the same as that of Figure B19

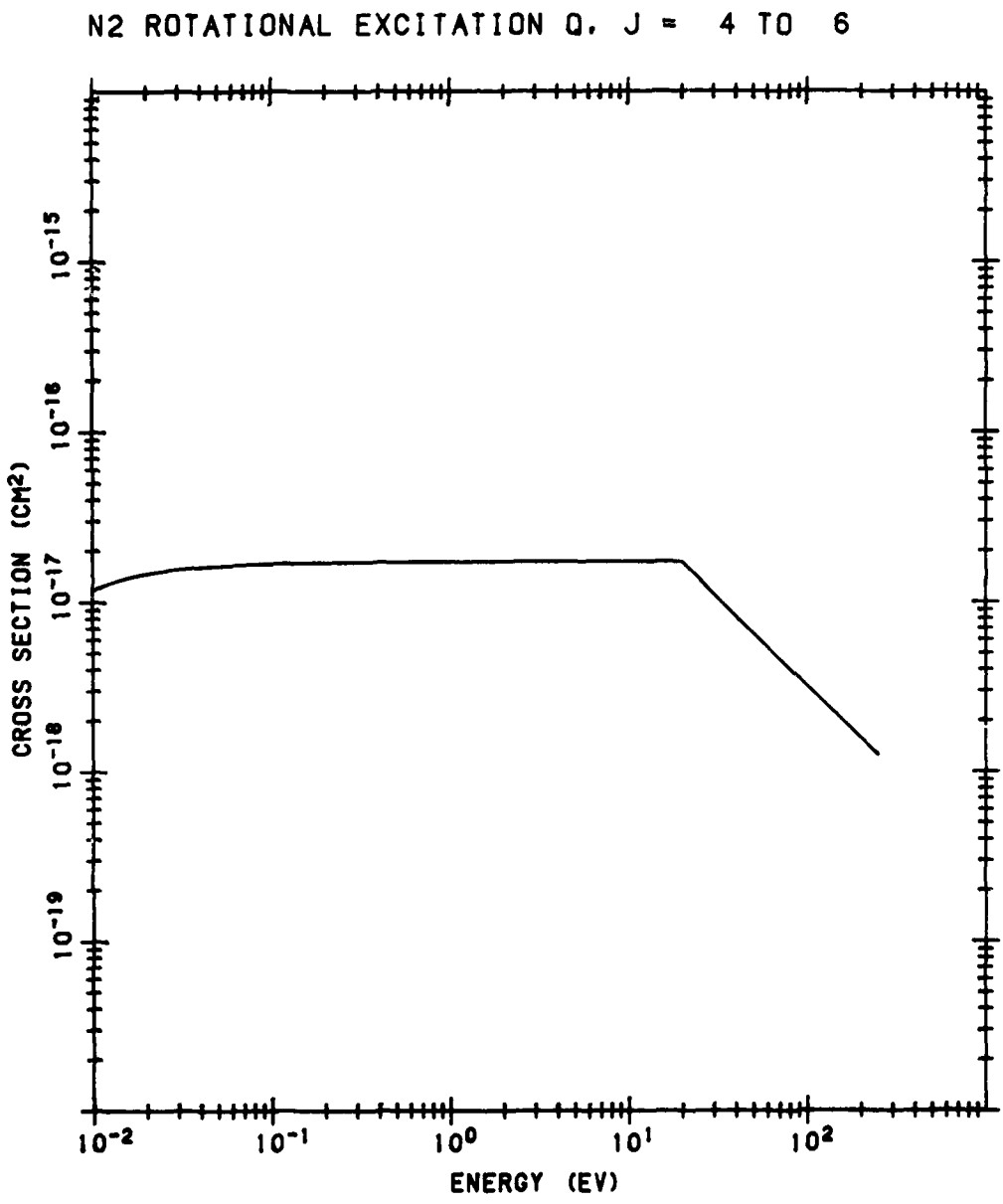


Figure B21. $N_2$ Rotational Excitation Cross Section from J of 4 to 6. The source of the data is the same as that of Figure B19

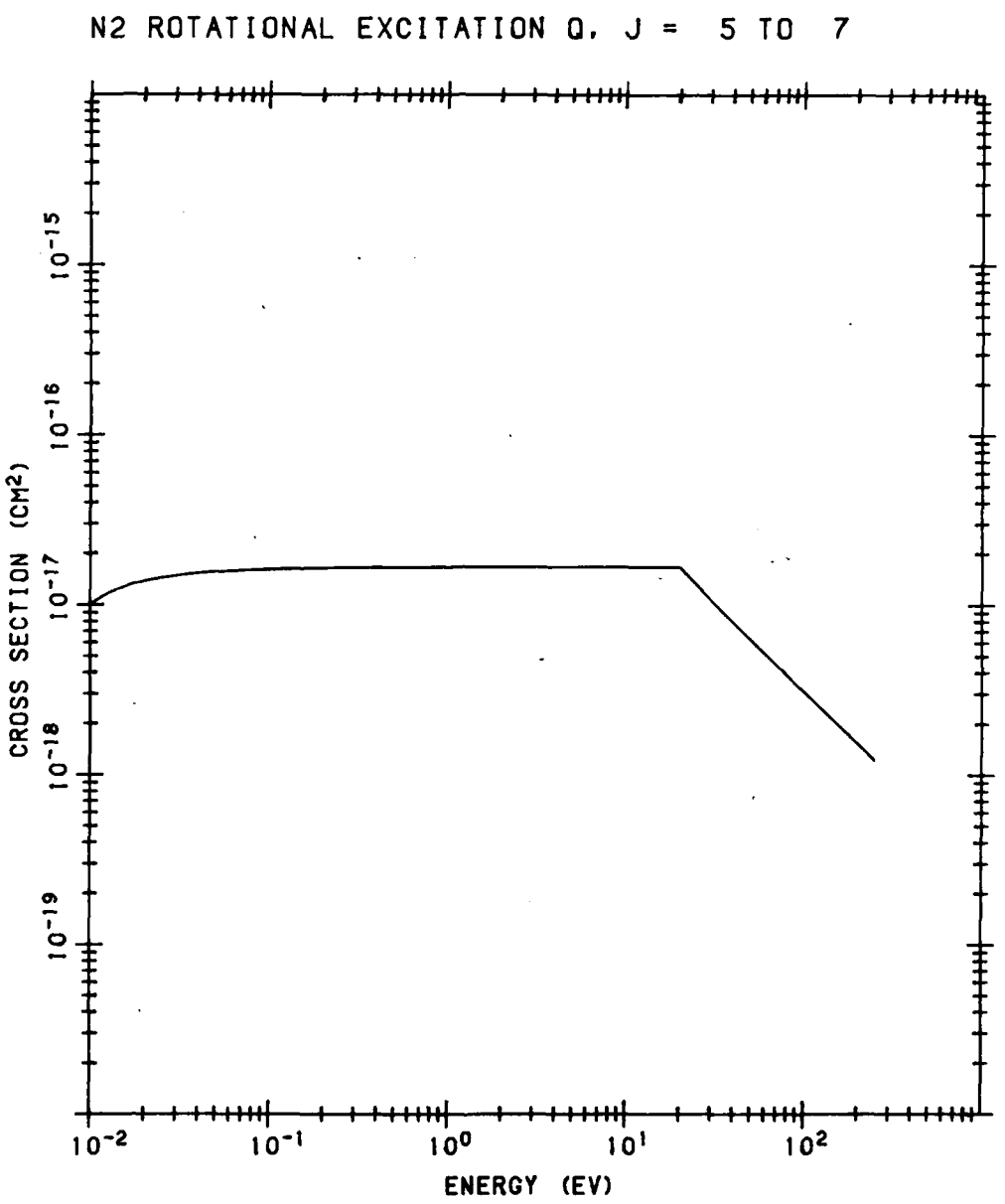


Figure B22. $N_2$ Rotational Excitation Cross Section from J of 5 to 7. The source of the data is the same as that of Figure B19

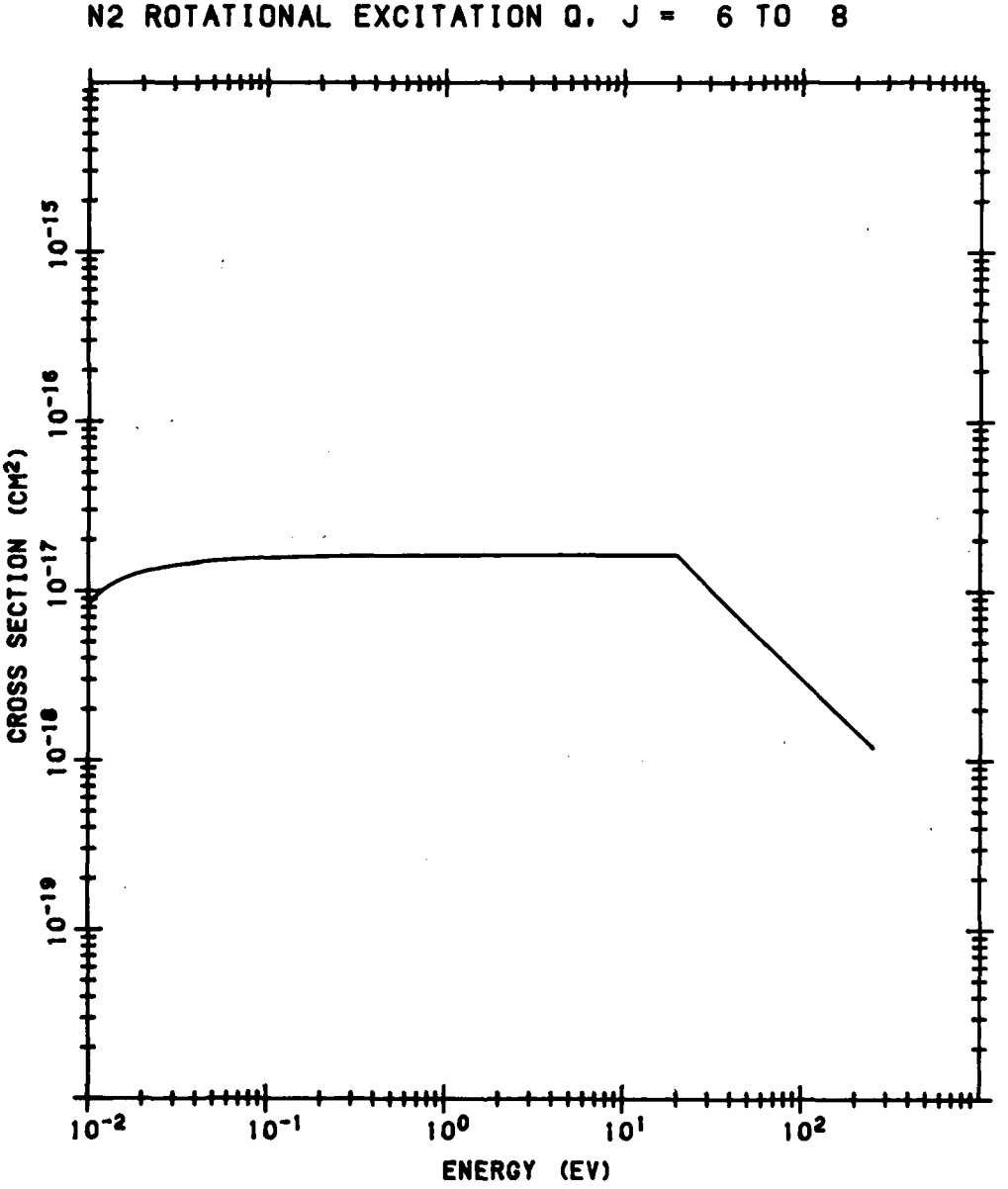


Figure B23. $N_2$ Rotational Excitation Cross Section from J of 6 to 8. The source of the data is the same as that of Figure B19

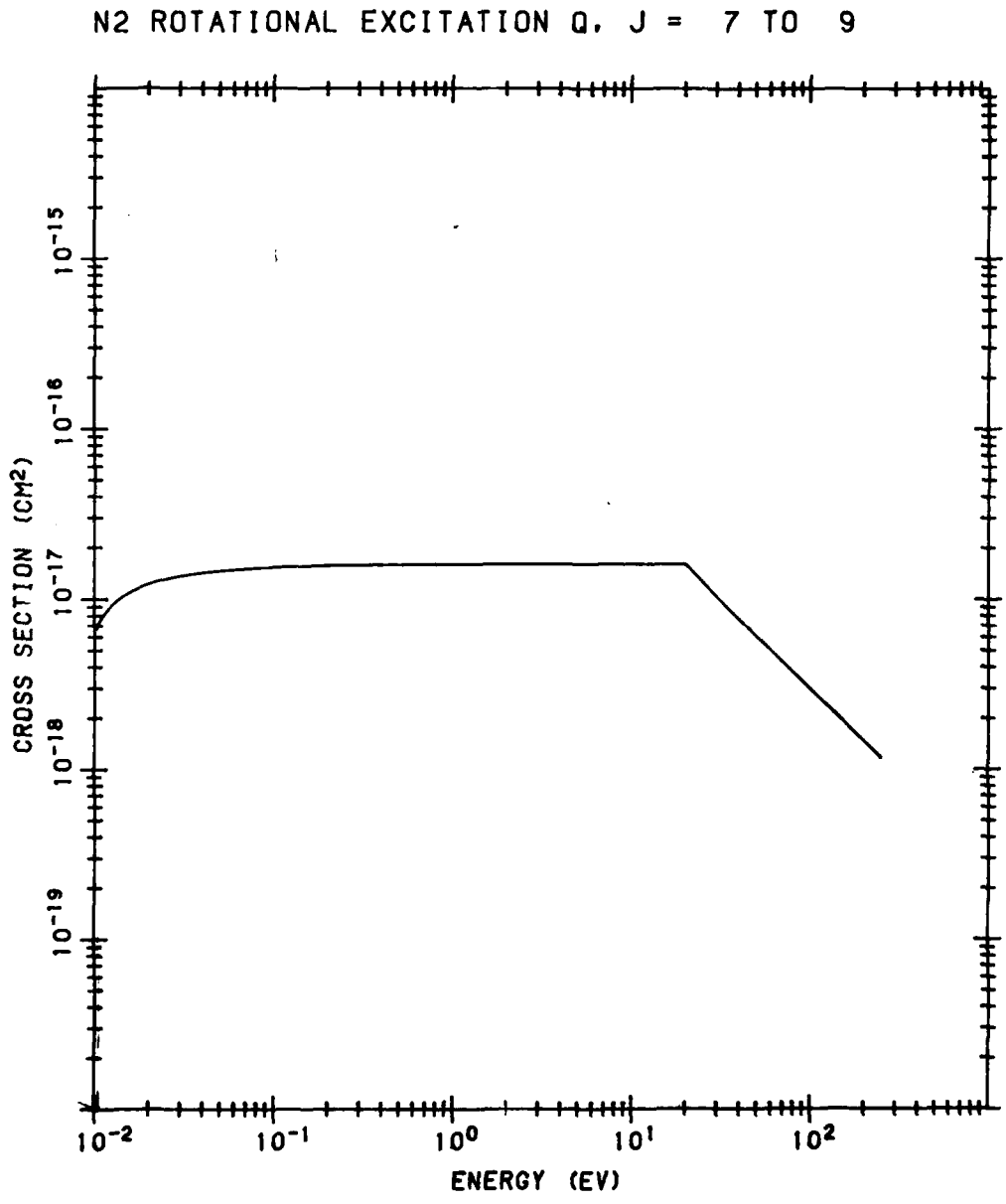


Figure B24. $N_2$ Rotational Excitation Cross Section from J of 7 to 9. The source of the data is the same as that of Figure B19

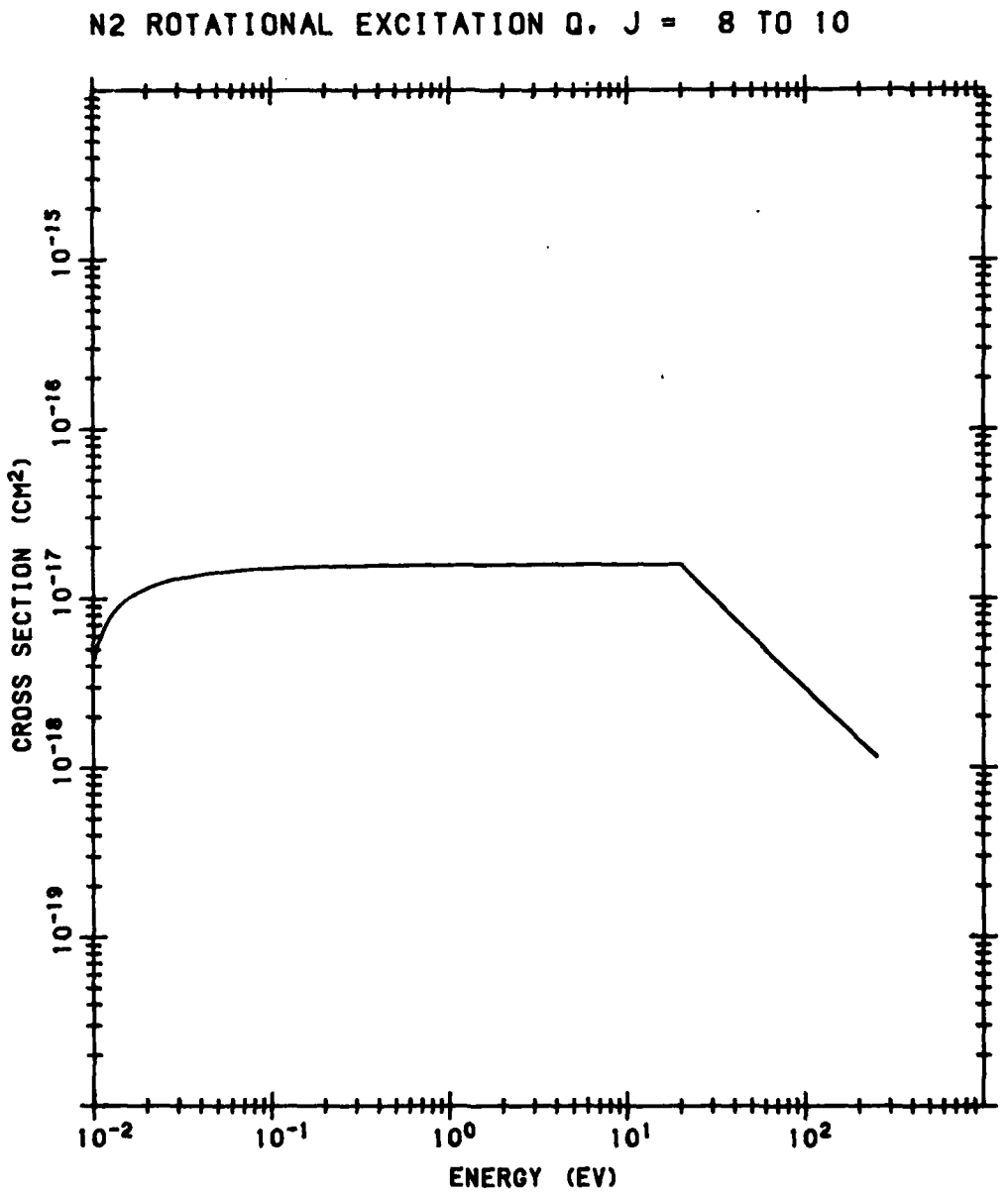


Figure B25. $N_2$ Rotational Excitation Cross Section from J of 9 to 10. The source of the data is the same as that of Figure B19

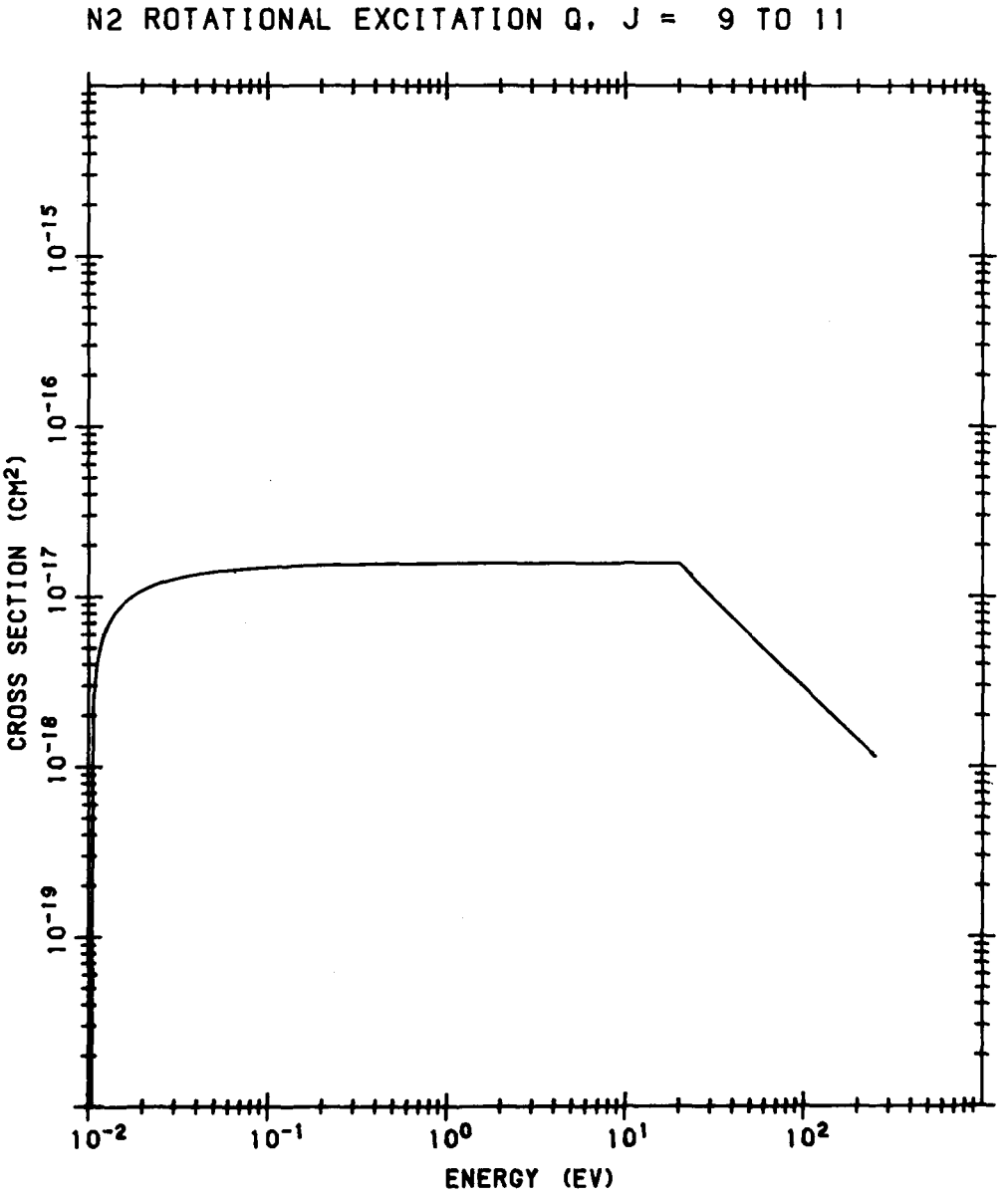


Figure B26. $N_2$ Rotational Excitation Cross Section from J of 10 to 12. The source of the data is the same as that of Figure B19

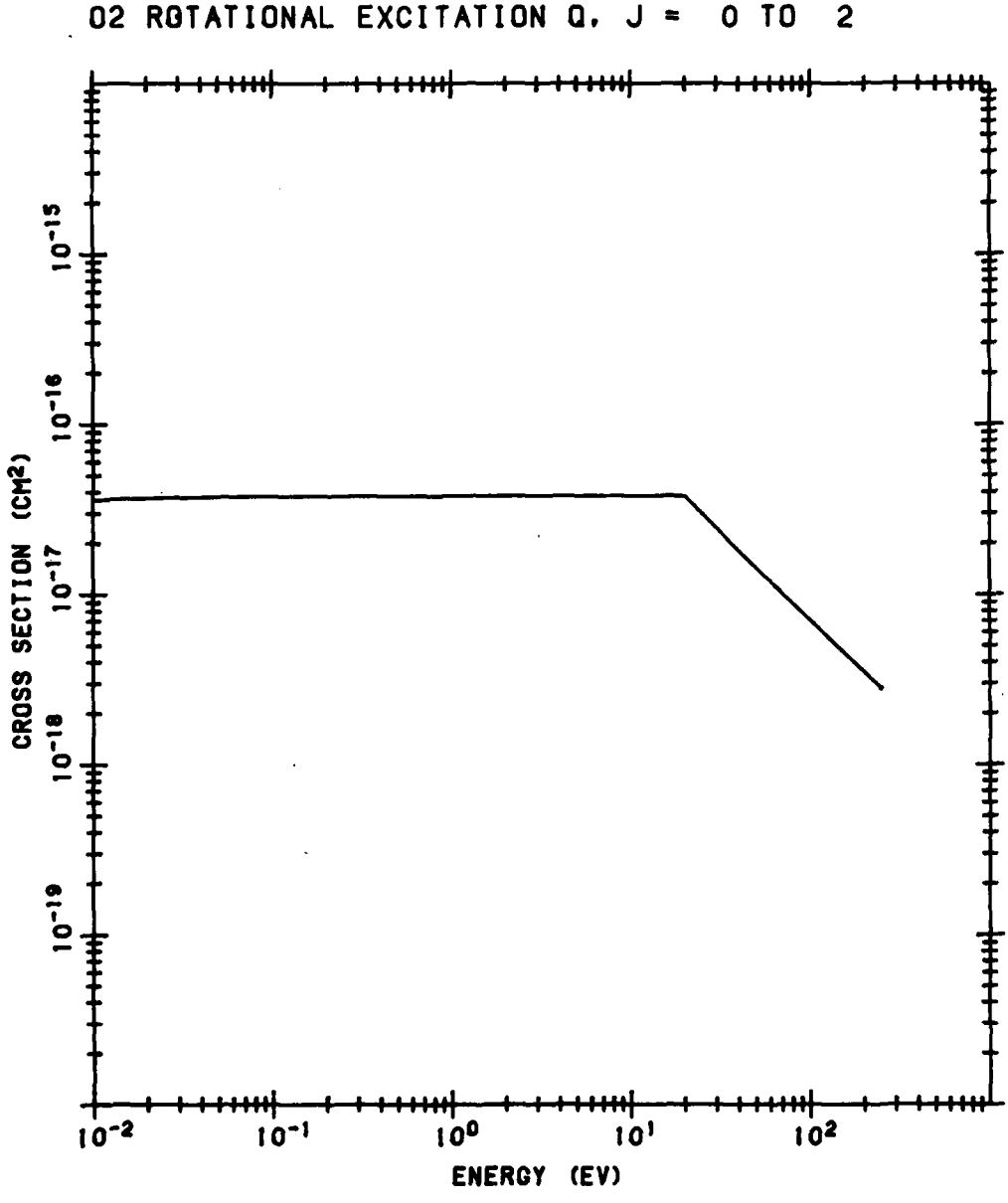


Figure B27. $O_2$ Rotational Excitation Cross Section from J of 0 to 2. The data are from the formula of Gerjuoy and Stein (1955)[B9] below 20 eV using a quadrupole moment of -1.1. The higher energies follow a 1/E extrapolation

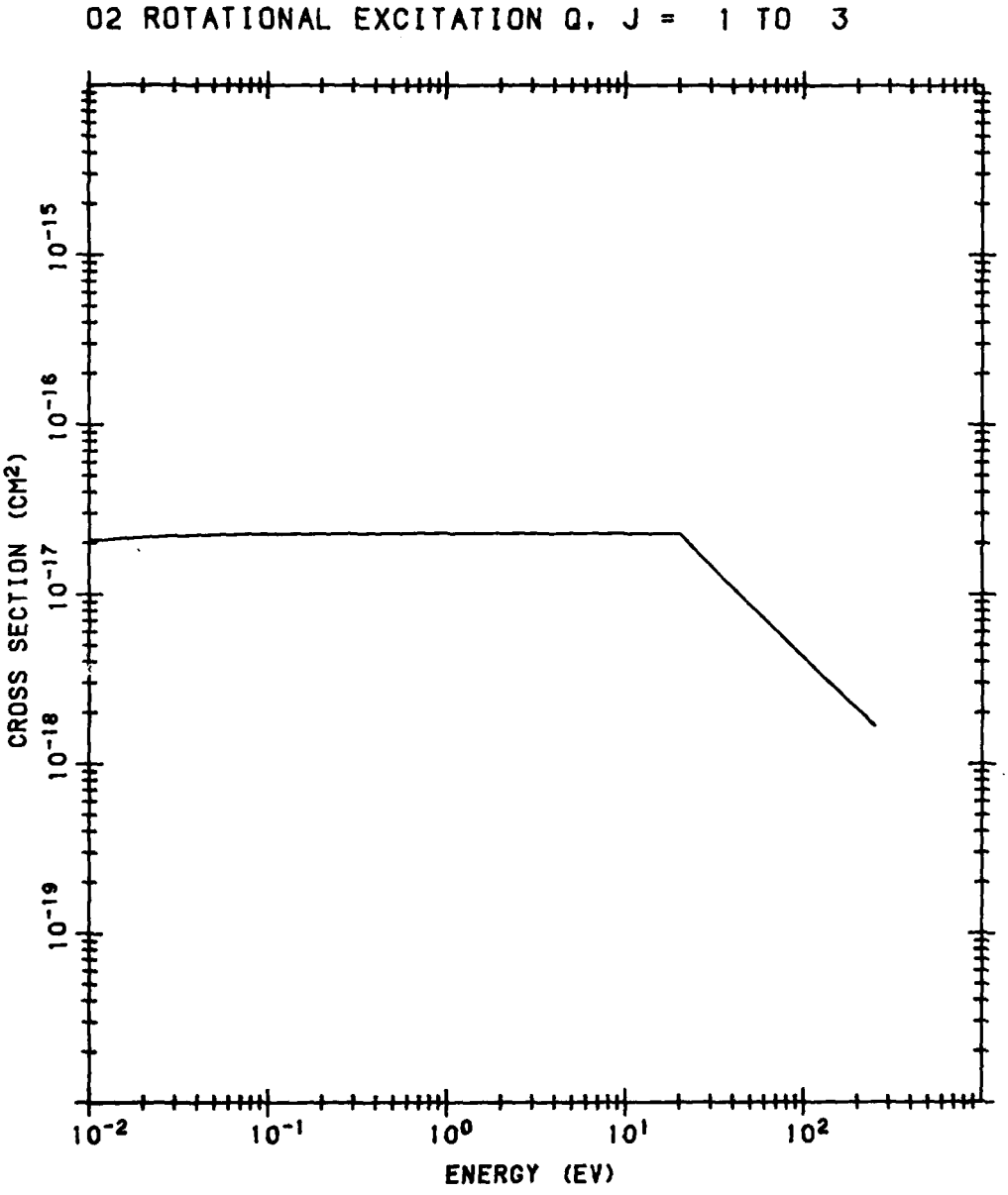


Figure B28. $O_2$ Rotational Excitation Cross Section from J of 1 to 3. The data source is the same as that of Figure B27

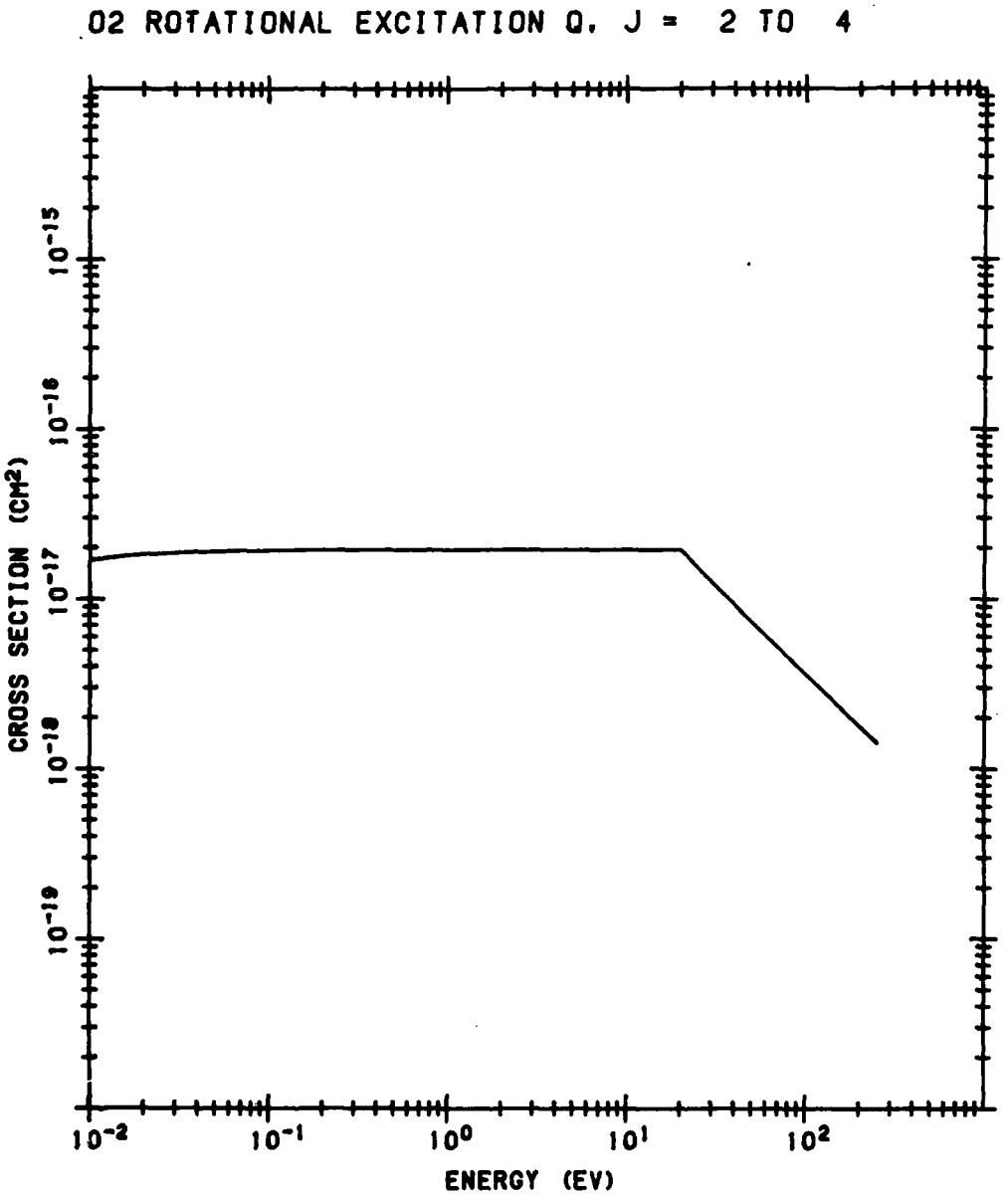


**Figure B29.** $O_2$ **Rotational Excitation Cross Section from J of 2 to 4. The data source is the same as that of Figure B27**

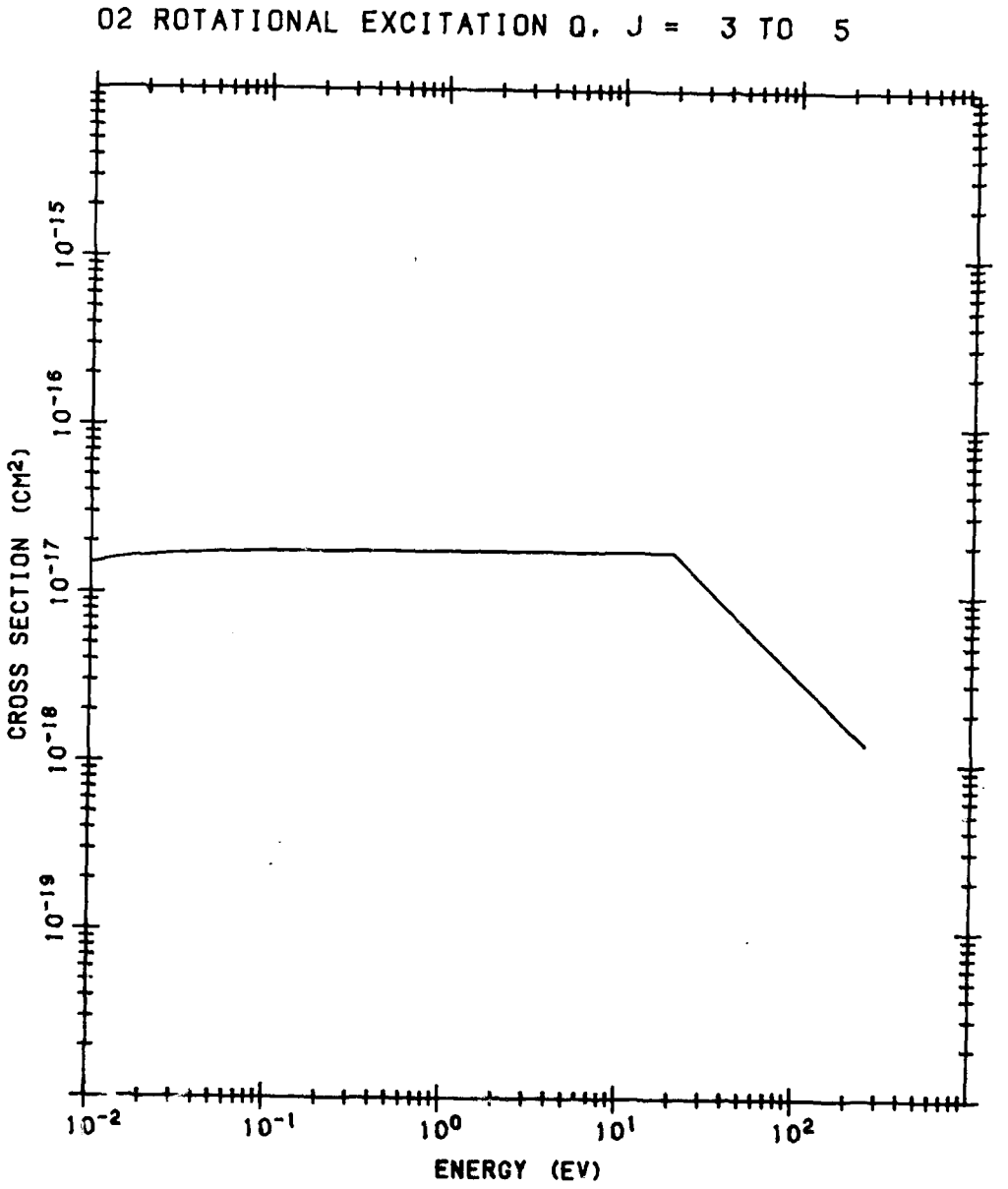


Figure B30. $O_2$ Rotational Excitation Cross Section from J of 3 to 5. The data source is the same as that of Figure B27

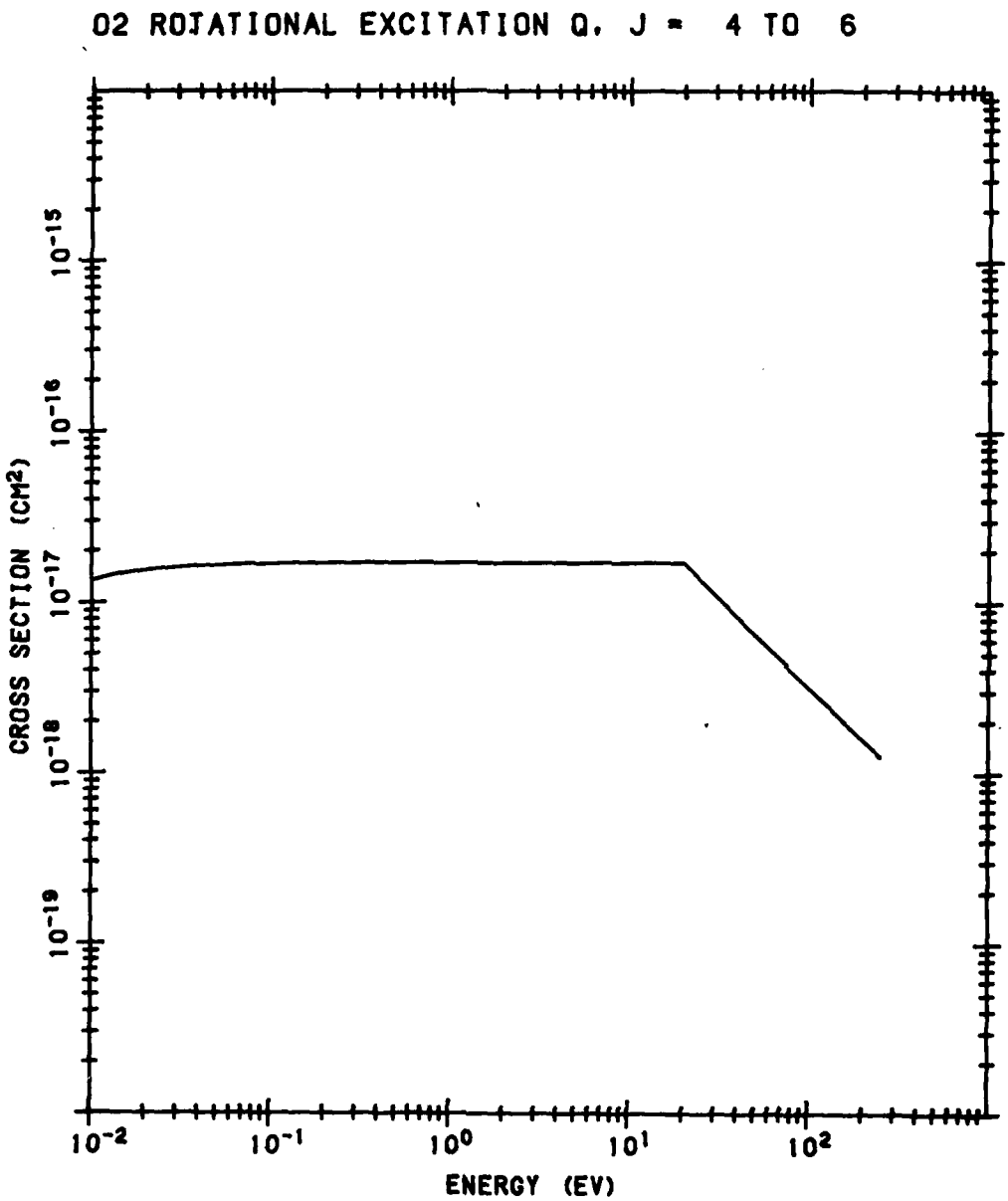


**Figure B31.** $O_2$ **Rotational Excitation Cross Section from J of 4 to 6. The data source is the same as that of Figure B27**

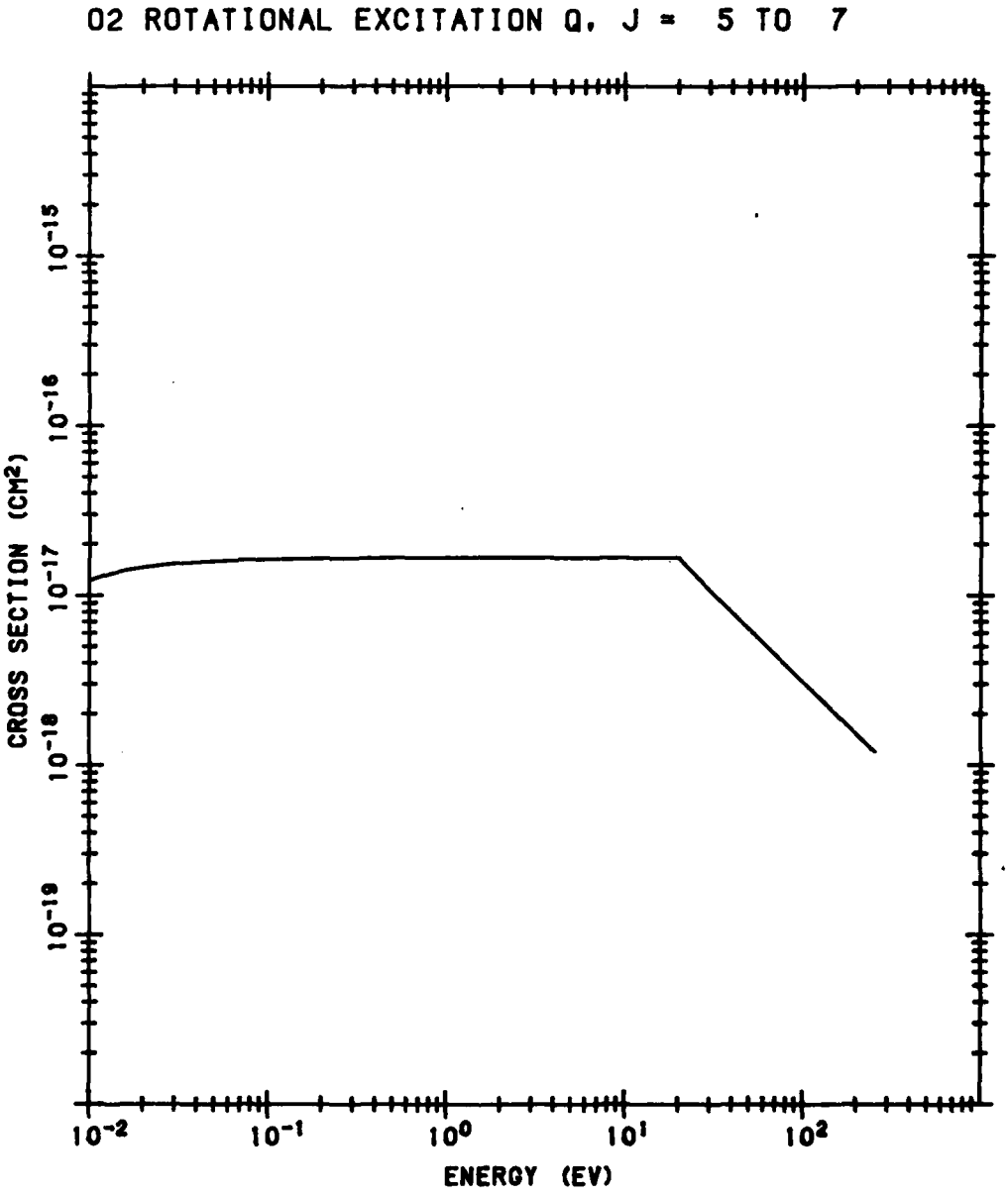


**Figure B32.** $O_2$ **Rotational Excitation Cross Section from J of 5 to 7. The data source is the same as that of Figure B27**

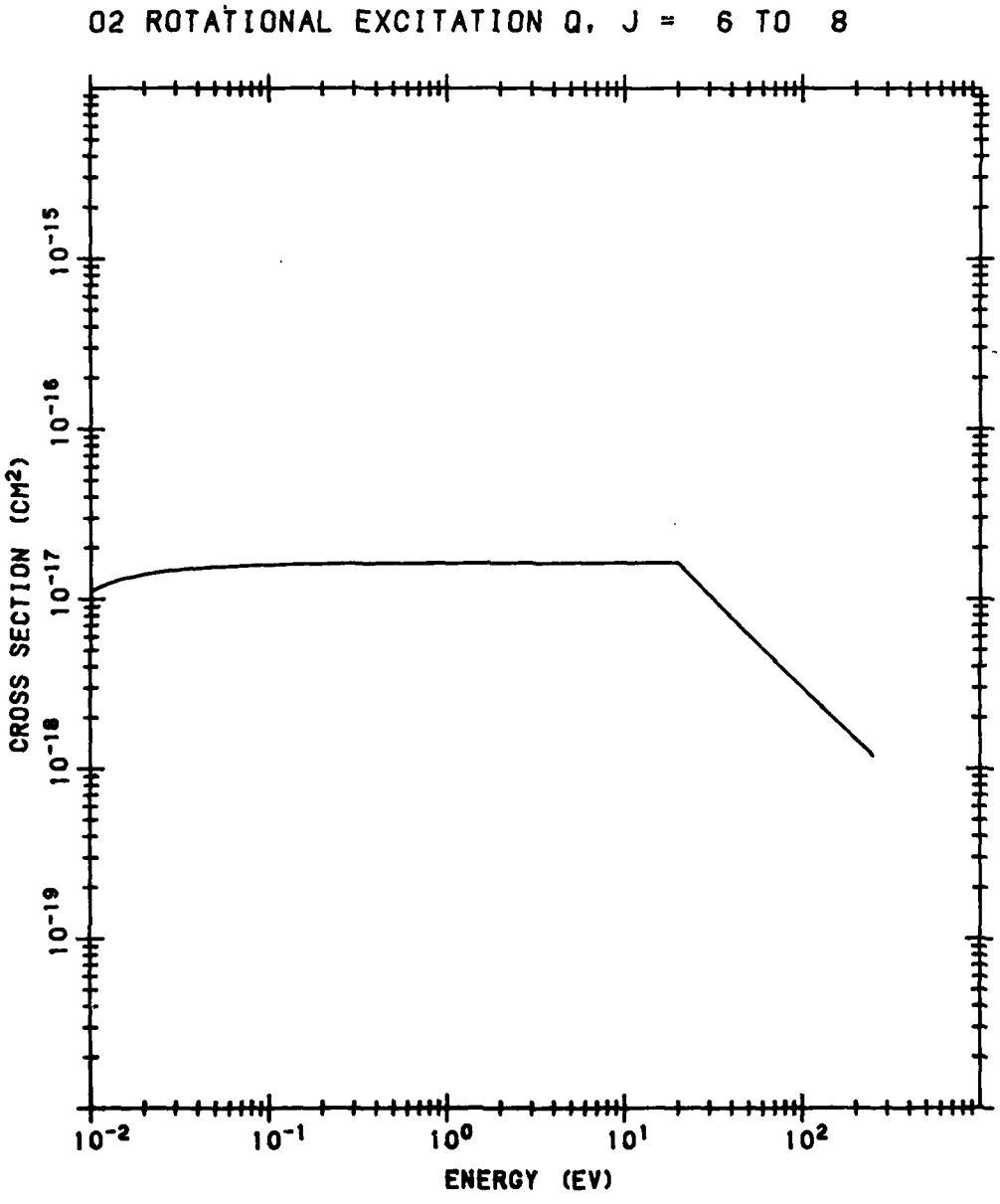


Figure B33. $O_2$ Rotational Excitation Cross Section from J of 6 to 8. The data source is the same as that of Figure B27

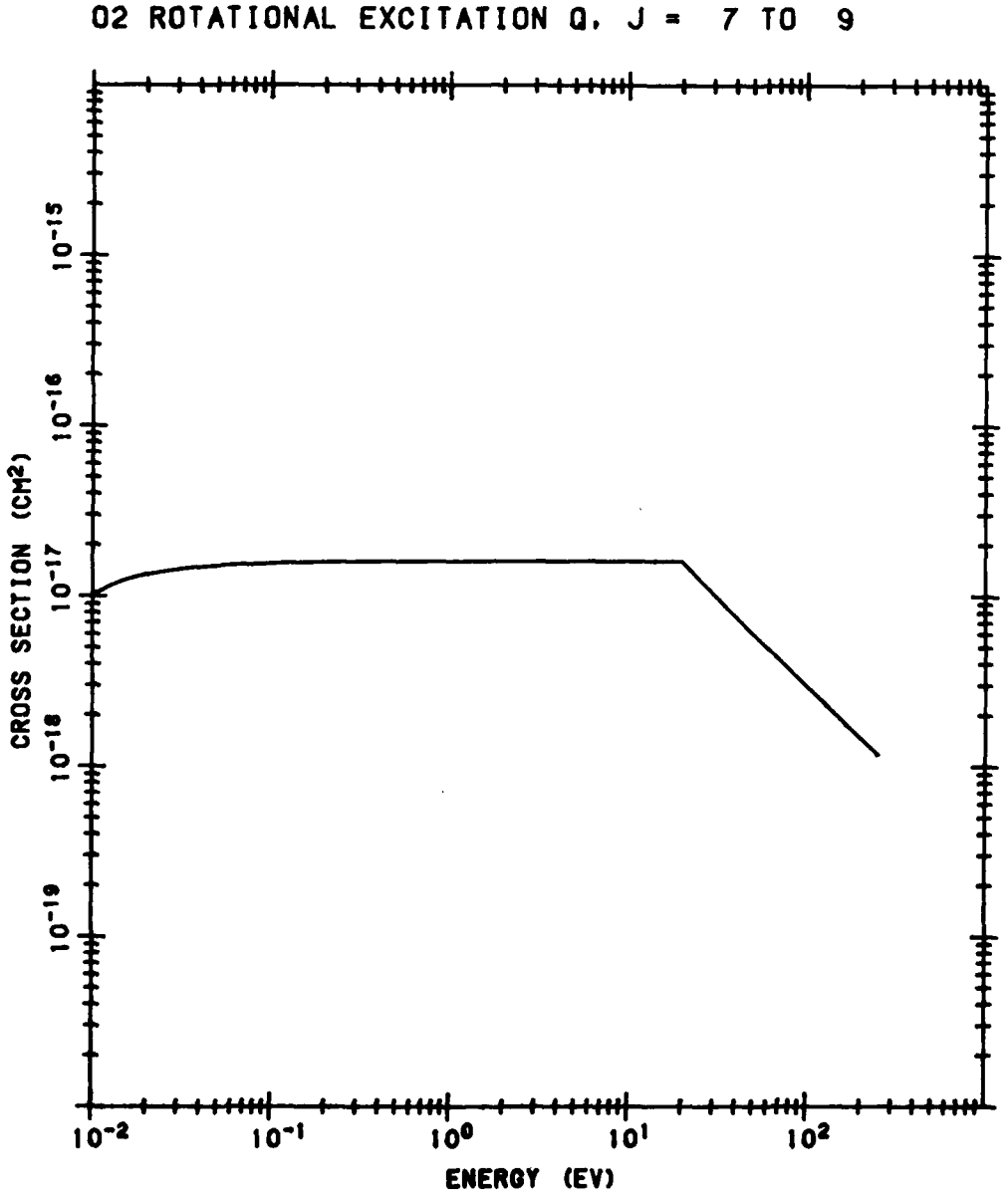


**Figure B34. $O_2$ Rotational Excitation Cross Section from J of 7 to 9. The data source is the same as that of Figure B27**

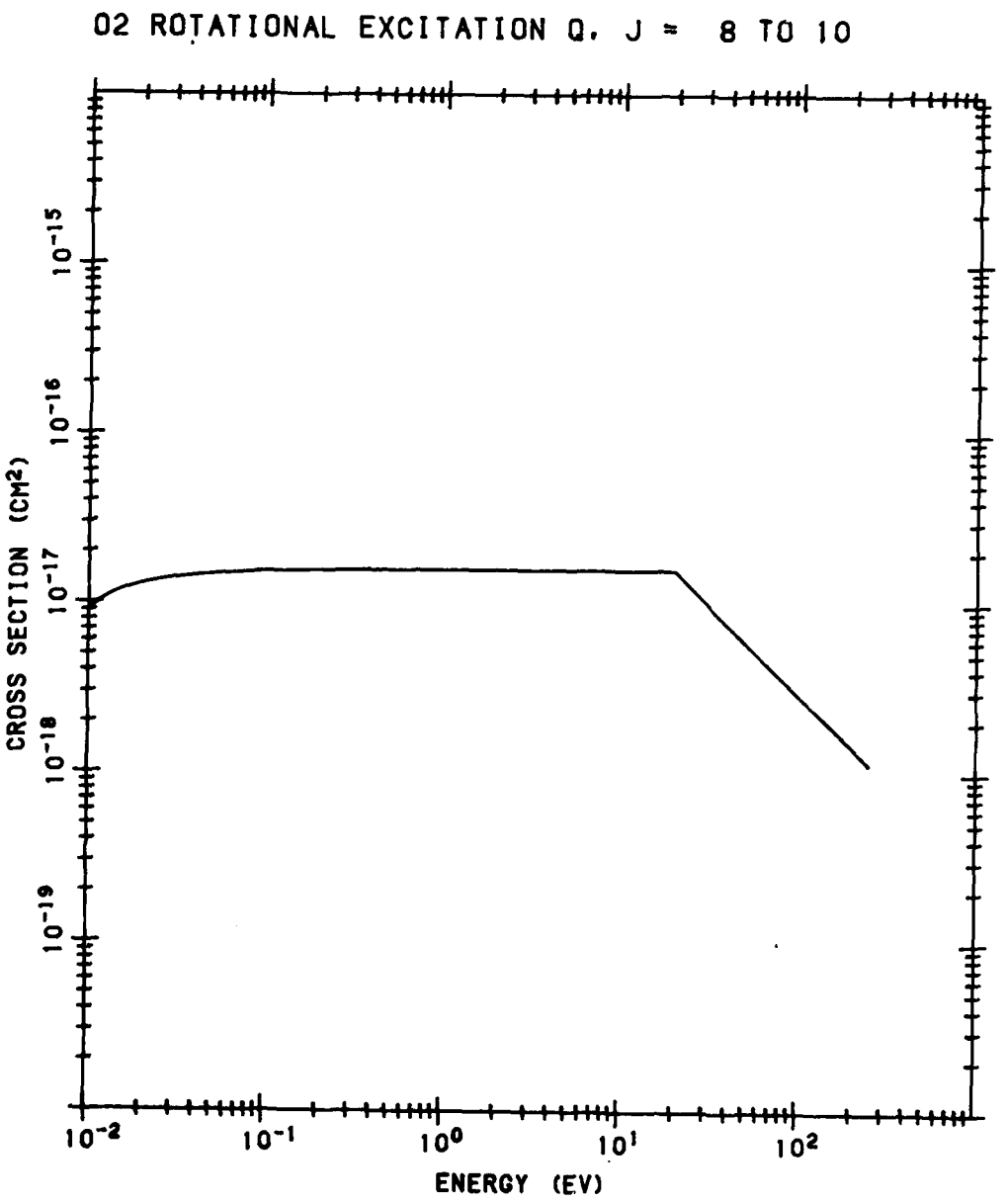


Figure B35. $O_2$ Rotational Excitation Cross Section from J of 8 to 10. The data source is the same as that of Figure B27

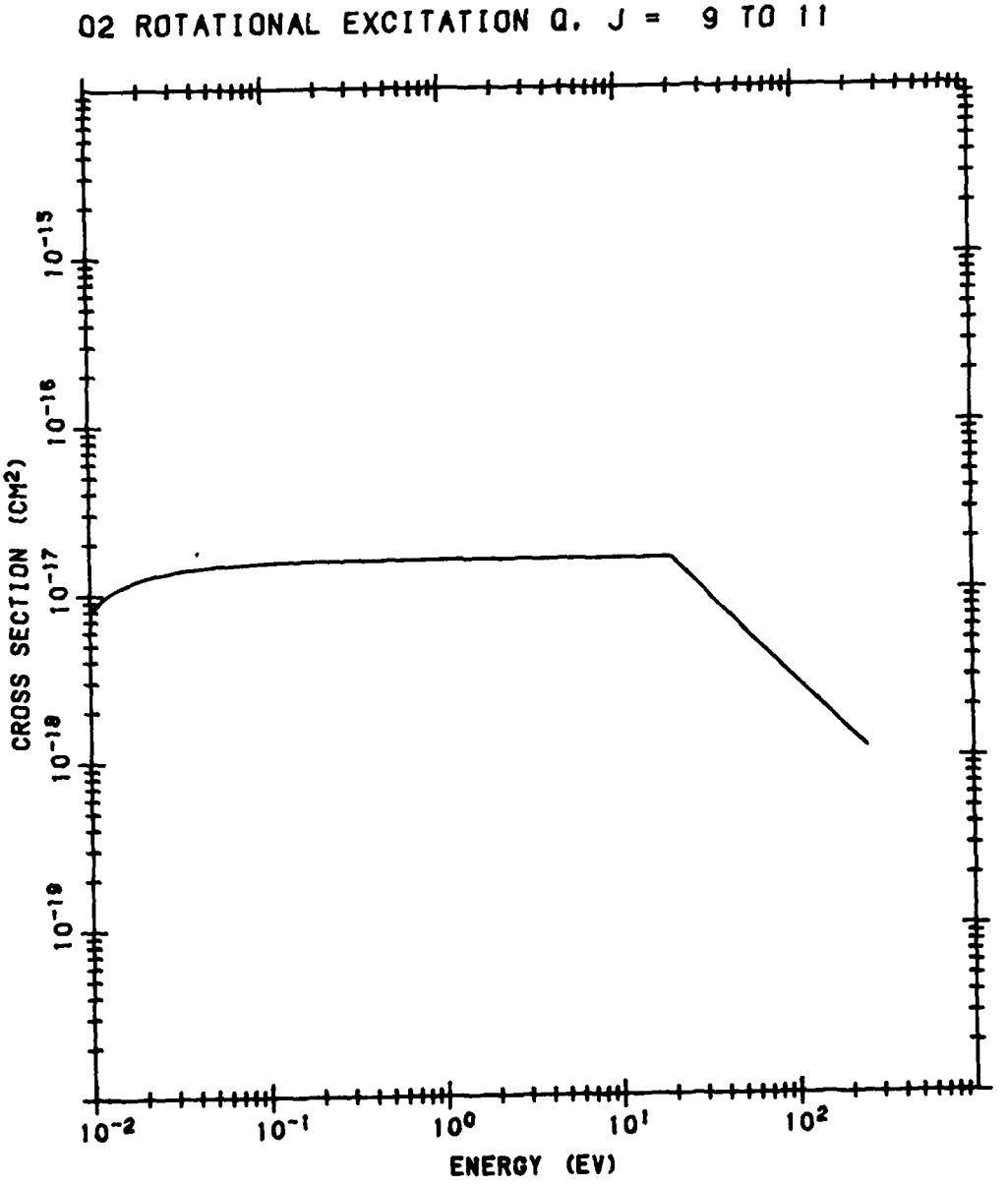


Figure B36. $O_2$ Rotational Excitation Cross Section from J of 9 to 11. The data source is the same as that of Figure B27

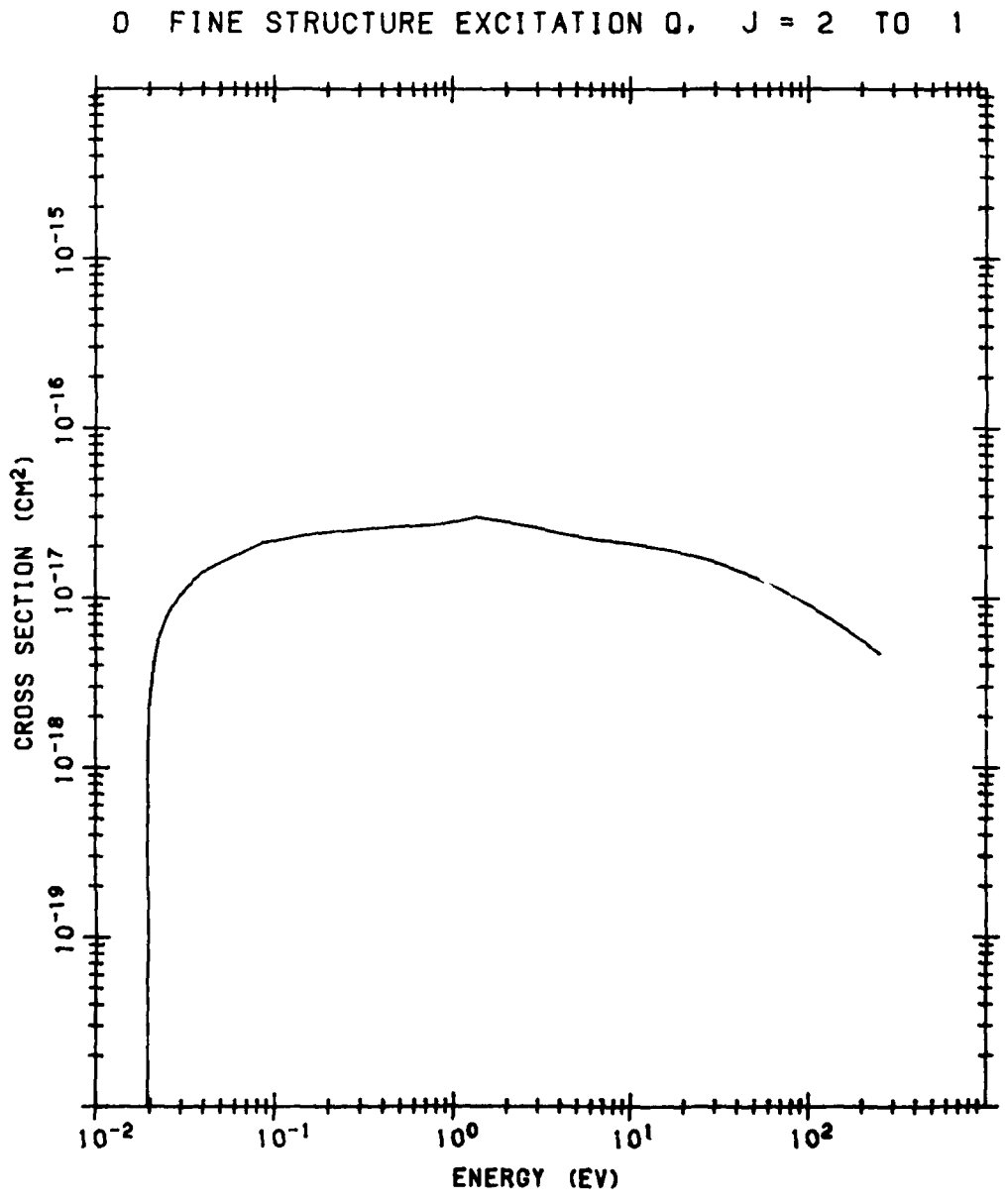


Figure B37. O Fine Structure Excitation Cross Section from J of 2 to 1. The data between 0.043 and 1.72 eV are from LeDourneuf and Nesbet (1976);[B11] between 2.72 and 9.52 eV from Tambe and Henry (1976).[B12] The data are extrapolated to the threshold and a 1/E extrapolation is used for high energies

B11. LeDournef, M., and Nesbet, R.K. (1976) J. Phys. B9:L241.

B12. Tambe, B.R., and Henry, R.J.W. (1976) Phys. Rev. A13:224.

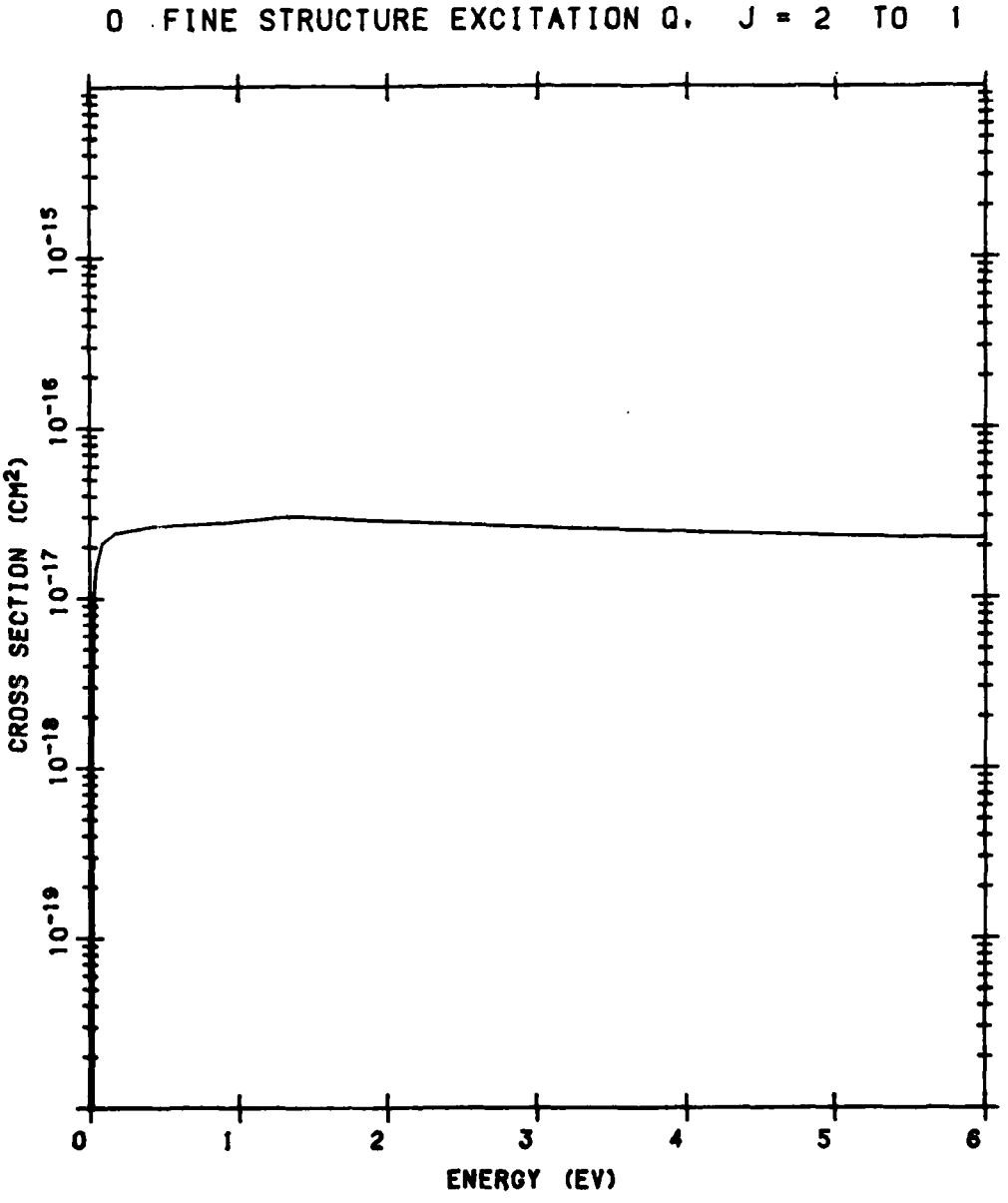


Figure B37. O Fine Structure Excitation Cross Section from J of 2 to 1. The data between 0.043 and 1.72 eV are from LeDourneuf and Nesbet (1976);[B11] between 2.72 and 9.52 eV from Tambe and Henry (1976).[B12] The data are extrapolated to the threshold and a 1/E extrapolation is used for high energies (Cont.)

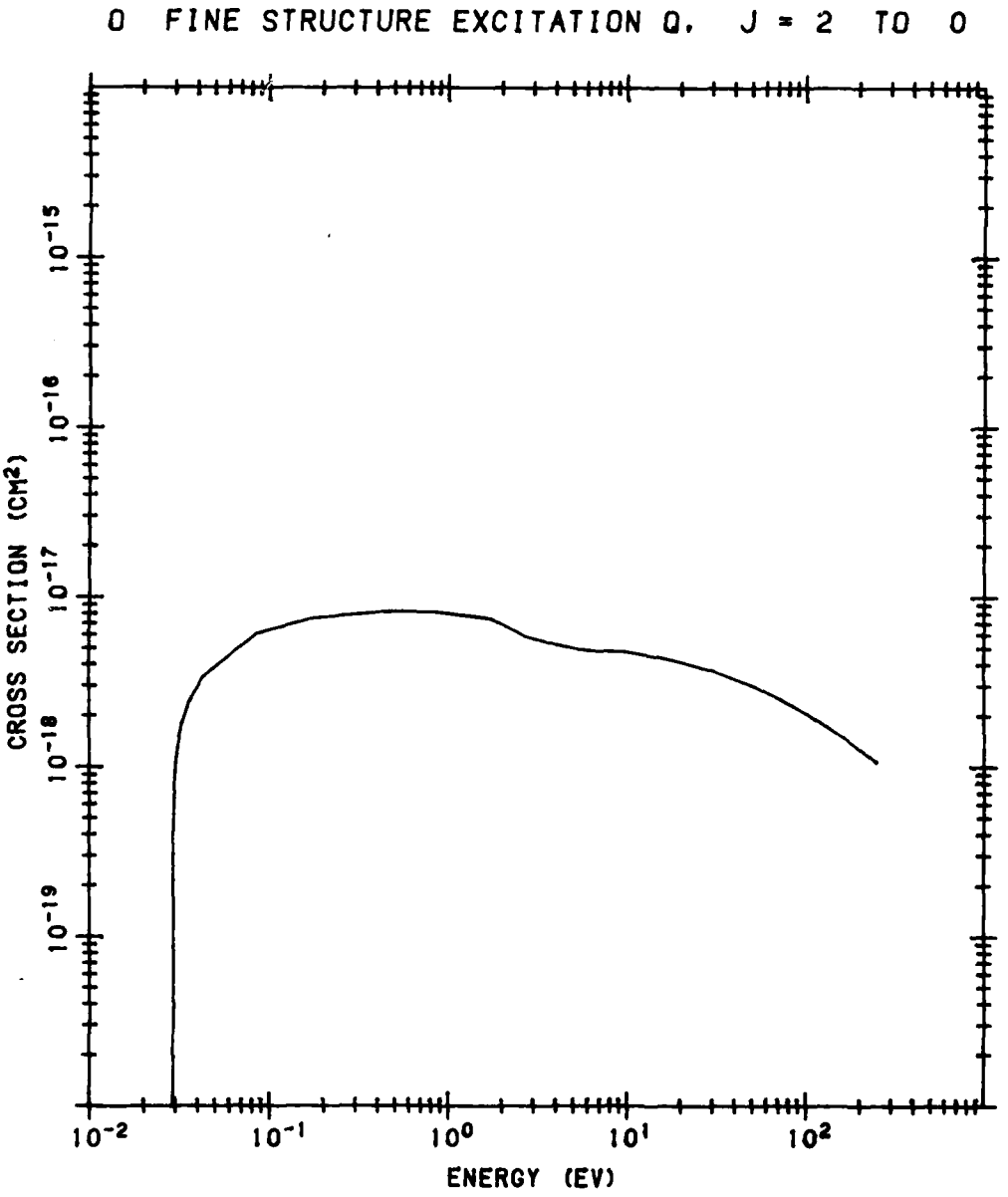


Figure B38. O Fine Structure Excitation Cross Section from J of 2 to 0. The data source is the same as that of Figure B37

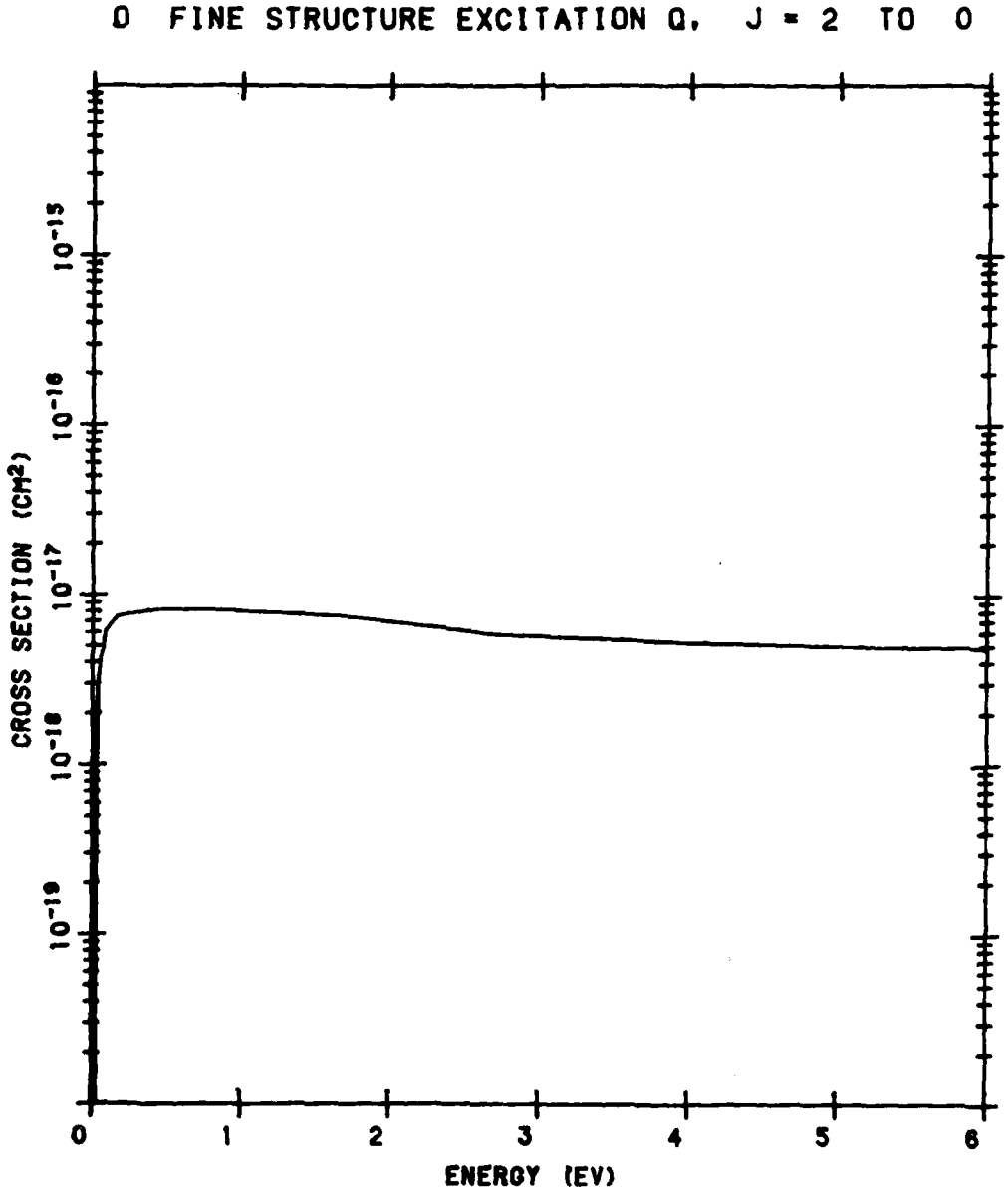


**Figure B38. O Fine Structure Excitation Cross Section from J of 2 to 0. The data source is the same as that of Figure B37 (Cont.)**

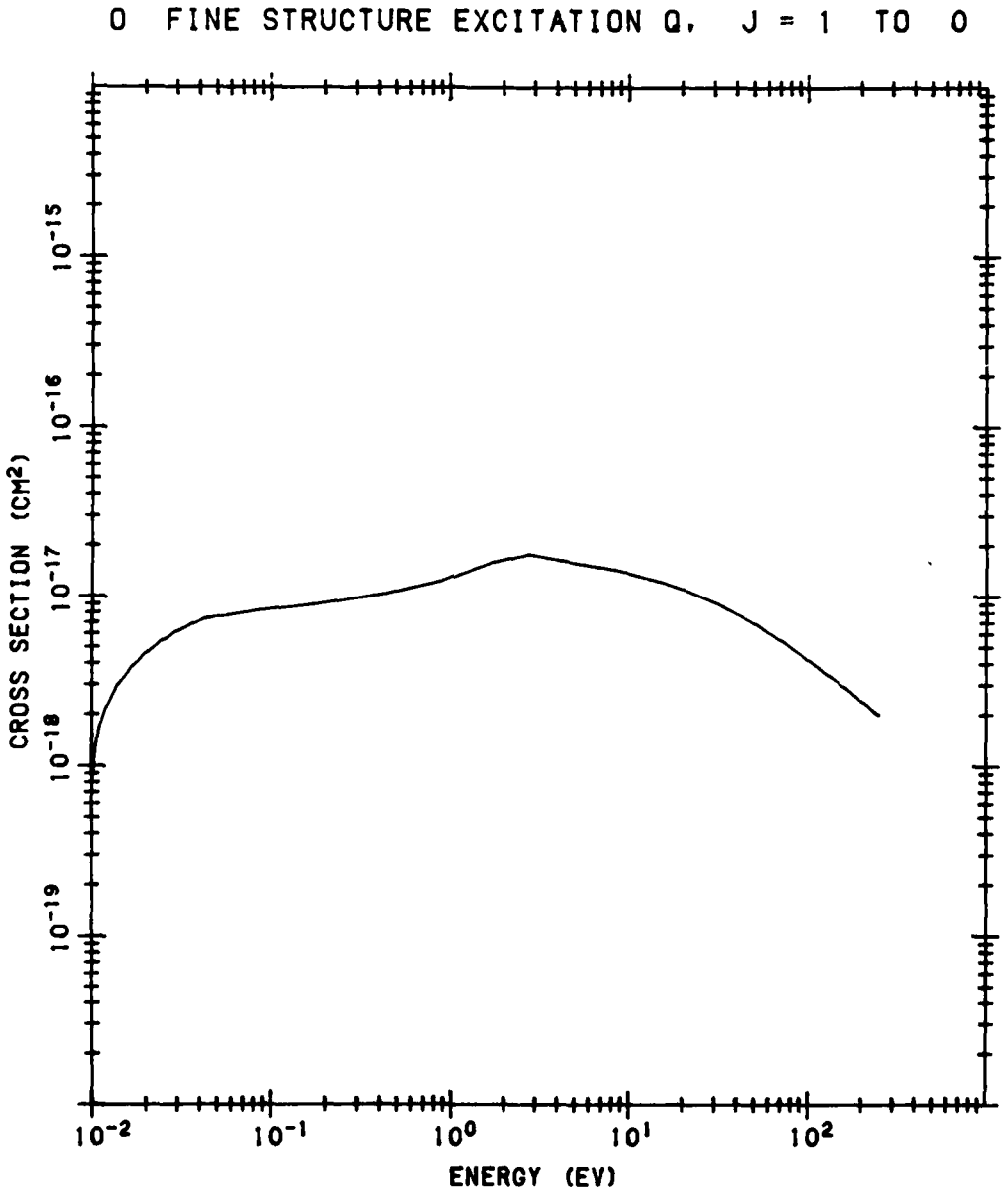


Figure B39. O Fine Structure Excitation Cross Section from J of 1 to 0. The data source is the same as that of Figure B37

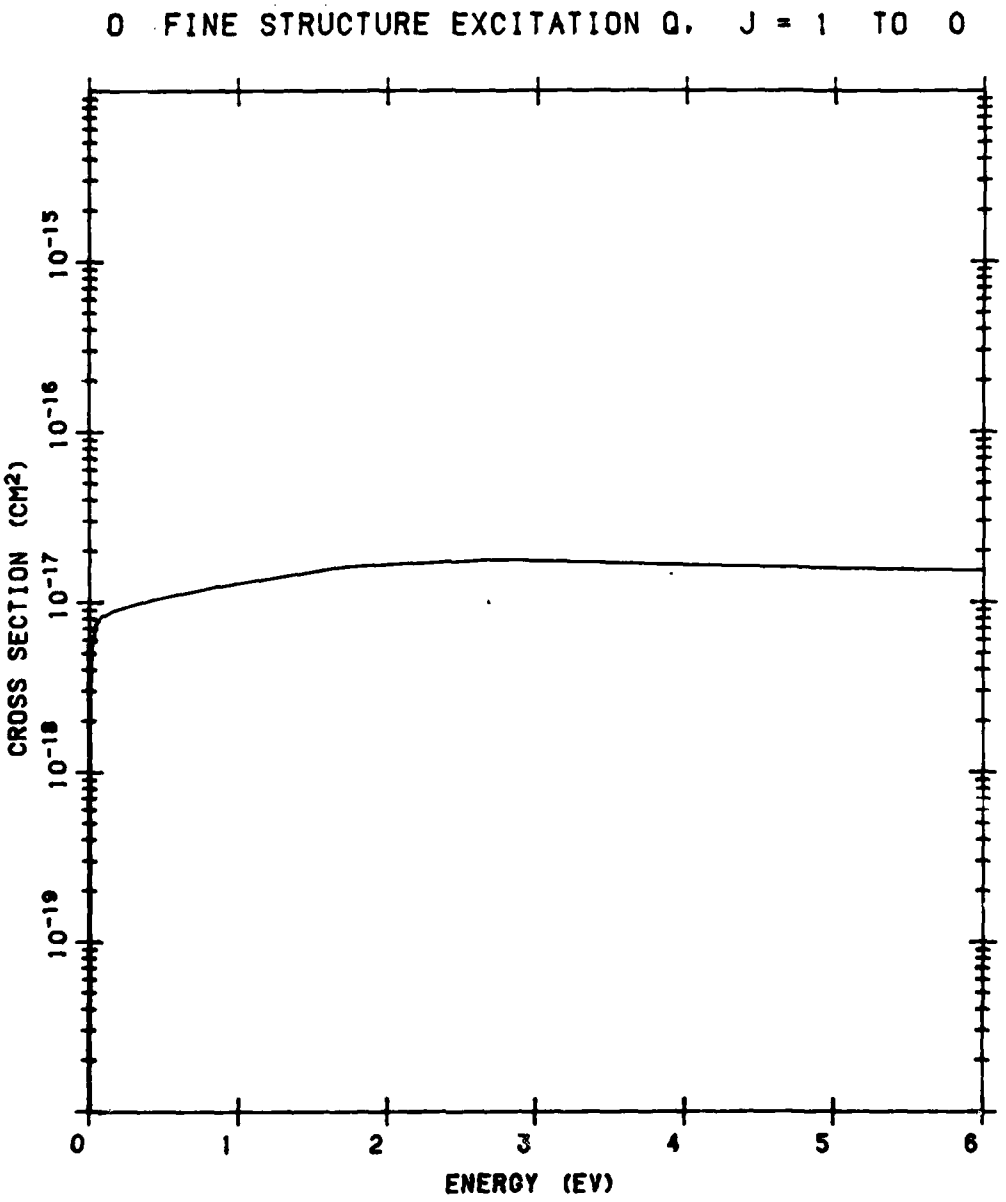


**Figure B39. O Fine Structure Excitation Cross Section from J of 1 to 0. The data source is the same as that of Figure B37 (Cont.)**

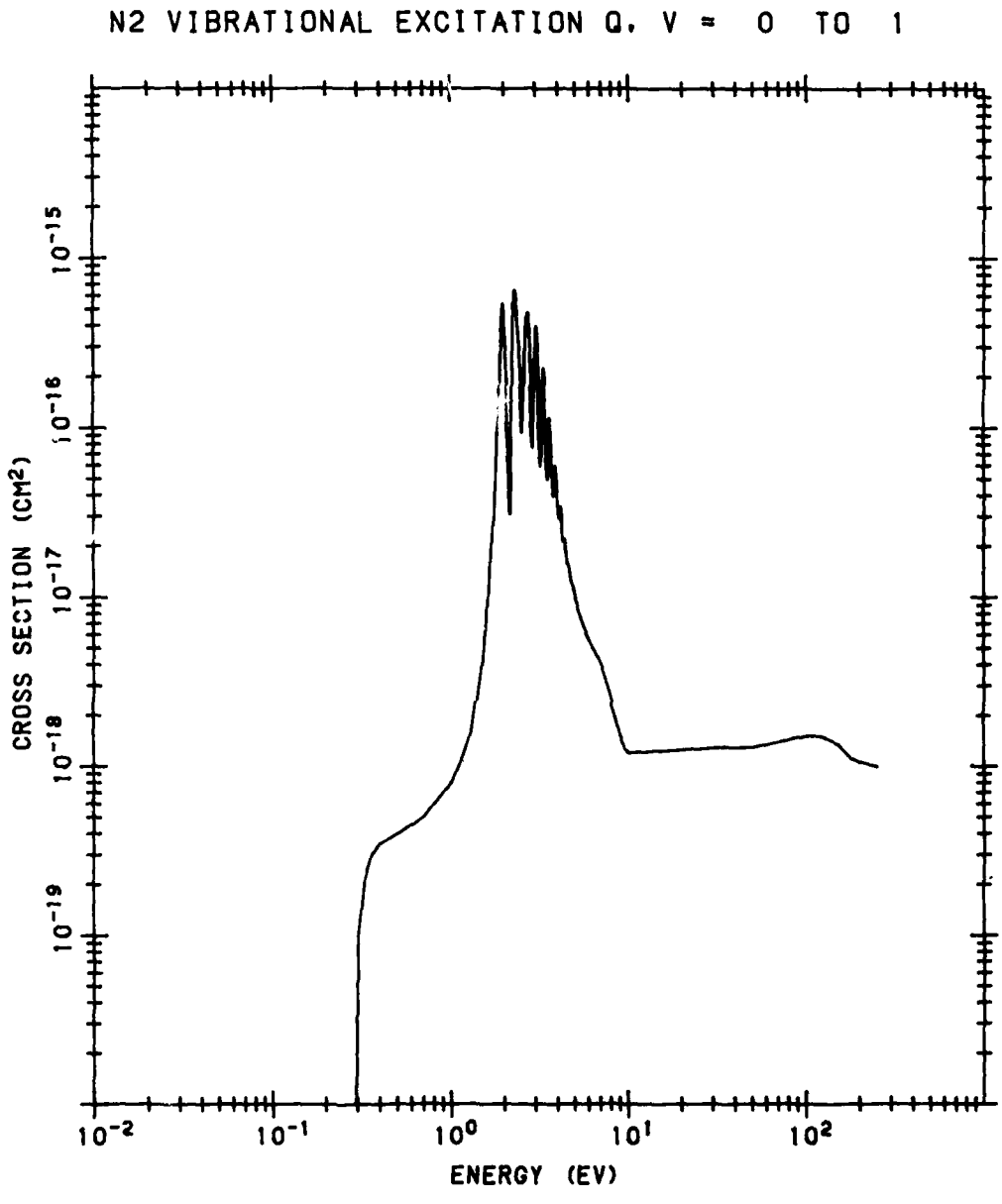


Figure B40. $N_2$ Vibrational Excitation Cross Section from v of 0 to 1. Below 1.5 eV the data are from Chen (1966a,[B13] 1966b[B14]); between 1.55 and 6.6 eV from Schneider (1980);[B15] from 10 to 50 eV from Truhlar et al (1977);[B16] and above 75 eV from Choi et al (1979)[B5]


B13. Chen, J.C.Y. (1966a) Phys. Rev. 146:61.

B14. Chen, J.C.Y. (1966b) J. Chem. Phys. 45:2710.

B15. Schneider, B.I. (1980) Private communication.

B16. Truhlar, D.G., Brandt, M.A. Srivastava, S.K., Trajmar, S., and Chutjian, A. (1977) J. Chem. Phys. 66:655.

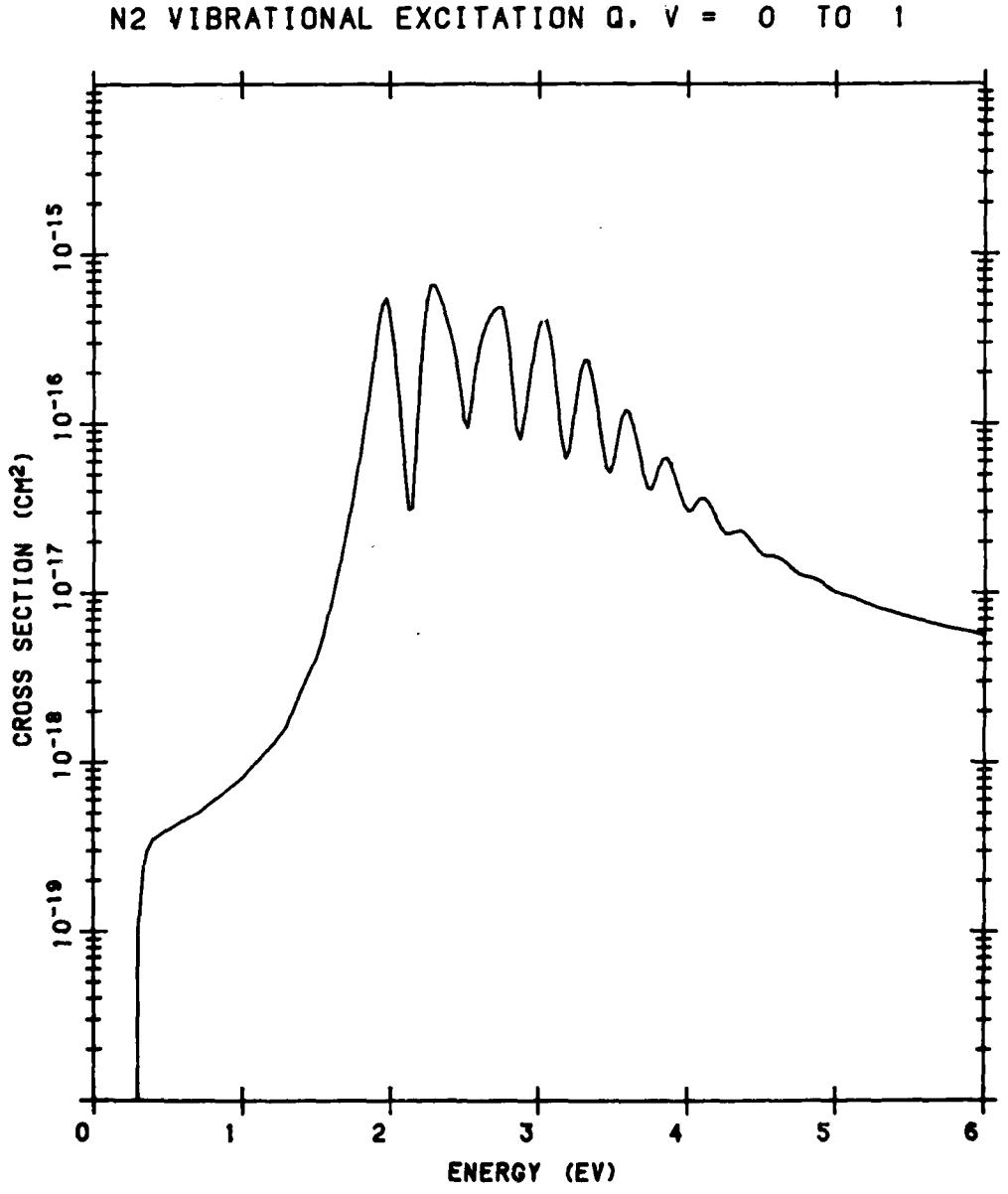


**Figure B40.** $N_2$ Vibrational Excitation Cross Section from v of 0 to 1. Below 1.5 eV the data are from Chen (1966a,[B13] 1966b[B14]); between 1.55 and 6.6 eV from Schneider (1980);[B15] from 10 to 50 eV from Truhlar et al (1977);[B16] and above 75 eV from Choi et al (1979)[B5] (Cont.)

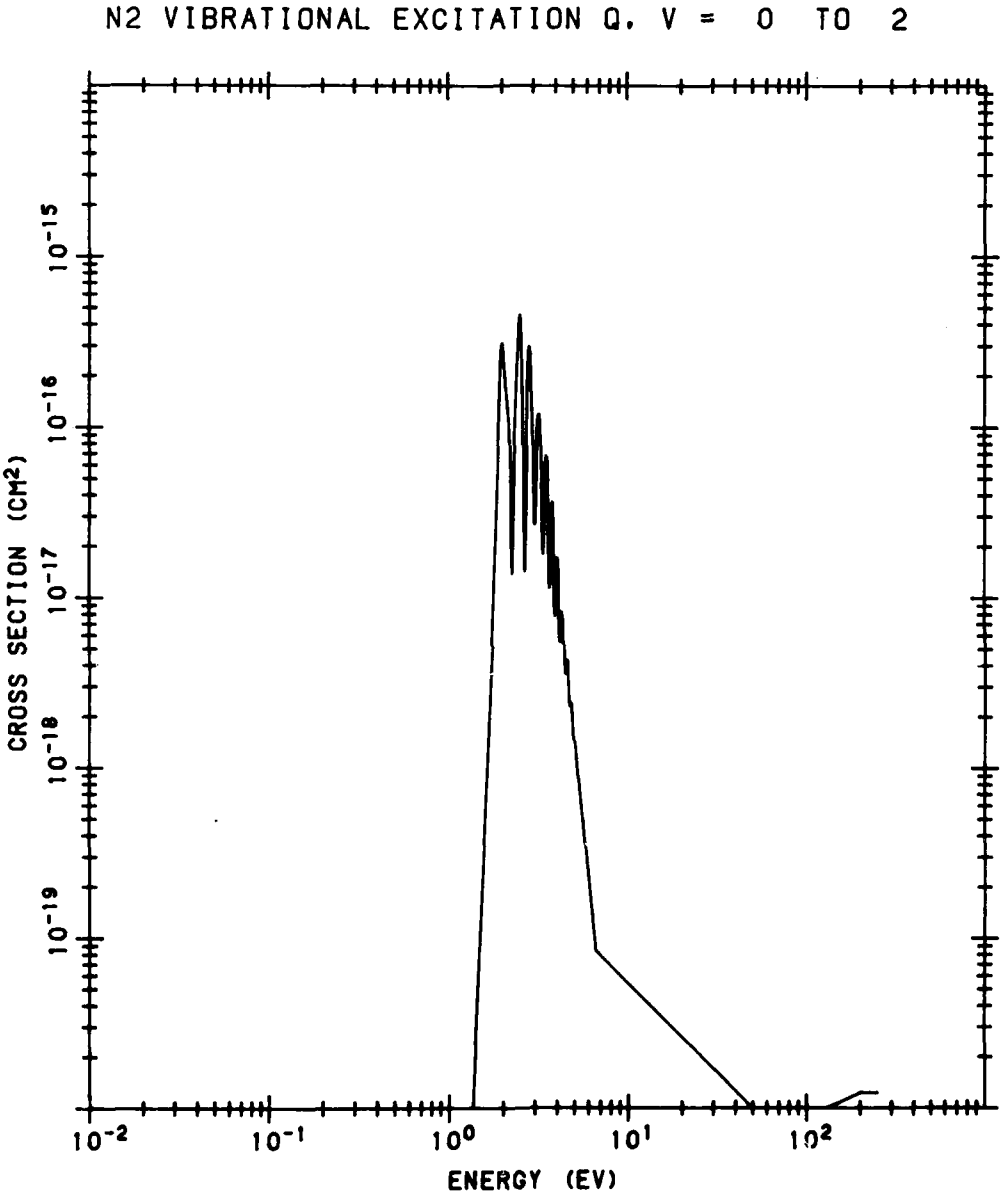


Figure B41. $N_2$ Vibrational Excitation Cross Section from v of 0 to 2. Between 1.0 and 8.6 eV the data are from Schneider (1980);[B15] and above 50 eV from Choi et al (1979)[B5]

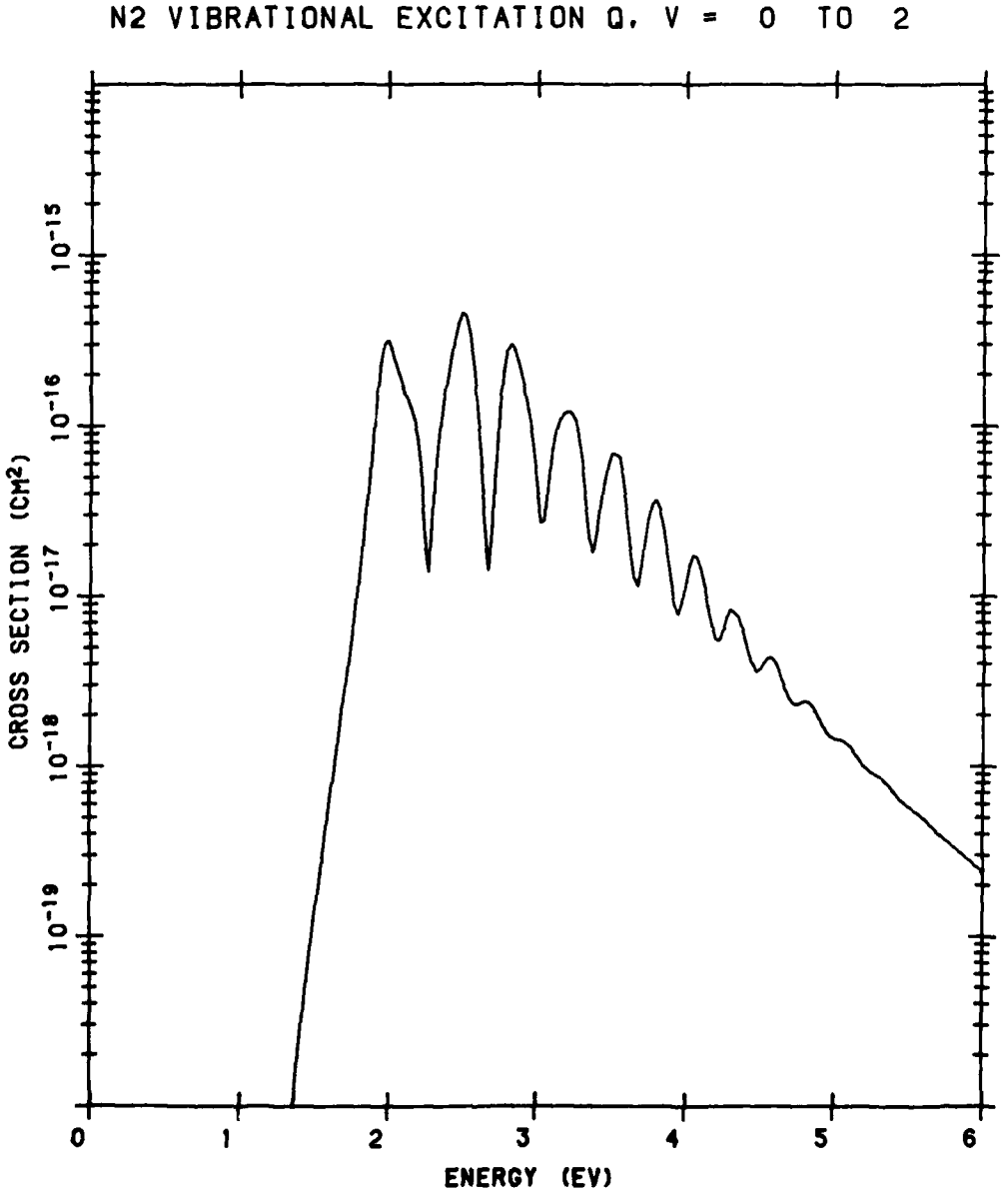


**Figure B41. $N_2$ Vibrational Excitation Cross Section from v of 0 to 2. Between 1.0 and 6.6 eV the data are from Schneider (1980);[B15] and above 50 eV from Choi et al (1979)[B5] (Cont.)**

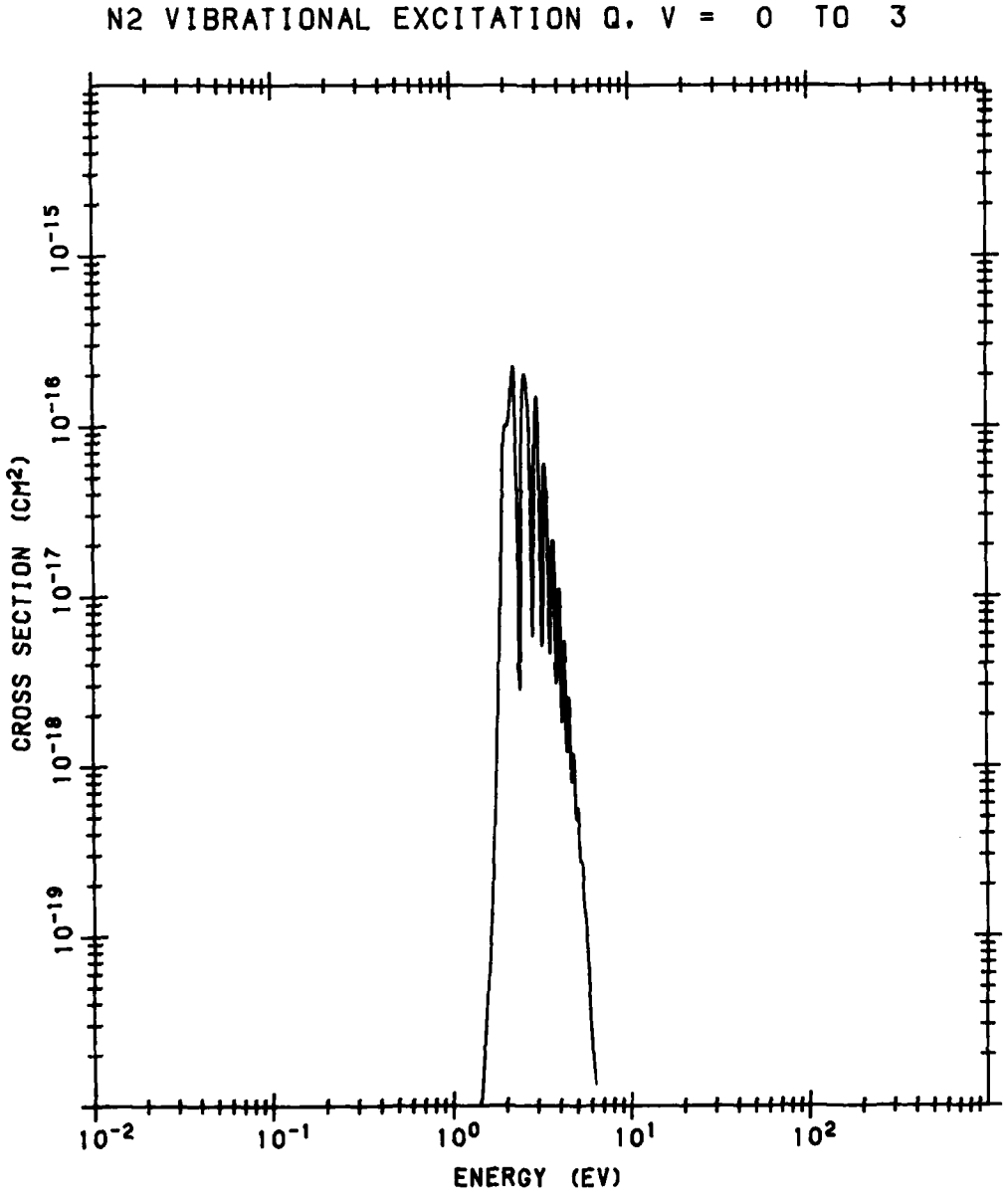


Figure B42. $N_2$ Vibrational Excitation Cross Section from v of 0 to 3. The data are from Schneider (1980)[B15]

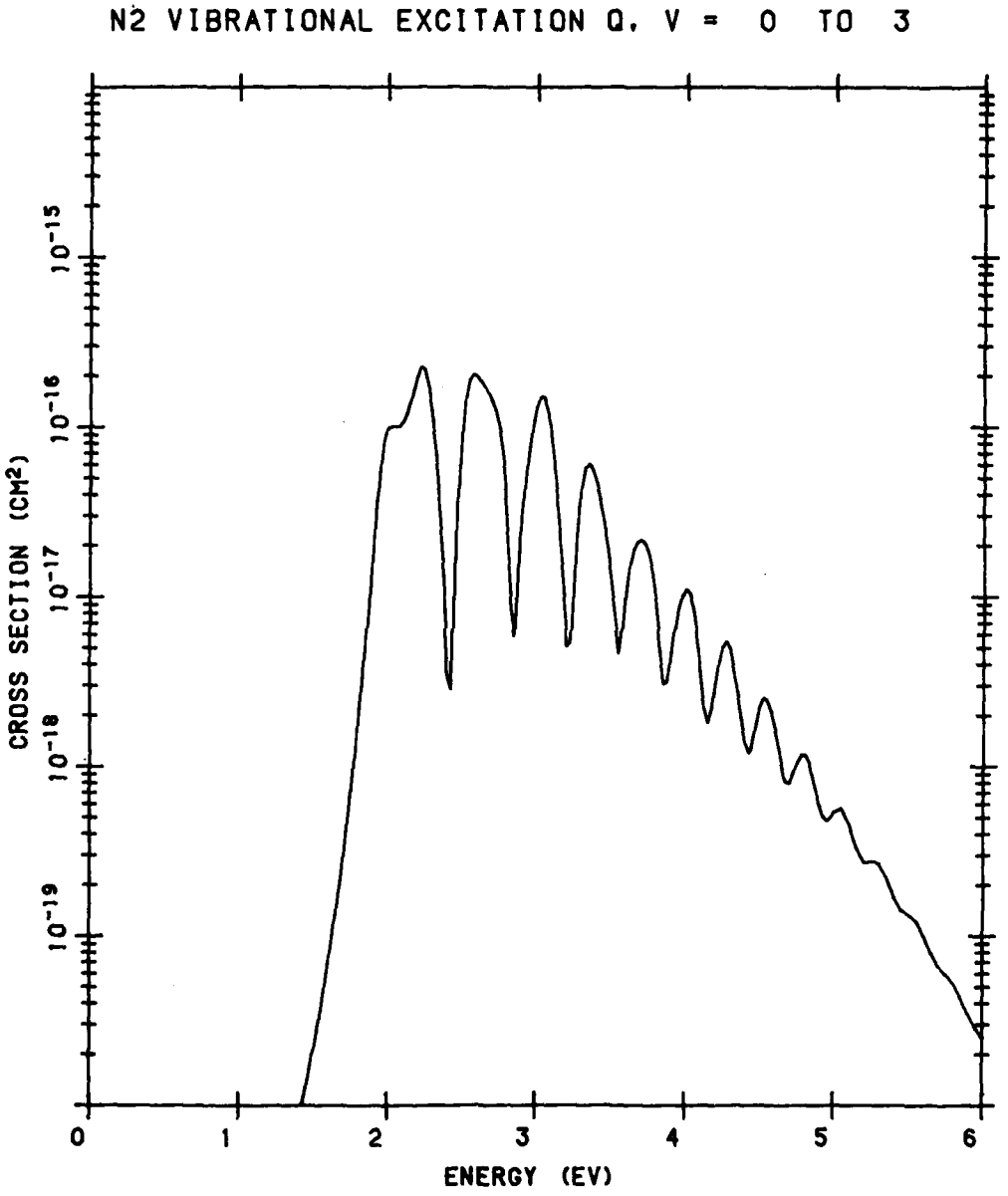


**Figure B42. $N_2$ Vibrational Excitation Cross Section from v of 0 to 3. The data are from Schneider (1980)[B15] (Cont.)**

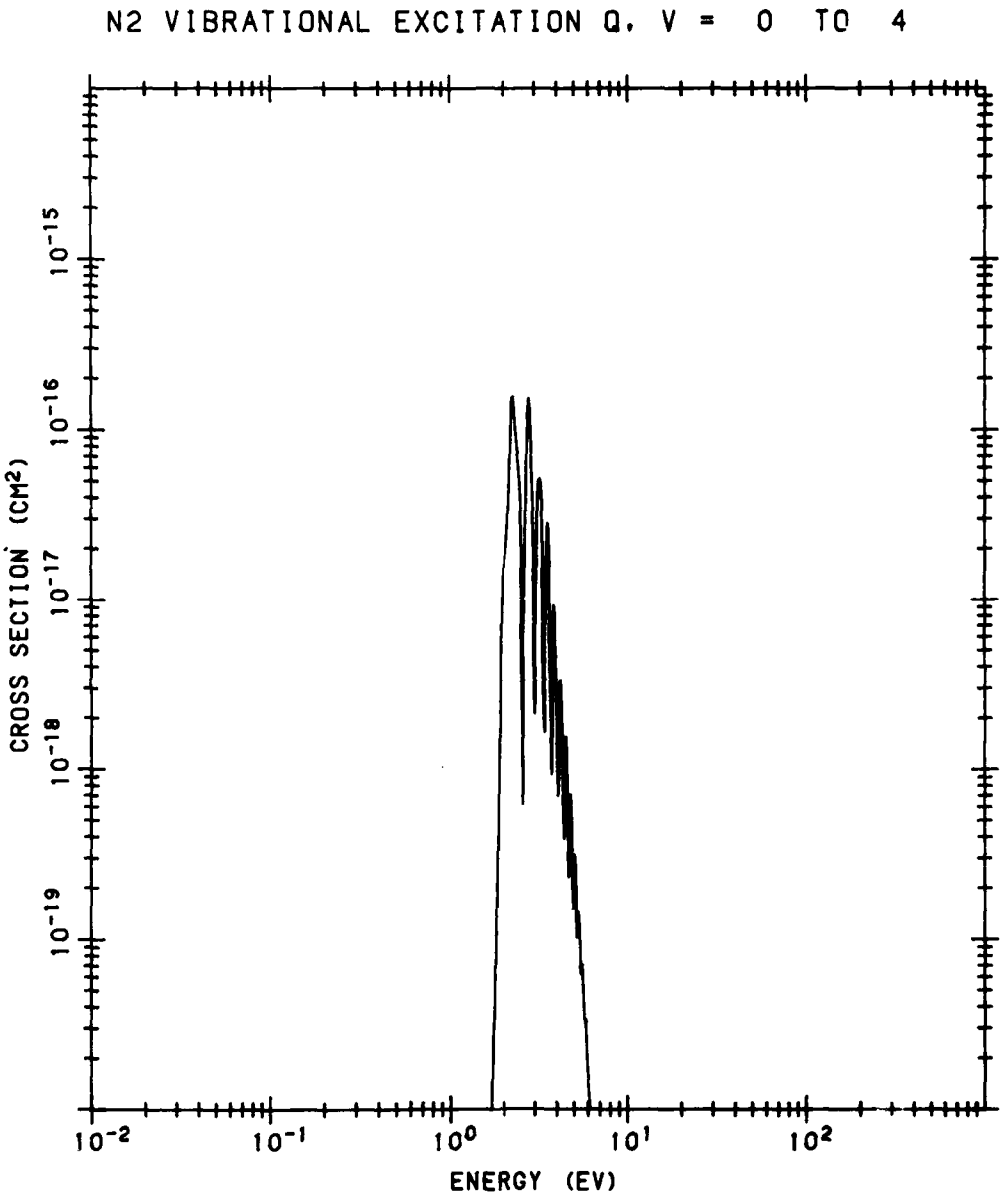


Figure B43. $N_2$ Vibrational Excitation Cross Section from v of 0 to 4. The source of the data is the same as in Figure B42

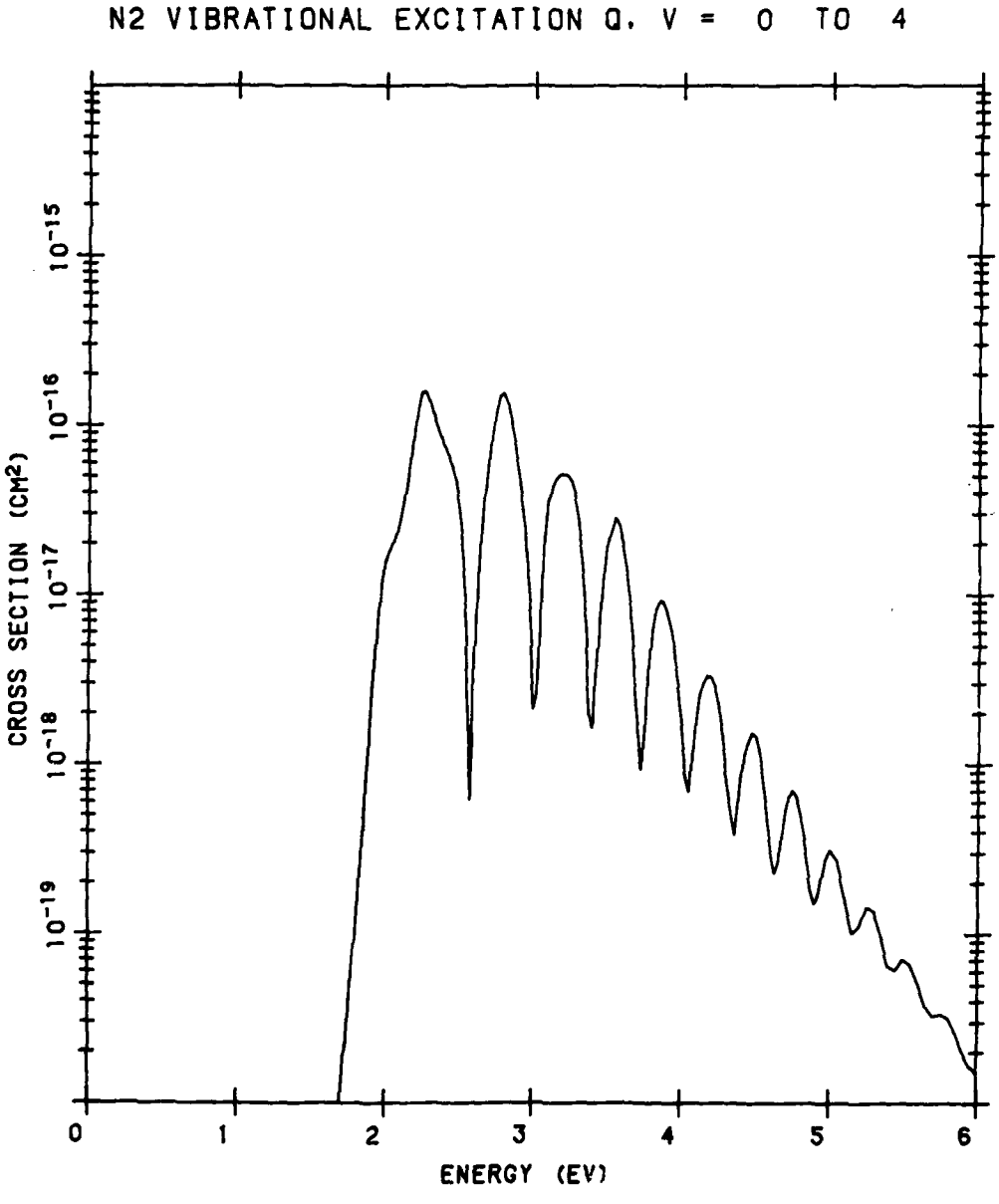


**Figure B43.** $N_2$ **Vibrational Excitation Cross Section from v of 0 to 4. The source of the data is the same as in Figure B42 (Cont.)**

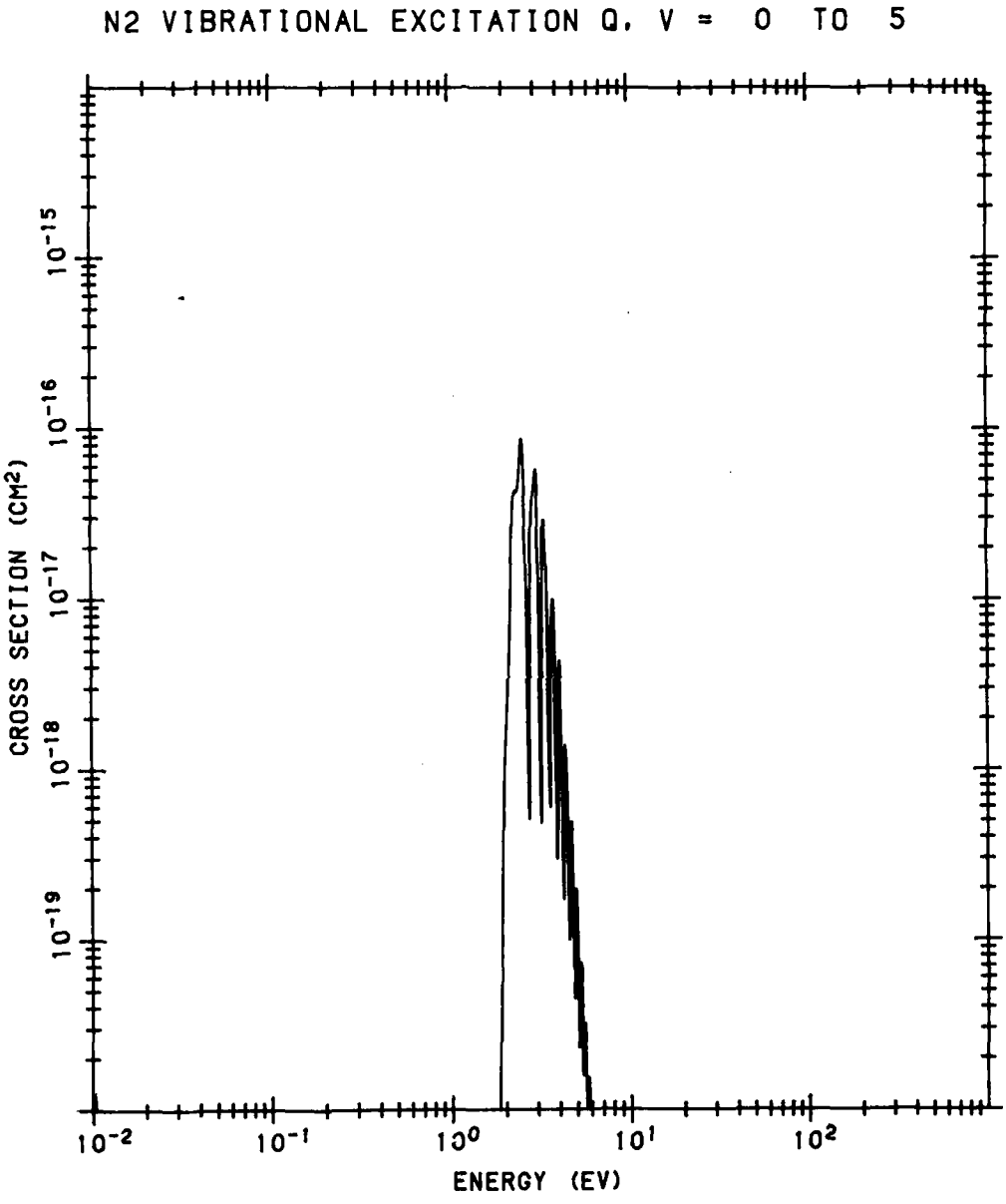


Figure B44. $N_2$ Vibrational Excitation Cross Section from v of 0 to 5. The source of the data is the same as in Figure B42

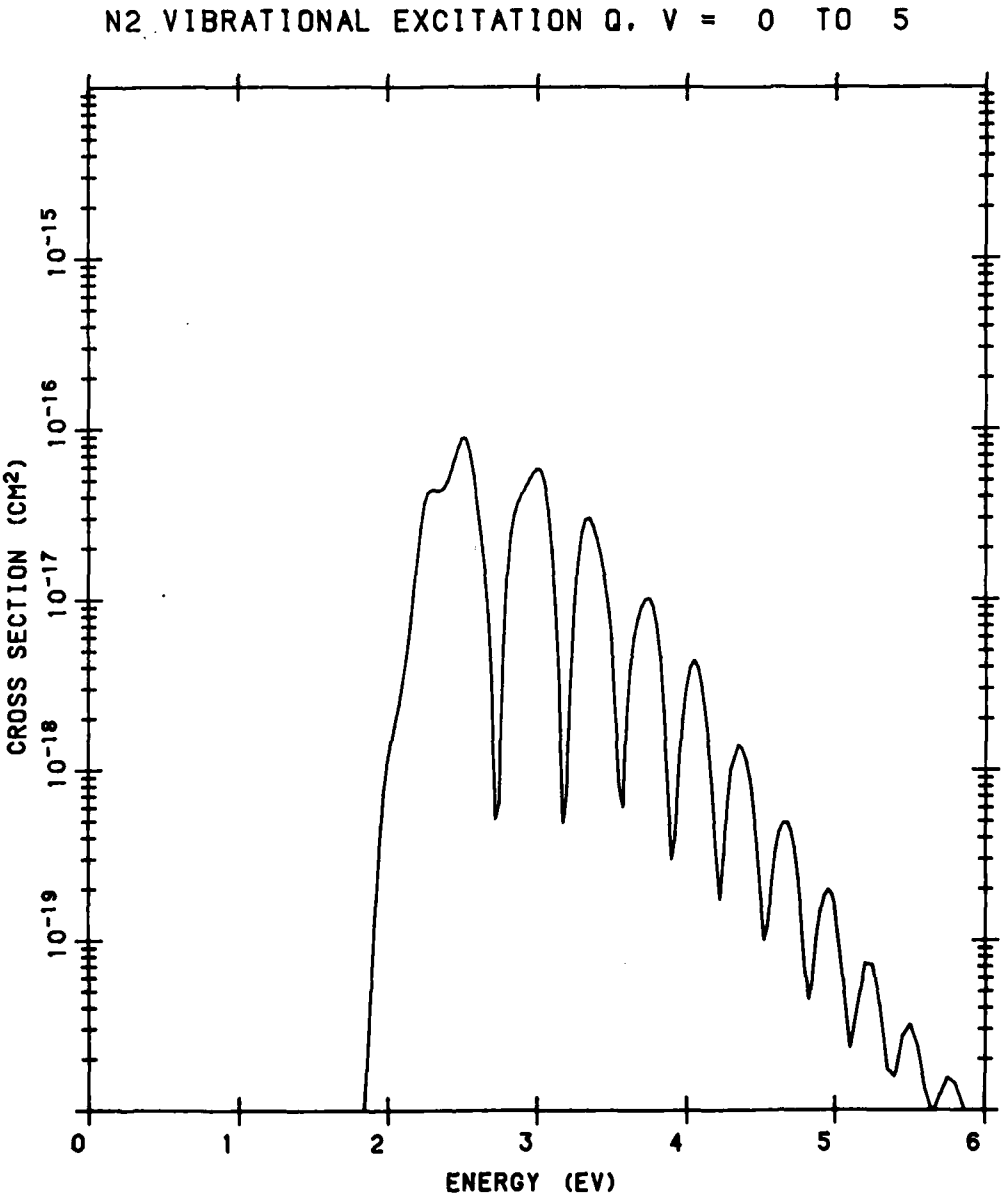


**Figure B44. $N_2$ Vibrational Excitation Cross Section from v of 0 to 5. The source of the data is the same as in Figure B42 (Cont.)**

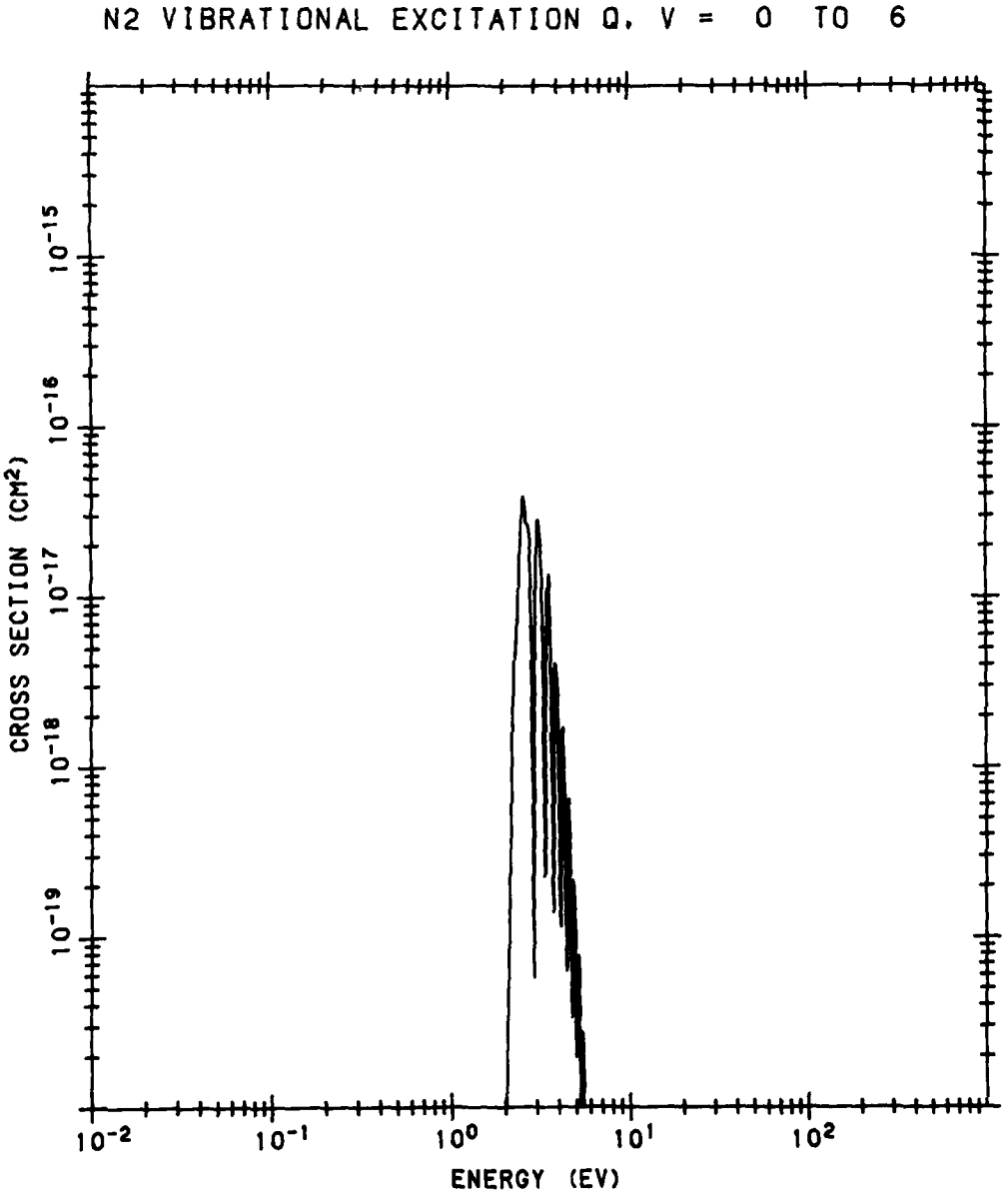


**Figure B45. $N_2$ Vibrational Excitation Cross Section from v of 0 to 6. The source of the data is the same as in Figure B42**

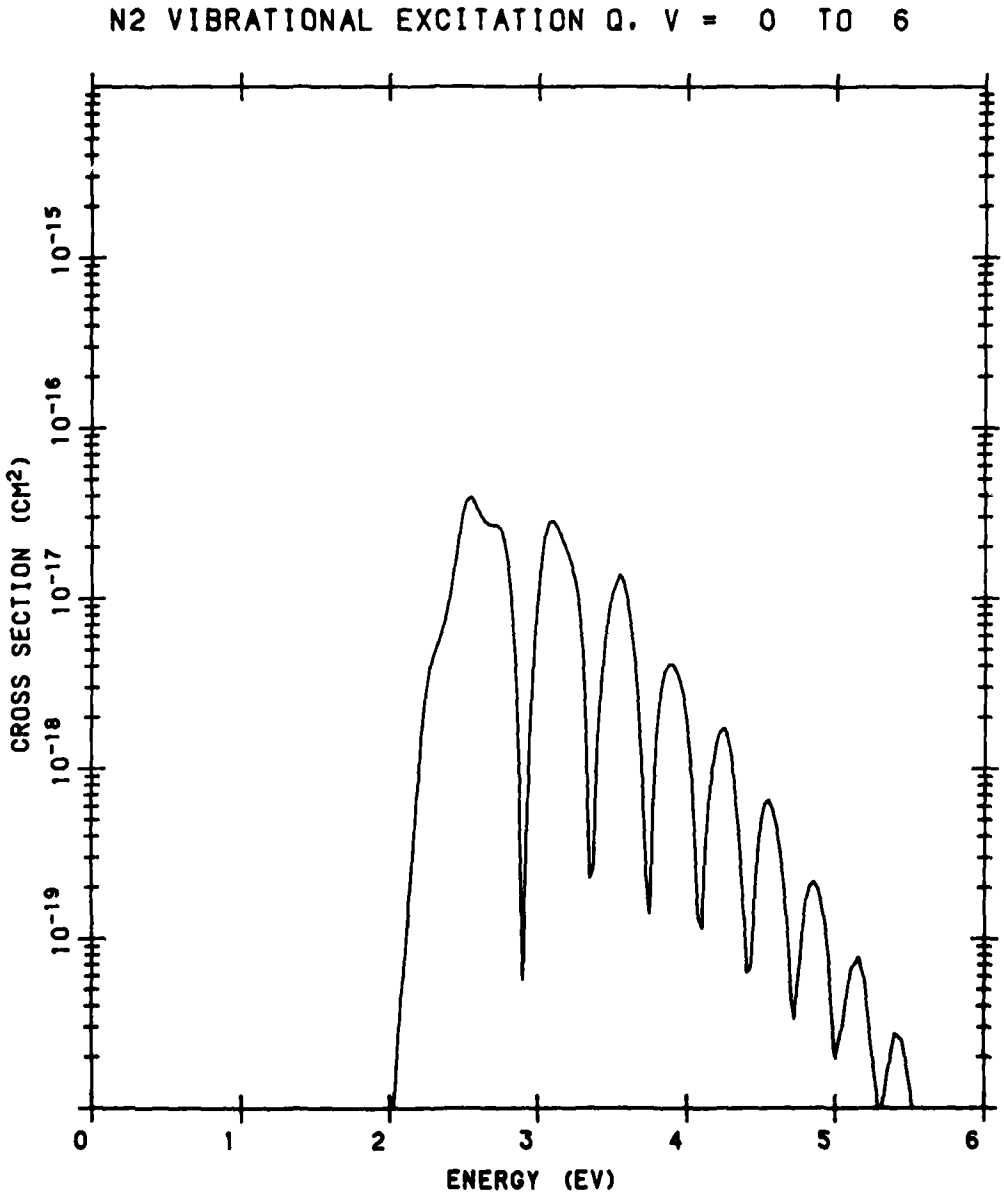


Figure B45. $N_2$ Vibrational Excitation Cross Section from v of 0 to 6. The source of the data is the same as in Figure B42 (Cont.)

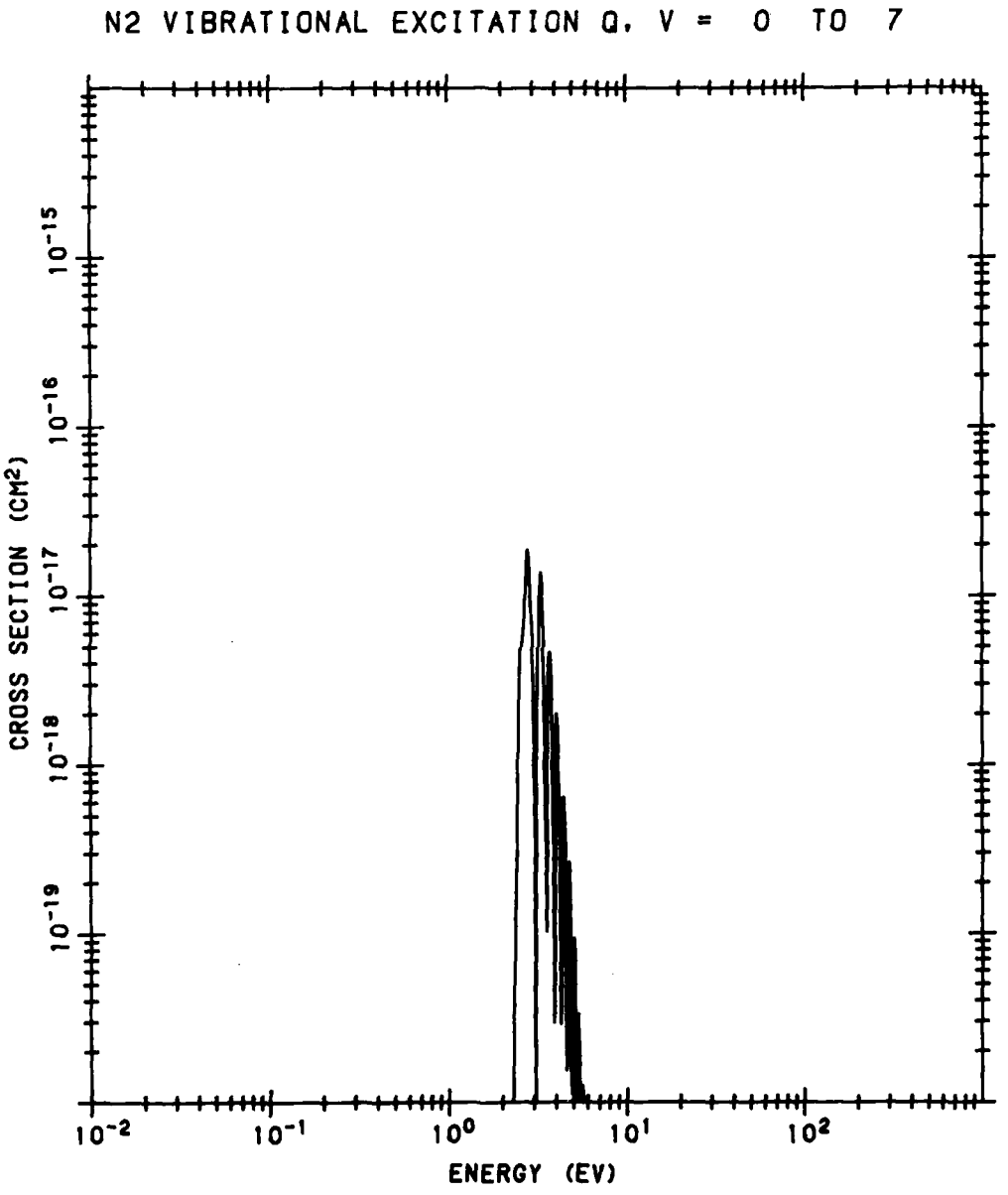


Figure B46. $N_2$ Vibrational Excitation Cross Section from v of 0 to 7. The source of the data is the same as in Figure B42

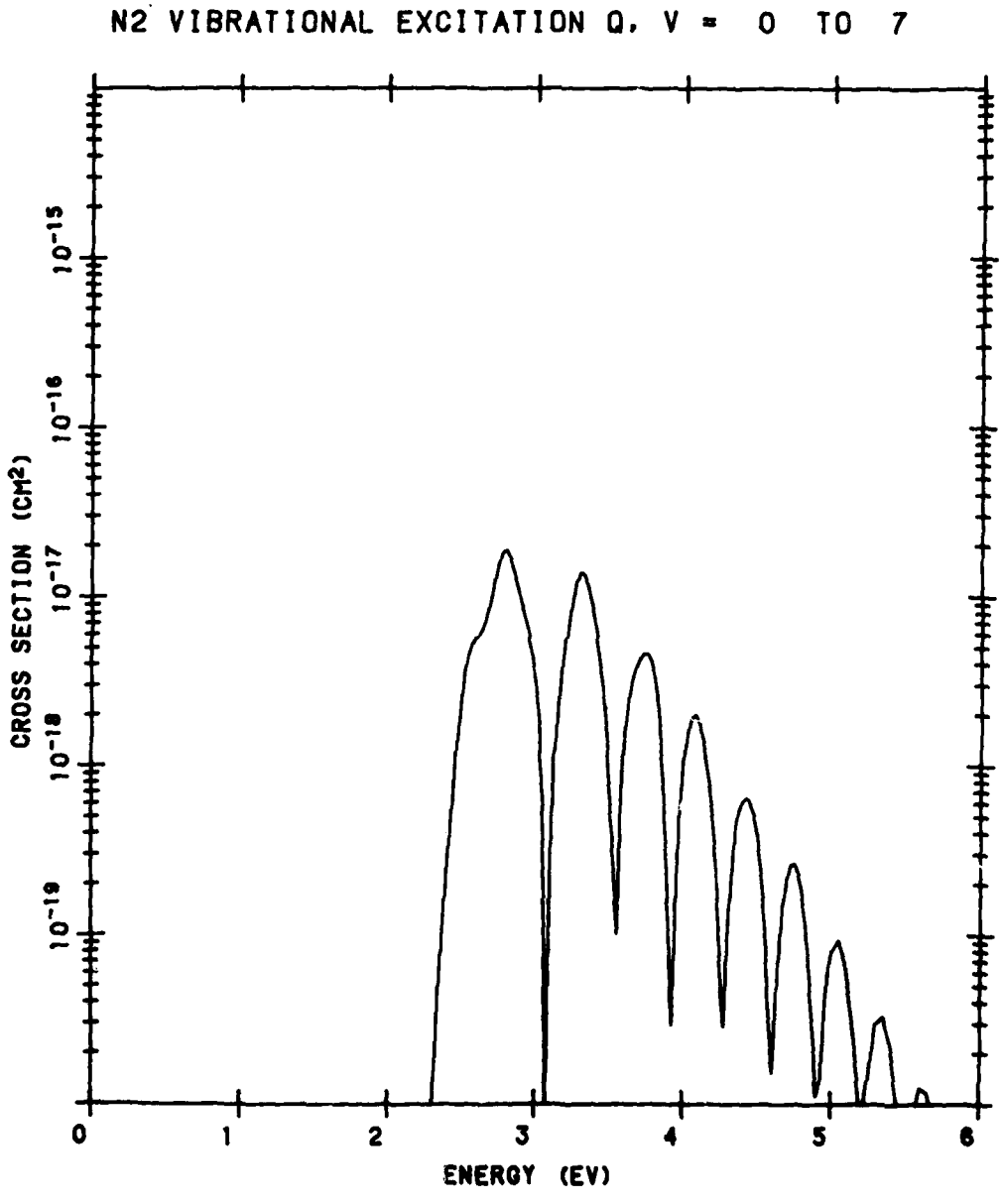


**Figure B46. $N_2$ Vibrational Excitation Cross Section from v of 0 to 7. The source of the data is the same as in Figure B42 (Cont.)**

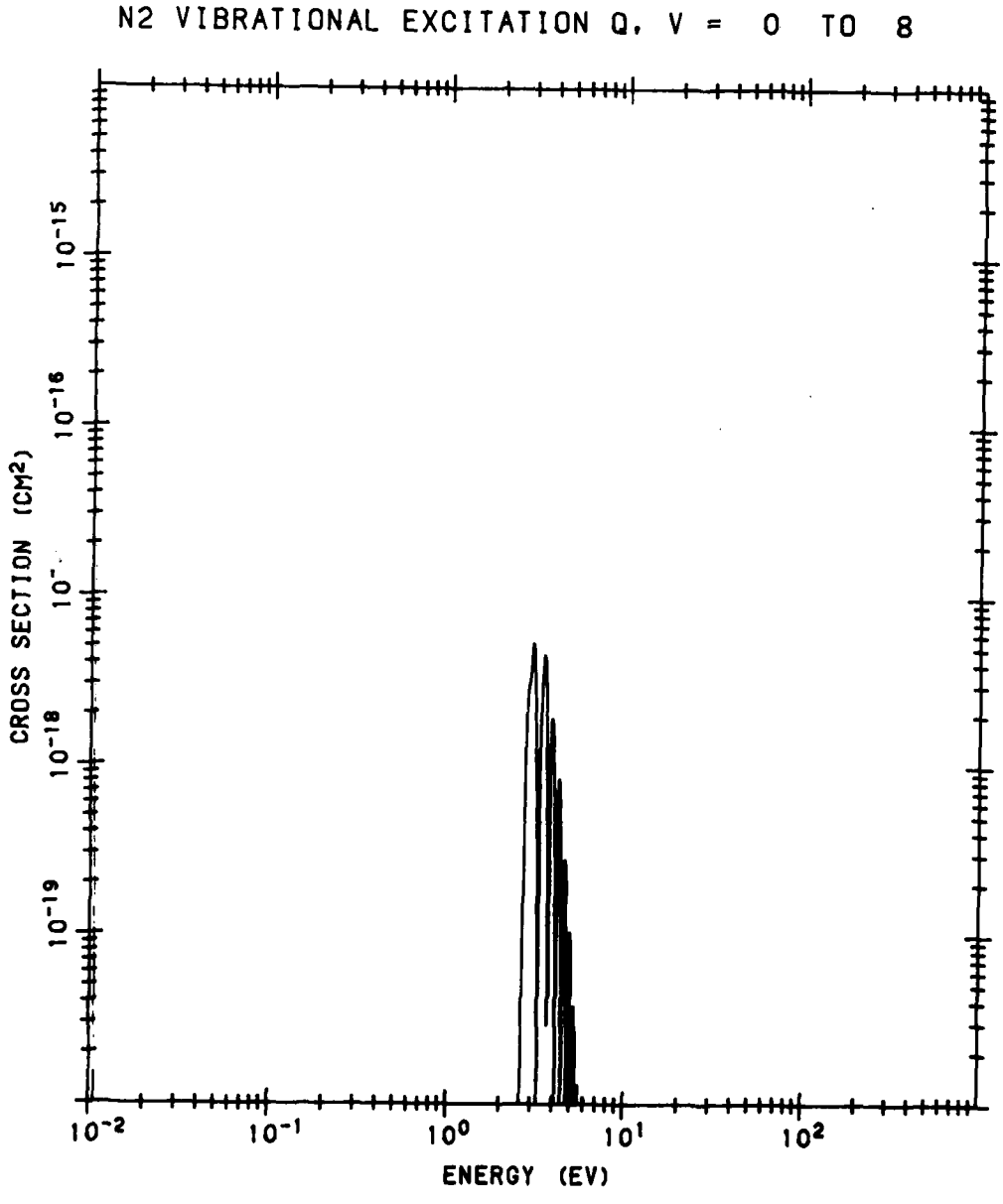


Figure B47. $N_2$ Vibrational Excitation Cross Section from v of 0 to 8. The source of the data is the same as in Figure B42

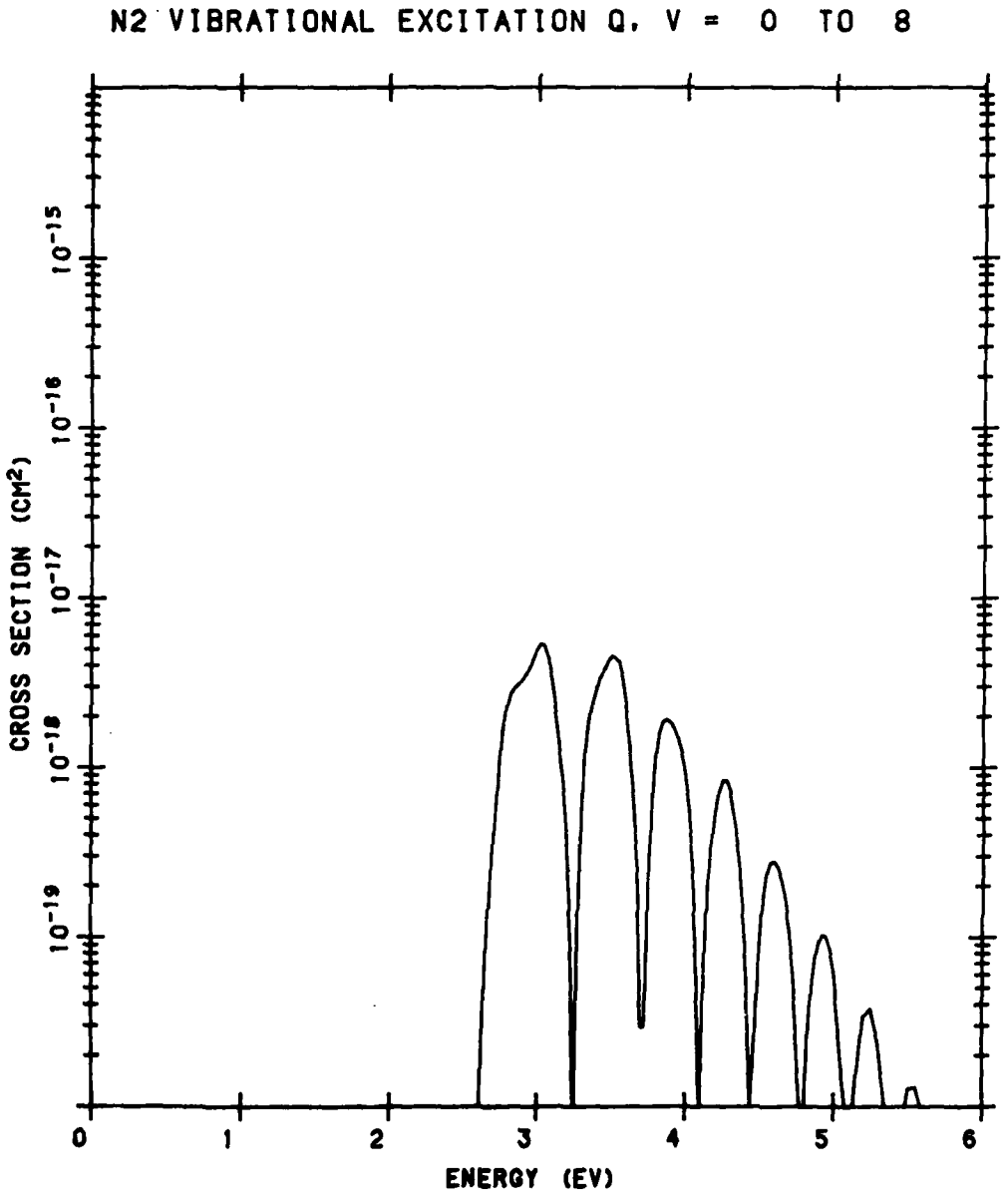


**Figure B47. $N_2$ Vibrational Excitation Cross Section from v of 0 to 8. The source of the data is the same as in Figure B42 (Cont.)**

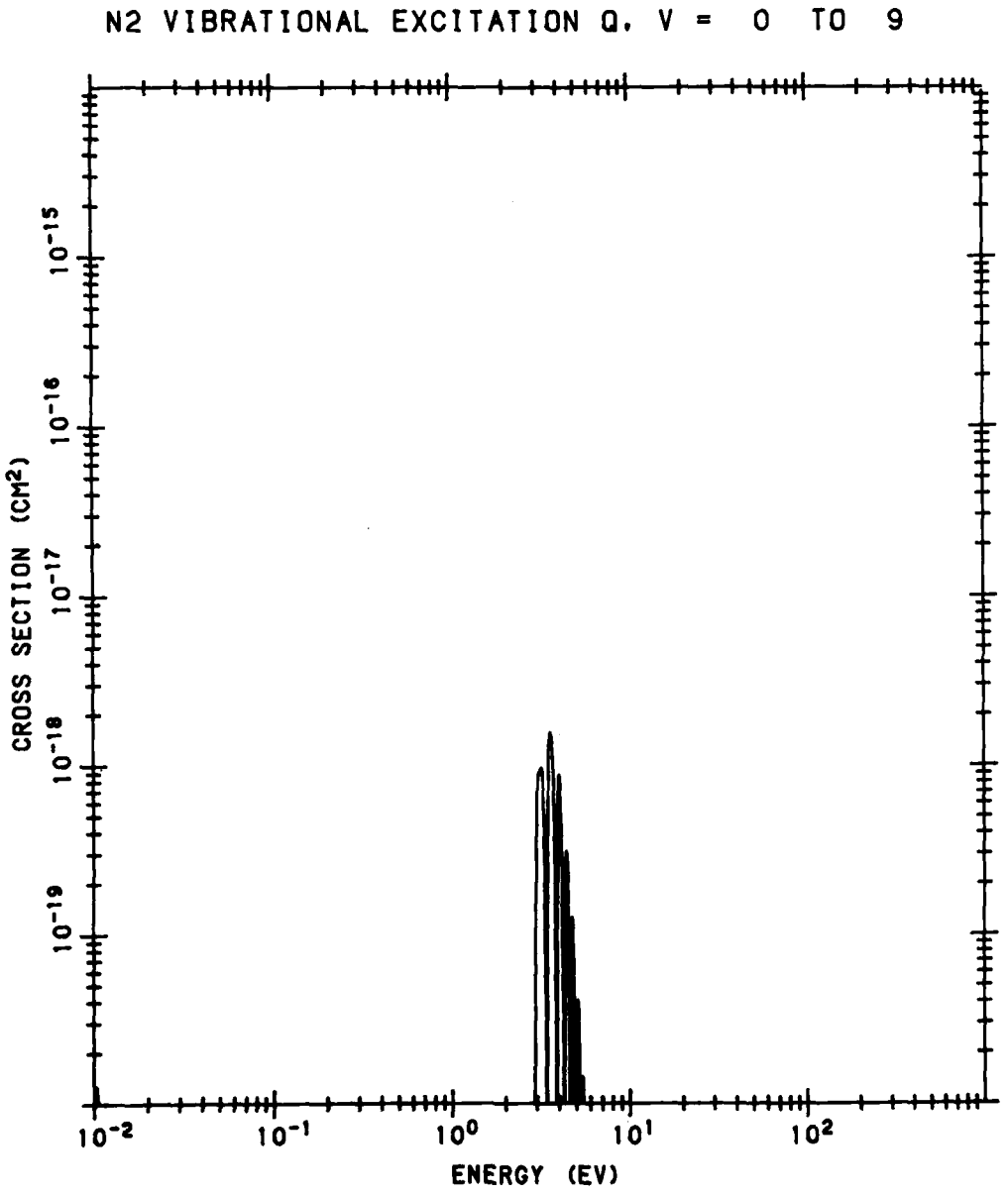


Figure B48. $N_2$ Vibrational Excitation Cross Section from v of 0 to 9. The source of the data is the same as in Figure B42

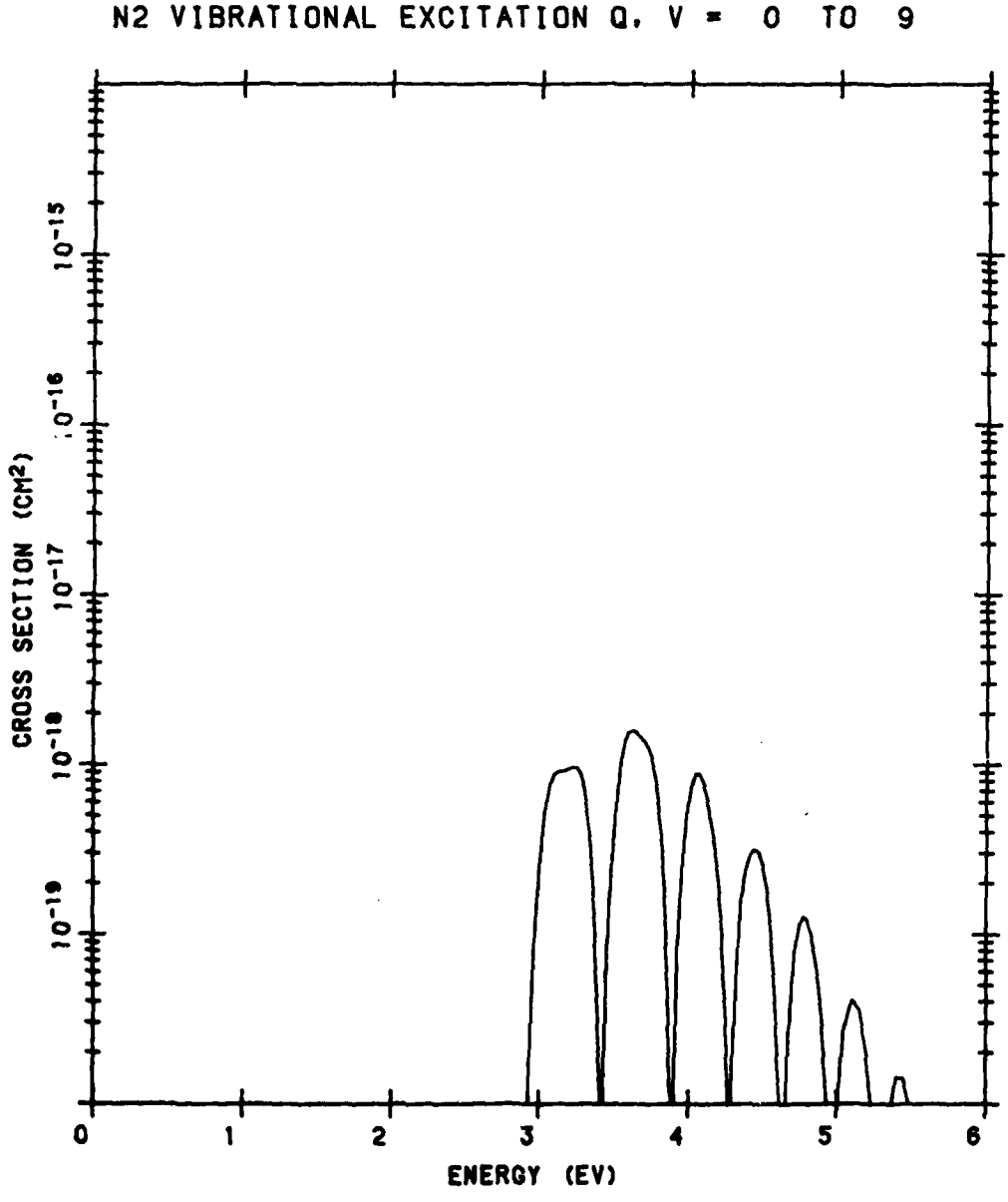


**Figure B48. $N_2$ Vibrational Excitation Cross Section from v of 0 to 9. The source of the data is the same as in Figure B42 (Cont.)**

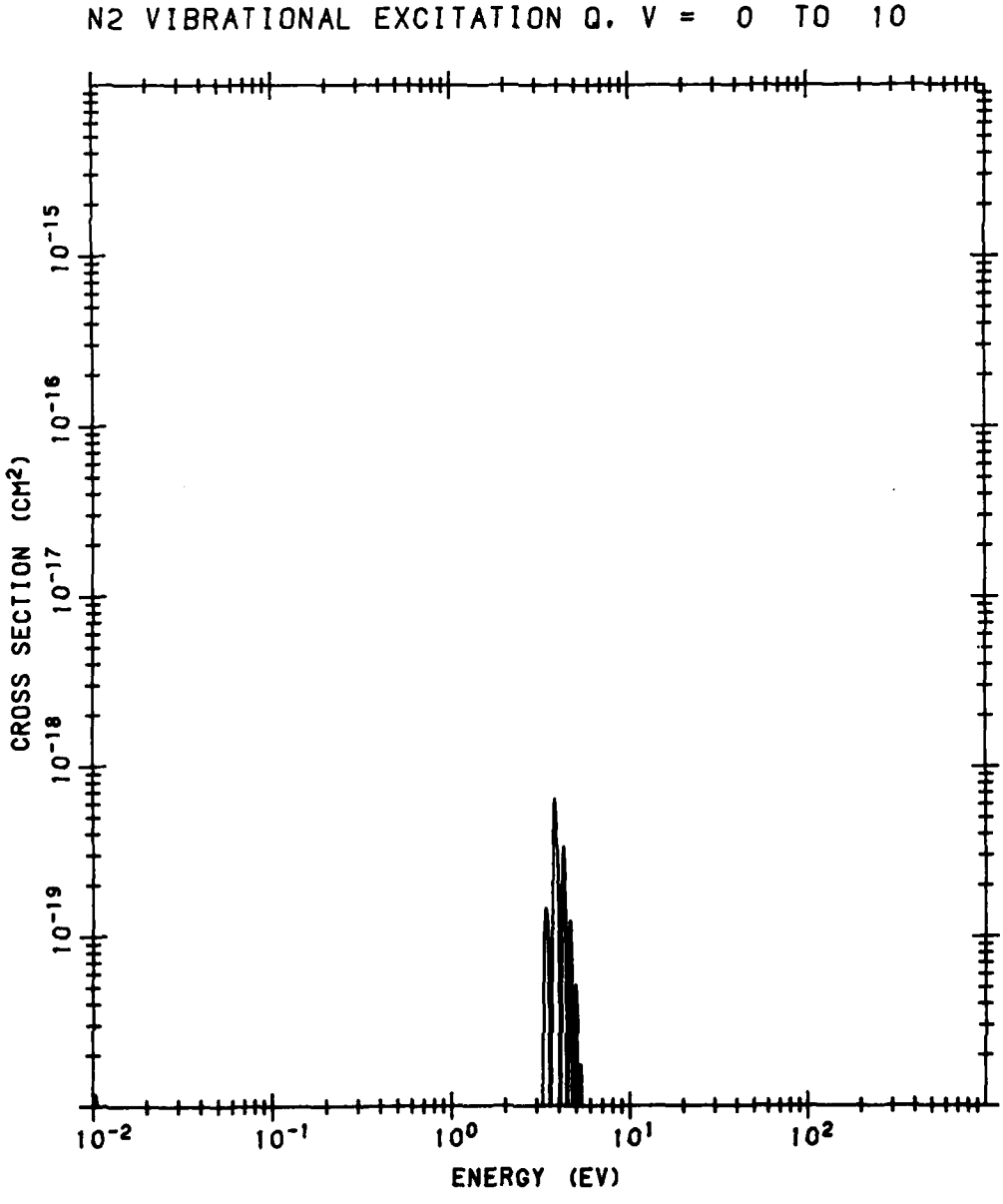


**Figure B49. $N_2$ Vibrational Excitation Cross Section from v of 0 to 10. The source of the data is the same as in Figure B42**

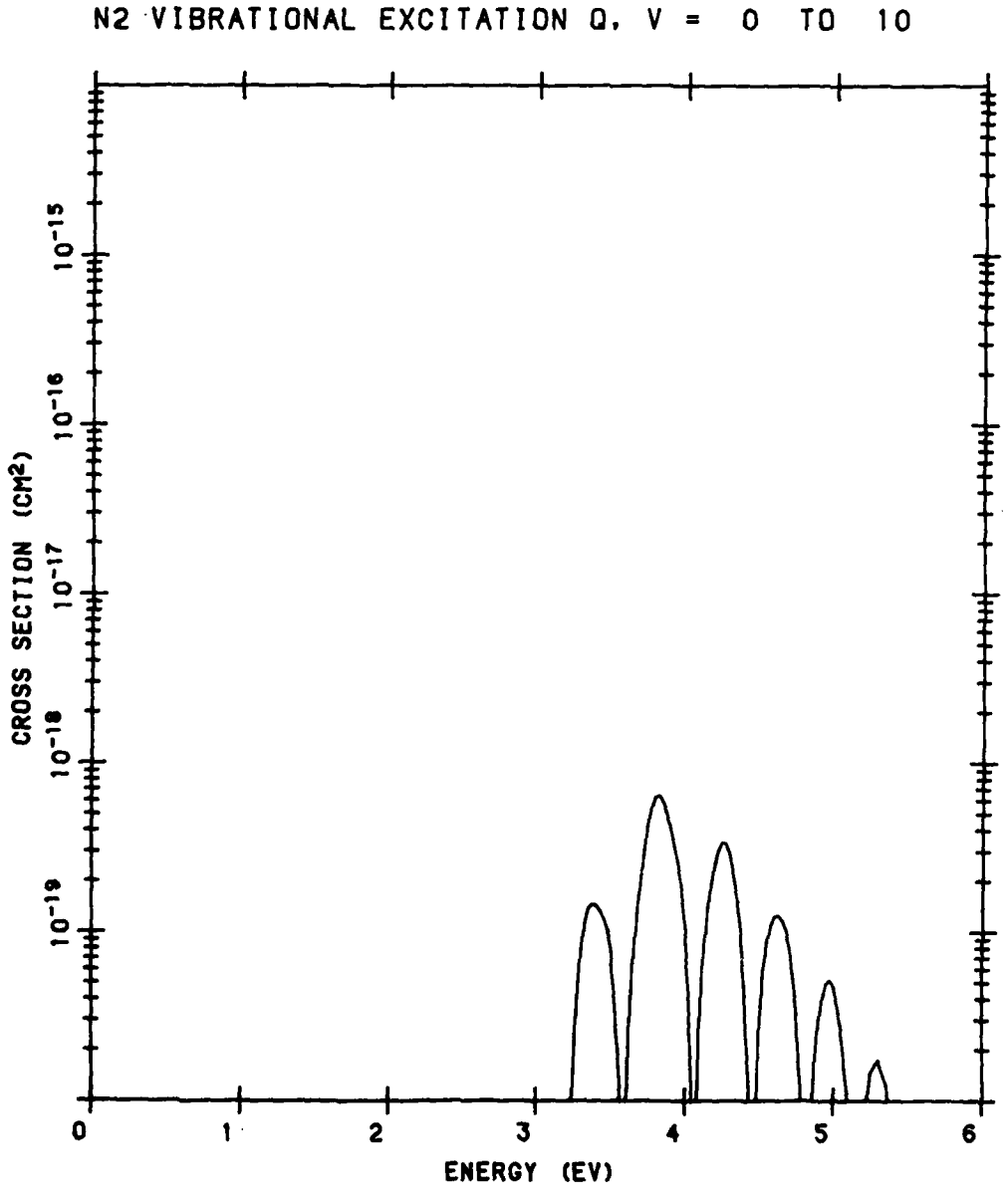


**Figure B49. $N_2$ Vibrational Excitation Cross Section from v of 0 to 10. The source of the data is the same as in Figure B42 (Cont.)**

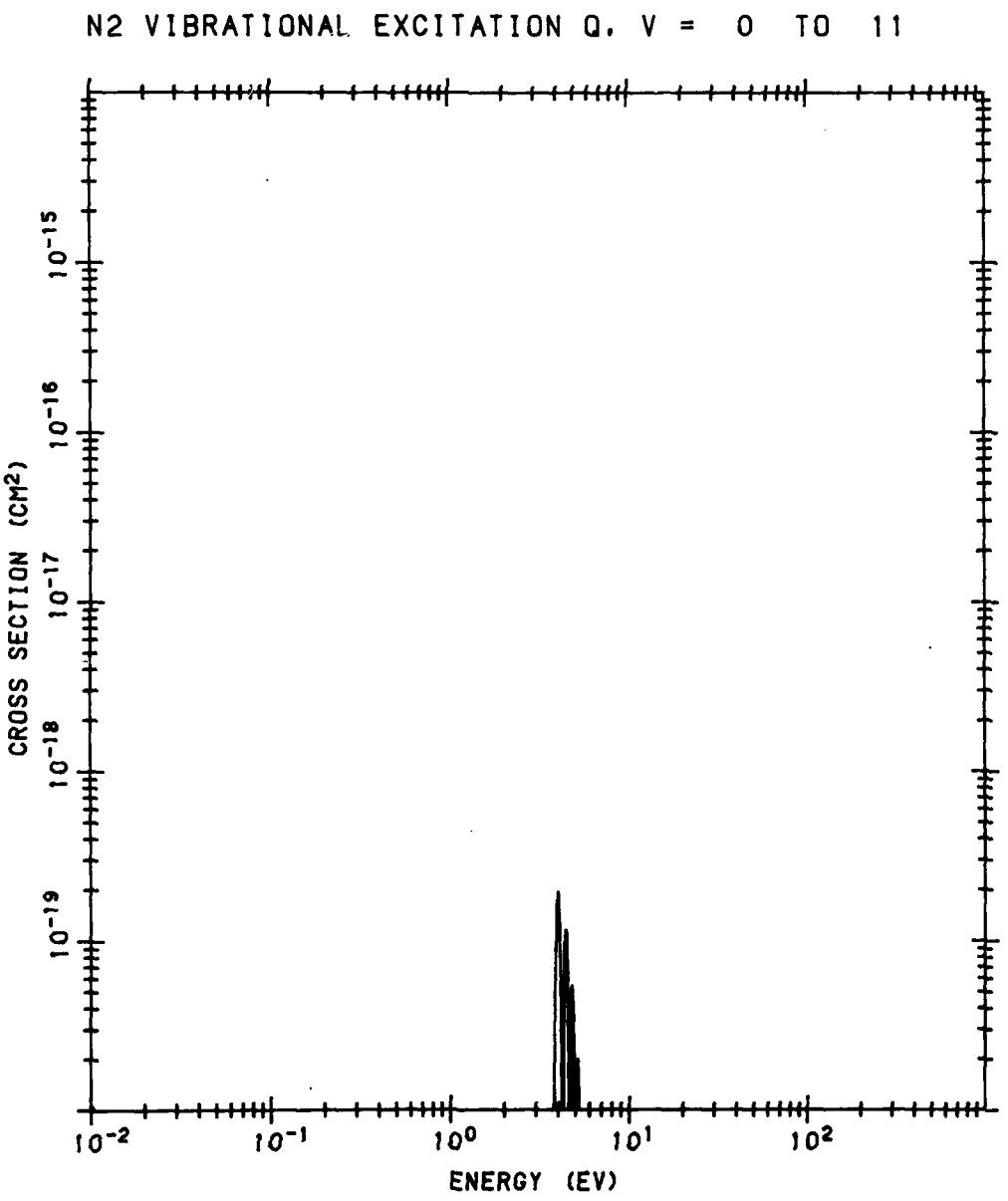


Figure B50. $N_2$ Vibrational Excitation Cross Section from v of 0 to 11. The source of the data is the same as in Figure B42

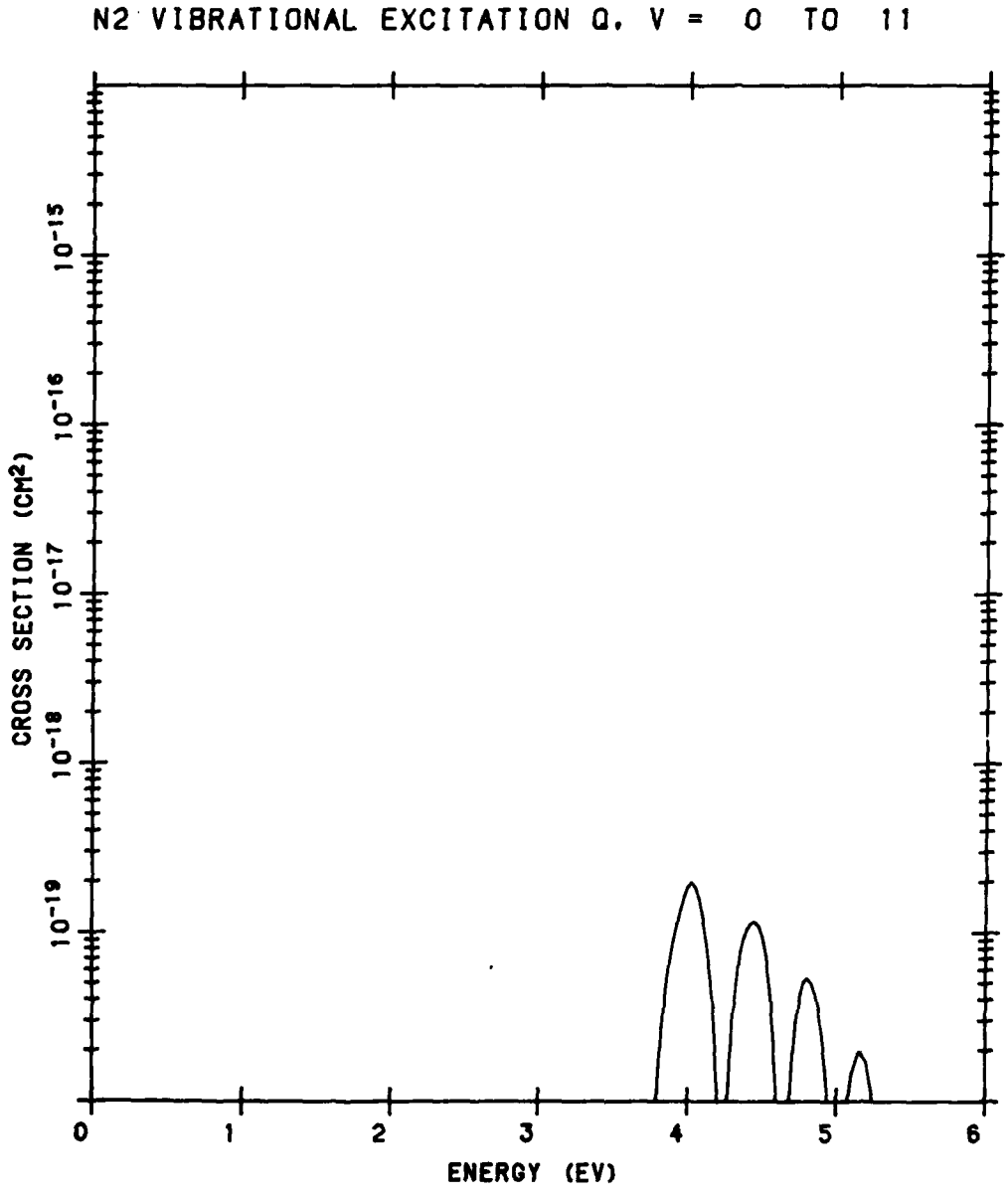


**Figure B50. $N_2$ Vibrational Excitation Cross Section from v of 0 to 11. The source of the data is the same as in Figure B42 (Cont.)**

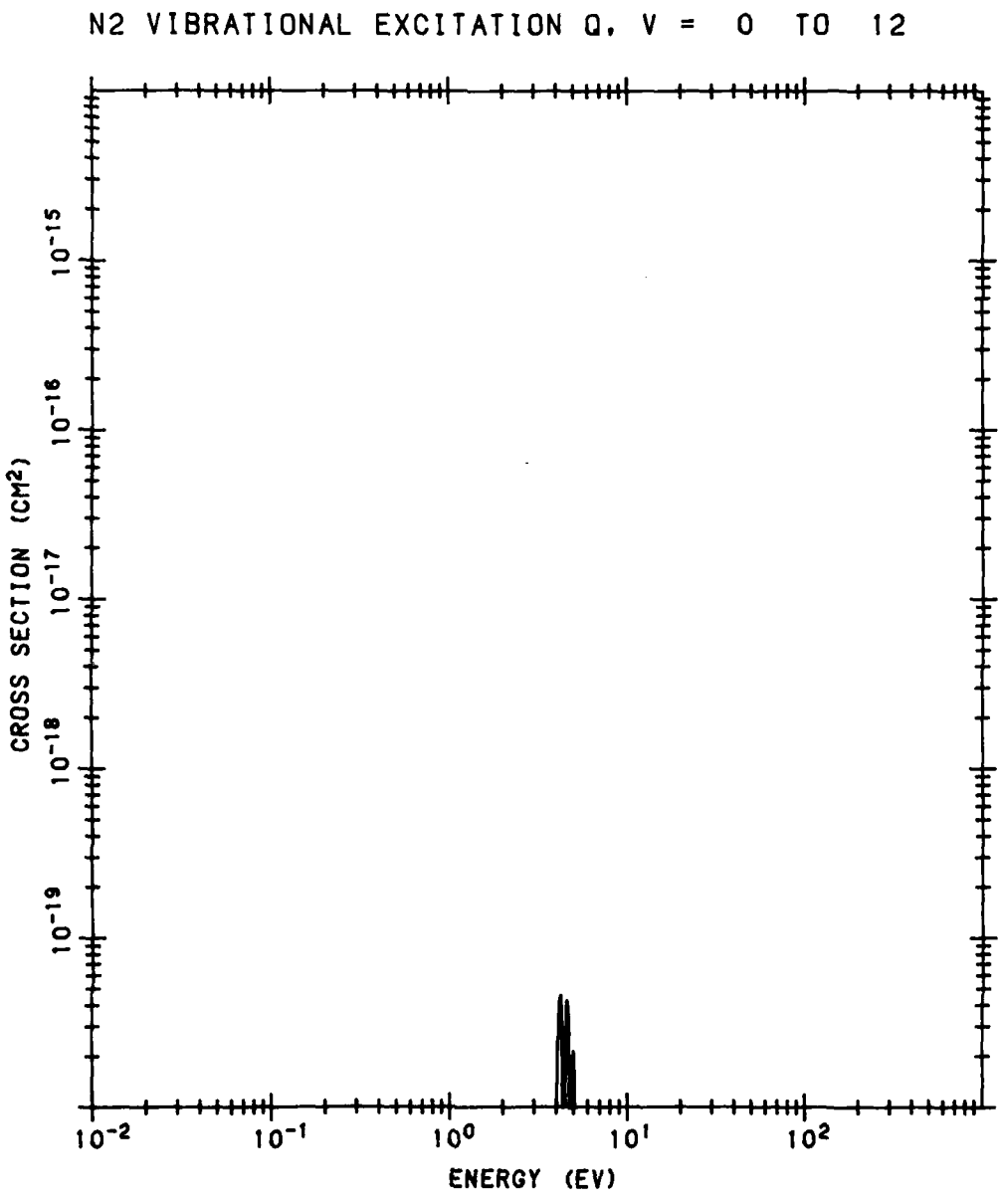


**Figure B51. $N_2$ Vibrational Excitation Cross Section from v of 0 to 12. The source of the data is the same as in Figure B42**

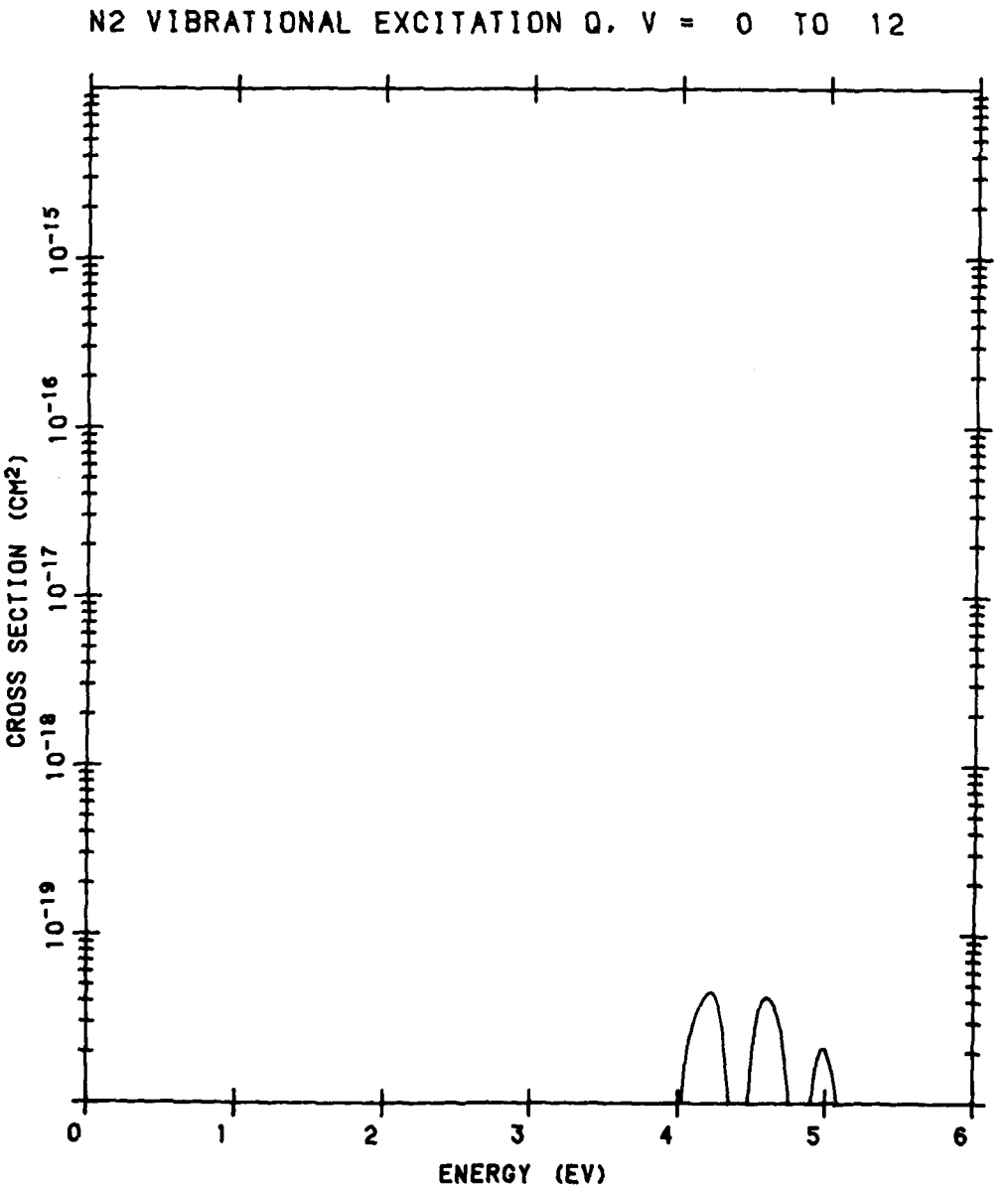


**Figure B51. $N_2$ Vibrational Excitation Cross Section from v of 0 to 12. The source of the data is the same as in Figure B42 (Cont.)**

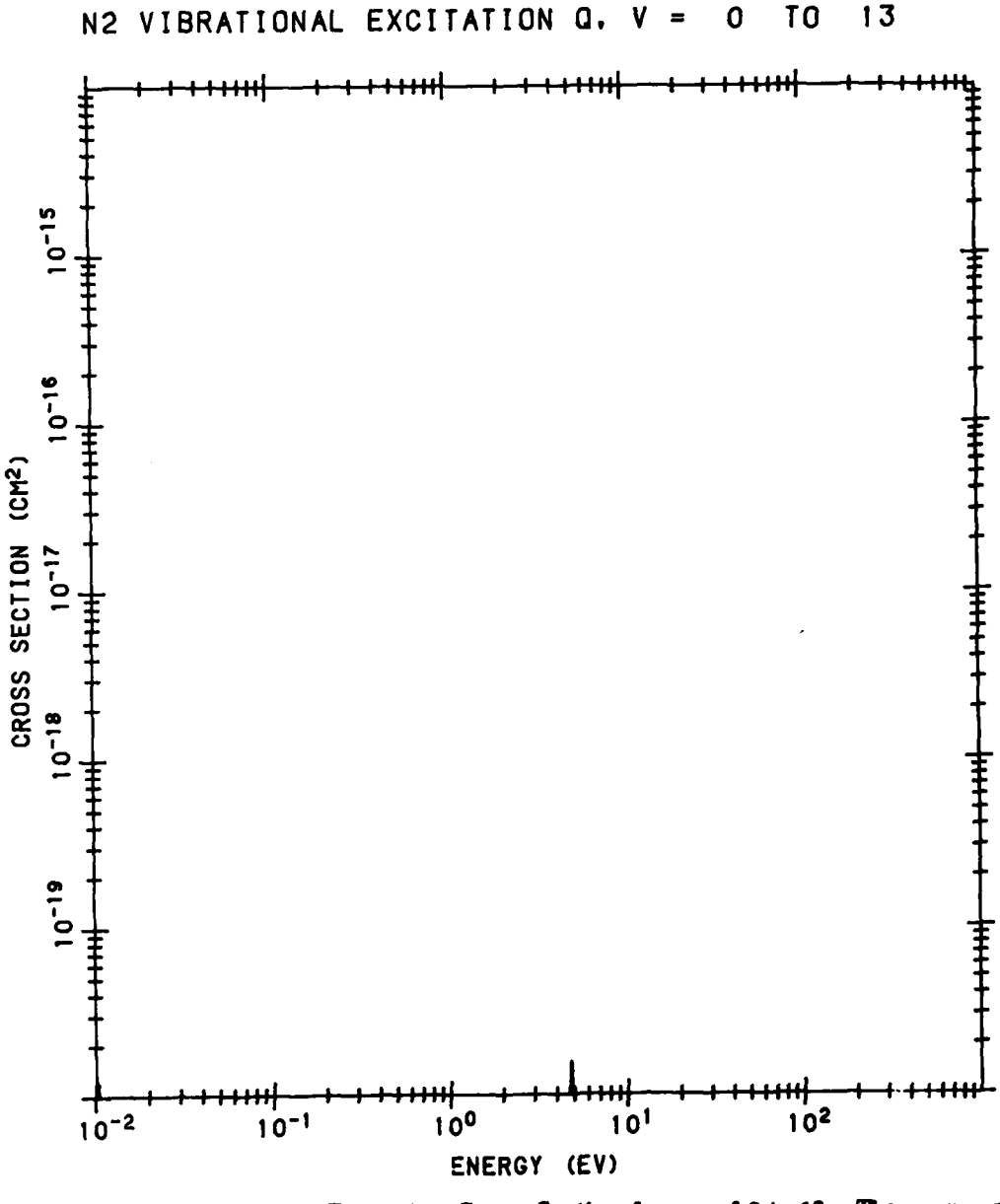


Figure B52. $N_2$ Vibrational Excitation Cross Section from v of 0 to 13. The source of the data is the same as in Figure B42

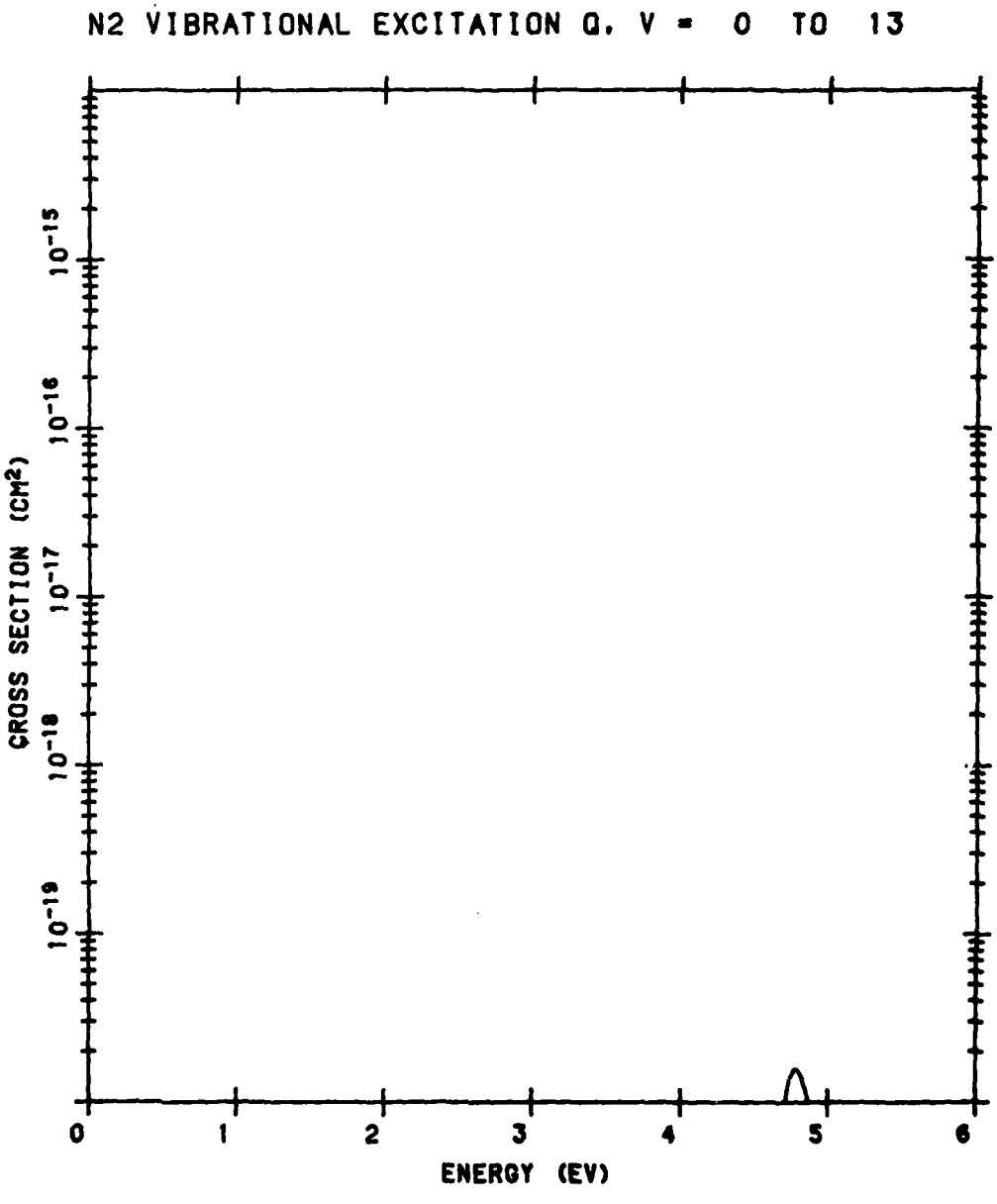


Figure B52. $N_2$ Vibrational Excitation Cross Section from v of 0 to 13. The source of the data is the same as in Figure B42 (Cont.)

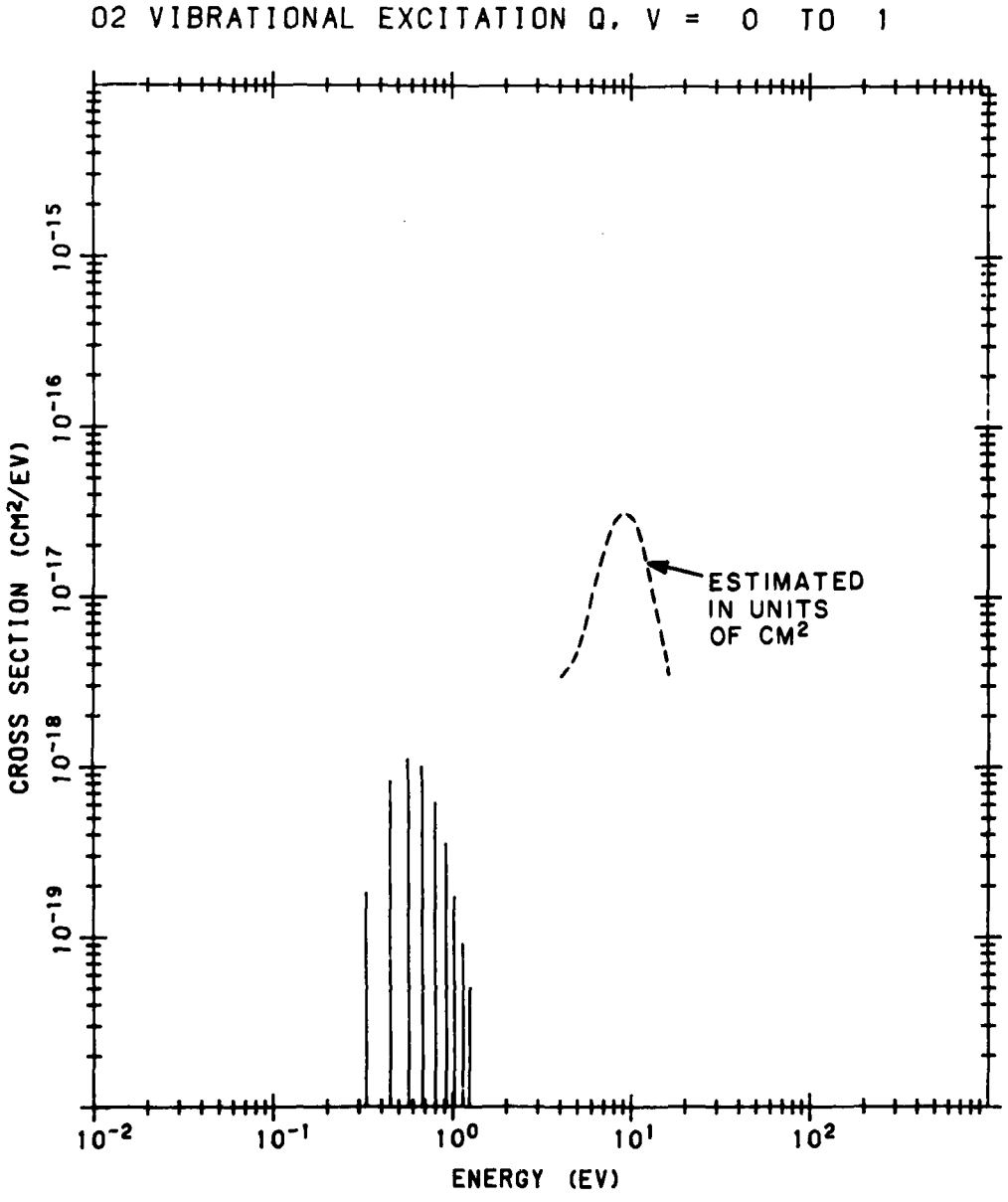


Figure B53. $O_2$ Vibrational Excitation Cross Sections from v of 0 to 1. The low energy data are from Linder and Schmidt (1971)[B17] and from Koike (1973)[B18]. Near 9.5 eV the cross section is estimated by integrating the differential cross section of Wong et al (1973)[B19], measured at 25°, assuming the same angular dependence as that for $N_2$ calculated by Chandra and Temkin (1976)[B8].


B17. Linder, F., and Schmidt, H. (1971) Z. Naturforsch 26:1617.

B18. Koike, F. (1973) J. Phys. Soc. Japan 35:1166.

B19. Wong, S.F., Boness, M.J.W., and Schulz, G.S. (1973) Phys. Rev. Lett. 31:699.

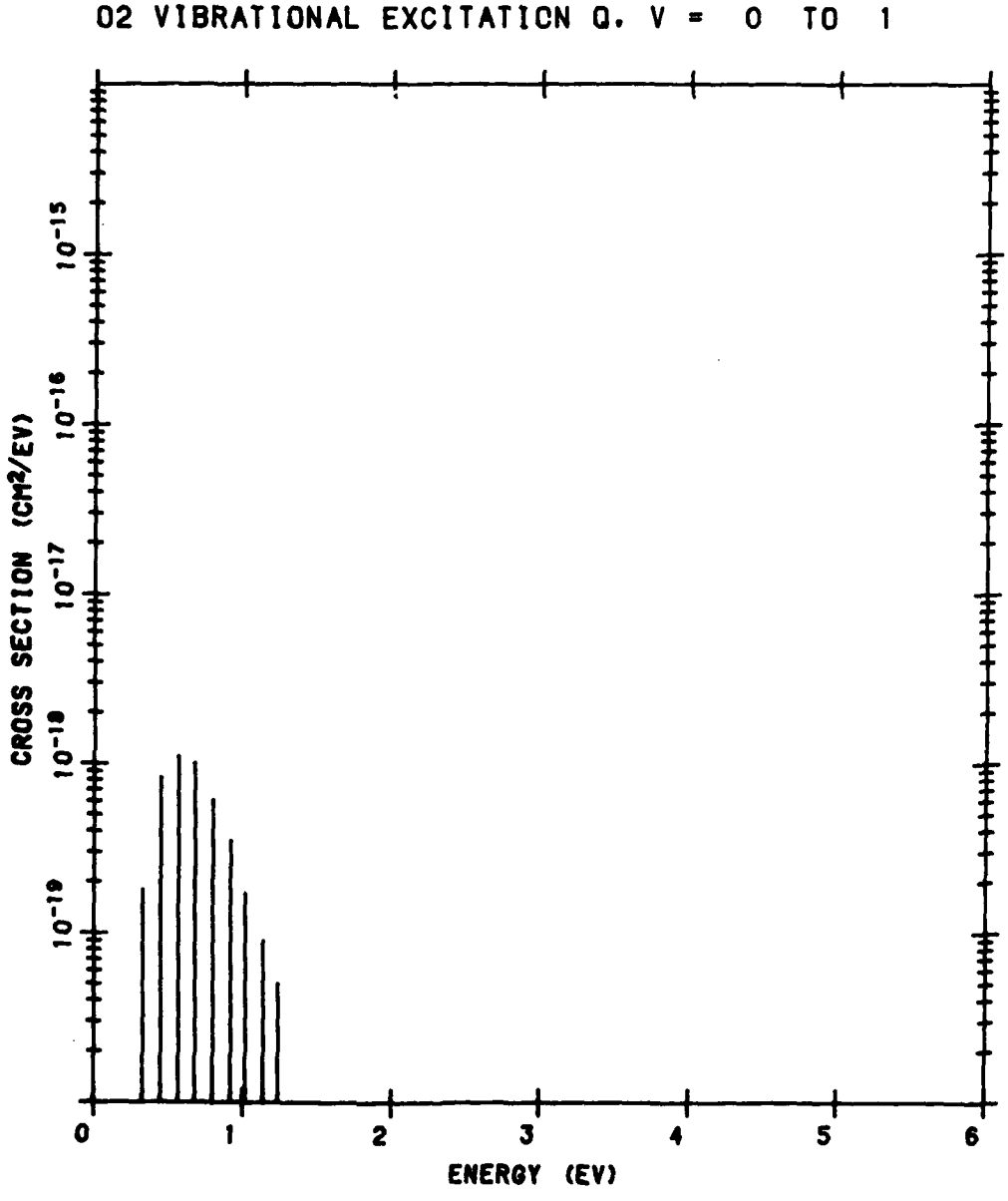


**Figure B53. $O_2$ Vibrational Excitation Cross Sections from v of 0 to 1. The data are from Linder and Schmidt (1971)[B17] and from Koike (1973)[B18] (Cont.)**

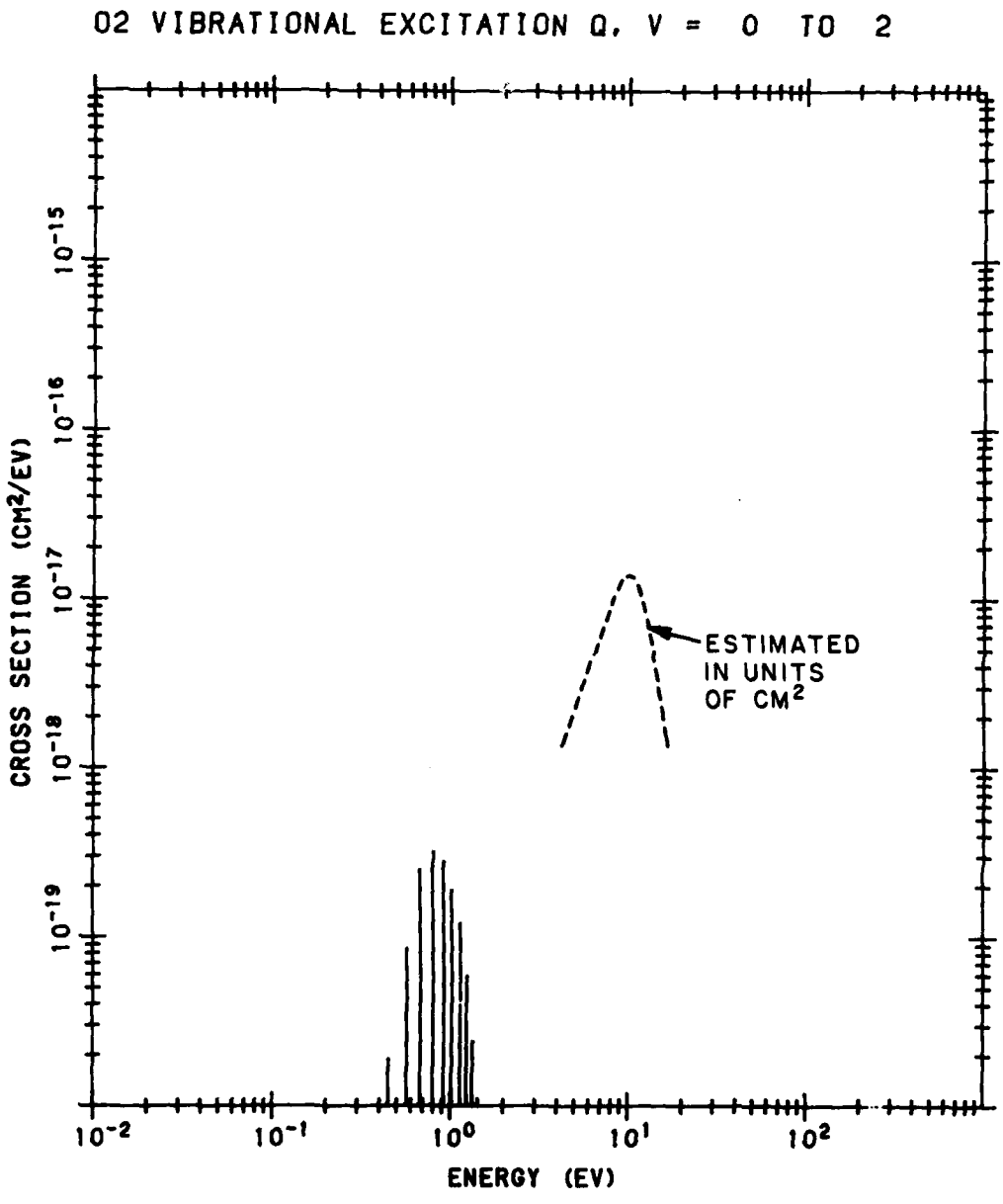


**Figure B54. $O_2$ Vibrational Excitation Cross Sections from v of 0 to 2. The source of the data is the same as in Figure B53**

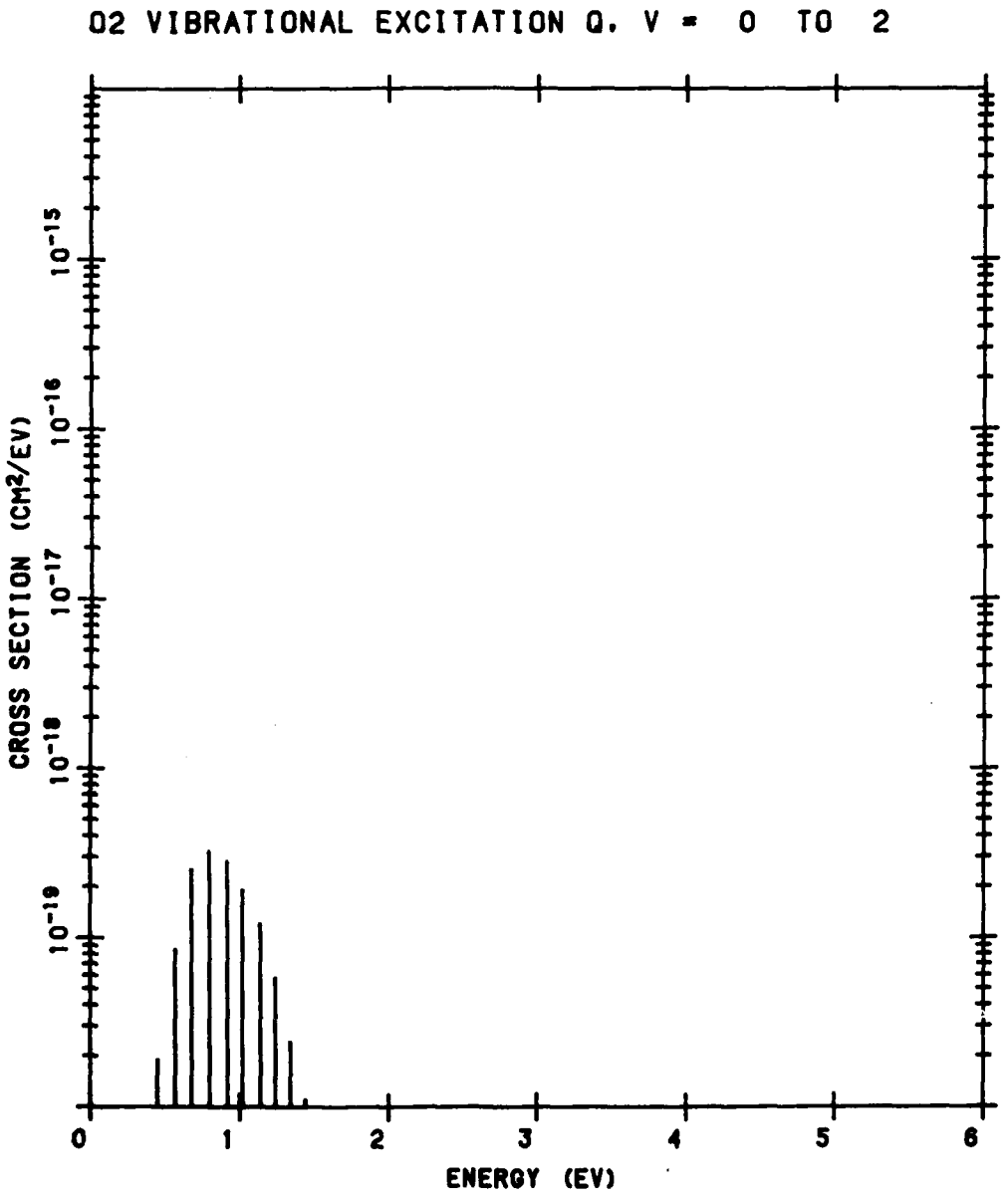


**Figure B54. $O_2$ Vibrational Excitation Cross Sections from v of 0 to 2. The source of the data is the same as in Figure B53 (Cont.)**

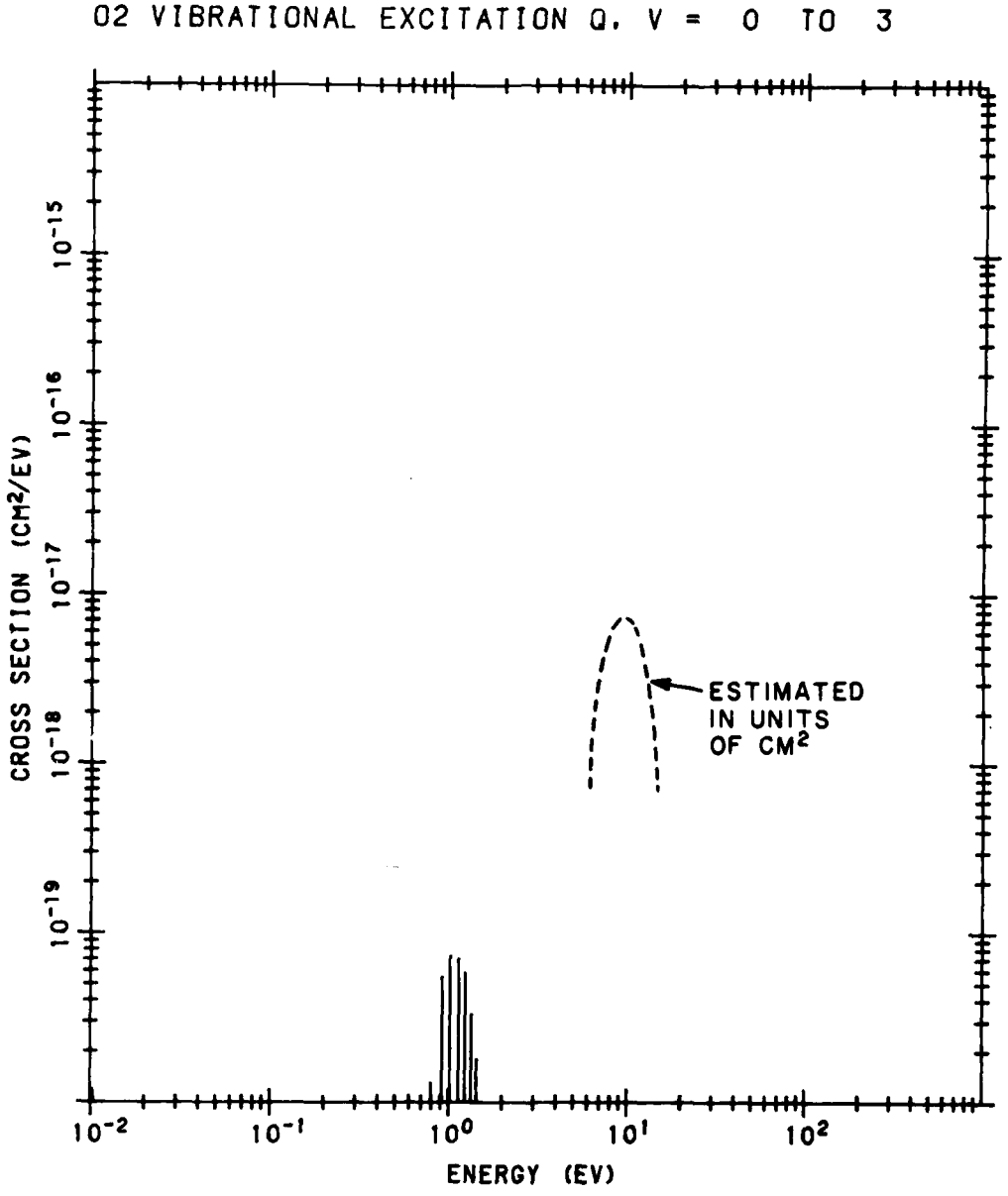


Figure B55. $O_2$ Vibrational Excitation Cross Section from v of 0 to 3. The low energy data are from Linder and Schmidt (1971)[B17]. Near 9.5 eV the cross section is estimated by integrating the differential cross section of Wong et al (1973)[B19], measured at 25°, assuming the same angular dependence as that for $N_2$ calculated by Chandra and Temkin (1976)[B8].

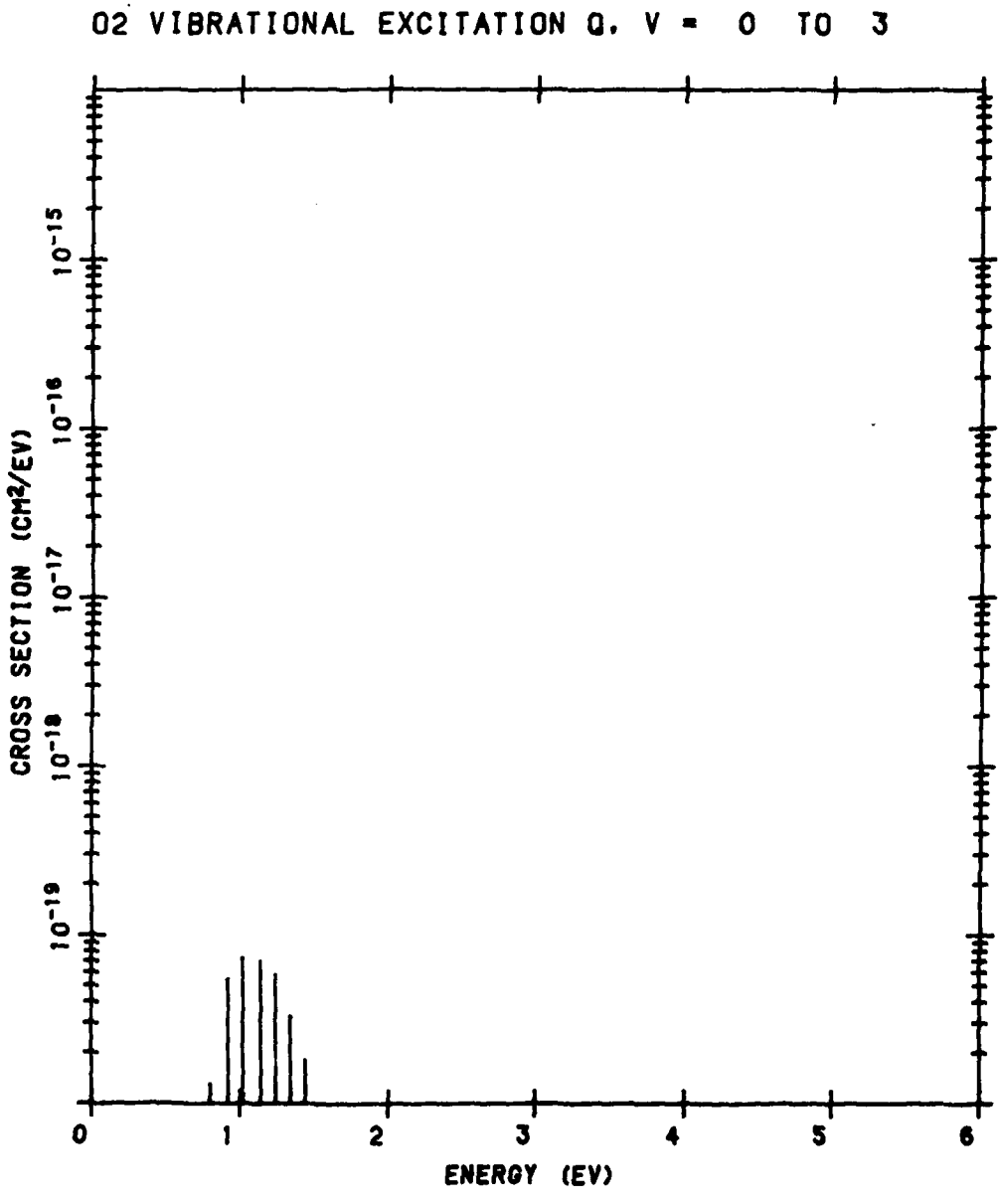


Figure B55. $O_2$ Vibrational Excitation Cross Sections from v of 0 to 3. The data are from Linder and Schmidt (1971)[B16] (Cont.)

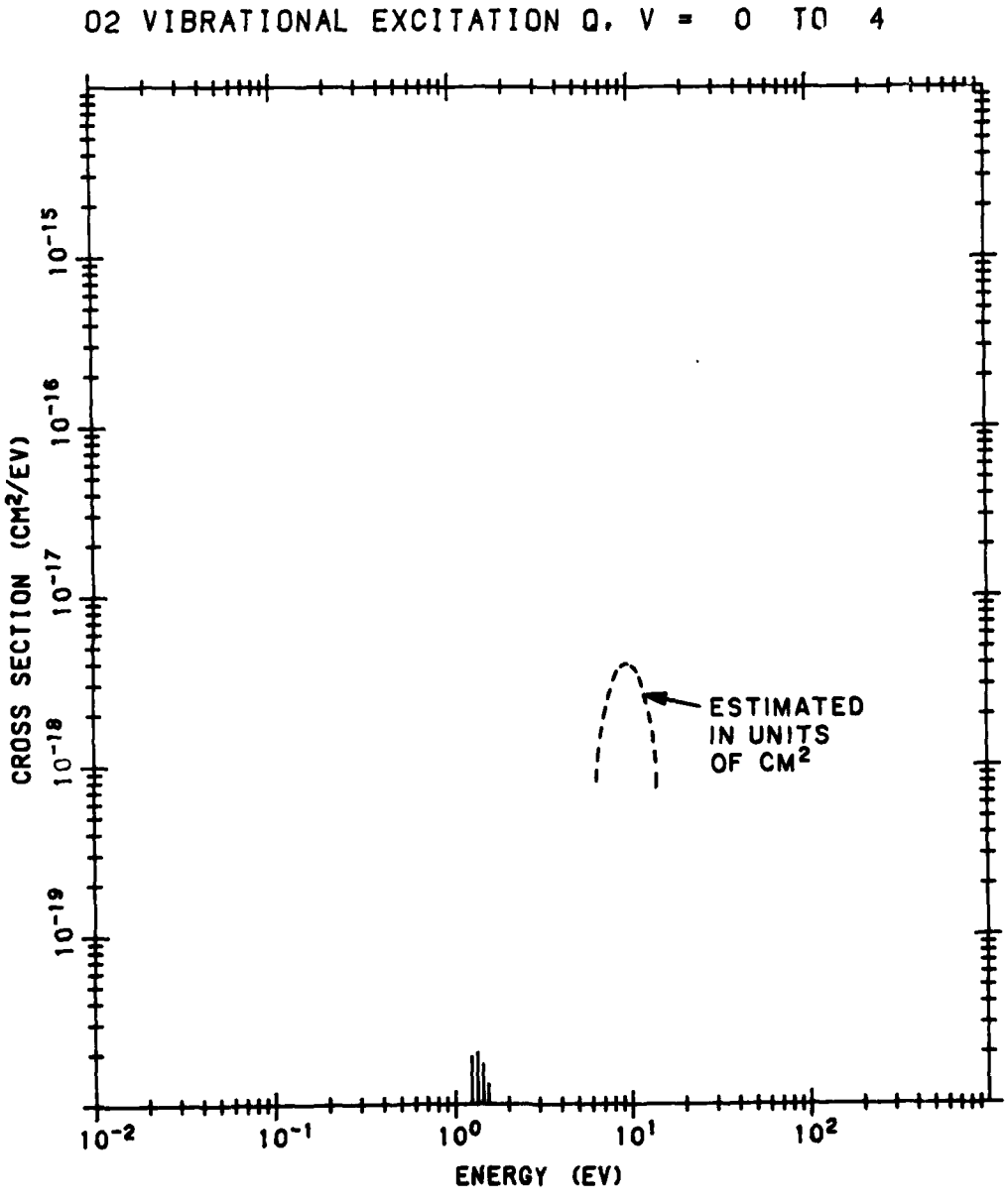


**Figure B56. $O_2$ Vibrational Excitation Cross Sections from v of 0 to 4. The source of the data is the same as in Figure B55**

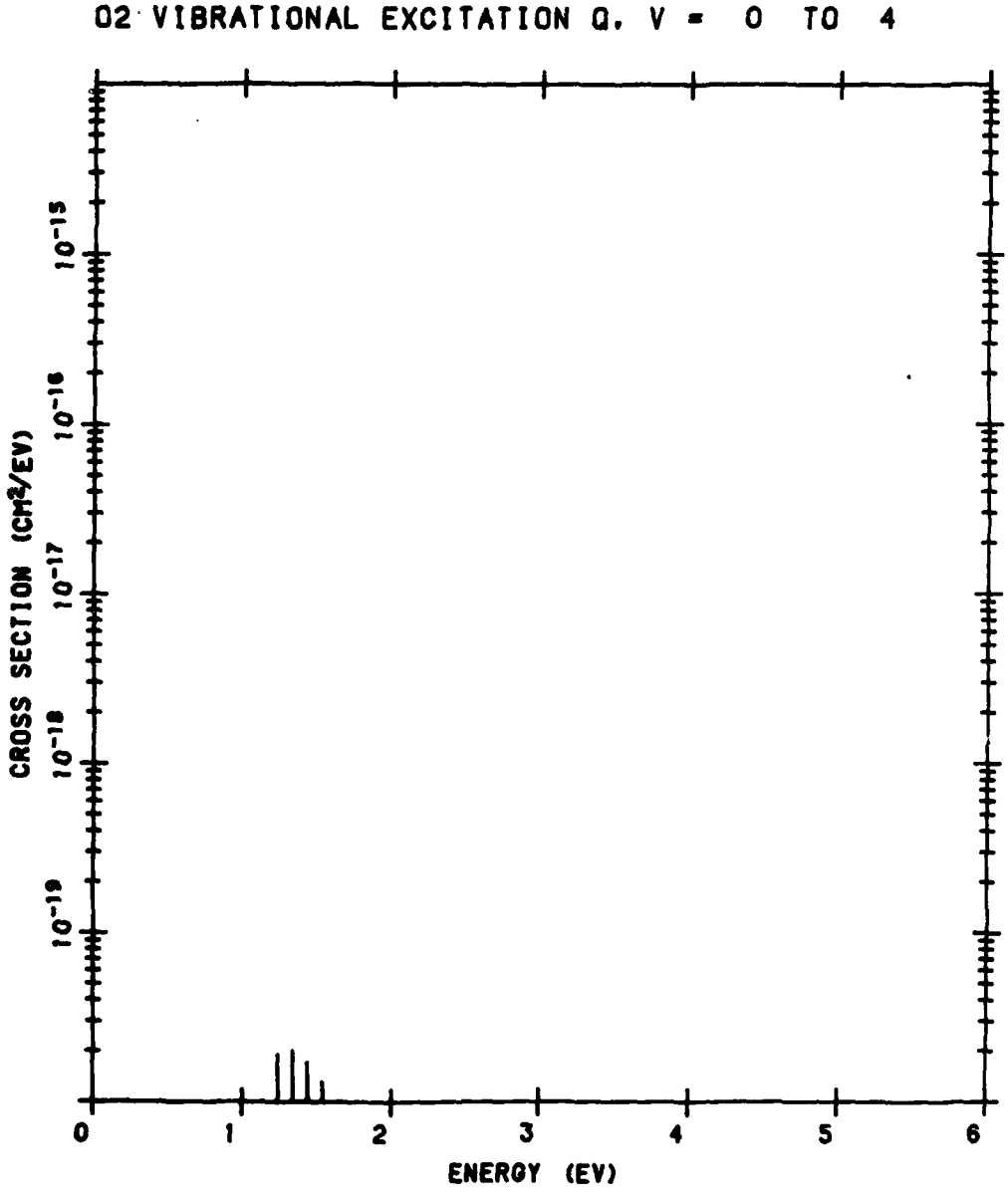


**Figure B56. $O_2$ Vibrational Excitation Cross Sections from v of 0 to 4. The source of the data is the same as in Figure B55 (Cont.)**

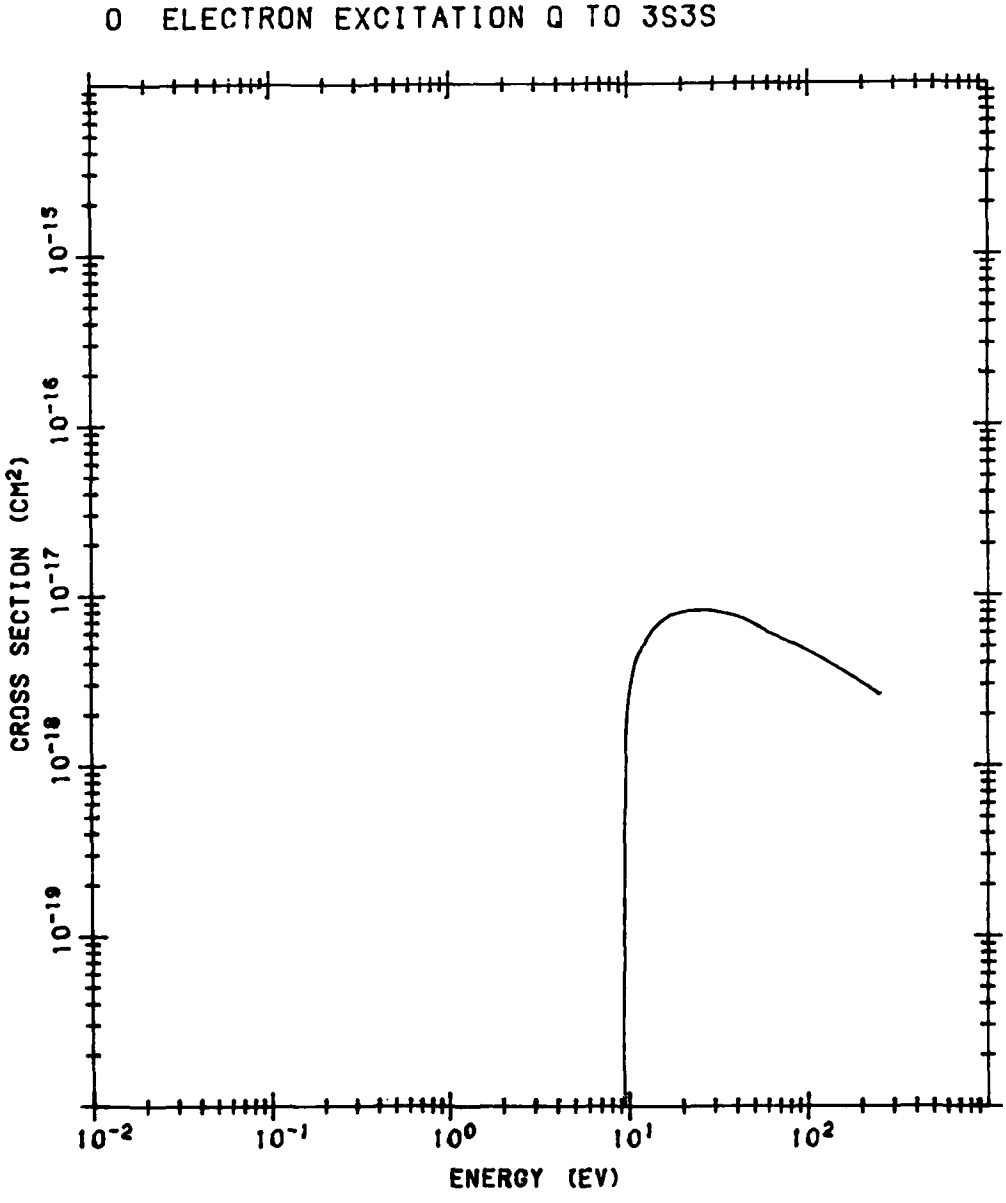


Figure B57. O Electron Excitation Cross Section to $(^4S^o)3s\ ^3S^o$. The data below 40.8 eV are from Smith (1976);[B20] at 60 eV from Rountree and Henry (1972);[B21] and extrapolated to higher energies using (log E)/E

B20. Smith, E.R. (1976) Phys. Rev. 13:A65.

B21. Rountree, S.P., and Henry, R.J.W. (1972) Phys. Rev. A6:2106.

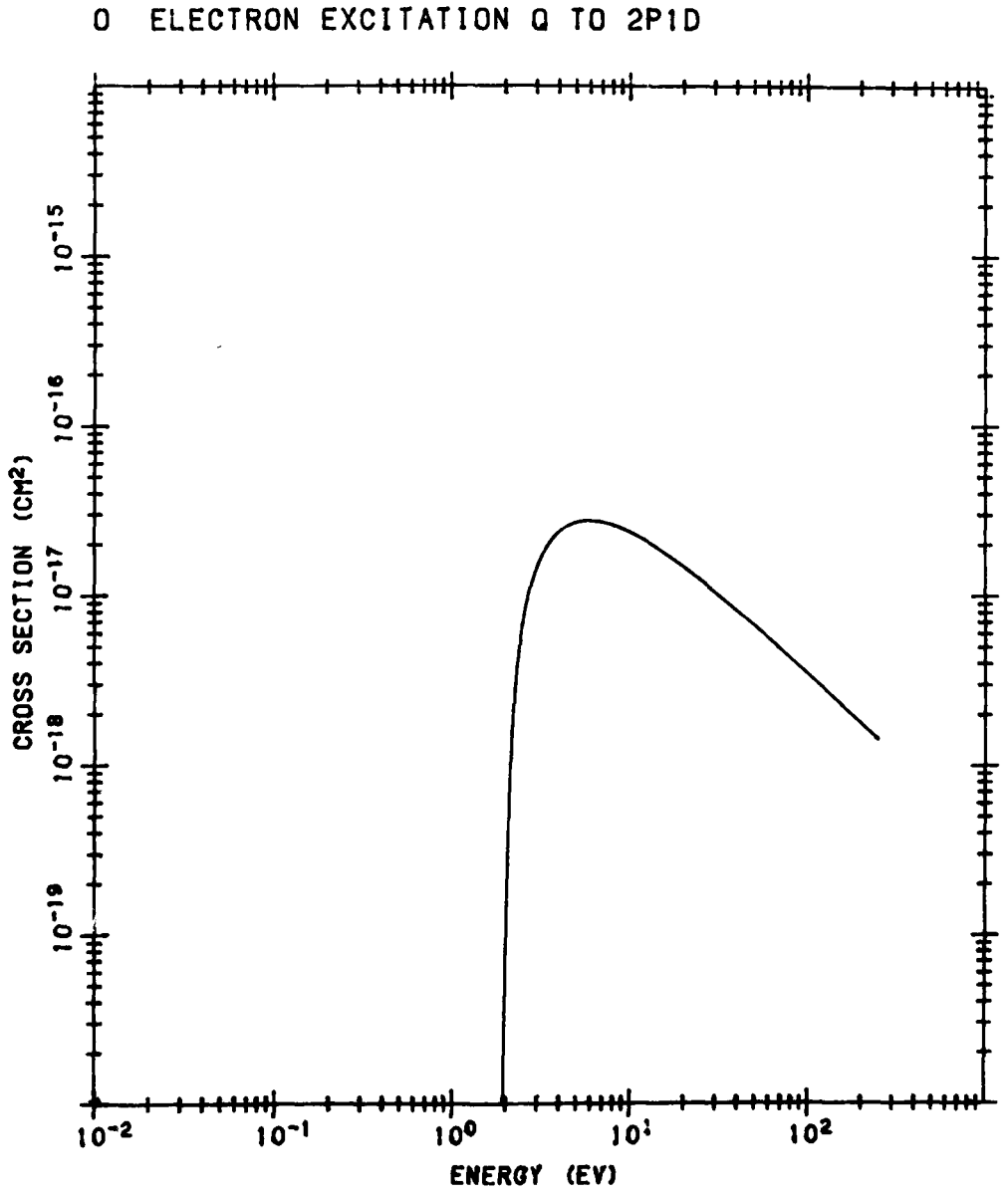


**Figure B58. O Electron Excitation Cross Section to $2p^4\ ^1D$. The data are from Jackman et al (1980)[B22] with the F parameter modified to 0.011 for better agreement with Vo Ky Lan et al (1972)[B23]**

B22. Jackman, C.H., Garvey, R.H., and Green, A.E.S. (1980) Private communication.

B23. Vo Ky Lan, Feautrier, N., LeDournef, M., and Regemorter, H. van (1972) J. Phys. 13:1506.

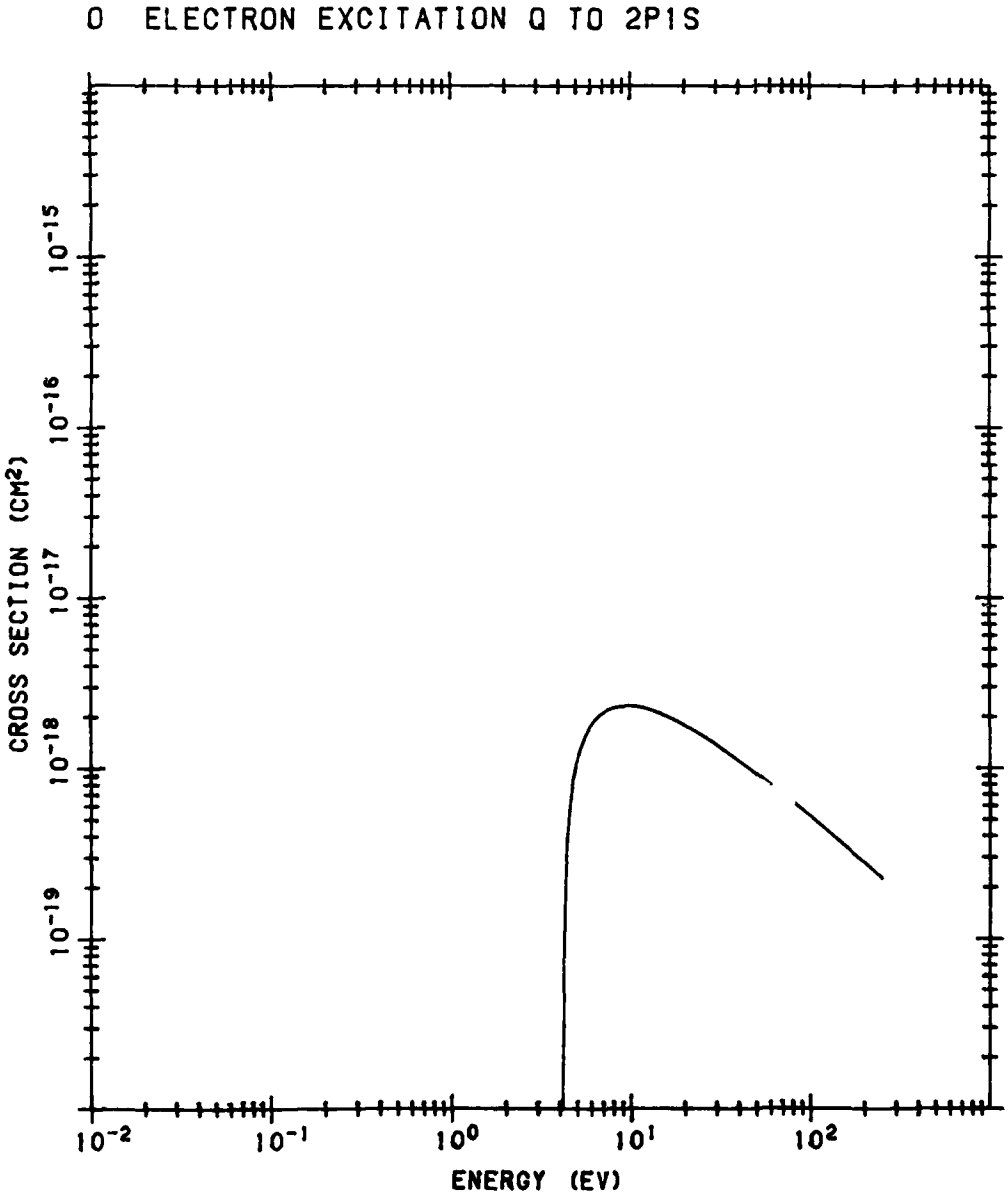


Figure B59. O Electron Excitation Cross Section to $2p^4\ ^1S$. The data are from Jackman et al (1980)[B22]

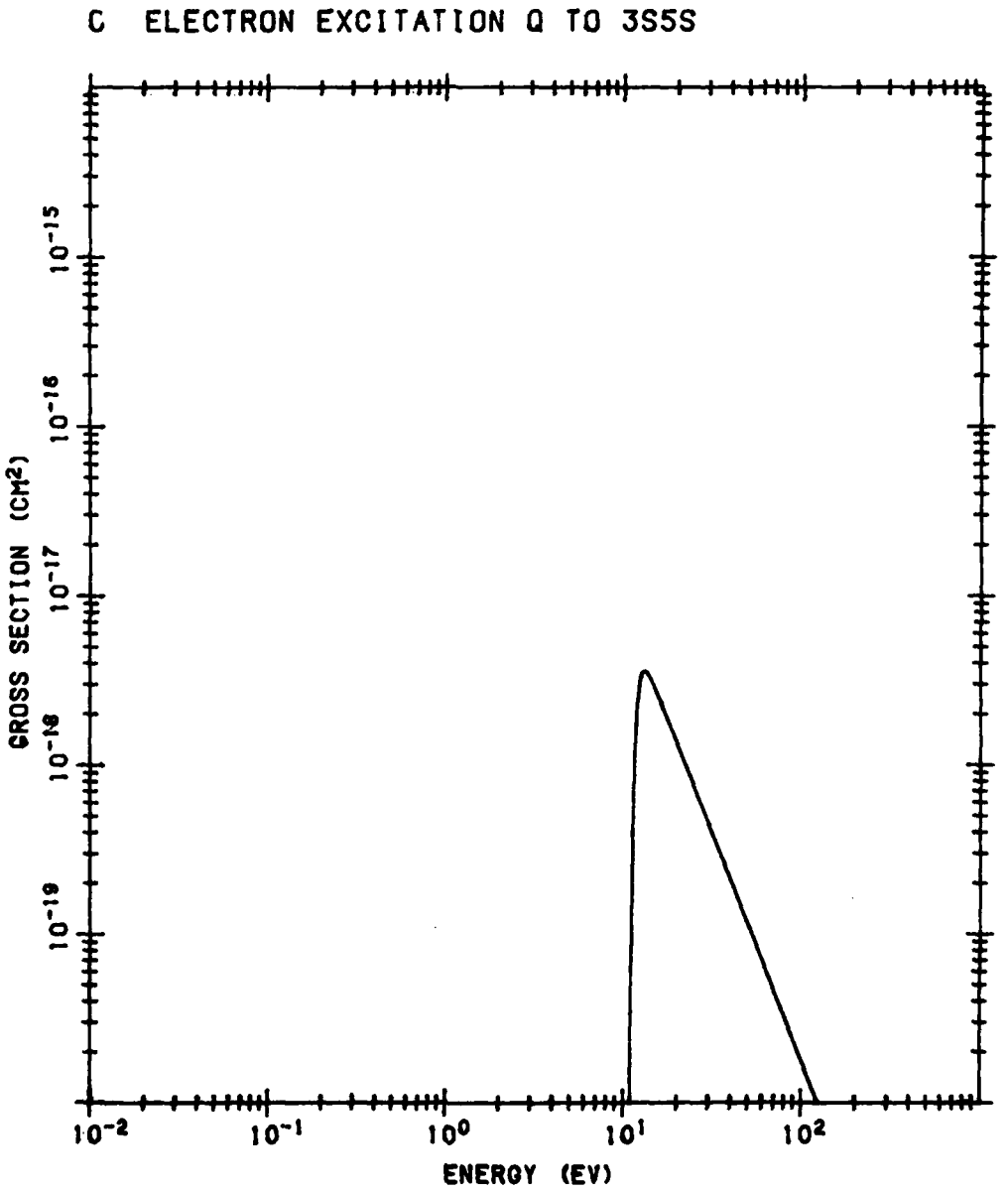


Figure B60. O Electron Excitation Cross Section to ($^4S^o$) 3s $^5S^o$. The source of the data is the same as in Figure B59

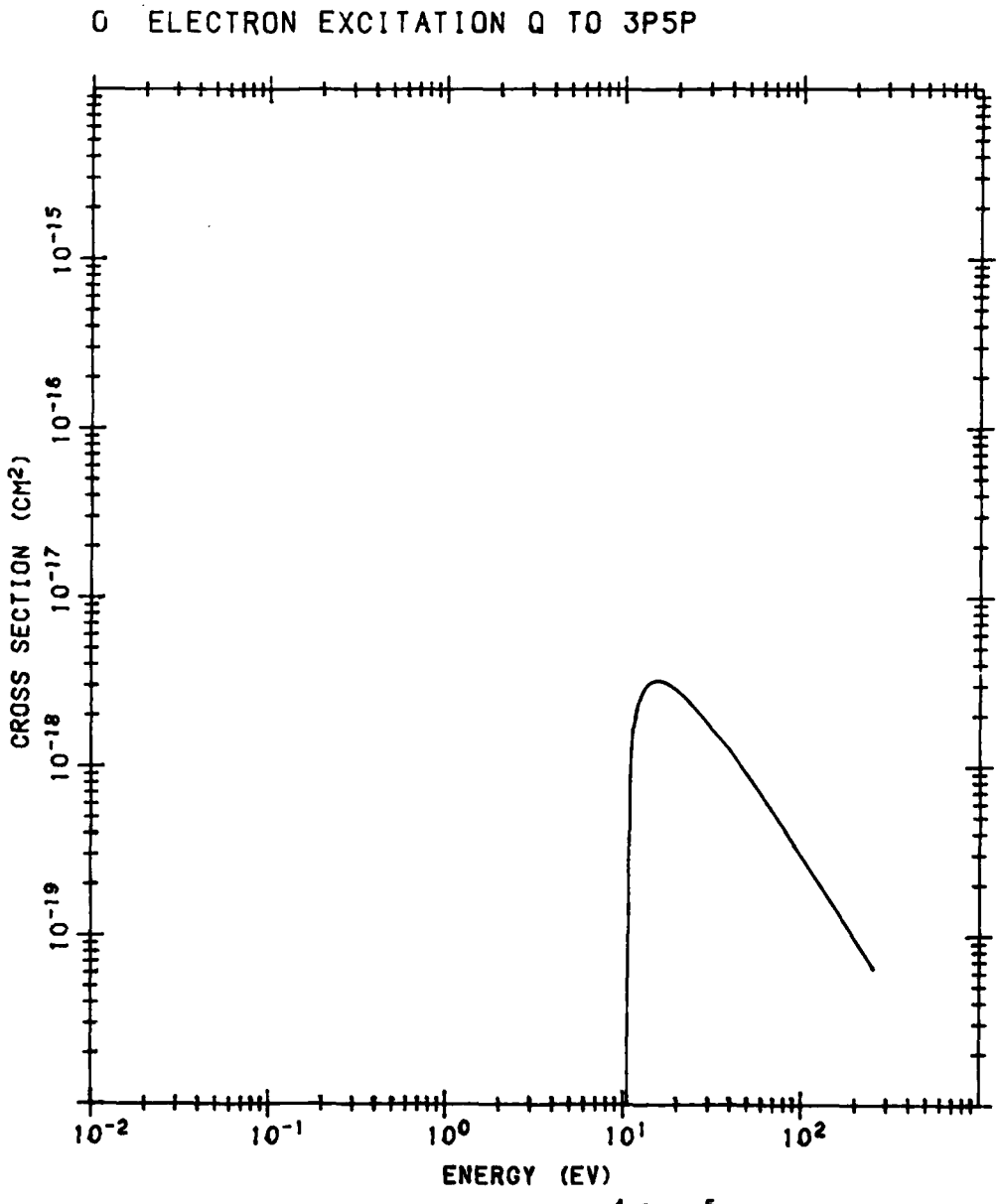


Figure B61. O Electron Excitation Cross Section to ($^4S^o$) 3p $^5P$. The source of the data is the same as in Figure B59

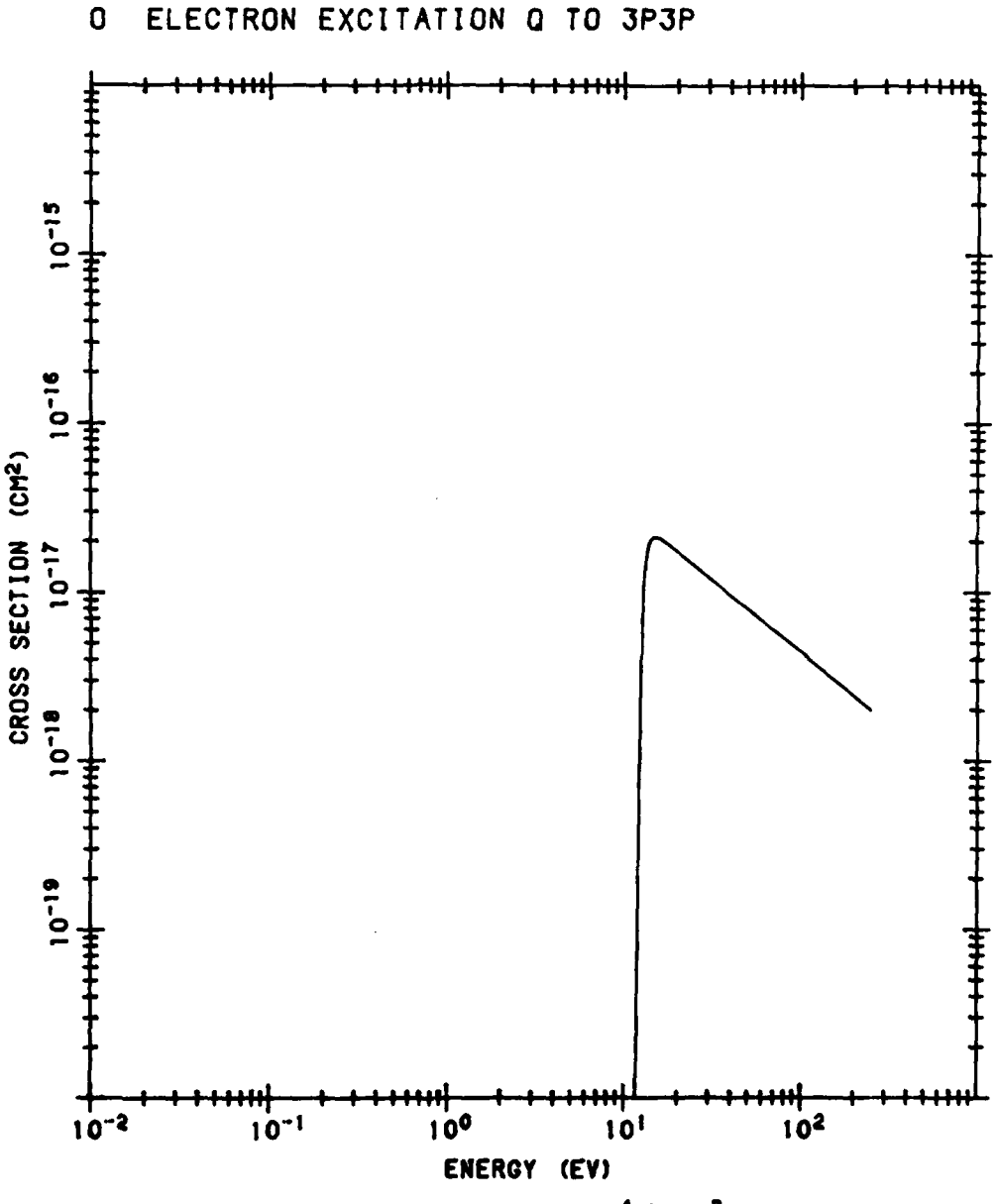


**Figure B62. O Electron Excitation Cross Section to ($^4S^o$) 3p $^3P$. The source of the data is the same as in Figure B59**

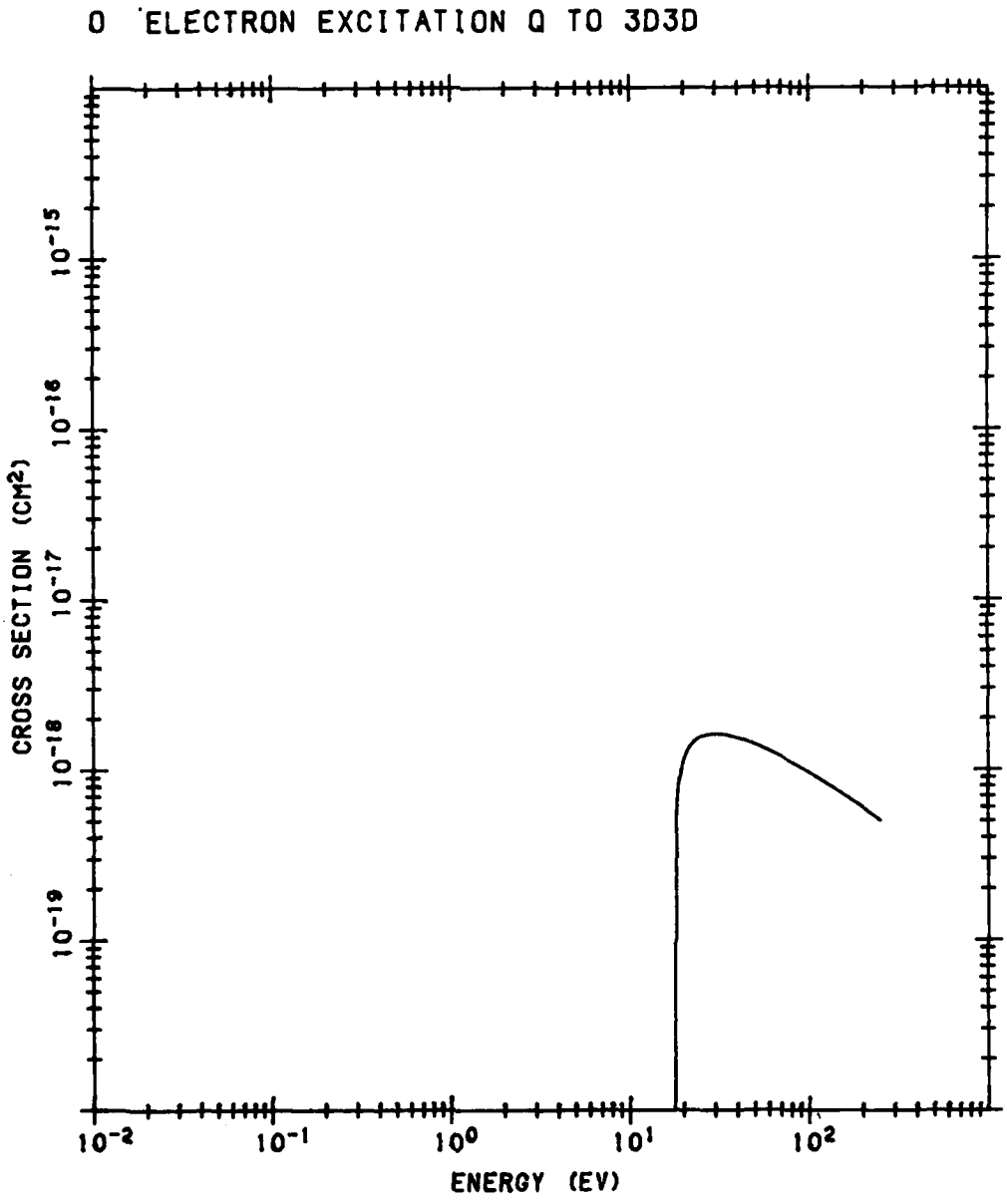


Figure B63. O Electron Excitation Cross Section to $(^4S^o)\,3d\,^3D^o$. The data are from Jackman et al (1980)[B22] with the F parameter modified to 0.009 for better agreement with Smith (1976)[B20]

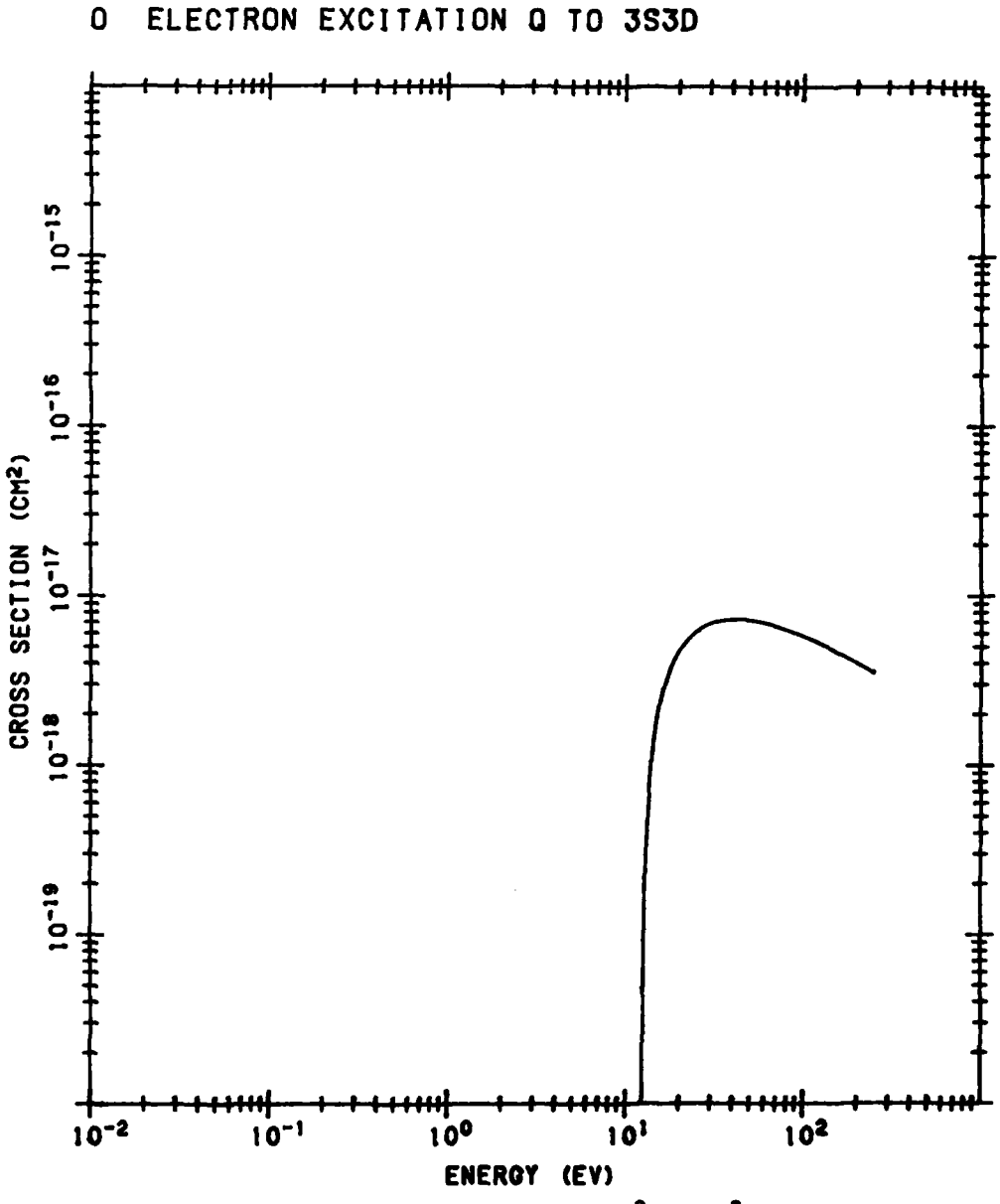


**Figure B64. O Electron Excitation Cross Section to ($^2D^o$) 3s $^3D^o$. The source of the data is the same as in Figure B59**

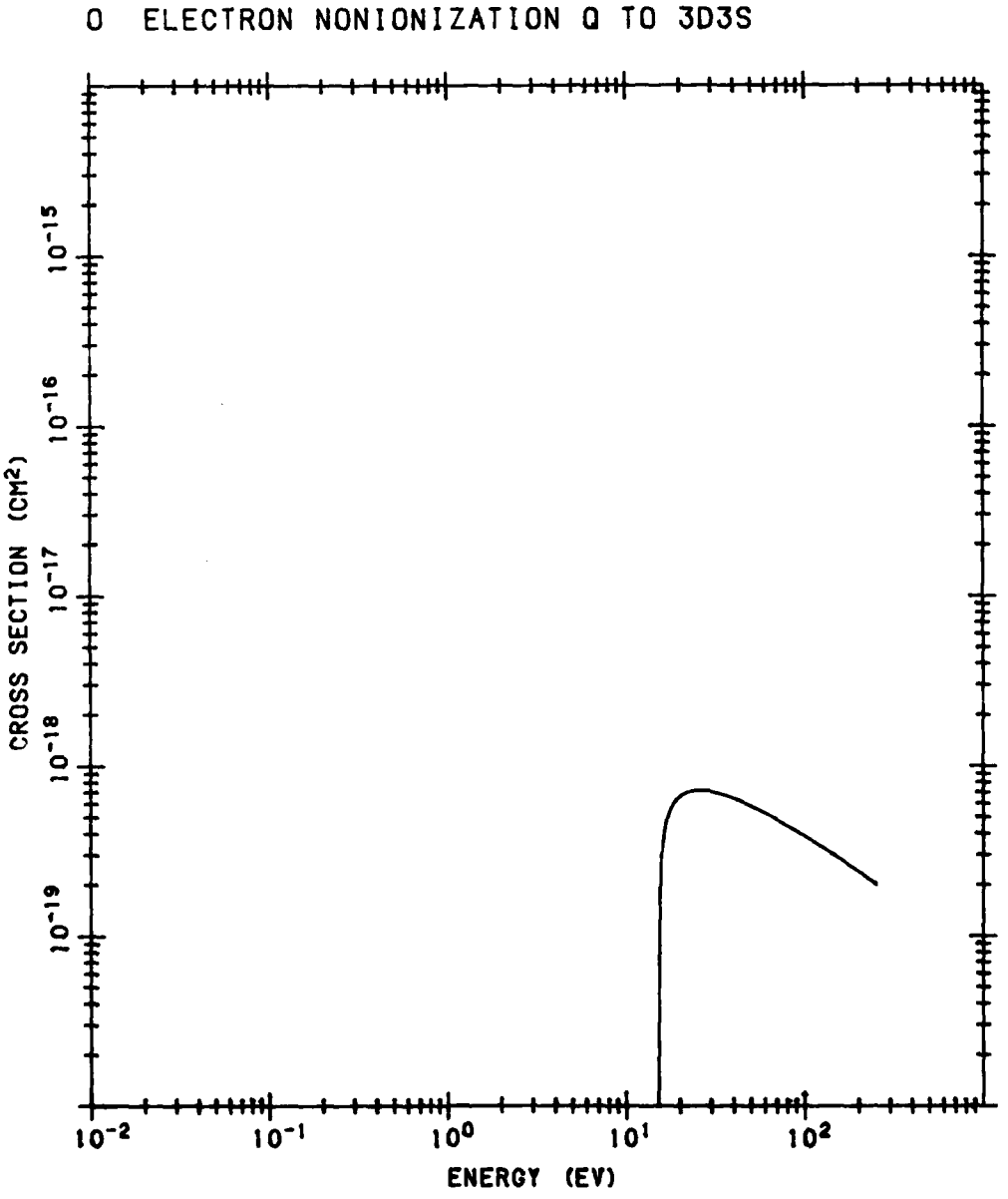


**Figure B65. O Electron Excitation Cross Section to ($^2D^o$) 3d $^3S^o$. The data are from Jackman et al (1980)[B22] weighted by the fraction of excitations that decay radiatively**

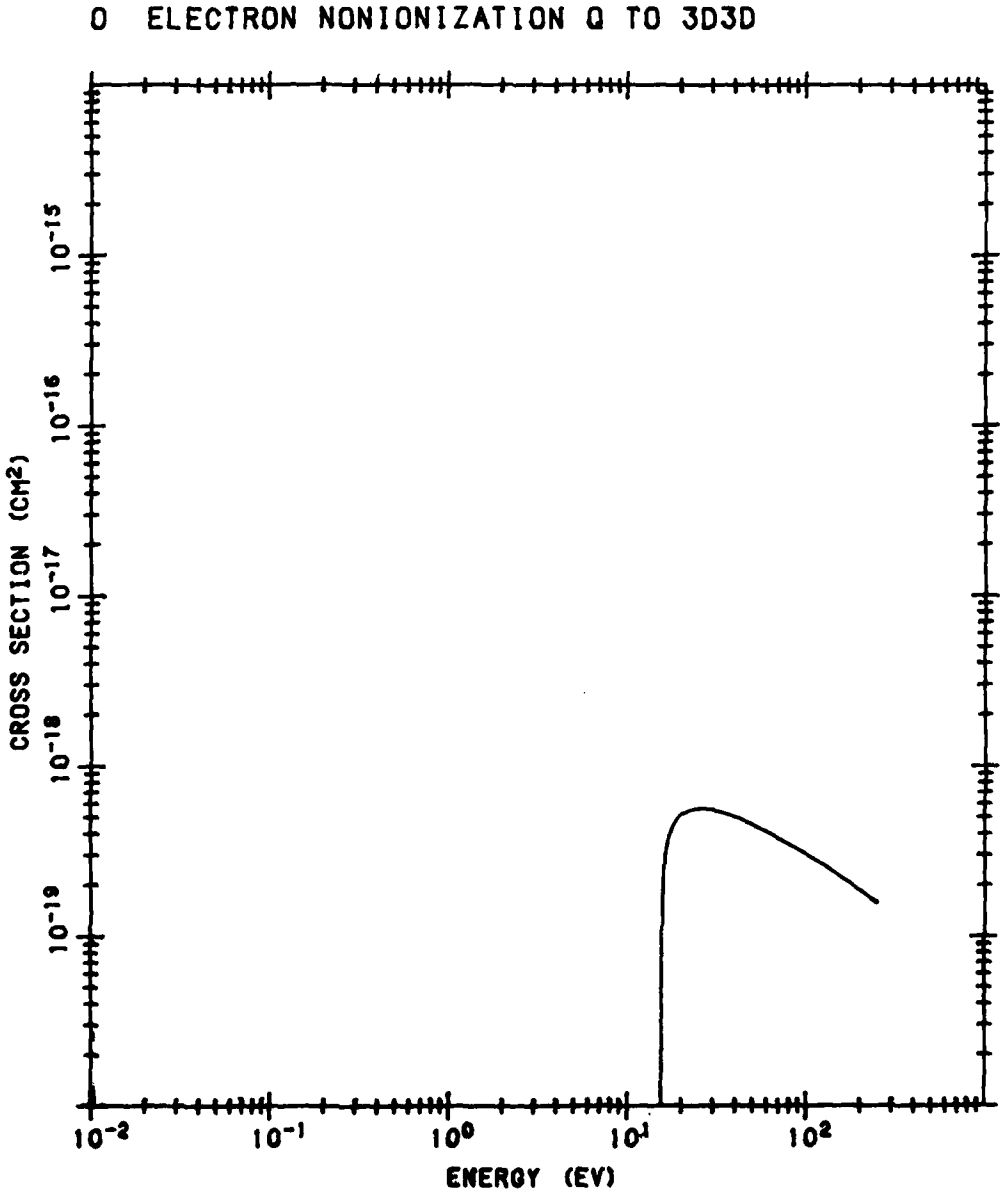


**Figure B66. O Electron Excitation Cross Section to ($^2D^o$) 3d $^3D^o$. The source of the data is the same as in Figure B65**

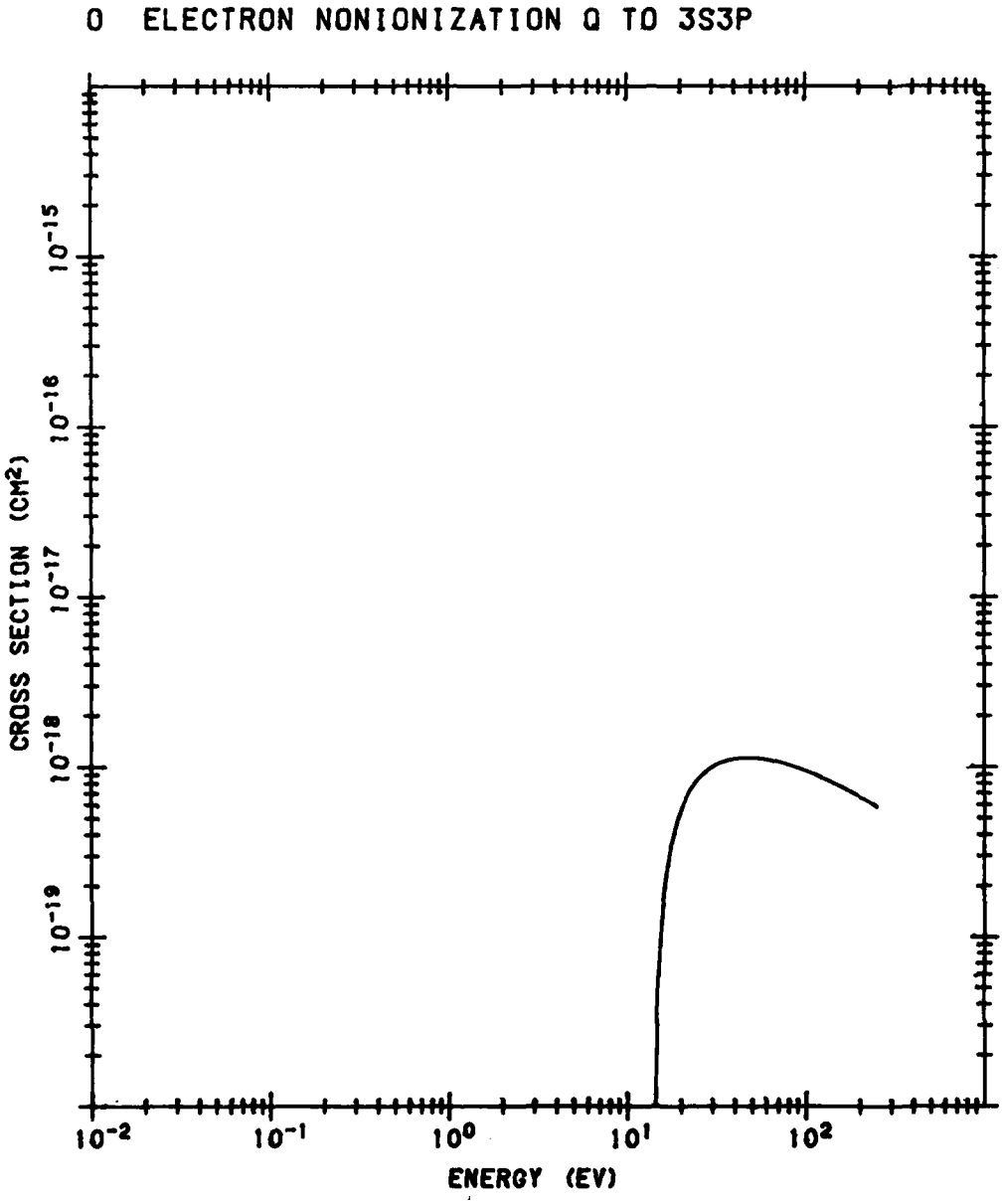


Figure B67. O Electron Excitation Cross Section to ($^2P^o$) 3s $^3P^o$. The source of the data is the same as in Figure B65

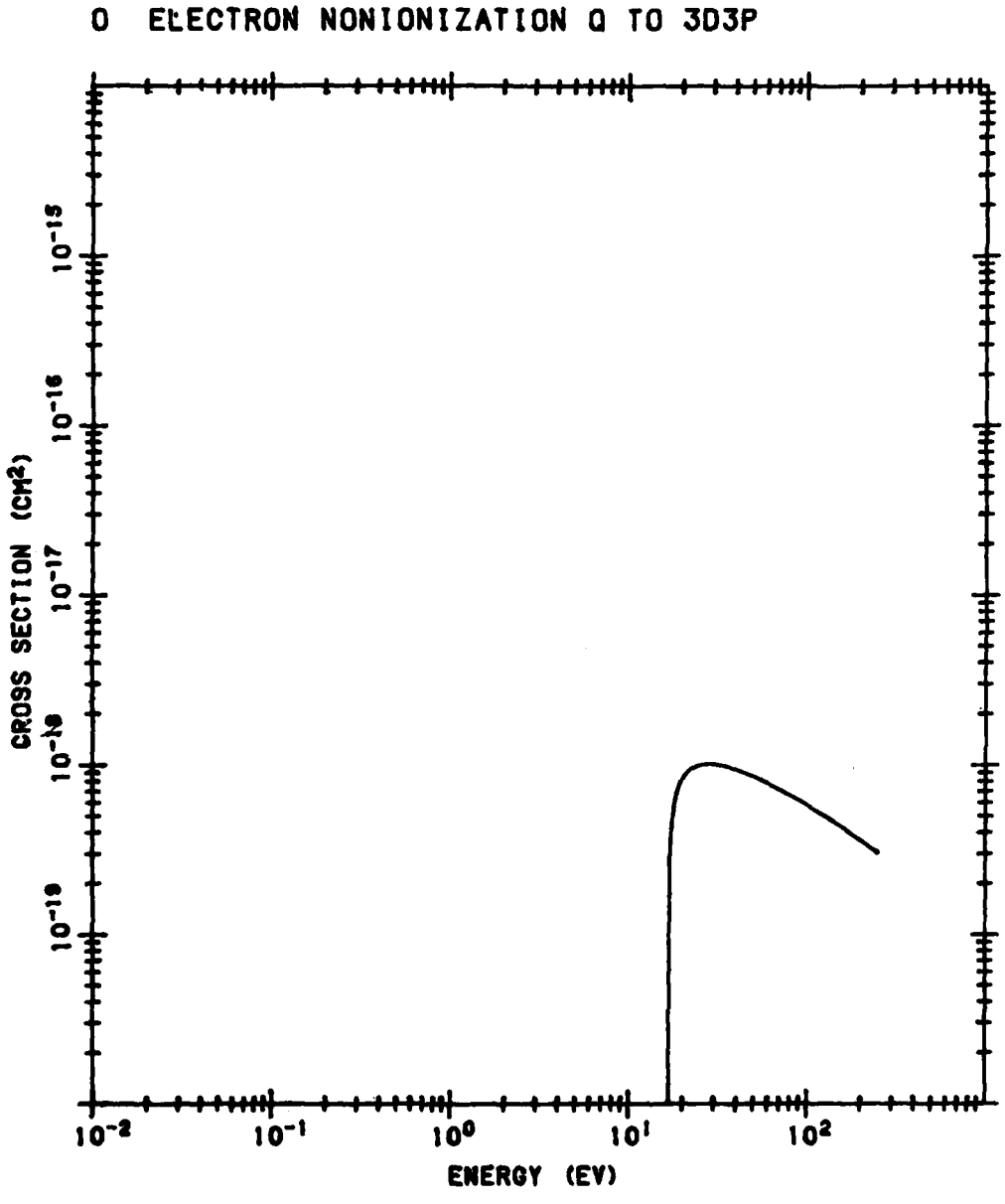


**Figure B68. O Electron Excitation Cross Section to ($^2P^o$) 3d $^3P^o$. The source of the data is the same as in Figure B65**

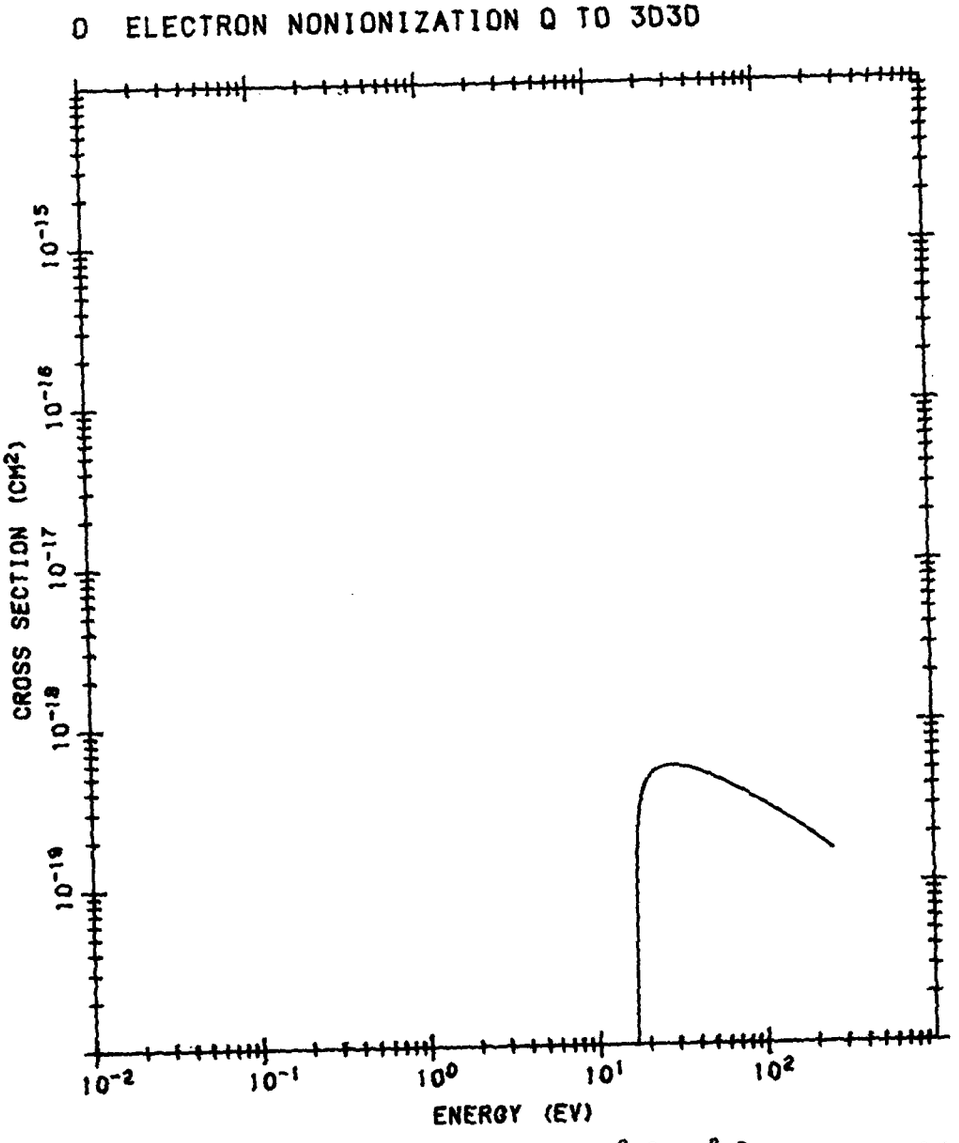


Figure B69. O Electron Excitation Cross Section to ($^2P^o$) 3d $^3D^o$. The source of the data is the same as in Figure B65

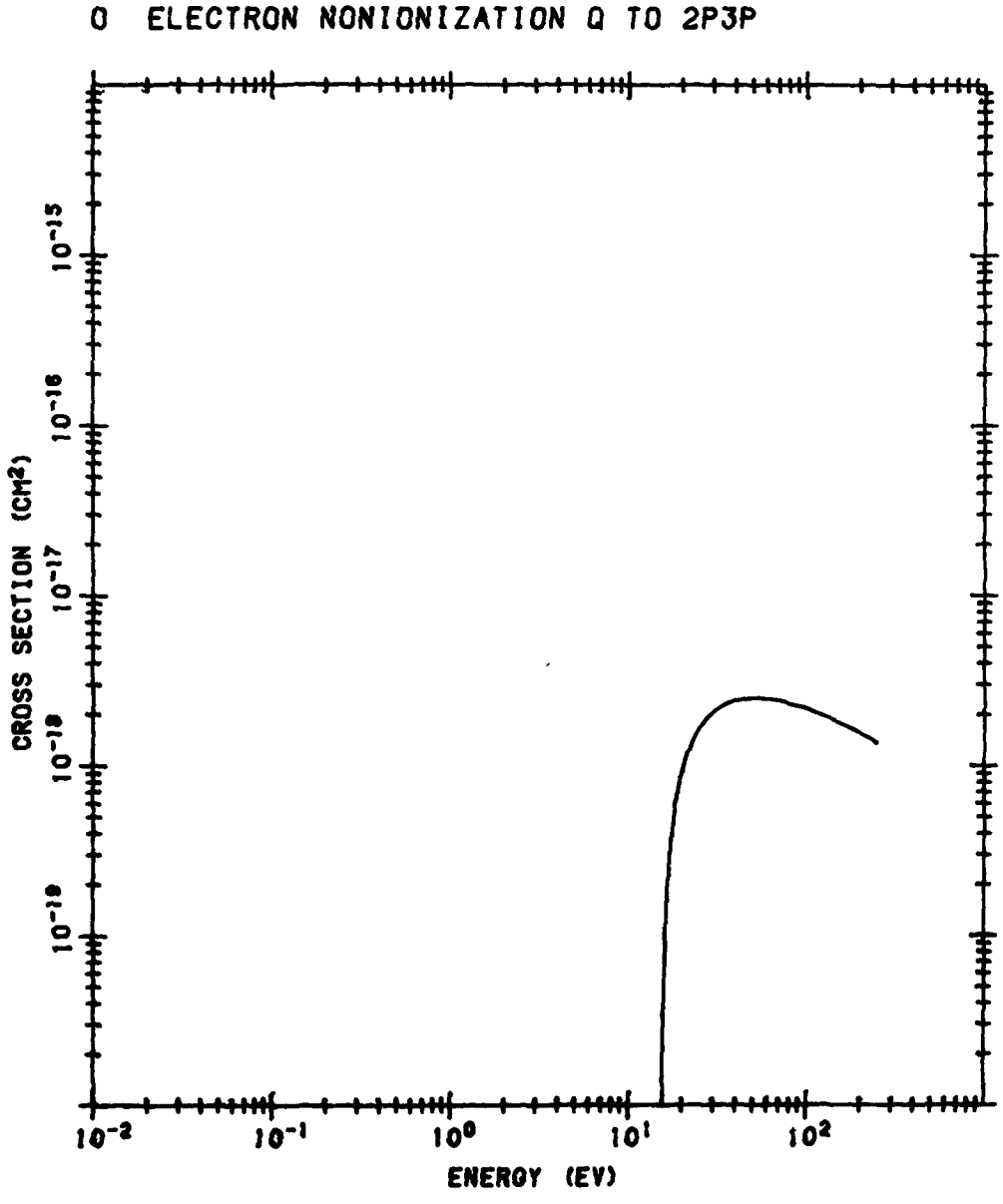


**Figure B70. O Electron Excitation Cross Section to $2p^5\ ^3P^o$. The source of the data is the same as in Figure B65**

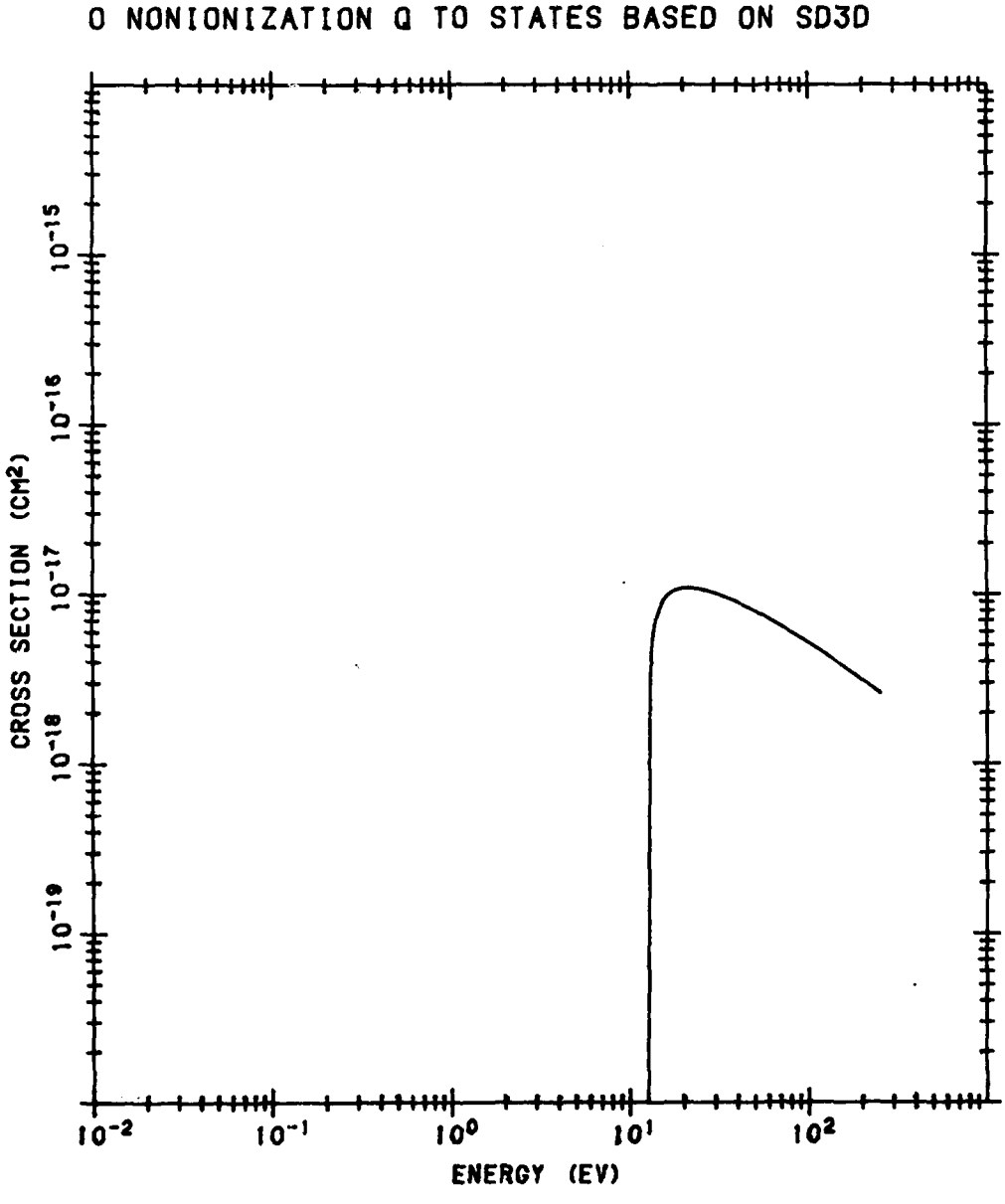


Figure B71: Sum of O Nonionizing Cross Sections to Rydberg States ($^4S^o$) nd $^3D^o$. The cross section data (Jackman et al, 1980)[B22] are weighted by the fraction of excitations which decay radiatively and summed from n equal to 4

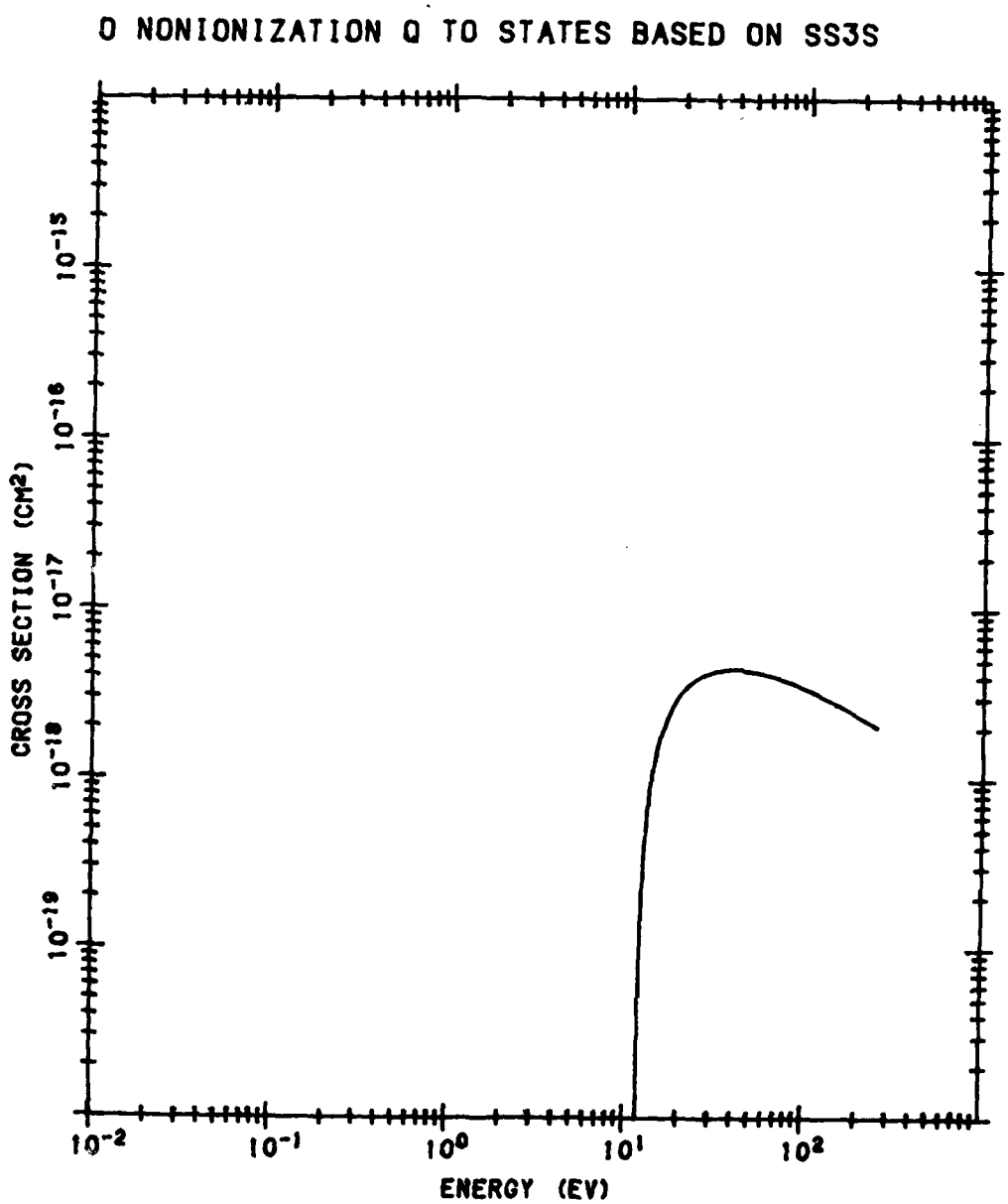


Figure B72. Sum of O Nonionizing Cross Sections to Rydberg States ($^4S^o$)ns $^3S^o$. The data source is the same as that of Figure B71

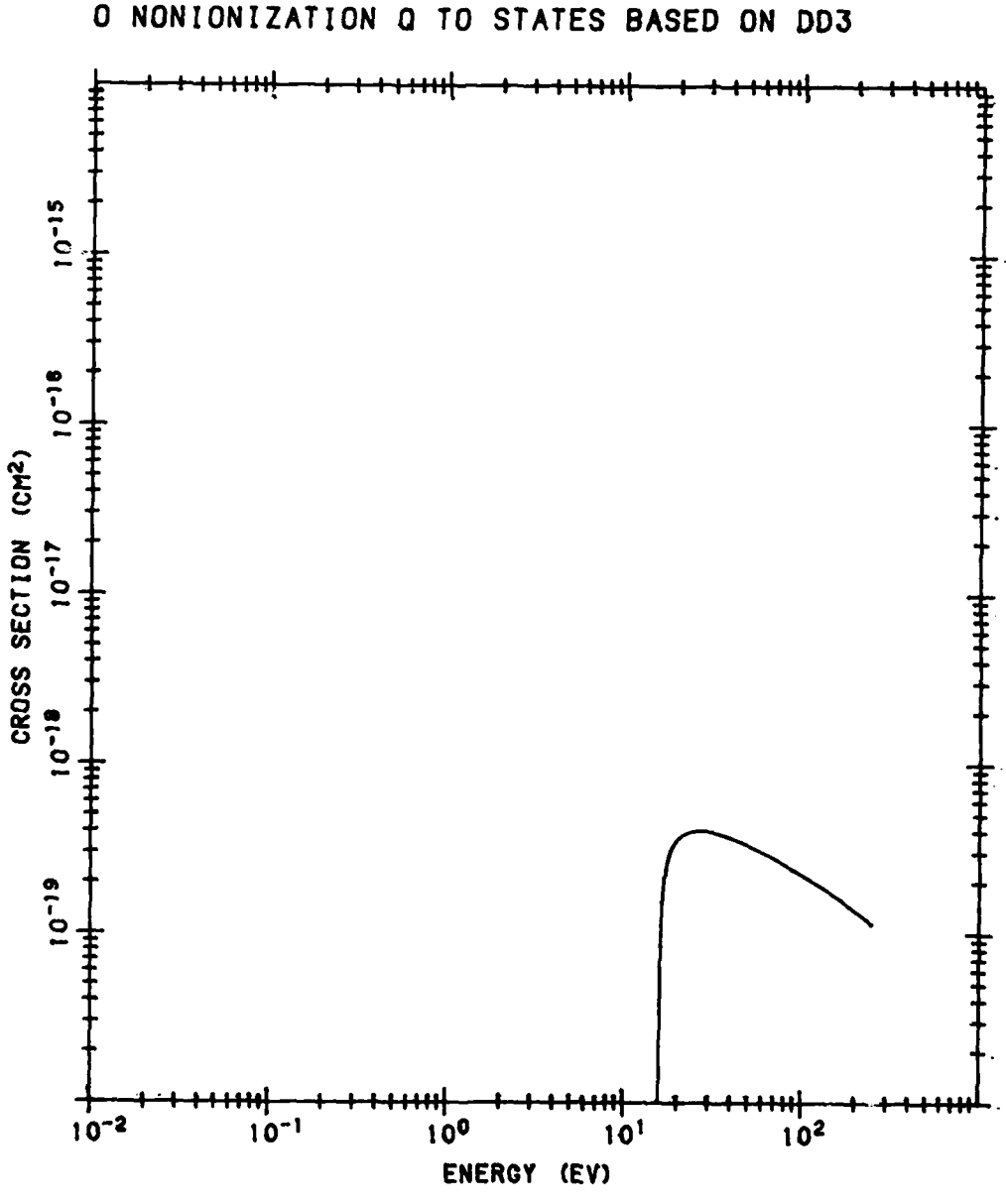


Figure B73. Sum of O Nonionizing Cross Sections to Rydberg States ($^2D^o$) nd $^3SPD^o$. The data source is the same as that of Figure B71

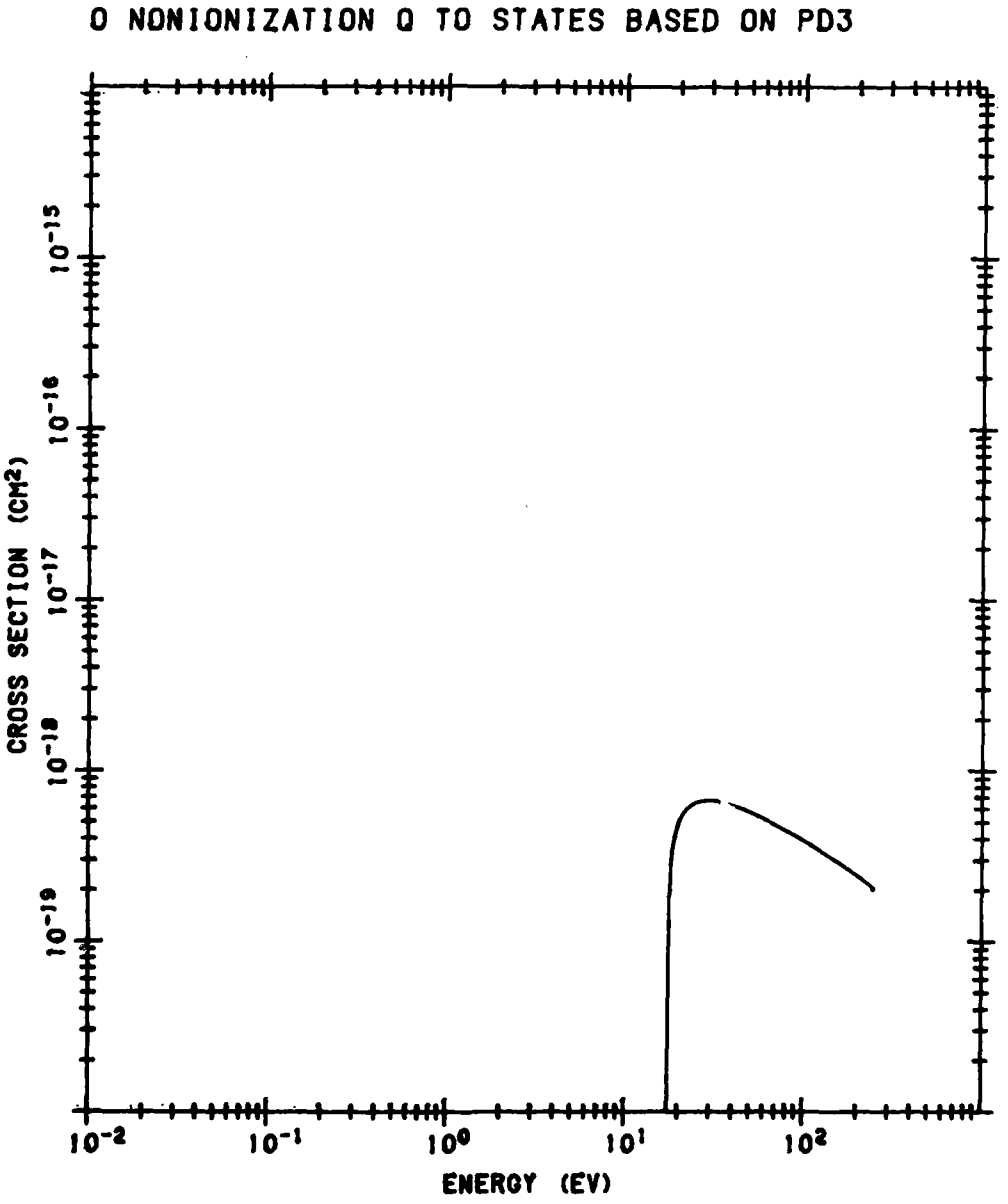


Figure B74. Sum of O Nonionizing Cross Sections to Rydberg States ($^2P^o$) nd $^3PD^o$. The data source is the same as that of Figure B71

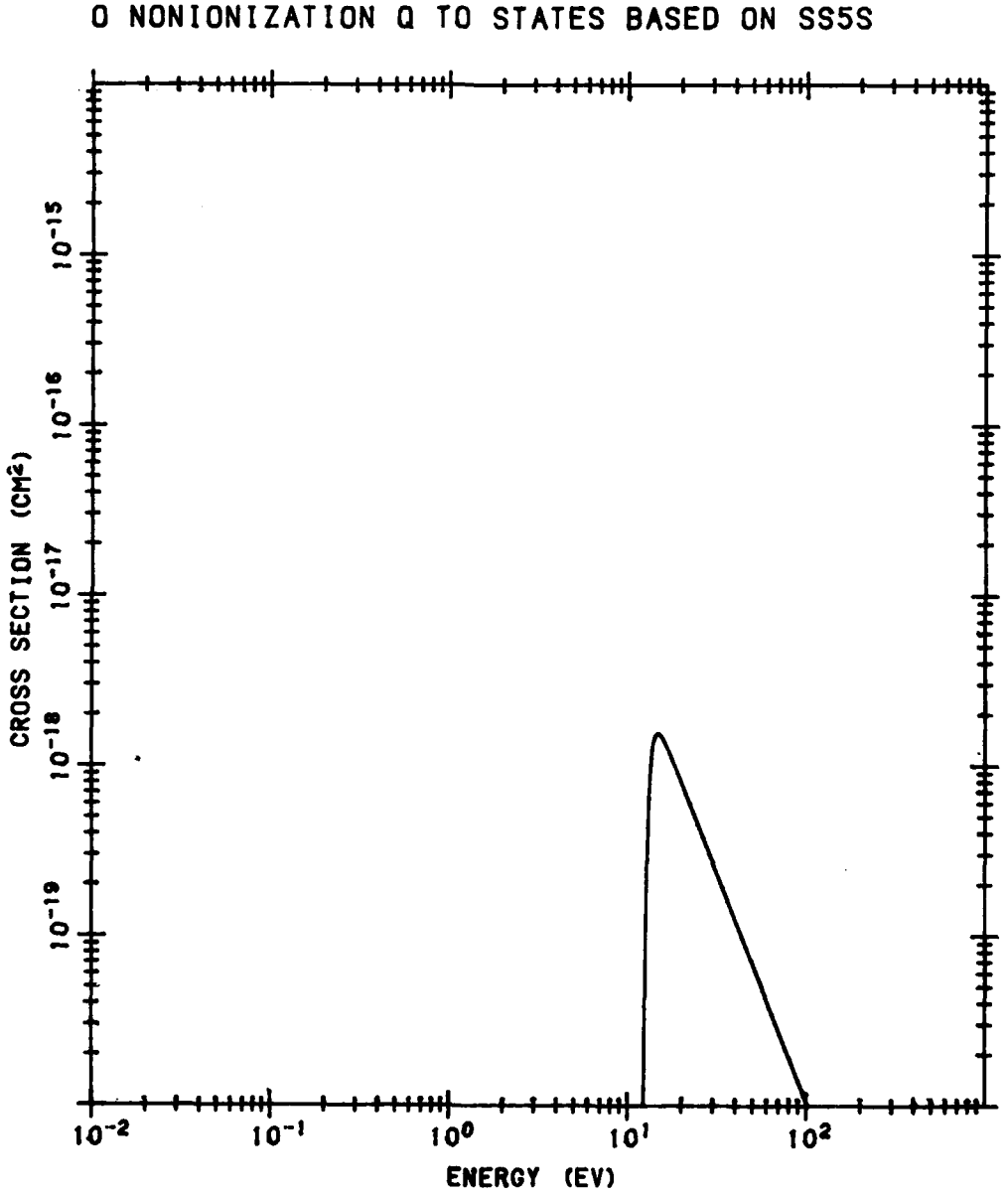


Figure B75. Sum of O Nonionizing Cross Sections to Rydberg States ($^4S^o$)ns $^5S^o$. The data source is the same as that of Figure B71

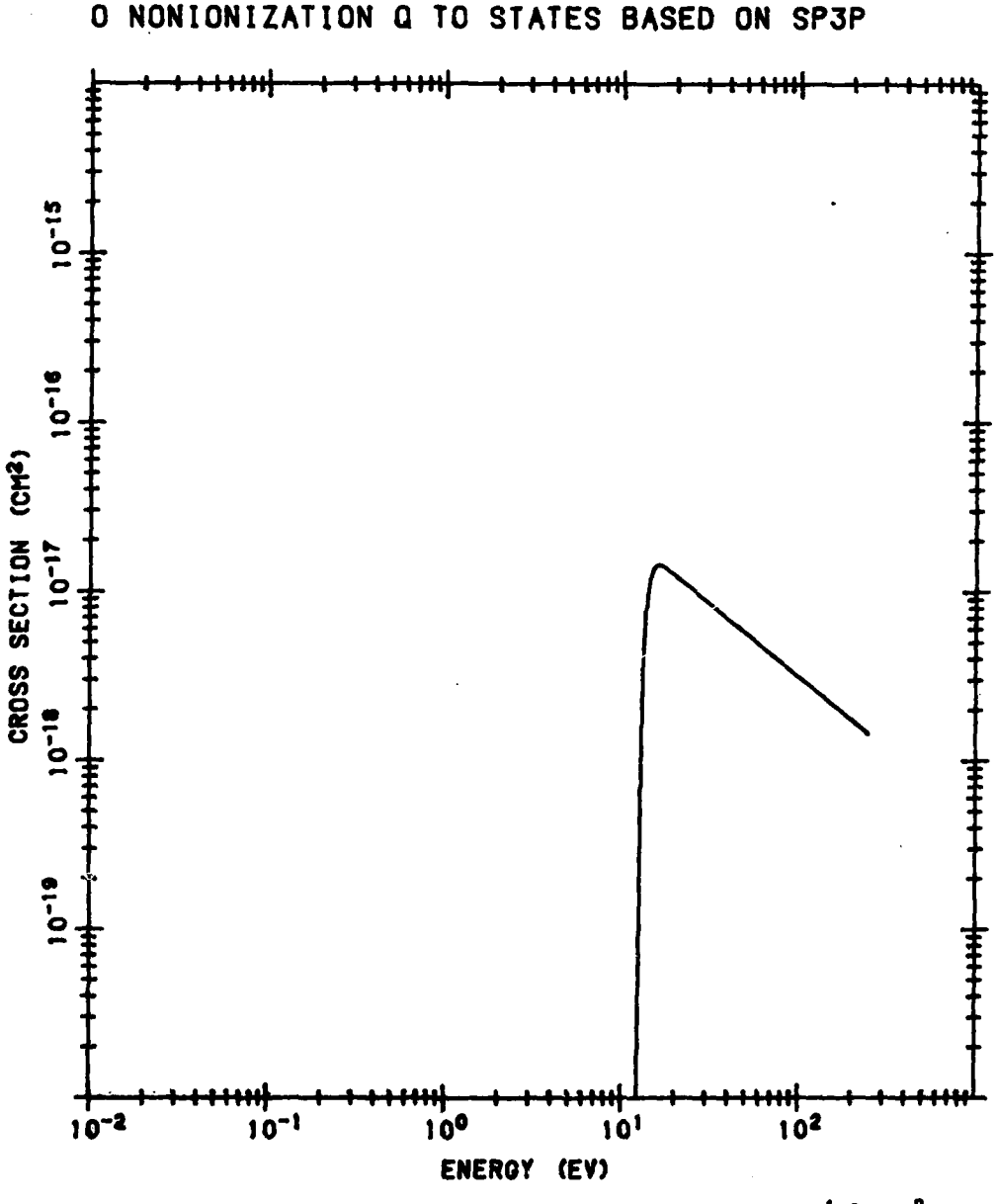


Figure B76. Sum of O Nonionizing Cross Sections to Rydberg States ($^4S^o$) np $^3P$. The data source is the same as that of Figure B71

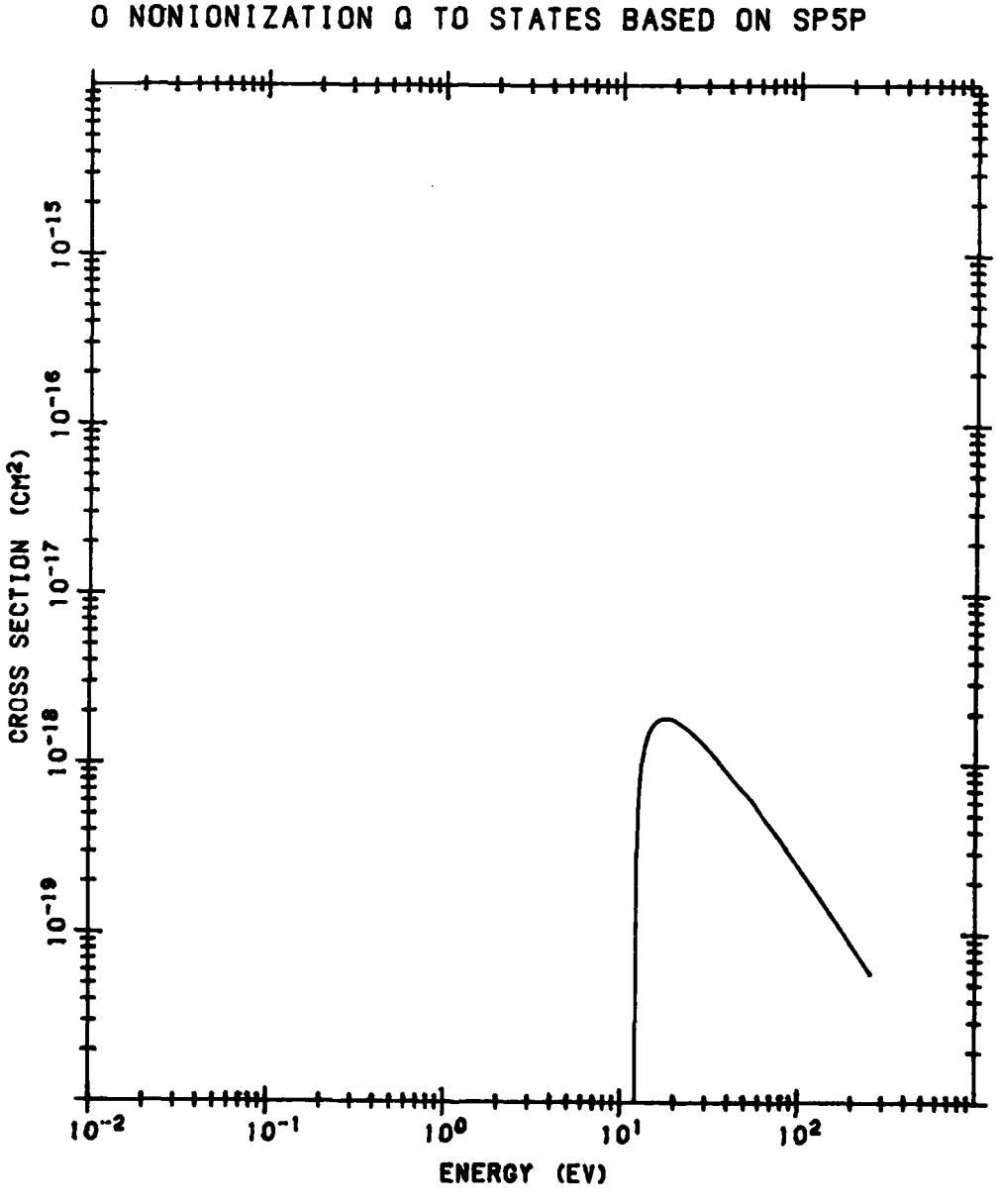


Figure B77. Sum of O Nonionizing Cross Sections to Rydberg States ($^4S^o$) np $^5P$. The data source is the same as that of Figure B71

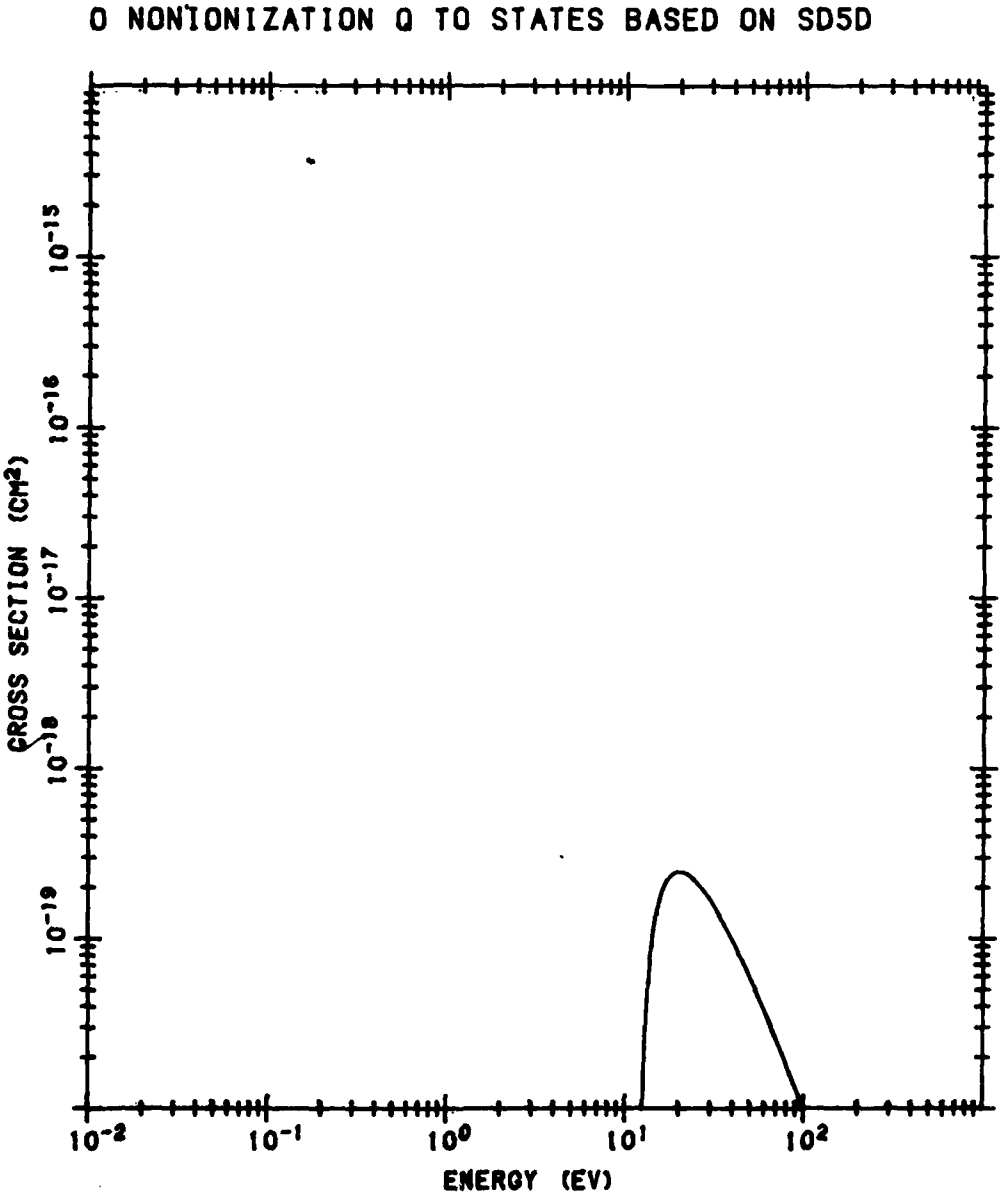


Figure B78. Sum of O Nonionizing Cross Section to Rydberg States ($^4S^o$) nd $^5D$. The cross section data (Jackman et al 1980[B22]) are weighted by the fraction of excitations that decay radiatively and summed from n equal to 3

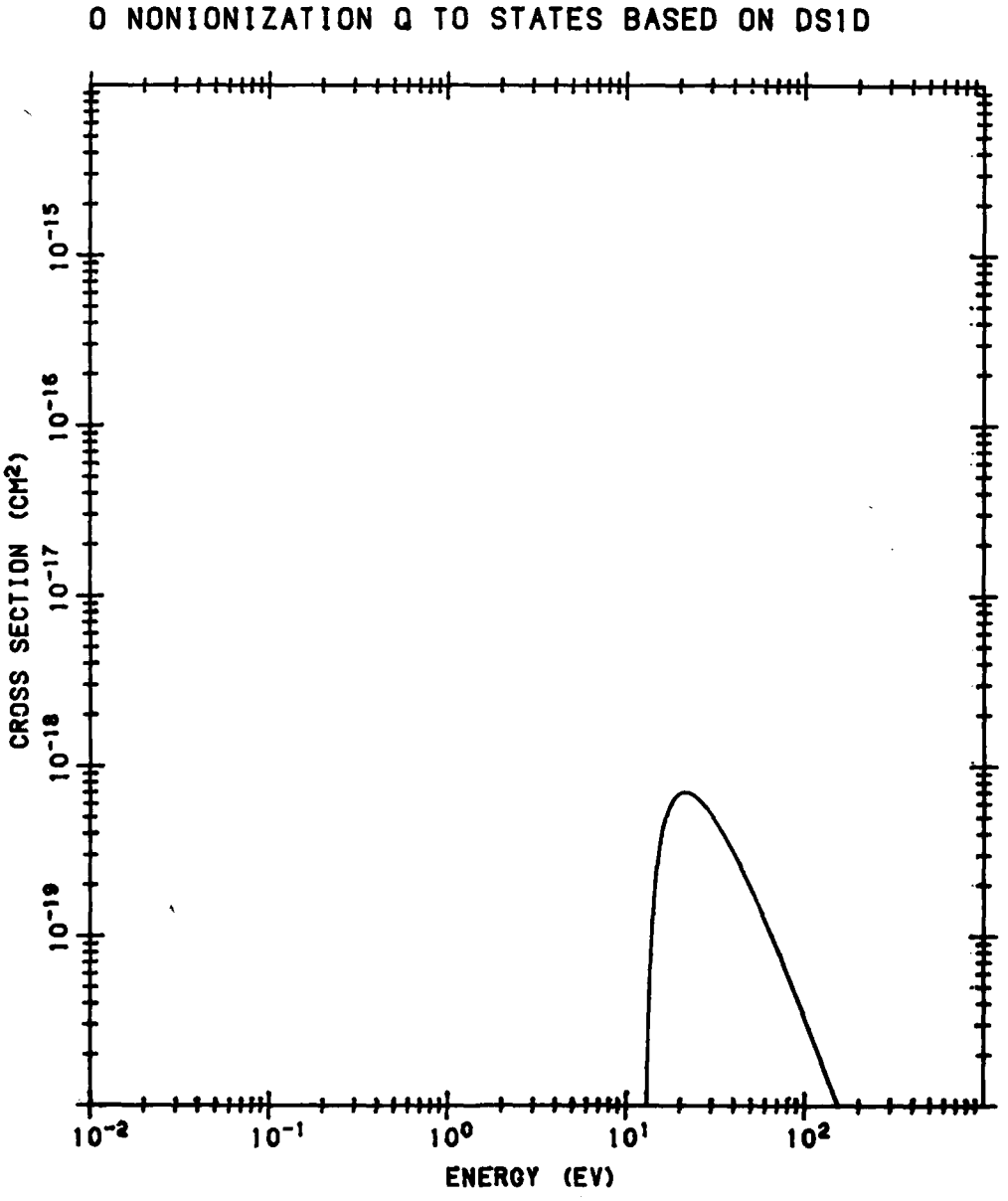


Figure B79. Sum of O Nonionizing Cross Section to Rydberg States ($^2D^o$) ns $^1D^o$. The data source is the same as that of Figure B78

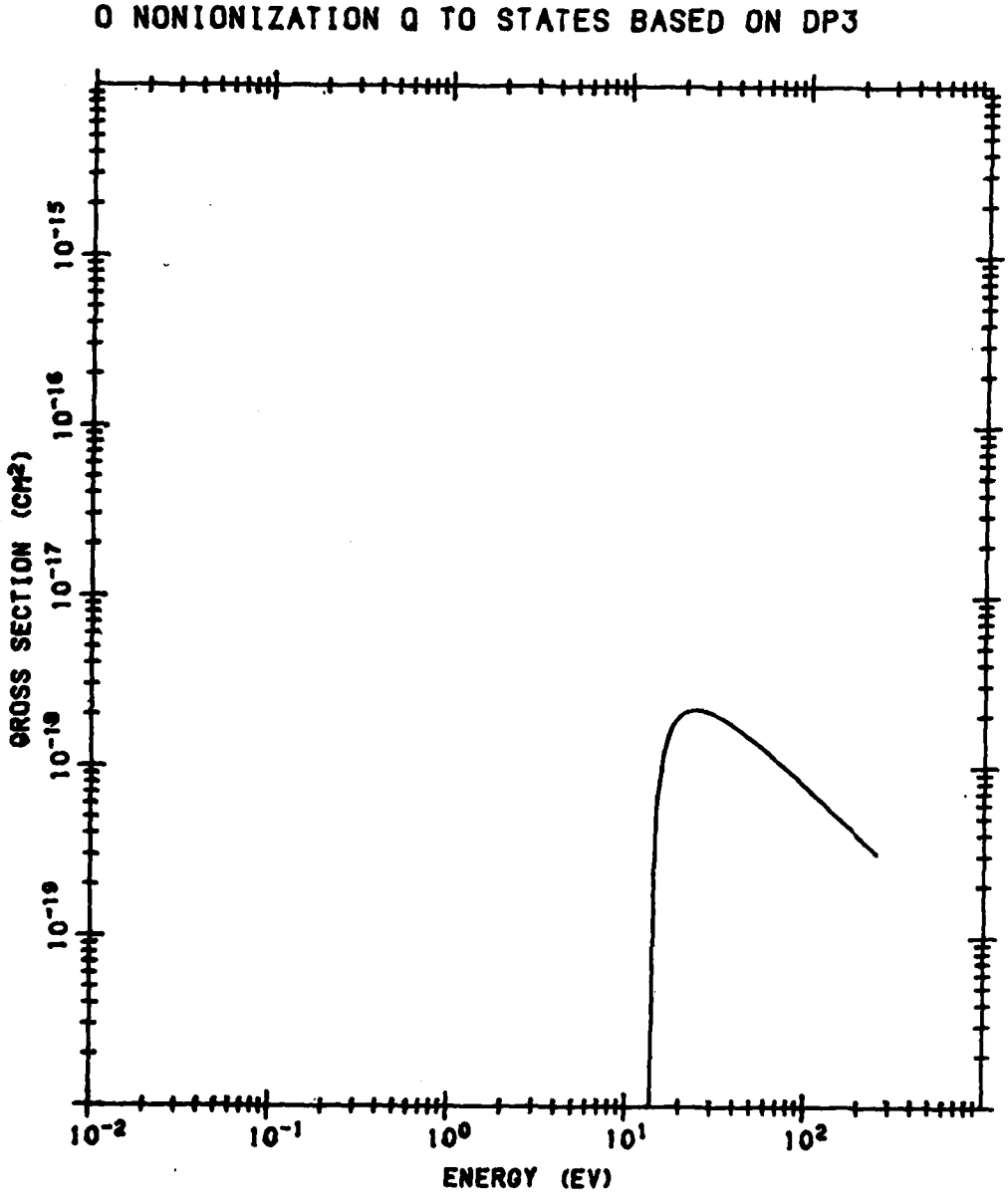


**Figure B80. Sum of O Nonionizing Cross Sections to Rydberg States ($^2D^o$) np $^3PDF$. The data source is the same as that of Figure B78**

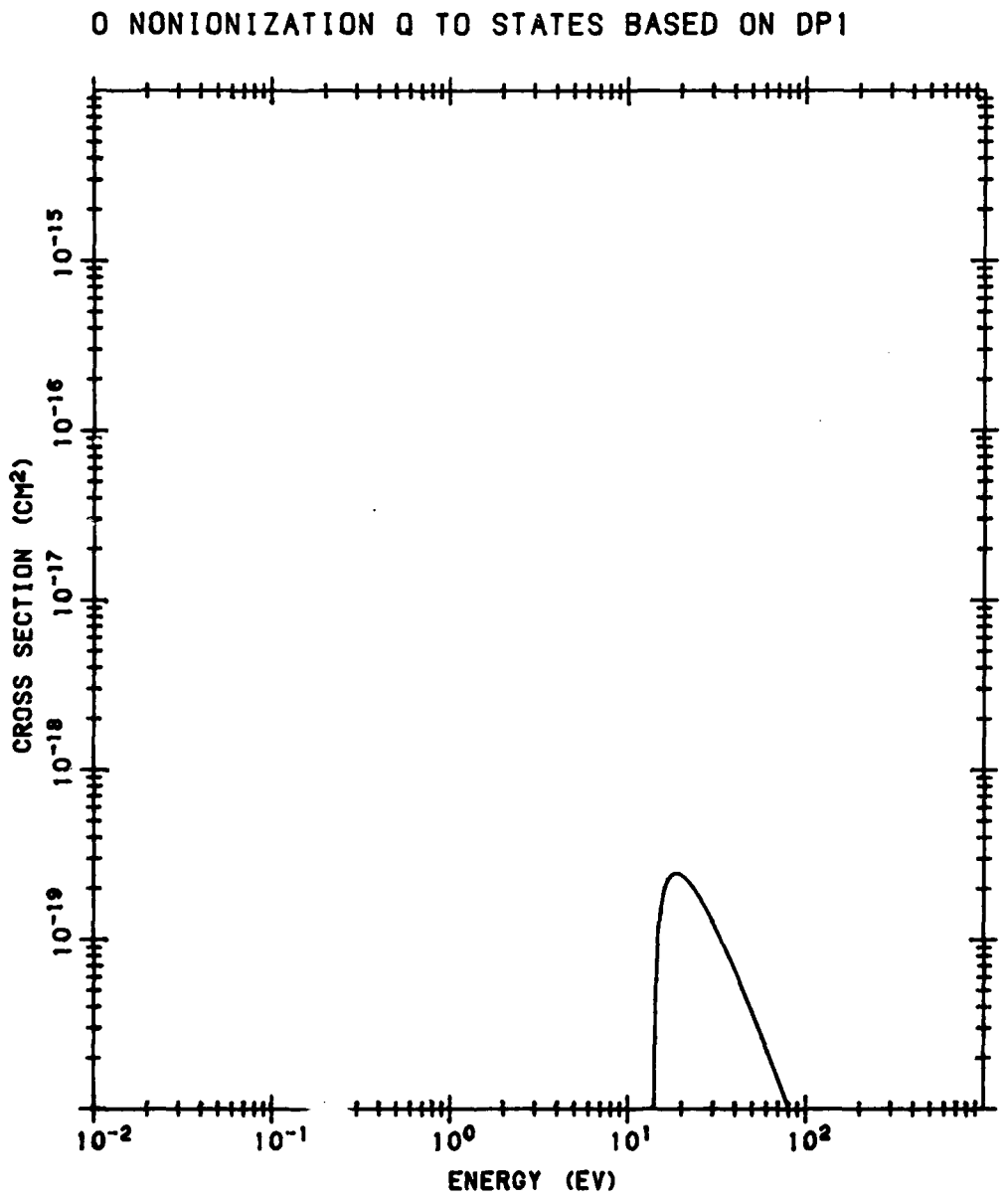


Figure B81. Sum of O Nonionizing Cross Sections to Rydberg States $(^2D^o)np\ ^1PDF$. The data source is the same as that of Figure B78

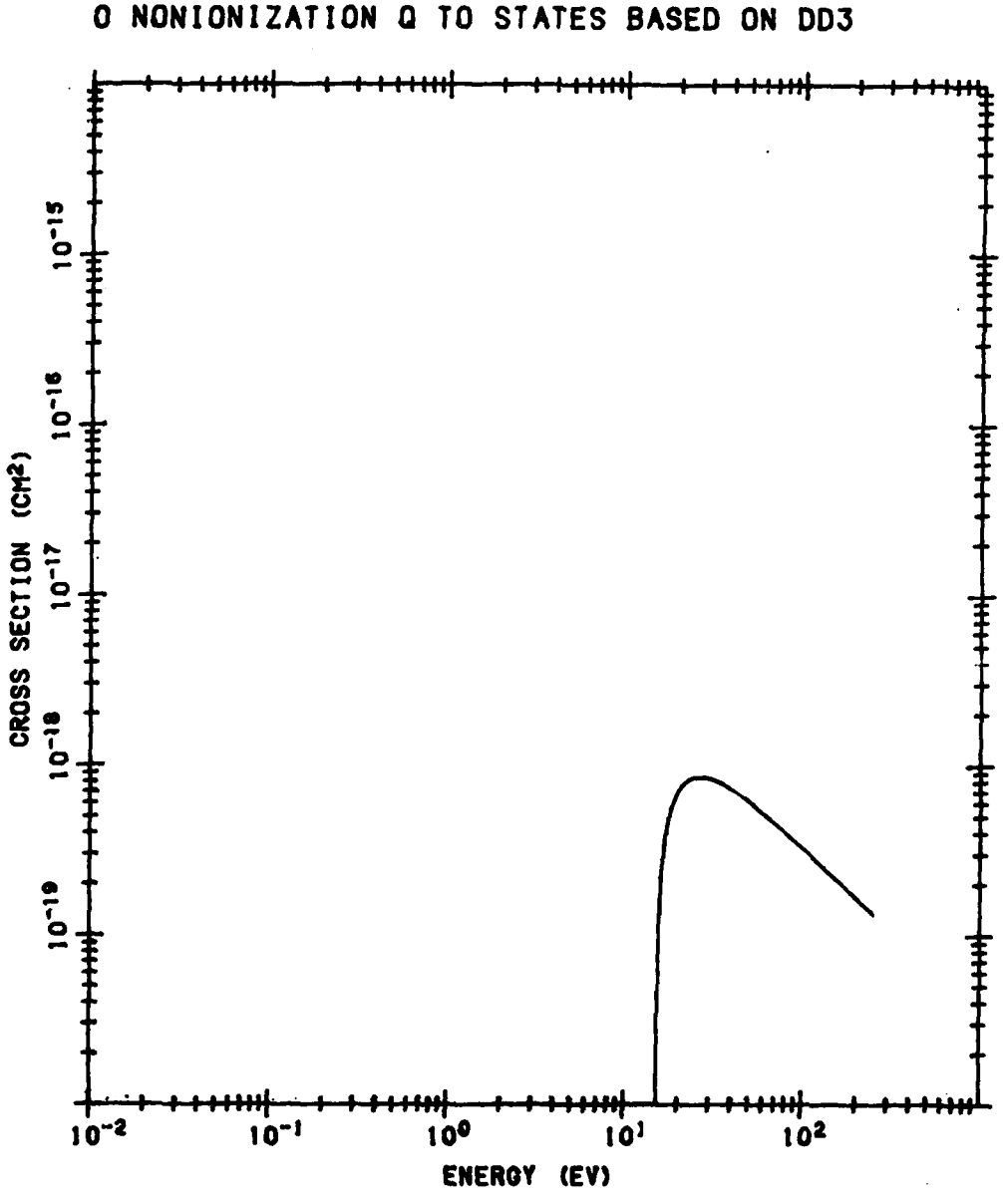


Figure B82. Sum of O Nonionizing Cross Sections to Rydberg States ($^2D^o$) nd $^3FG^o$. The data source is the same as that of Figure B78

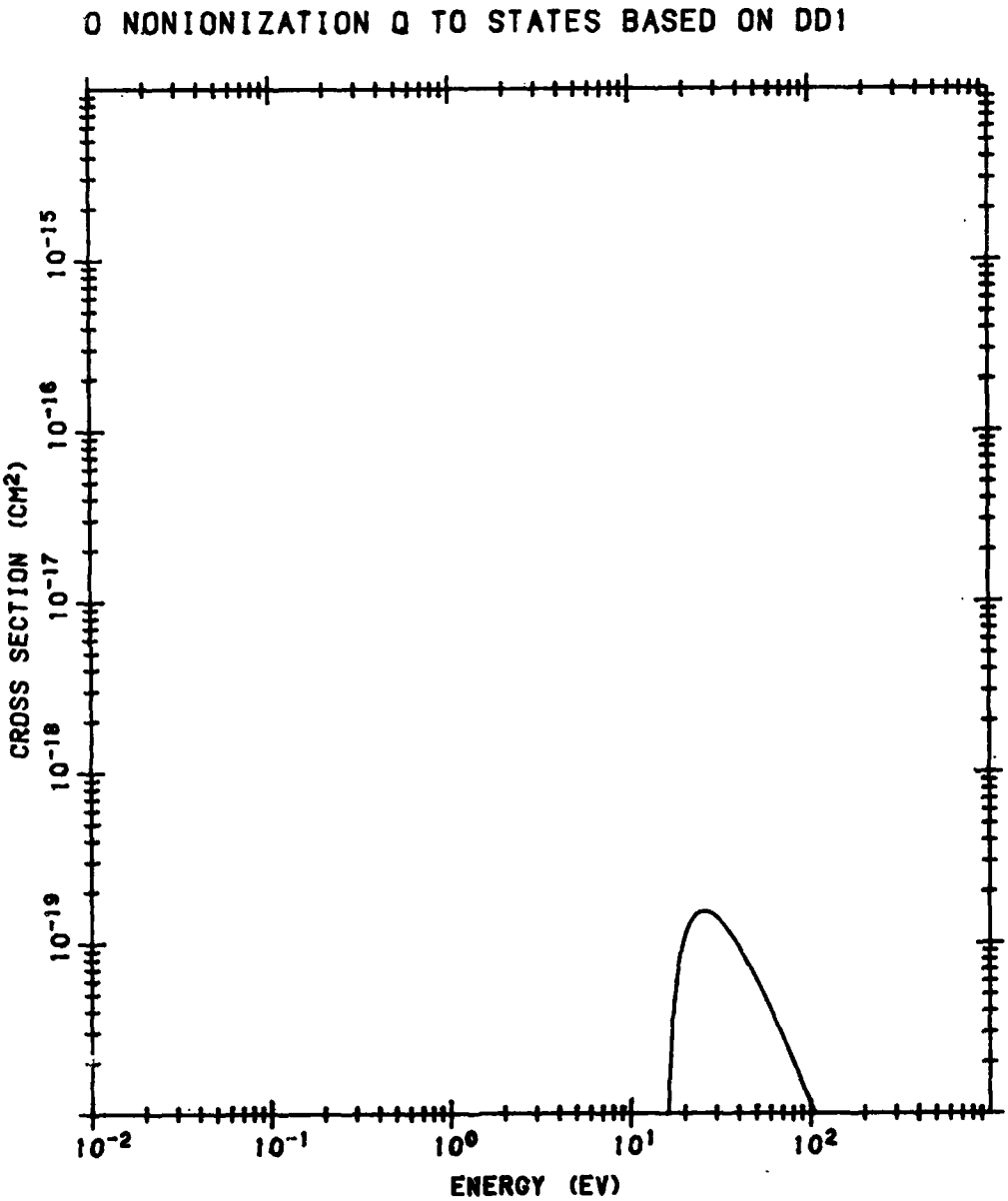


**Figure B83. Sum of O Nonionizing Cross Sections to Rydberg States ($^2D^o$) nd $^1SPDFG^o$. The data source is the same as that of Figure B78**

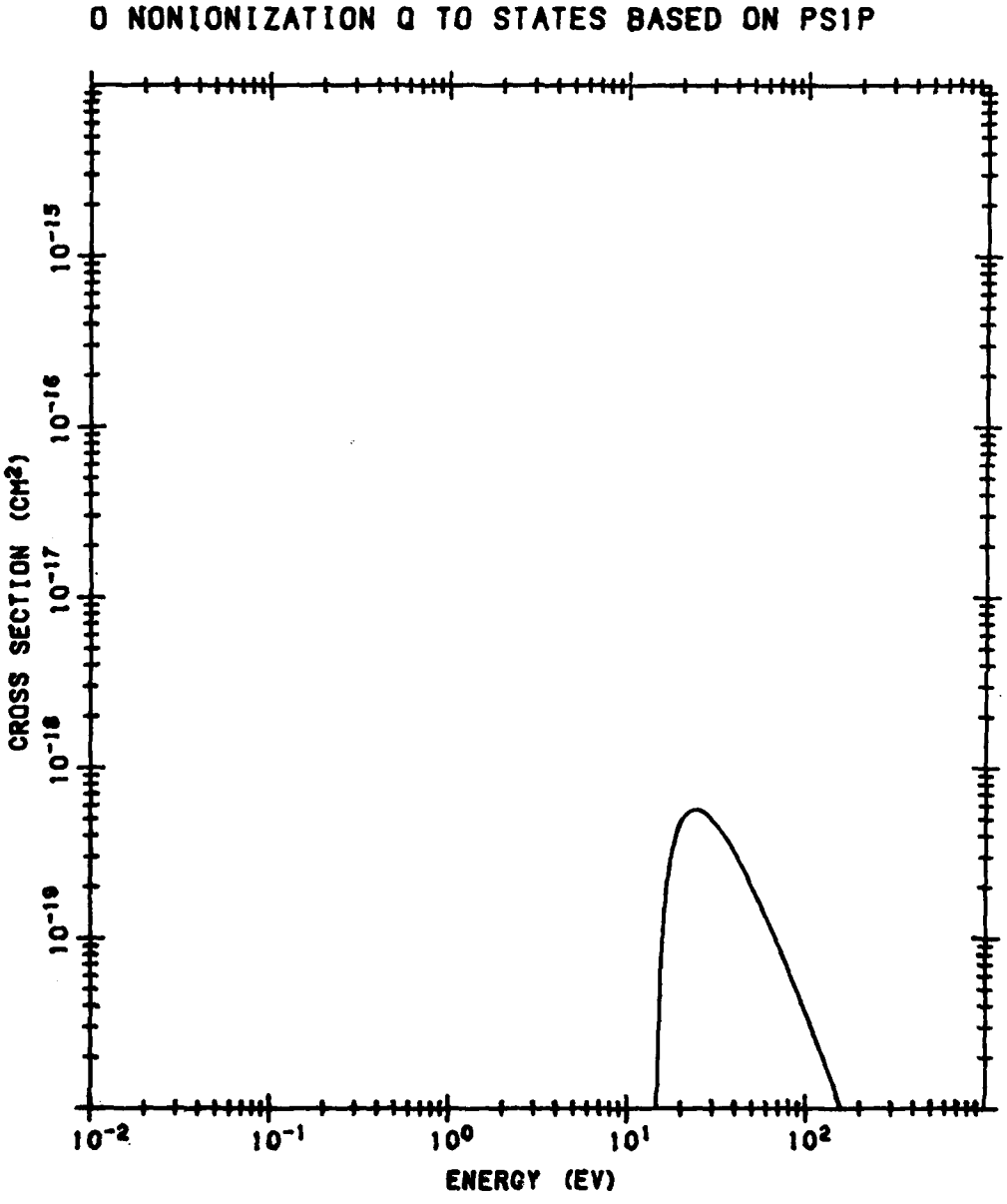


**Figure B64. Sum of O Nonionizing Cross Sections to Rydberg States ($^2P^o$) ns $^1P^o$. The data source is the same as that of Figure B78**

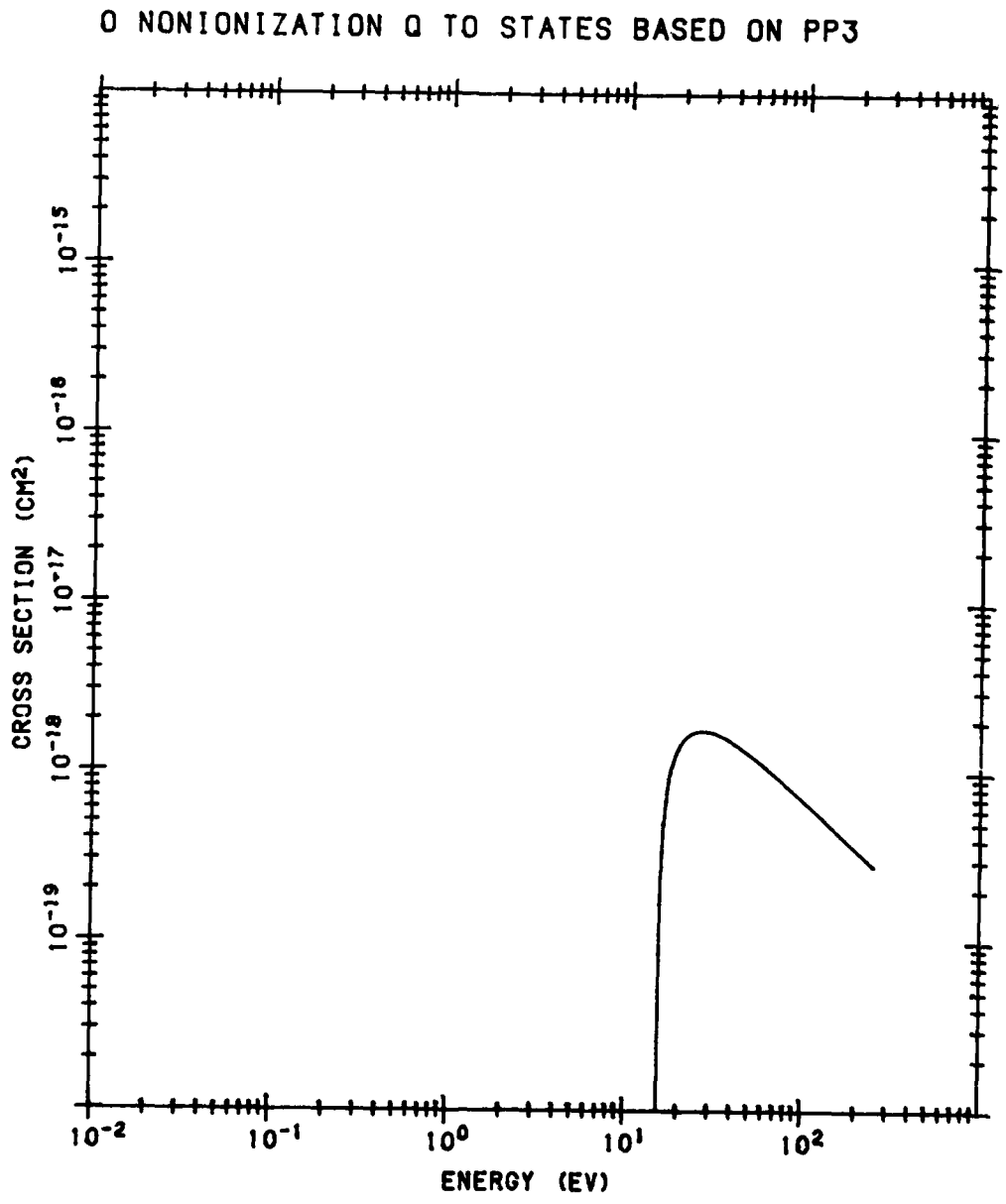


Figure B85. Sum of O Nonionizing Cross Sections to Rydberg States ($^2P^o$) np $^3SPD$. The data source is the same as that of Figure B78

AD-A118 921 BEDFORD RESEARCH ASSOCIATES MA F/G 4/1
LOW ENERGY ELECTRON AND PHOTON CROSS SECTIONS FOR O, N2, AND O2--ETC(U)
JAN 82 H T WADZINSKI, J R JASPERSE F19628-80-C-0216
UNCLASSIFIED AFGL-TR-82-0008 NL

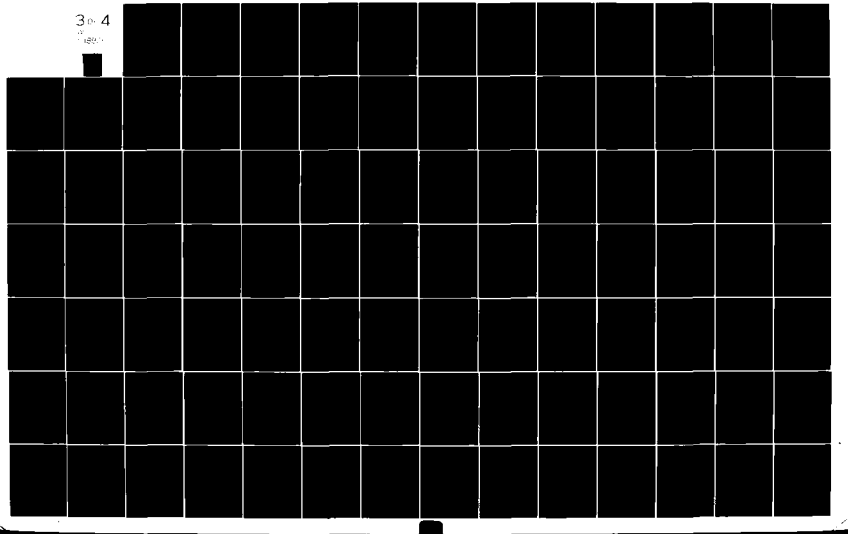

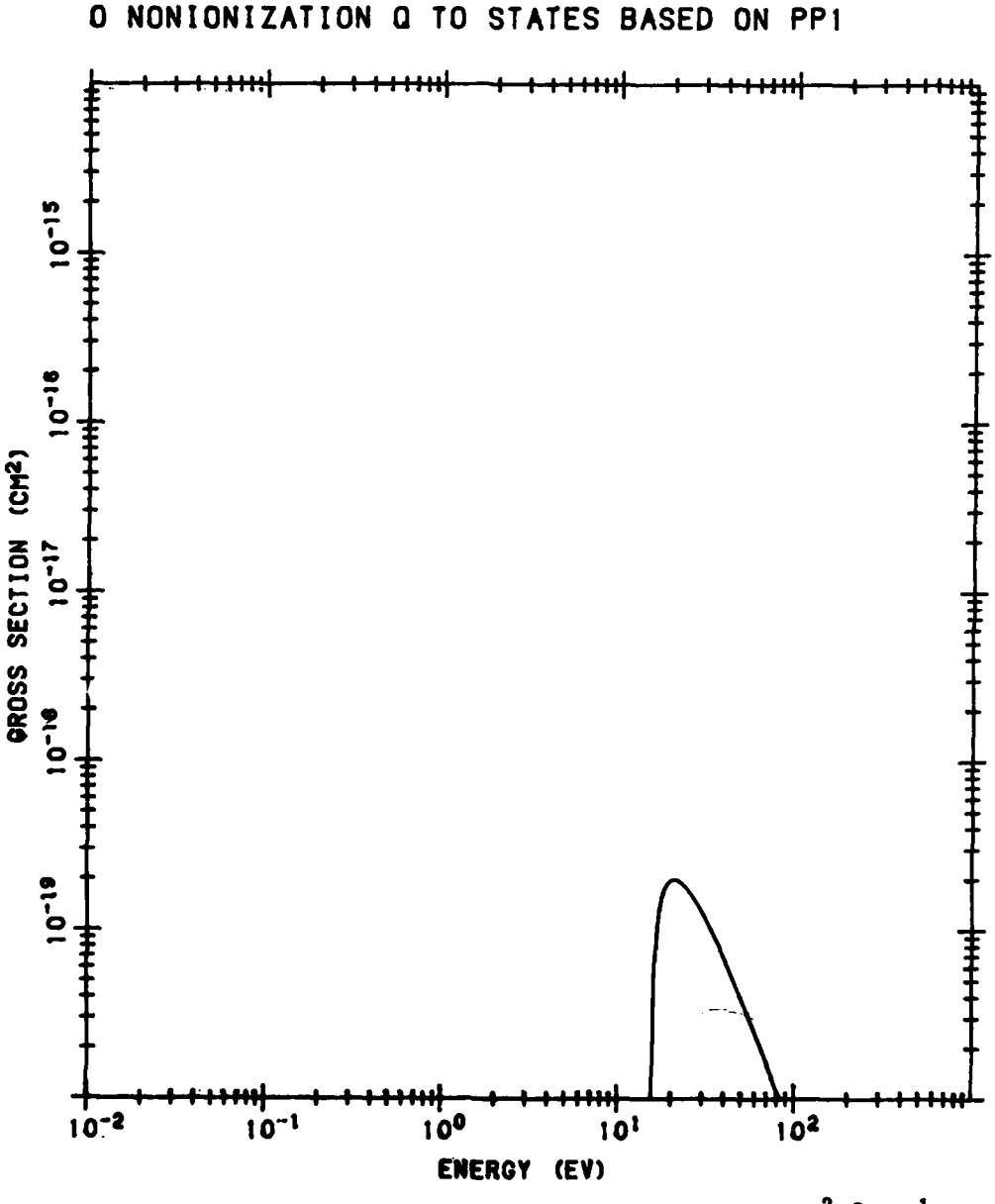


Figure B86. Sum of O Nonionizing Cross Sections to Rydberg States ($^2P^o$) np $^1$SPD. The data source is the same as that of Figure B78

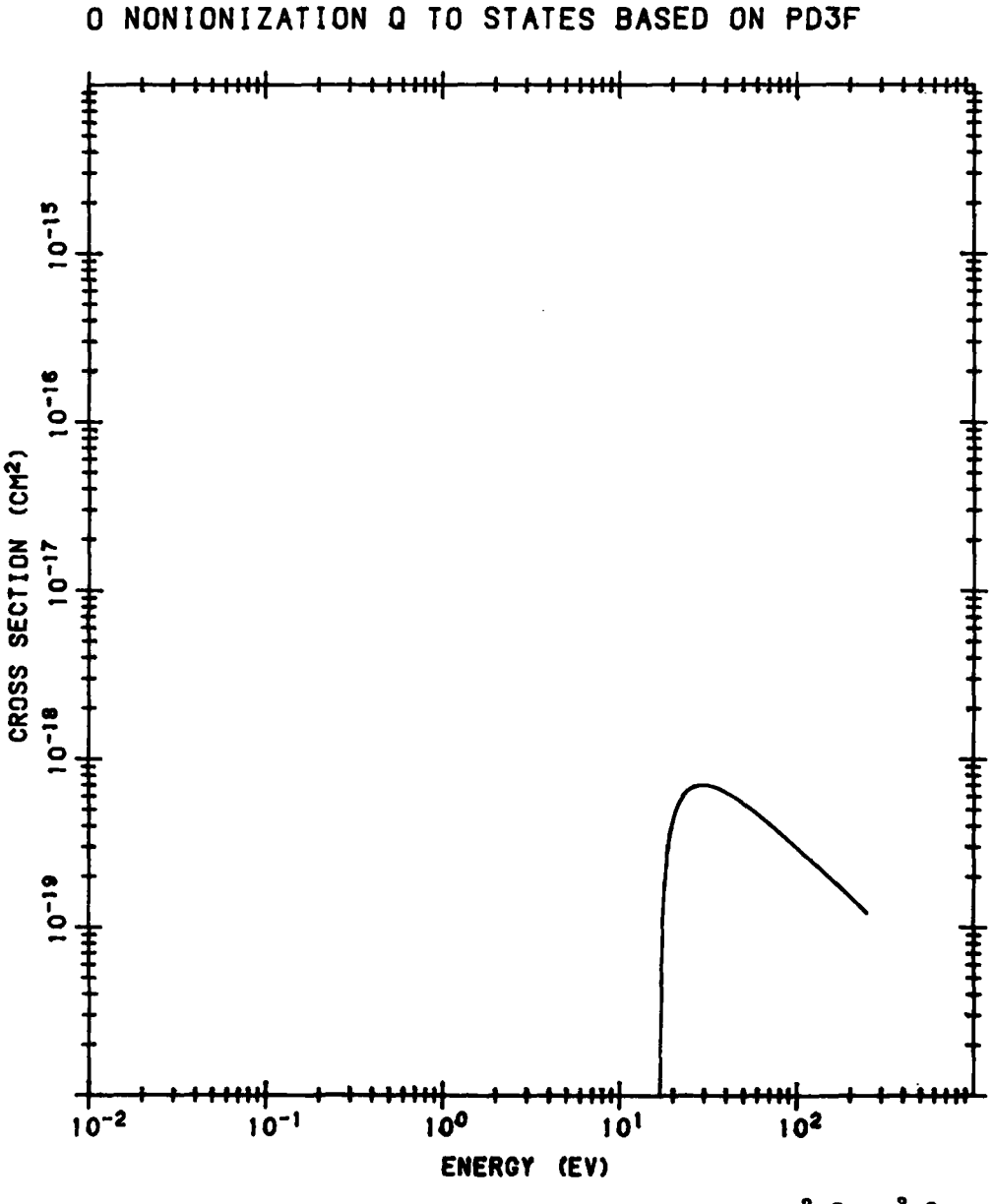


Figure B87. Sum of O Nonionizing Cross Sections to Rydberg States ($^2P^o$) nd $^3F^o$. The data source is the same as that of Figure B78

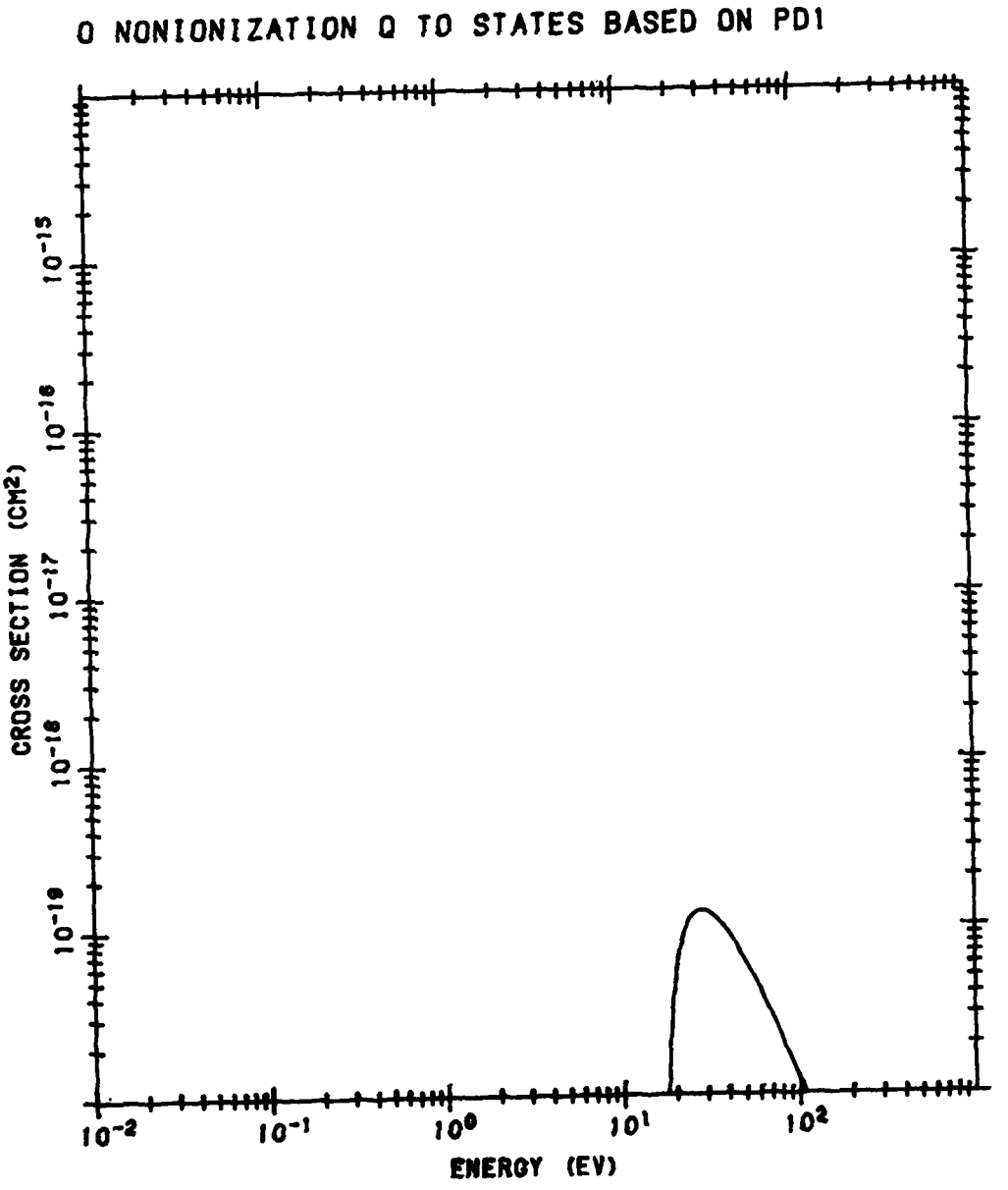


Figure B86. *Sum of O Nonionizing Cross Sections* to Rydberg States ($^2P^o$) nd $^1PDF^o$. The data source is the same as that of Figure B78

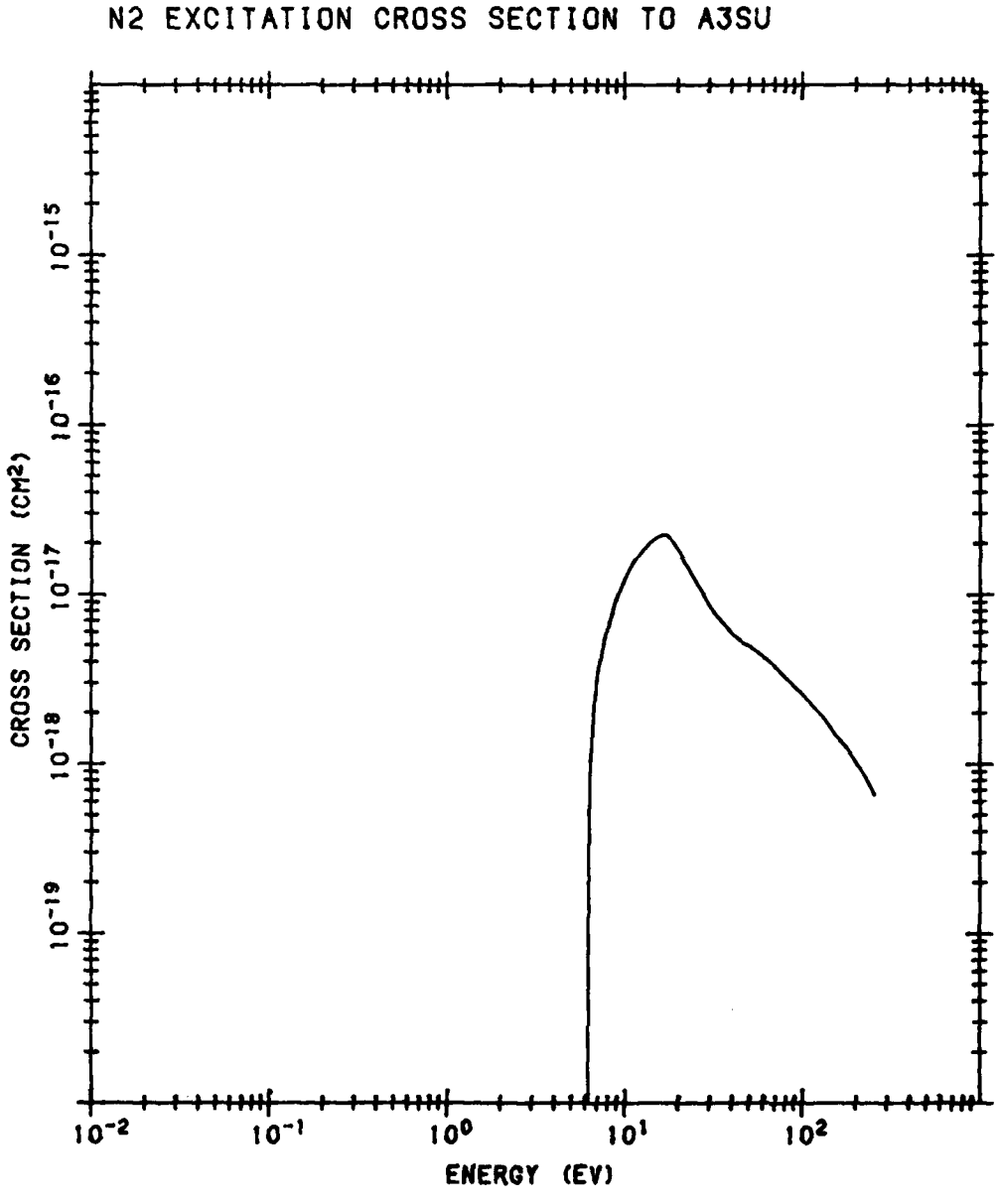


Figure B89. $N_2$ Electron Excitation Cross Section to A $^3\Sigma_u^+$. The data below 50 eV are from Cartwright et al (1977)[B24] and extrapolated as $1/E^3$ to higher energies

B24. Cartwright, D. C., Trajmar, S., Chutjian, A., and Williams, W. (1977) Phys. Rev. A16:1041.

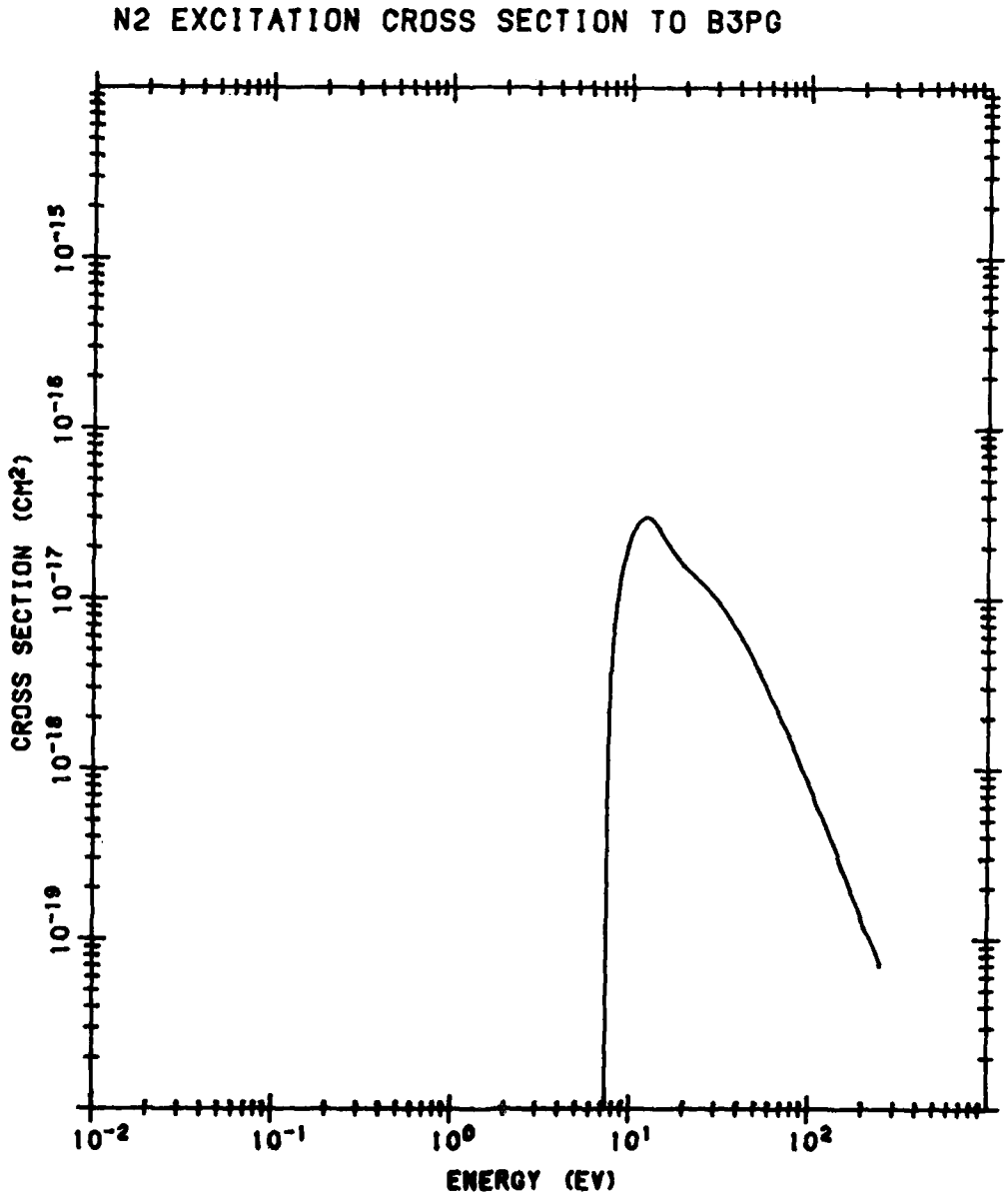


Figure B90. $N_2$ Electron Excitation Cross Section to B $^3\Pi_g$. The data source is the same as that of Figure B89

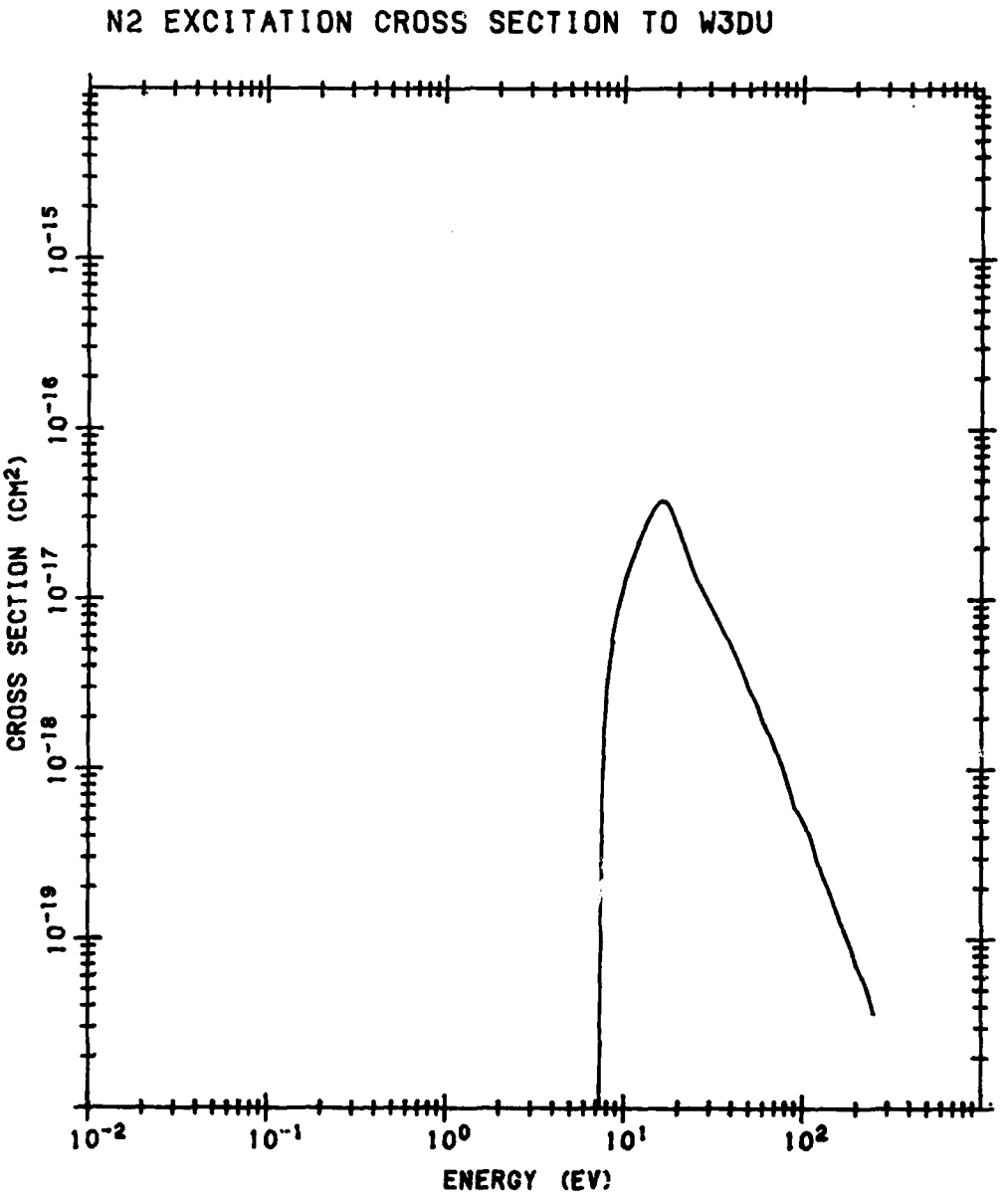


Figure B91. $N_2$ Electron Excitation Cross Section to W $^3\Delta_u$. The data source is the same as that of Figure B89

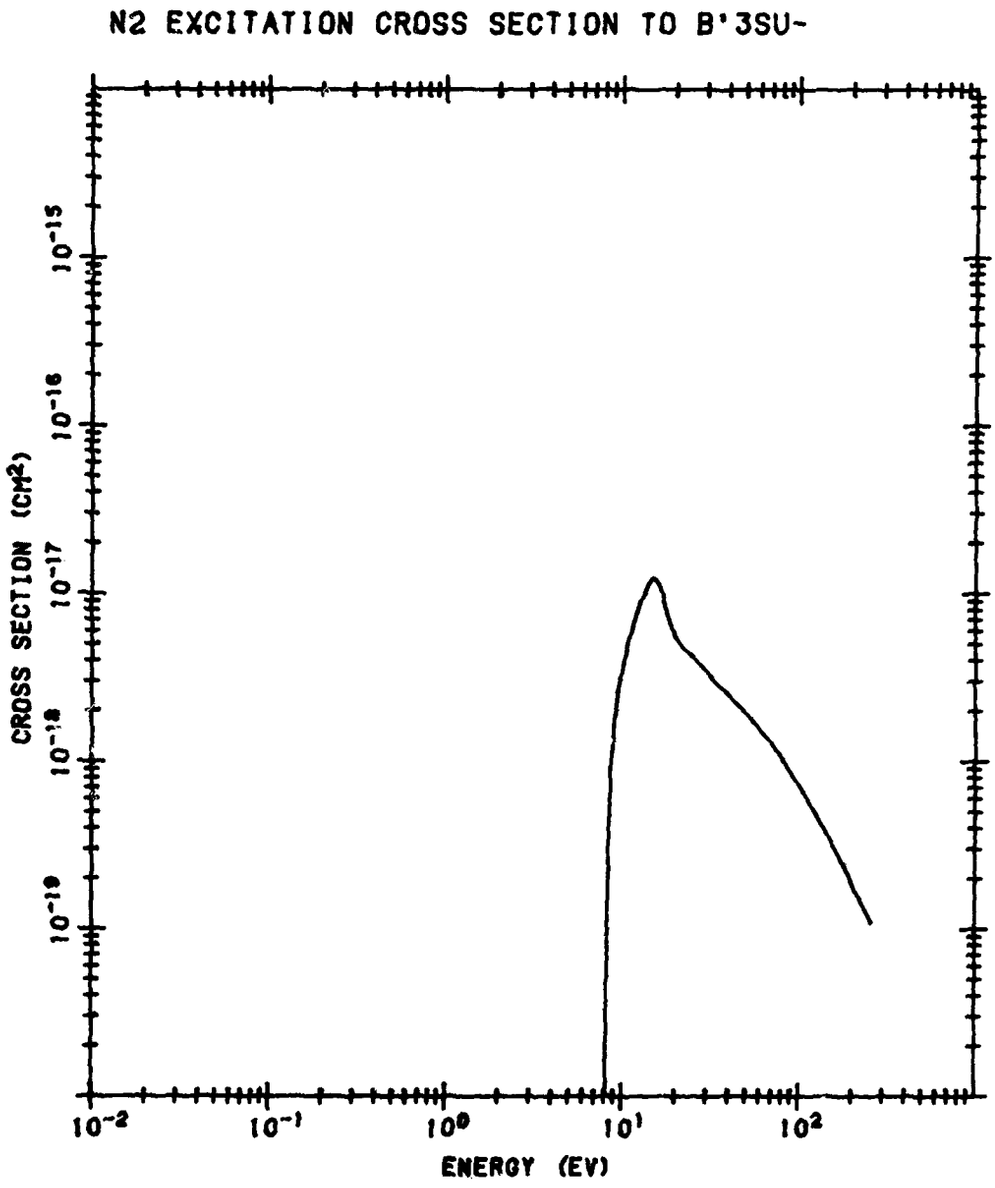


Figure B92. $N_2$ Electron Excitation Cross Section to $B'\ ^3\Sigma_u^-$. The data source is the same as that of Figure B89

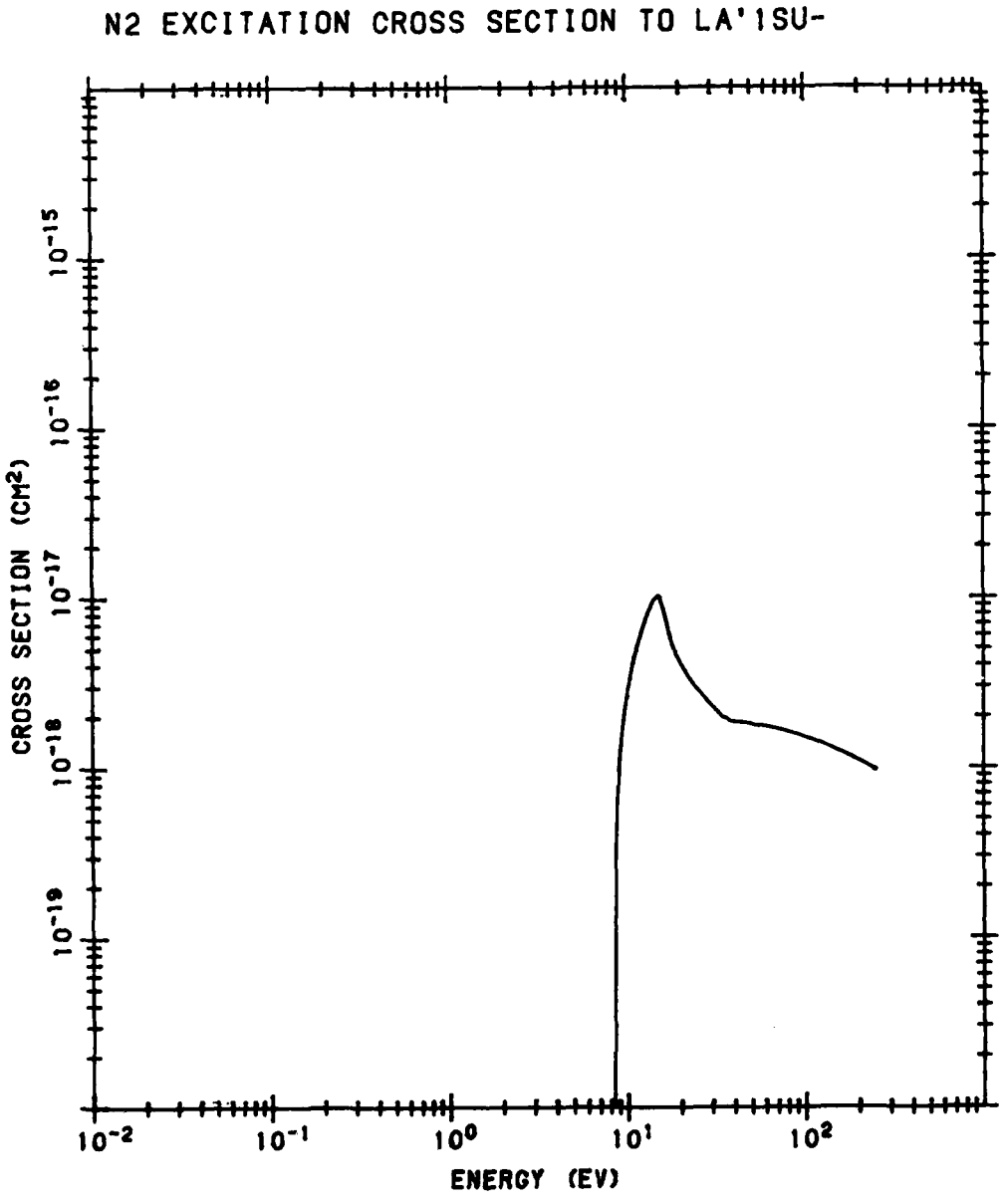


Figure B93. $N_2$ Electron Excitation Cross Section to a' $^1\Sigma_u^-$. The data below 50 eV are from Cartwright et al (1977)[B24] and extrapolated as (log E)/E to higher energies

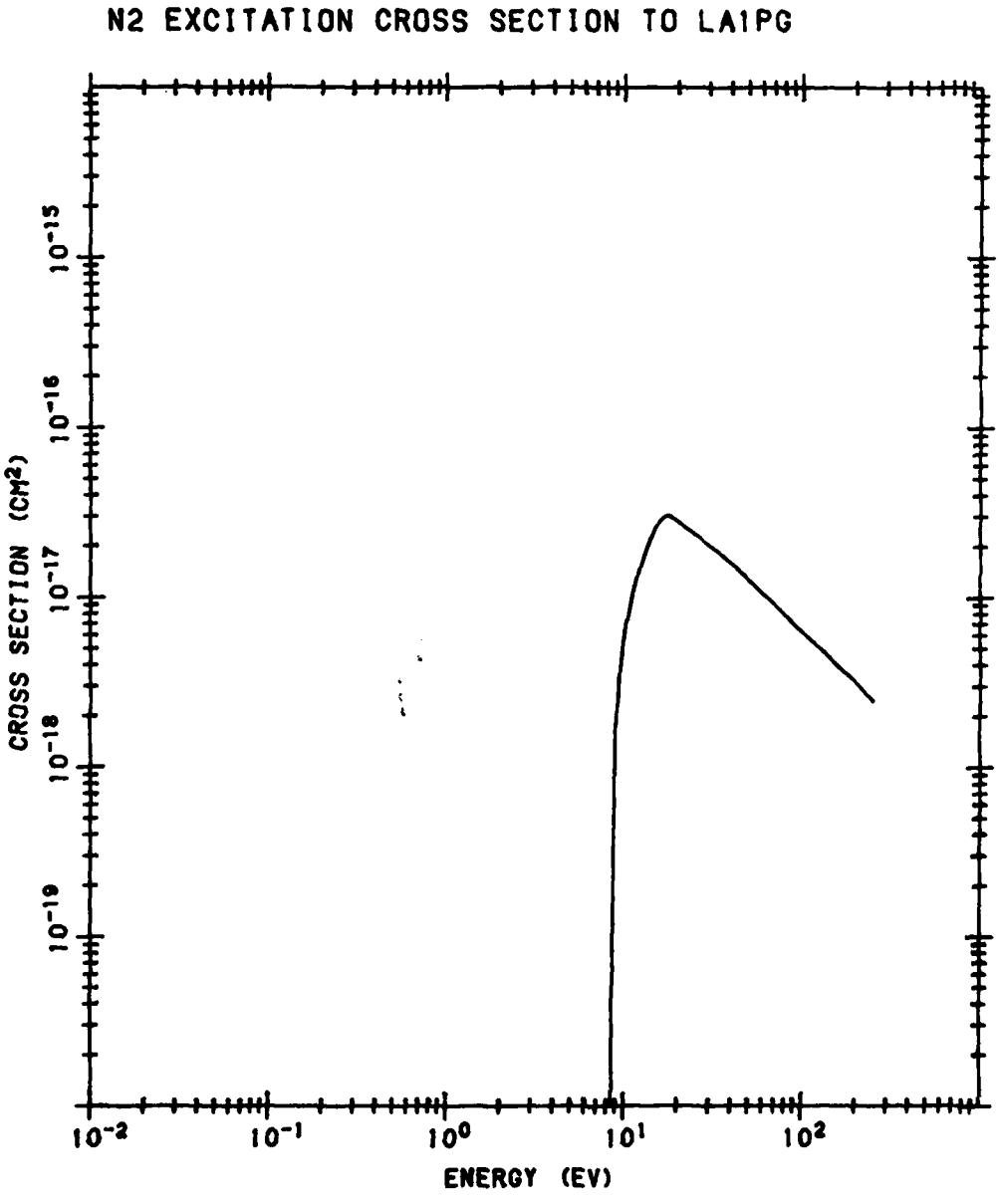


Figure B94. $N_2$ Electron Excitation Cross Section to a $^1\Pi_g$. The data below 50 eV are from Cartwright et al (1977)[B24] and extrapolated as 1/E to higher energies

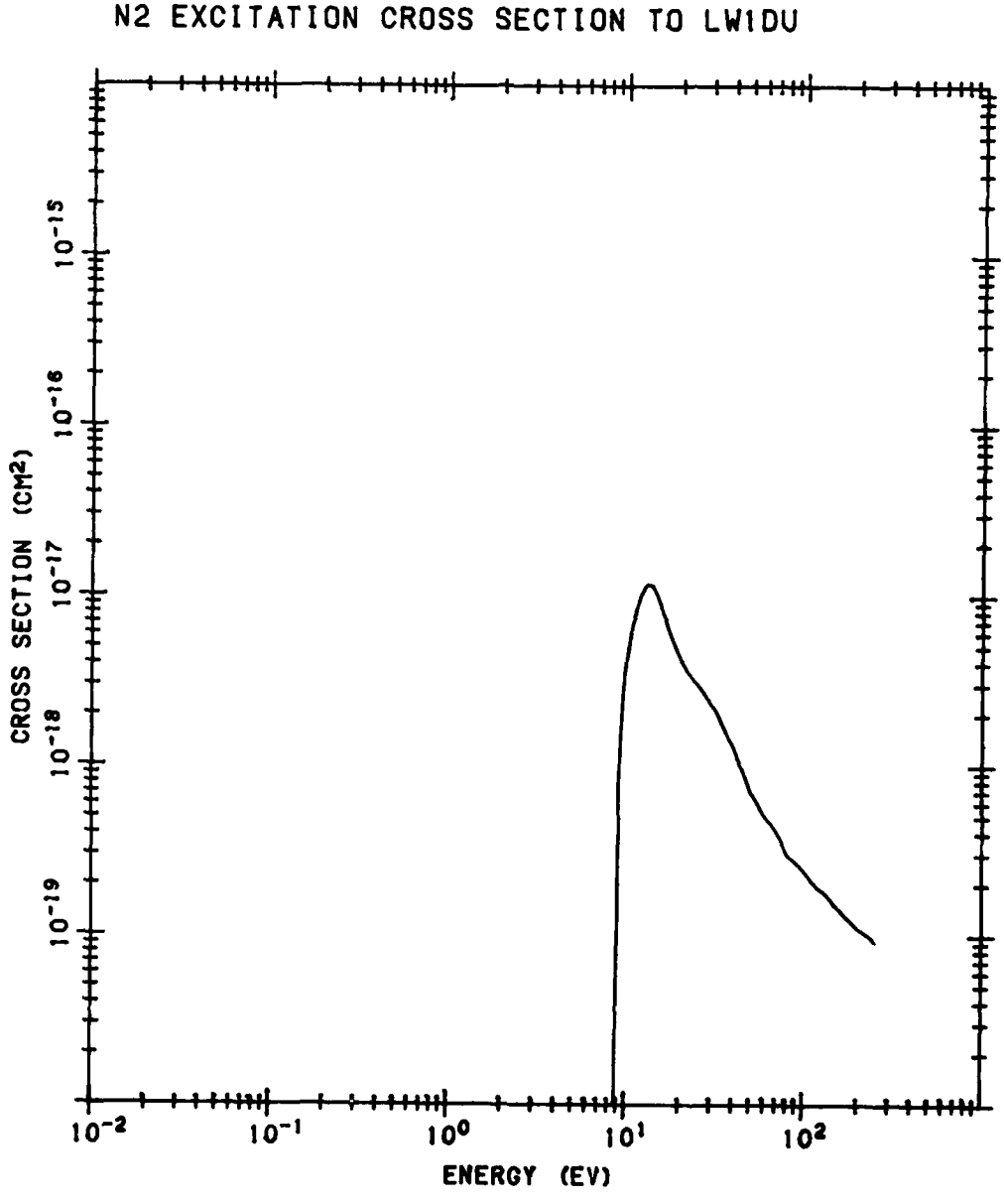


Figure B95. $N_2$ Electron Excitation Cross Section to W $^1\Delta_u$. The data source is the same as that of Figure B93

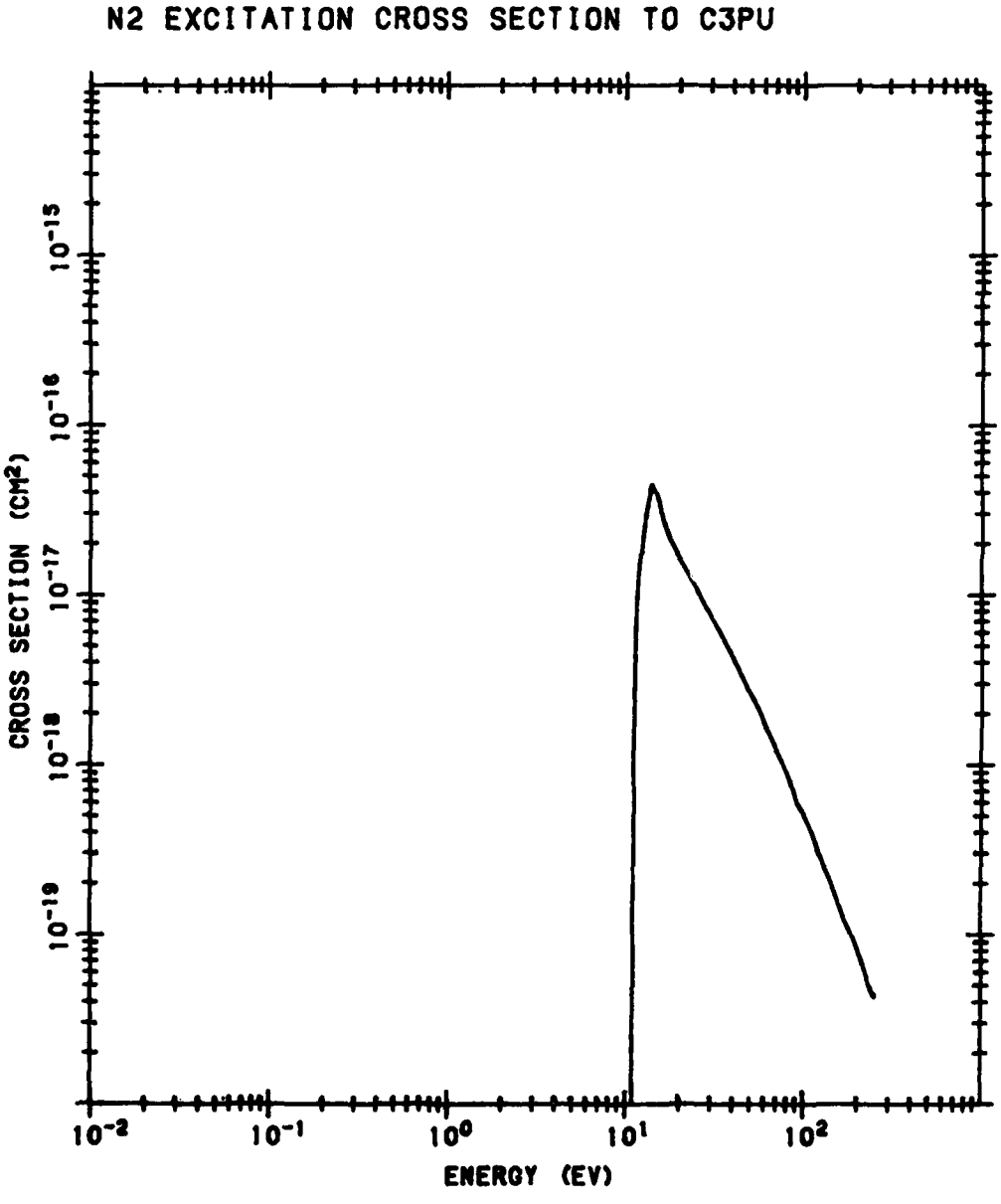


**Figure B96.** $N_2$ Electron Excitation Cross Section to C $^3\Pi_u$. The data source is the same as that of Figure B89

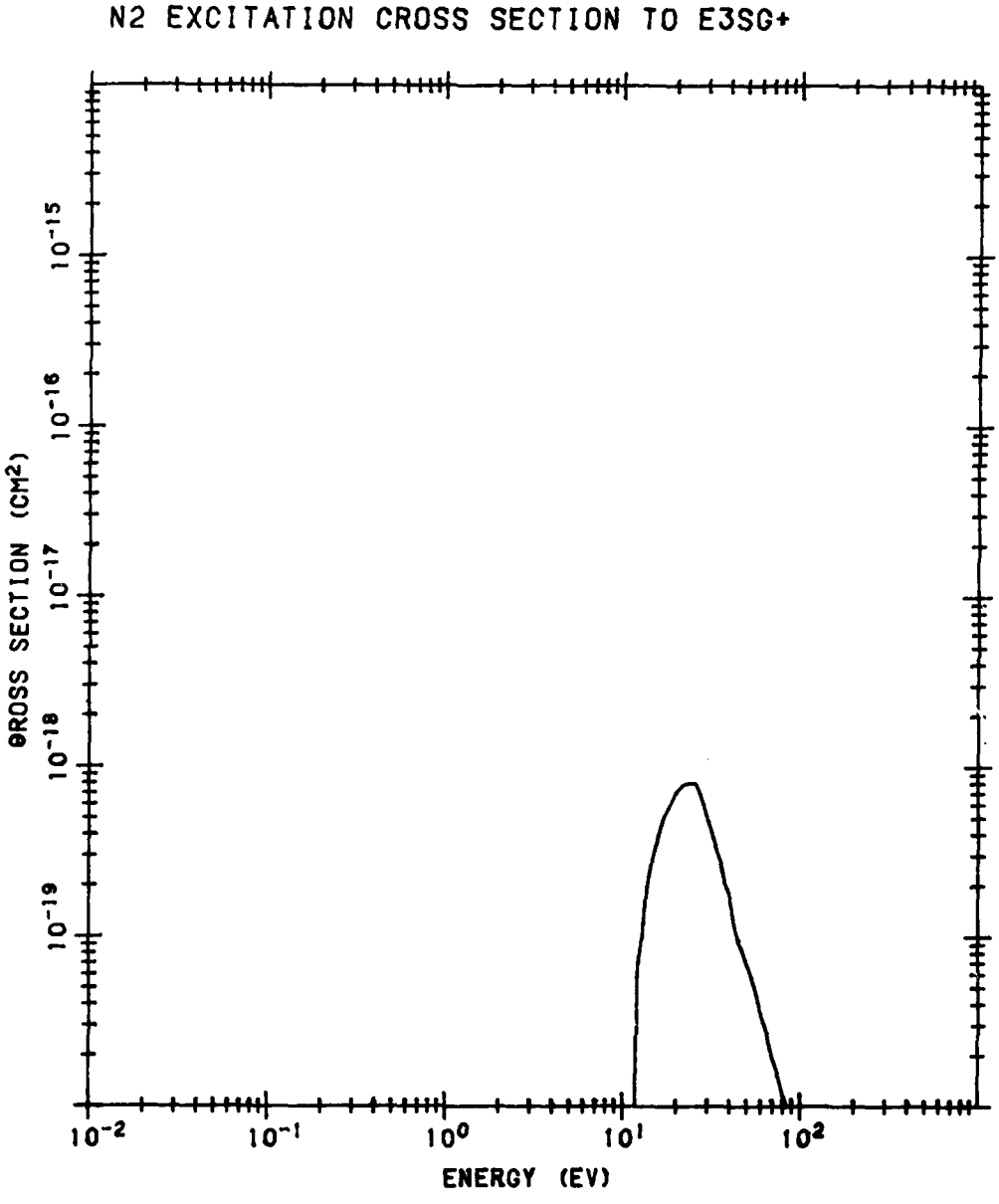


Figure B97. $N_2$ Electron Excitation Cross Section to E $^3\Sigma_g^+$. The data source is the same as that of Figure B89

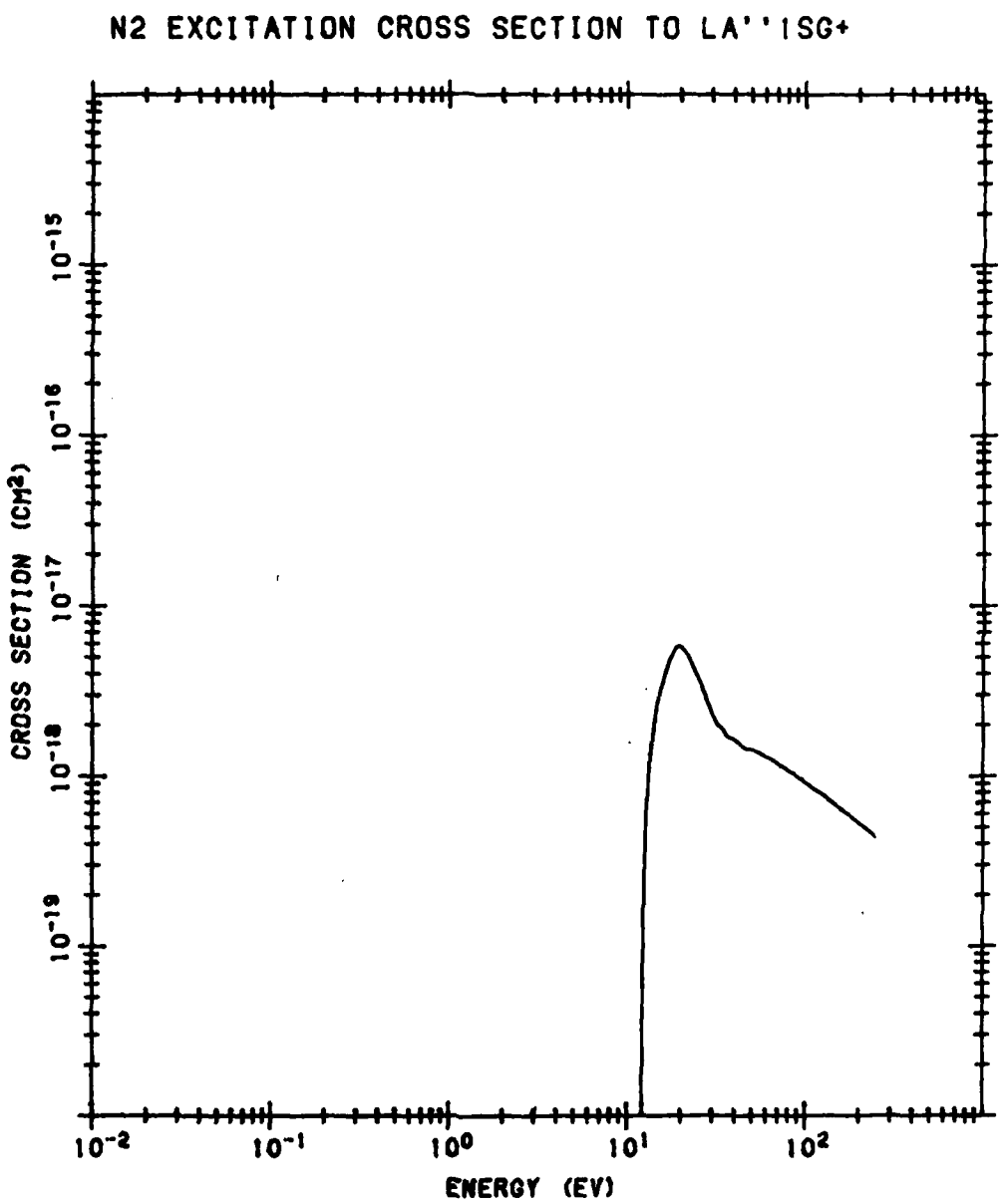


Figure B98. $N_2$ Electron Excitation Cross Section to a" $^1\Sigma_g^+$. The data source is the same as that of Figure B94

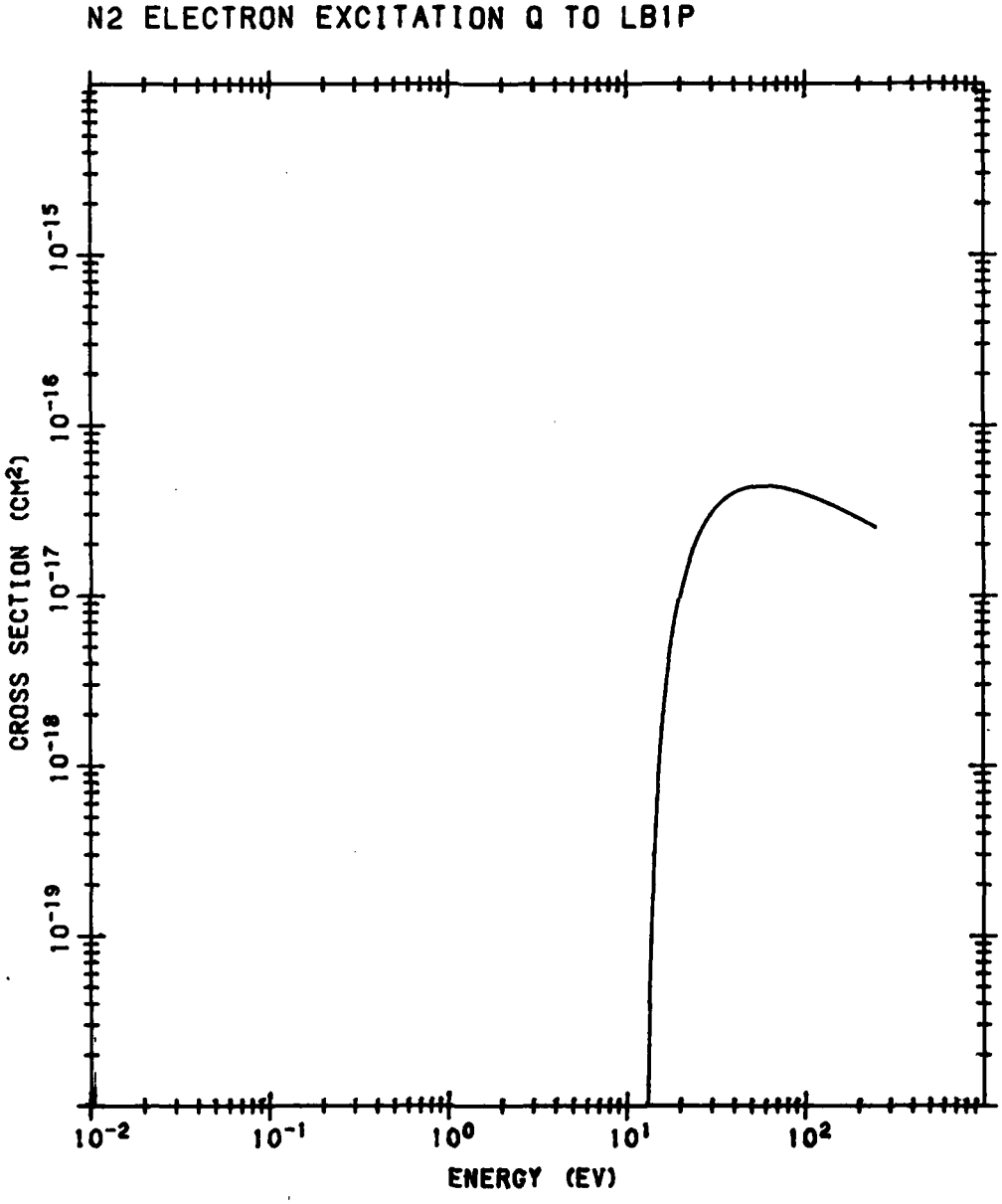


Figure B99. $N_2$ Electron Excitation Cross Section to b $^1\Pi_u$. The data are from Jackman et al (1980)[B22]

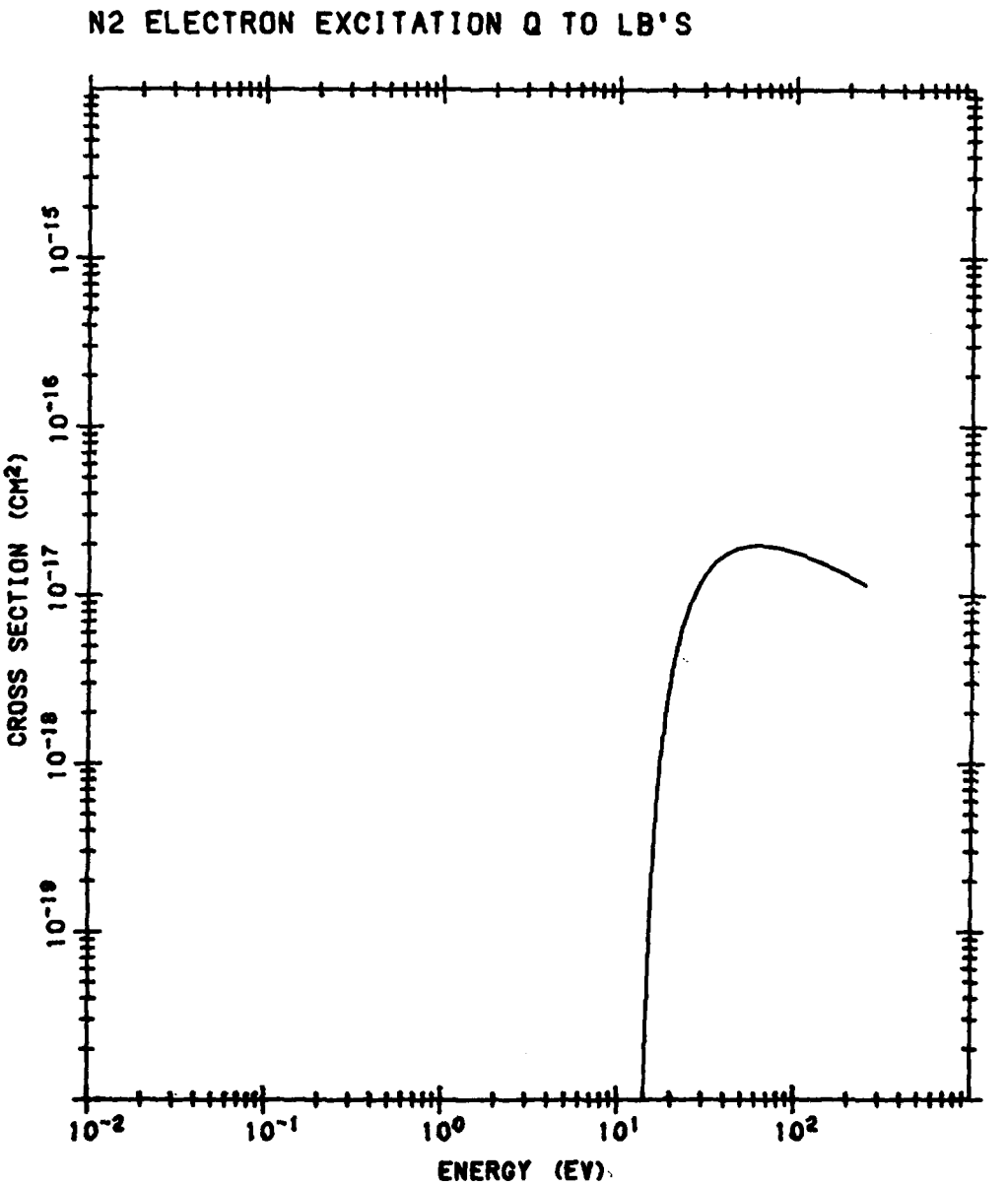


Figure B100. $N_2$ Electron Excitation Cross Section to b' $^1\Sigma_u^+$. The data are from Jackman et al (1980)[B22]

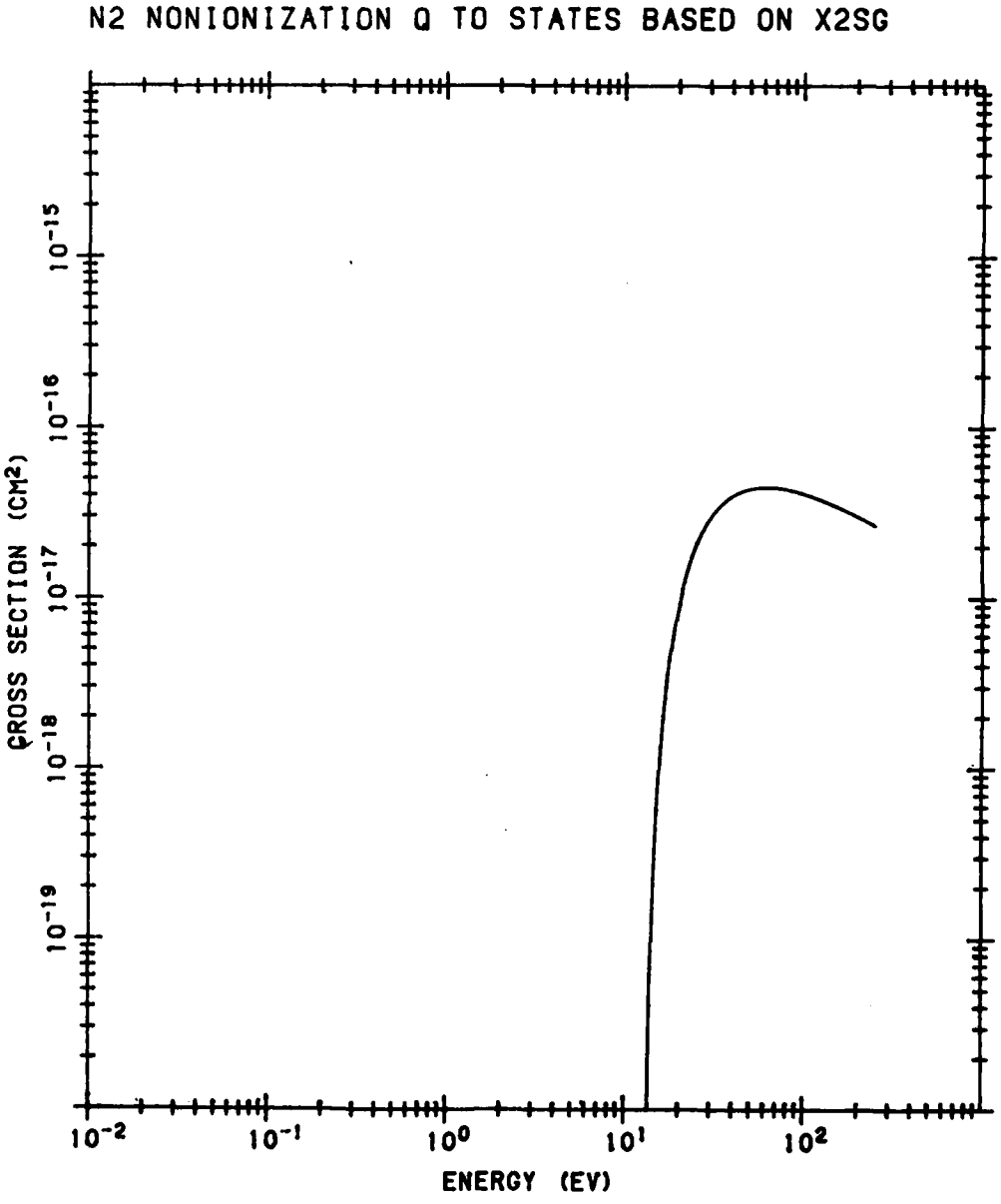


Figure B101. Sum of $N_2$ Nonionizing Cross Sections to Rydberg States Based on $N_2^+ X\,^2\Sigma_g^+$. The cross section data (Jackman et al 1980 [B22]) are weighted by the fraction of excitations which decay radiatively and summed from an n of 3

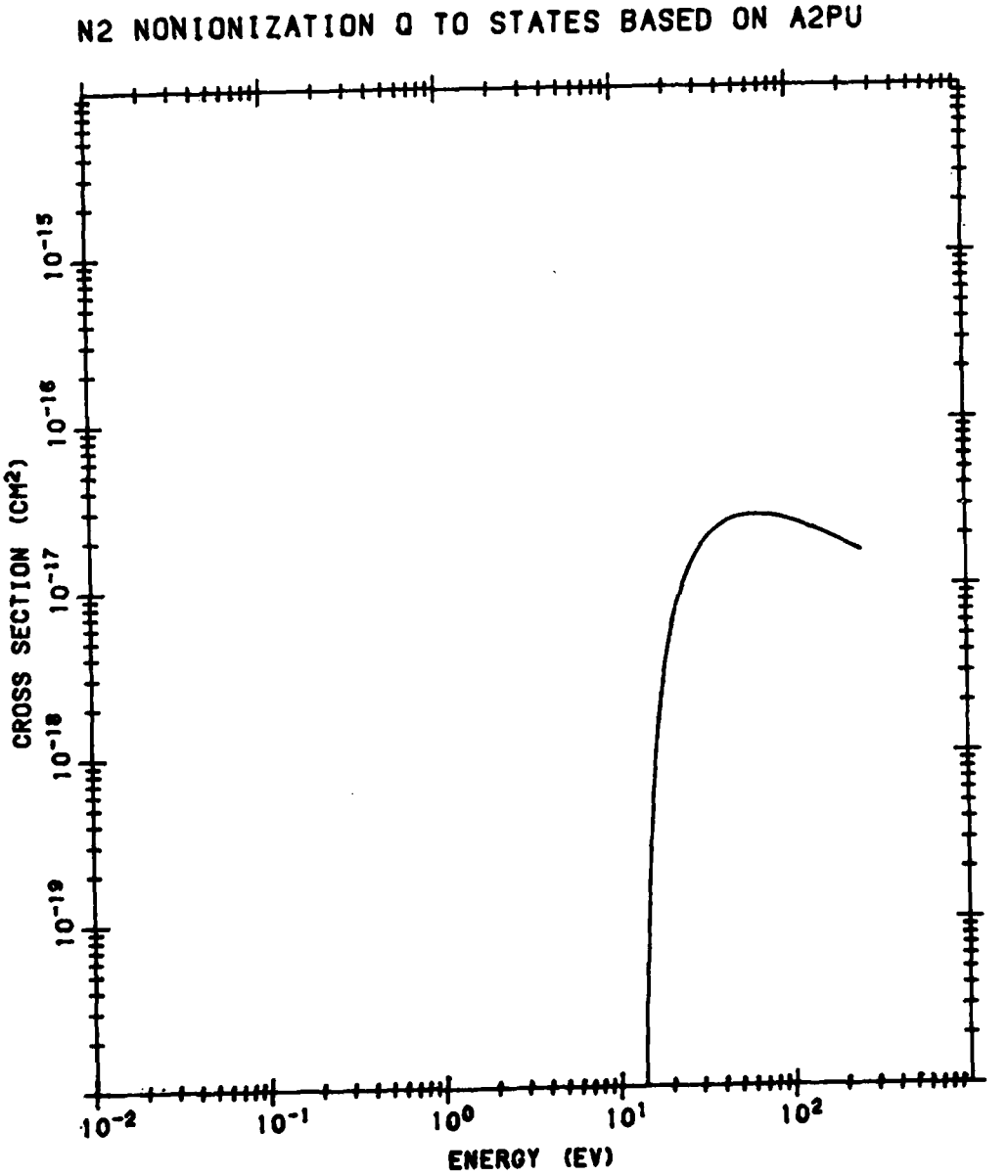


Figure B102. Sum of $N_2$ Nonionizing Cross Sections to Rydberg States based on $N_2^+$ A $\Pi_u$. The data source is the same as that of Figure B101

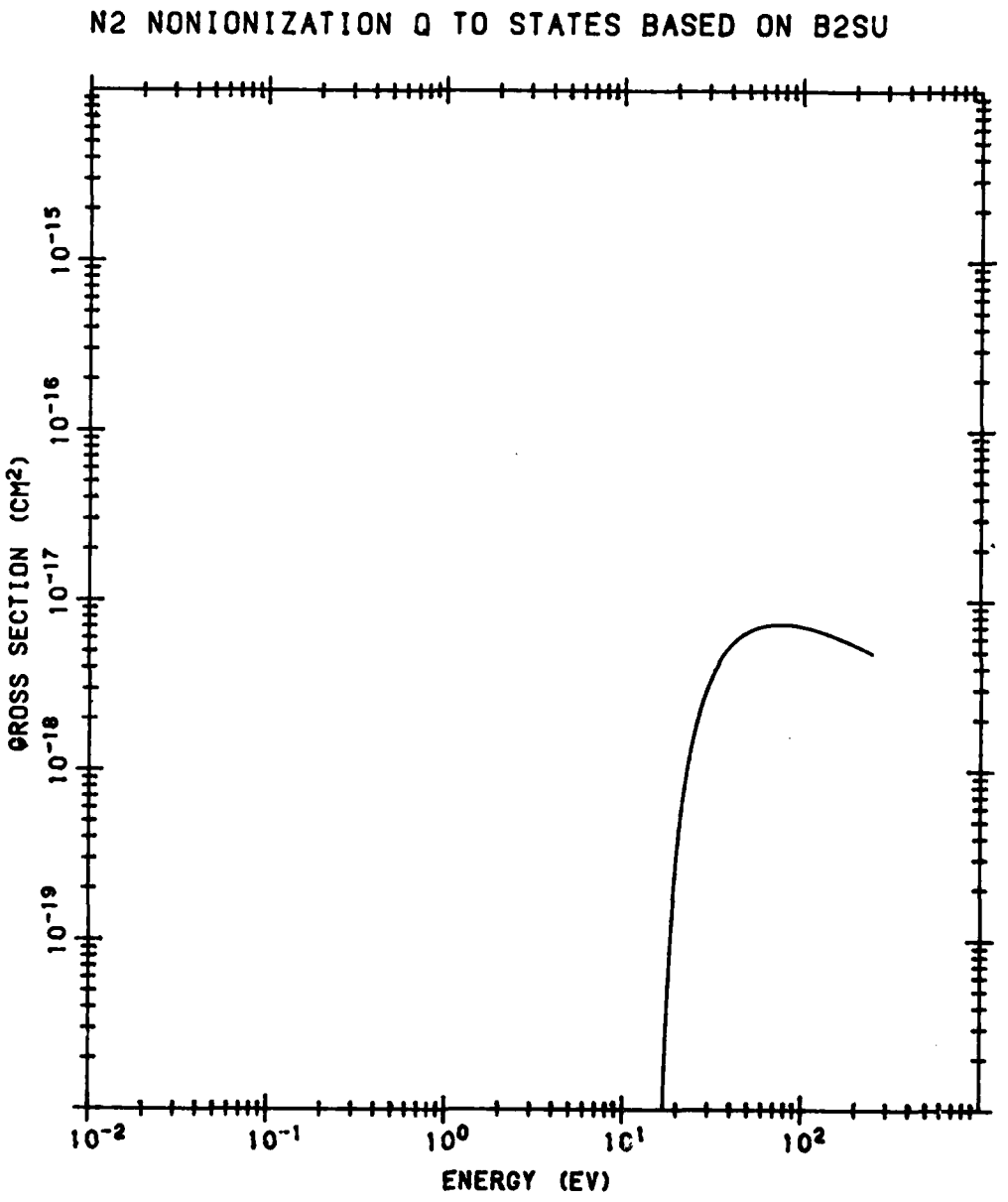


Figure B103. Sum of $N_2$ Nonionizing Cross Sections to Rydberg States Based on $B\,^2\Sigma_u^+$. The data source is the same as that of Figure B101

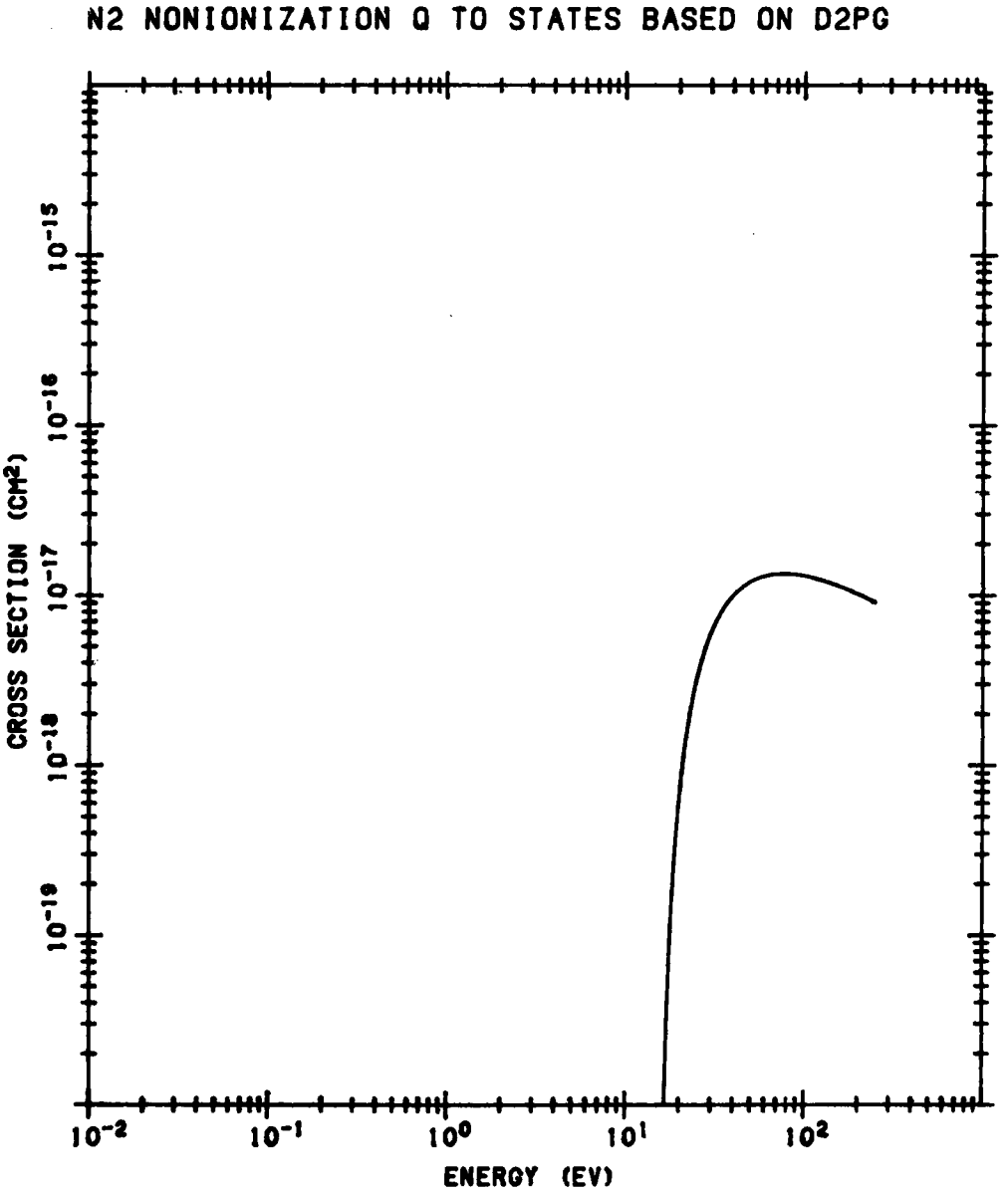


Figure B104. Sum of $N_2$ Nonionizing Cross Sections to Rydberg States Based on D $^2\Pi_g$. The data source is the same as that of Figure B101

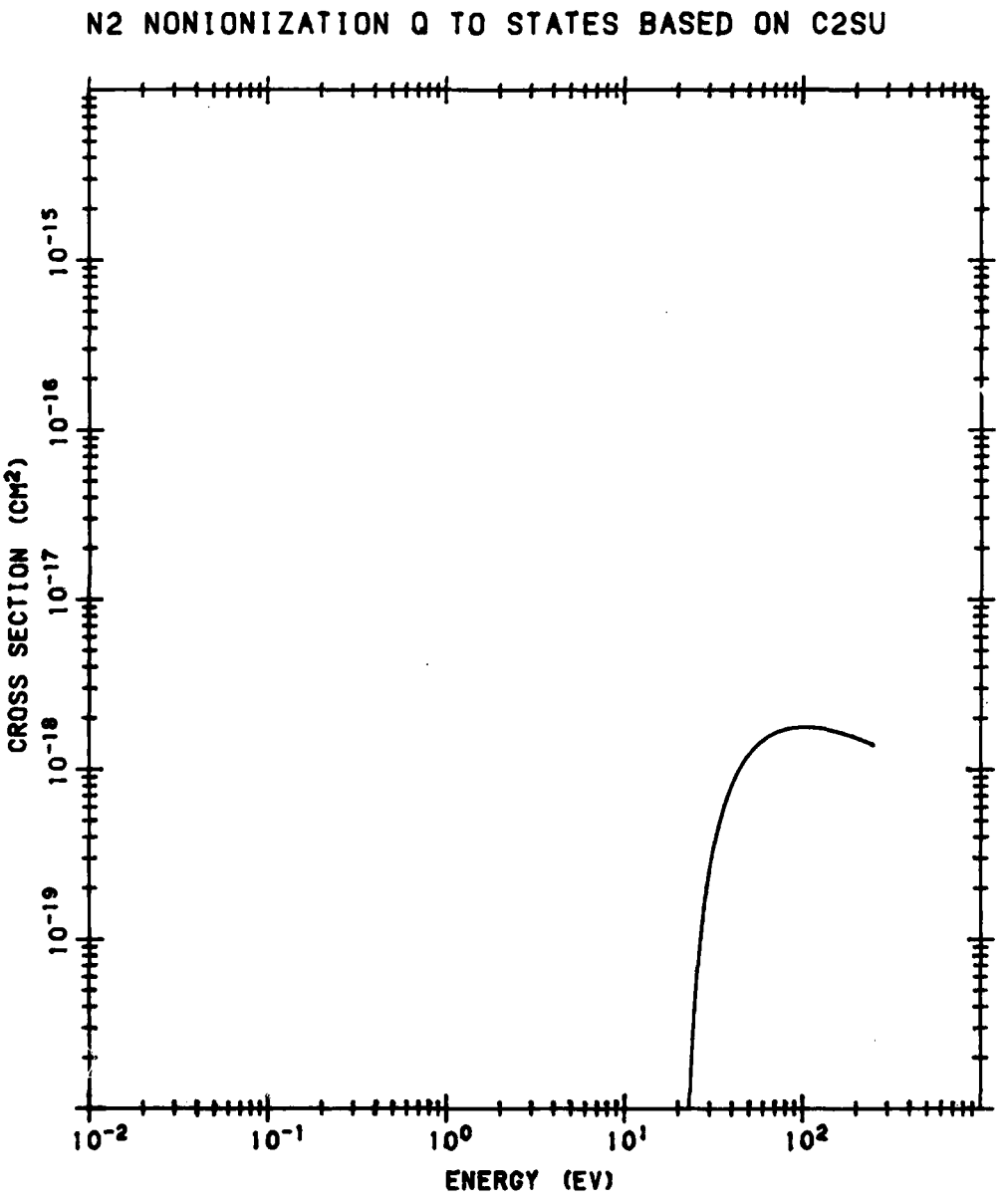


Figure B105. Sum of $N_2$ Nonionizing Cross Sections to Rydberg States Based on C $^2\Sigma_u^+$. The data source is the same as that of Figure B101

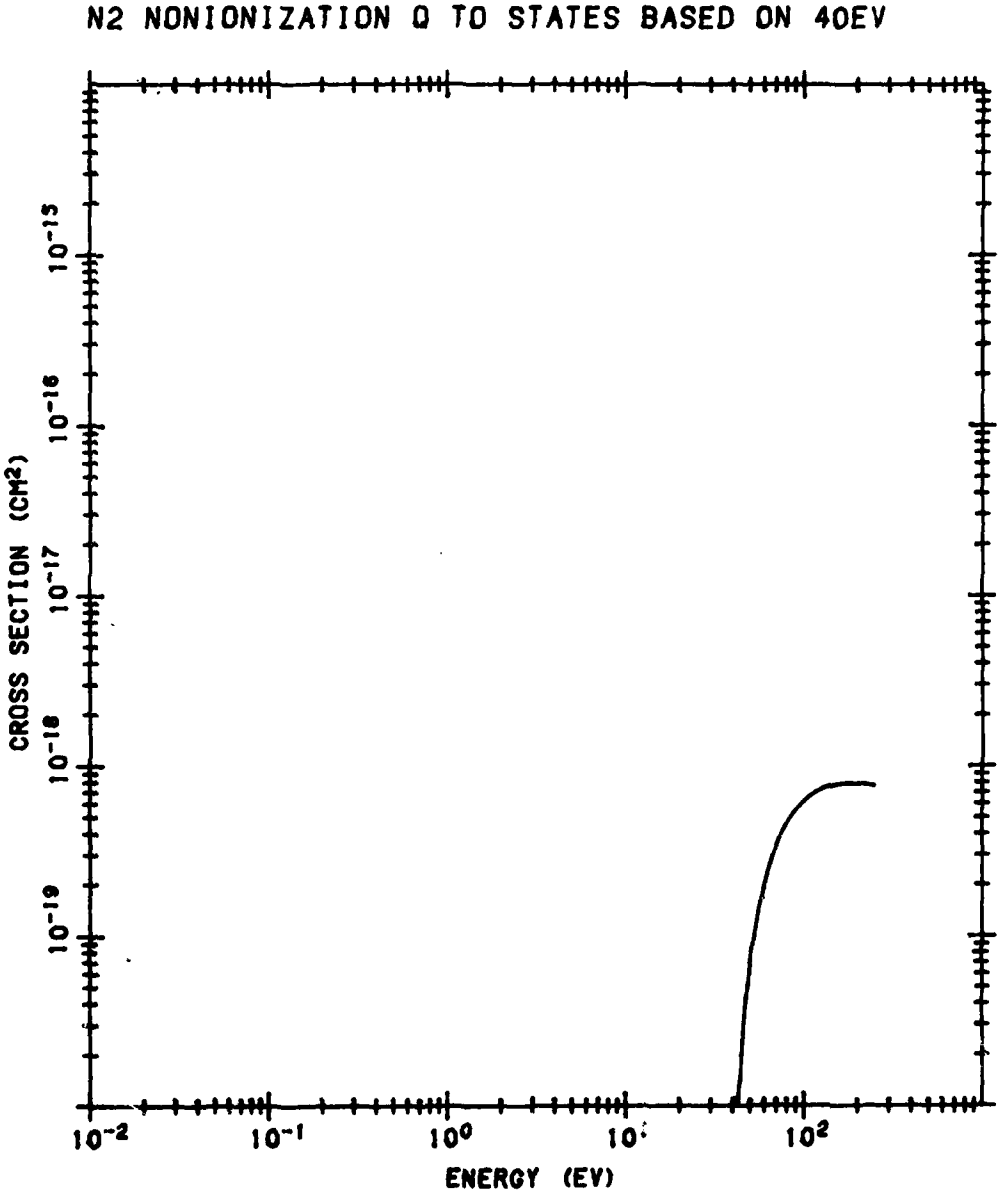


Figure B106. Sum of $N_2$ Nonionizing Cross Sections to Rydberg States Based on an $N_2^+$ State Hypothesized at 40 eV. The data source is the same as that of Figure B101

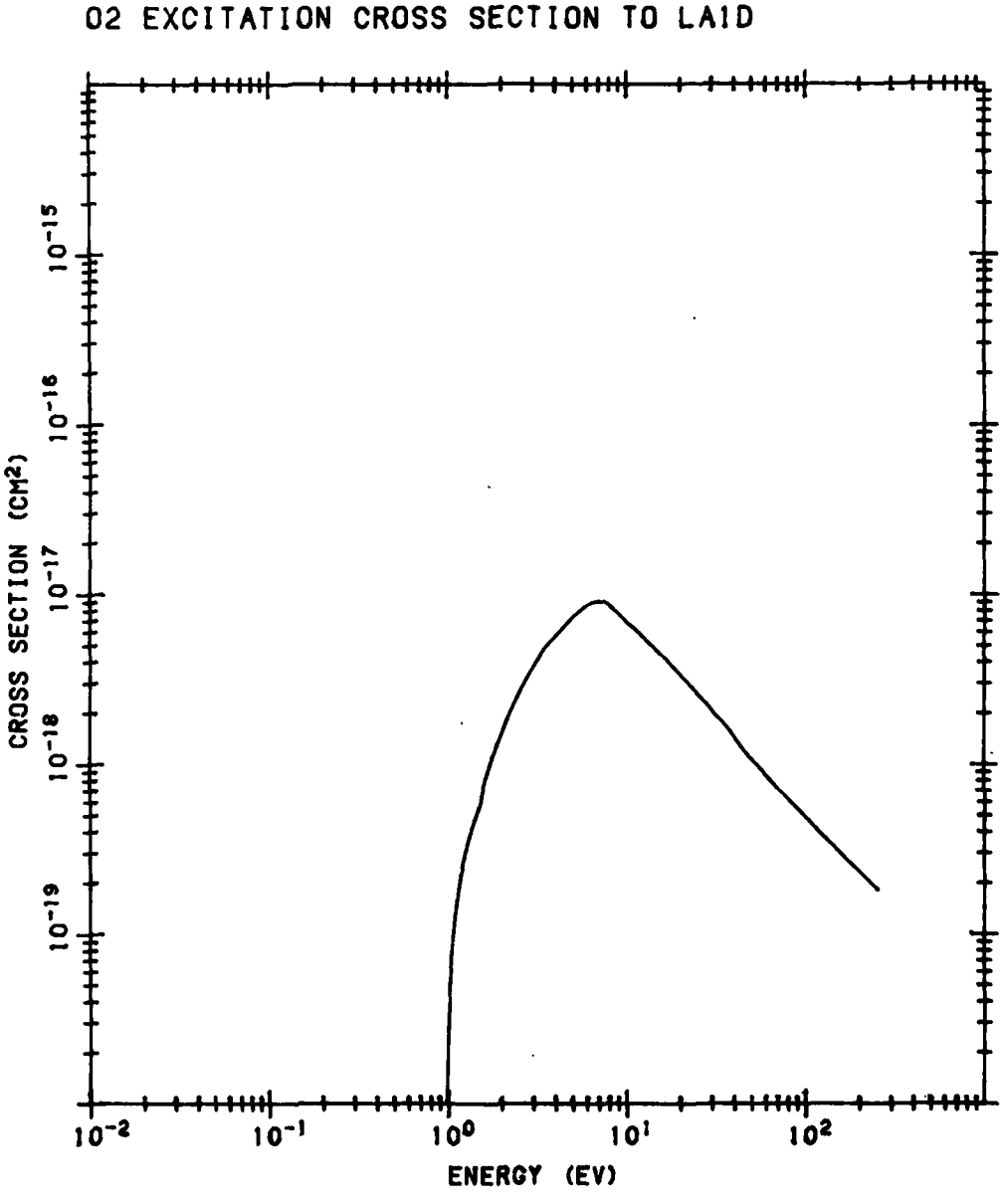


Figure B107. $O_2$ Electron Excitation Cross Section to a $^1\Delta_g$. Below 3.5 eV the data are from Linder and Schmidt (1971);[B16] between 4 and 45 eV from Trajmar et al (1971),[B25] and extrapolated to higher energies using 1/E

B25. Trajmar, S., Cartwright, D.C., and Williams, W. (1971) Phys. Rev. A4:1462.

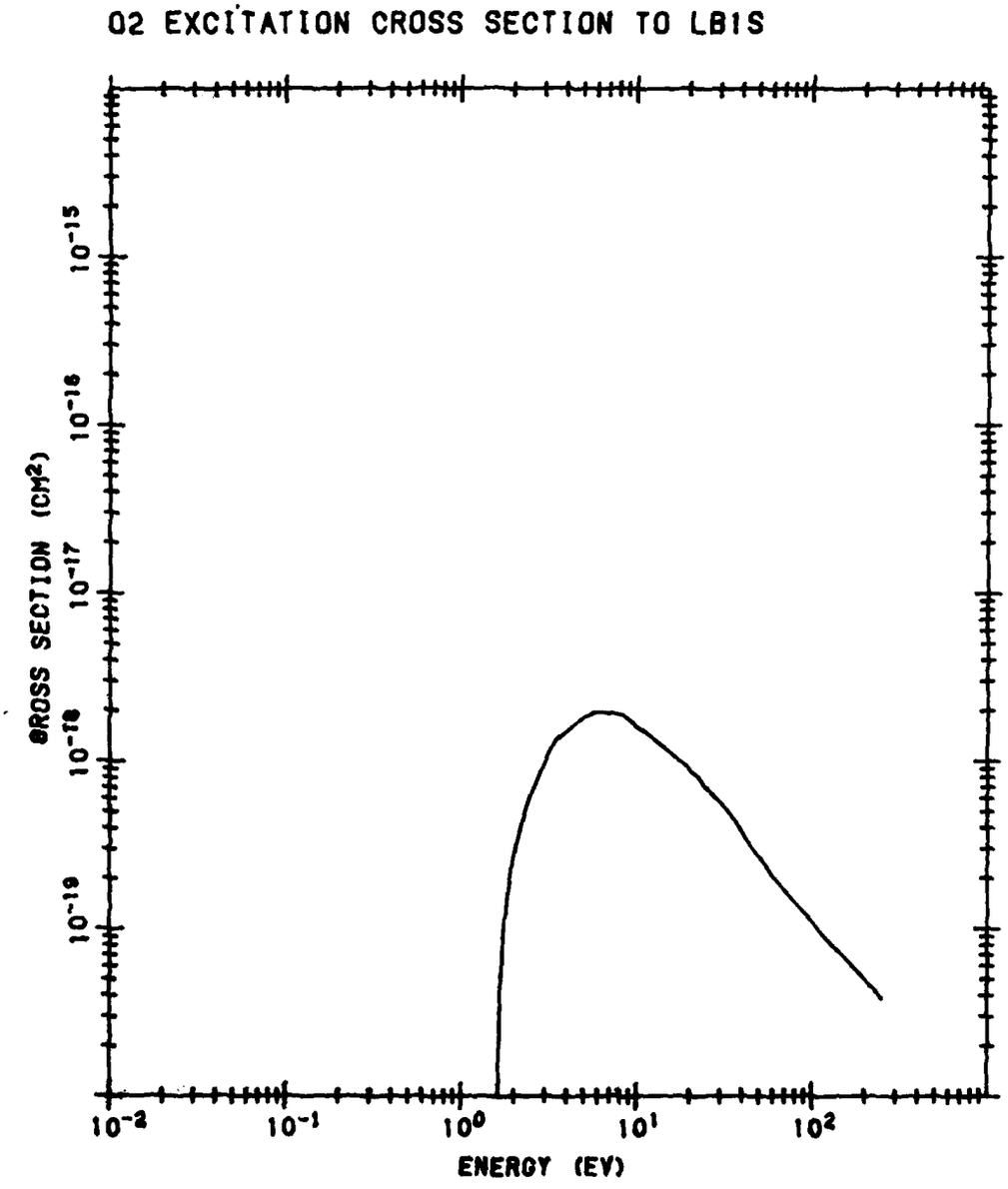


Figure B108. $O_2$ Electron Excitation Cross Section to b $^1\Sigma_g^+$. The data source is the same as that of Figure B107

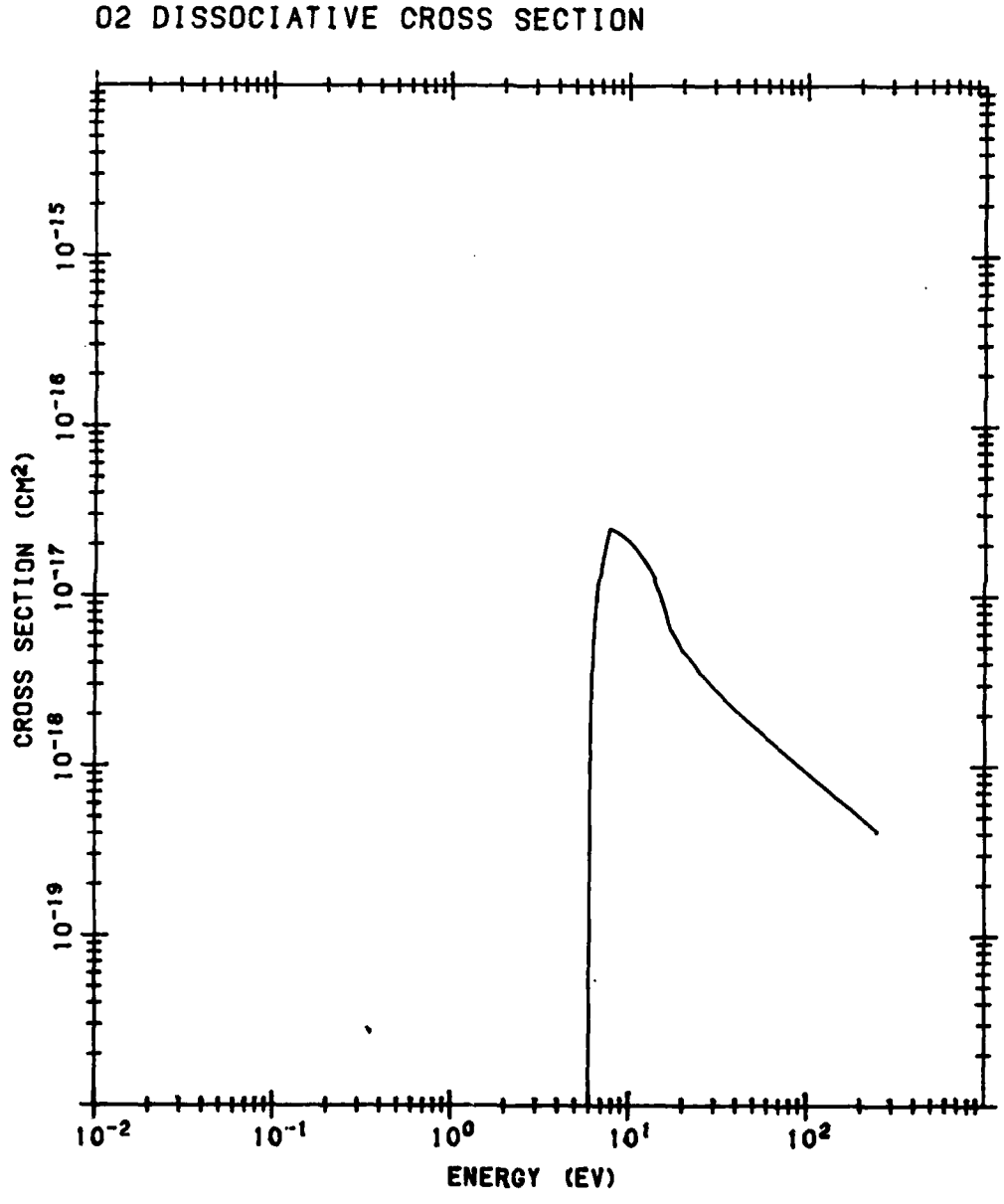


**Figure B109. $O_2$ Nonionizing Dissociative Cross Section. The data are from the Linder and Schmidt (1971)[B17] cross section with an energy loss of 6 eV**

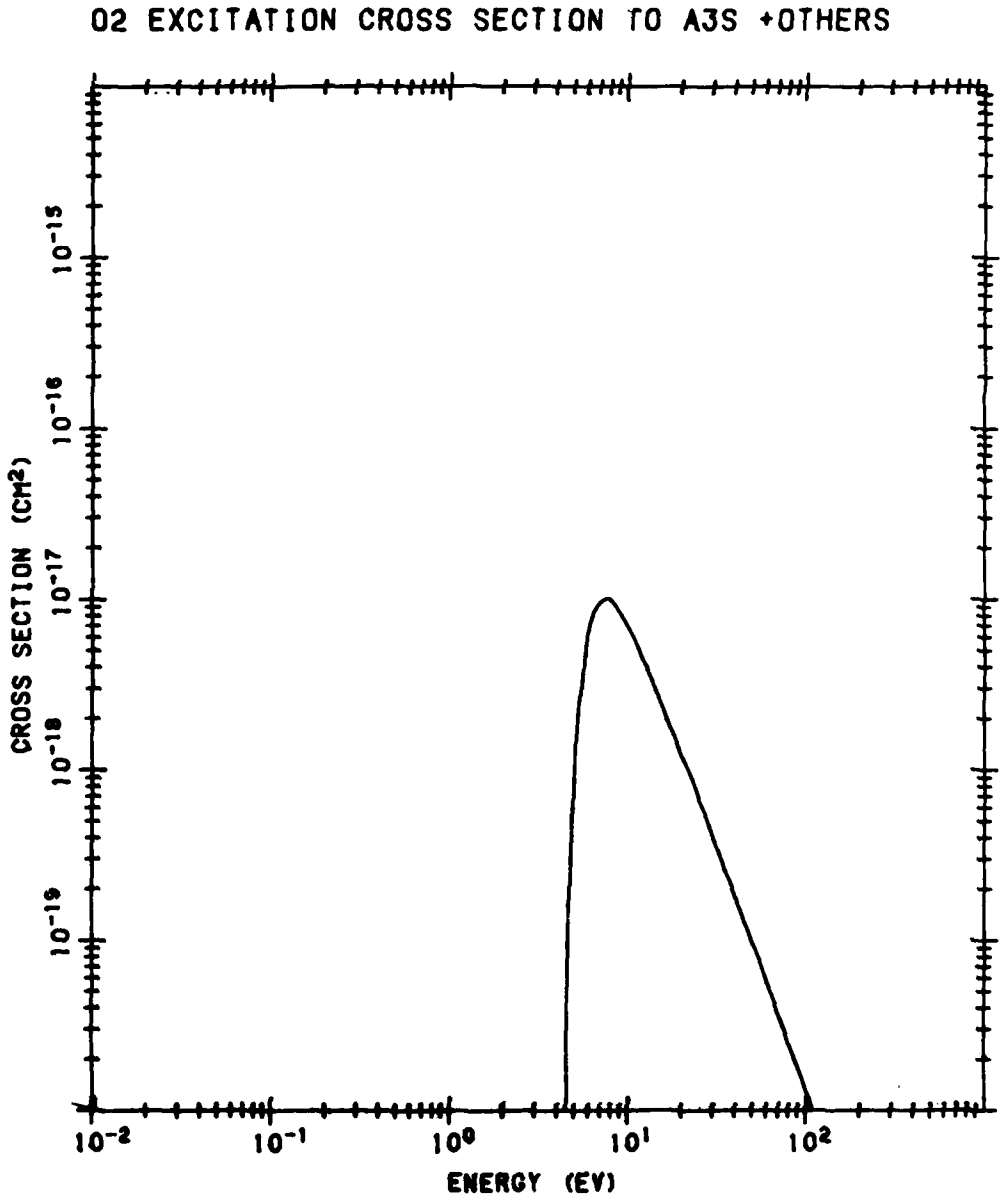


**Figure B110.** $O_2$ **Electron Excitation Cross Section to A** $^3\Sigma_u^+$ **and Similar States. The data are from the Linder and Schmidt (1971)[B17] cross section with an energy loss of 4.5 eV**

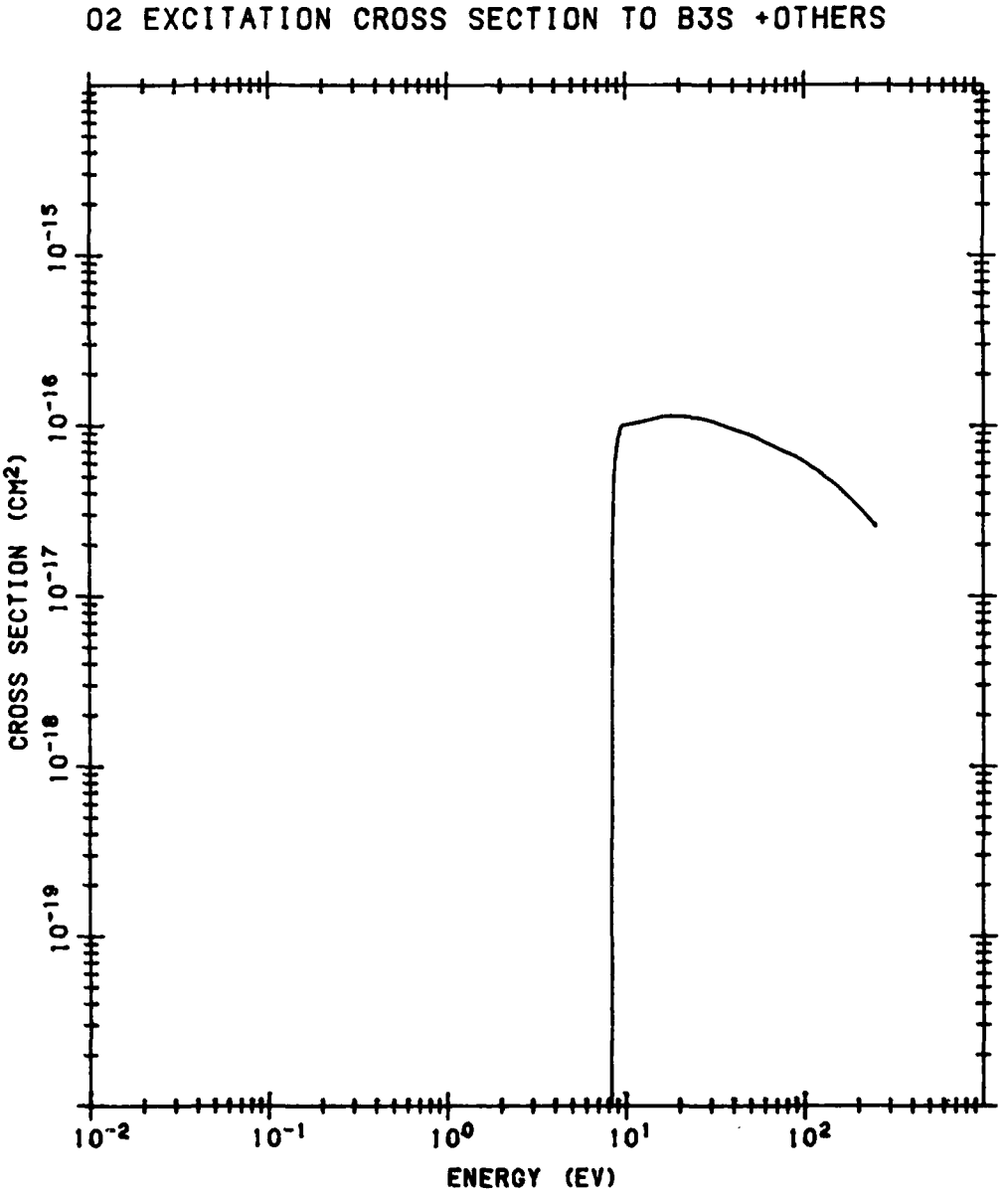


Figure B111. $O_2$ Electron Excitation Cross Section to B $^3\Sigma_u^-$ and Similar States. The data are from the Linder and Schmidt (1971)[B17] cross section with an energy loss of 8.4 eV minus the Rydberg state cross sections in Figures B112 through B118

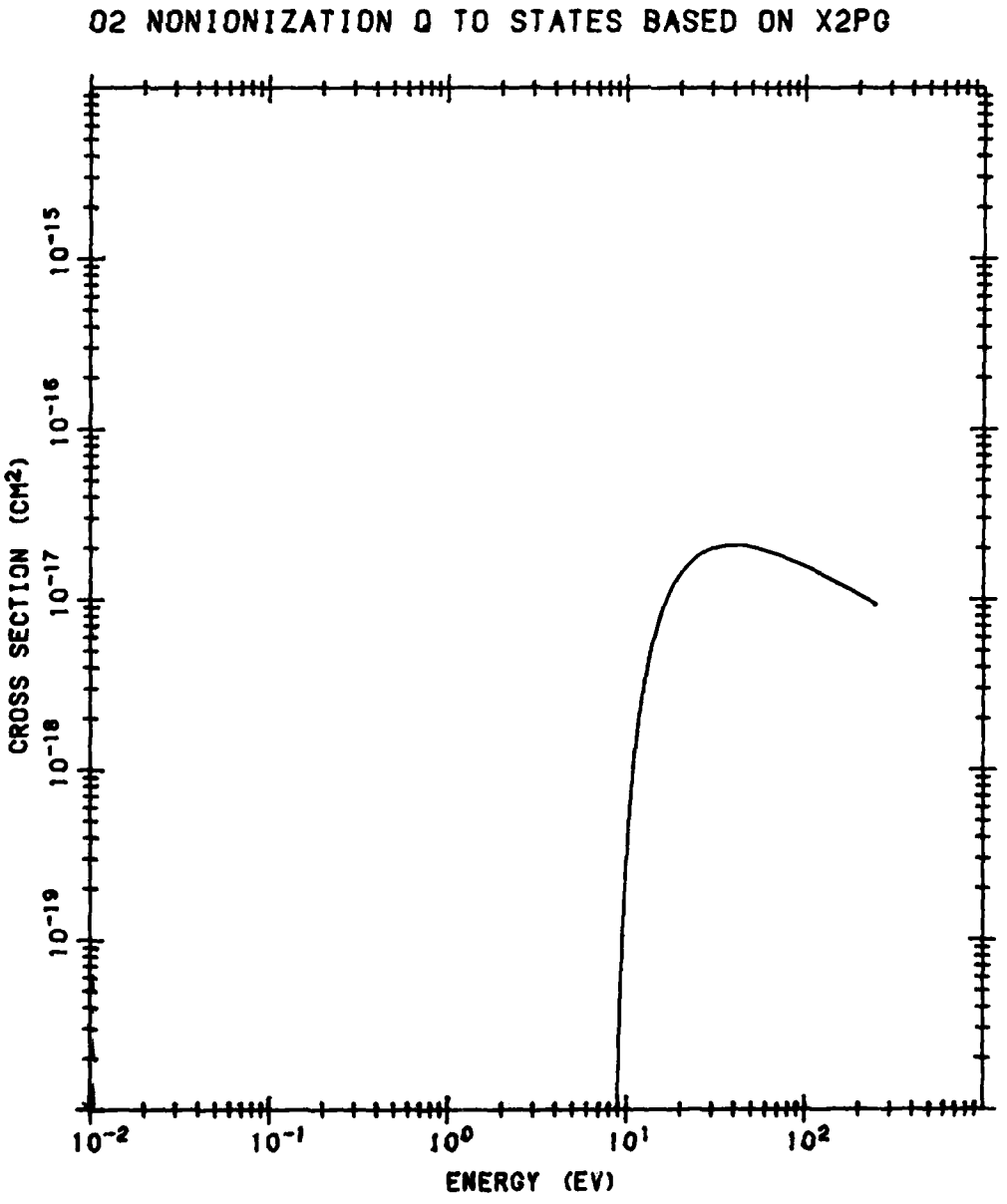


Figure B112. Sum of $O_2$ Nonionizing Cross Sections to Rydberg States Based on $O_2$ $X\,^2\Sigma g$. The cross section data from Jackman et al (1980)[B22] are weighted by the fraction of excitations which decay radiatively and summed from an n of 3

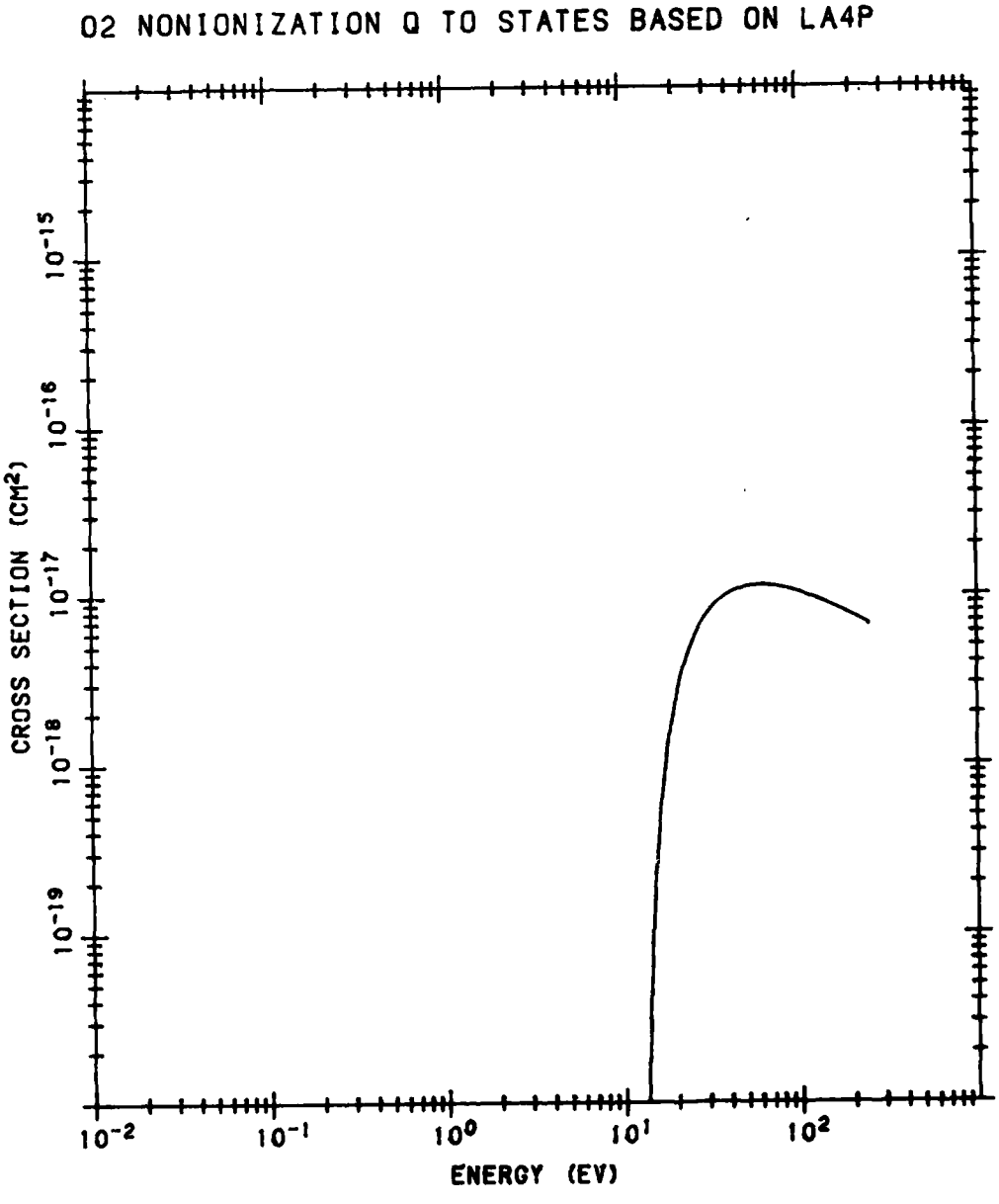


Figure B113. Sum of $O_2$ Nonionizing Cross Sections to Rydberg States Based on $O_2^+$ a $^4\Pi_u$. The data source is the same as that of Figure B112

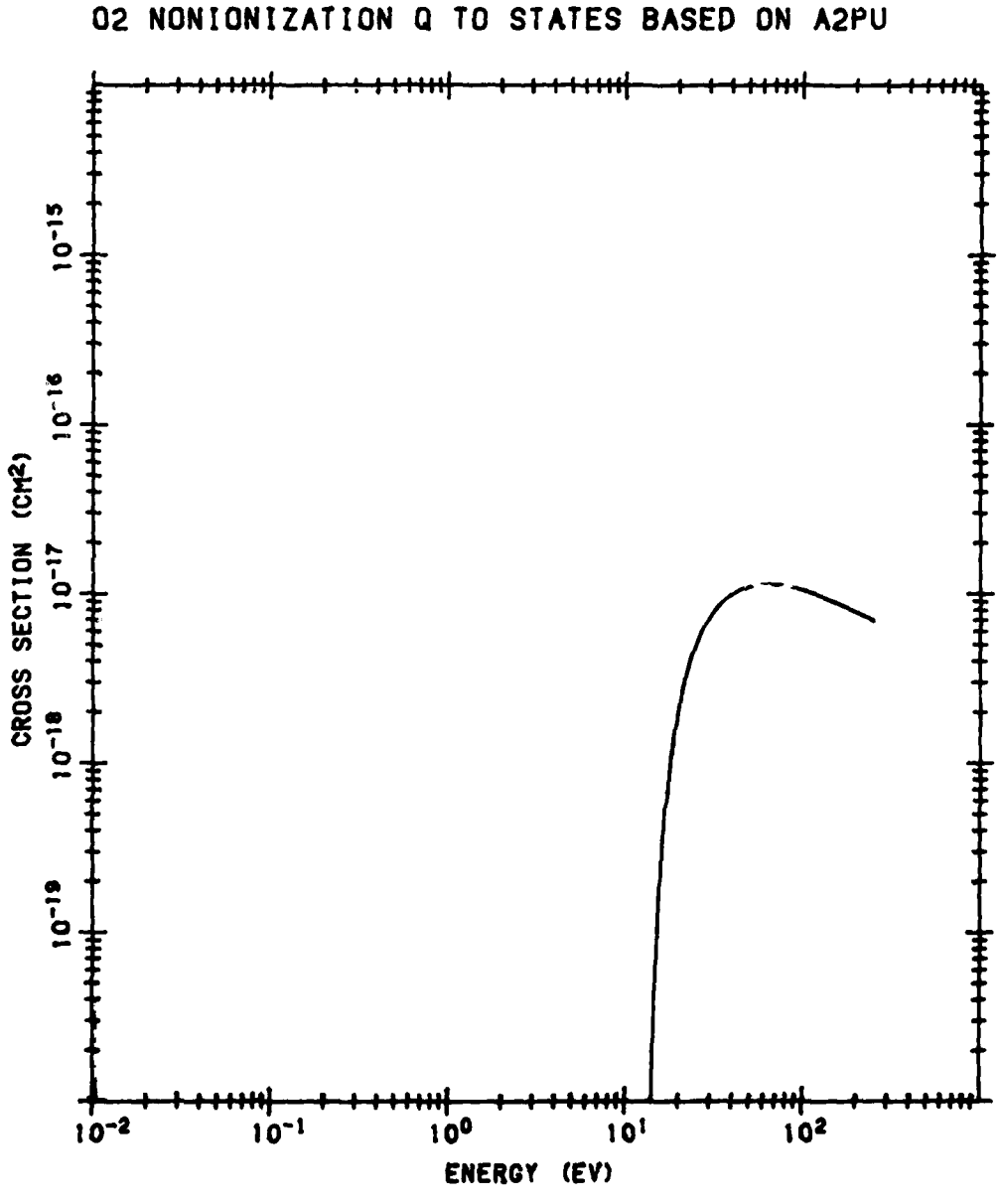


Figure B114. Sum of $O_2$ Nonionizing Cross Sections to Rydberg States Based on A $^2\Pi_u$. The data source is the same as that of Figure B112

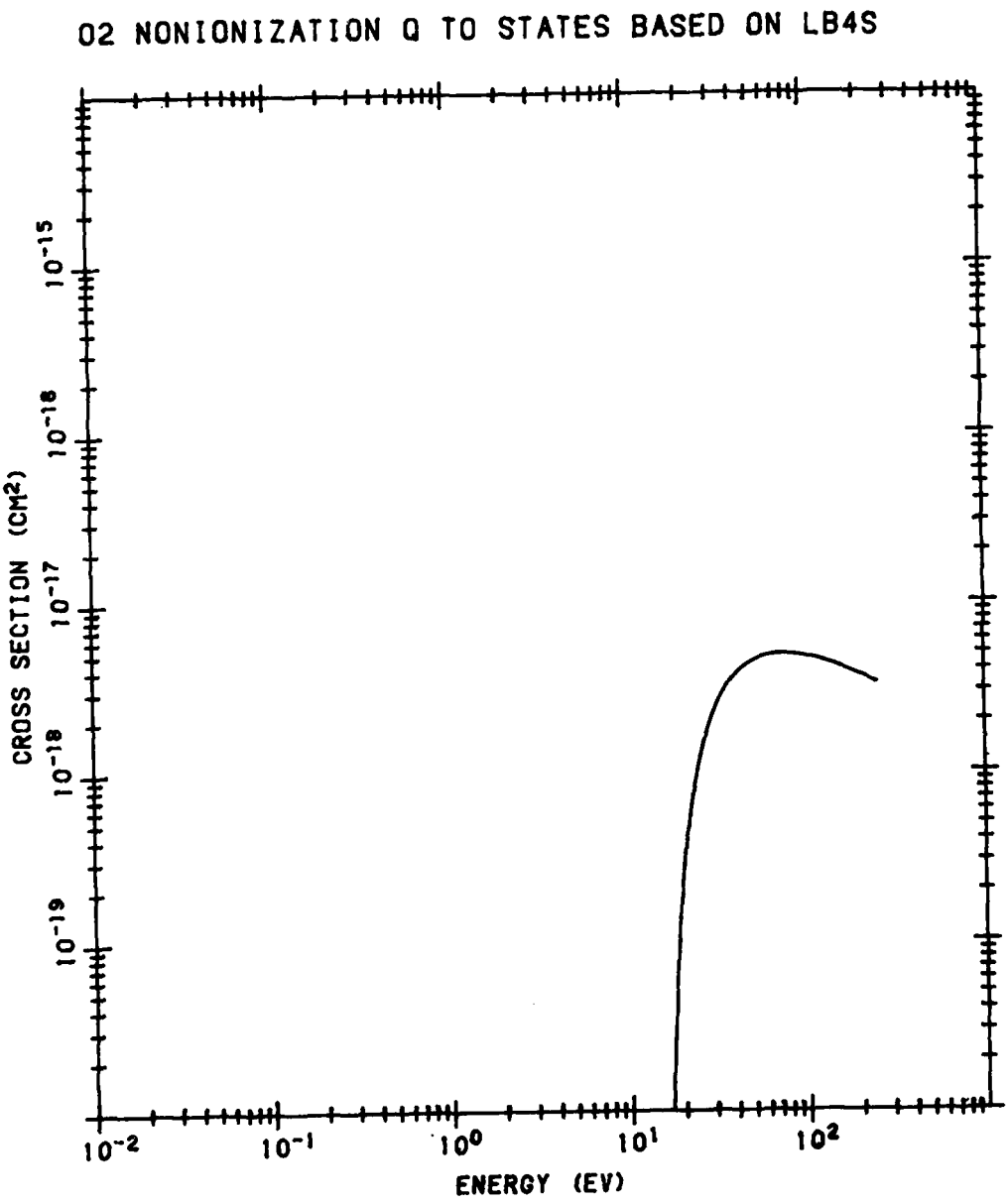


Figure B115. Sum of $O_2$ Nonionizing Cross Sections to Rydberg States Based on b $^4\Sigma_g^-$. The data source is the same as that of Figure B112

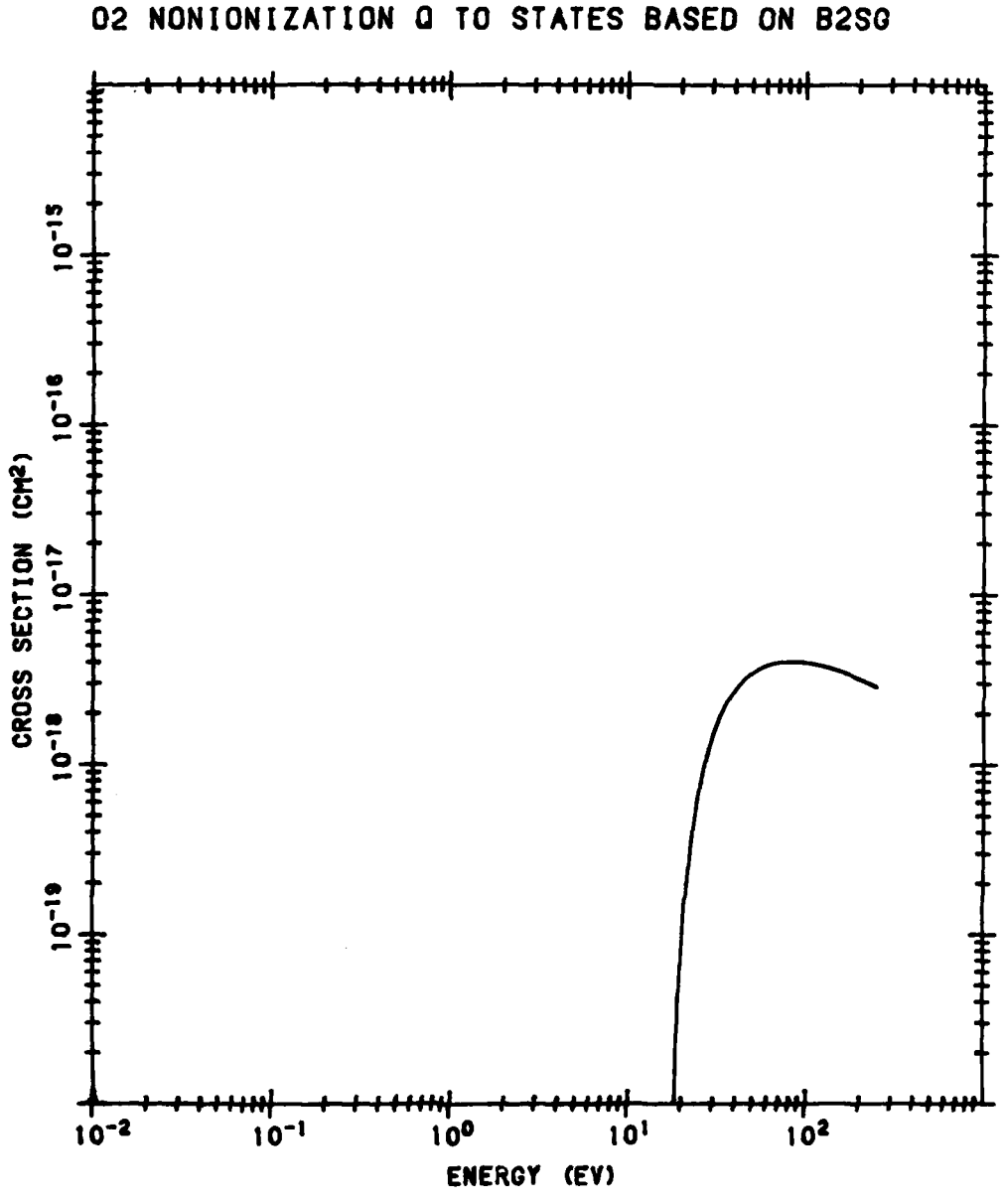


Figure B116. Sum of $O_2$ Nonionizing Cross Sections to Rydberg States Based on B $^2\Sigma_g^-$. The data source is the same as that of Figure B112

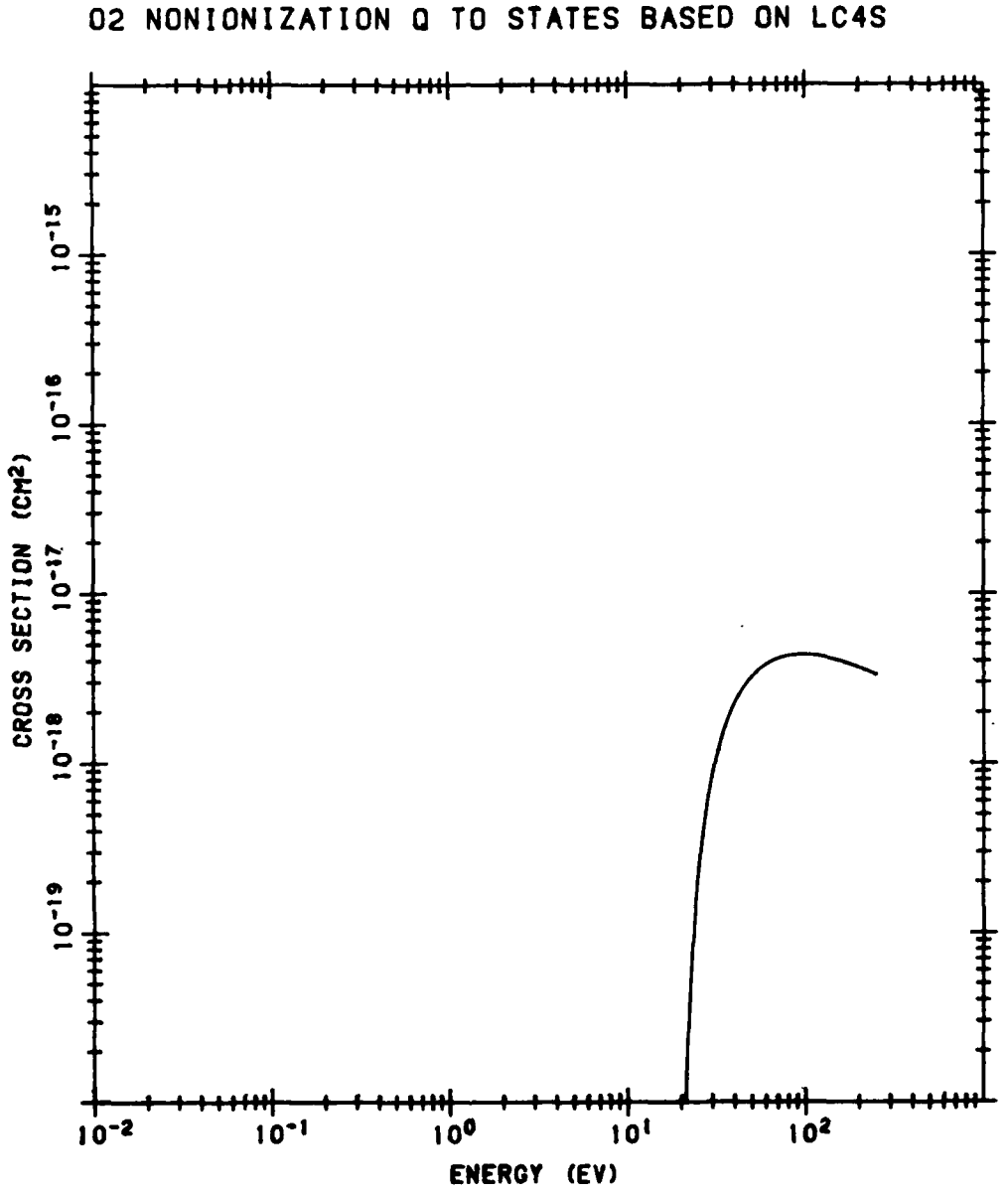


Figure B117. Sum of $O_2$ Nonionizing Cross Sections to Rydberg States Based on c $^4\Sigma_u^-$. The data source is the same as that of Figure B112

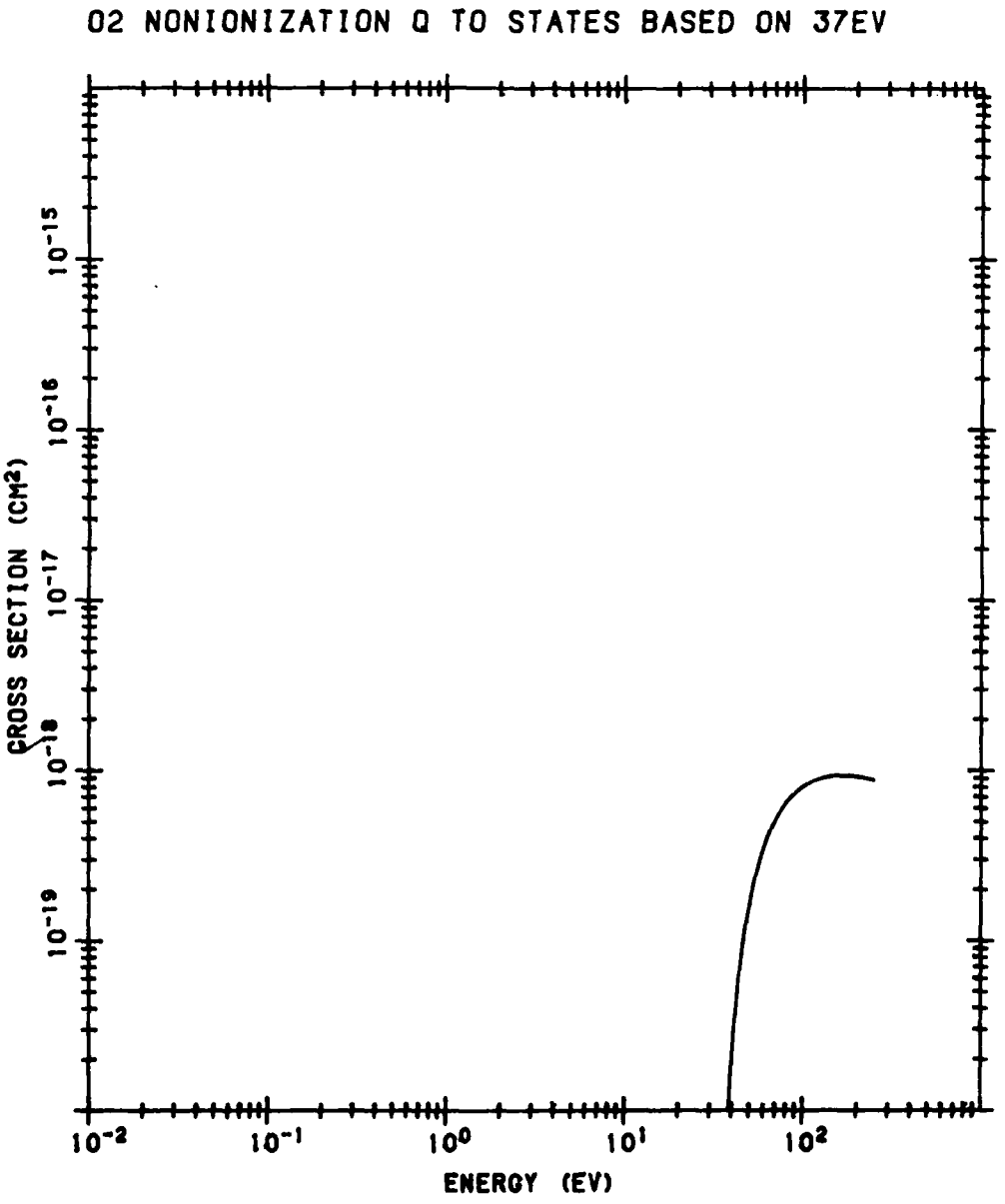


Figure B118. Sum of Nonionizing Cross Sections to Rydberg States Based on an $O_2^+$ State Hypothesized at 37 eV. The data source is the same as that of Figure B112

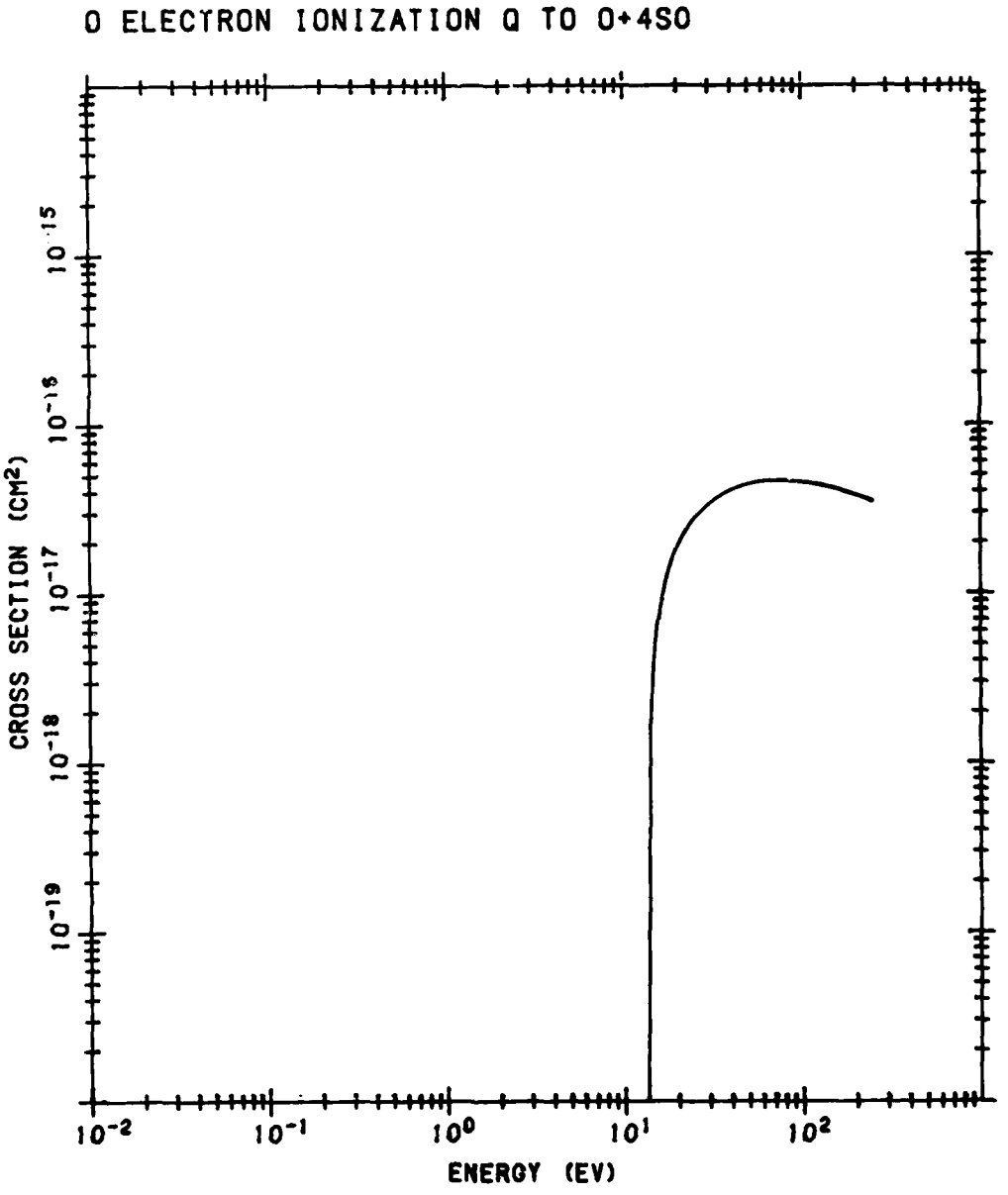


Figure B119. O Ionization Cross Section to $O^+$ State $^4S^o$. The data are from Jackman et al (1980)[322]

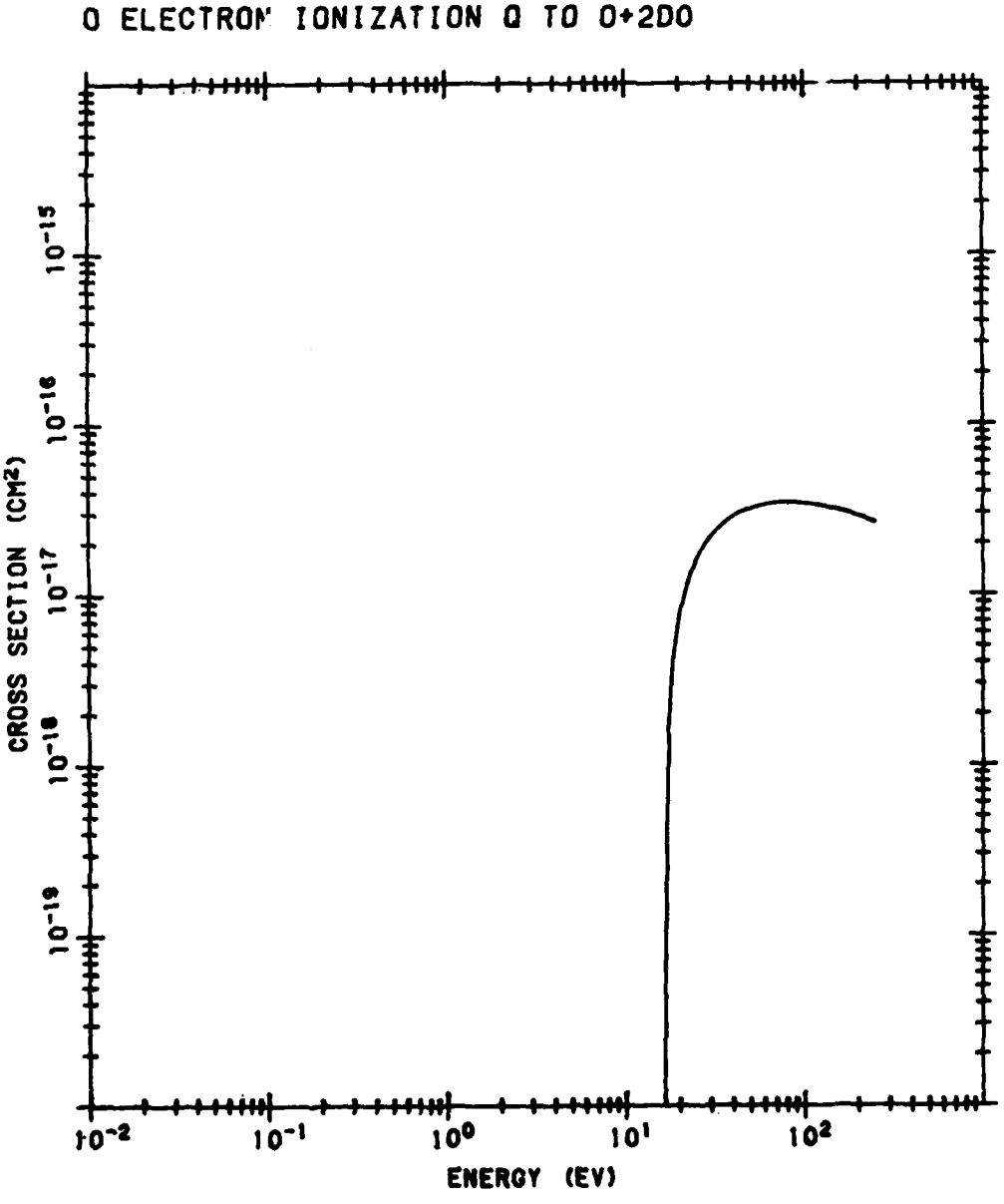


Figure B120. O Ionization Cross Section to $O^+$ State $^2D^o$. The data source is the same as that of Figure B119

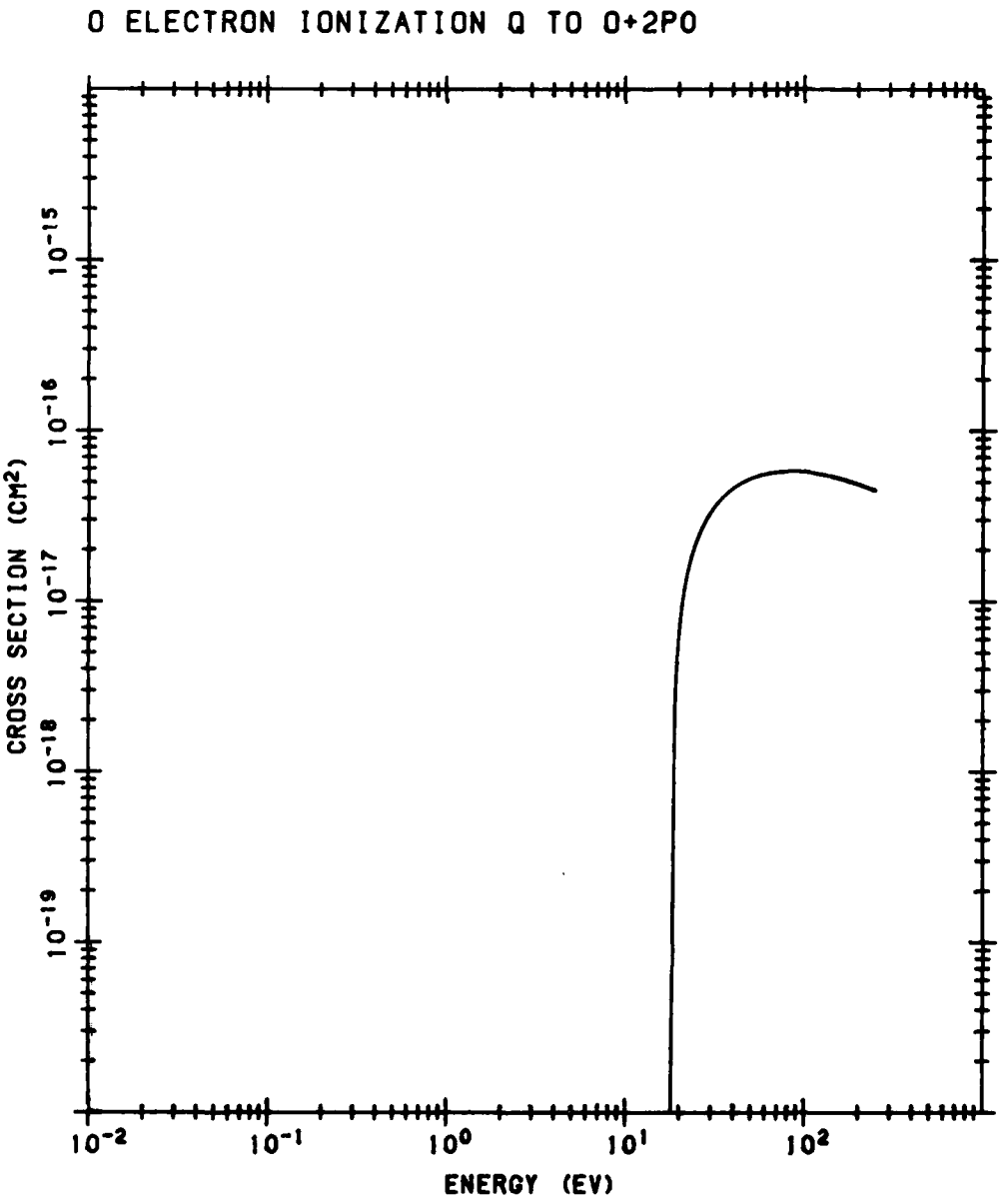


**Figure B121. O Ionization Cross Section to $O^+$ State $^2P^o$. The data source is the same as that of Figure B119**

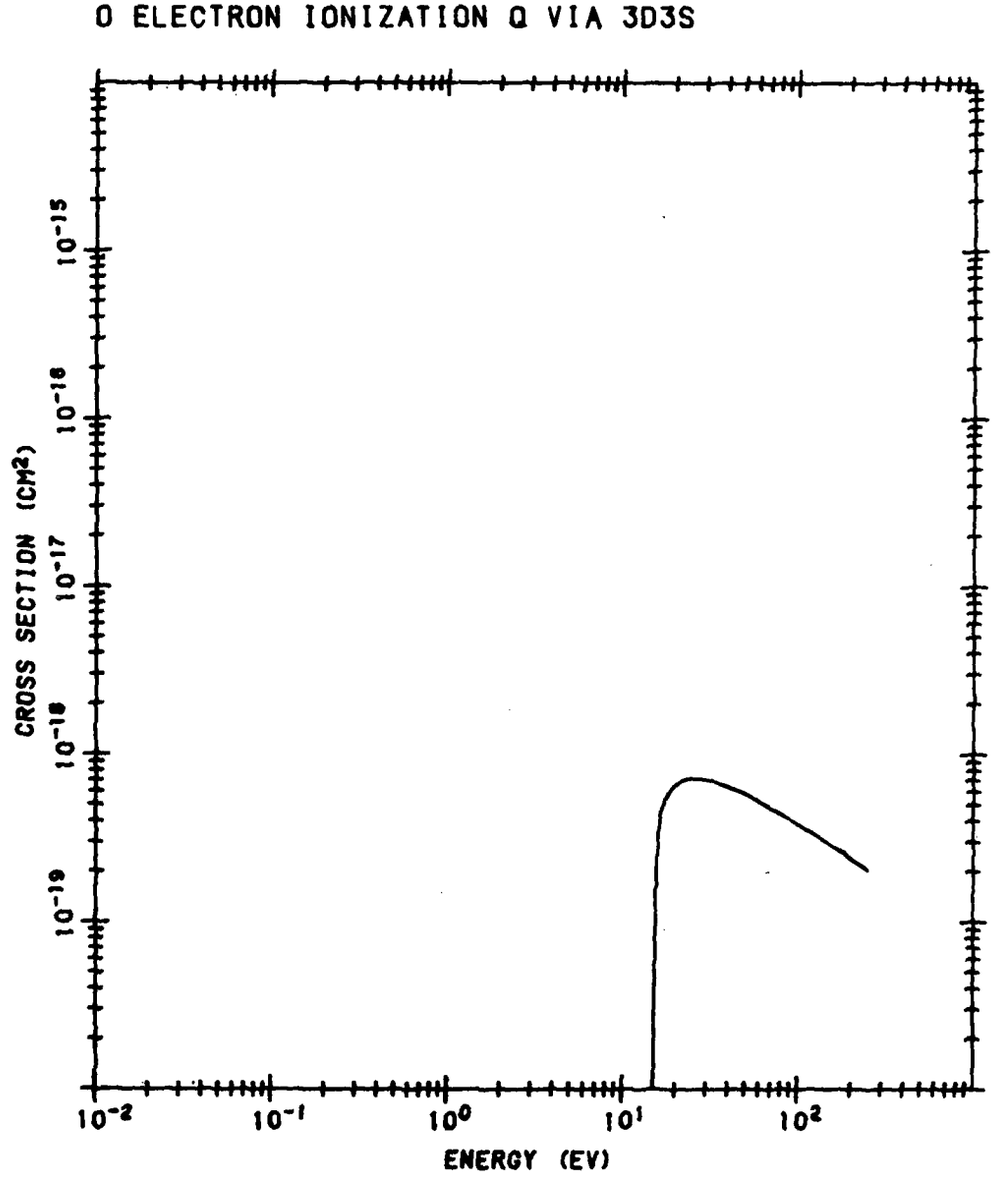


Figure B122. O Ionization Cross Section via State ($^2D^o$) 3d $^3S^o$. The data are from Jackman et al (1980)[B22] weighted by the fraction of excitations which ionize

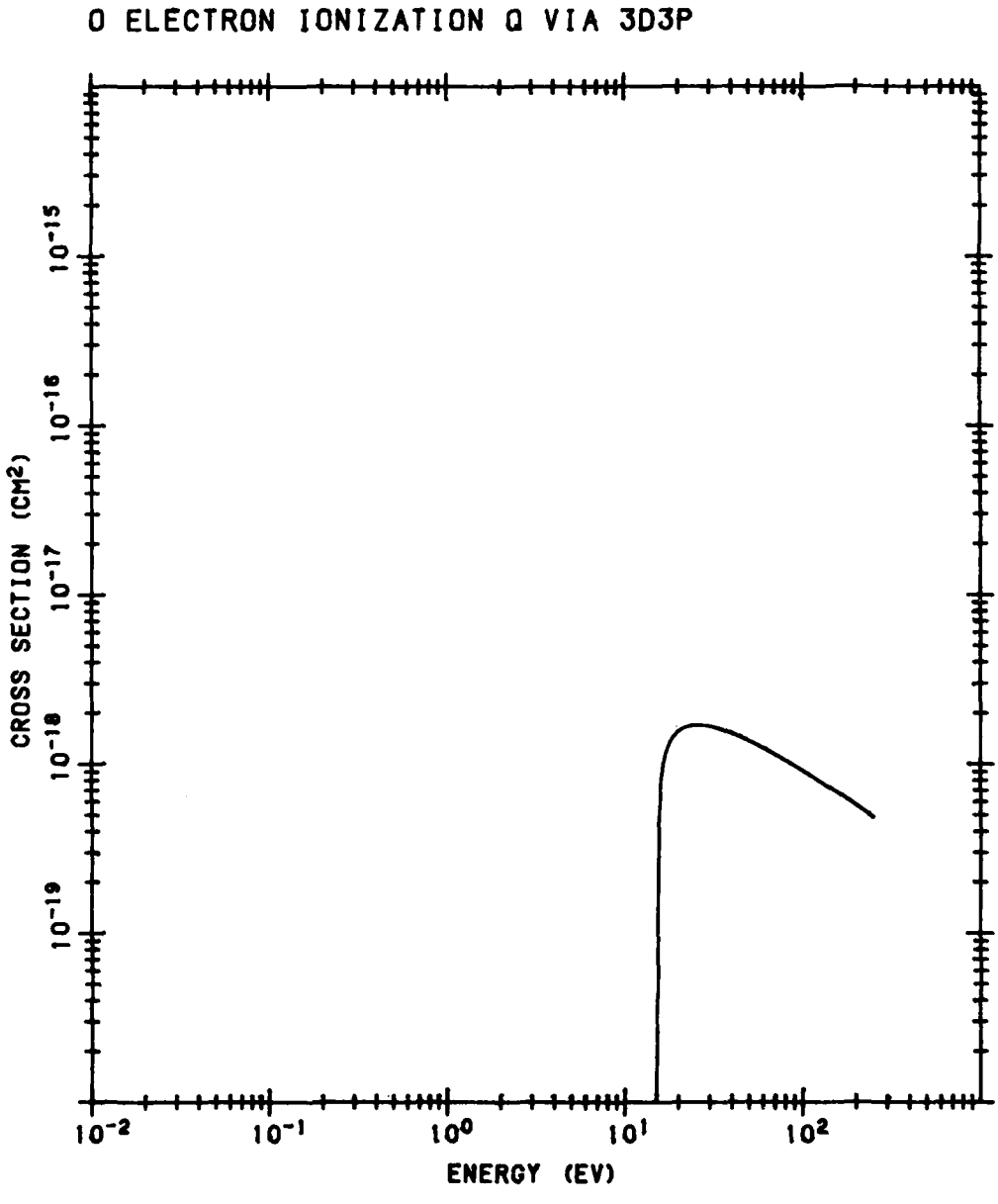


Figure B123. O Ionization Cross Section via State ($^2D^o$) 3d $^3P^o$. The data source is the same as that of Figure B122

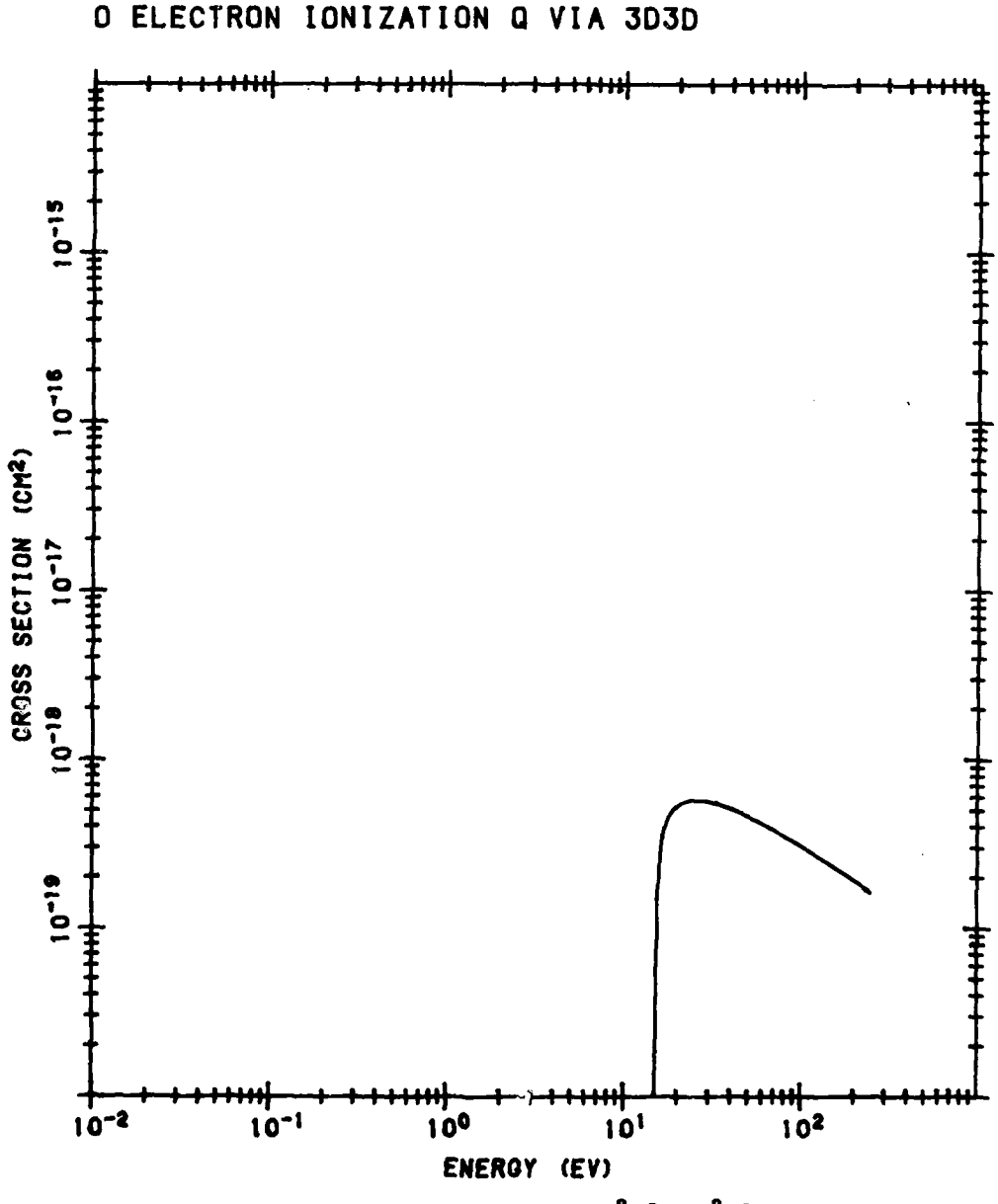


Figure B124. O Ionization Cross Section via State ($^2D^o$) 3d $^3D^o$. The data source is the same as that of Figure B122

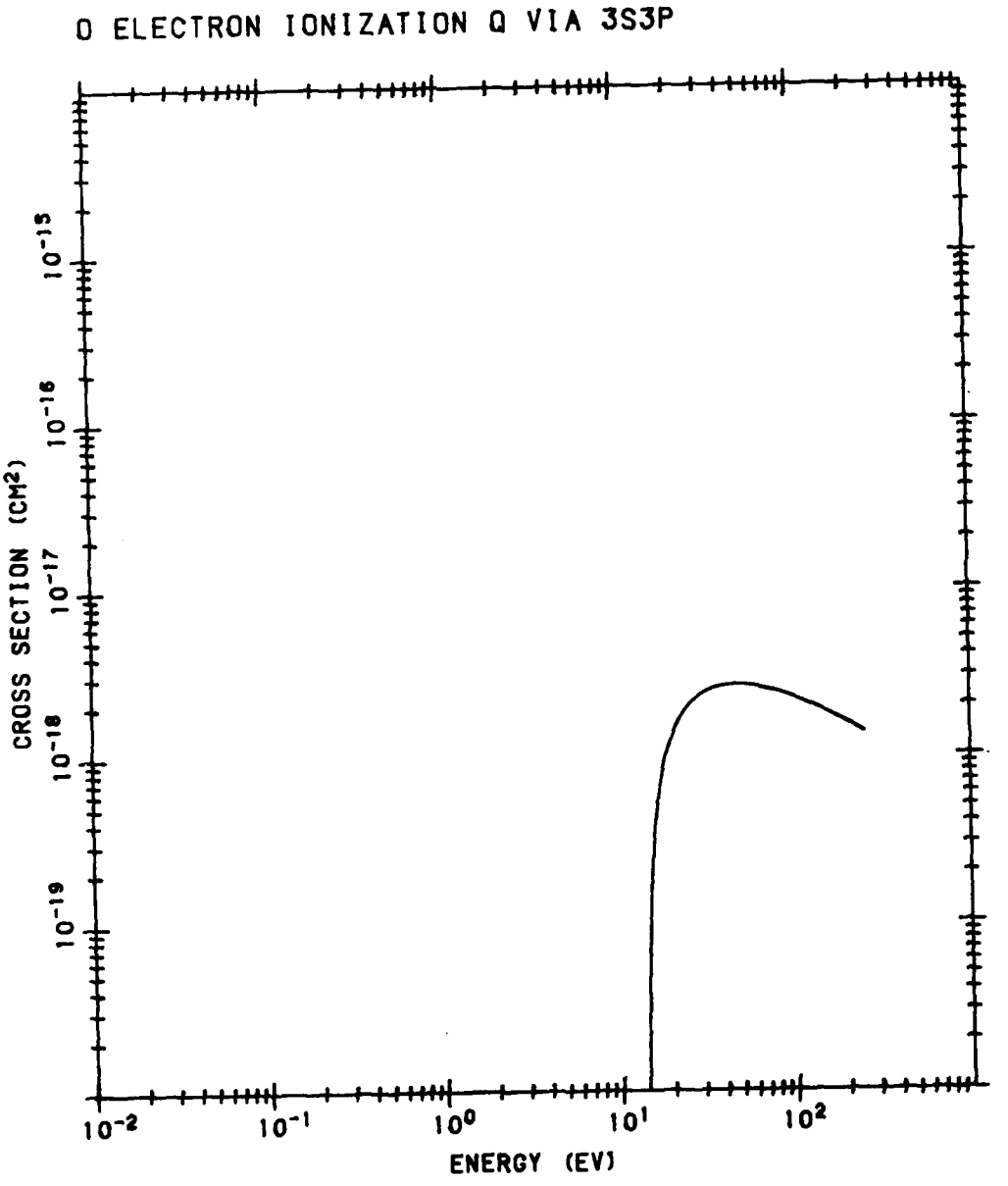


Figure B125. O Ionization Cross Section via State ($^2P^o$) 3s $^3P^o$. The data source is the same as that of Figure B122

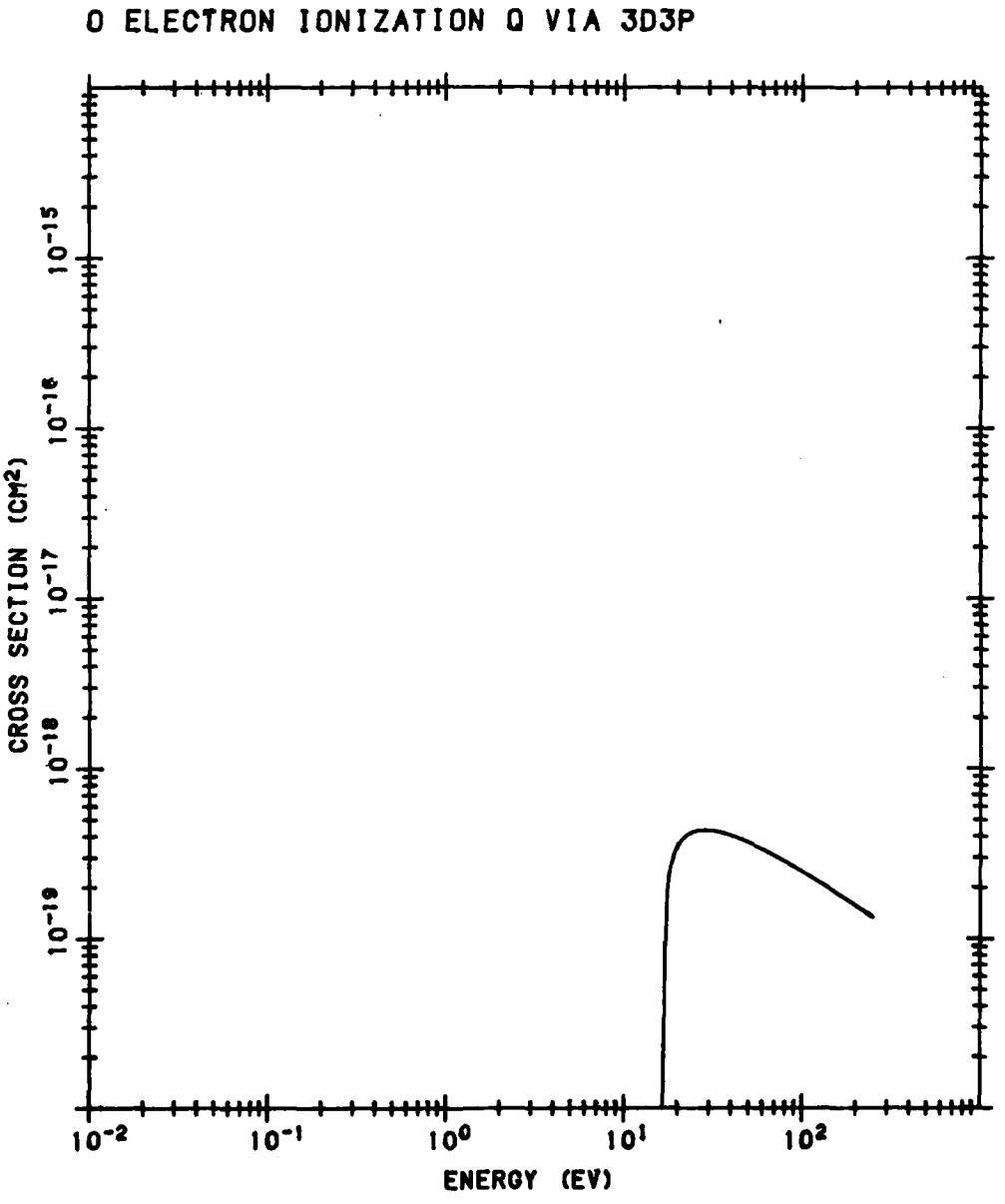


Figure B126. O Ionization Cross Section via State ($^2P^o$) 3d $^3P^o$. The data source is the same as that of Figure B122

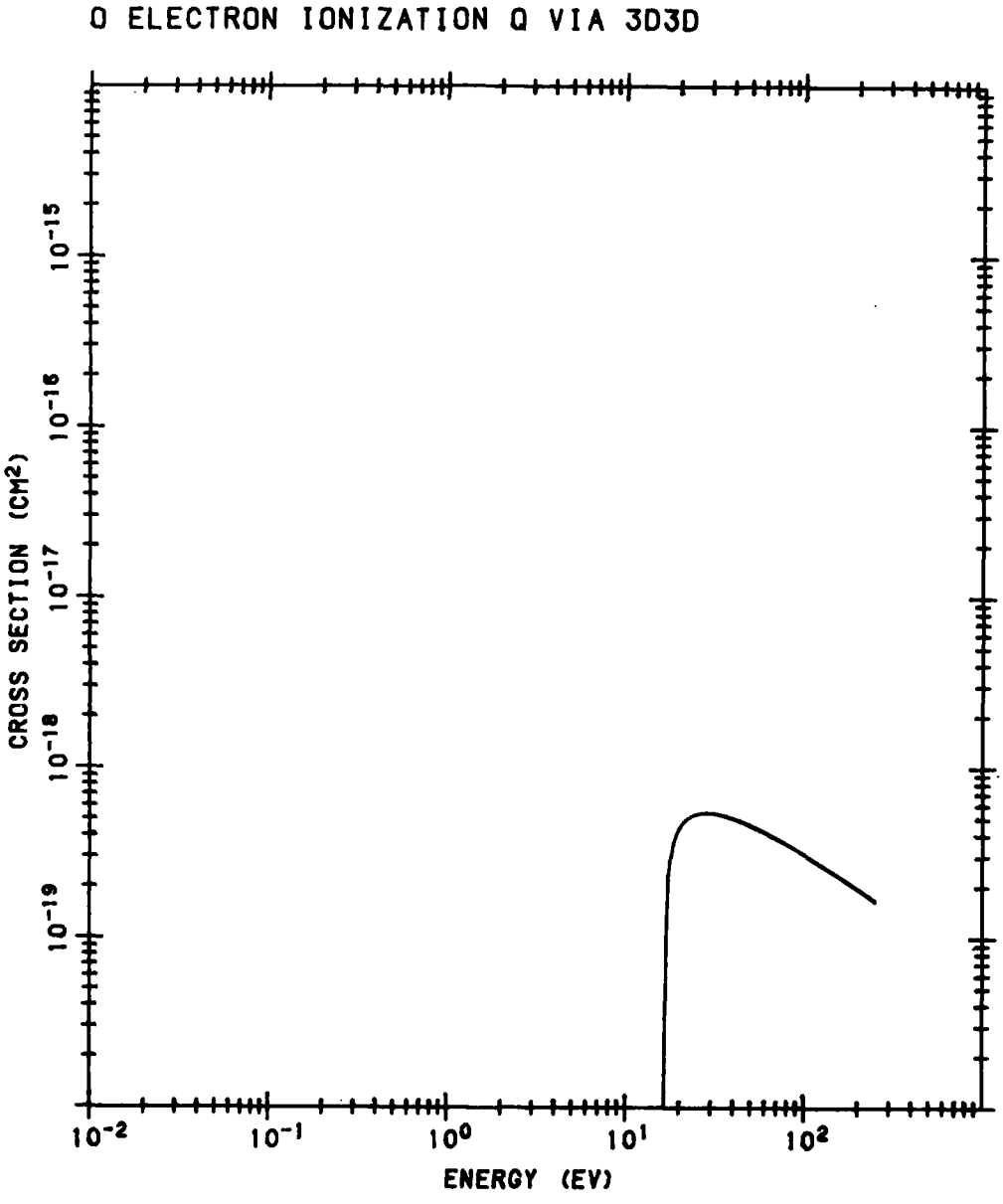


Figure B127. O Ionization Cross Section via State ($^2P^o$) 3d $^3D^o$. The data source is the same as that of Figure B122.

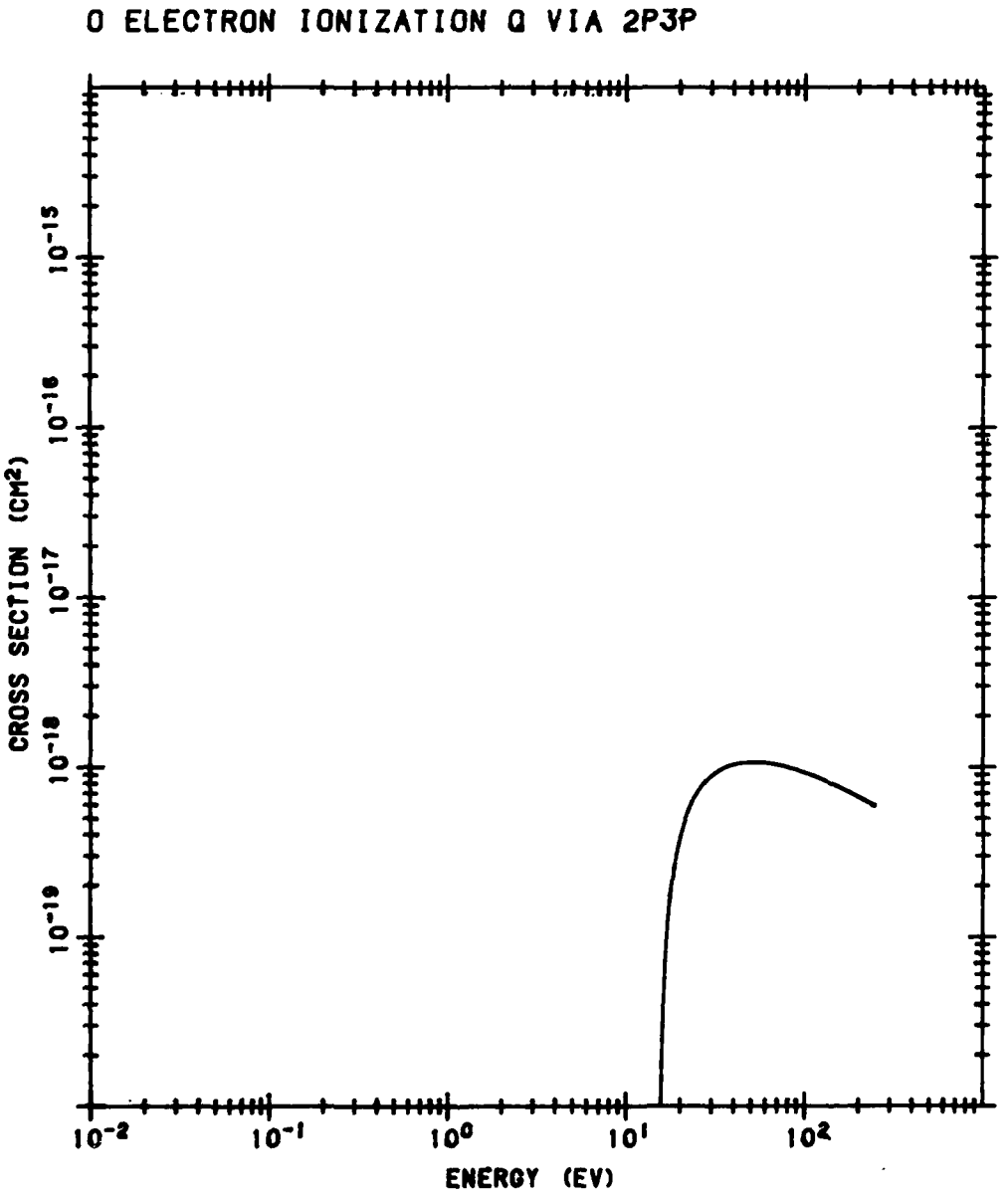


**Figure B128. O Ionization Cross Section via State $2p^5\ ^3P^o$. The data source is the same as that of Figure B122**

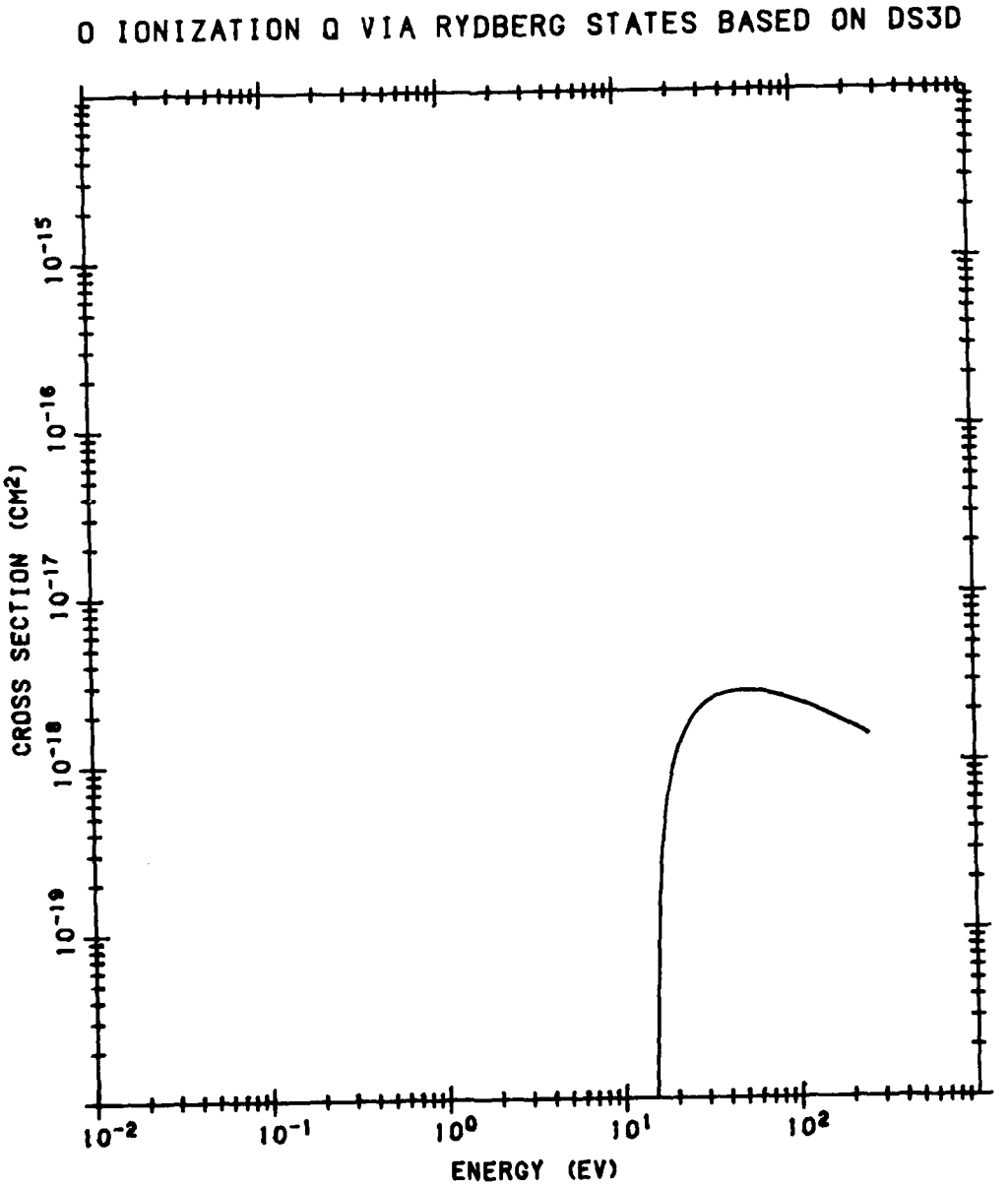


Figure B129. Sum of O Ionization Cross Sections via Rydberg States ($^2D^o$) ns $^3D^o$. The cross section data of Jackman et al (1980)[B22] are weighted by the fraction of excitations which ionize and summed from n equal to 3

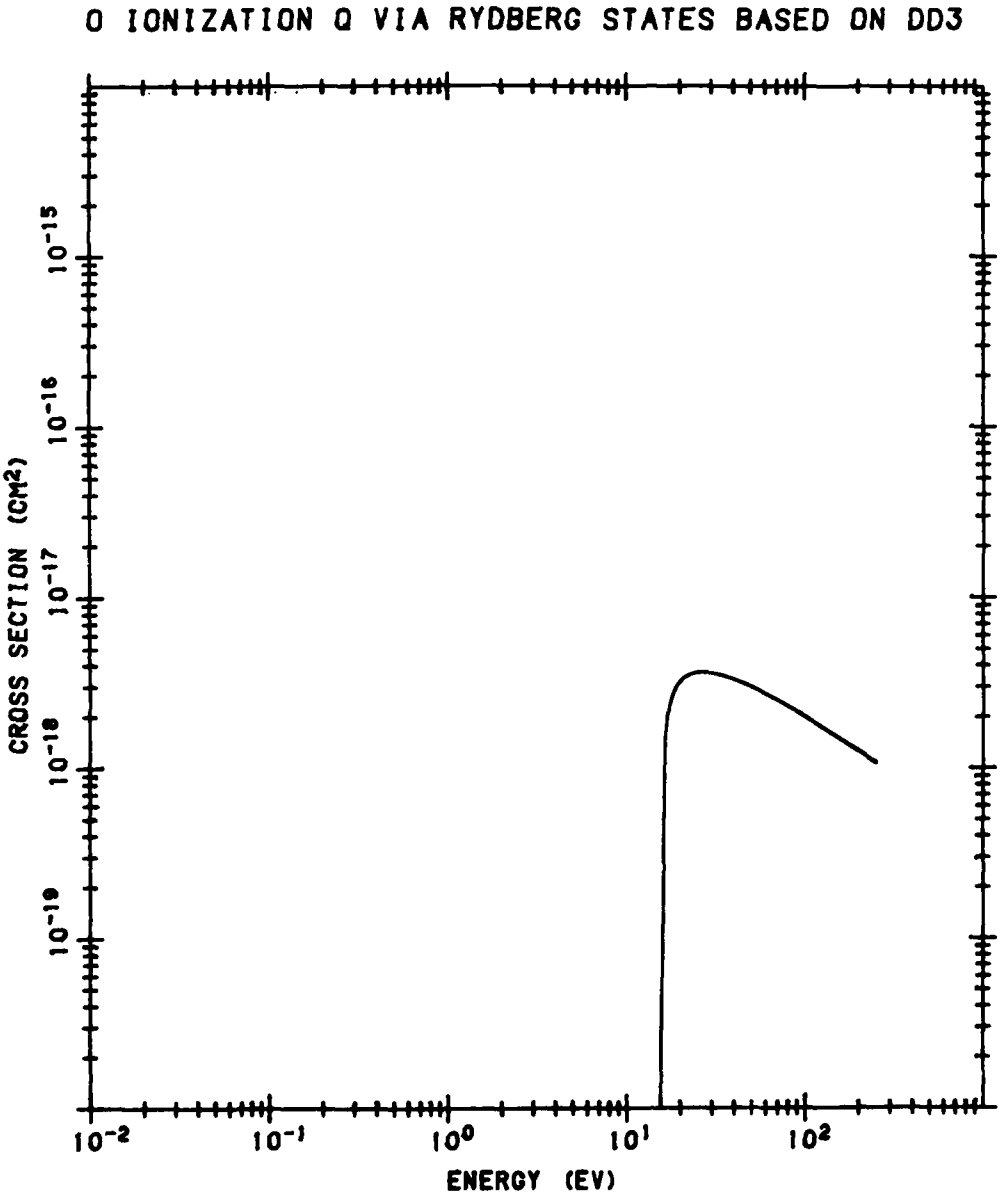


**Figure B130. Sum of O Ionization Cross Sections via Rydberg States ($^2D^o$) nd $^3SPD^o$. The data source is the same as that of Figure B129**

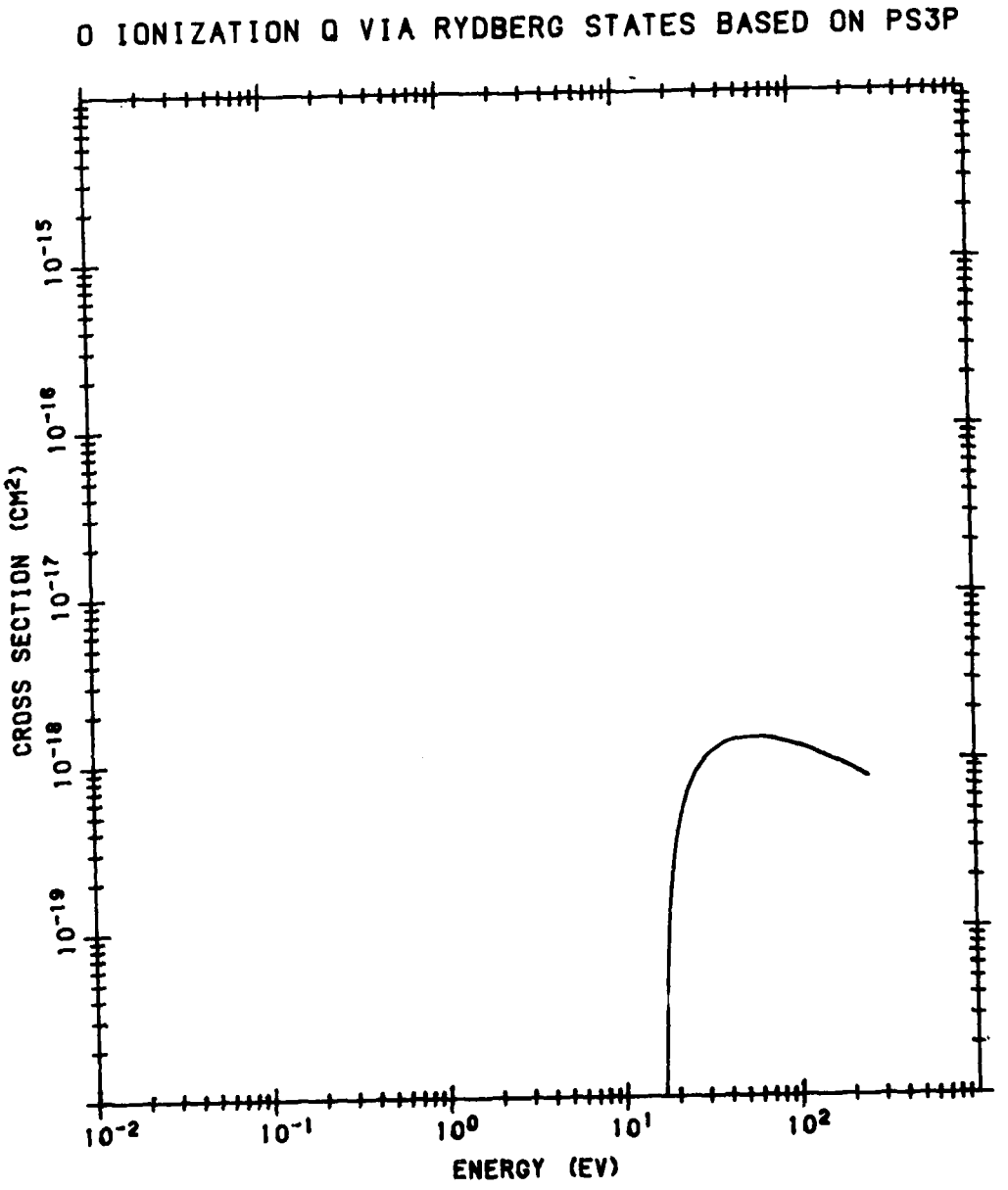


Figure B131. Sum of O Ionization Cross Sections via Rydberg States ($^2P^o$) ns $^3P^o$. The data source is the same as that of Figure B129

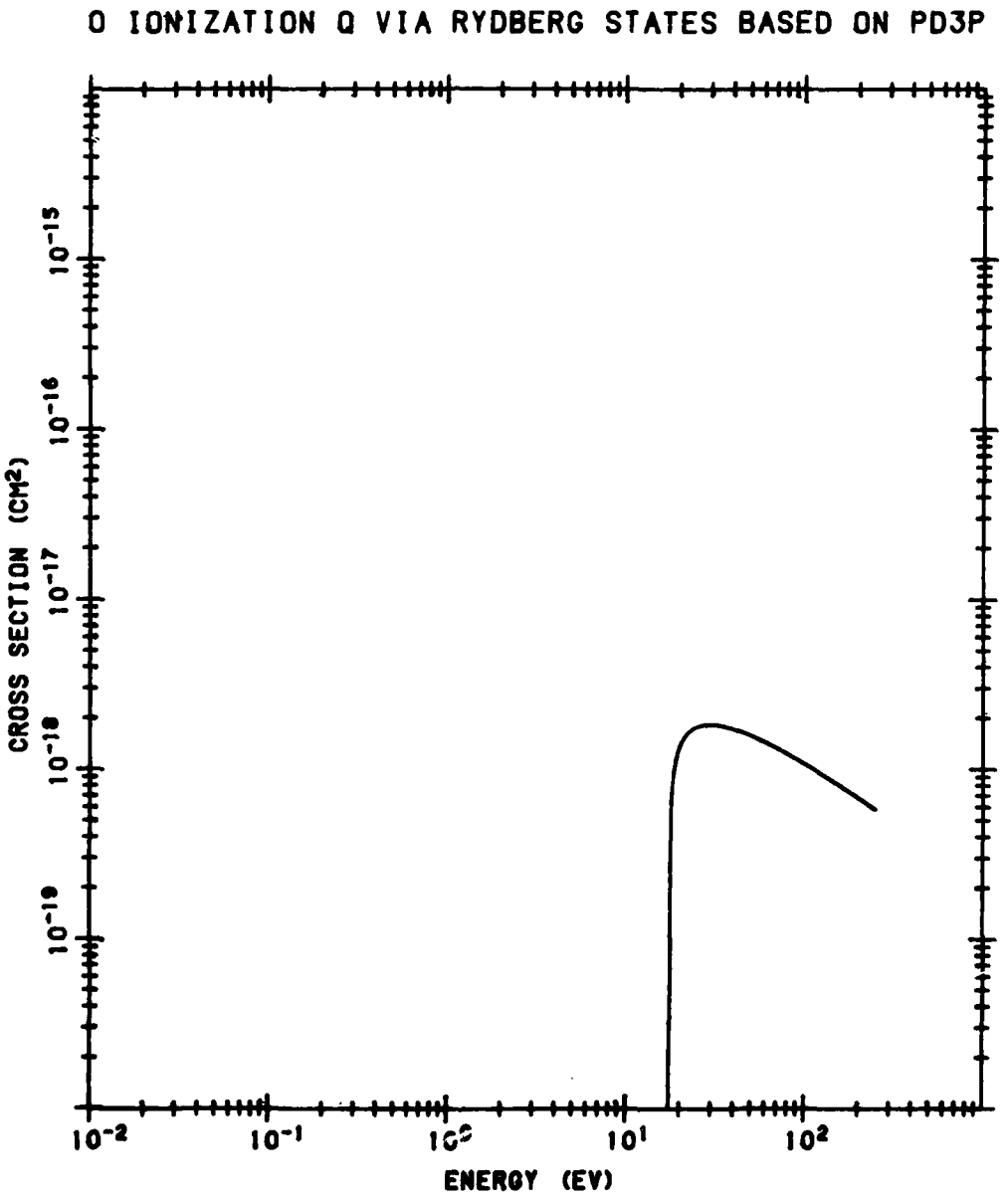


Figure B132. Sum of O Ionization Cross Sections via Rydberg States ($^2P^o$) nd $^3PD^o$. The data source is the same as that of Figure B129.

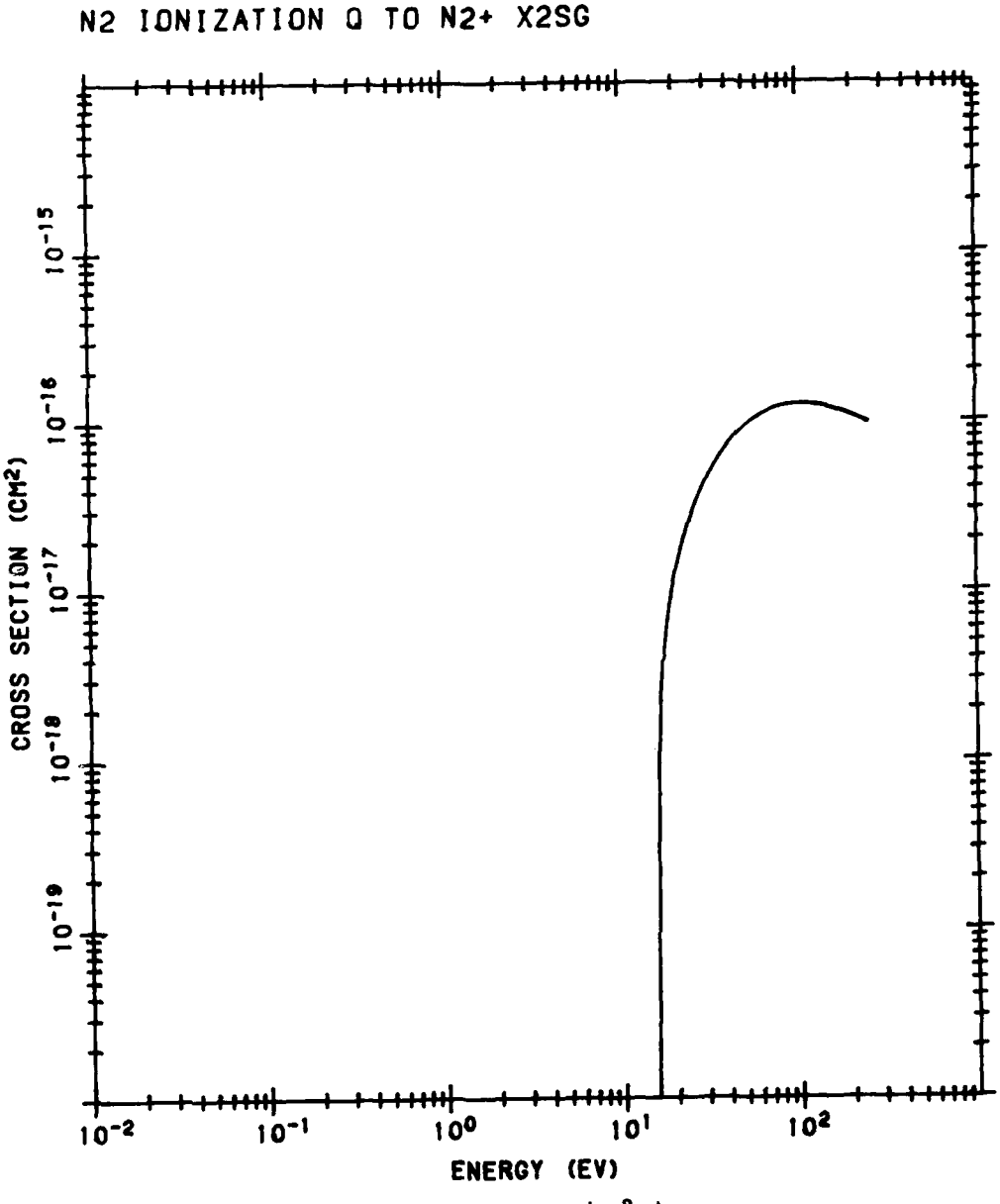


Figure B133. $N_2$ Ionization Cross Section to $N_2^+ X\,^2\Sigma_g^+$. The data are from Jackman et al (1980)[B22]

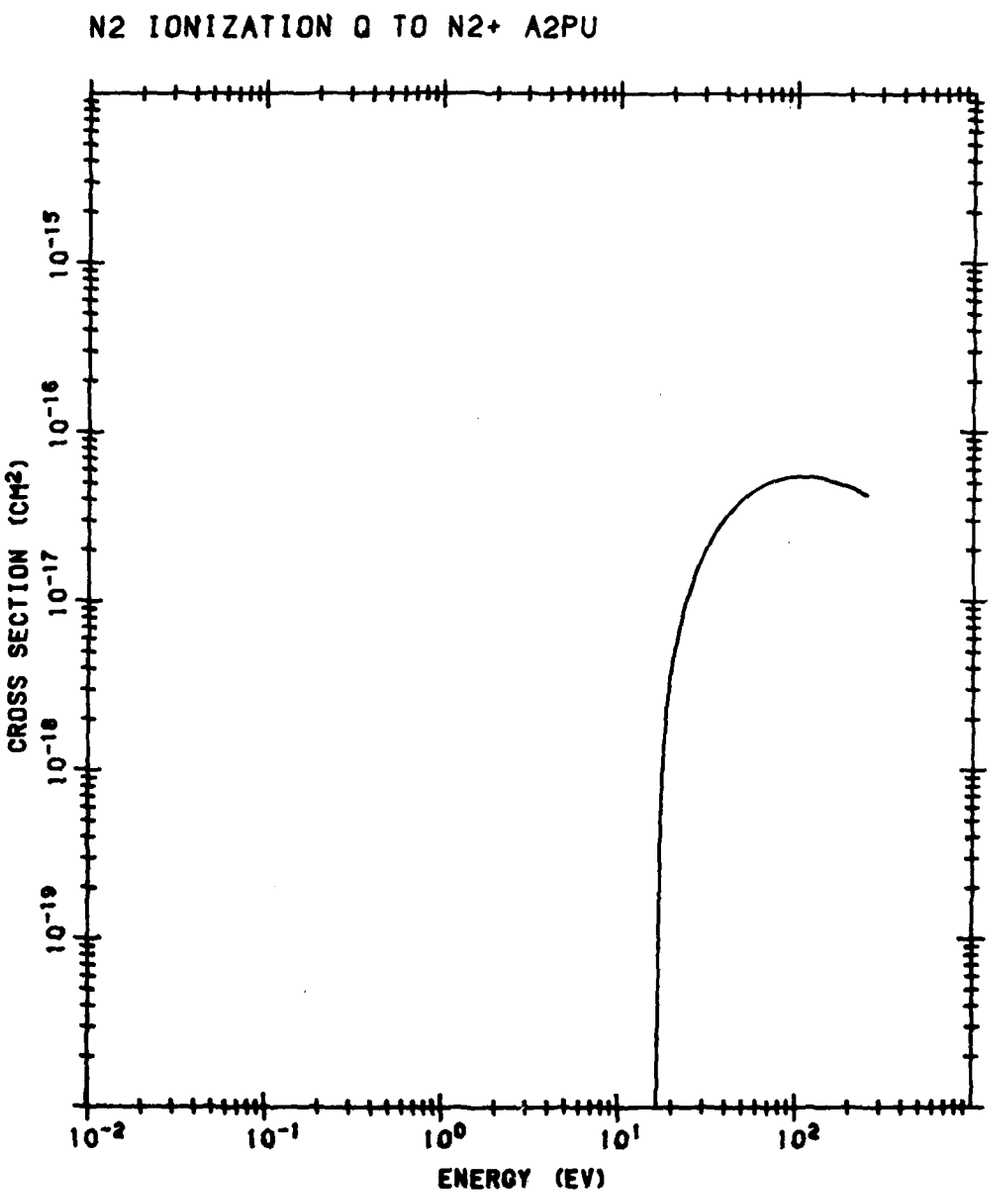


Figure B134. $N_2$ Ionization Cross Section to A $^2\Pi_u$. The data are from Jackman et al (1980)[B22]

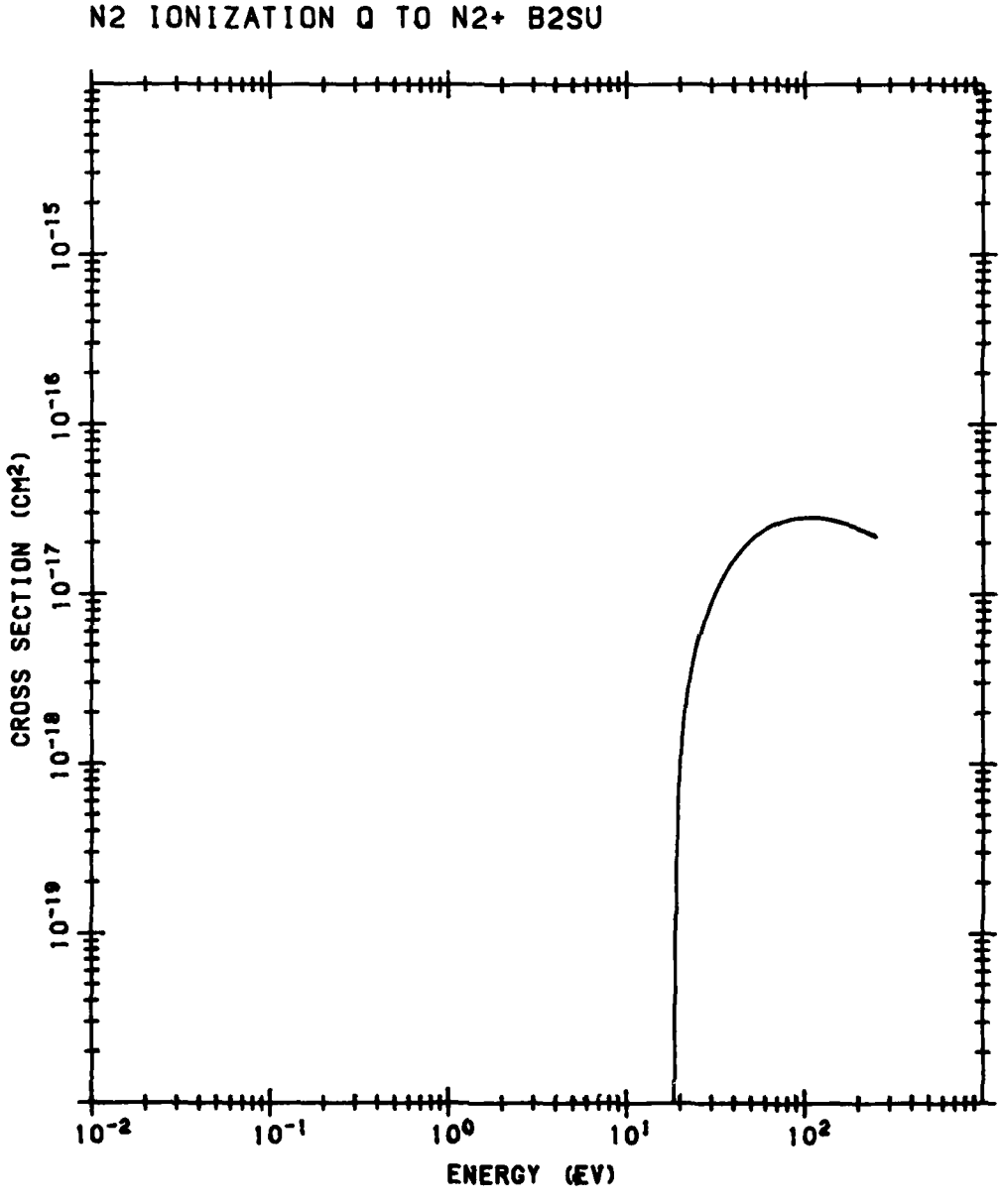


Figure B135. $N_2$ Ionization Cross Section to B $^2\Sigma_u^+$. The data are from Jackman et al (1980)[B22]

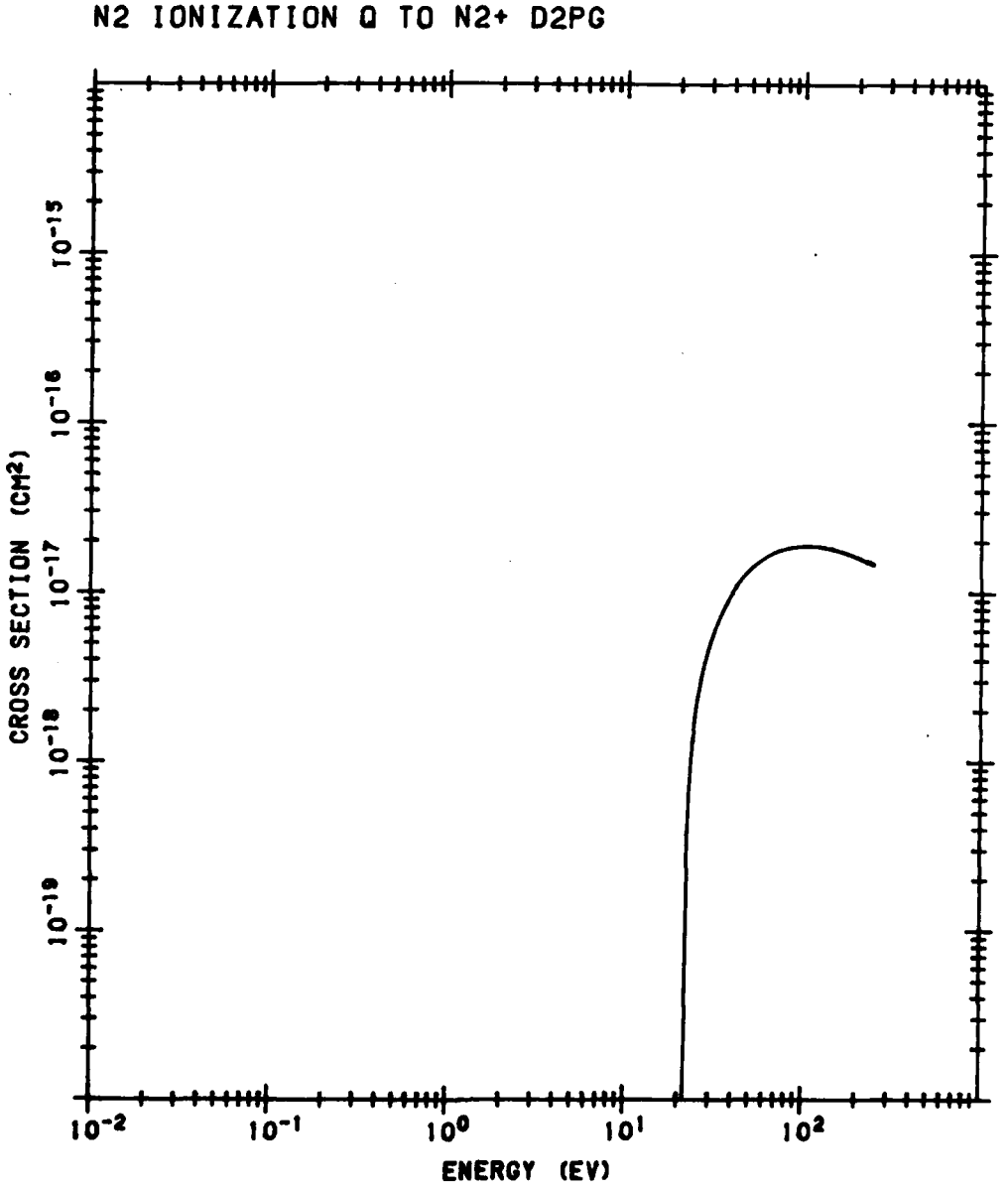


Figure B136. $N_2$ Ionization Cross Section to D $^2\Pi_g$. The data are from Jackman et al (1980)[B22]

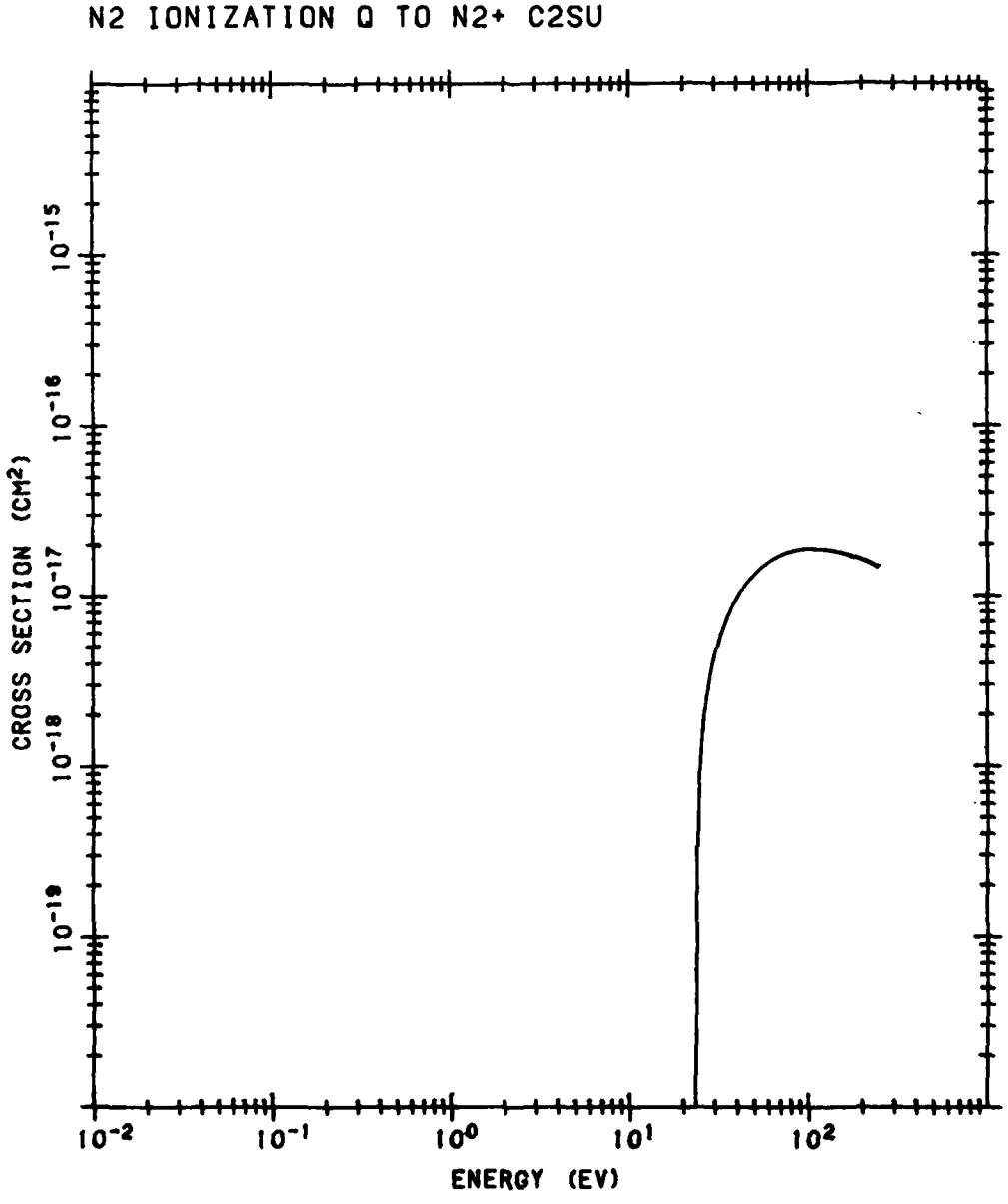


Figure B137. $N_2$ Ionization Cross Section to C $^2\Sigma_u^+$. The data are from Jackman et al (1980)[B22]

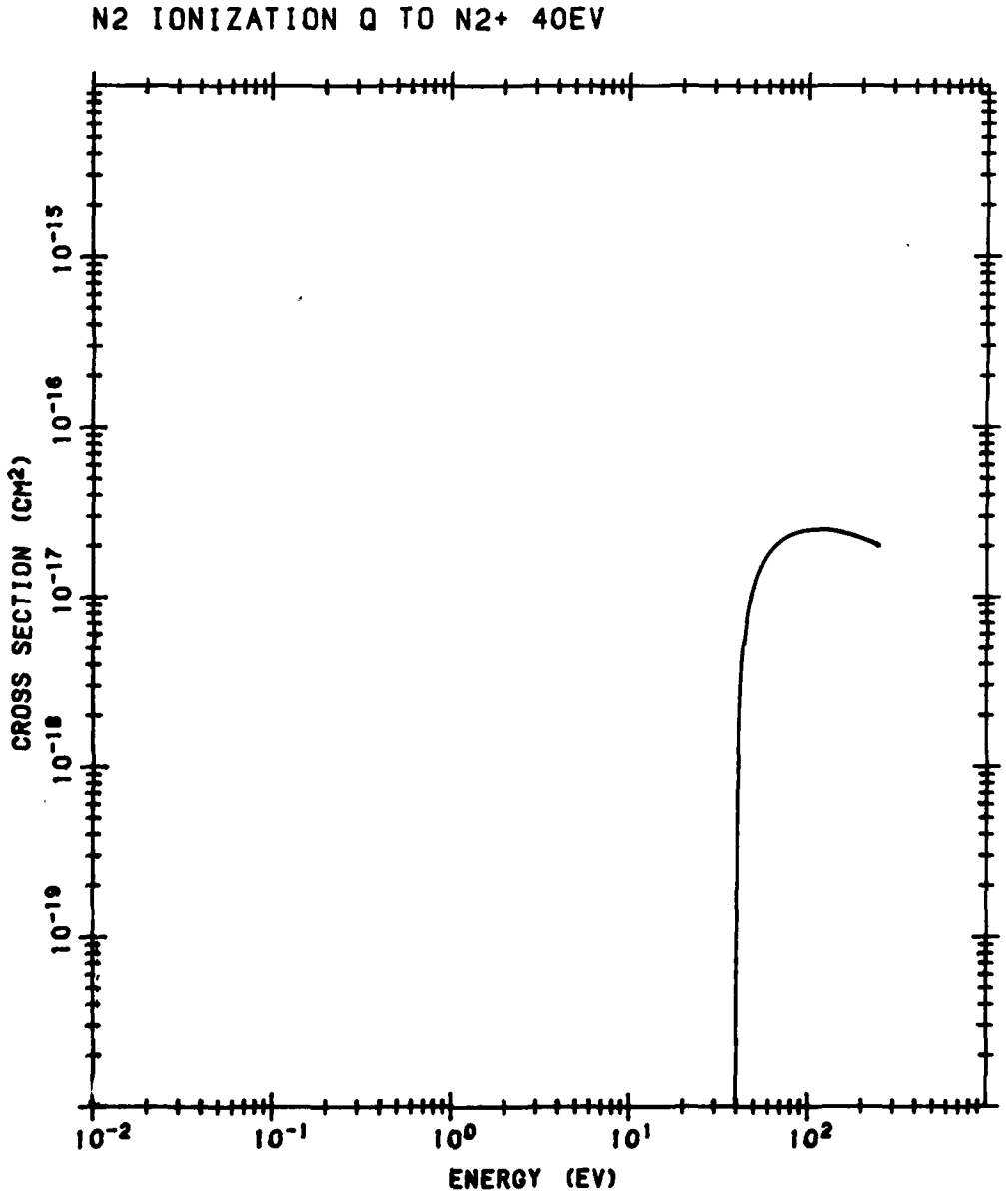


Figure B138. $N_2$ Ionization Cross Section to an $N_2^+$ State Hypothesized at 40 eV. The data are from Jackman et al (1980)[B22]

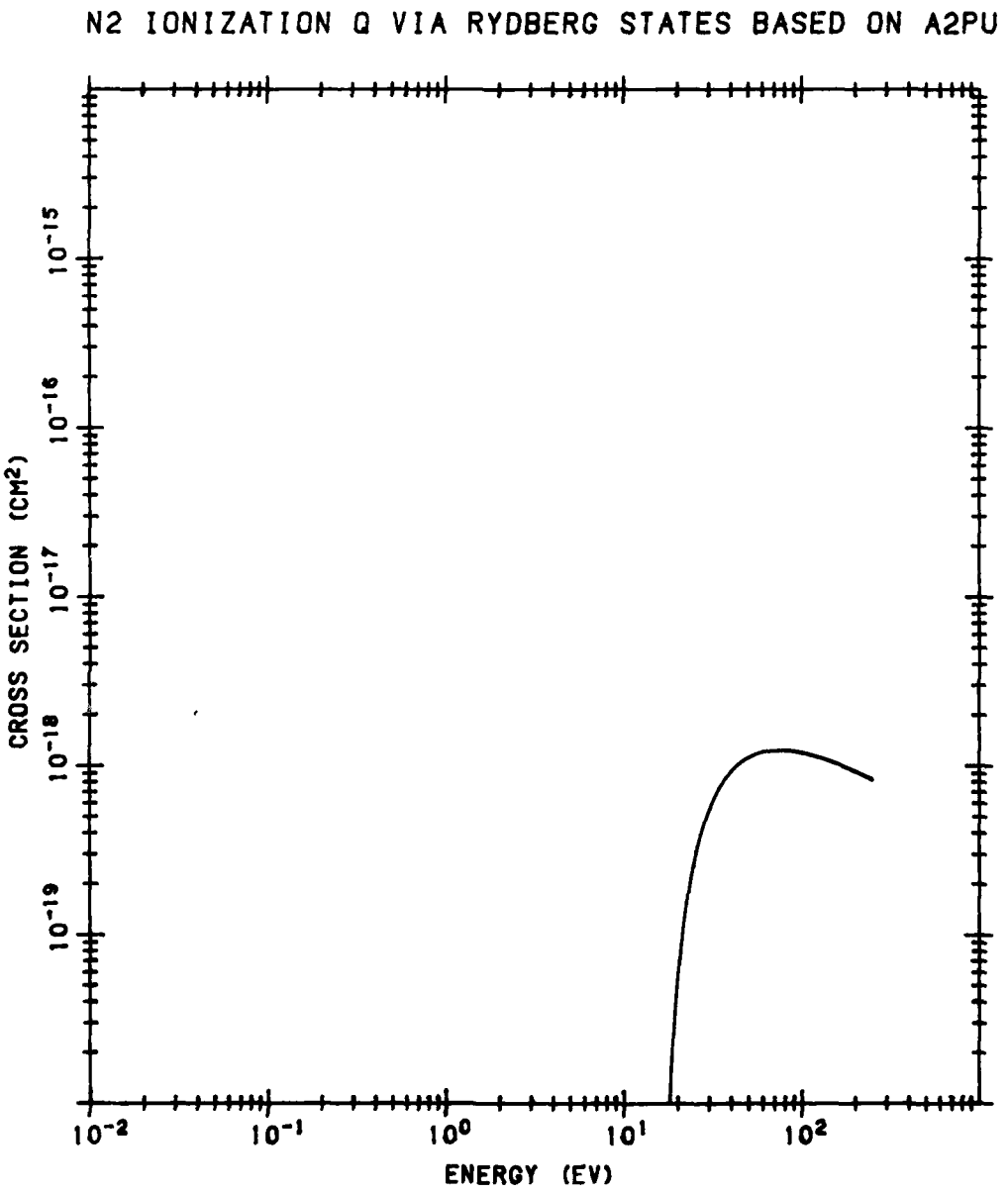


Figure B139. Sum of $N_2$ Ionization Cross Sections via Rydberg States Based on $N_2^+ A\,^2\Pi_u$. The cross section data of Jackman et al (1980)[B22] are weighted by the fraction of excitations which ionize and summed from n equal to 3

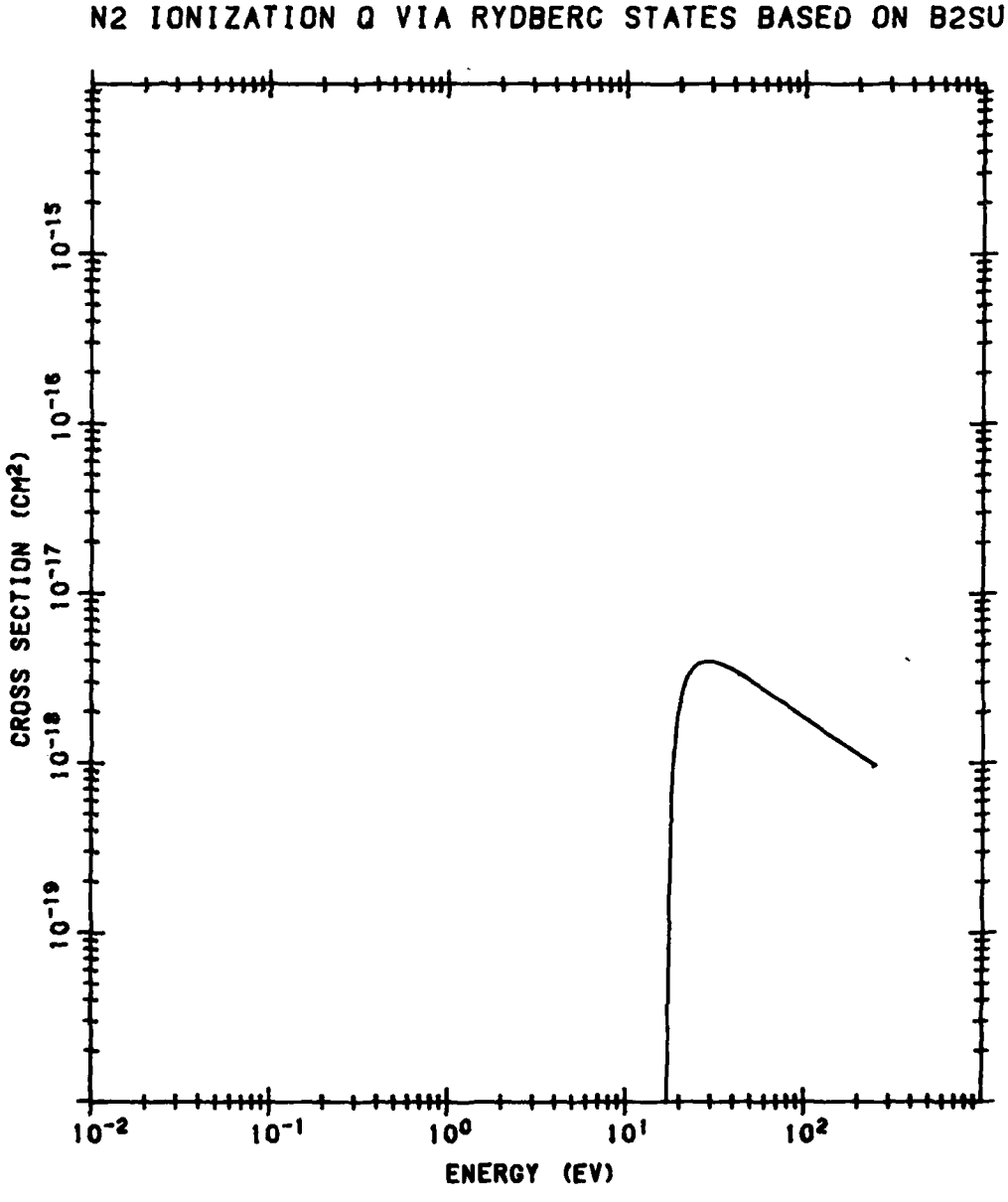


Figure B140. Sum of $N_2$ Ionization Cross Sections via Rydberg States Based on $N_2^+$ B $^2\Sigma_u^+$. The data source is the same as that of Figure B139

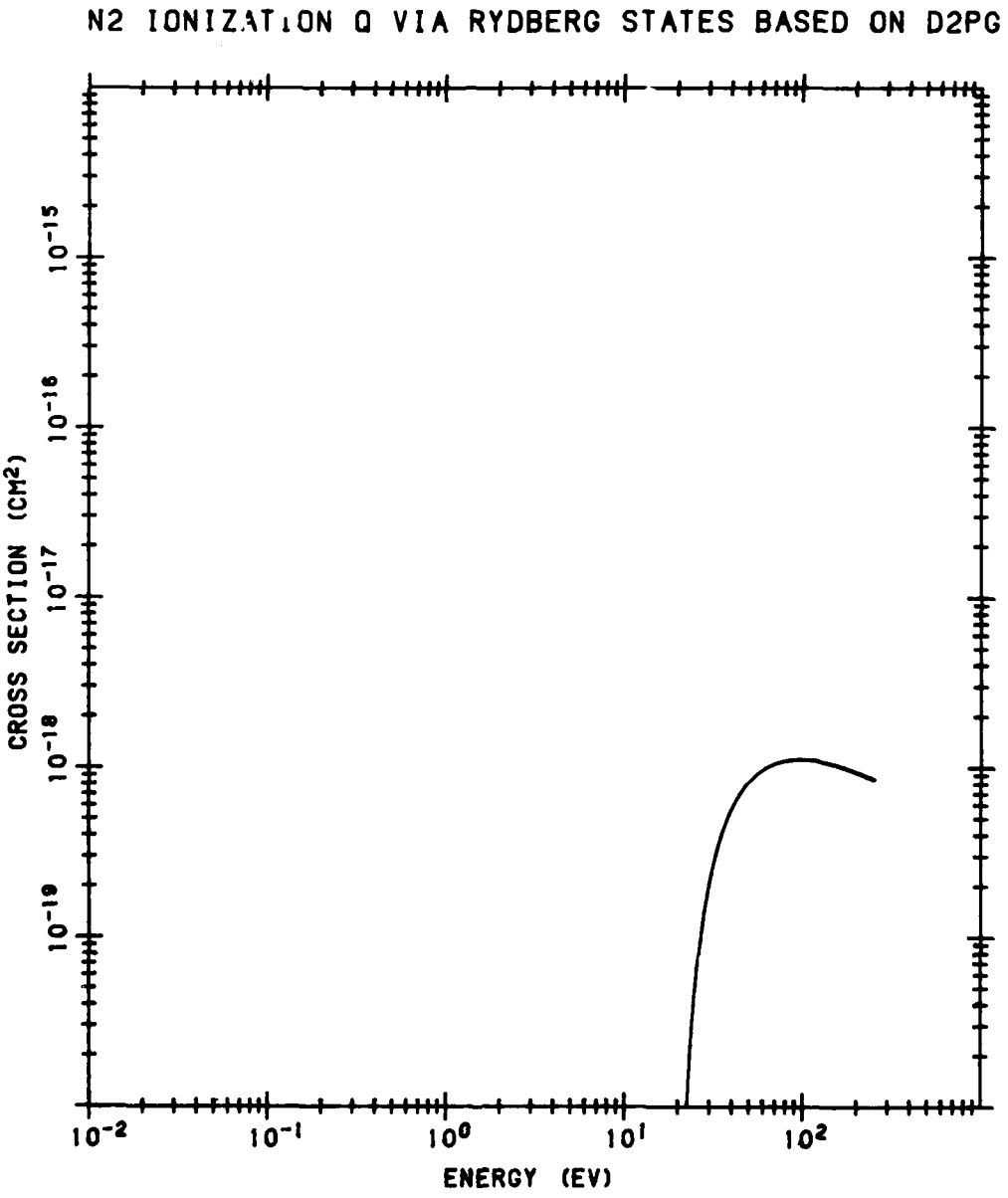


Figure B141. Sum of $N_2$ Ionization Cross Sections via Rydberg States Based on $D\ ^2\Pi_g$. The data source is the same as that of Figure B139

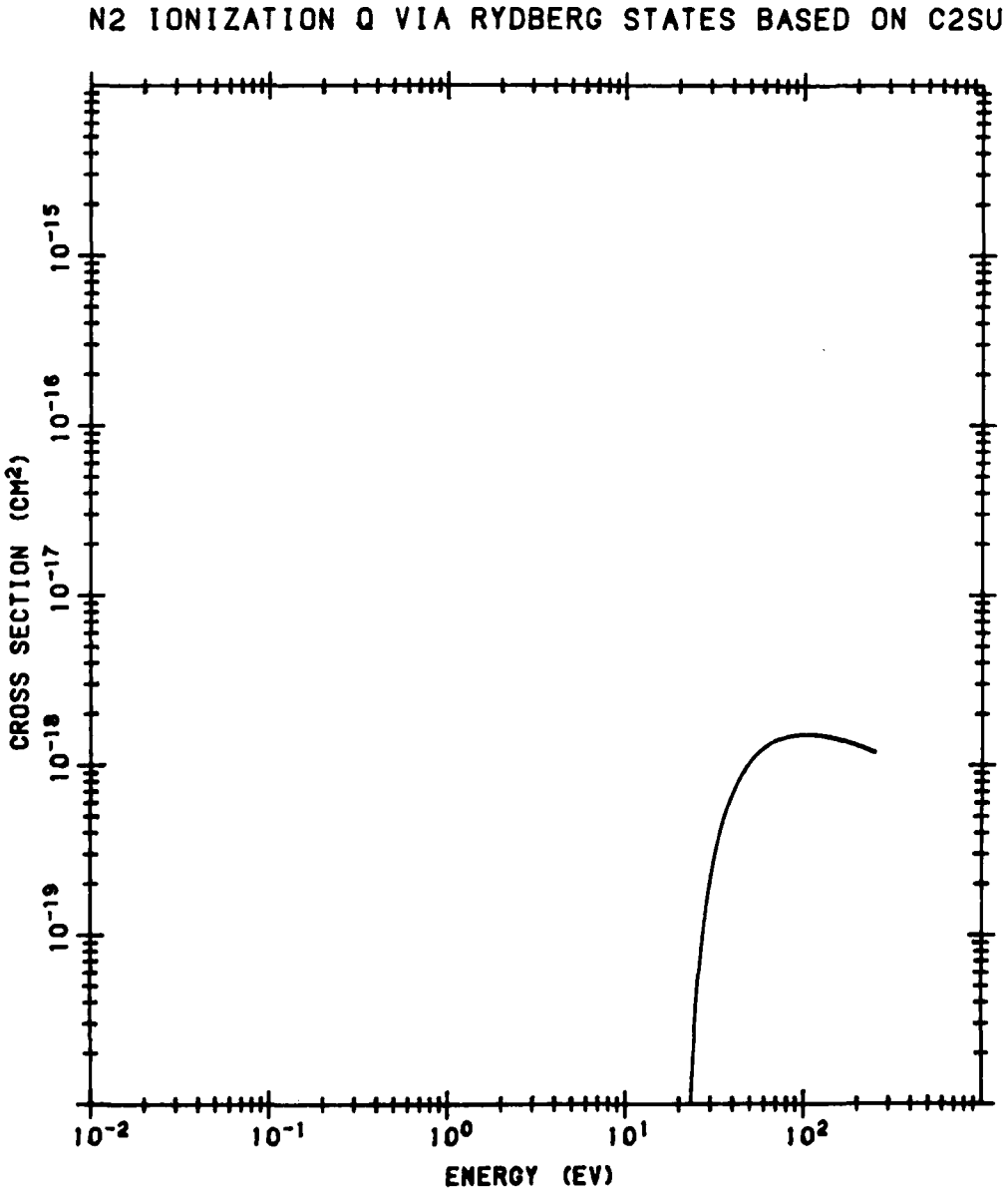


Figure B142. Sum of $N_2$ Ionization Cross Sections via Rydberg States Based on C $^2\Sigma_u^+$. The data source is the same as that of Figure B139

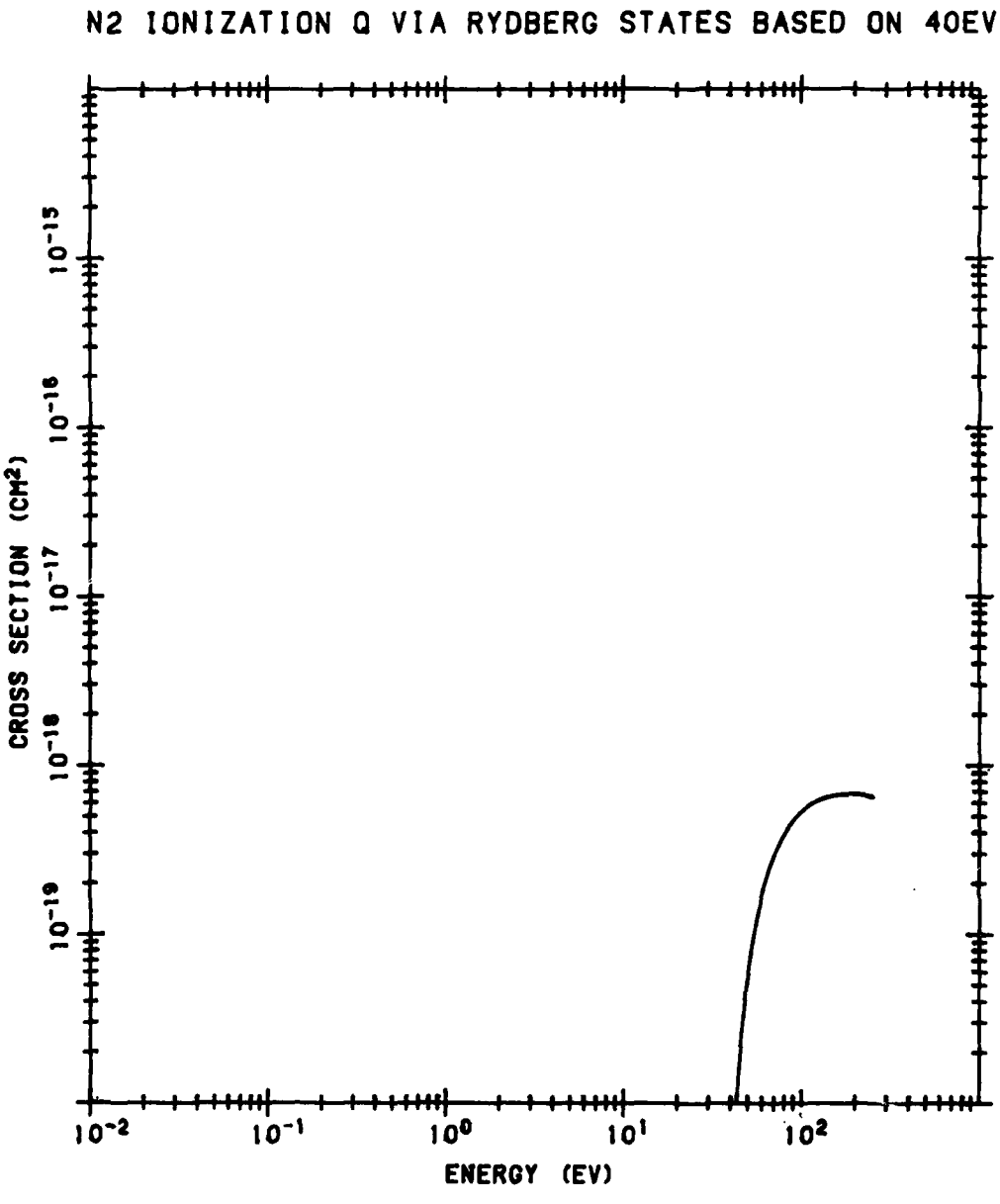


Figure B143. Sum of $N_2$ Ionization Cross Sections via Rydberg States Based on an $N_2^+$ State Hypothesized at 40 eV. The data source is the same as that of Figure B139

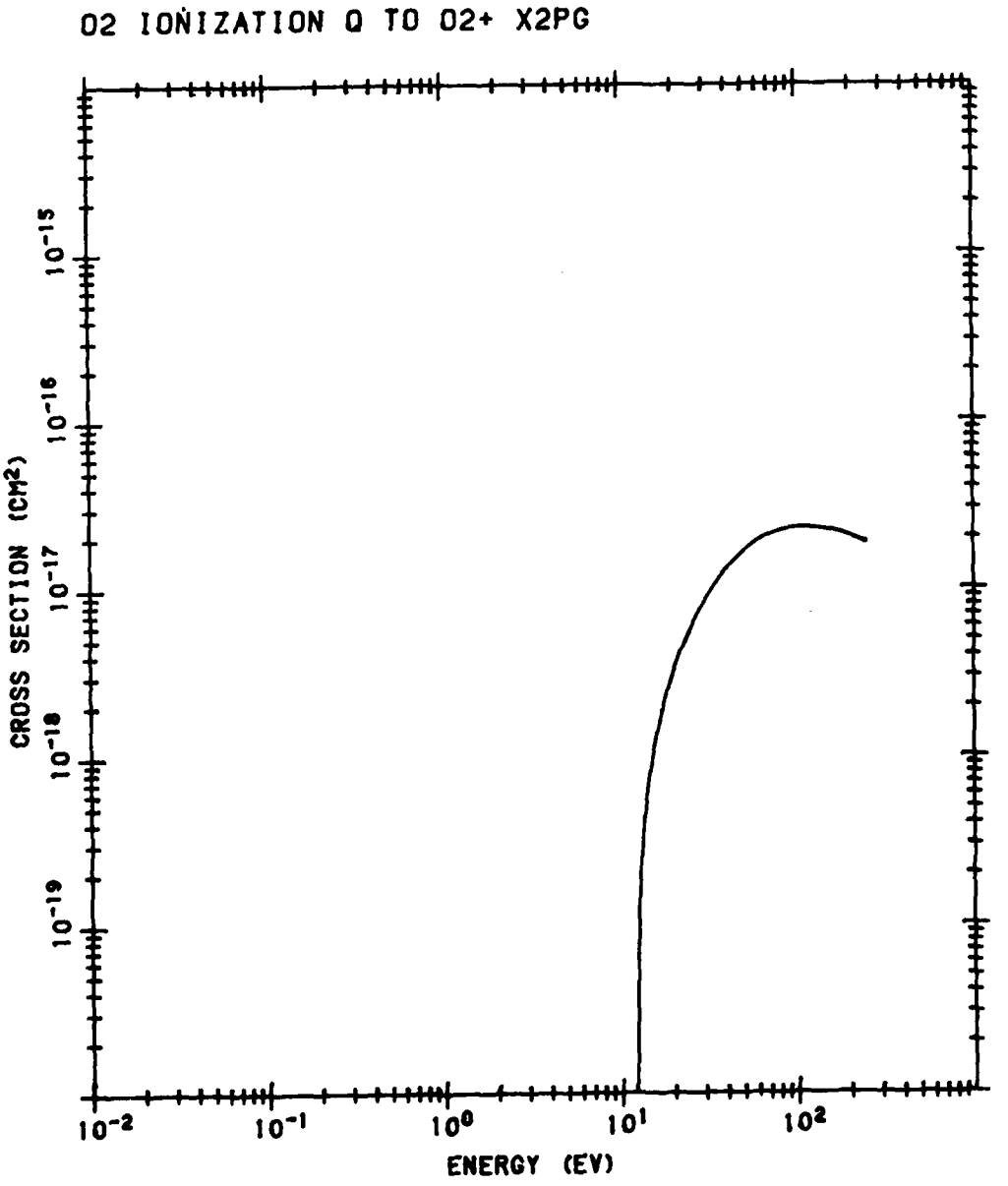


Figure B144. $O_2$ Ionization Cross Section to $O_2^+ X\,^2\Pi_g$. The data are from Jackman et al (1980)[B22]

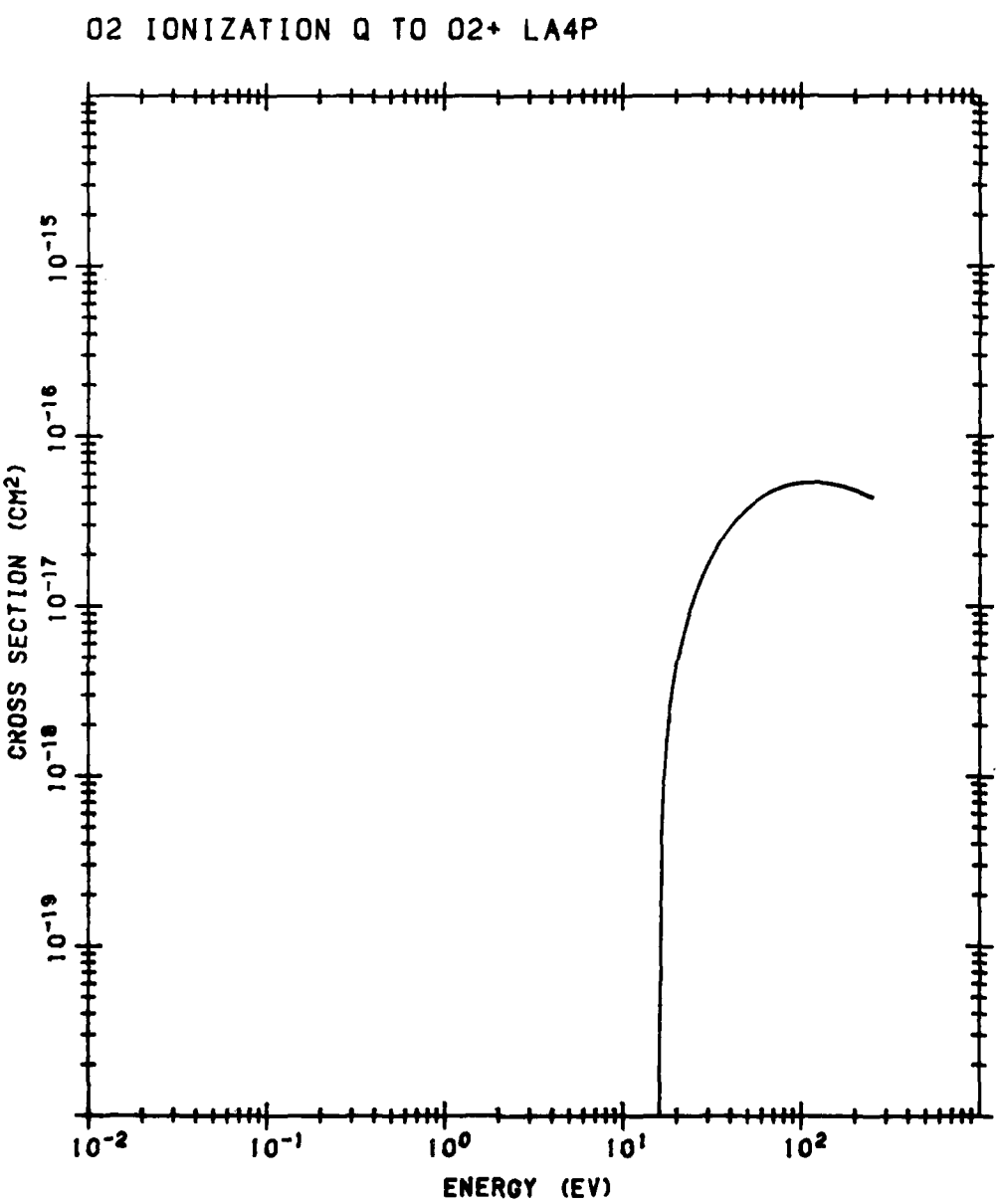


Figure B145. $O_2$ Ionization Cross Section to $O_2^+$ a $^4\Pi_u$. The data are from Jackman et al (1980)[B22]

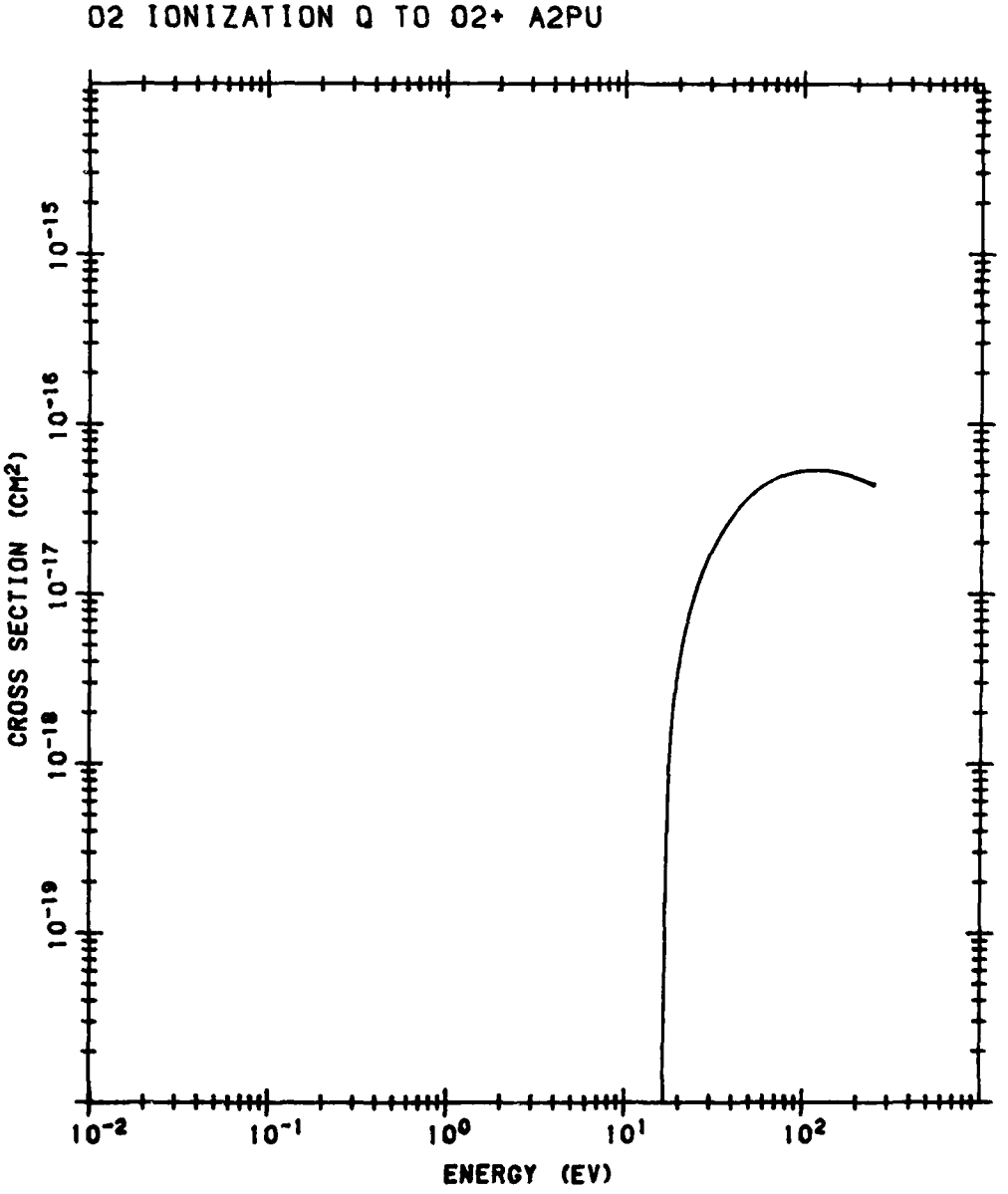


Figure B146. $O_2$ Ionization Cross Section to $O_2^+$ A $^2\Pi_u$. The data are from Jackman et al (1980)[B22]

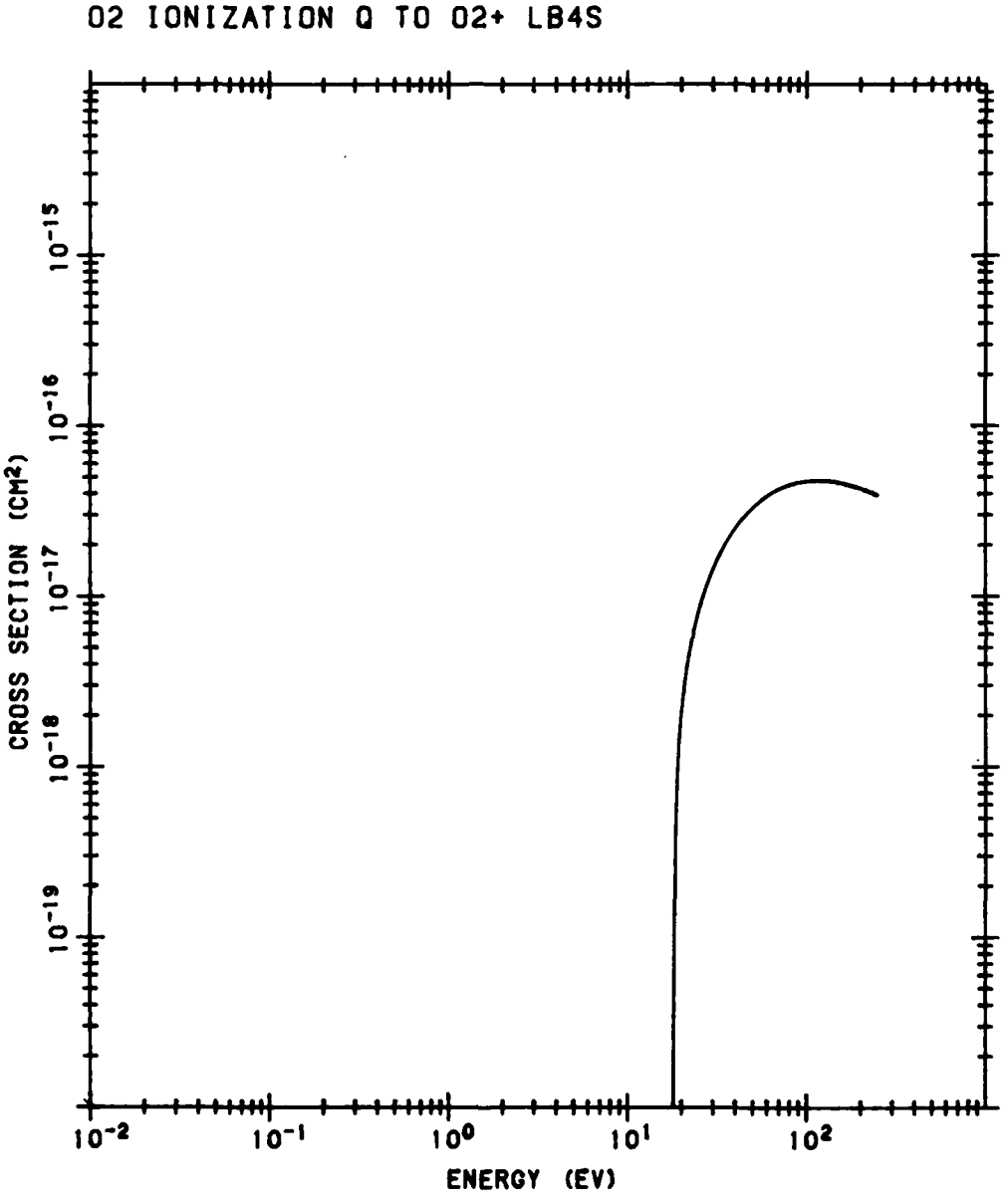


Figure B147. $O_2$ Ionization Cross Section to $O_2^+$ b $^4\Sigma_g^-$. The data are from Jackman et al (1980)[B22]

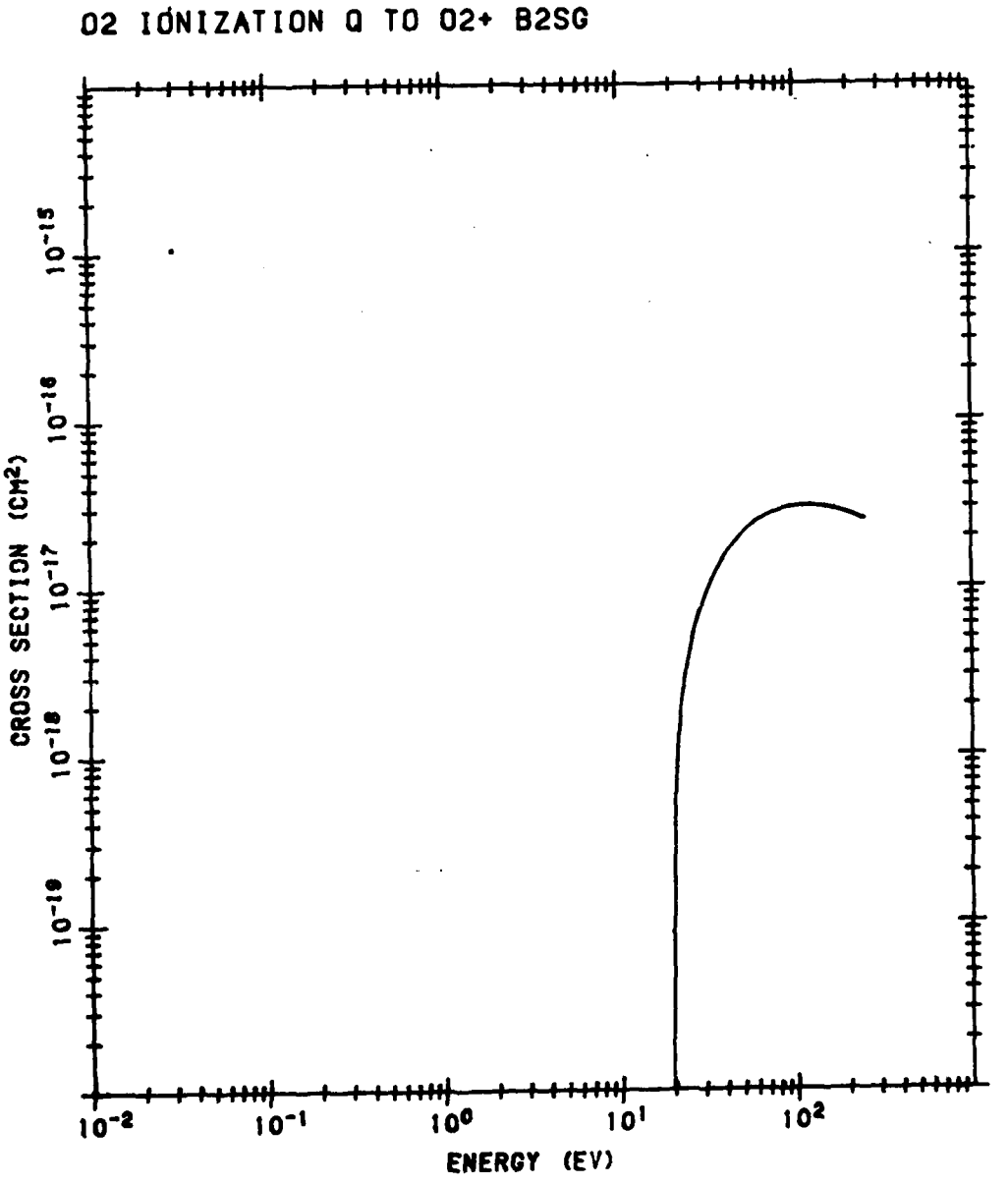


Figure B148. $O_2$ Ionization Cross Section to B $^2\Sigma_g^-$. The data are from Jackman et al (1980)[B22]

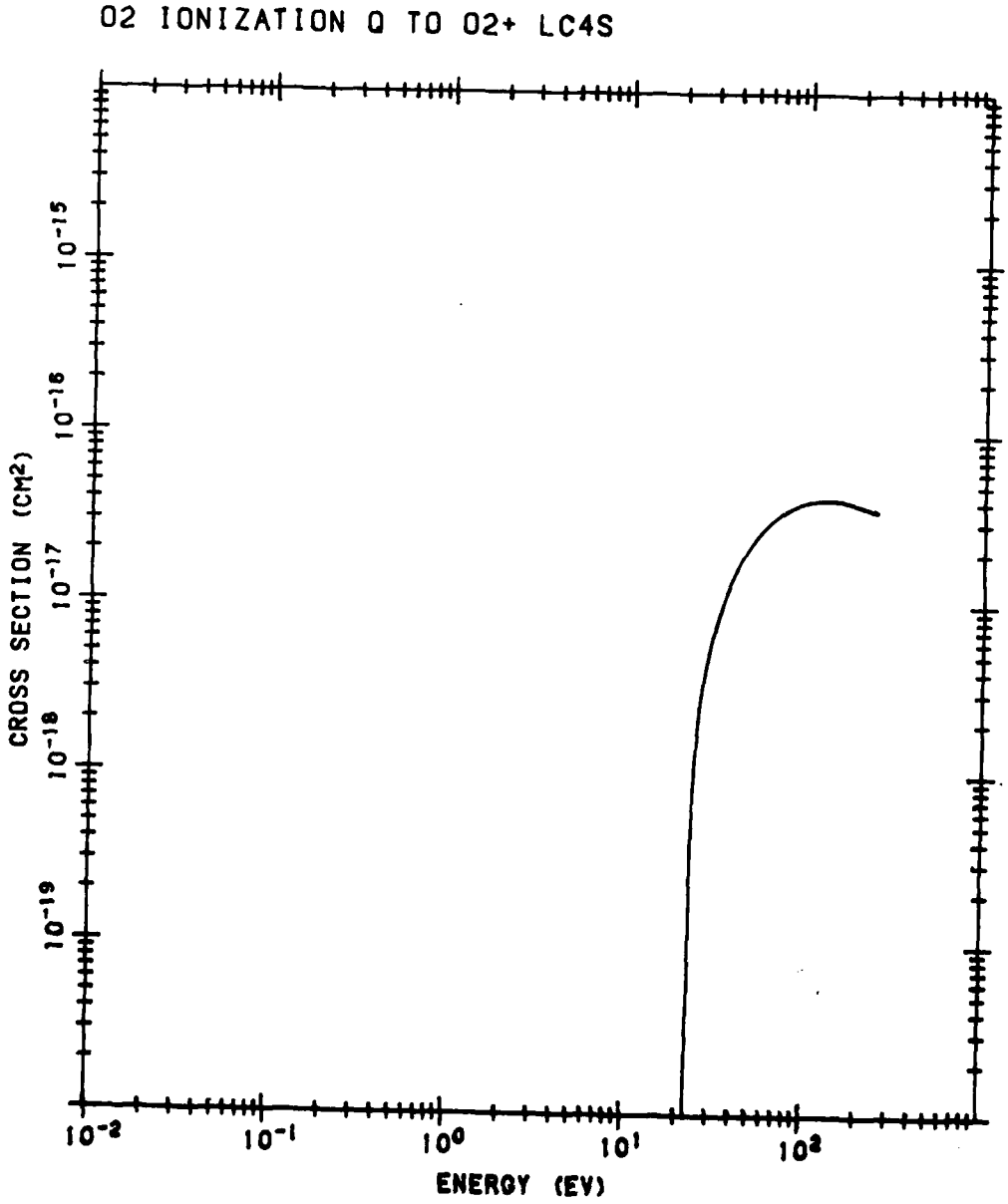


Figure B149. $O_2$ Ionization Cross Section to c $^4\Sigma_u^-$. The data are from Jackman et al (1980)[B22]

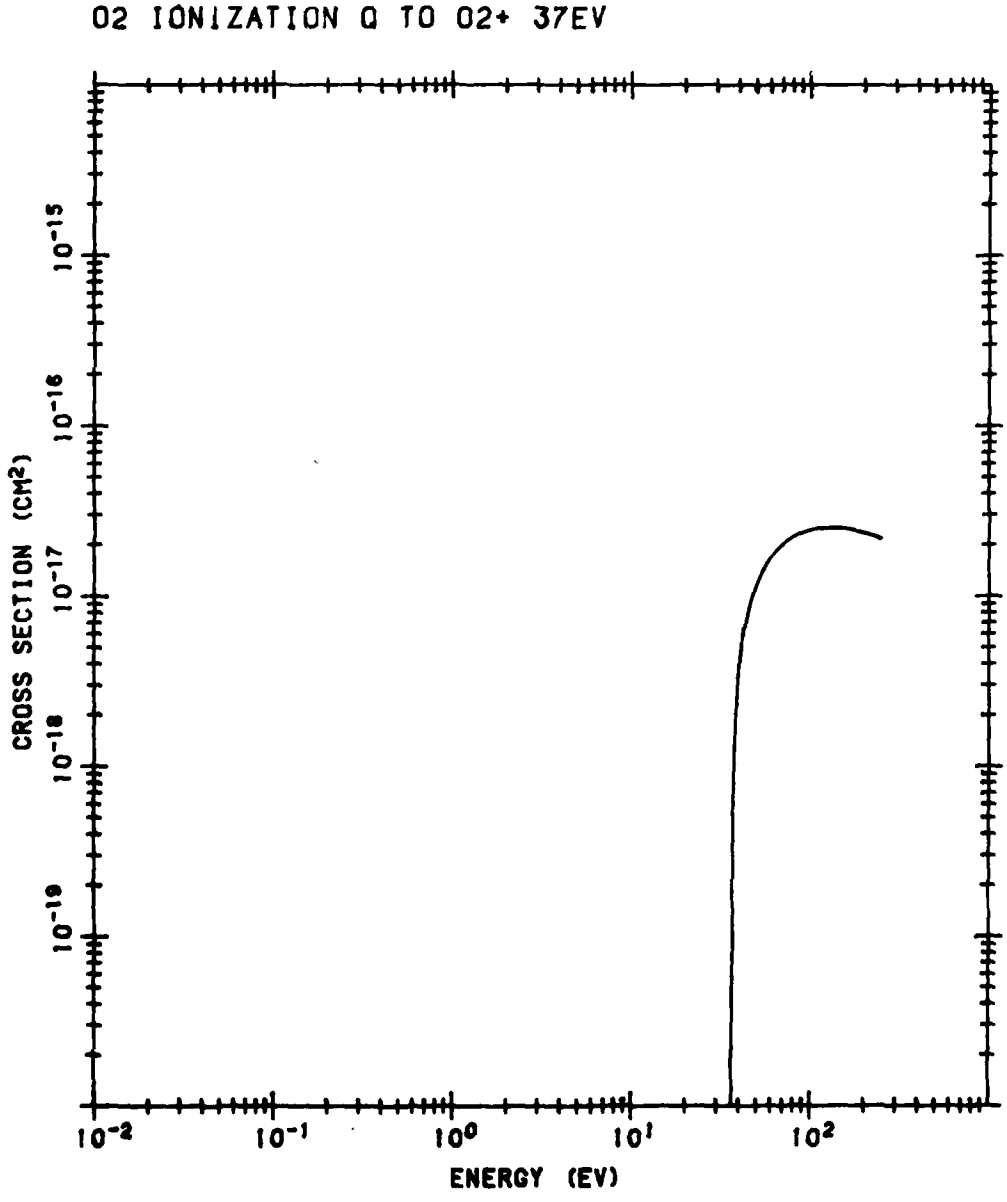


Figure B150. $O_2$ Ionization Cross Section to an $O_2^+$ State Hypothesized at 37 eV. The data are from Jackman et al (1980)[B22]

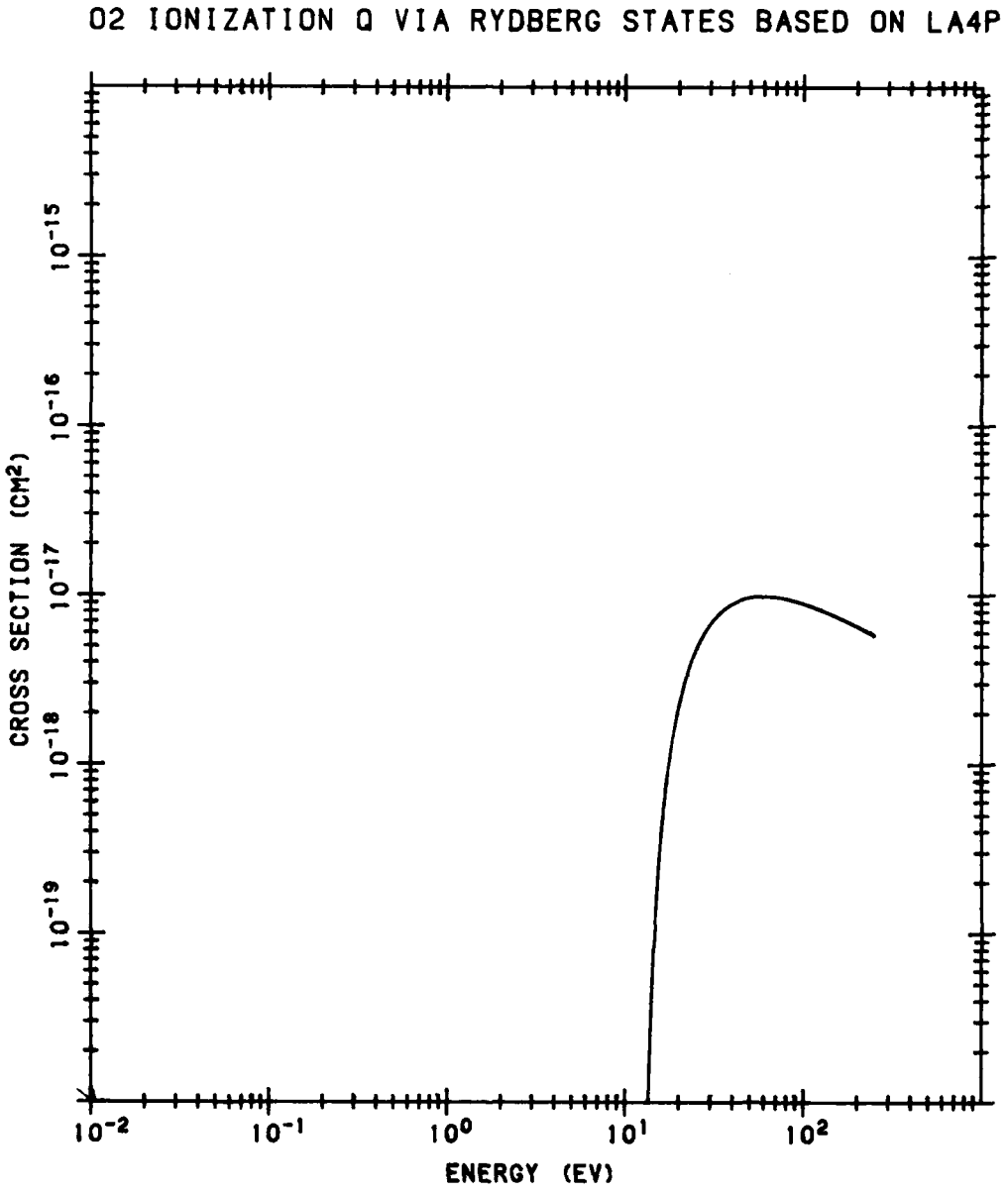


Figure B151. Sum of $O_2$ Ionization Cross Sections via Rydberg States Based on $O_2^+$ a $^4\Pi_u$. The cross section data of Jackman et al (1980)[B22] are weighted by the fraction of excitations which ionize and summed from n equal to 3

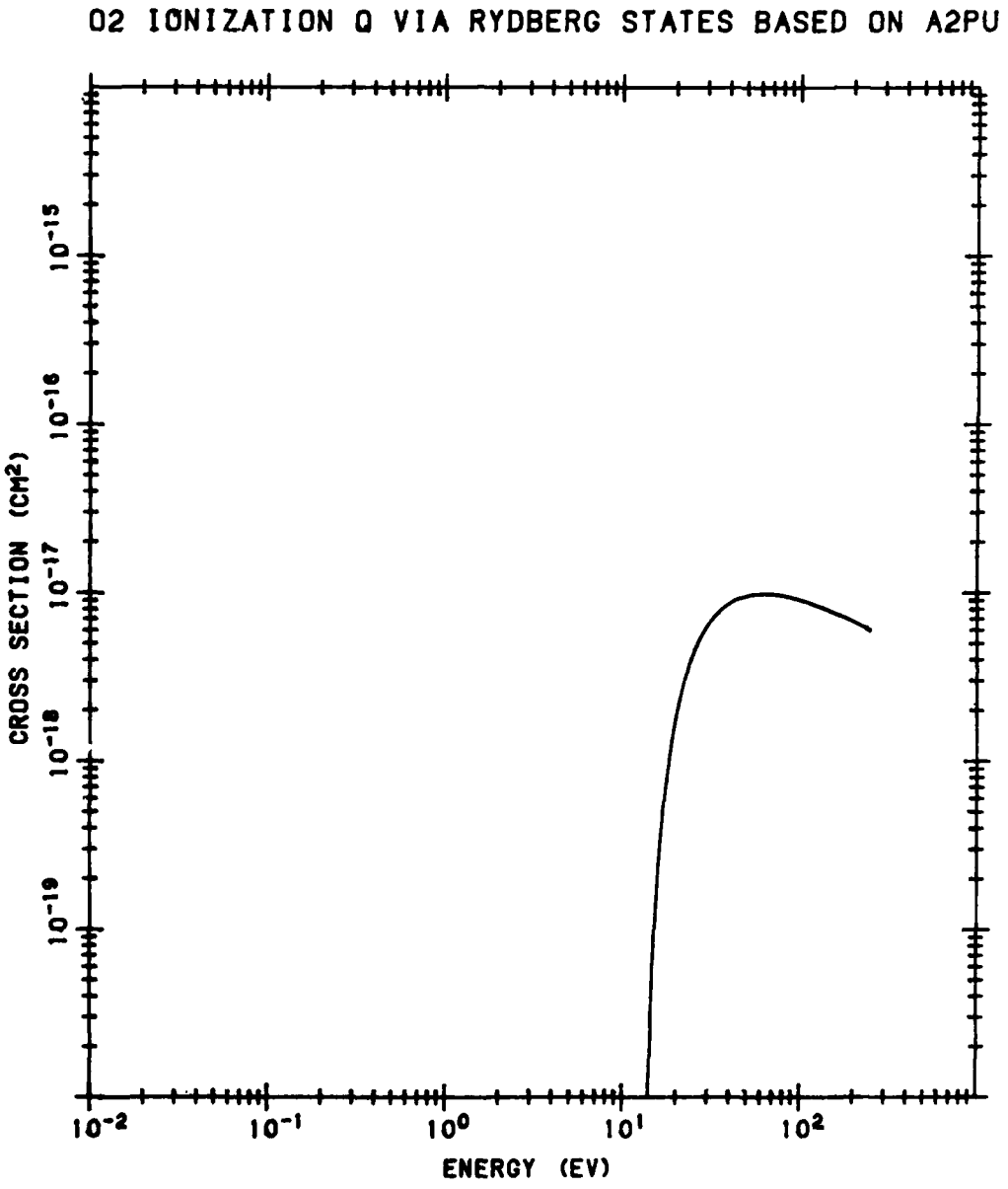


Figure B152. Sum of $O_2$ Ionization Cross Sections via Rydberg States Based on $O_2^+ A\,^2\Pi_u$. The data source is the same as that of Figure B151

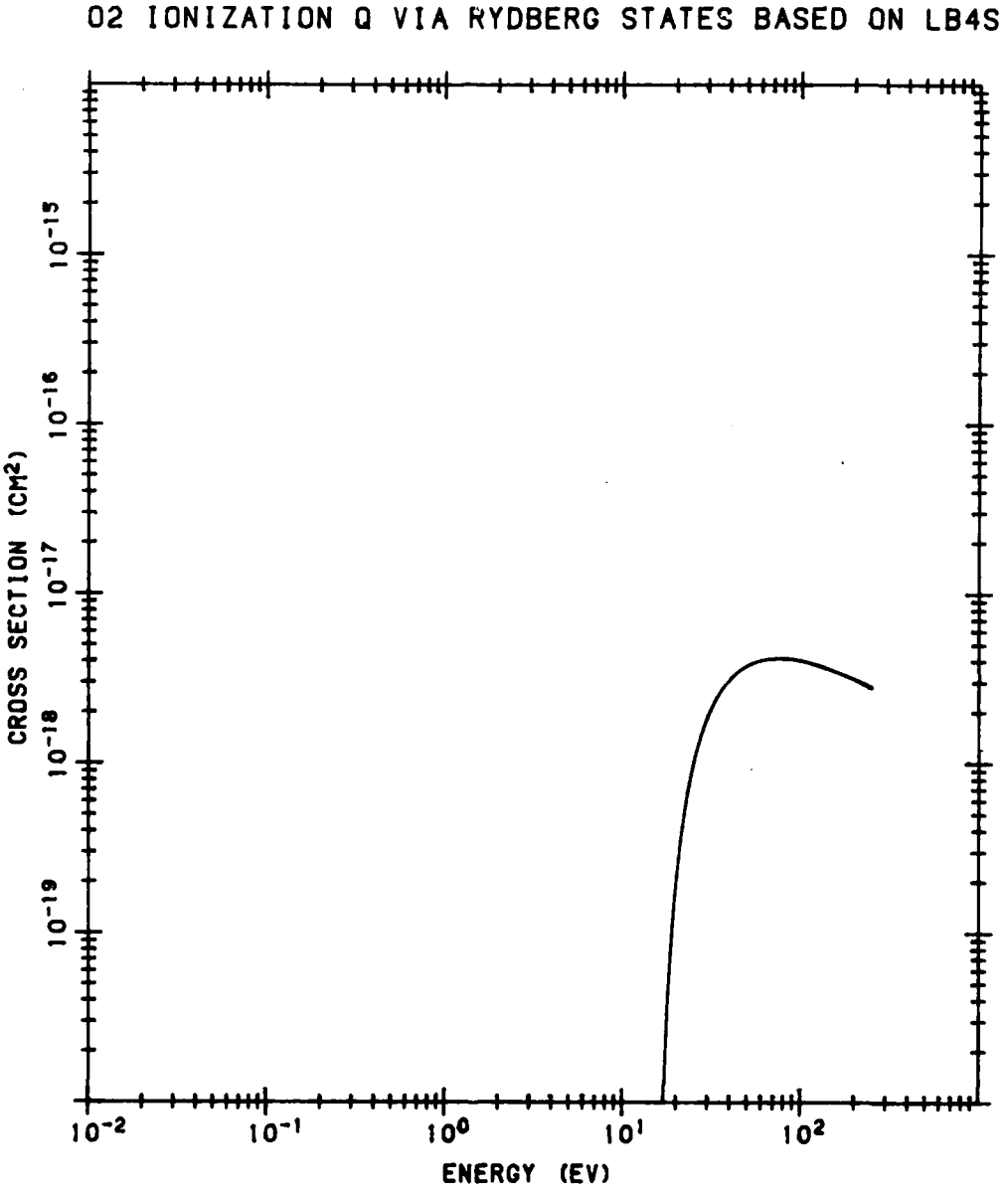


Figure B153. Sum of $O_2$ Ionization Cross Sections via Rydberg States Based on $O_2^+ b\,^4\Sigma_g^-$. The data source is the same as that of Figure B151

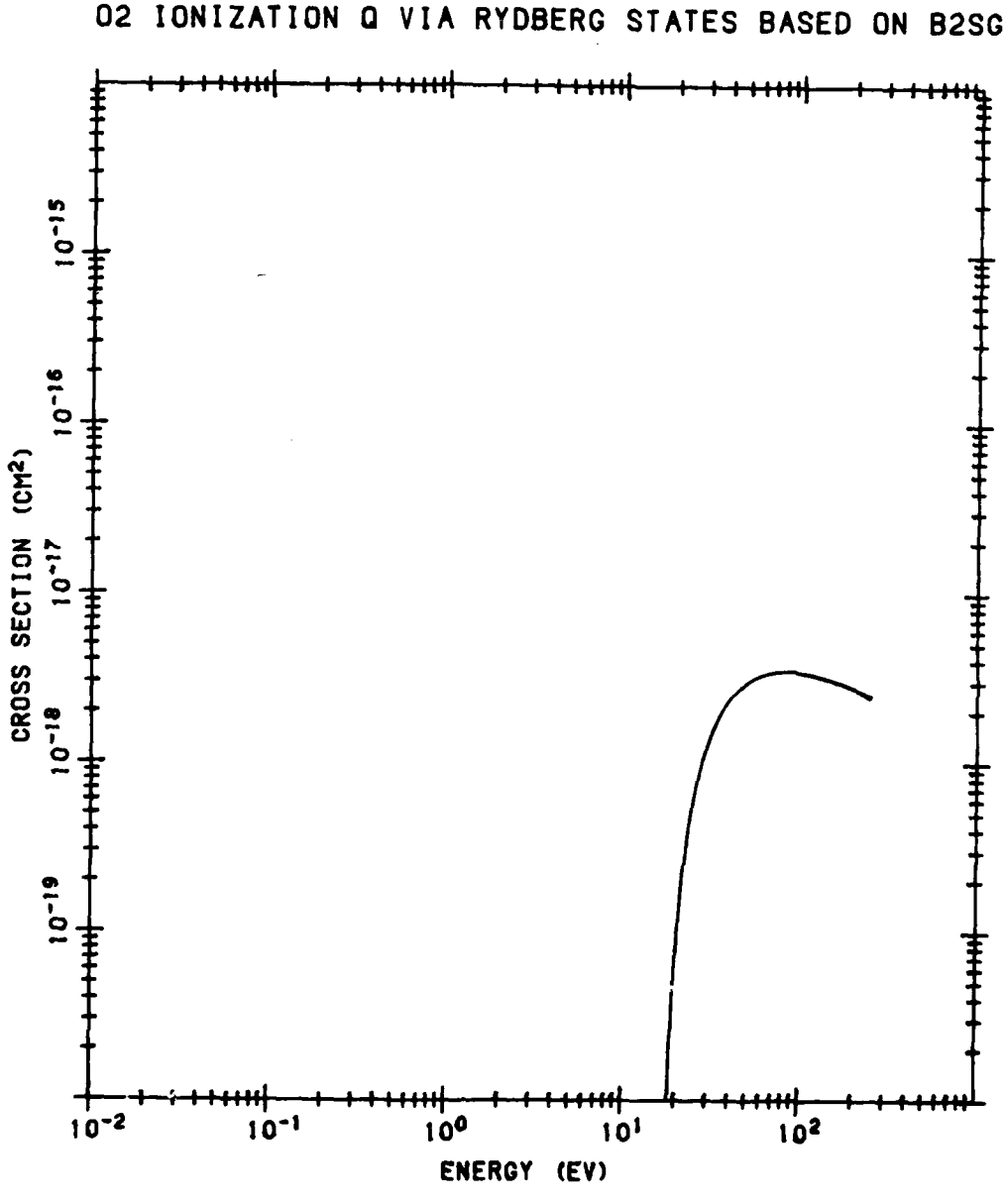


Figure B154. Sum of $O_2$ Ionization Cross Sections via Rydberg States Based on $O_2^+ B\,^2\Sigma_g^-$. The data source is the same as that of Figure B151

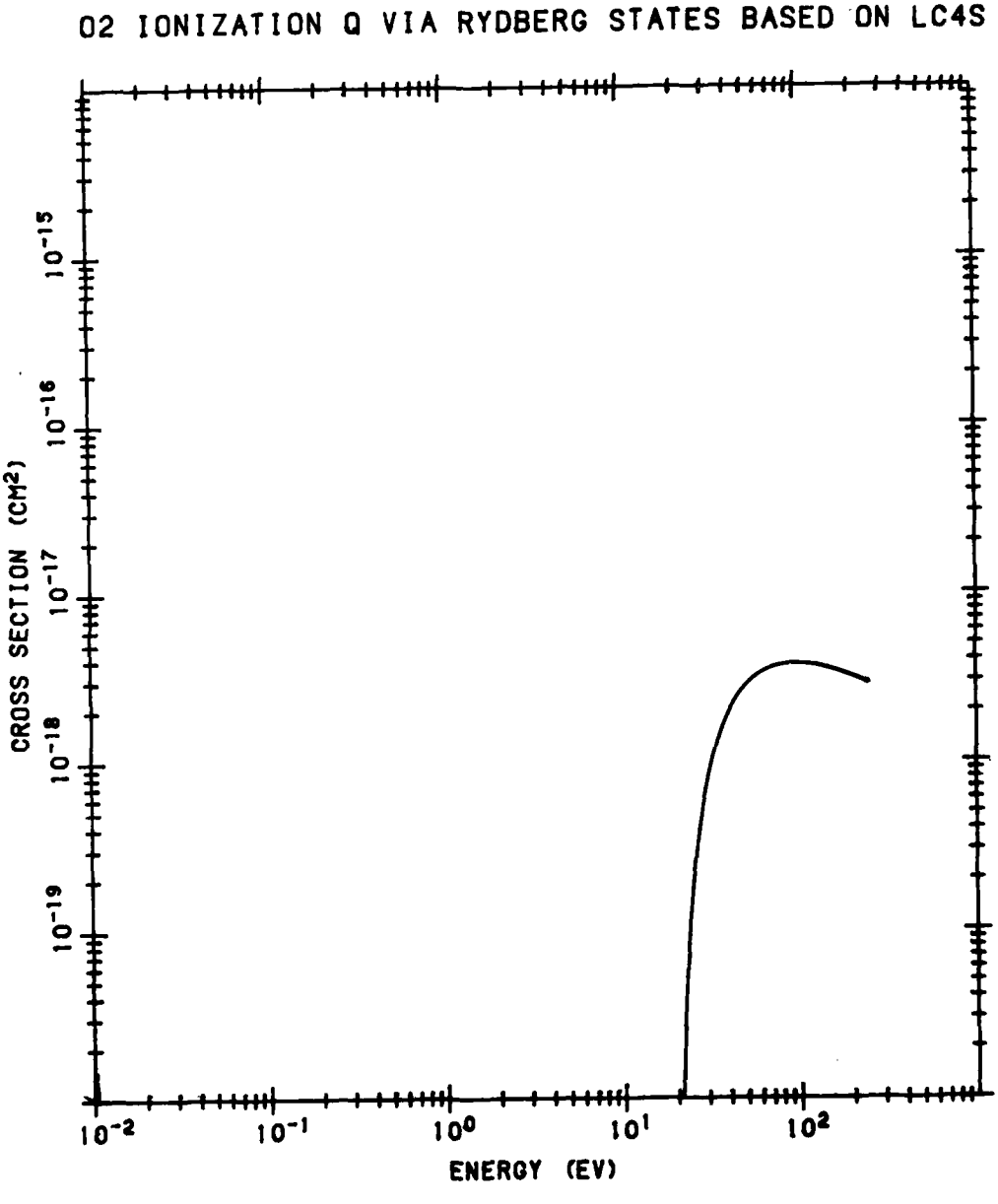


Figure B155. Sum of $O_2$ Ionization Cross Sections via Rydberg States Based on $O_2^+$ c $^4\Sigma_u^-$. The data source is the same as that of Figure B151

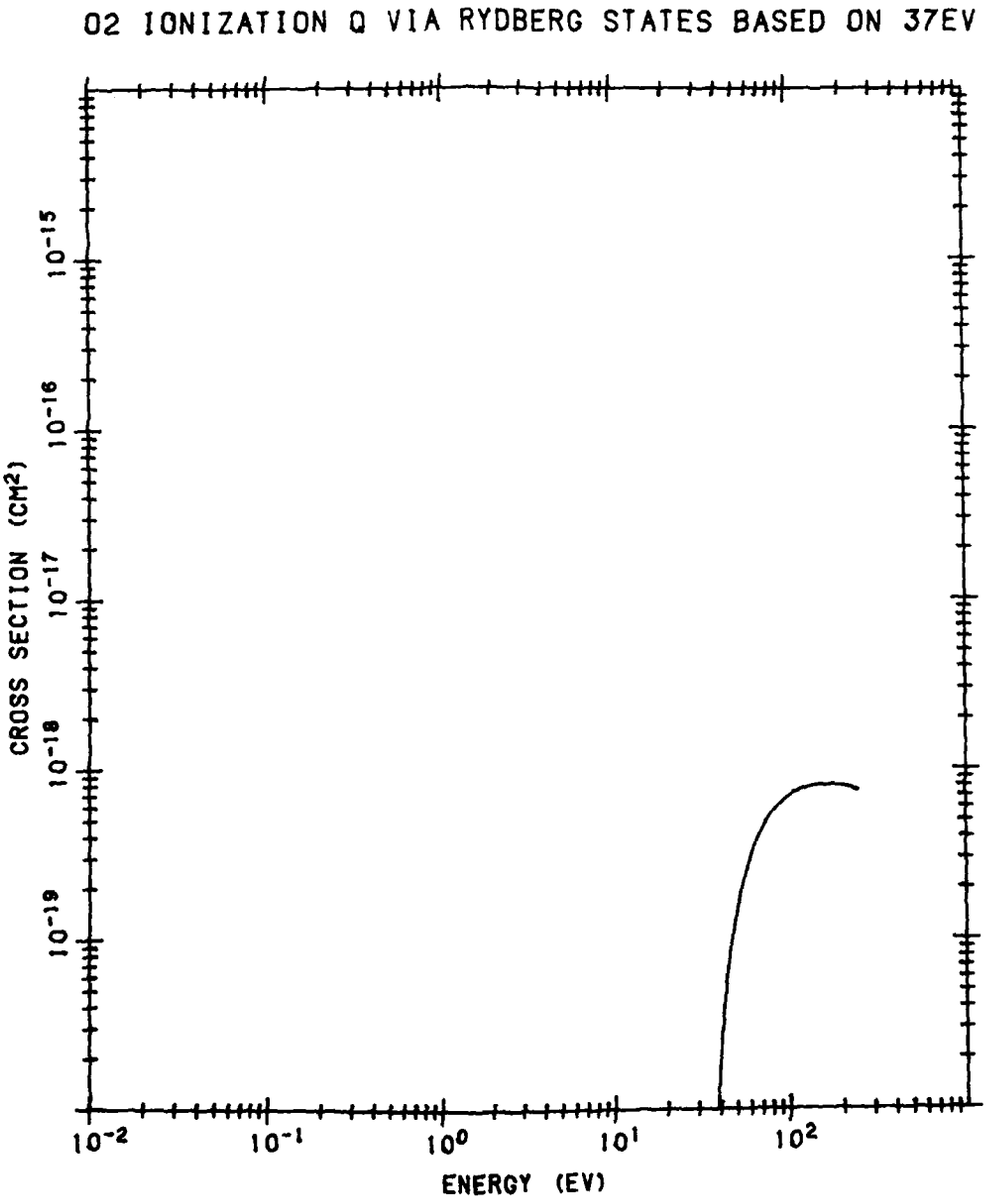


Figure B156. Sum of $O_2$ Ionization Cross Sections via Rydberg States Based on an $O_2^+$ State Hypothesized at 37 eV. The data source is the same as that of Figure B151

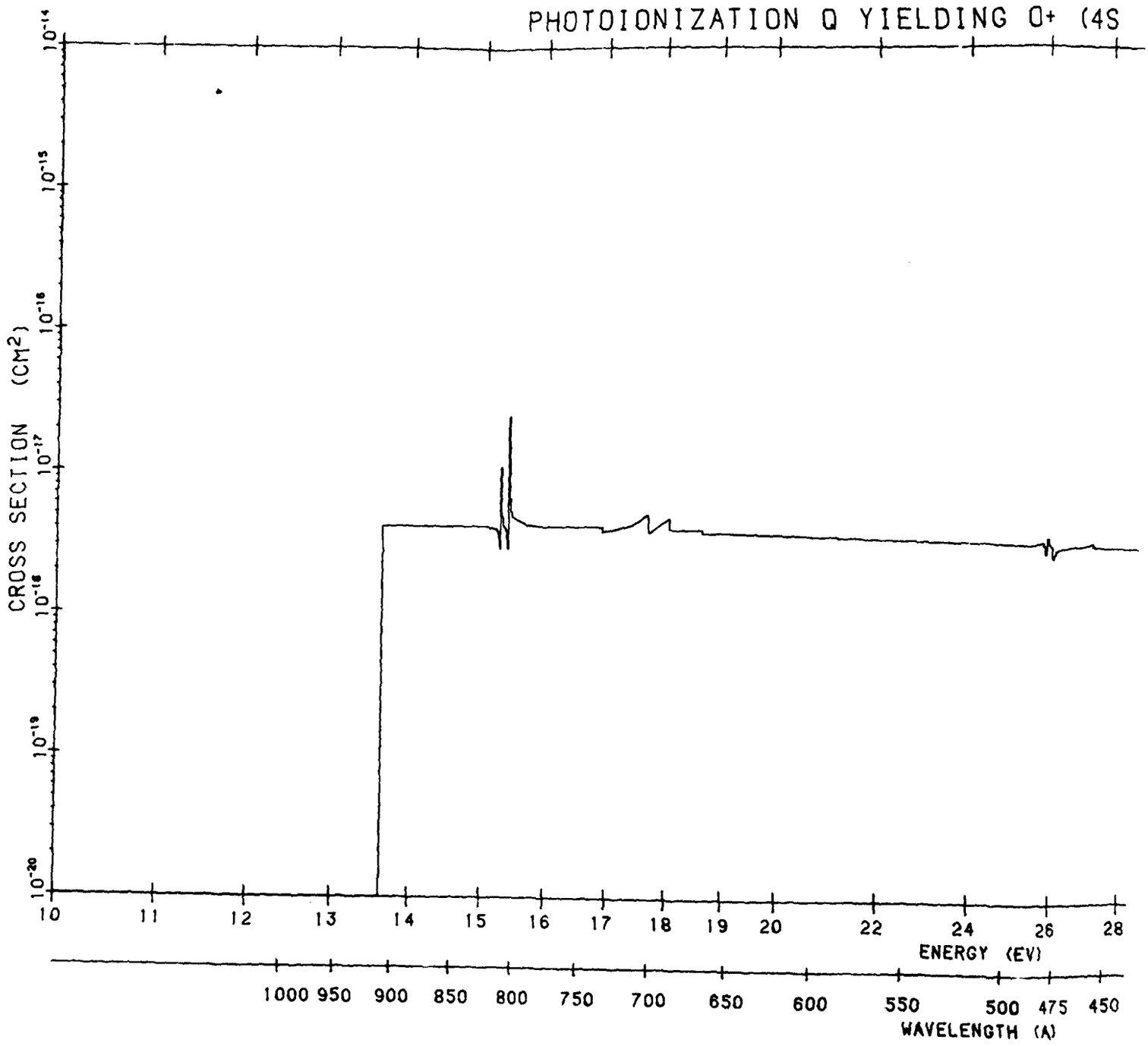
PHOTOIONIZATION Q YIELDING O+ (4S
CROSS SECTION (CM2)
10-14
10-15
10-16
10-17
10-18
10-19
10-20
10 11 12 13 14 15 16 17 18 19 20 22 24 26 28
ENERGY (EV)
1000 950 900 850 800 750 700 650 600 550 500 475 450
WAVELENGTH (A)

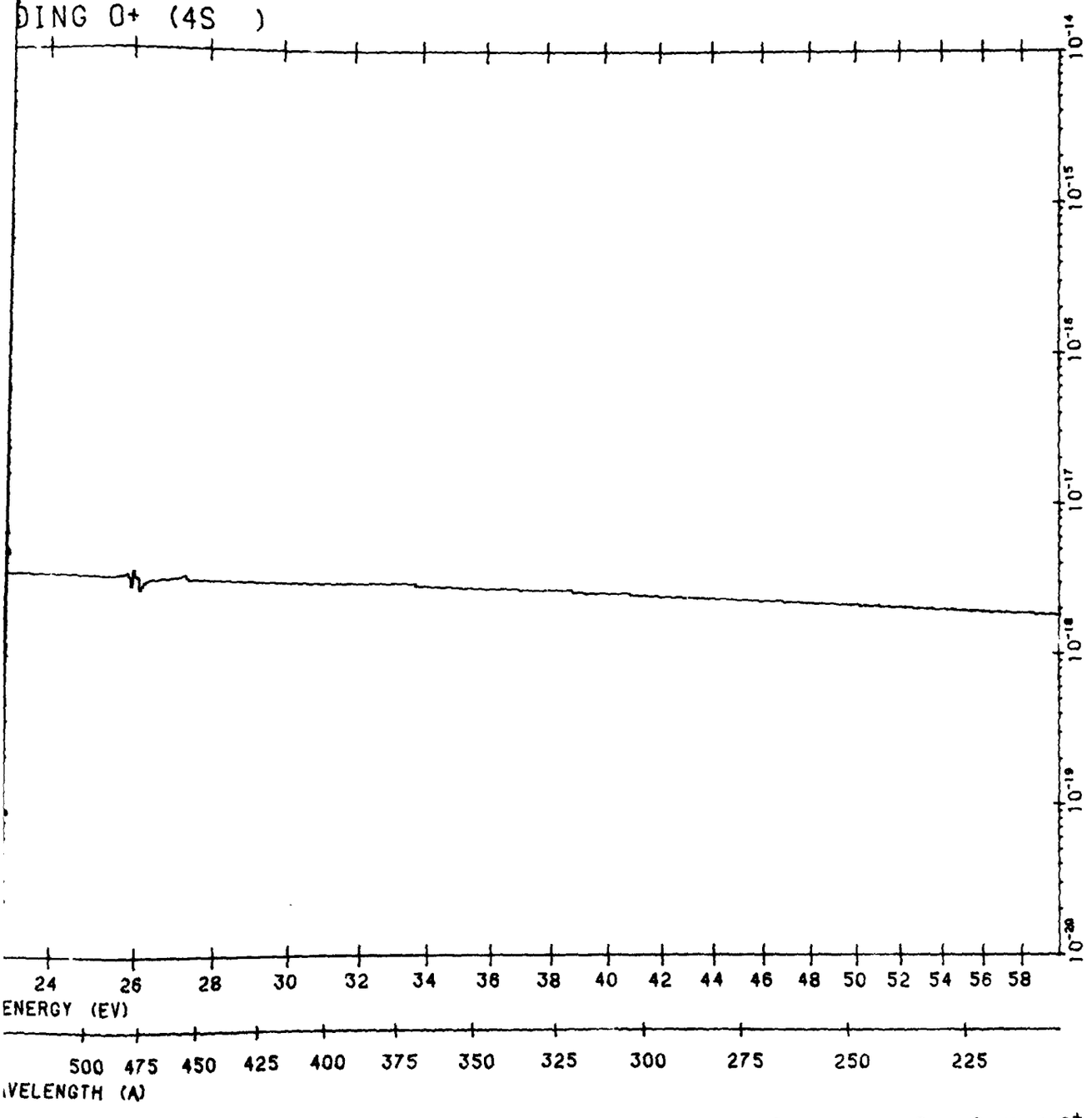


Figure B157. O Photoionization Cross Section to $O^+$ State $^4S^o$. The data are from Kirby et al (1979)[B26]

B26. Kirby, K., Constantinides, E.R., Babeu, S., Oppenheimer, M., and Victor, G.A. (1979) Atomic Data and Nuclear Data Tables 23:63.

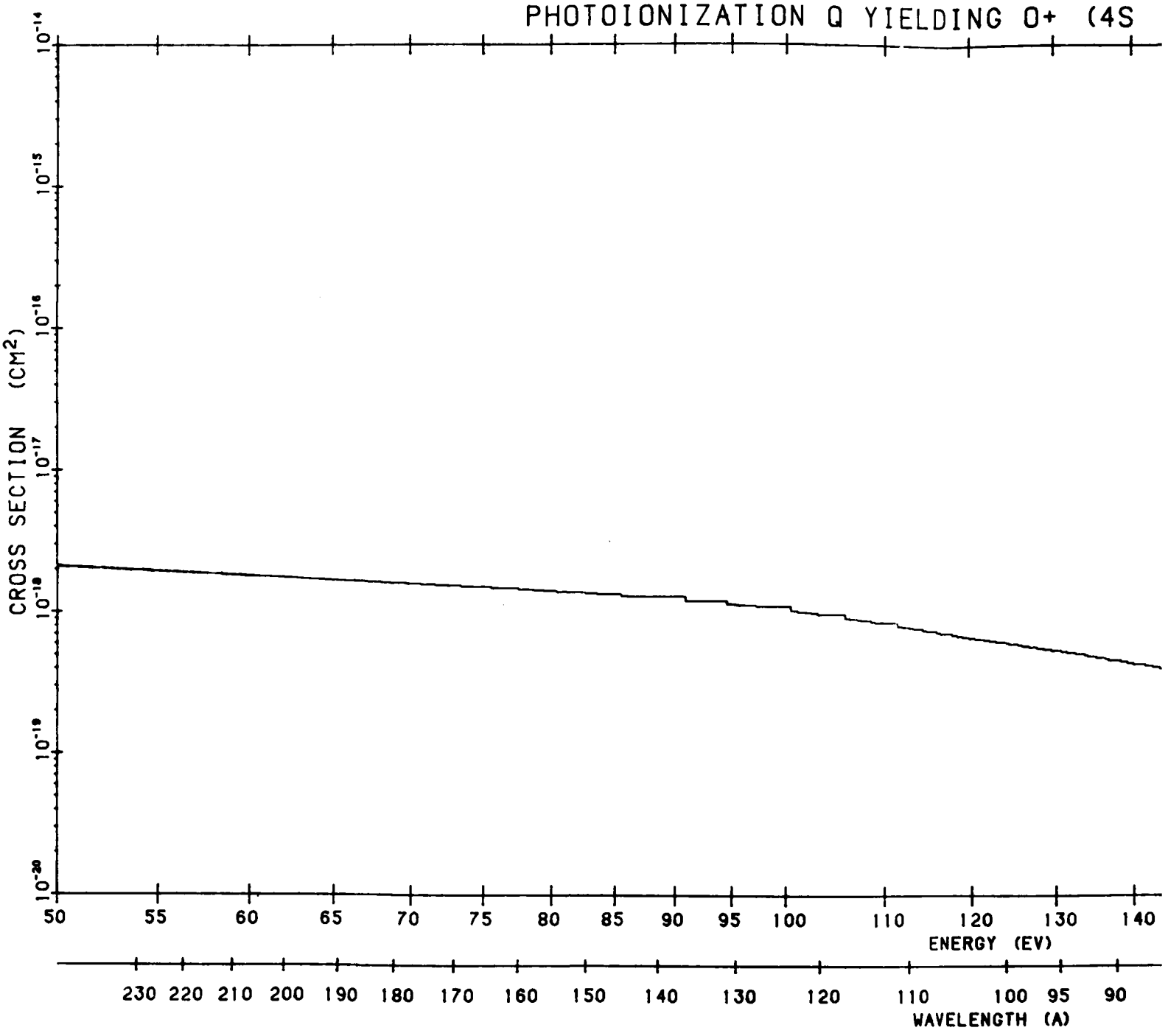
PHOTOIONIZATION Q YIELDING O+ (4S
CROSS SECTION (CM2)
10-14
10-15
10-16
10-17
10-18
10-19
10-20
50 55 60 65 70 75 80 85 90 95 100 110 120 130 140
ENERGY (EV)
230 220 210 200 190 180 170 160 150 140 130 120 110 100 95 90
WAVELENGTH (A)

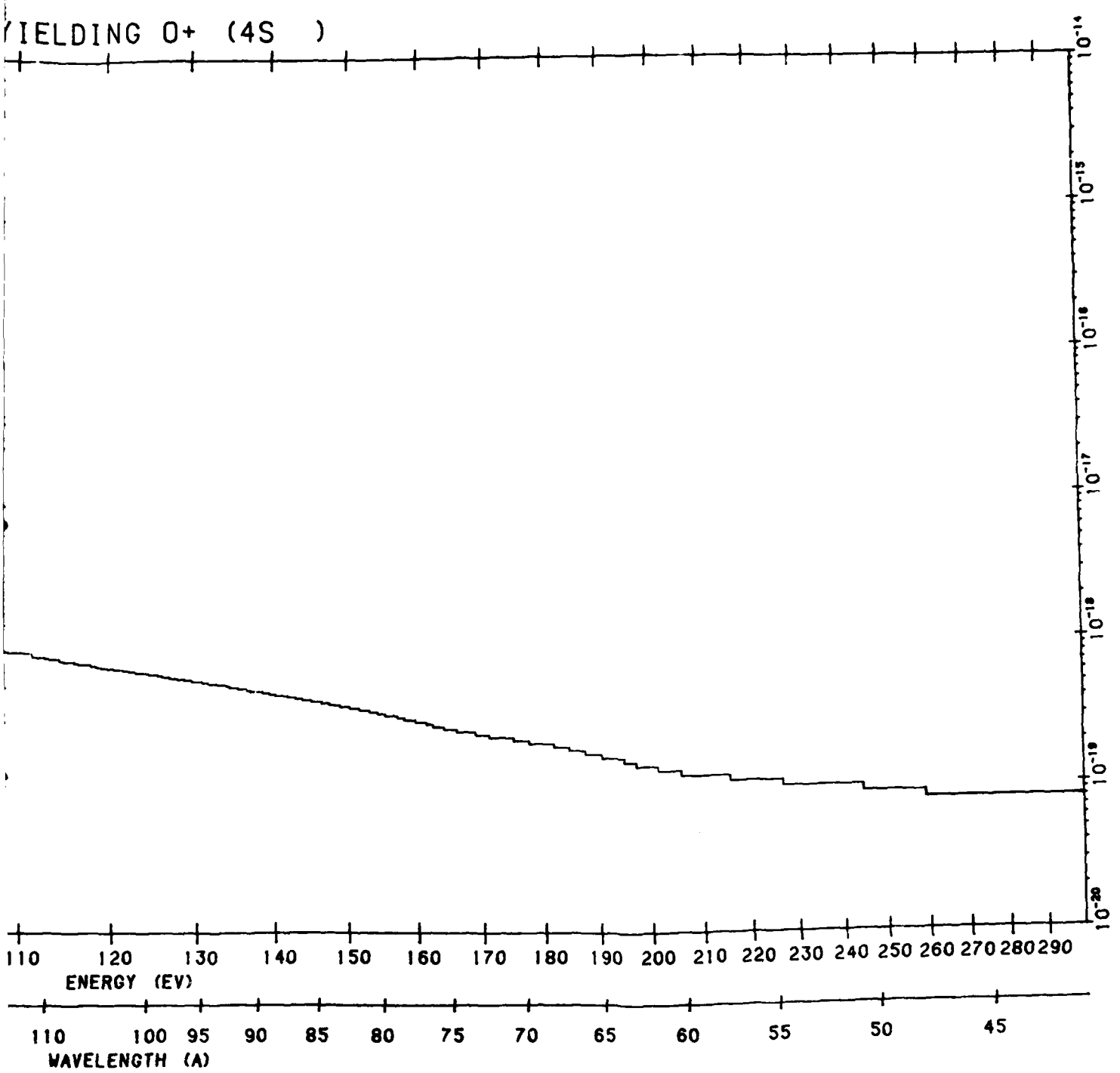


Figure B157. O Photoionization Cross Section to $O^+$ State $^4S^o$. The data are from Kirby et al (1979)[B26] (Cont.)

2

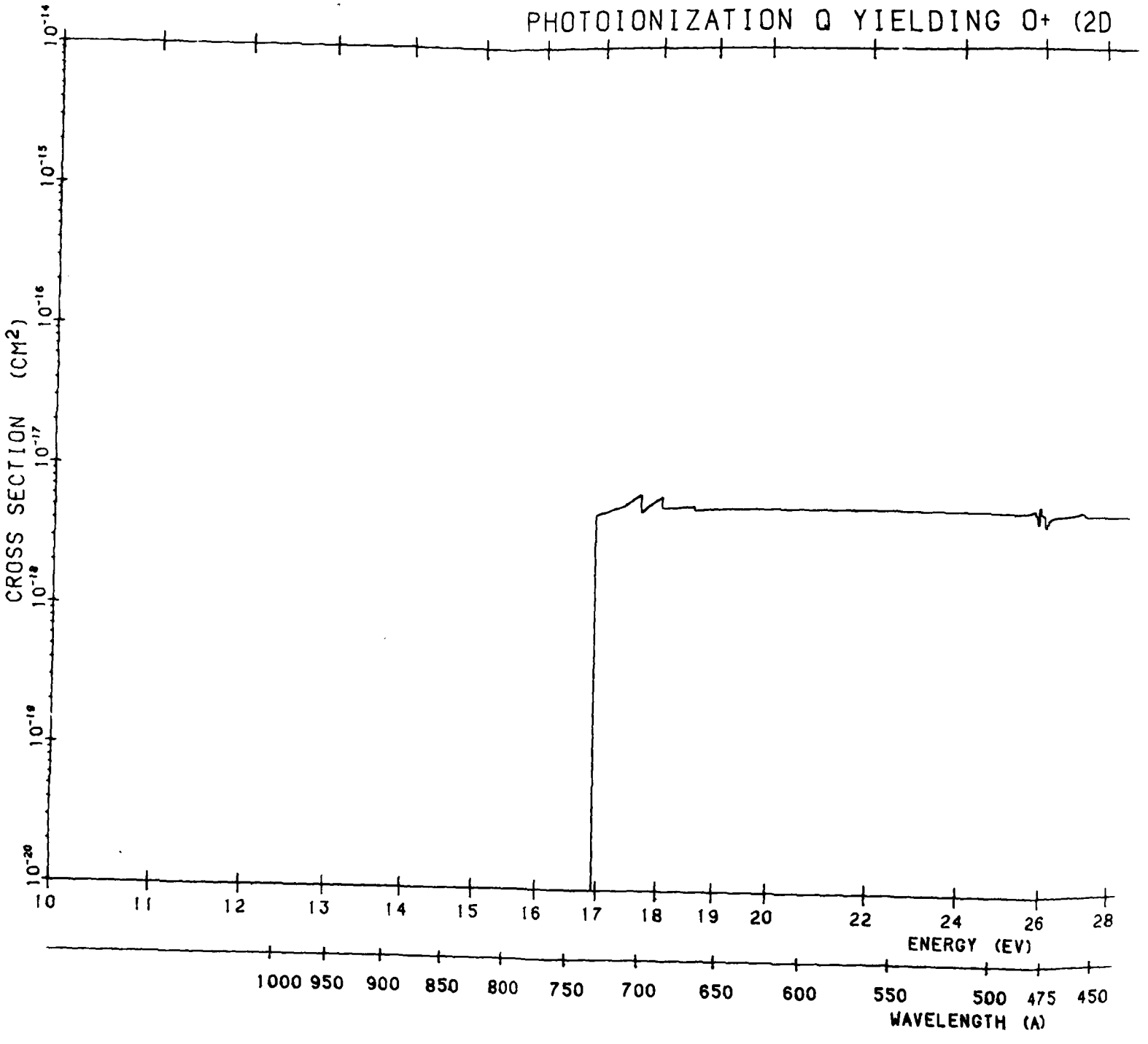
PHOTOIONIZATION Q YIELDING O+ (2D
CROSS SECTION (CM2)
10-14
10-15
10-16
10-17
10-18
10-19
10-20
10 11 12 13 14 15 16 17 18 19 20 22 24 26 28
ENERGY (EV)
1000 950 900 850 800 750 700 650 600 550 500 475 450
WAVELENGTH (A)

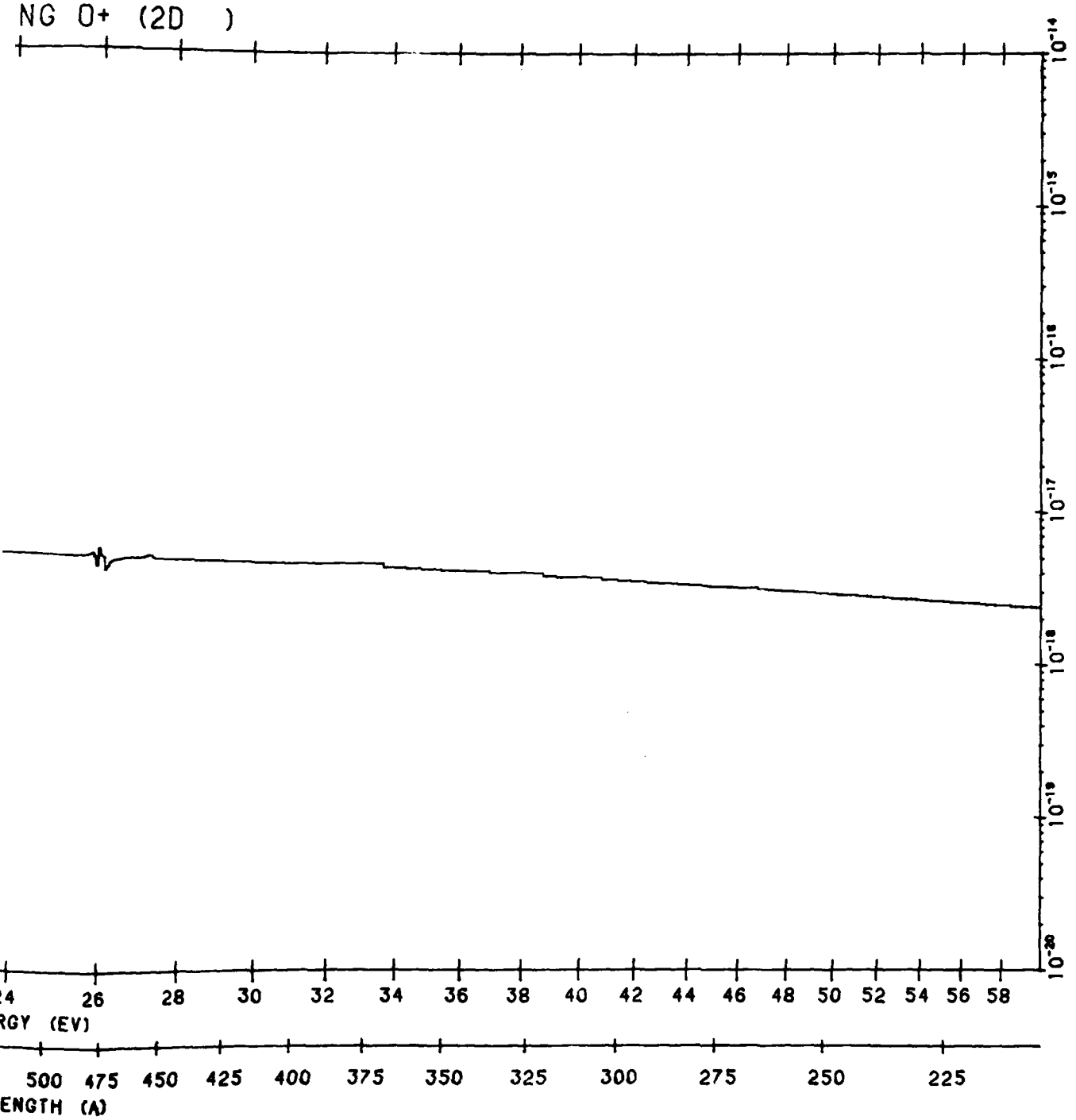


Figure B158. O Photoionization Cross Section to $O^+$ State $^2D^o$. The data source is the same as that of Figure B157

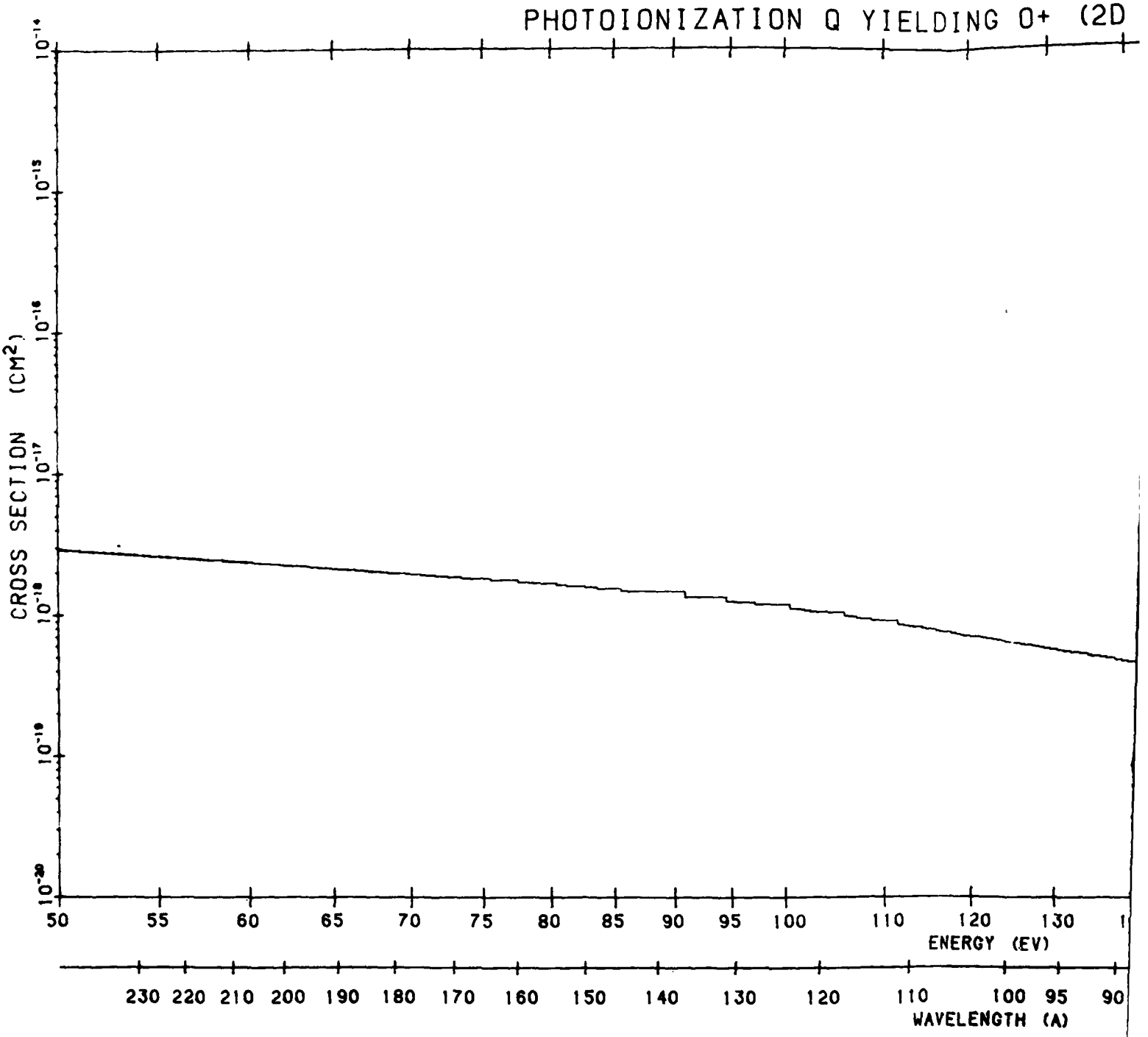
PHOTOIONIZATION Q YIELDING O+ (2D
CROSS SECTION (CM2)
10-14
10-15
10-16
10-17
10-18
10-19
10-20
50 55 60 65 70 75 80 85 90 95 100 110 120 130
ENERGY (EV)
230 220 210 200 190 180 170 160 150 140 130 120 110 100 95 90
WAVELENGTH (A)

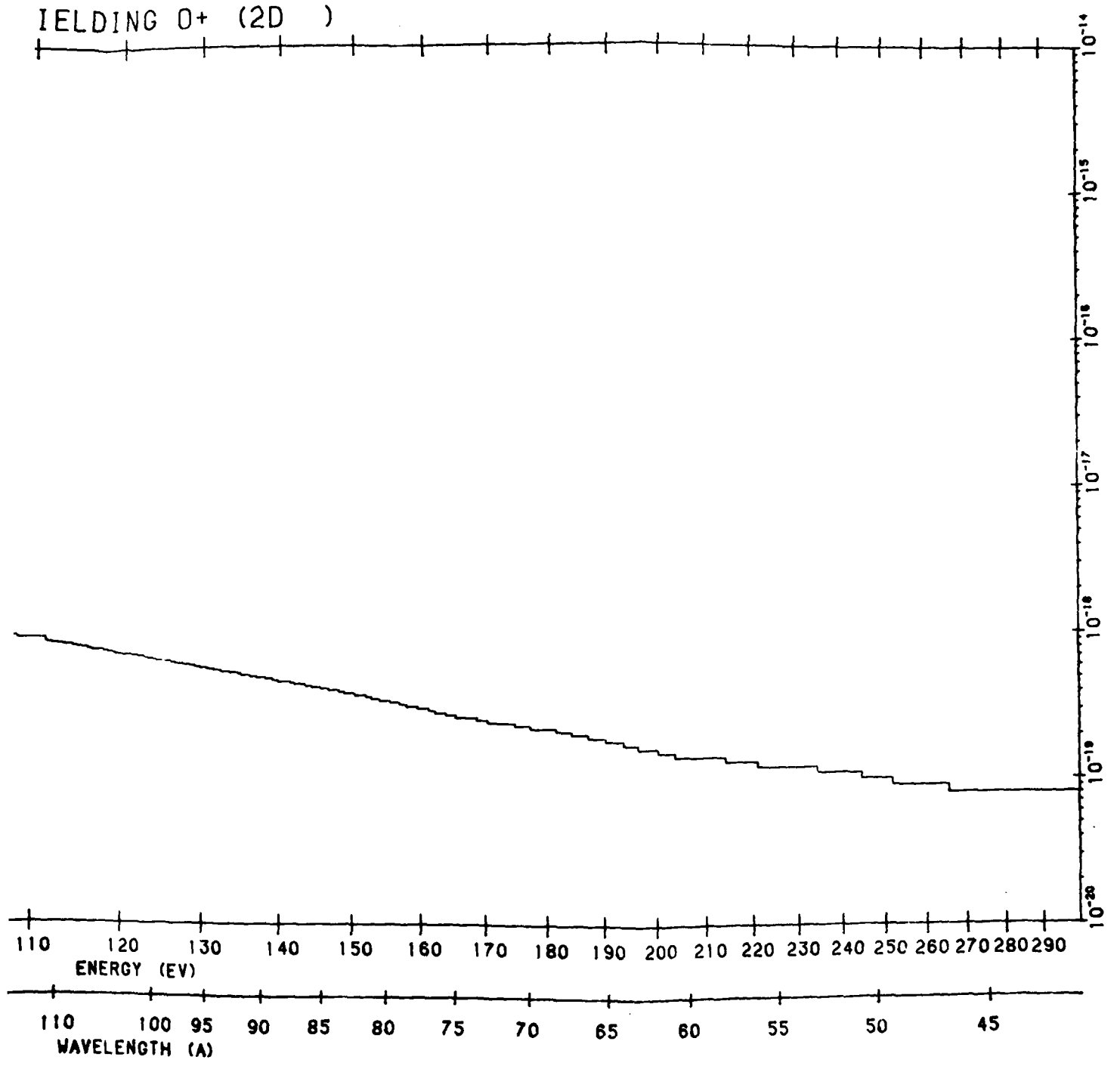


Figure B158. O Photoionization Cross Section to $O^+$ State $^2D^o$. The data source is the same as that of Figure B157 (Cont.)

2

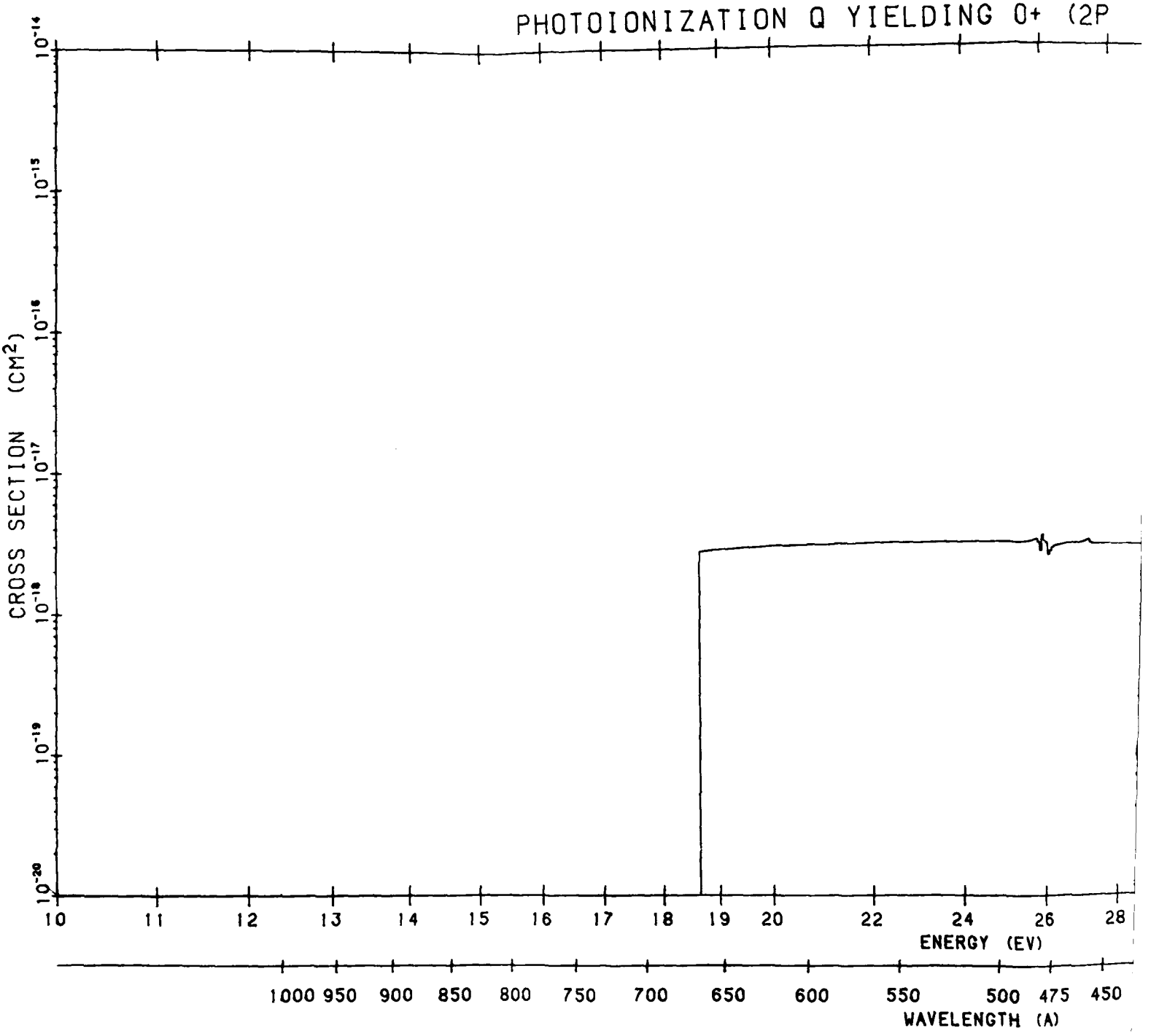
PHOTOIONIZATION Q YIELDING O+ (2P
CROSS SECTION (CM2)
10-14
10-15
10-16
10-17
10-18
10-19
10-20
10 11 12 13 14 15 16 17 18 19 20 22 24 26 28
ENERGY (EV)
1000 950 900 850 800 750 700 650 600 550 500 475 450
WAVELENGTH (A)

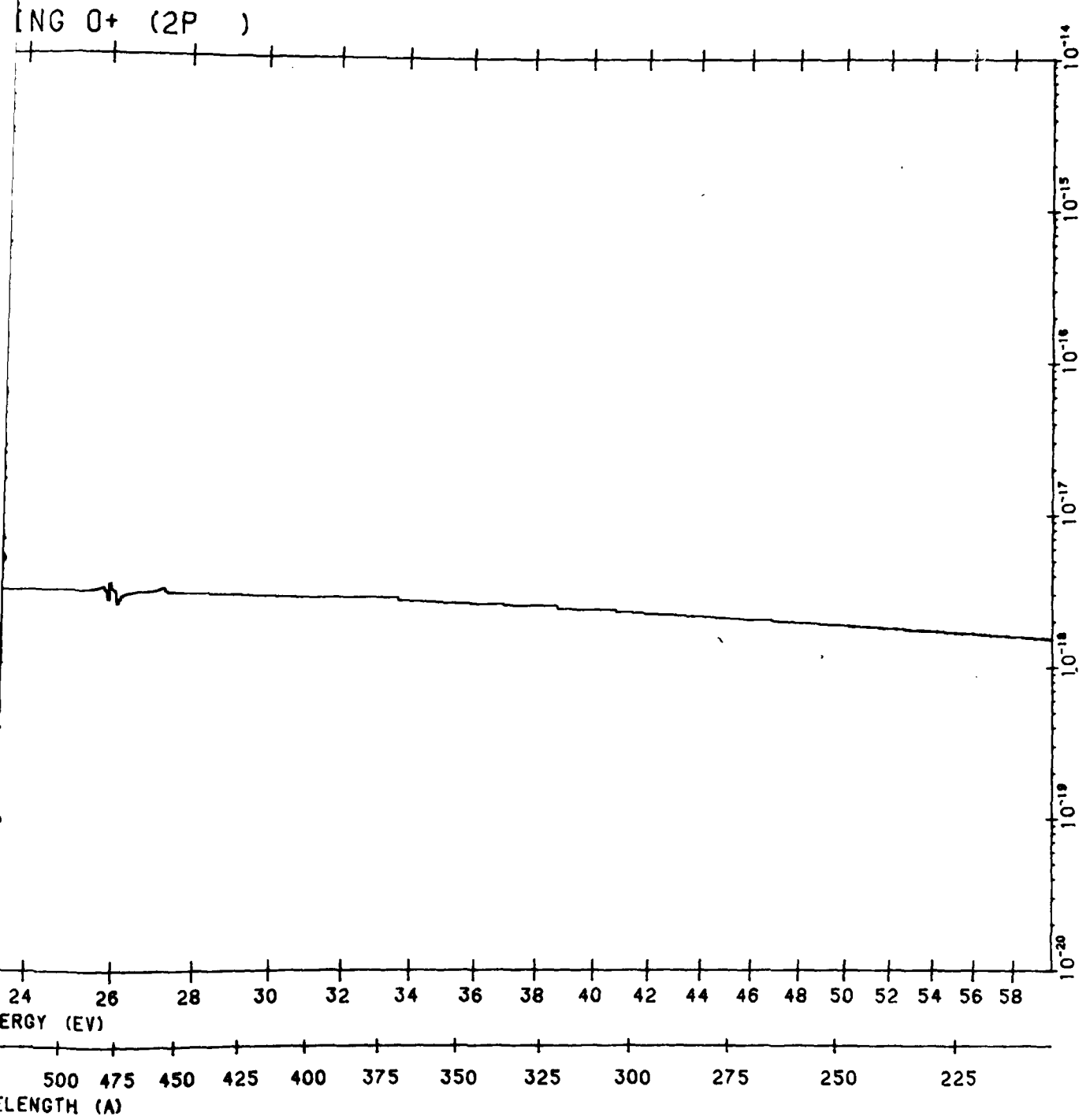


Figure B159. O Photoionization Cross Section to $^2P^o$. The data source is the same as that of Figure B157

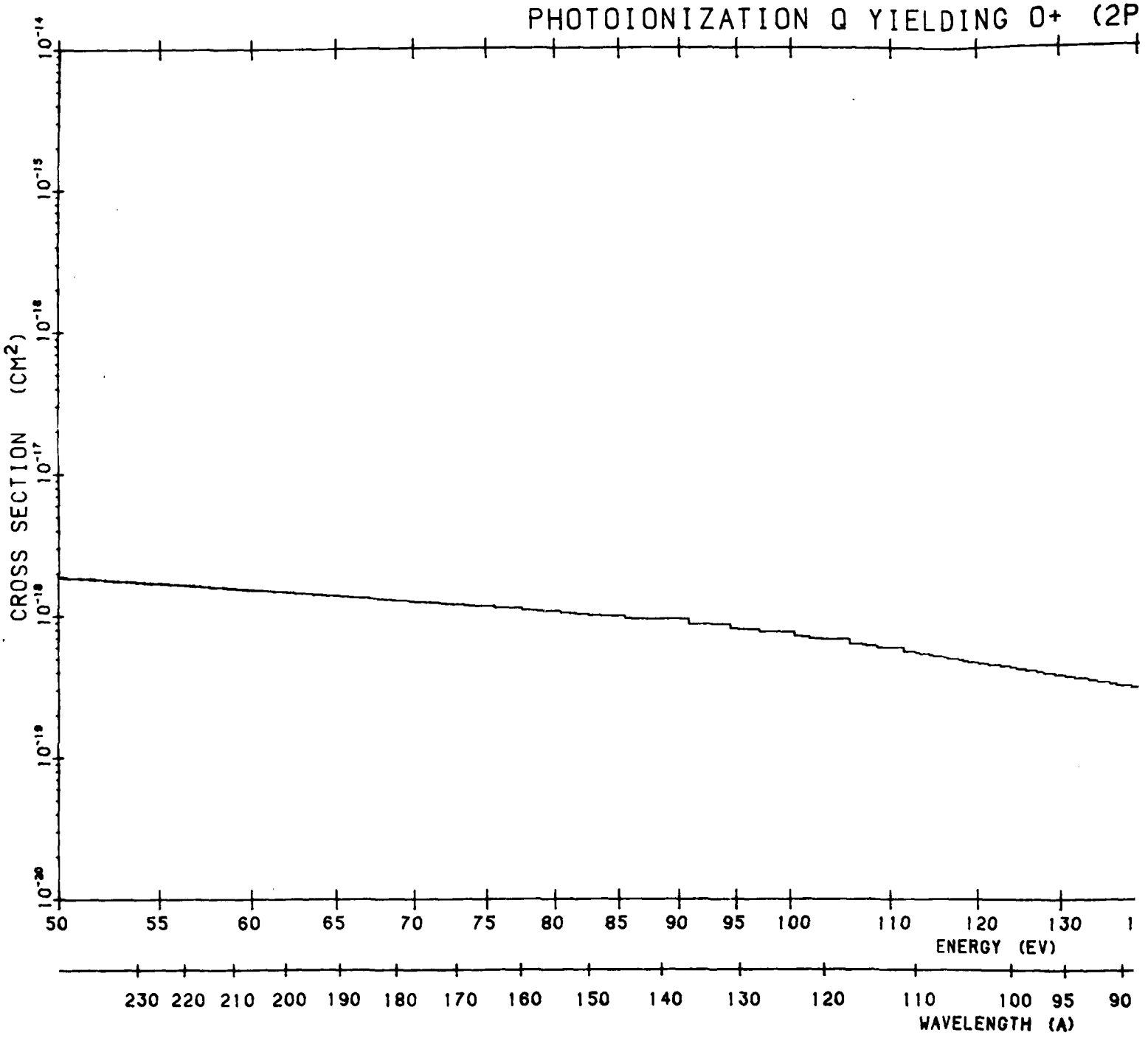
PHOTOIONIZATION Q YIELDING O+ (2P
CROSS SECTION (CM2)
10-14
10-15
10-16
10-17
10-18
10-19
10-20
50 55 60 65 70 75 80 85 90 95 100 110 120 130
ENERGY (EV)
230 220 210 200 190 180 170 160 150 140 130 120 110 100 95 90
WAVELENGTH (A)

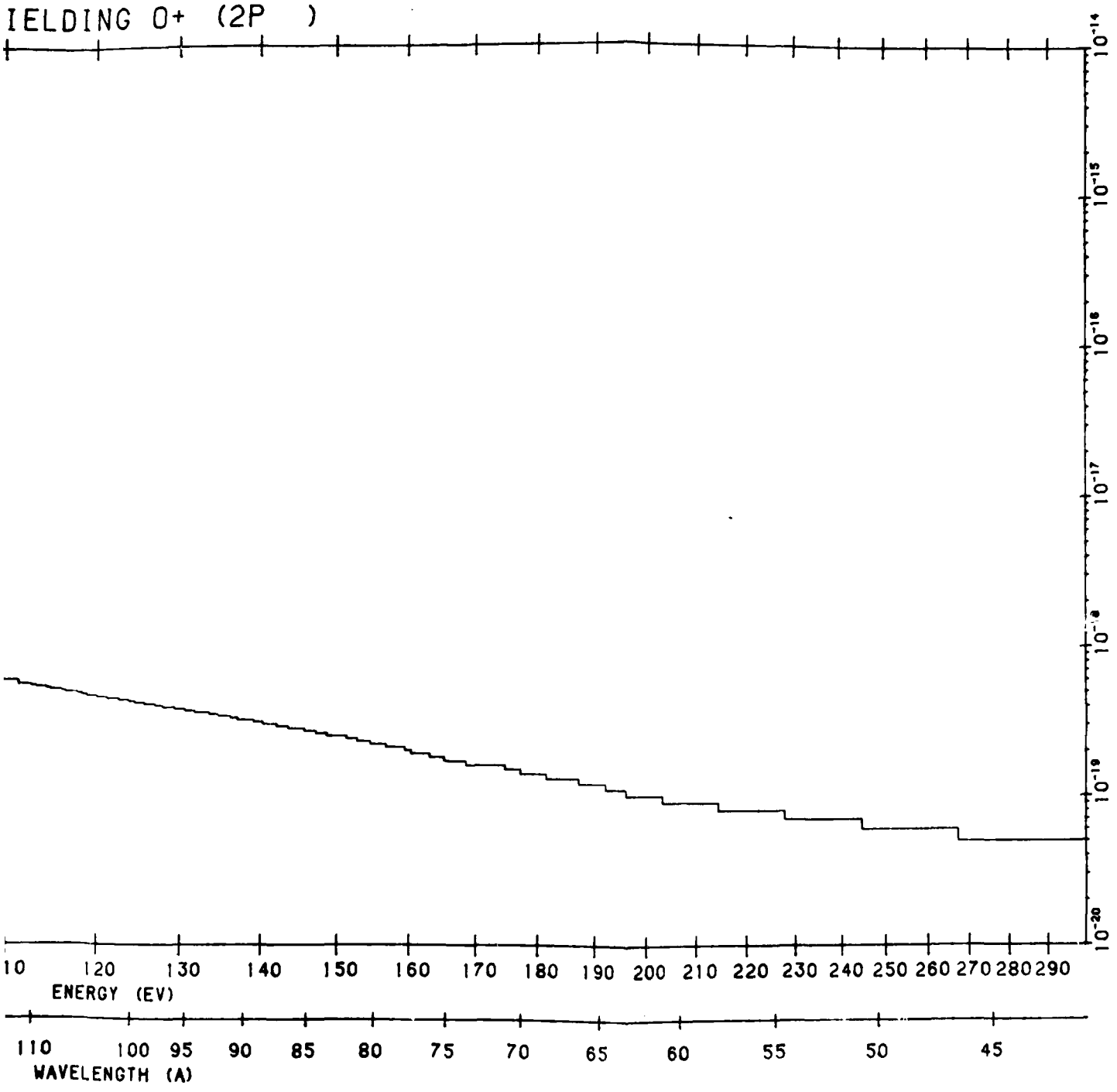


Figure B159. O Photoionization Cross Section to $^2P^o$. The data source is the same as that of Figure B157 (Cont.)

2

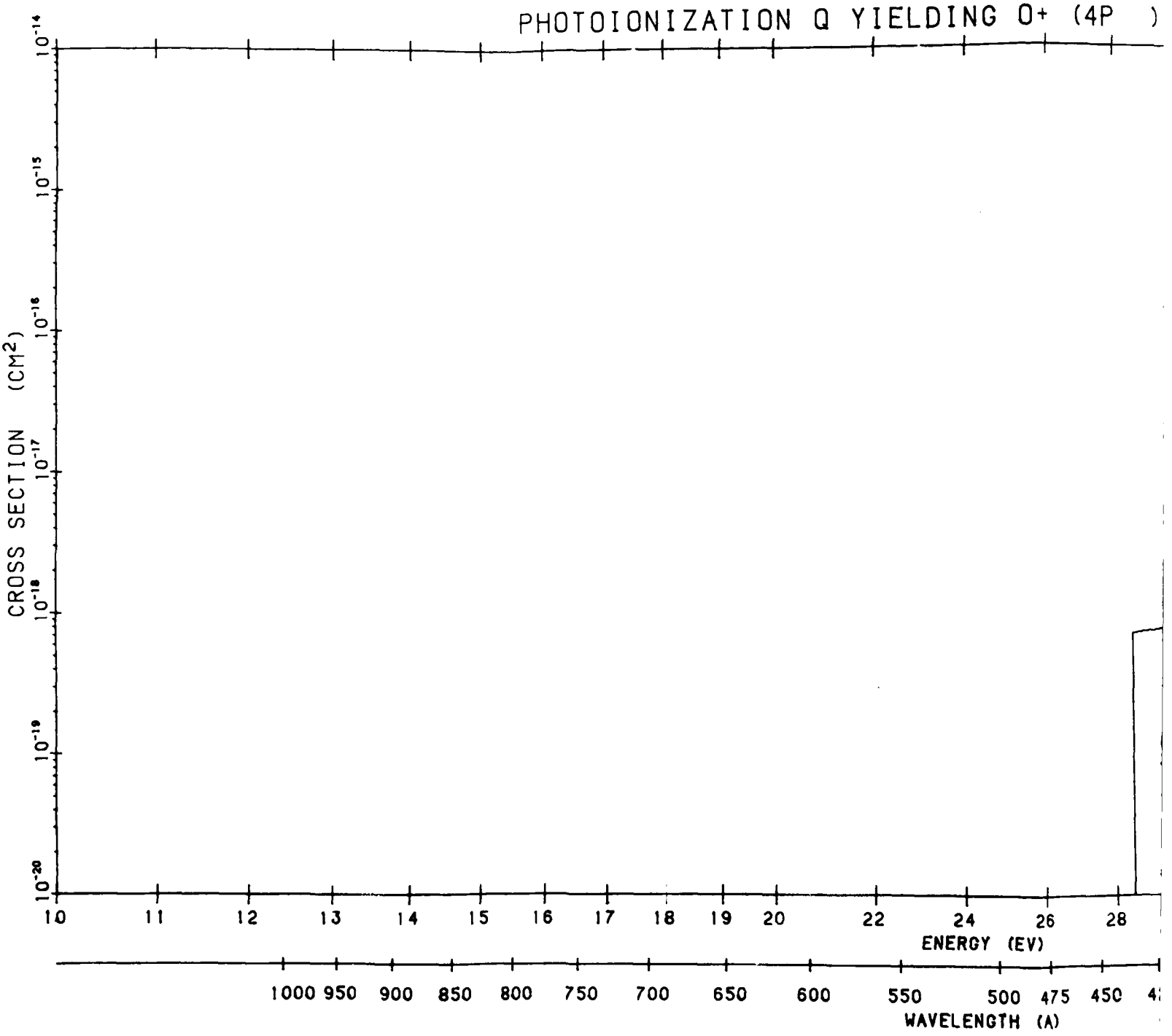
PHOTOIONIZATION Q YIELDING O+ (4P )
CROSS SECTION (CM2)
10-14
10-15
10-16
10-17
10-18
10-19
10-20
10 11 12 13 14 15 16 17 18 19 20 22 24 26 28
ENERGY (EV)
1000 950 900 850 800 750 700 650 600 550 500 475 450
WAVELENGTH (A)

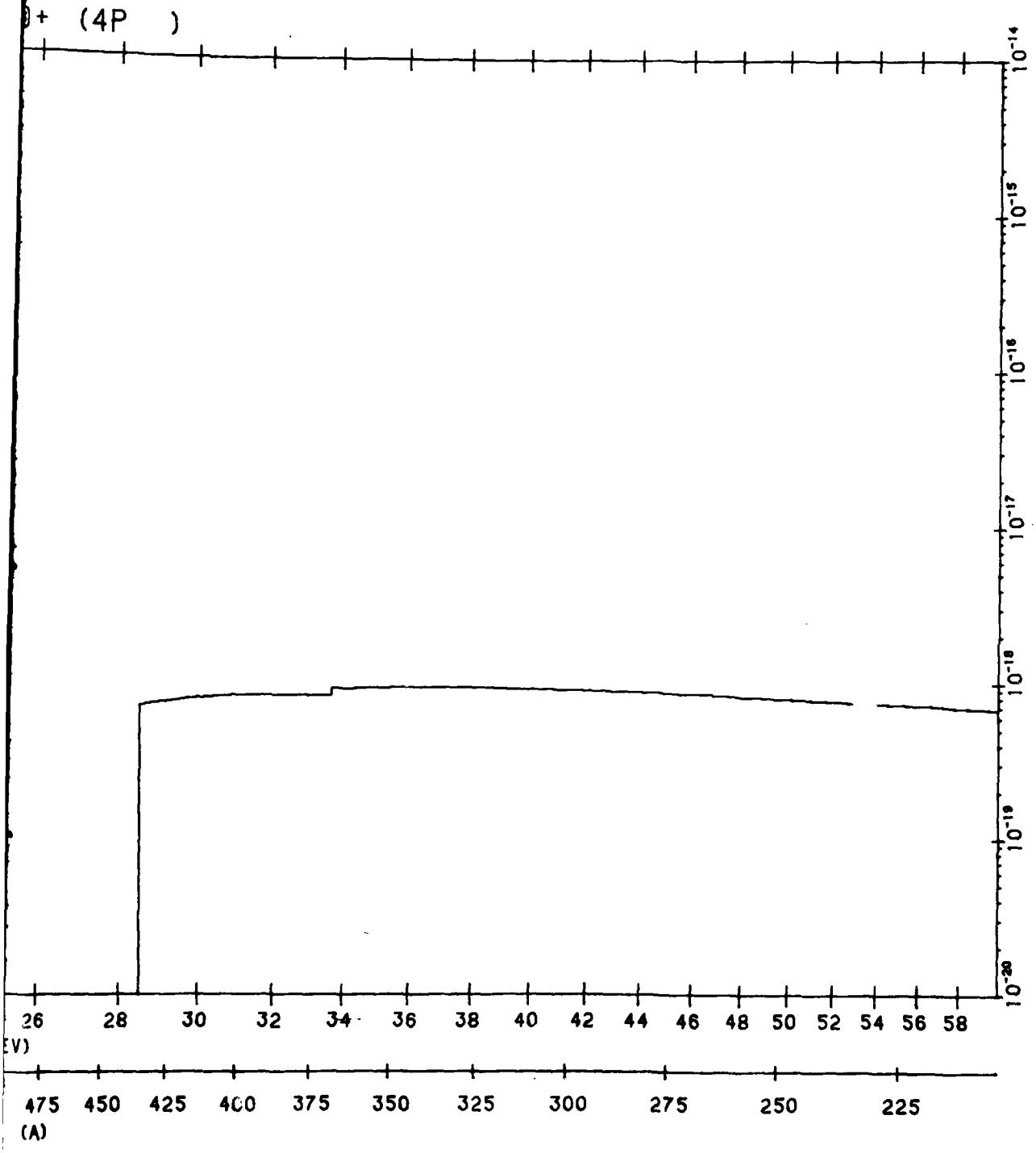


Figure B160. O Photoionization Cross Section to $^4P^e$. The data source is the same as that of Figure B157

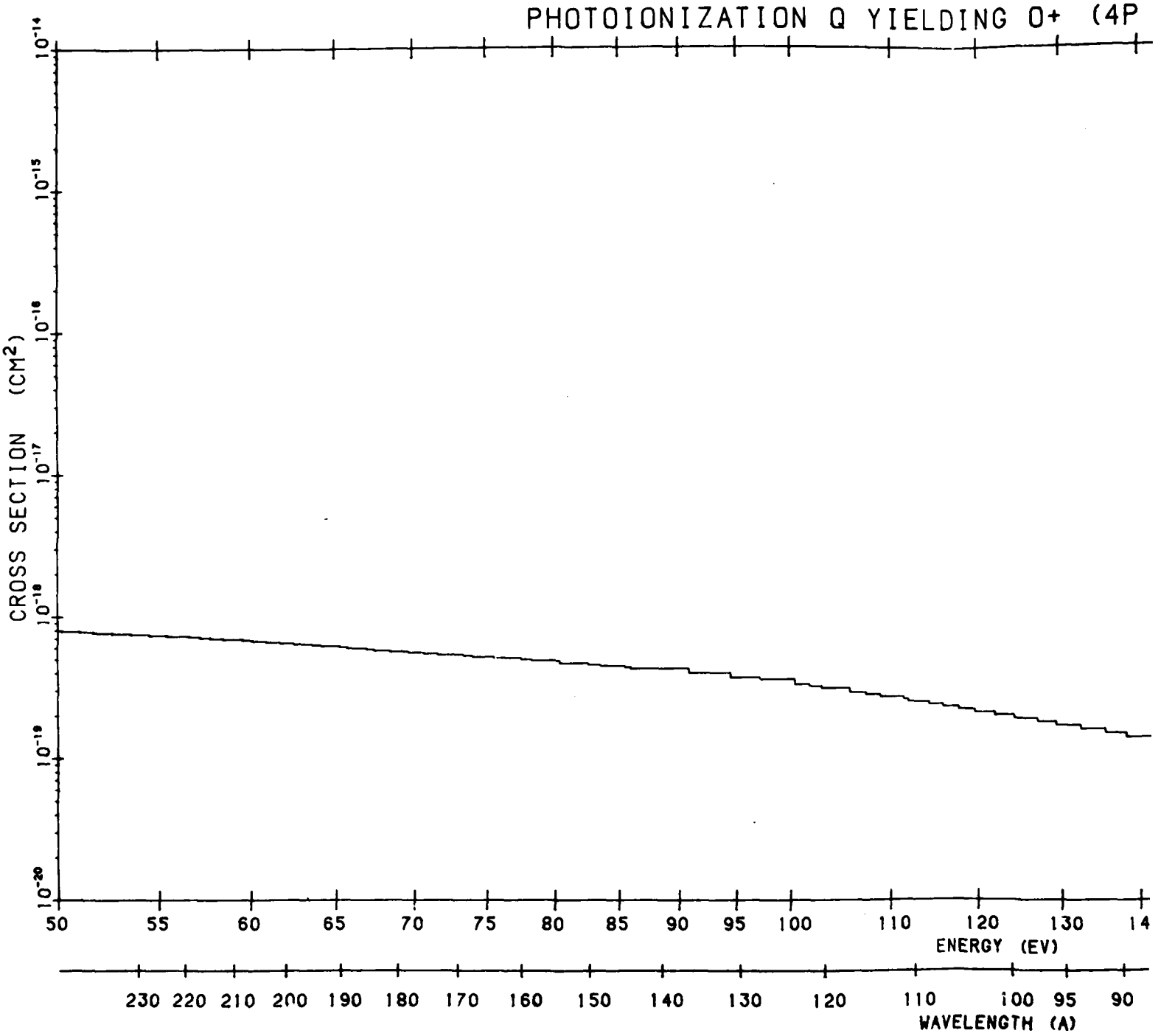
PHOTOIONIZATION Q YIELDING O+ (4P
CROSS SECTION (CM2)
10-14
10-15
10-16
10-17
10-18
10-19
10-20
50 55 60 65 70 75 80 85 90 95 100 110 120 130 14
ENERGY (EV)
230 220 210 200 190 180 170 160 150 140 130 120 110 100 95 90
WAVELENGTH (A)

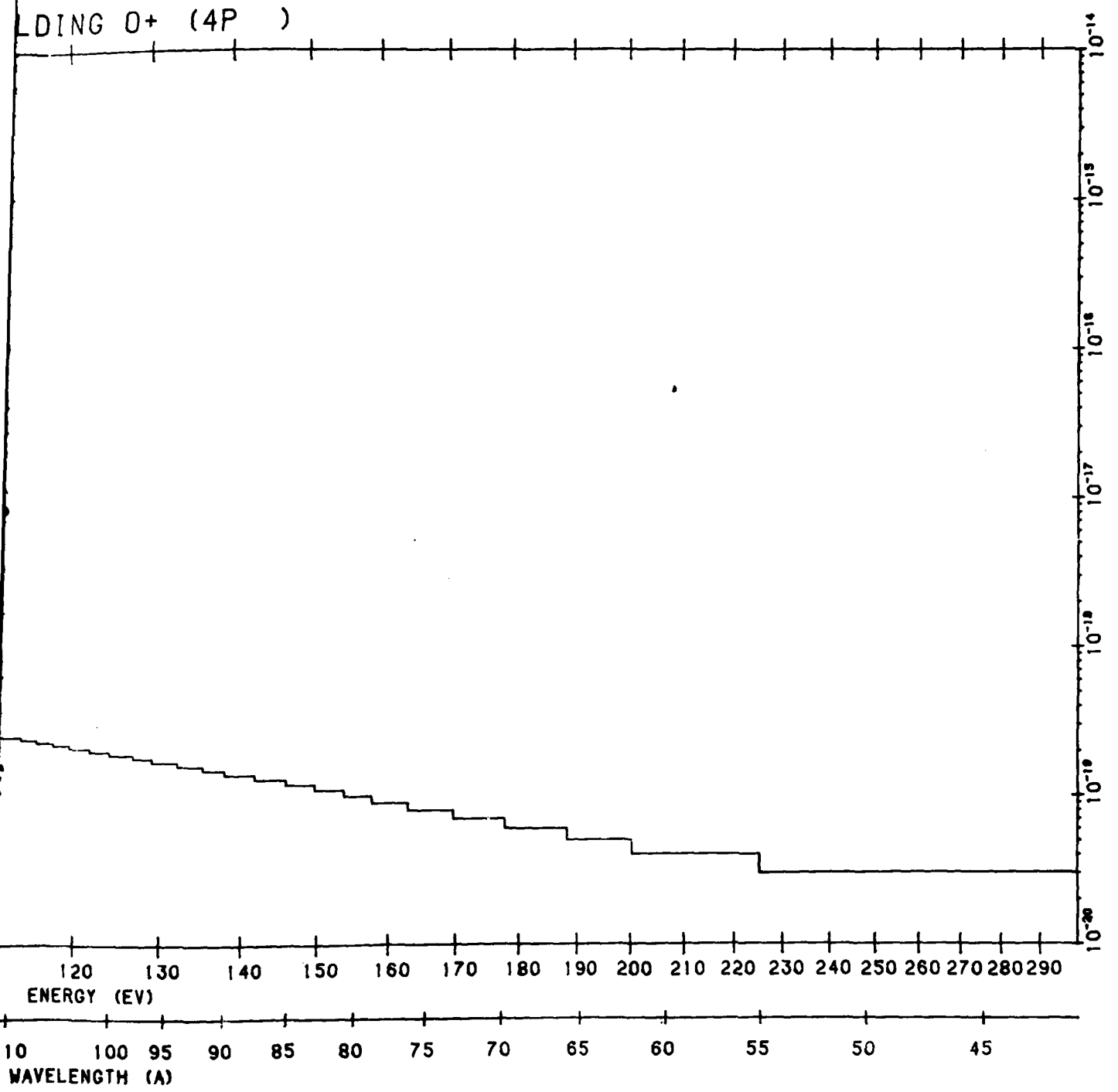


Figure B160. O Photoionization Cross Section to $^4P^e$. The data source is the same as that of Figure B157 (Cont.)

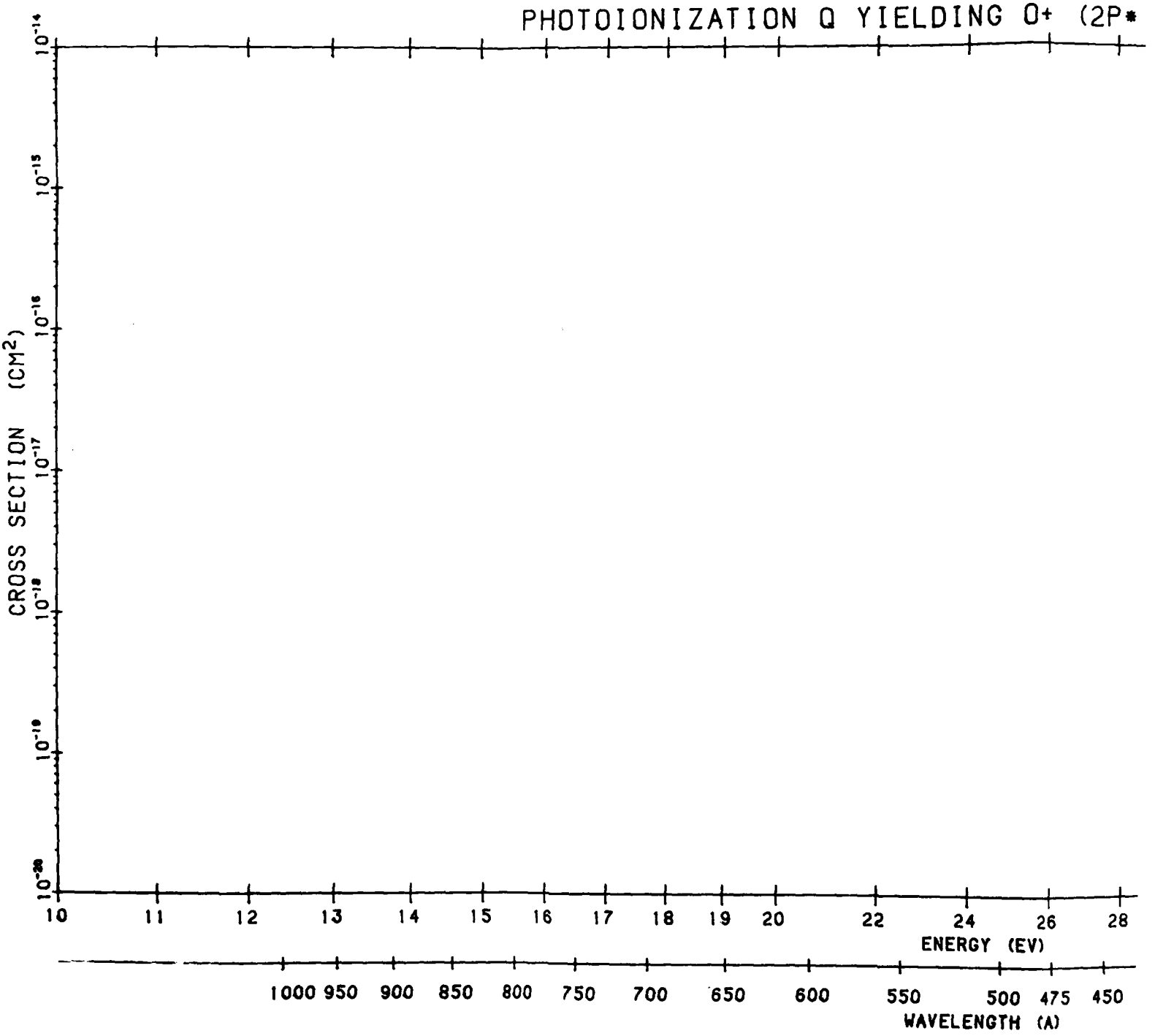
PHOTOIONIZATION Q YIELDING O+ (2P*
CROSS SECTION (CM2)
10-14
10-15
10-16
10-17
10-18
10-19
10-20
10 11 12 13 14 15 16 17 18 19 20 22 24 26 28
ENERGY (EV)
1000 950 900 850 800 750 700 650 600 550 500 475 450
WAVELENGTH (A)

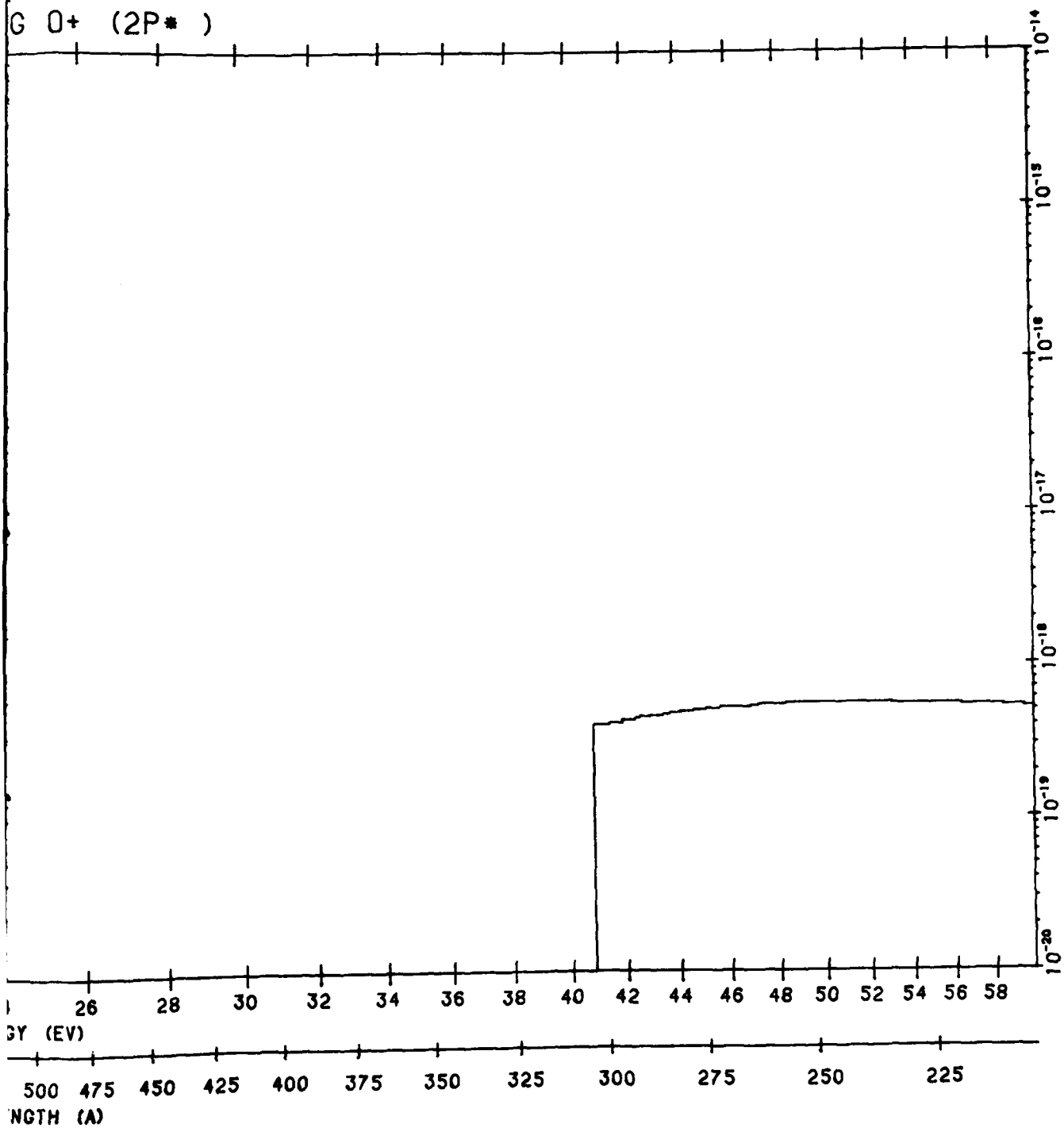


Figure B161. O Photoionization Cross Section to $^2P^e$. The data source is the same as that of Figure B157

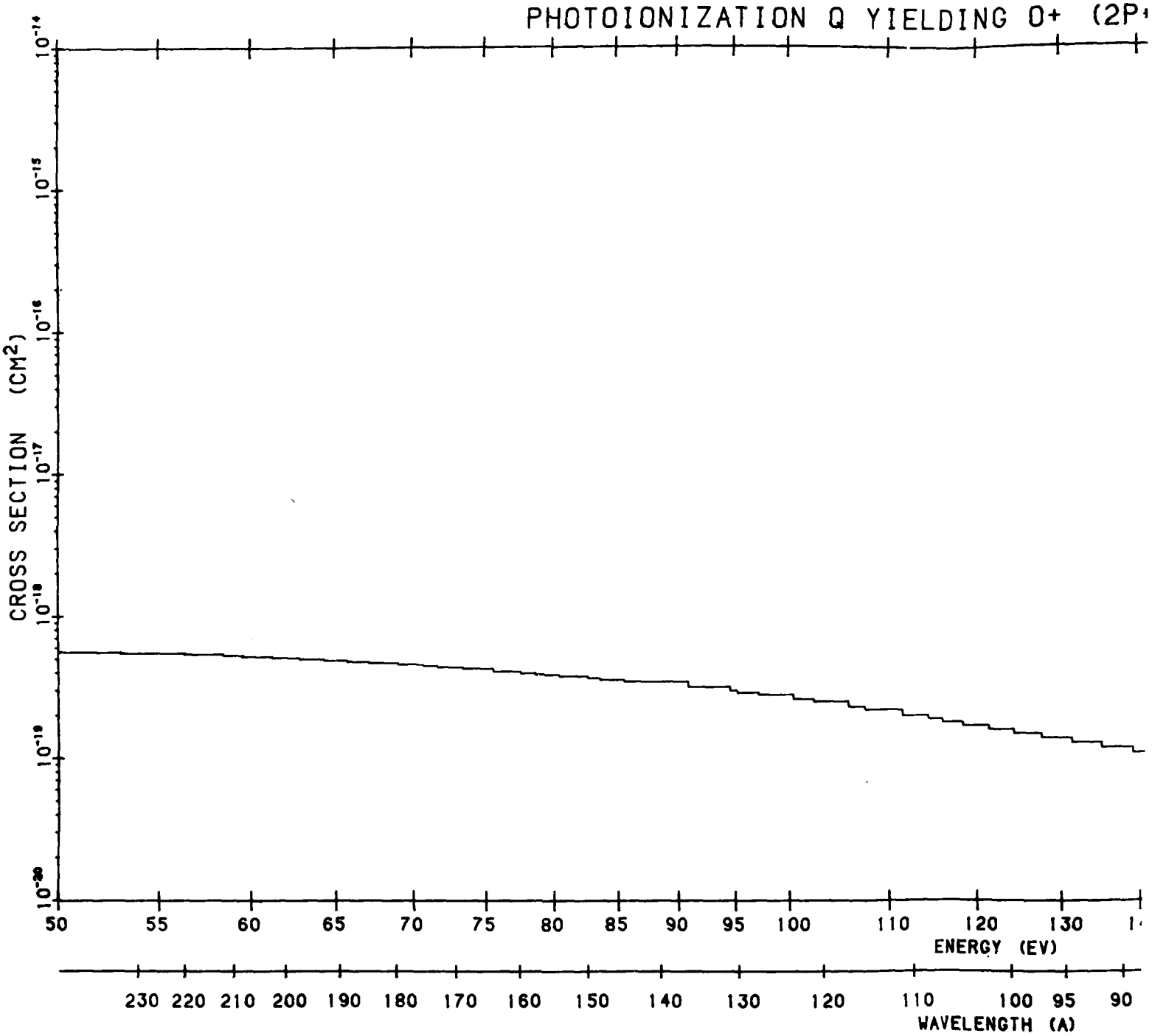
PHOTOIONIZATION Q YIELDING O+ (2P
CROSS SECTION (CM2)
10-14
10-15
10-16
10-17
10-18
10-19
10-20
50 55 60 65 70 75 80 85 90 95 100 110 120 130
ENERGY (EV)
230 220 210 200 190 180 170 160 150 140 130 120 110 100 95 90
WAVELENGTH (A)

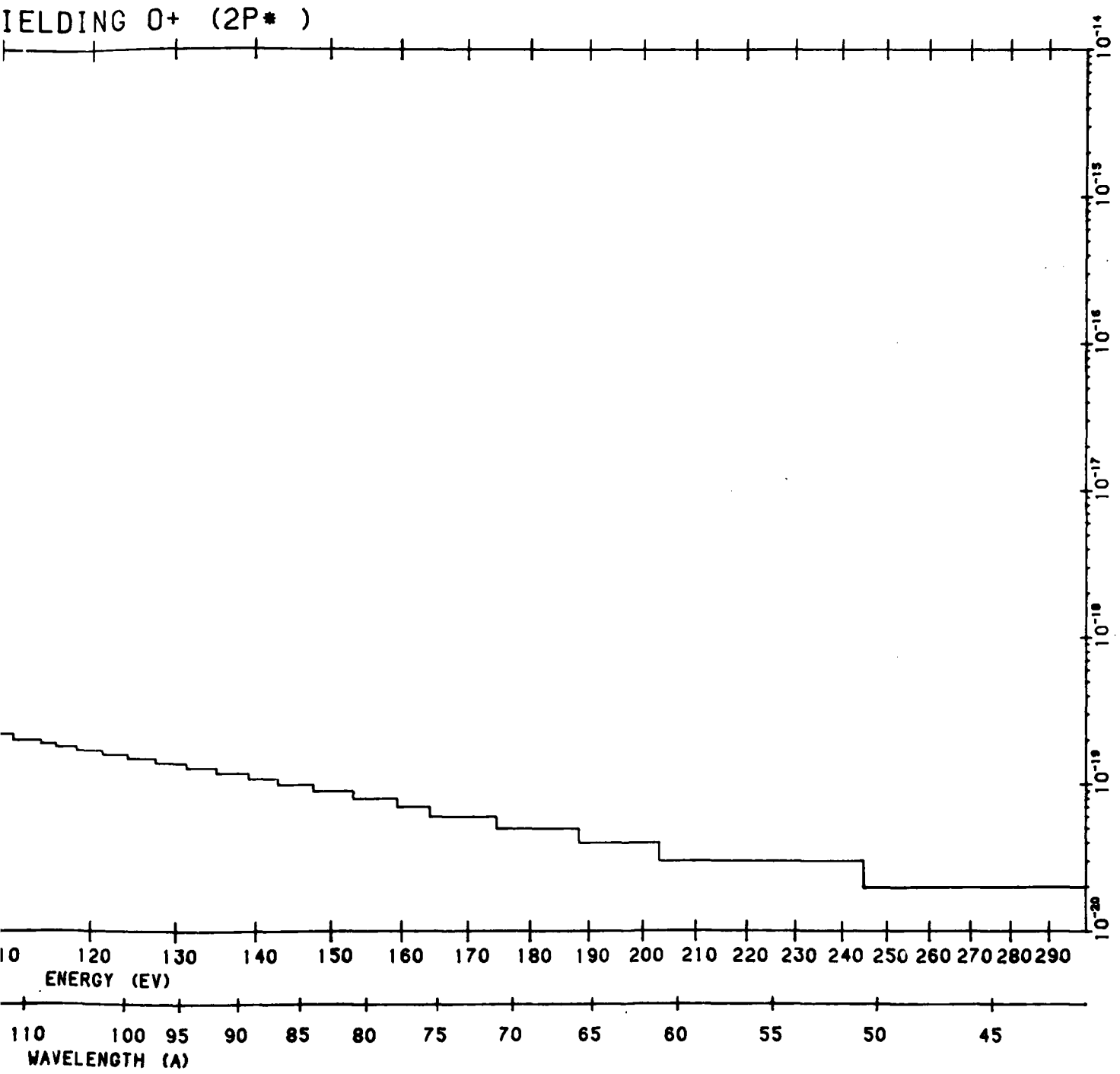


Figure B161. O Photoionization Cross Section to $^2P^e$. The data source is the same as that of Figure B157 (Cont.)

2

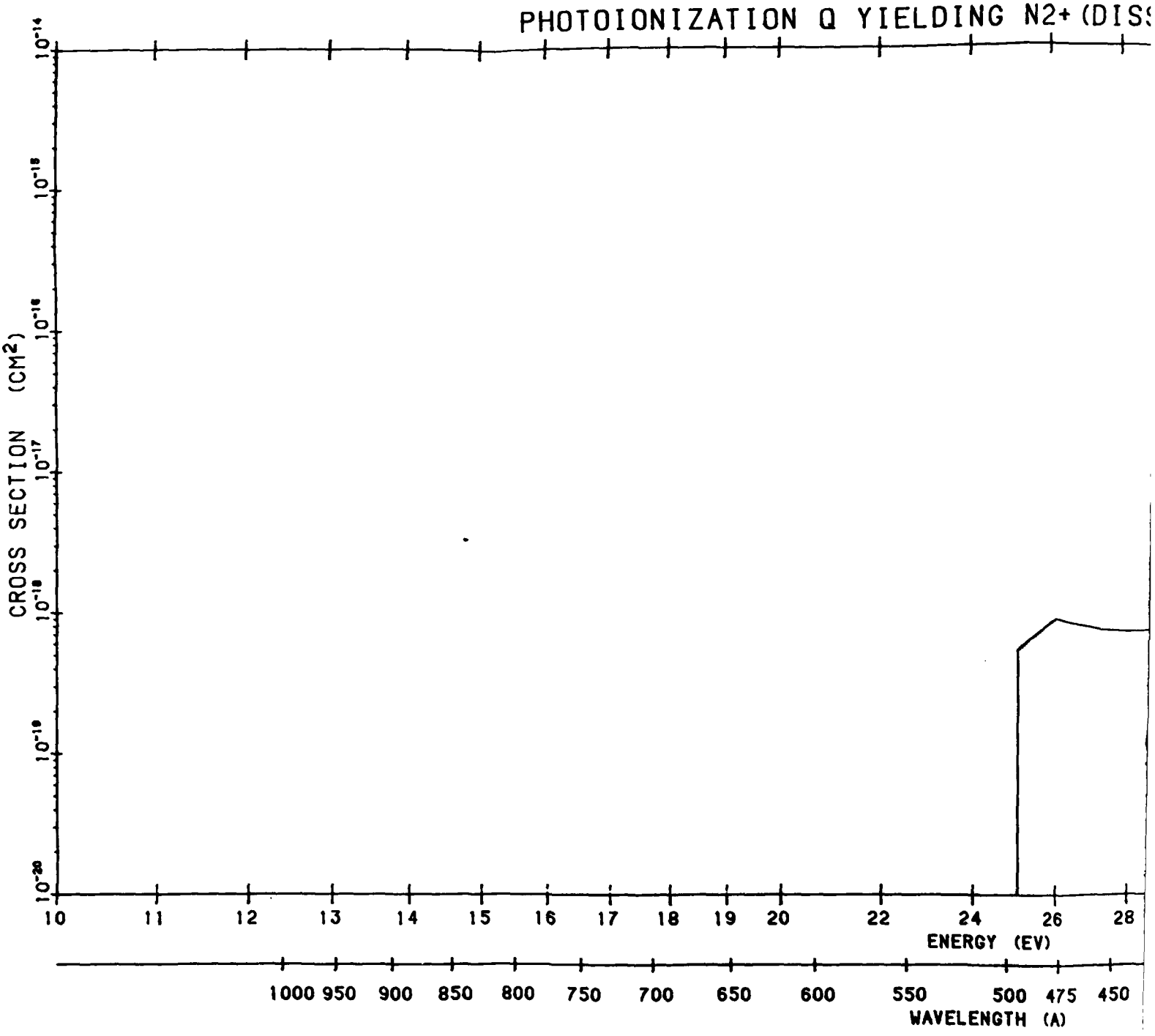
PHOTOIONIZATION Q YIELDING N2+ (DISS
CROSS SECTION (CM2)
10-14
10-15
10-16
10-17
10-18
10-19
10-20
10 11 12 13 14 15 16 17 18 19 20 22 24 26 28
ENERGY (EV)
1000 950 900 850 800 750 700 650 600 550 500 475 450
WAVELENGTH (A)

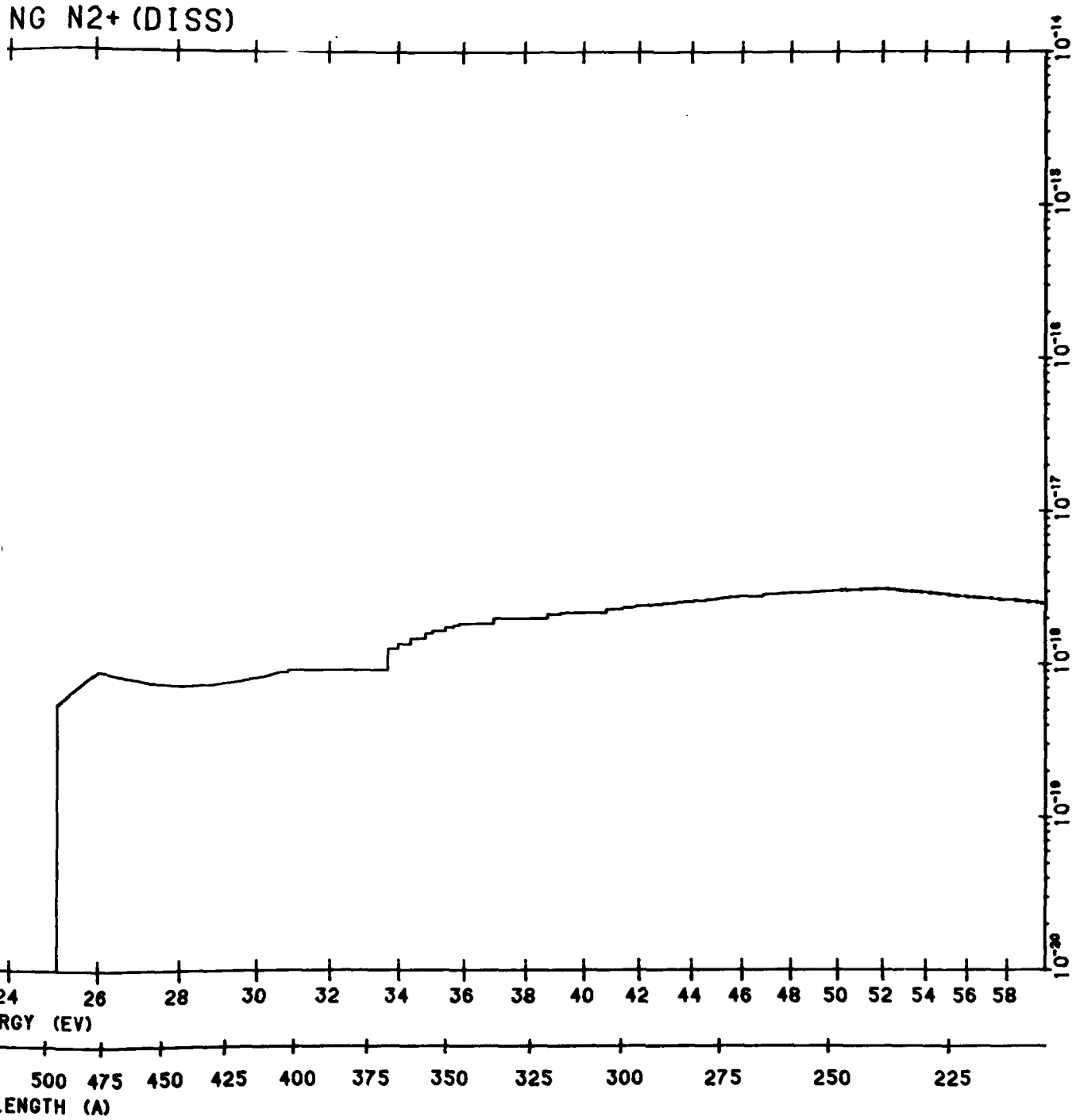


Figure B162. $N_2$ Dissociative Photoionization Cross Section. The data source is the same as that of Figure B157

2

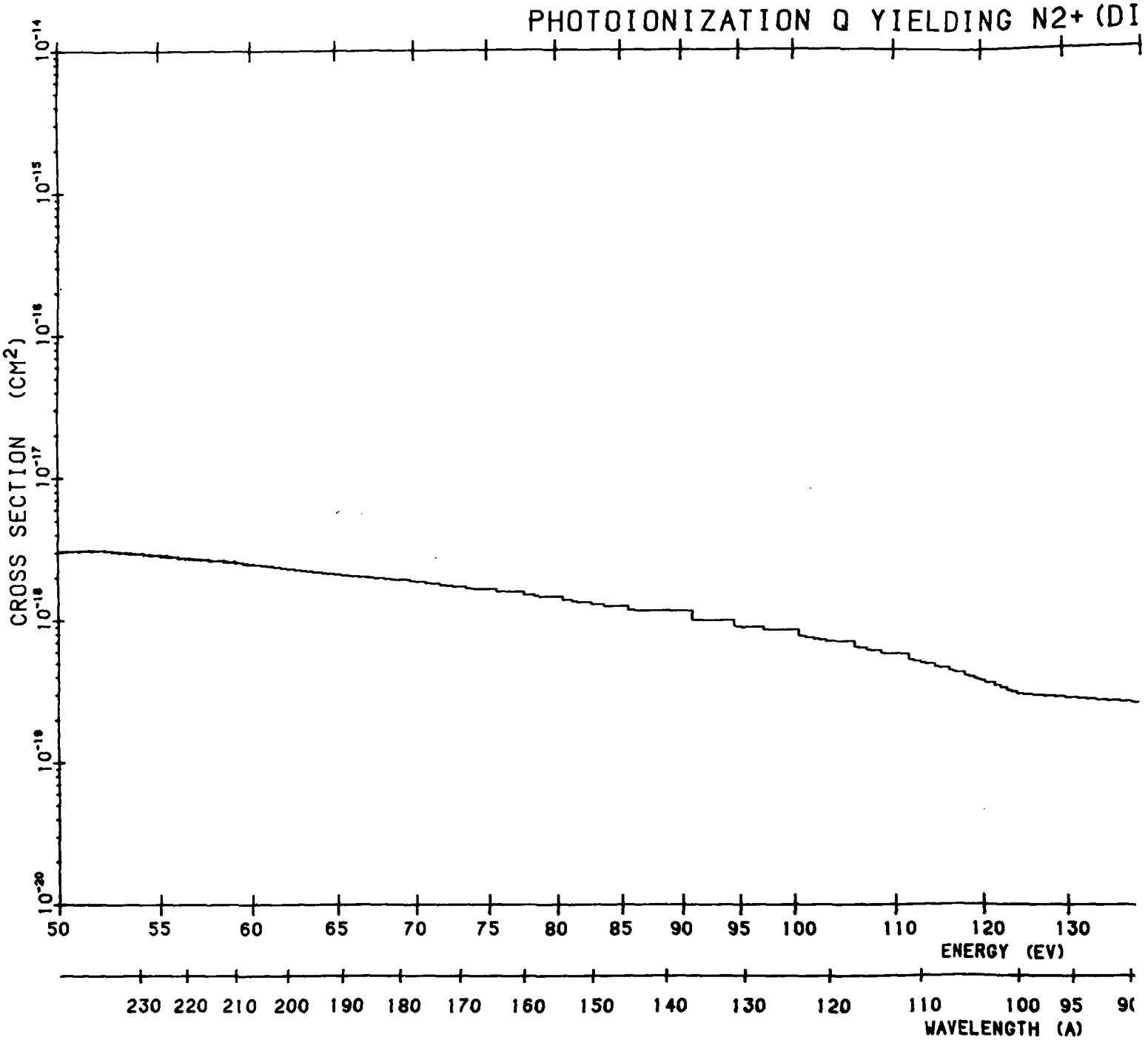
PHOTOIONIZATION Q YIELDING N2+ (DI
CROSS SECTION (CM2)
10-14
10-15
10-16
10-17
10-18
10-19
10-20
50 55 60 65 70 75 80 85 90 95 100 110 120 130
ENERGY (EV)
230 220 210 200 190 180 170 160 150 140 130 120 110 100 95 90
WAVELENGTH (A)

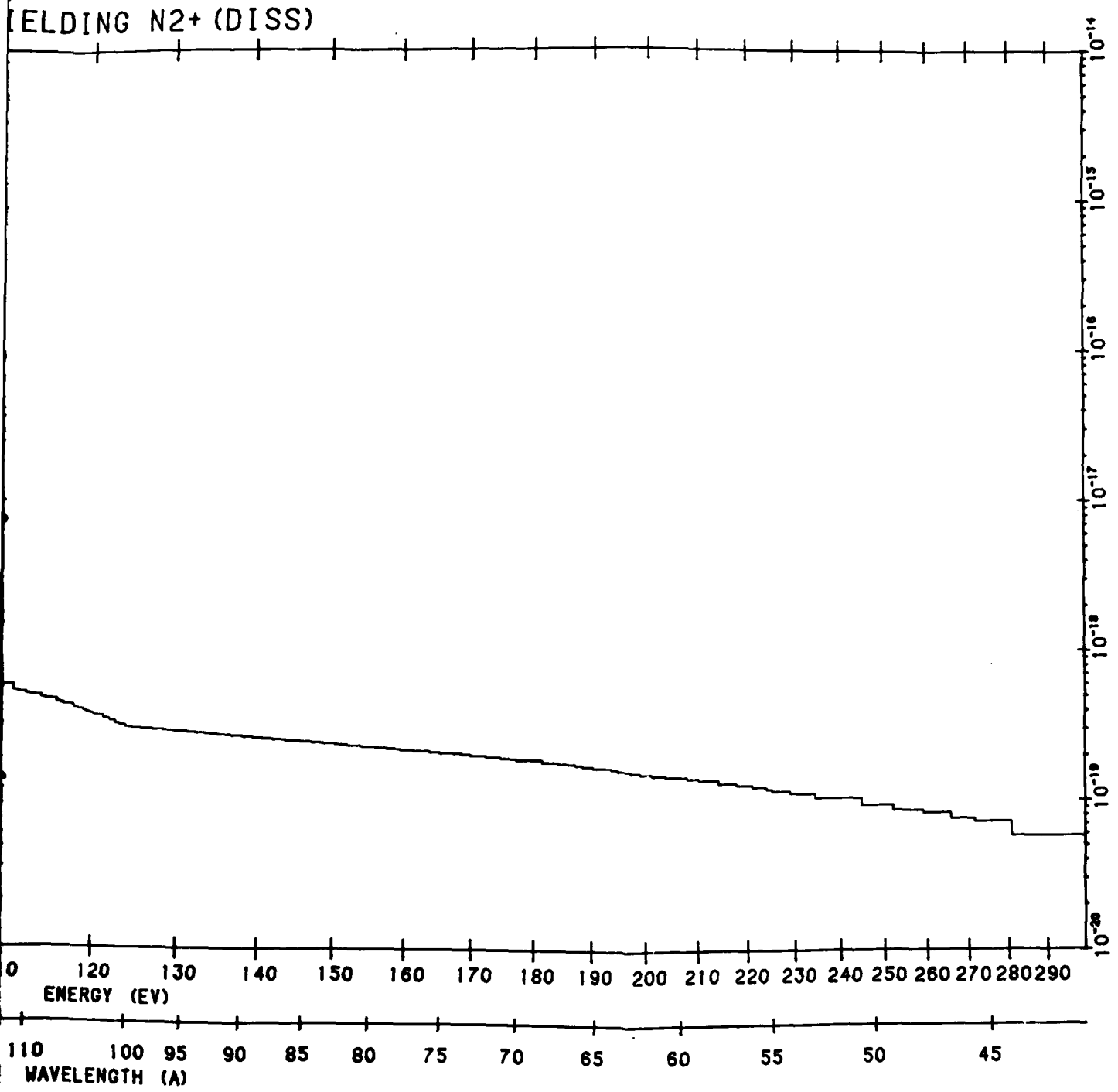


Figure B162. $N_2$ Dissociative Photoionization Cross Section. The data source is the same as that of Figure B157 (Cont.)

2

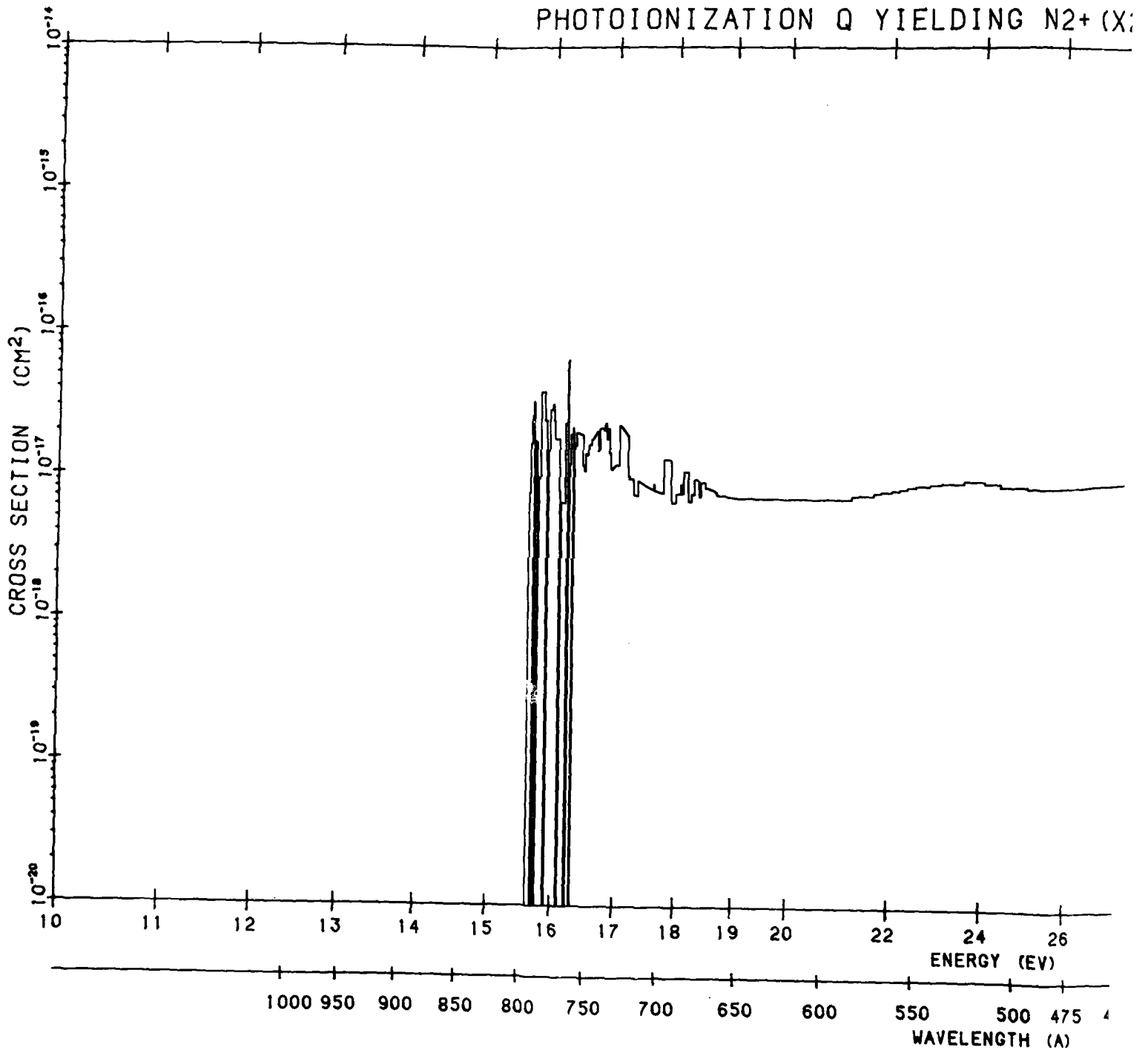
PHOTOIONIZATION Q YIELDING N2+ (X
CROSS SECTION (CM2)
10-14
10-15
10-16
10-17
10-18
10-19
10-20
10 11 12 13 14 15 16 17 18 19 20 22 24 26
ENERGY (EV)
1000 950 900 850 800 750 700 650 600 550 500 475
WAVELENGTH (A)

AD-A118 921 BEDFORD RESEARCH ASSOCIATES MA F/G 4/1
LOW ENERGY ELECTRON AND PHOTON CROSS SECTIONS FOR O, N2, AND O2--ETC(U)
JAN 82 H T WADZINSKI, J R JASPERSE F19628-80-C-0216
UNCLASSIFIED AFGL-TR-82-0008 NL

4 of 4

END
DATE FILMED
10 82
DTIC

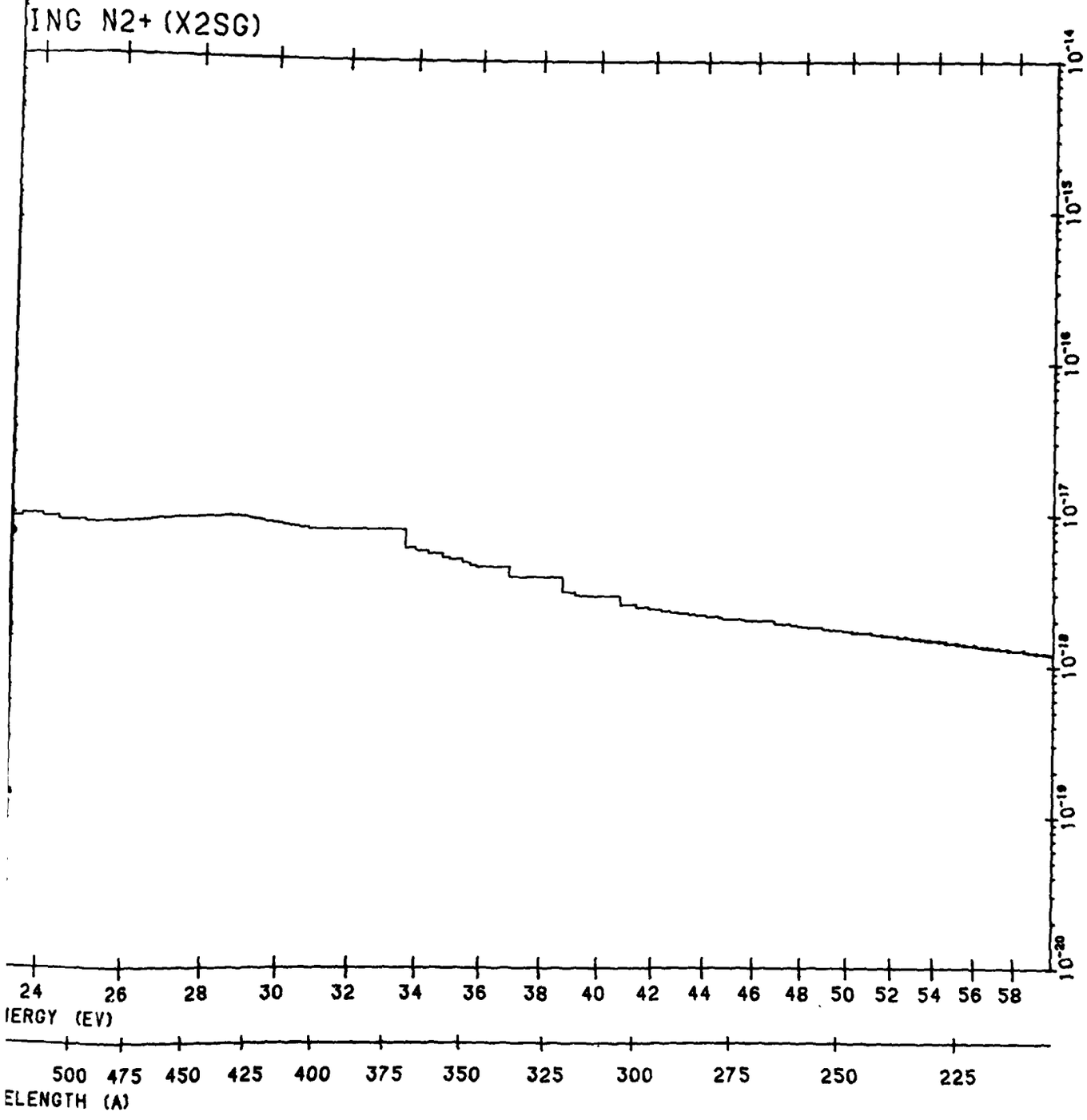


Figure B163. $N_2$ Photoionization Cross Section to $N_2^+ X\ ^2\Sigma_g^+$. The data source is the same as that of Figure B157

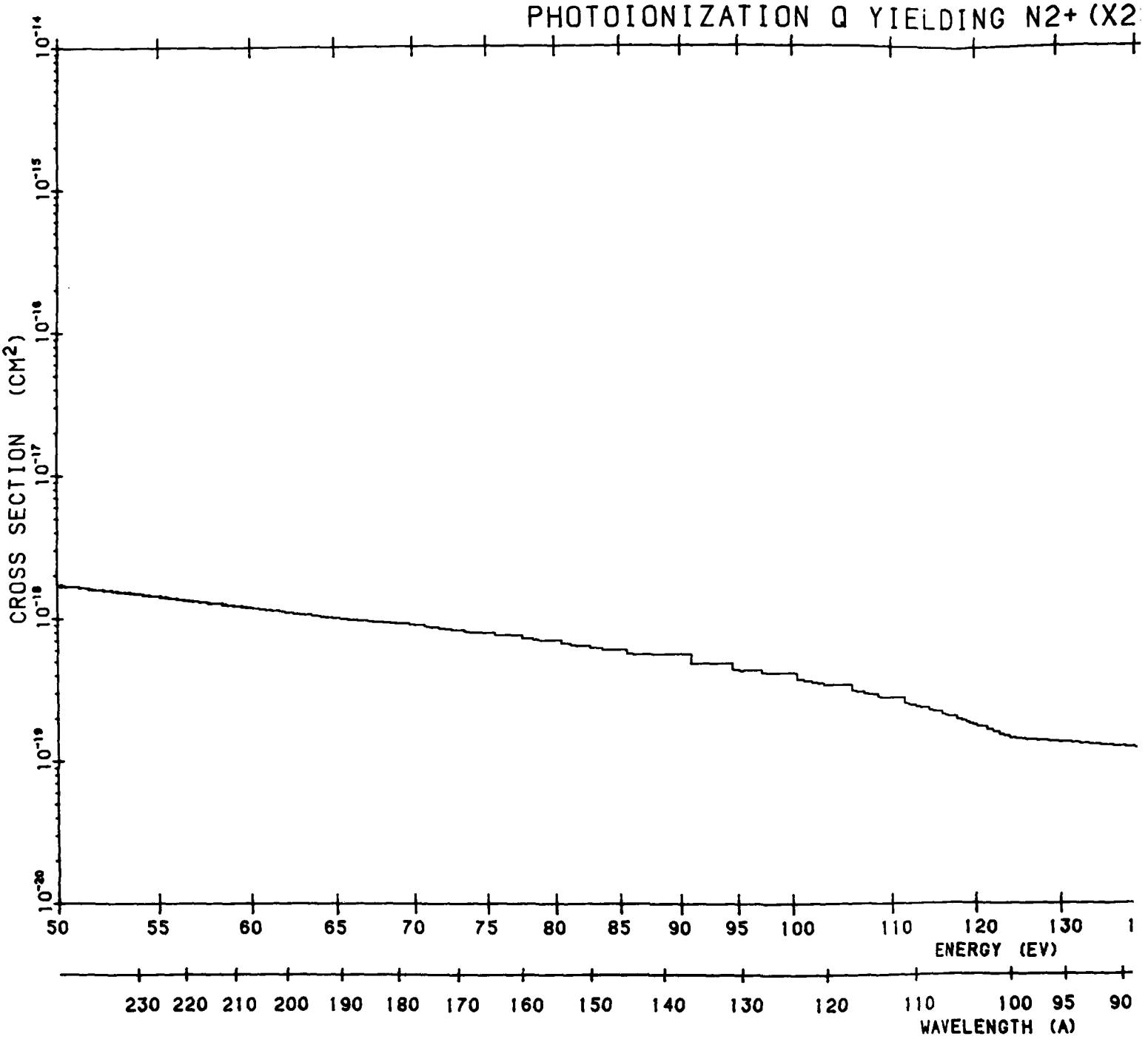
PHOTOIONIZATION Q YIELDING N2+ (X2
CROSS SECTION (CM2)
10-14
10-15
10-16
10-17
10-18
10-19
10-20
50 55 60 65 70 75 80 85 90 95 100 110 120 130
ENERGY (EV)
230 220 210 200 190 180 170 160 150 140 130 120 110 100 95 90
WAVELENGTH (A)

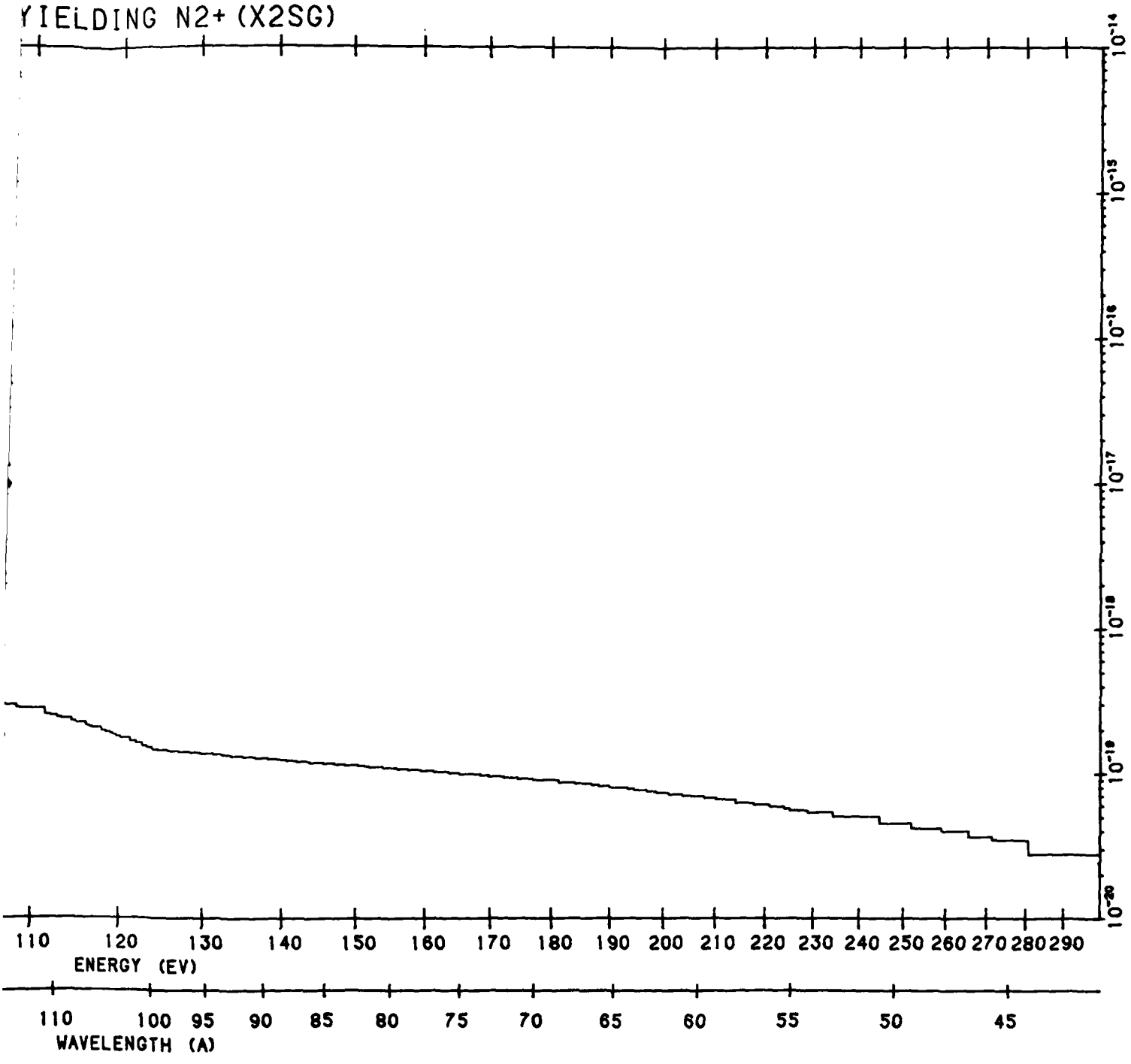


Figure B163. $N_2$ Photoionization Cross Section to $N_2^+ X\ ^2\Sigma_g^+$. The data source is the same as that of Figure B157 (Cont.)

2

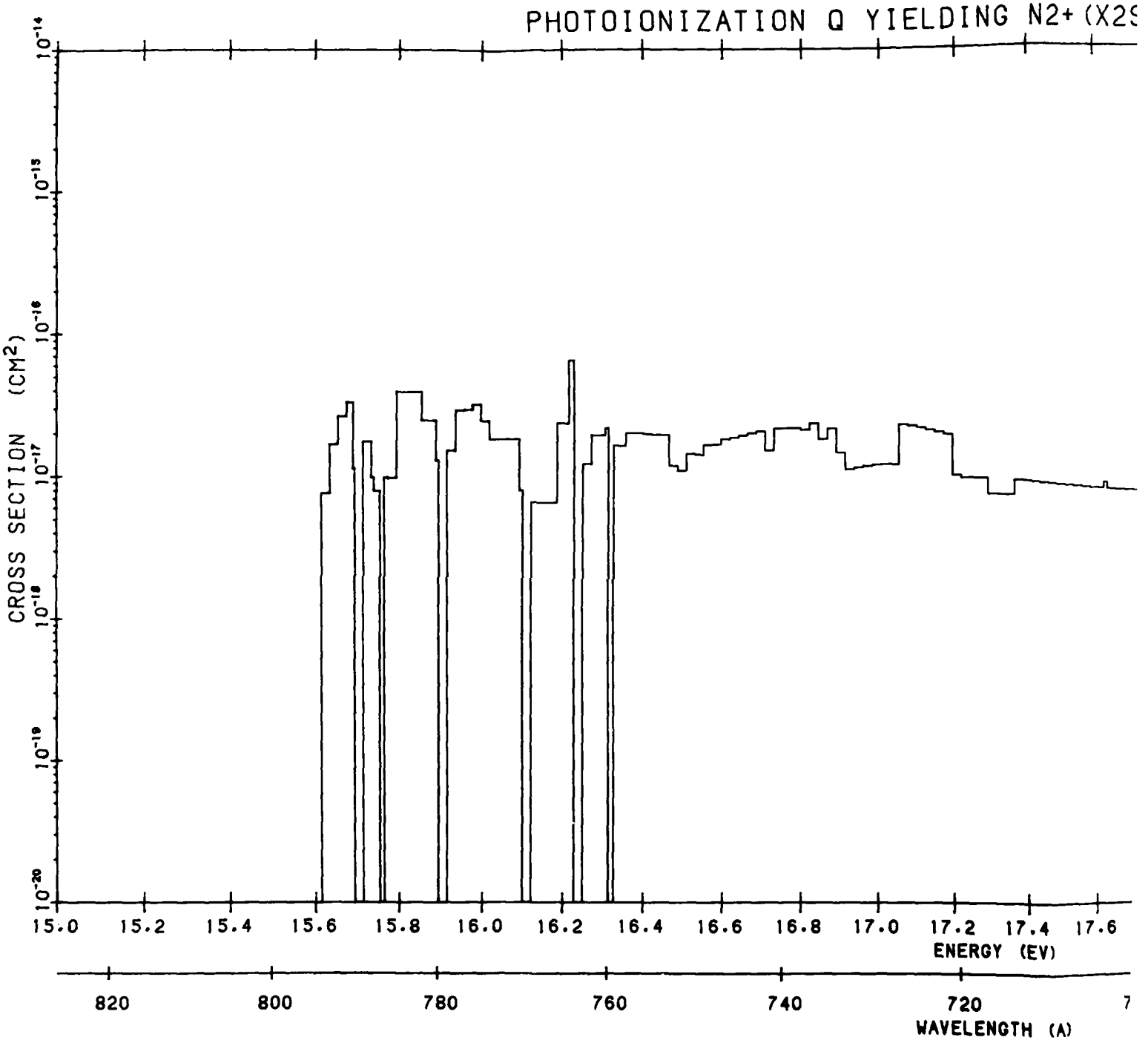
PHOTOIONIZATION Q YIELDING N2+ (X2S
CROSS SECTION (CM2)
10-14
10-15
10-16
10-17
10-18
10-19
10-20
15.0
15.2
15.4
15.6
15.8
16.0
16.2
16.4
16.6
16.8
17.0
17.2
17.4
17.6
ENERGY (EV)
820
800
780
760
740
720
WAVELENGTH (A)

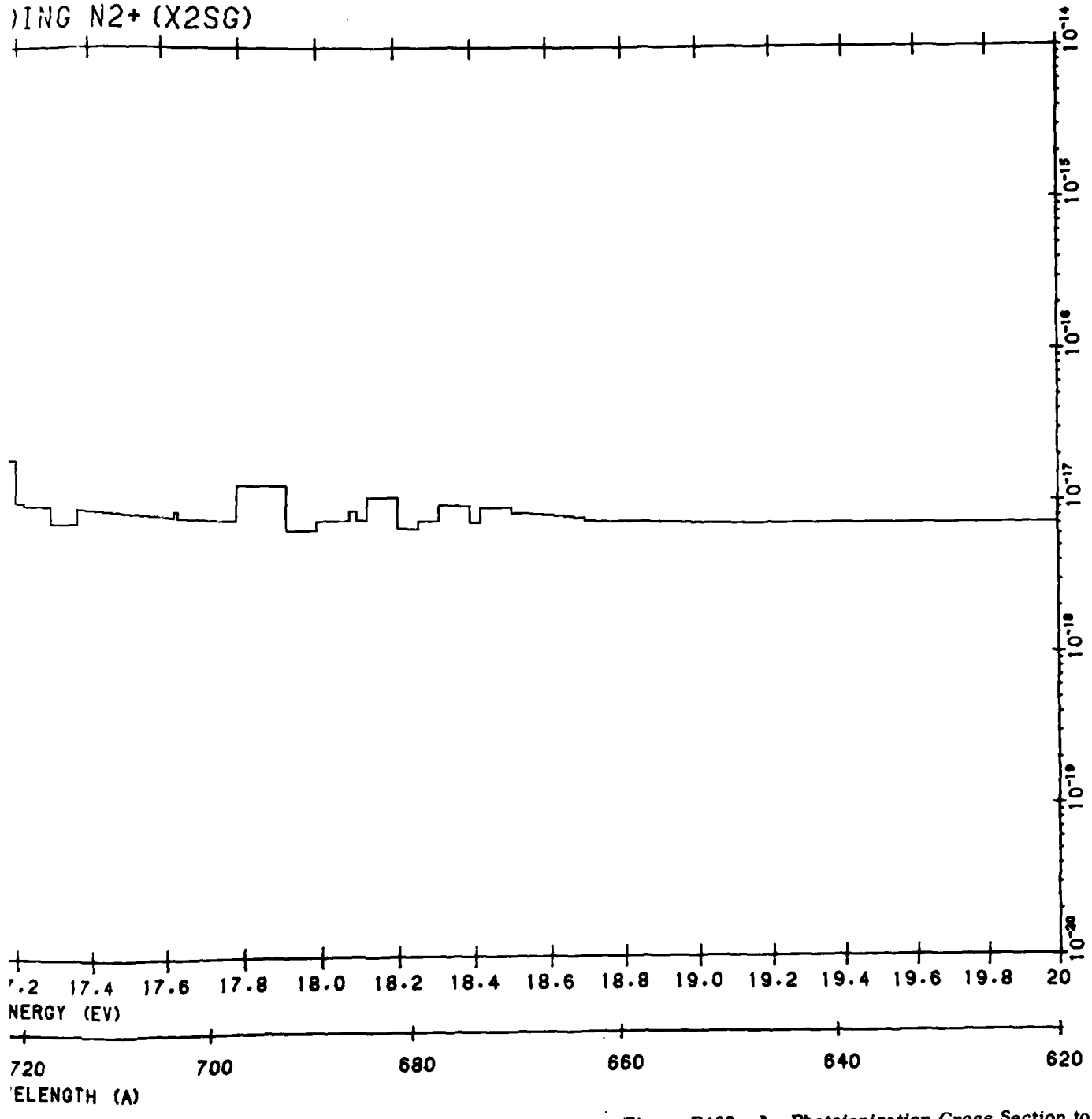


Figure B163. $N_2$ Photoionization Cross Section to $N_2^+ X\ ^2\Sigma_g^+$. The data source is the same as that of Figure B157 (Cont.)

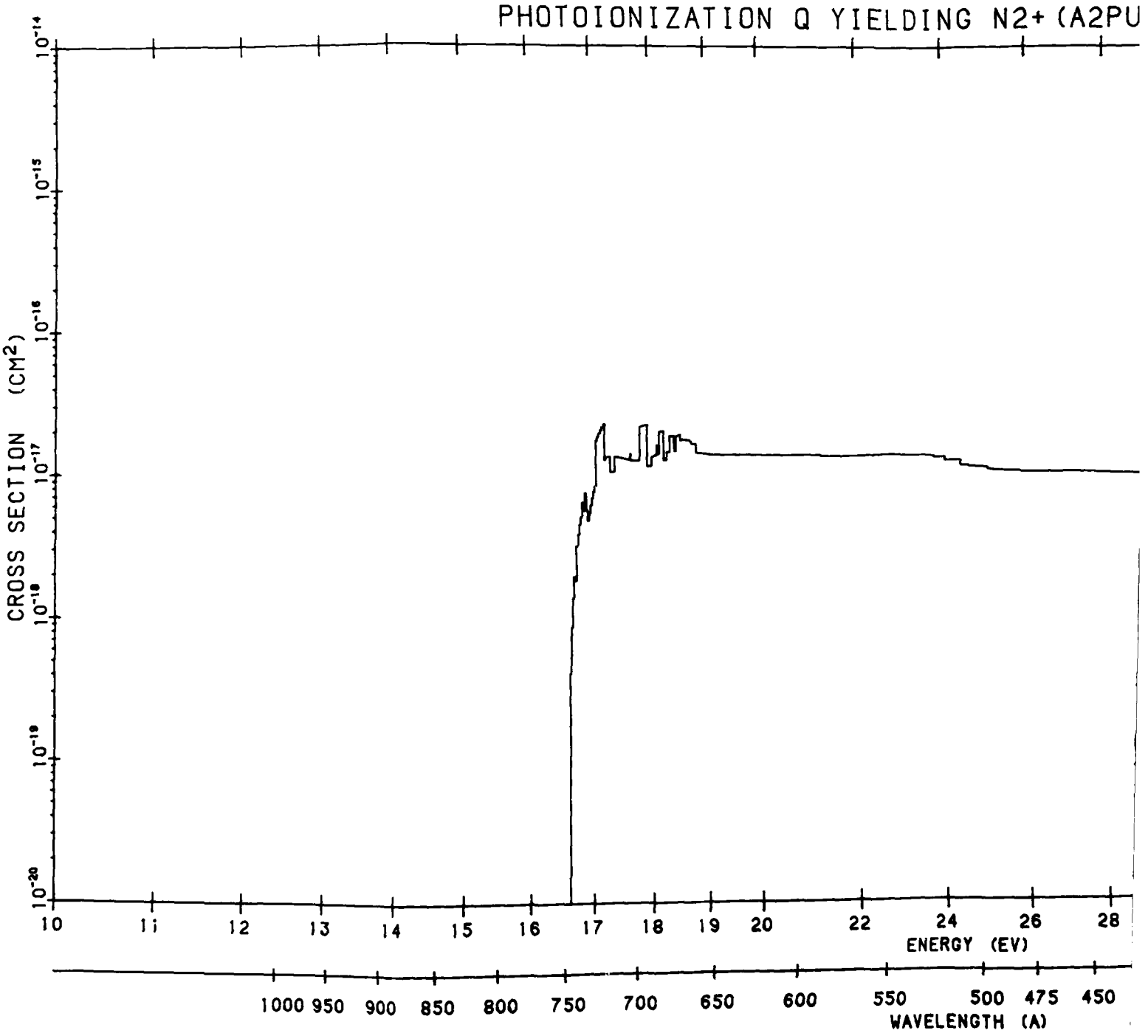
PHOTOIONIZATION Q YIELDING N2+ (A2PU
CROSS SECTION (CM2)
10^-14
10^-15
10^-16
10^-17
10^-18
10^-19
10^-20
10 11 12 13 14 15 16 17 18 19 20 22 24 26 28
ENERGY (EV)
1000 950 900 850 800 750 700 650 600 550 500 475 450
WAVELENGTH (A)

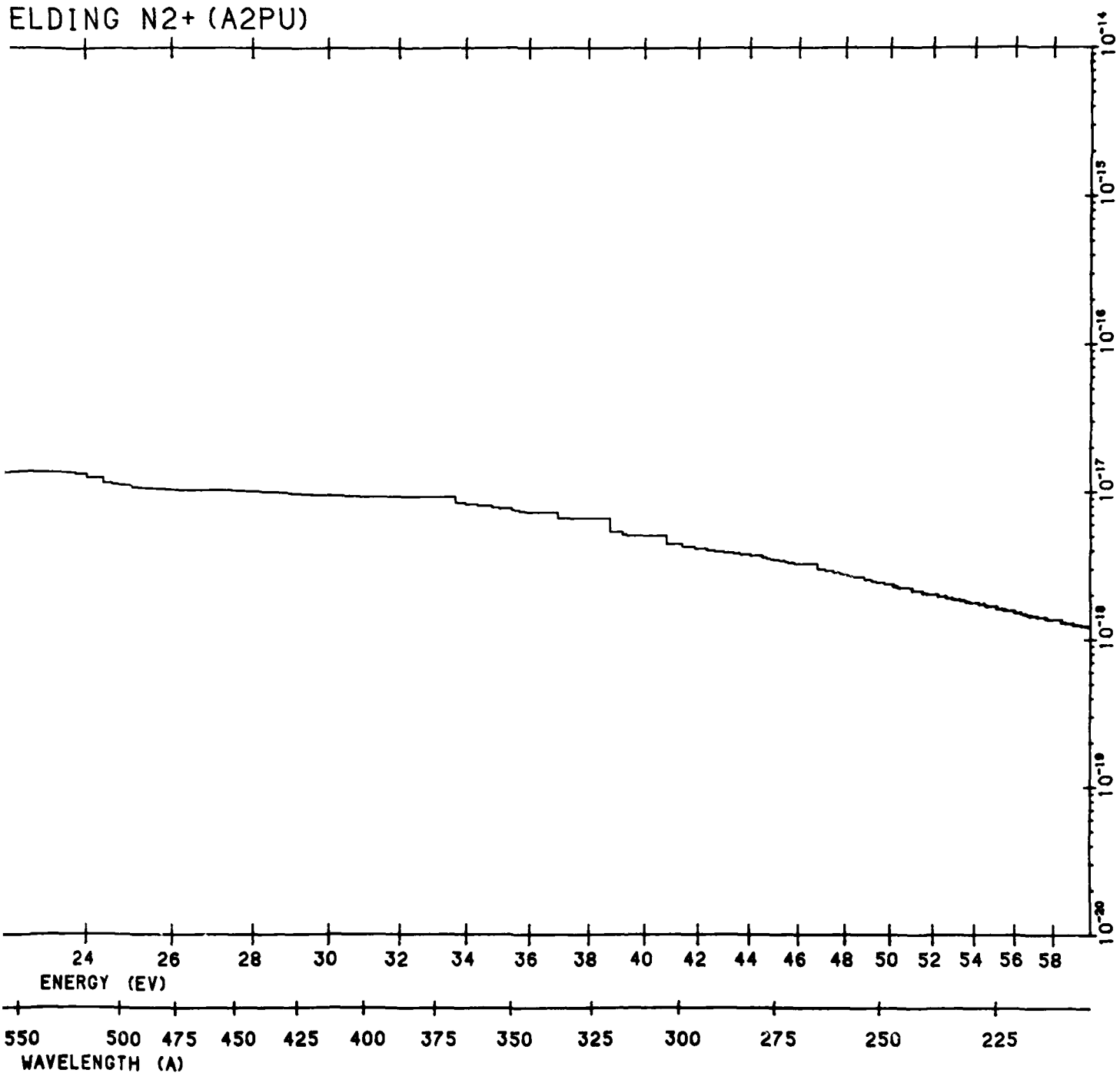


Figure B164. $N_2$ Photoionization Cross Section to A $^2\Pi_u$. The data source is the same as that of Figure B157

2

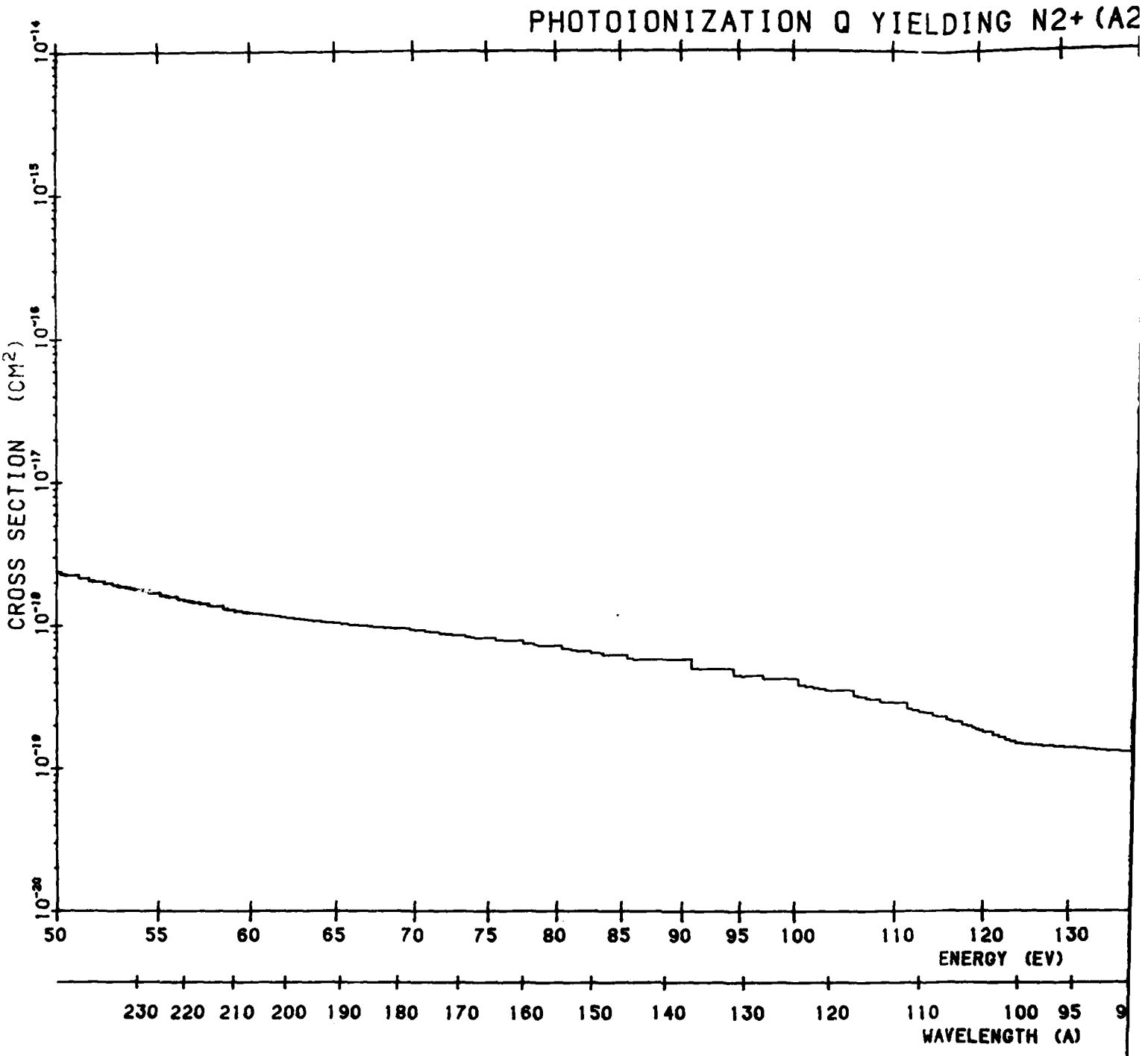
PHOTOIONIZATION Q YIELDING N2+ (A2
CROSS SECTION (CM2)
10-14
10-15
10-16
10-17
10-18
10-19
10-20
50 55 60 65 70 75 80 85 90 95 100 110 120 130
ENERGY (EV)
230 220 210 200 190 180 170 160 150 140 130 120 110 100 95 9
WAVELENGTH (A)

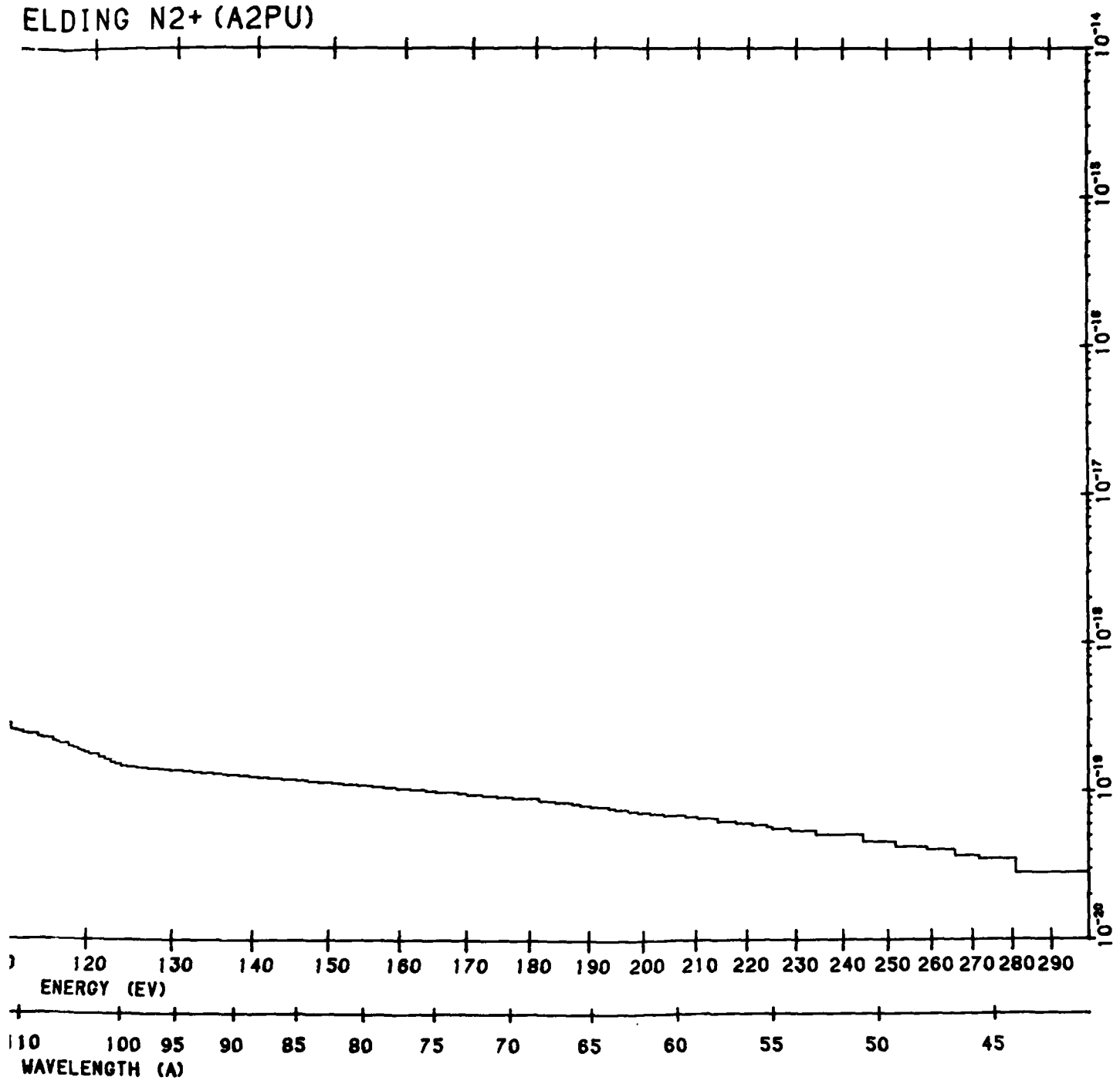


Figure B164. $N_2$ Photoionization Cross Section to A $^2\Pi_u$. The data source is the same as that of Figure B157 (Cont.)

2

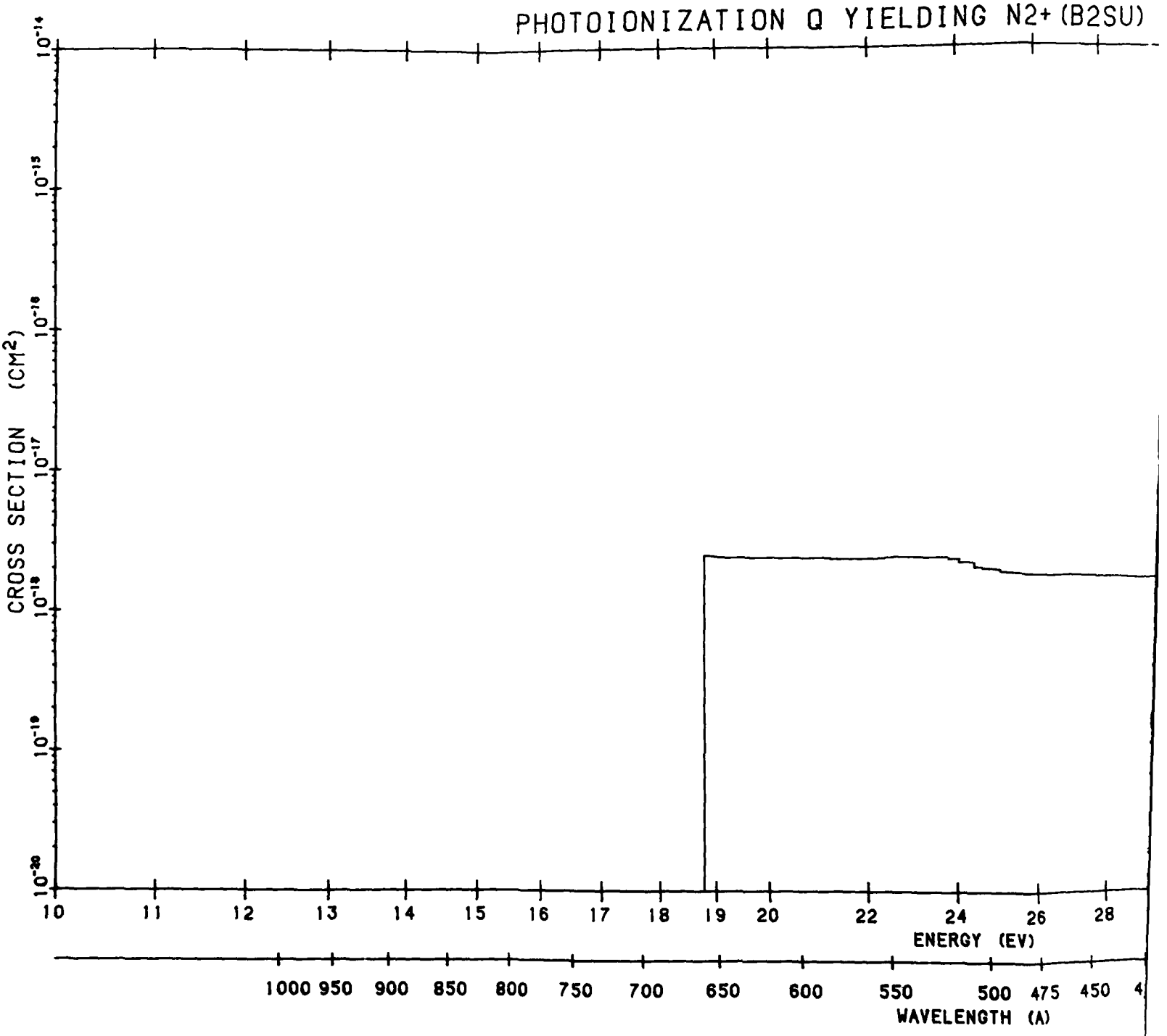
PHOTOIONIZATION Q YIELDING N2+ (B2SU)
CROSS SECTION (CM2)
10-14
10-15
10-16
10-17
10-18
10-19
10-20
10 11 12 13 14 15 16 17 18 19 20 22 24 26 28
ENERGY (EV)
1000 950 900 850 800 750 700 650 600 550 500 475 450
WAVELENGTH (A)

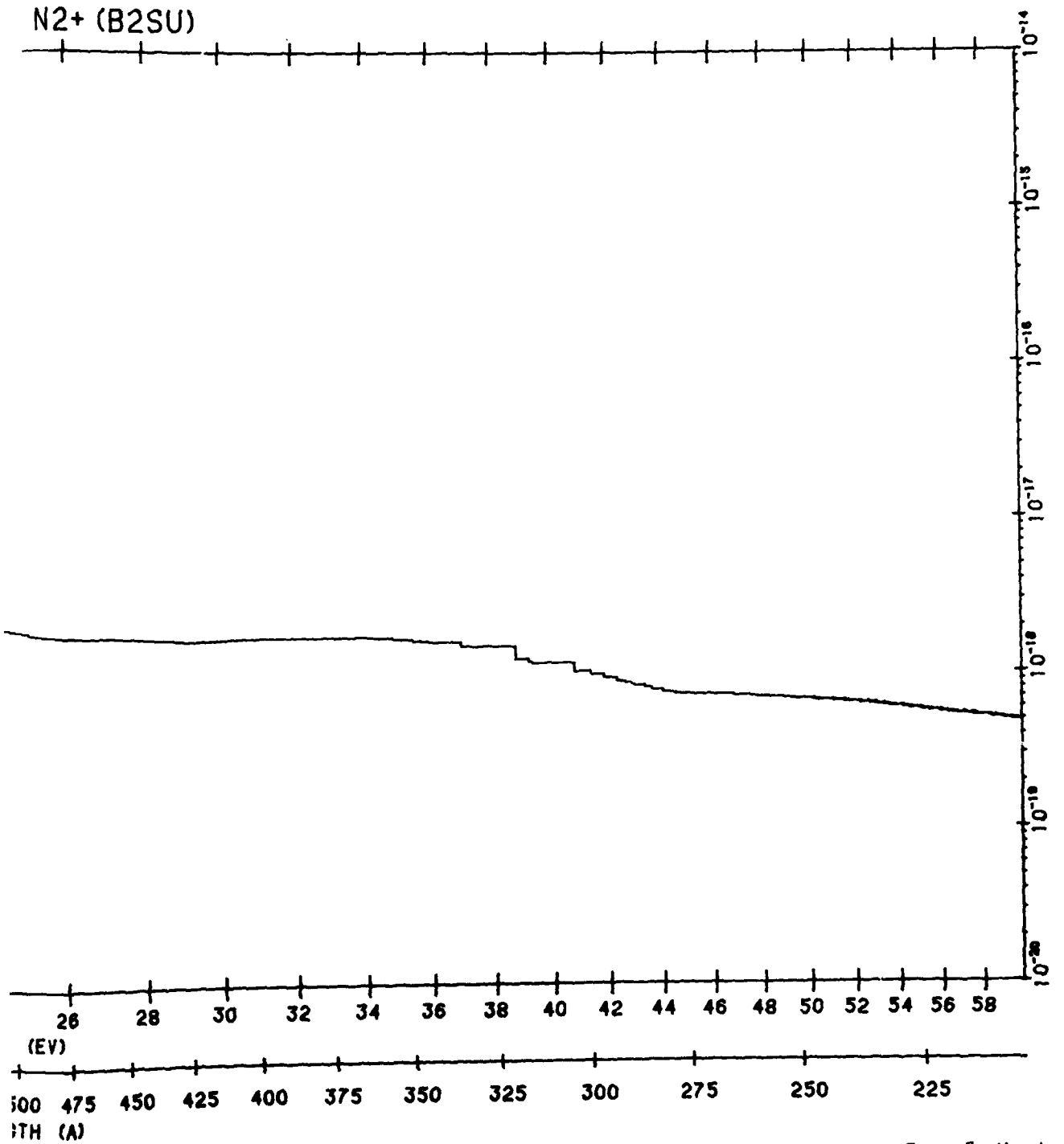


Figure B165. $N_2$ Photoionization Cross Section to B $^2\Sigma_u^+$. The data source is the same as that of Figure B157

2

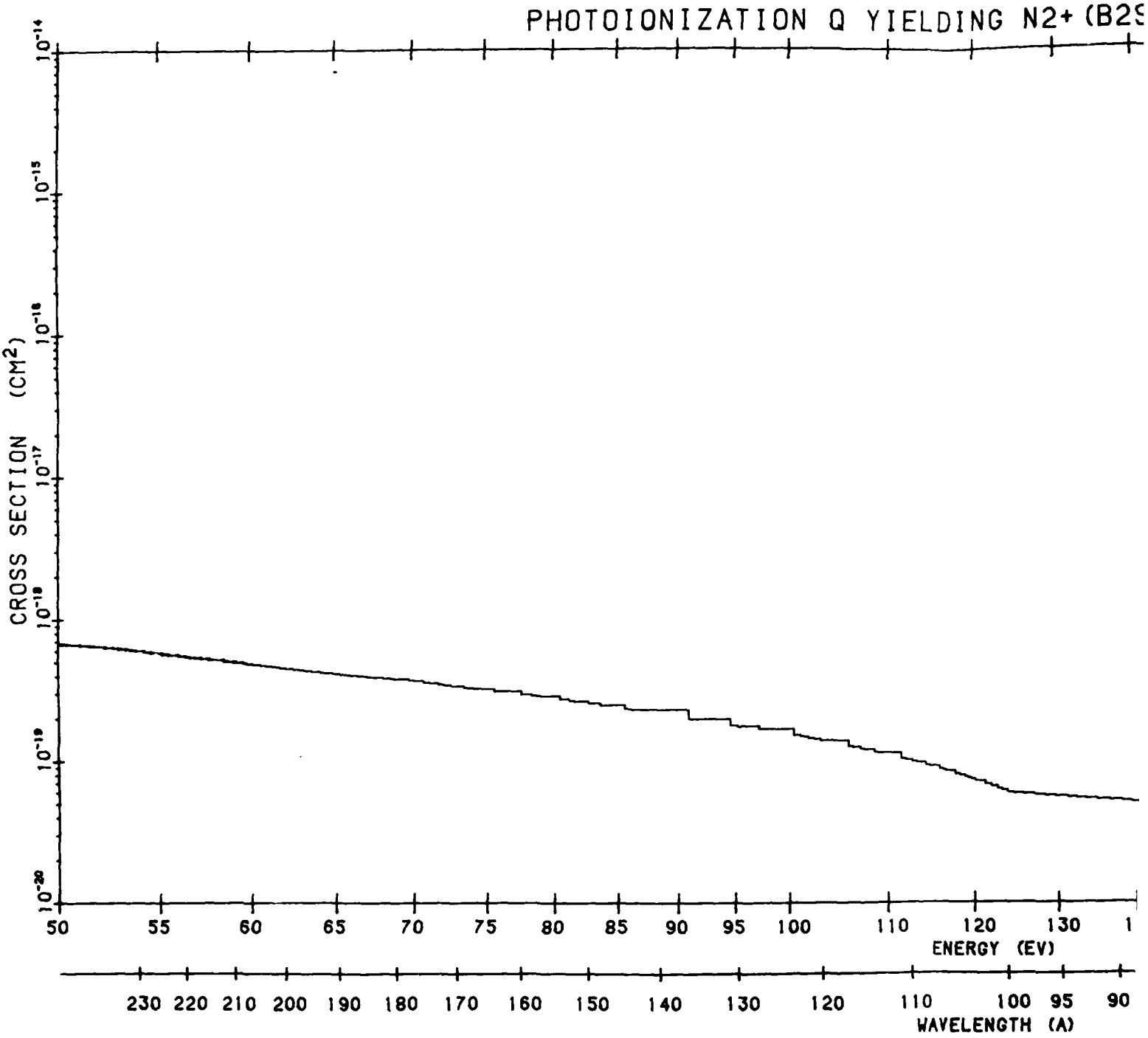
PHOTOIONIZATION Q YIELDING N2+ (B2S
CROSS SECTION (CM2)
10-14
10-15
10-16
10-17
10-18
10-19
10-20
50 55 60 65 70 75 80 85 90 95 100 110 120 130
ENERGY (EV)
230 220 210 200 190 180 170 160 150 140 130 120 110 100 95 90
WAVELENGTH (A)

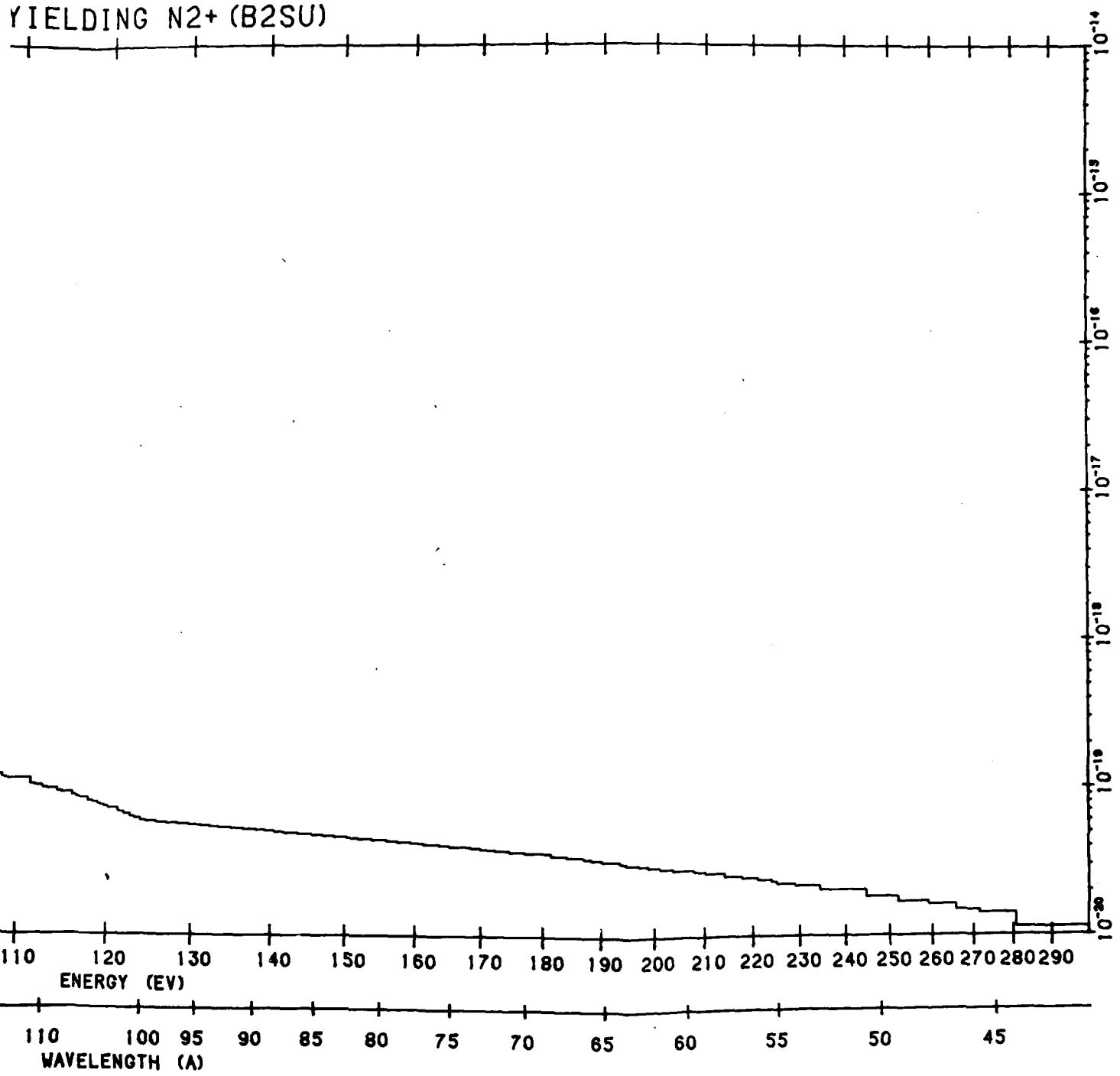


Figure B165. $N_2$ Photoionization Cross Section to $B\ ^2\Sigma_u^+$. The data source is the same as that of Figure B157 (Cont.)

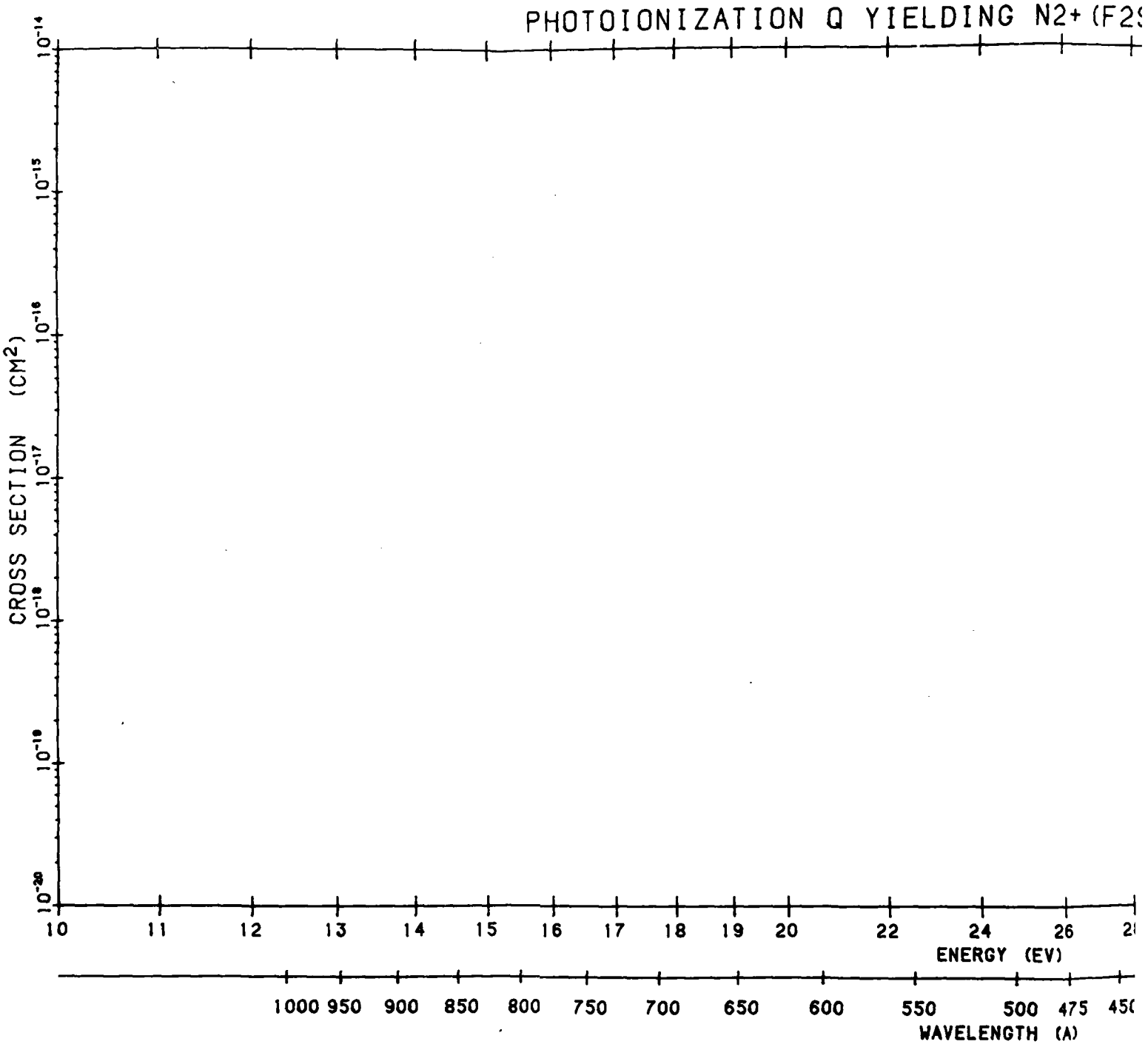
PHOTOIONIZATION Q YIELDING N2+ (F2
CROSS SECTION (CM2)
10-14
10-15
10-16
10-17
10-18
10-19
10-20
10 11 12 13 14 15 16 17 18 19 20 22 24 26
ENERGY (EV)
1000 950 900 850 800 750 700 650 600 550 500 475
WAVELENGTH (A)

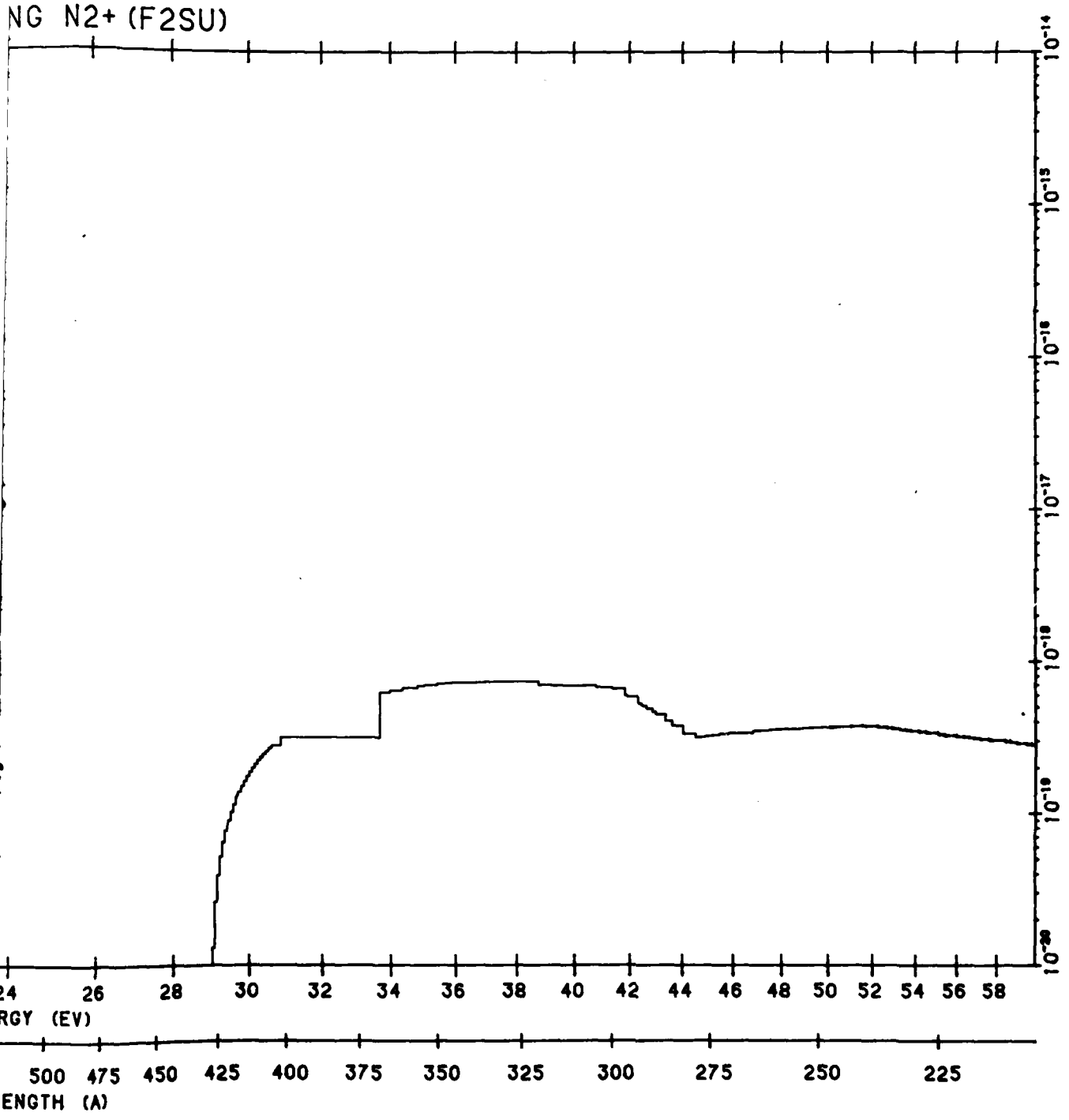


Figure B166. $N_2$ Photoionization Cross Section to F $^2\Sigma_g^+$. The data source is the same as that of Figure B157

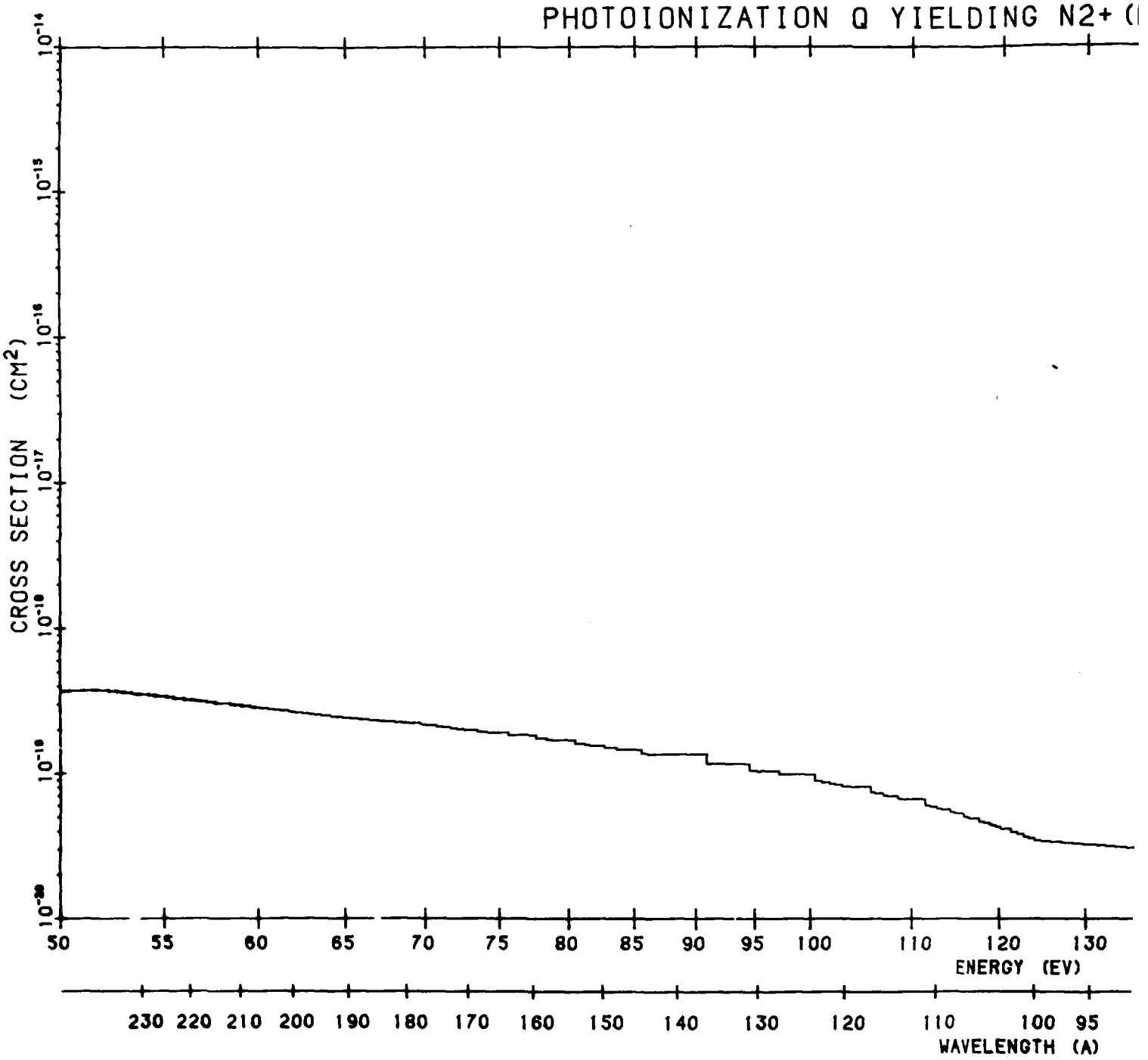
PHOTOIONIZATION Q YIELDING N2+ (
CROSS SECTION (CM2)
10-14
10-15
10-16
10-17
10-18
10-19
10-20
50
55
60
65
70
75
80
85
90
95
100
110
120
130
ENERGY (EV)
230
220
210
200
190
180
170
160
150
140
130
120
110
100
95
WAVELENGTH (A)

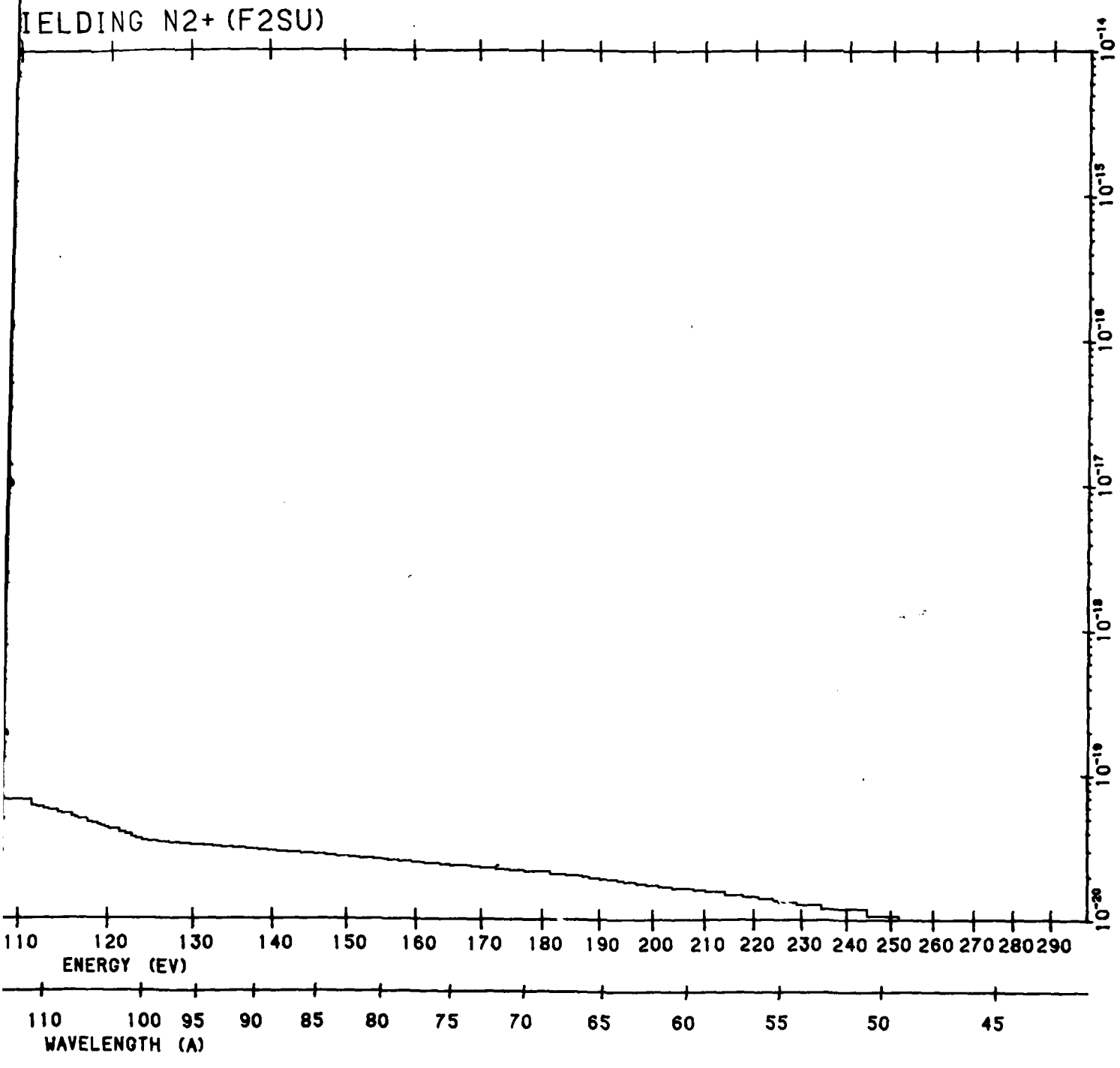


Figure B166. $N_2$ Photoionization Cross Section to F $^2\Sigma_g^+$. The data source is the same as that of Figure B157 (Cont.)

2

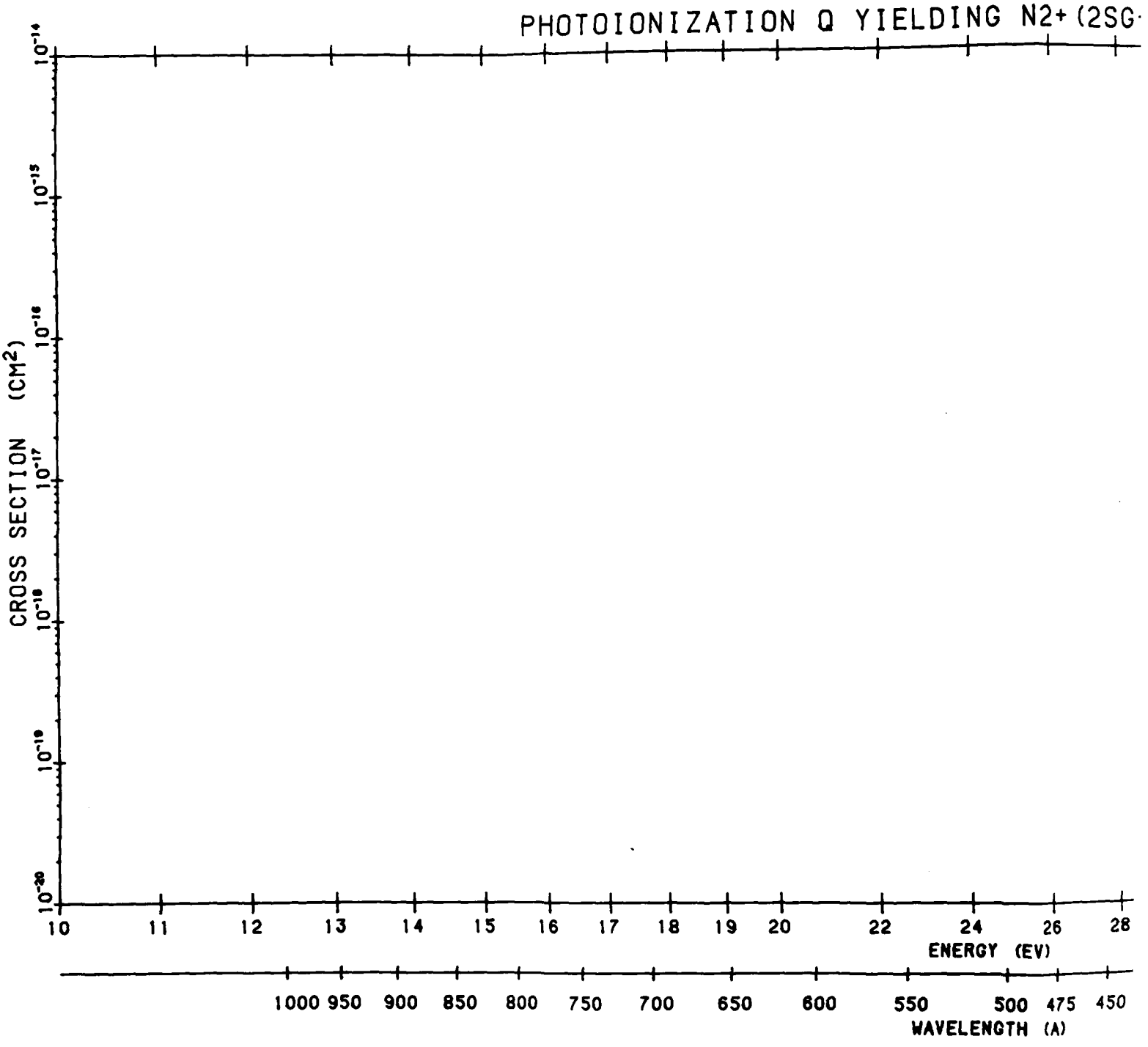
PHOTOIONIZATION Q YIELDING N2+ (2SG
CROSS SECTION (CM2)
10-14
10-15
10-16
10-17
10-18
10-19
10-20
10 11 12 13 14 15 16 17 18 19 20 22 24 26 28
ENERGY (EV)
1000 950 900 850 800 750 700 650 600 550 500 475 450
WAVELENGTH (A)

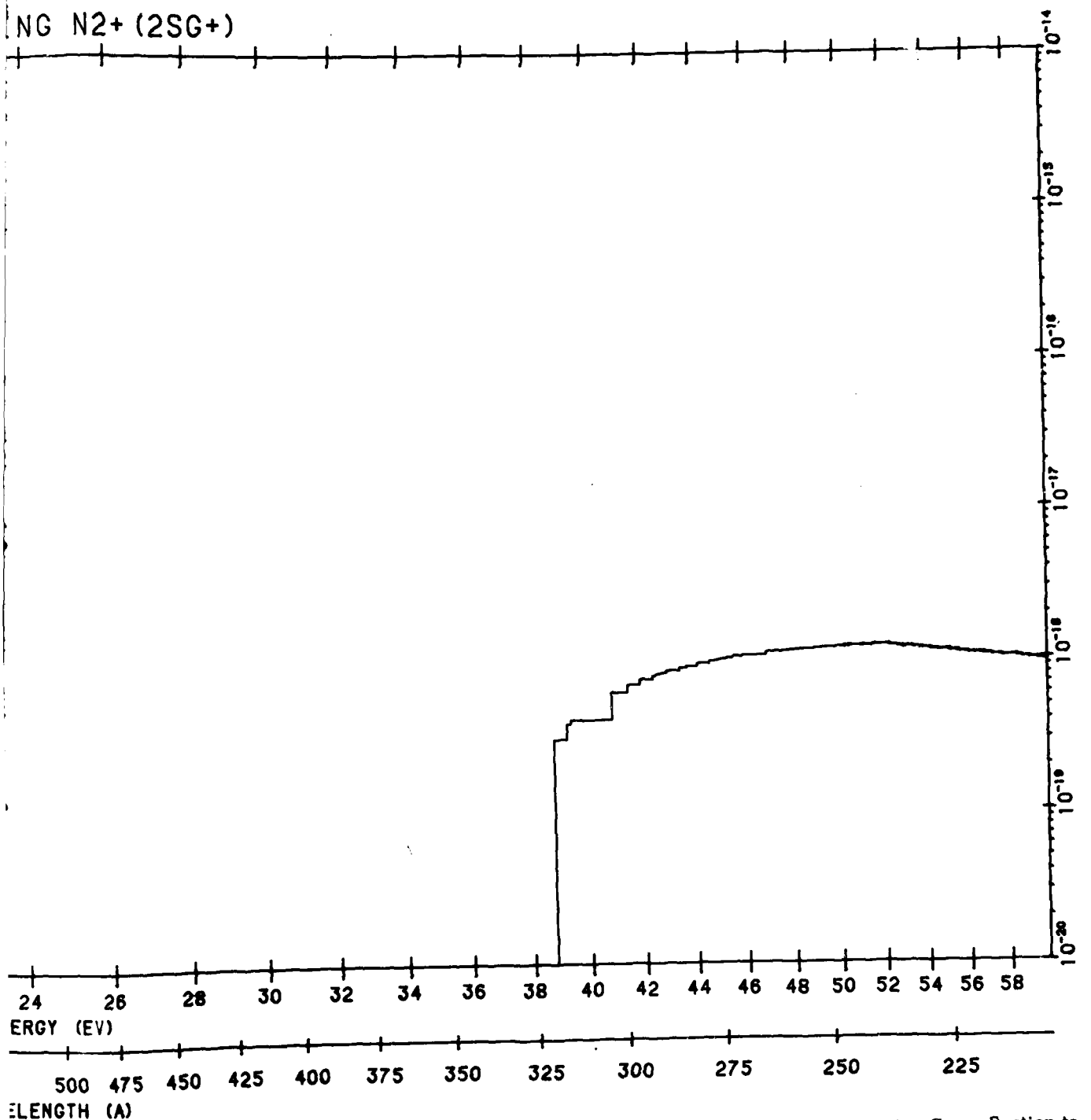


Figure B167. $N_2$ Photoionization Cross Section to $^2\Sigma_g^+$. The data source is the same as that of Figure B157

2

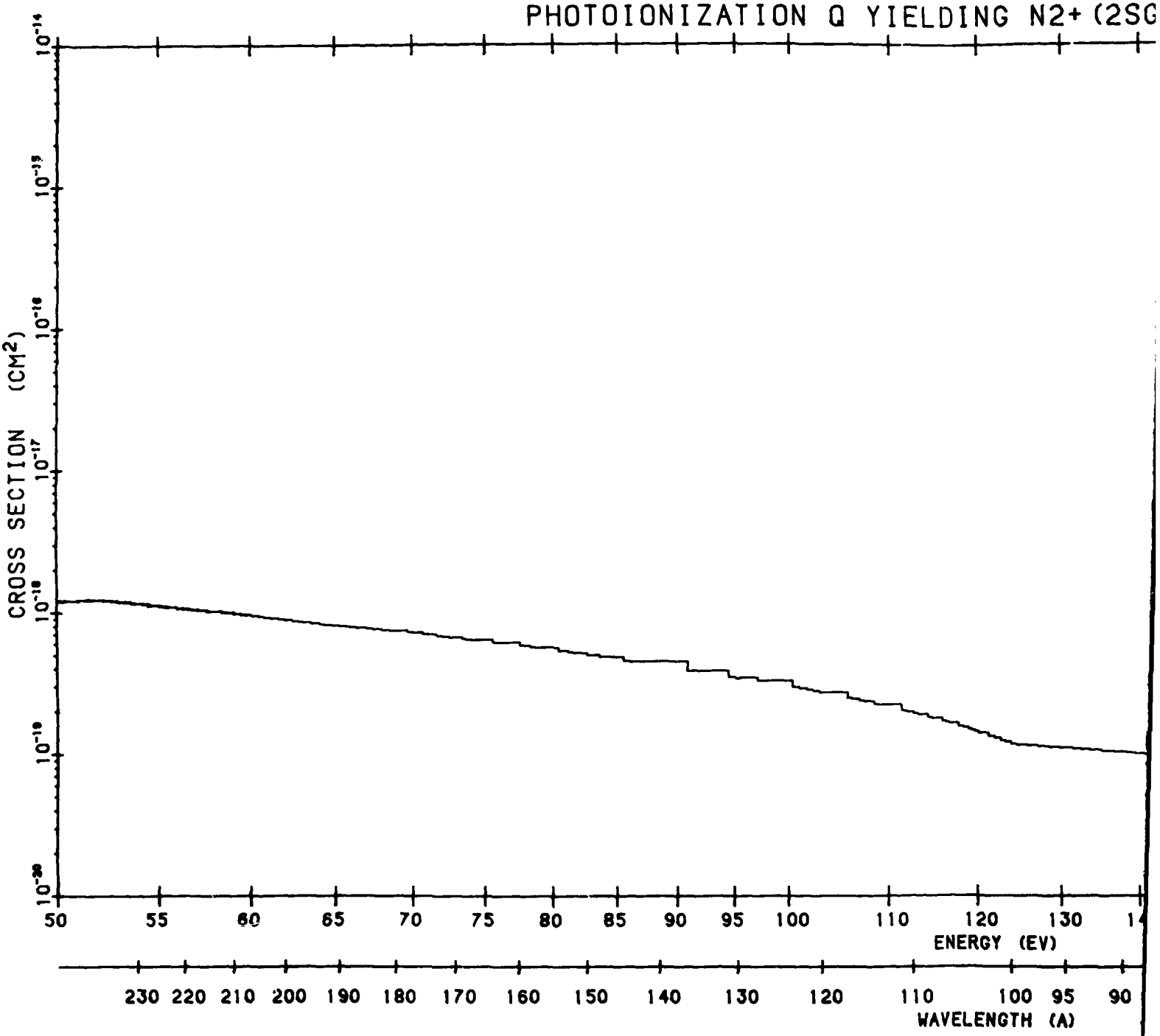
PHOTOIONIZATION Q YIELDING N2+ (2SG
CROSS SECTION (CM2)
10-14
10-15
10-16
10-17
10-18
10-19
10-20
50 55 60 65 70 75 80 85 90 95 100 110 120 130
ENERGY (EV)
230 220 210 200 190 180 170 160 150 140 130 120 110 100 95 90
WAVELENGTH (A)

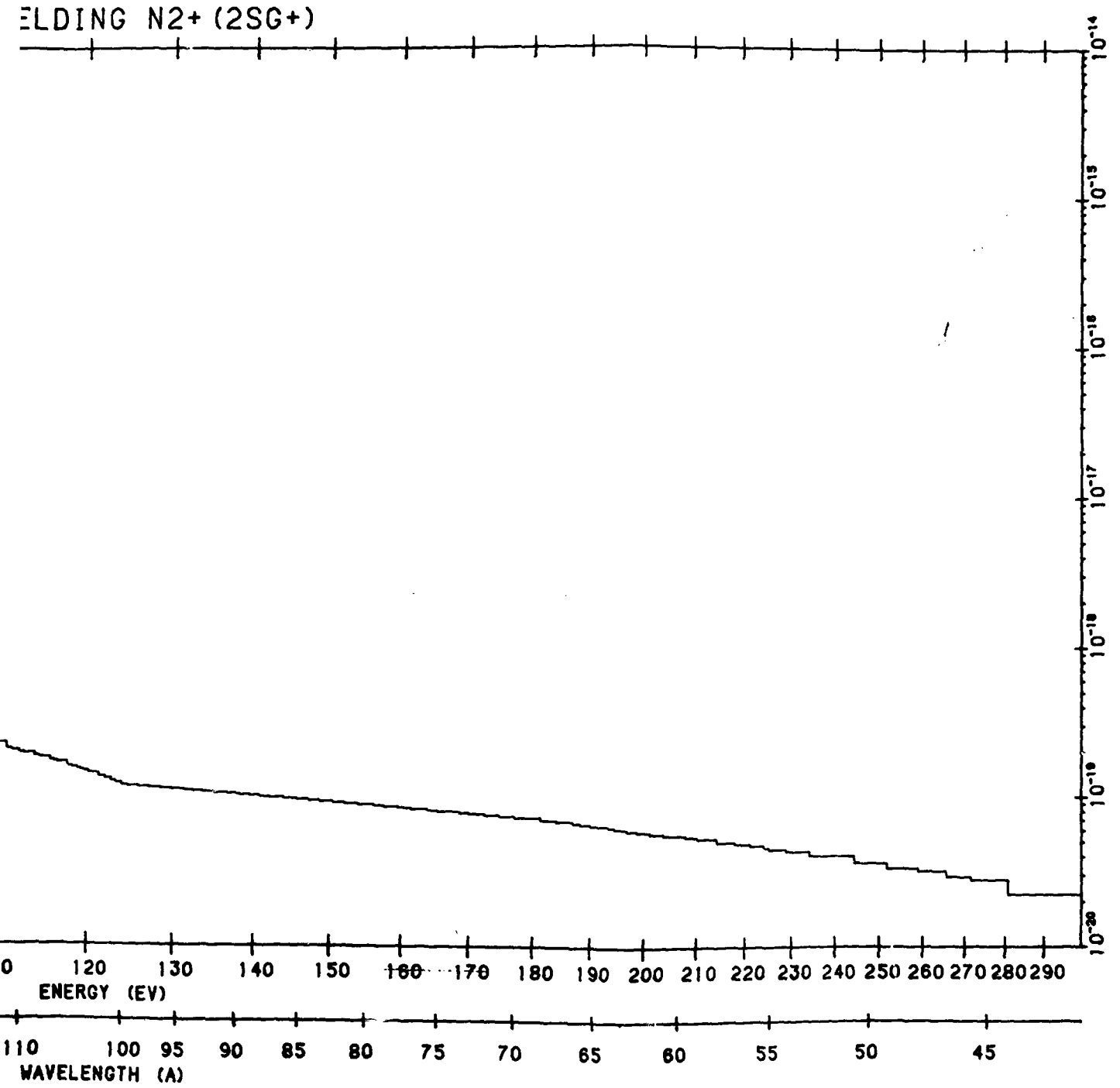


Figure B167. $N_2$ Photoionization Cross Section to $^2\Sigma_g^+$. The data source is the same as that of Figure B157 (Cont.)

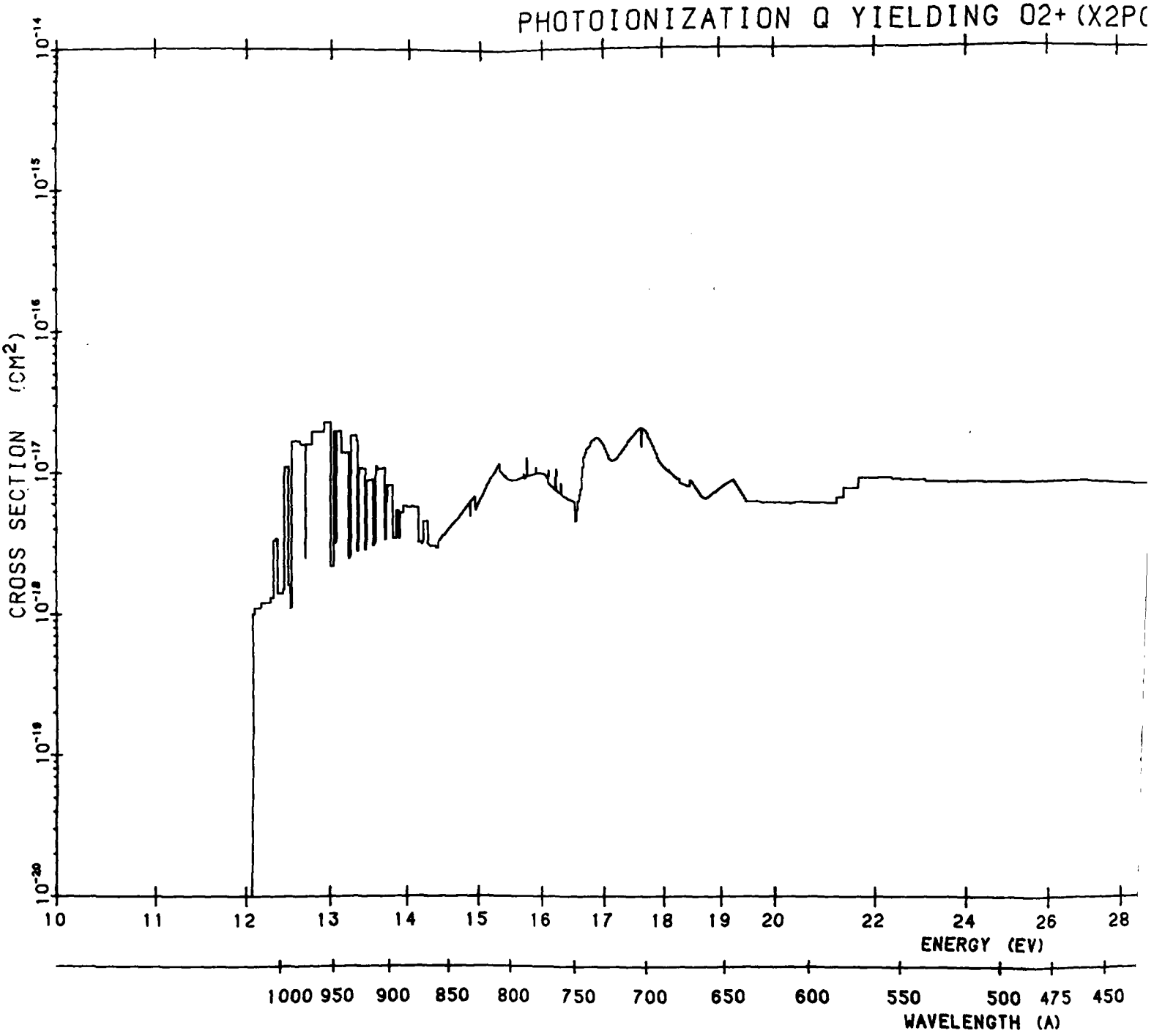
PHOTOIONIZATION Q YIELDING O2+ (X2P(
CROSS SECTION (CM2)
10^-14
10^-15
10^-16
10^-17
10^-18
10^-19
10^-20
10 11 12 13 14 15 16 17 18 19 20 22 24 26 28
ENERGY (EV)
1000 950 900 850 800 750 700 650 600 550 500 475 450
WAVELENGTH (A)

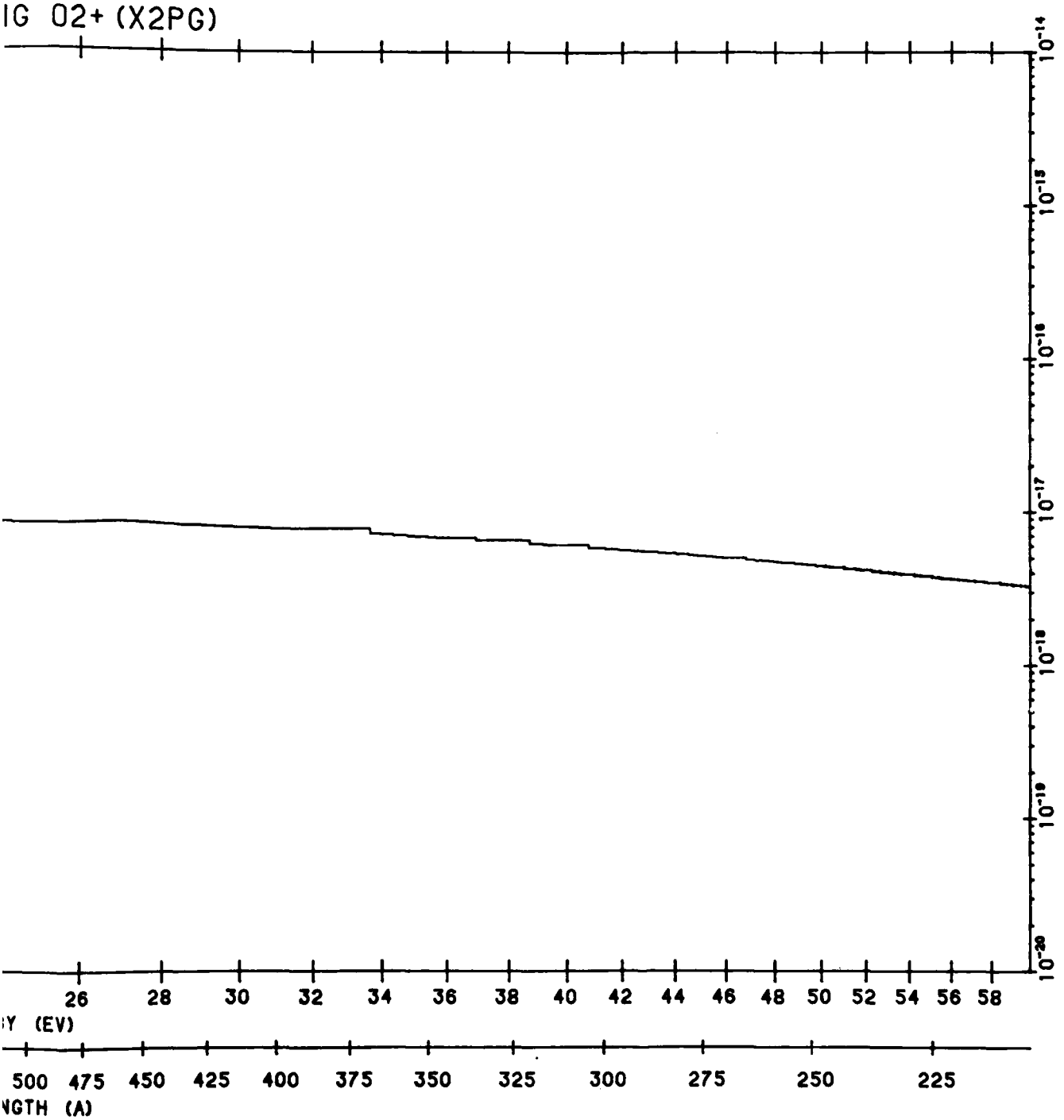


Figure B168. $O_2$ Photoionization Cross Section to $O_2^+ X\ ^2\Pi_g$. The data source is the same as that of Figure B157

2

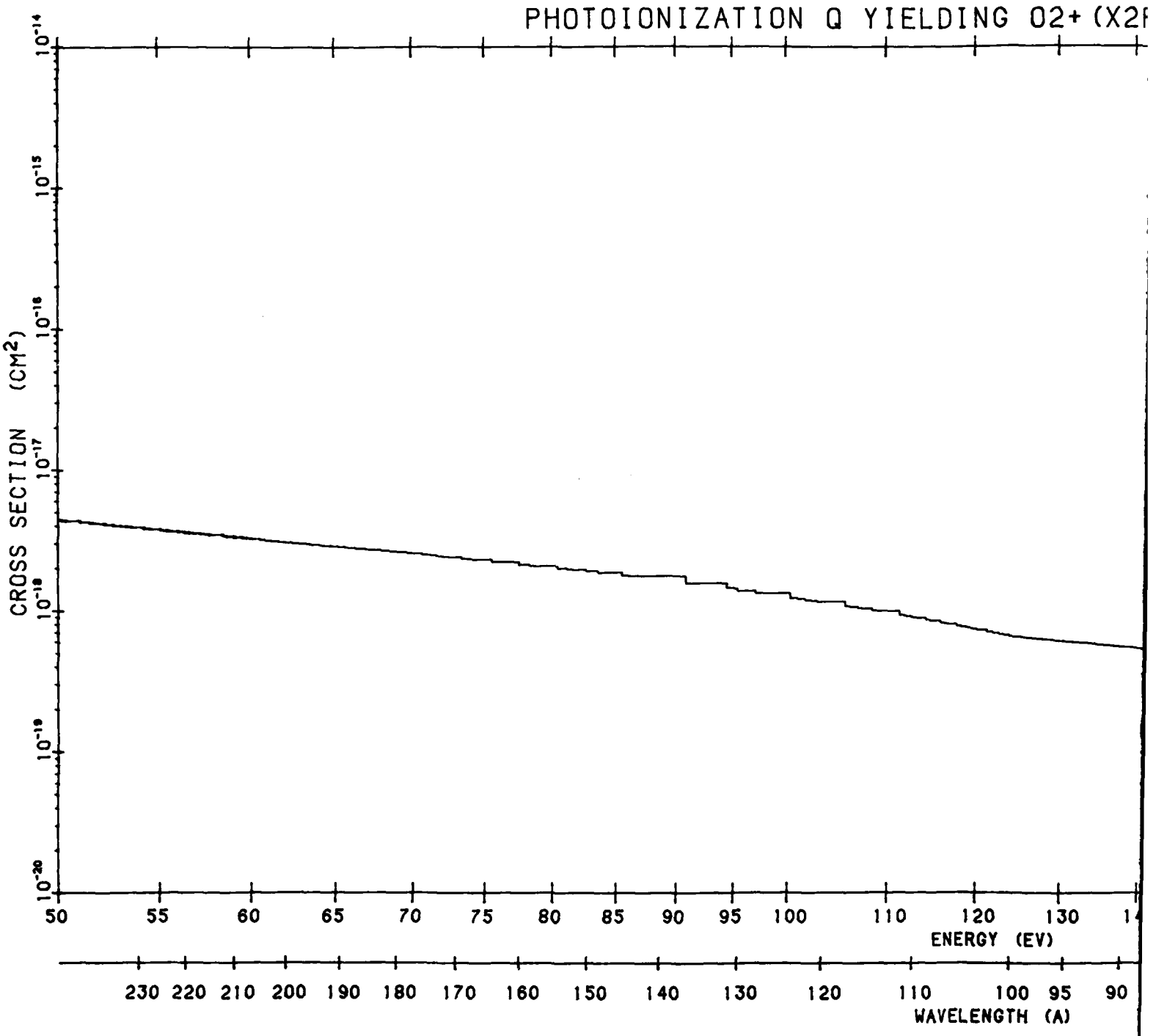
PHOTOIONIZATION Q YIELDING O2+ (X2
CROSS SECTION (CM2)
10-14
10-15
10-16
10-17
10-18
10-19
10-20
50 55 60 65 70 75 80 85 90 95 100 110 120 130
ENERGY (EV)
230 220 210 200 190 180 170 160 150 140 130 120 110 100 95 90
WAVELENGTH (A)

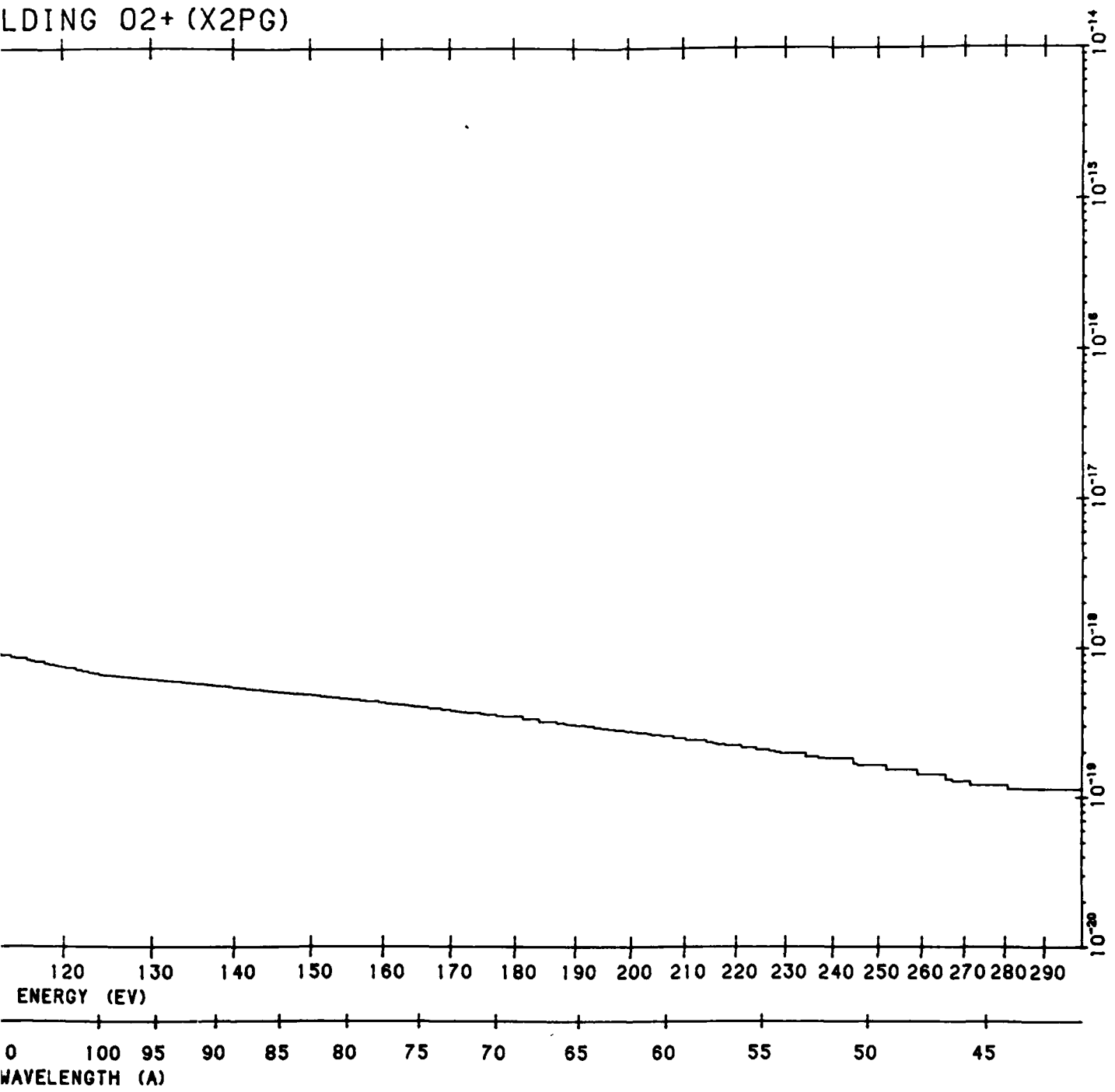


Figure B168. $O_2$ Photoionization Cross Section to $O_2^+ X\,^2\Pi_g$. The data source is the same as that of Figure B157 (Cont.)

2

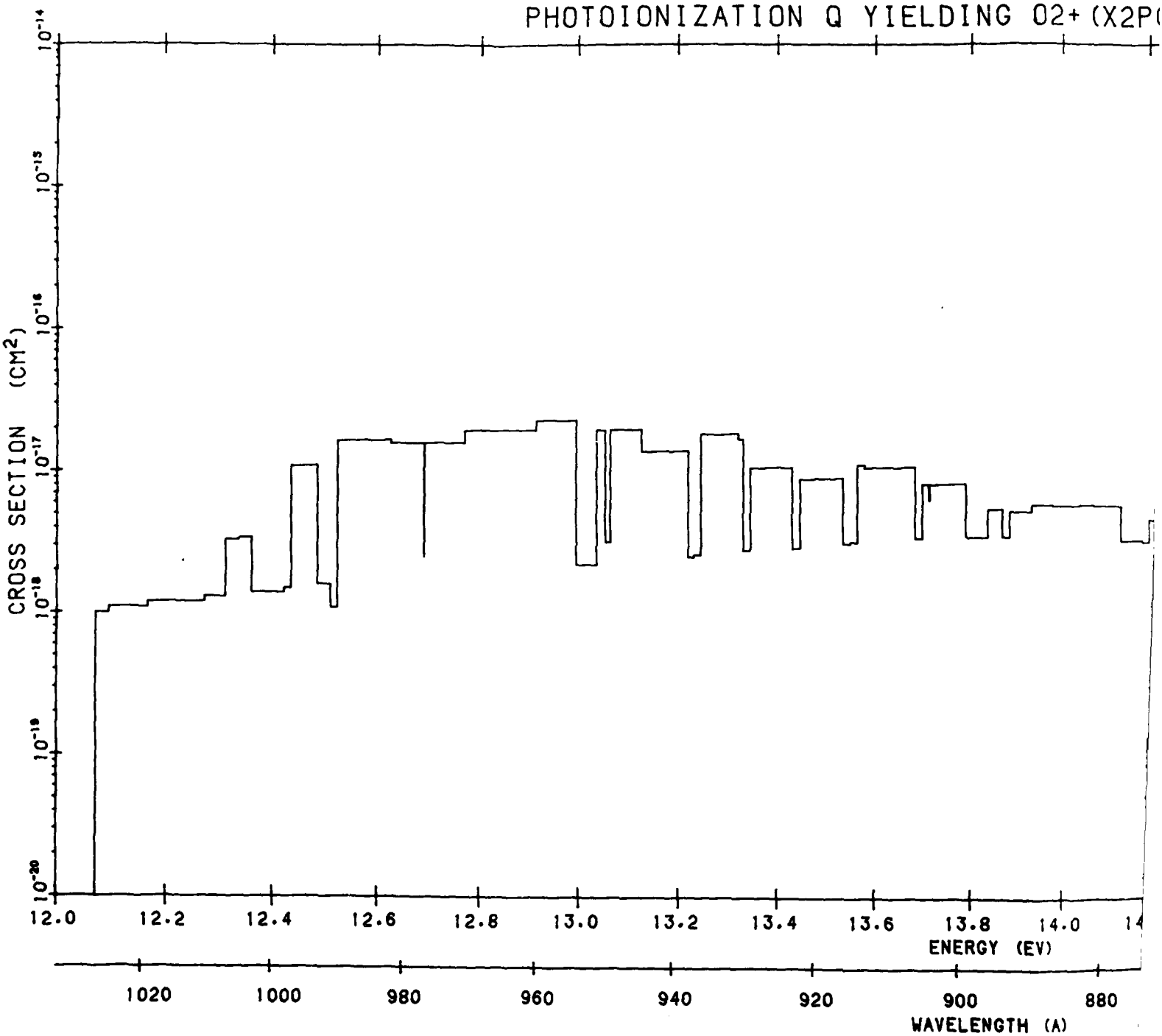
PHOTOIONIZATION Q YIELDING O2+ (X2P(
CROSS SECTION (CM2)
10-14
10-15
10-16
10-17
10-18
10-19
10-20
12.0
12.2
12.4
12.6
12.8
13.0
13.2
13.4
13.6
13.8
14.0
ENERGY (EV)
1020
1000
980
960
940
920
900
880
WAVELENGTH (A)

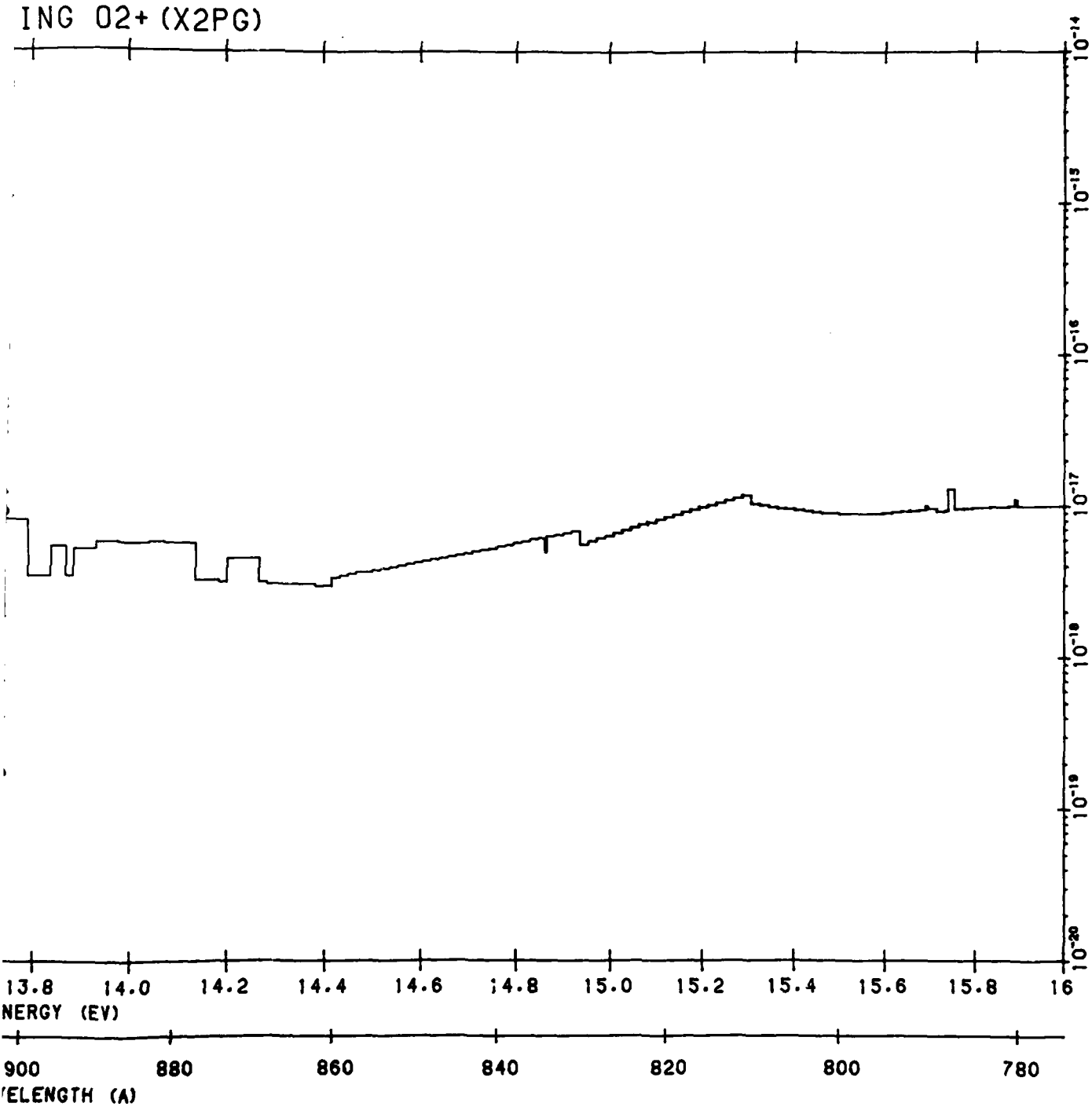


Figure B168. $O_2$ Photoionization Cross Section to $O_2^+ X\ ^2\Pi_g$. The data source is the same as that of Figure B157 (Cont.)

2

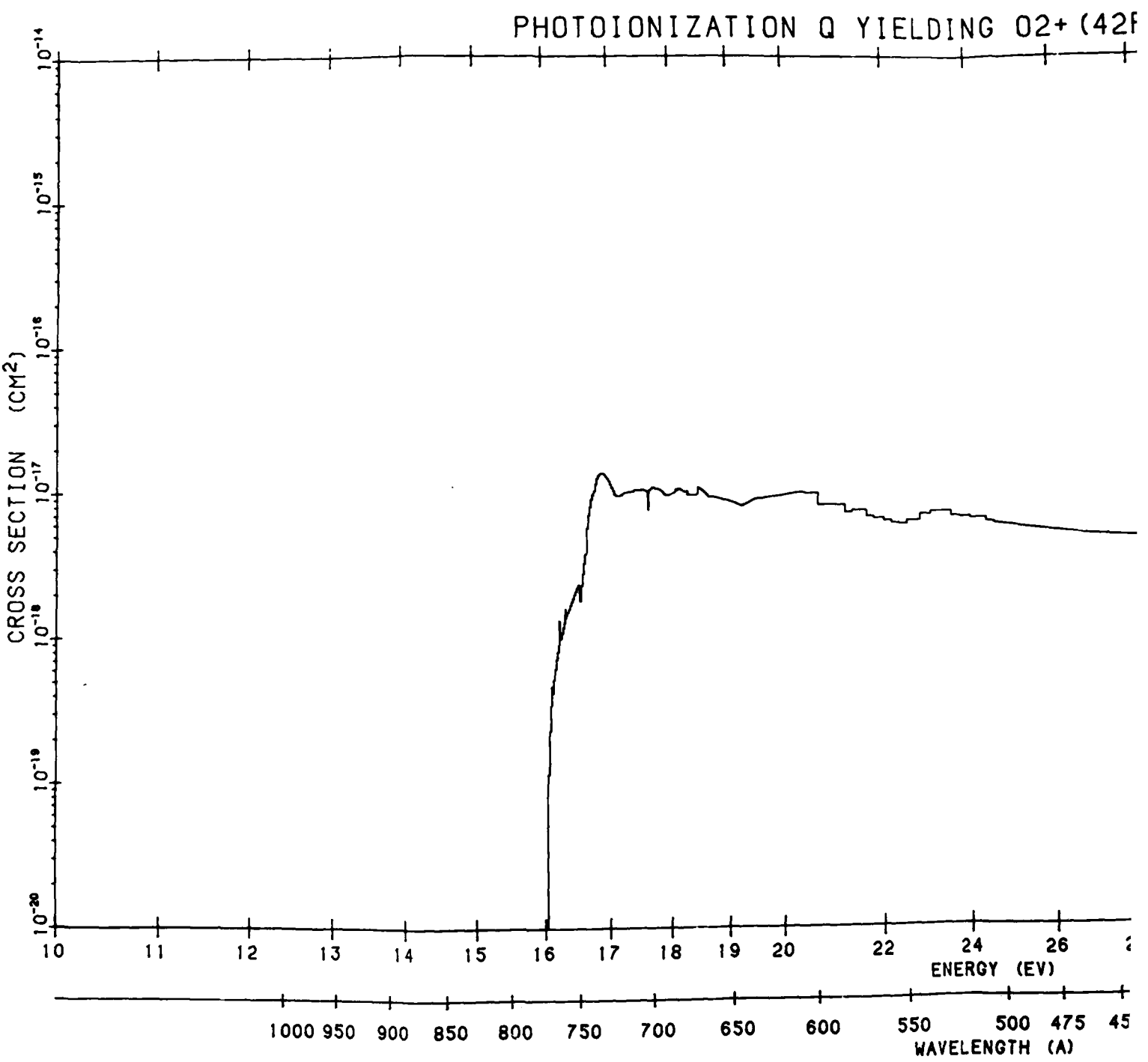
PHOTOIONIZATION Q YIELDING O2+ (42F
CROSS SECTION (CM2)
10-14
10-15
10-16
10-17
10-18
10-19
10-20
10 11 12 13 14 15 16 17 18 19 20 22 24 26
ENERGY (EV)
1000 950 900 850 800 750 700 650 600 550 500 475 45
WAVELENGTH (A)

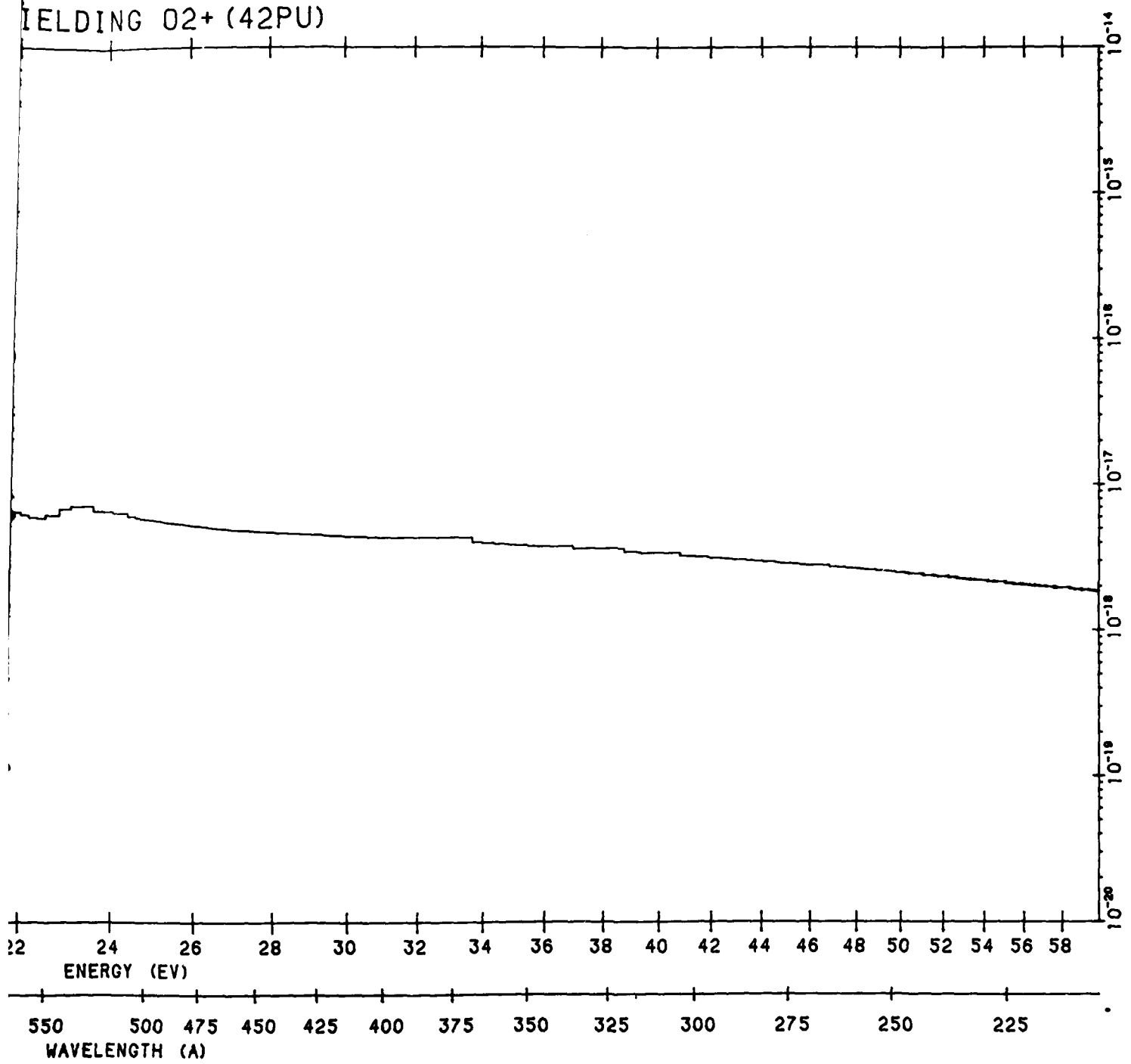


Figure B169. $O_2$ Photoionization Cross Section to $O_2^+$ States a $^4\Pi_u$ and A $^2\Pi_u$. The data source is the same as that of Figure B157

2

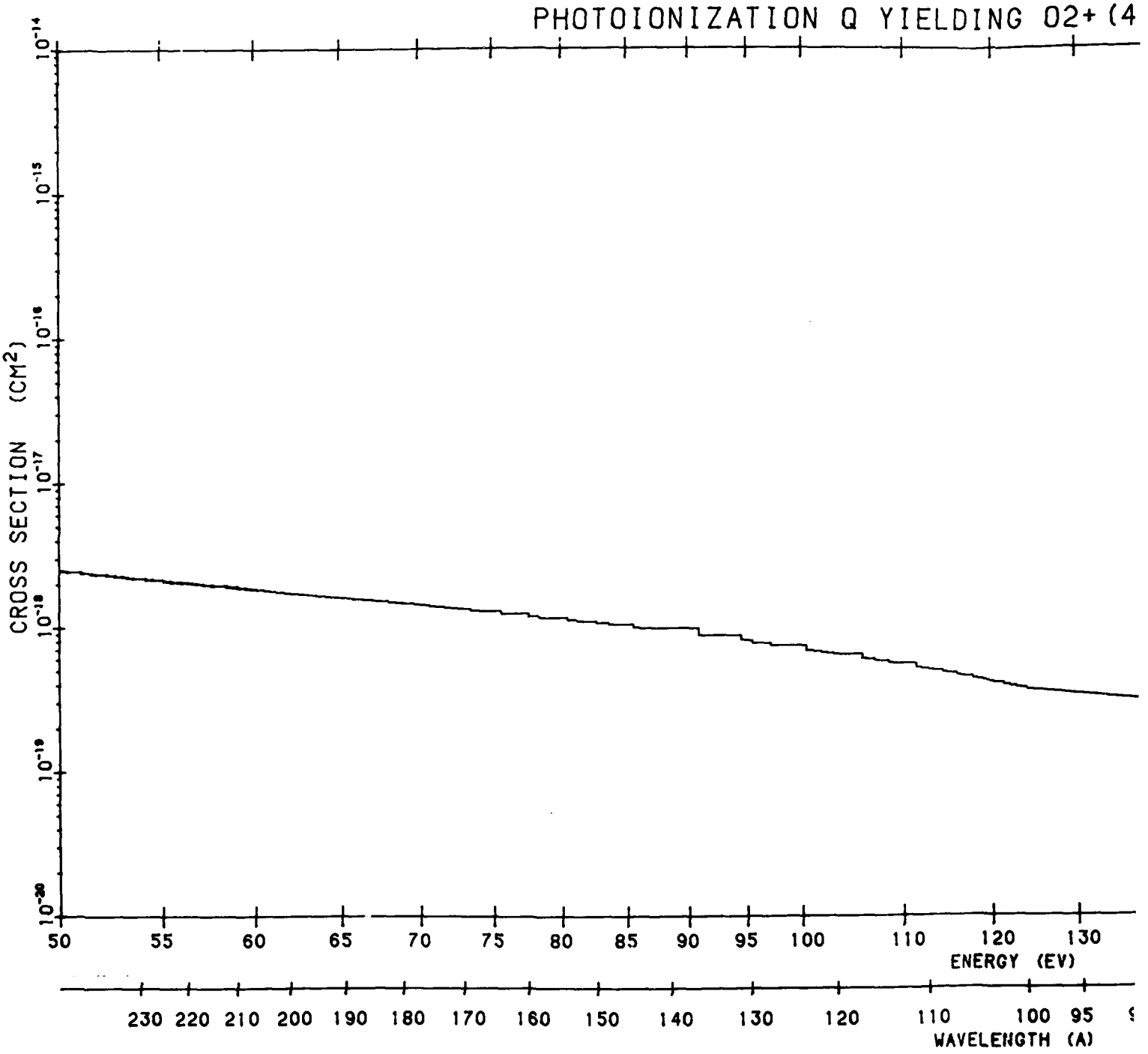
PHOTOIONIZATION Q YIELDING O2+ (4
CROSS SECTION (CM2)
10-14
10-15
10-16
10-17
10-18
10-19
10-20
50 55 60 65 70 75 80 85 90 95 100 110 120 130
ENERGY (EV)
230 220 210 200 190 180 170 160 150 140 130 120 110 100 95
WAVELENGTH (A)

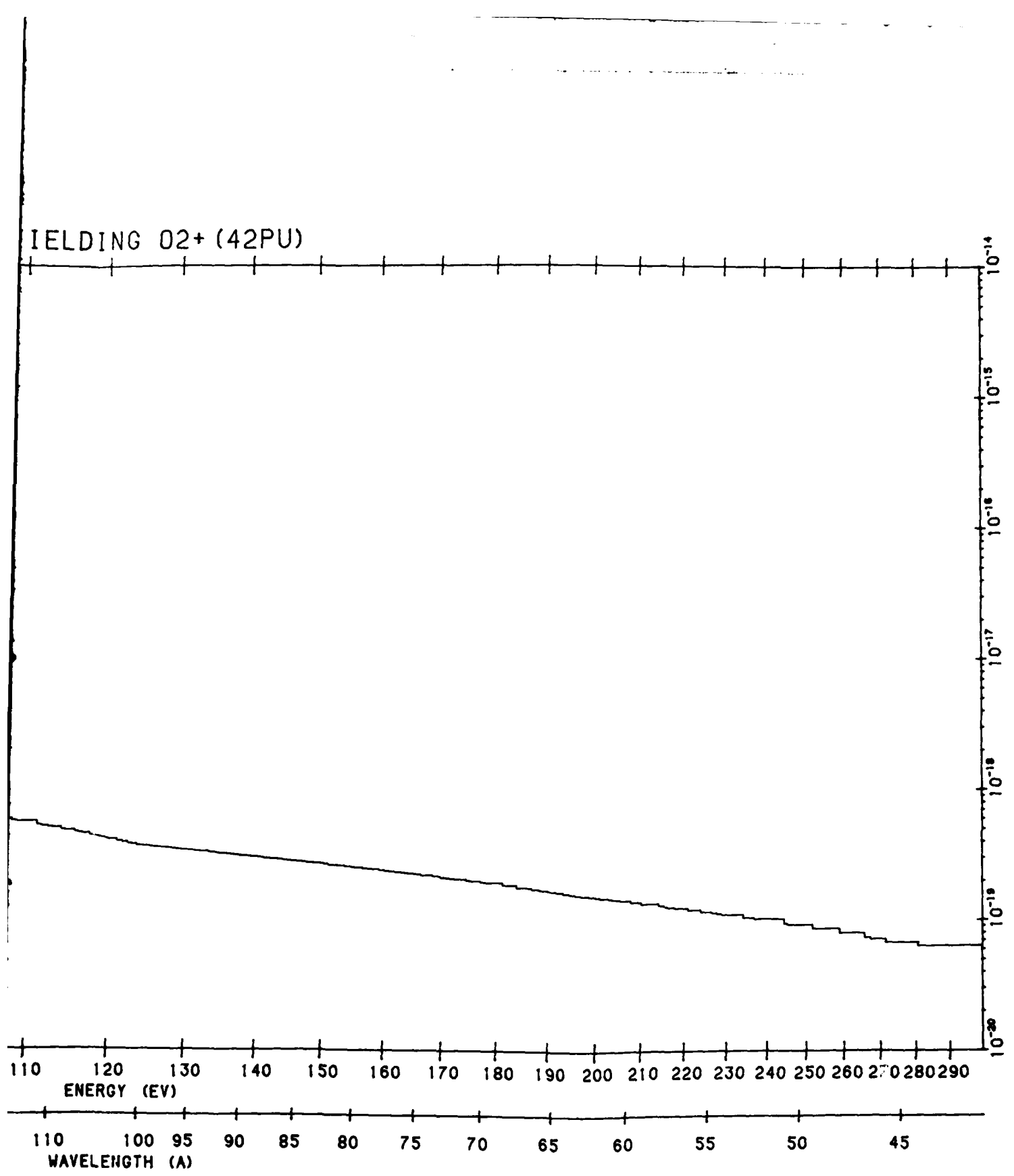


Figure B169. $O_2$ Photoionization Cross Section to $O_2^+$ States a $^4\Pi_u$ and A $^2\Pi_u$. The data source is the same as that of Figure B157 (Cont.)

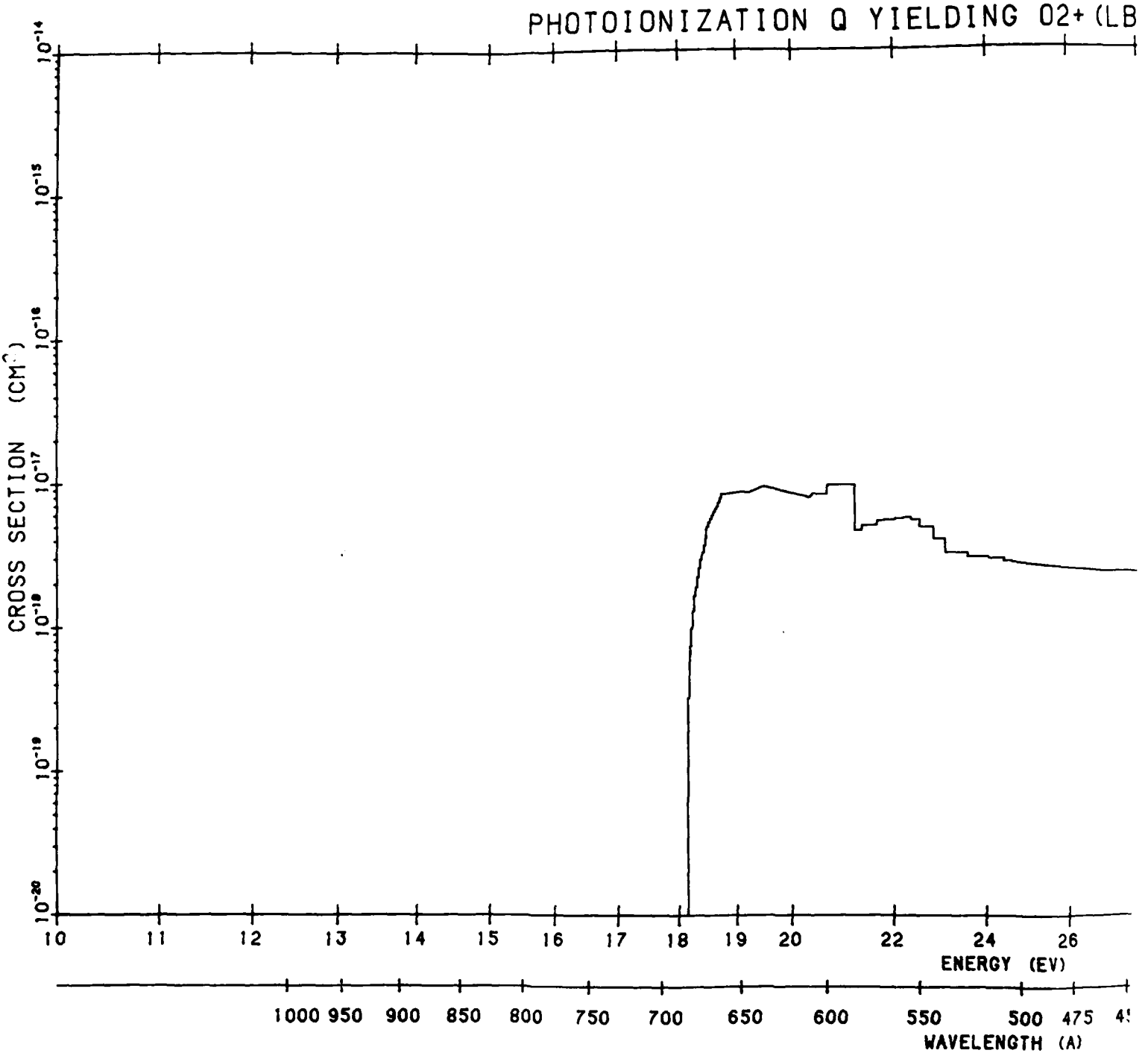
PHOTOIONIZATION Q YIELDING O2+ (LB
CROSS SECTION (CM²)
10⁻¹⁴
10⁻¹⁵
10⁻¹⁶
10⁻¹⁷
10⁻¹⁸
10⁻¹⁹
10⁻²⁰
10 11 12 13 14 15 16 17 18 19 20 22 24 26
ENERGY (EV)
1000 950 900 850 800 750 700 650 600 550 500 475
WAVELENGTH (A)

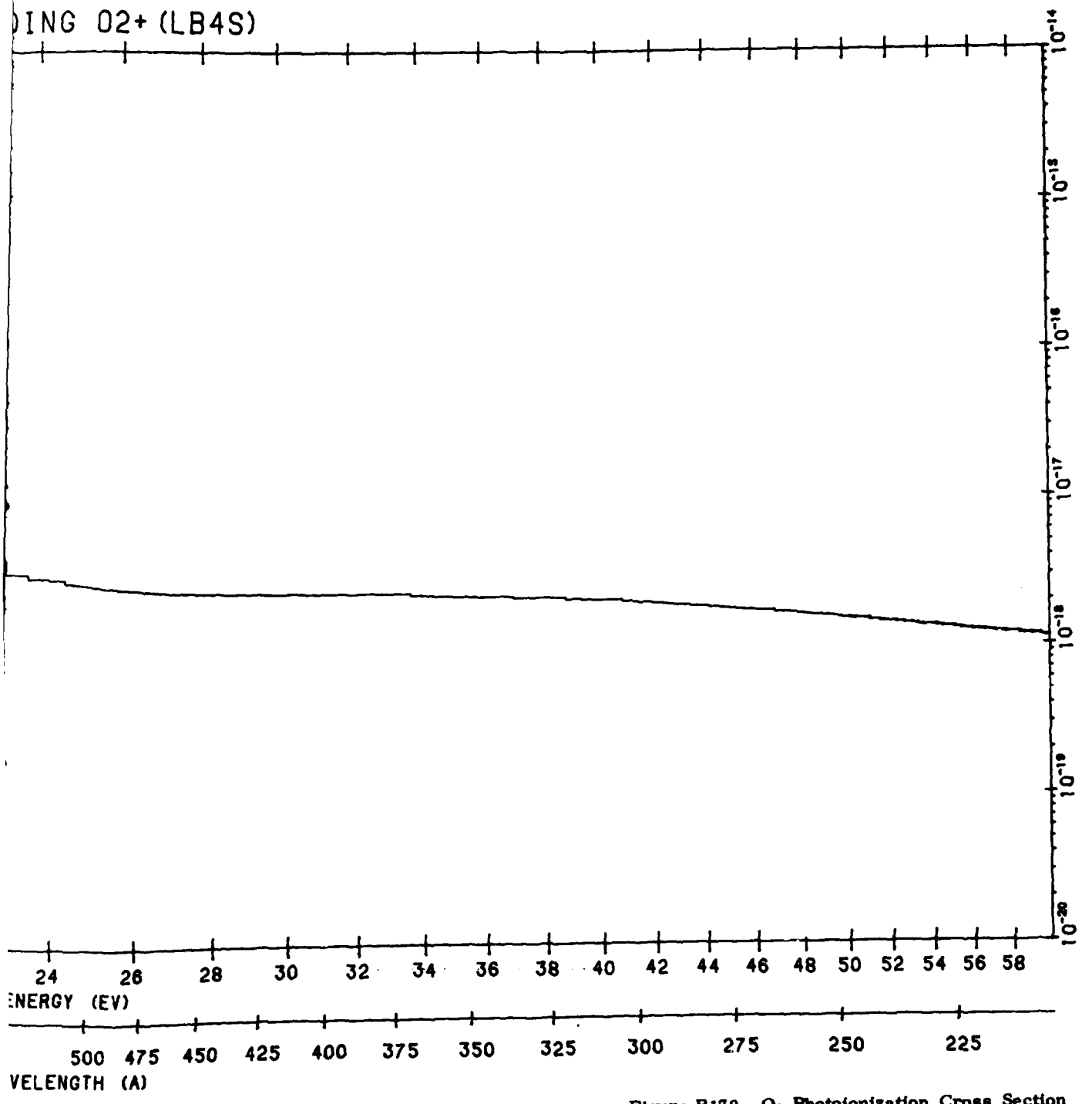


Figure B170. $O_2$ Photoionization Cross Section to $O_2^+$ b $^4\Sigma_g$. The data source is the same as that of Figure B157

2

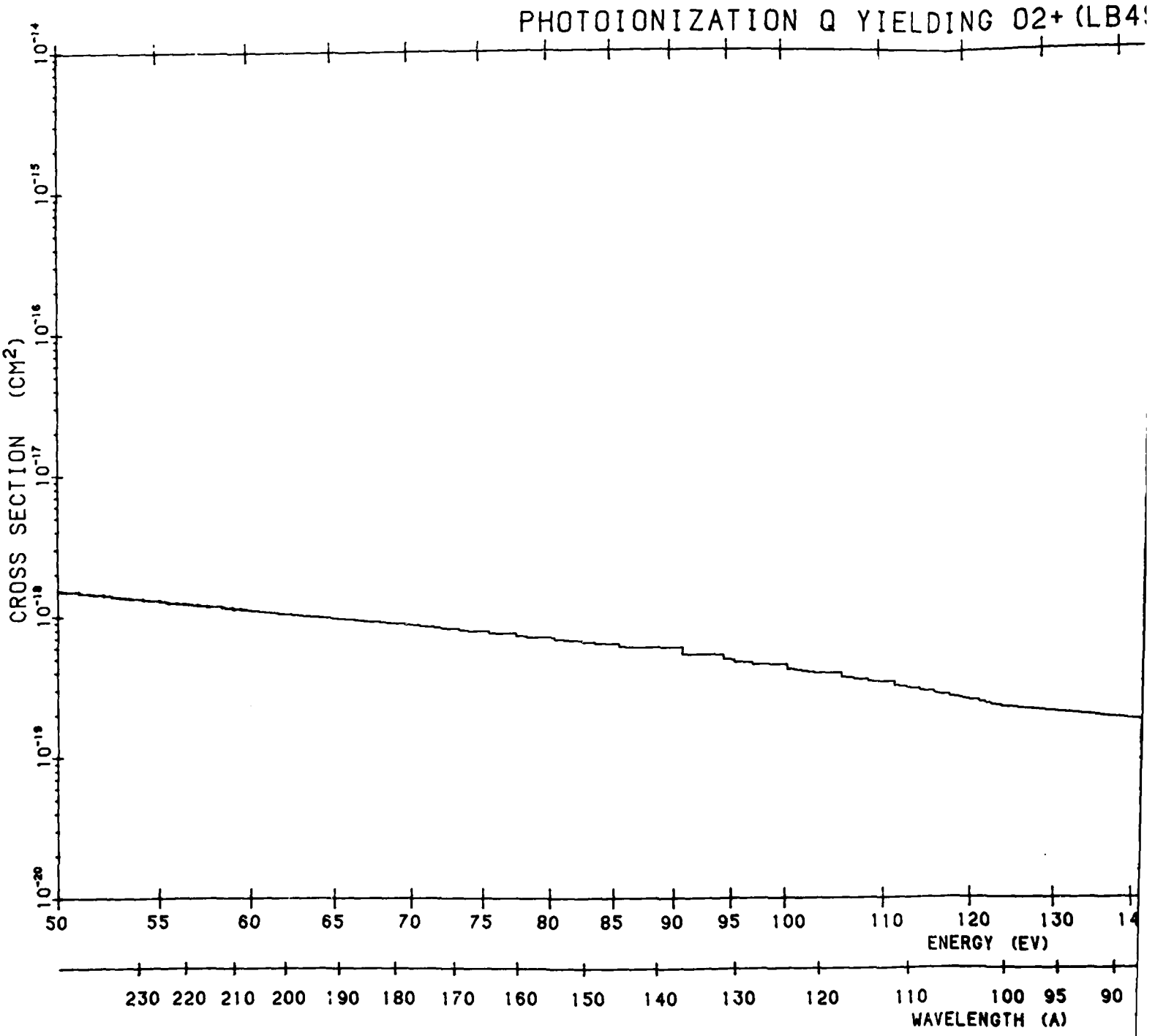
PHOTOIONIZATION Q YIELDING O2+ (LB4
CROSS SECTION (CM2)
10-14
10-15
10-16
10-17
10-18
10-19
10-20
50 55 60 65 70 75 80 85 90 95 100 110 120 130
ENERGY (EV)
230 220 210 200 190 180 170 160 150 140 130 120 110 100 95 90
WAVELENGTH (A)

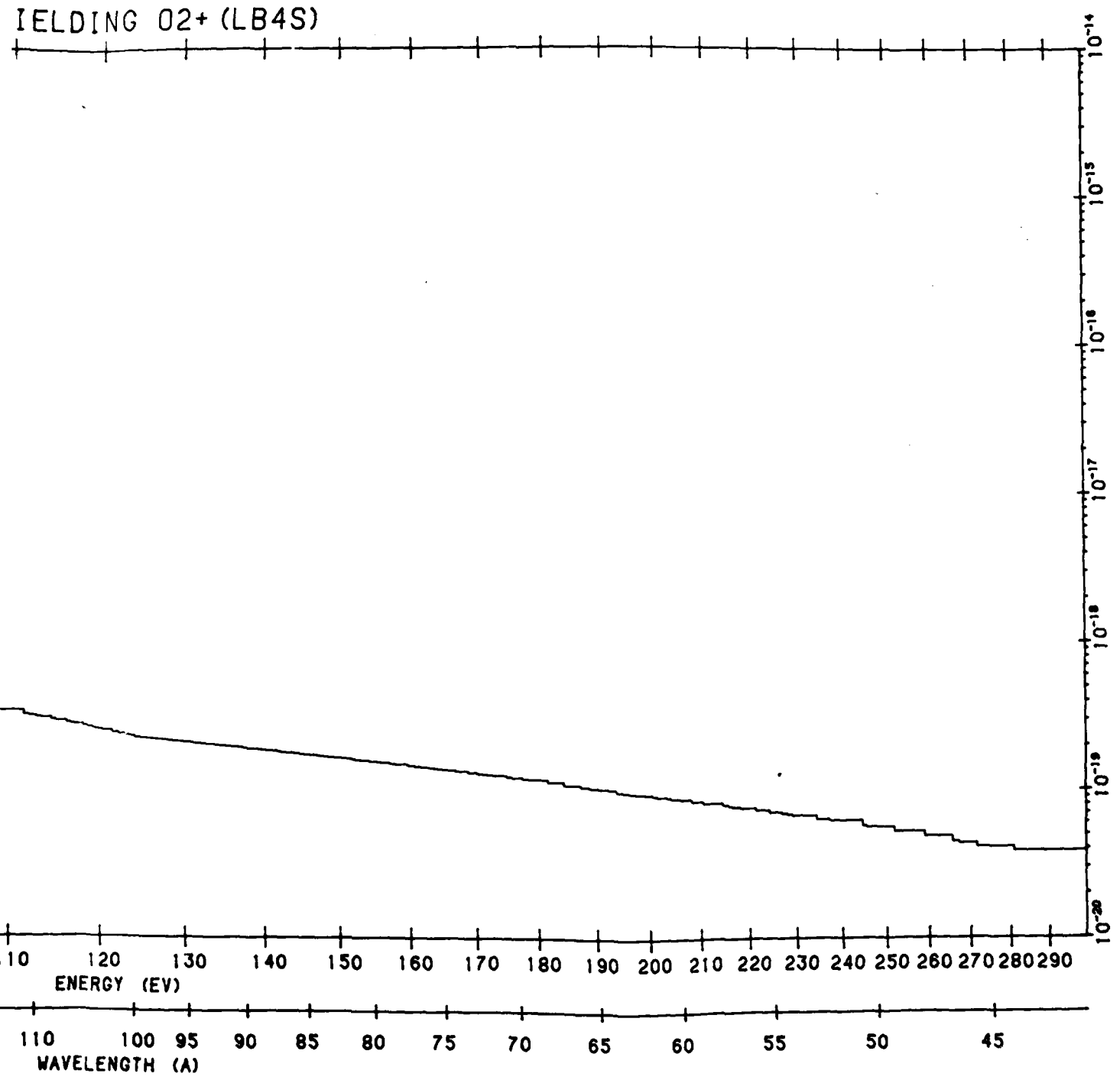


Figure B170. $O_2$ Photoionization Cross Section to $O_2^+$ b $^4\Sigma_g$. The data source is the same as that of Figure B157 (Cont.)

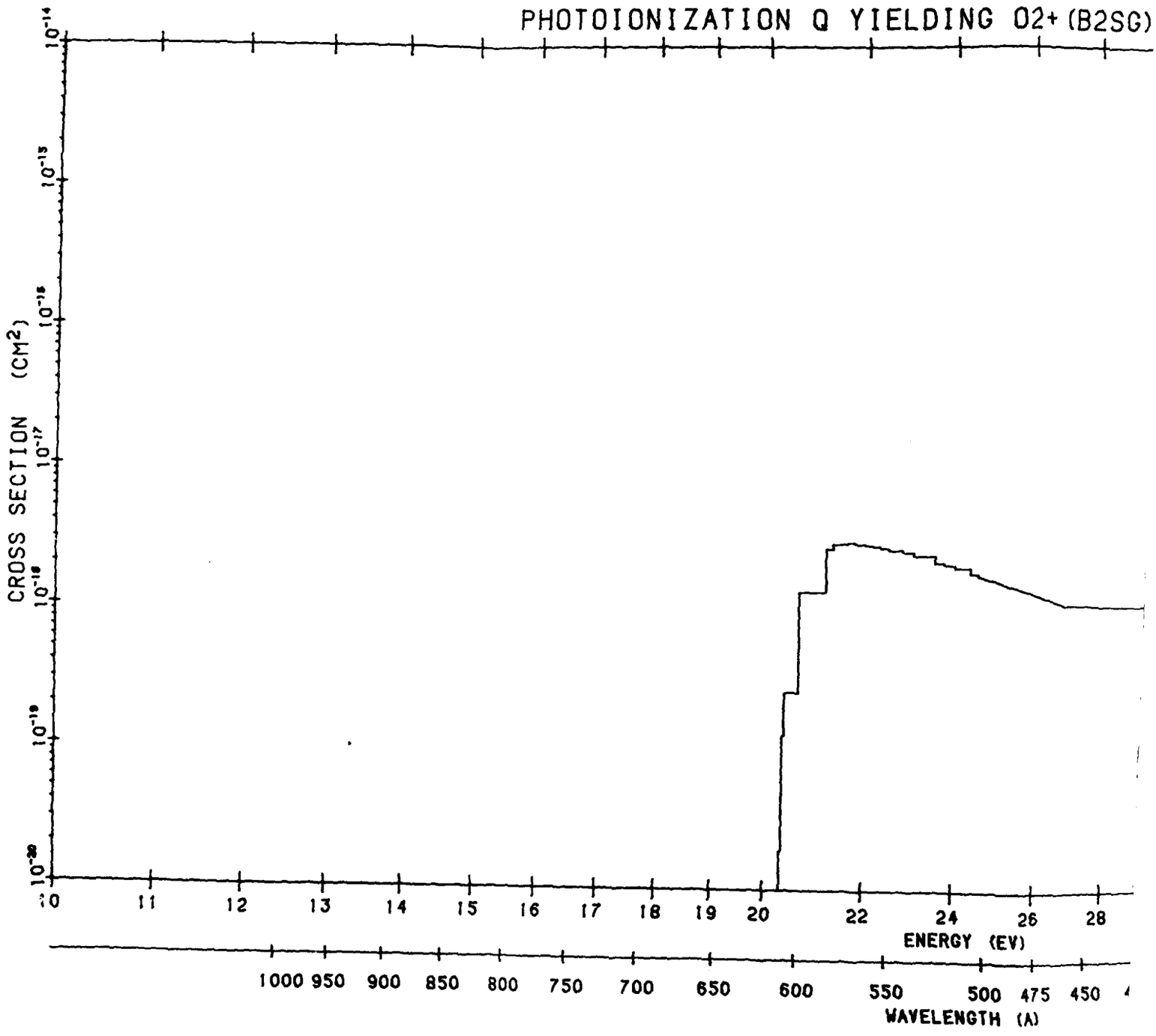
PHOTOIONIZATION Q YIELDING O2+ (B2SG)
CROSS SECTION (CM2)
10-14
10-15
10-16
10-17
10-18
10-19
10-20
10
11
12
13
14
15
16
17
18
19
20
22
24
26
28
ENERGY (EV)
1000
950
900
850
800
750
700
650
600
550
500
475
450
WAVELENGTH (A)

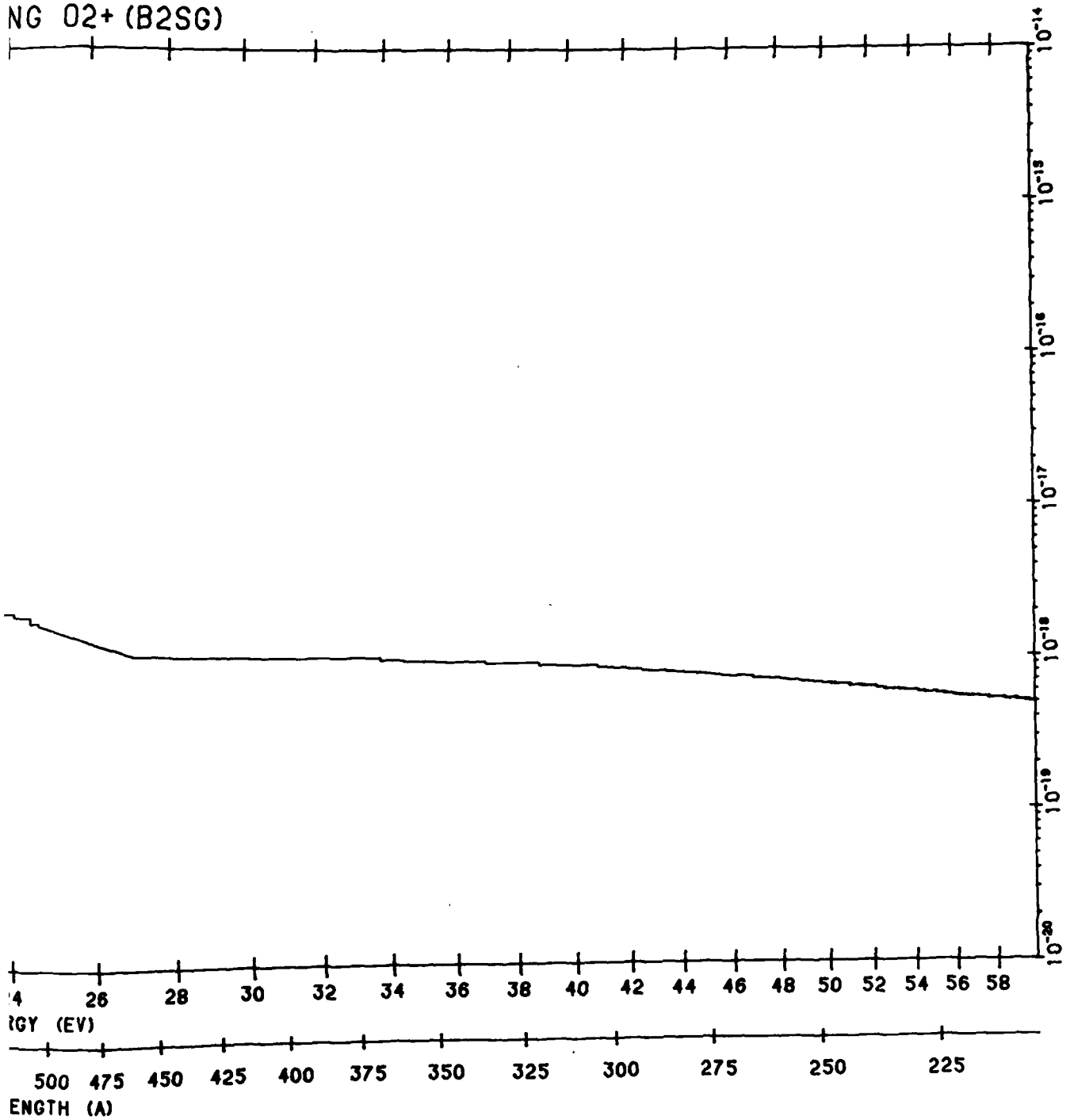


Figure B171. $O_2$ Photoionization Cross Section to B $^2\Sigma_g^-$. The data source is the same as that of Figure B157

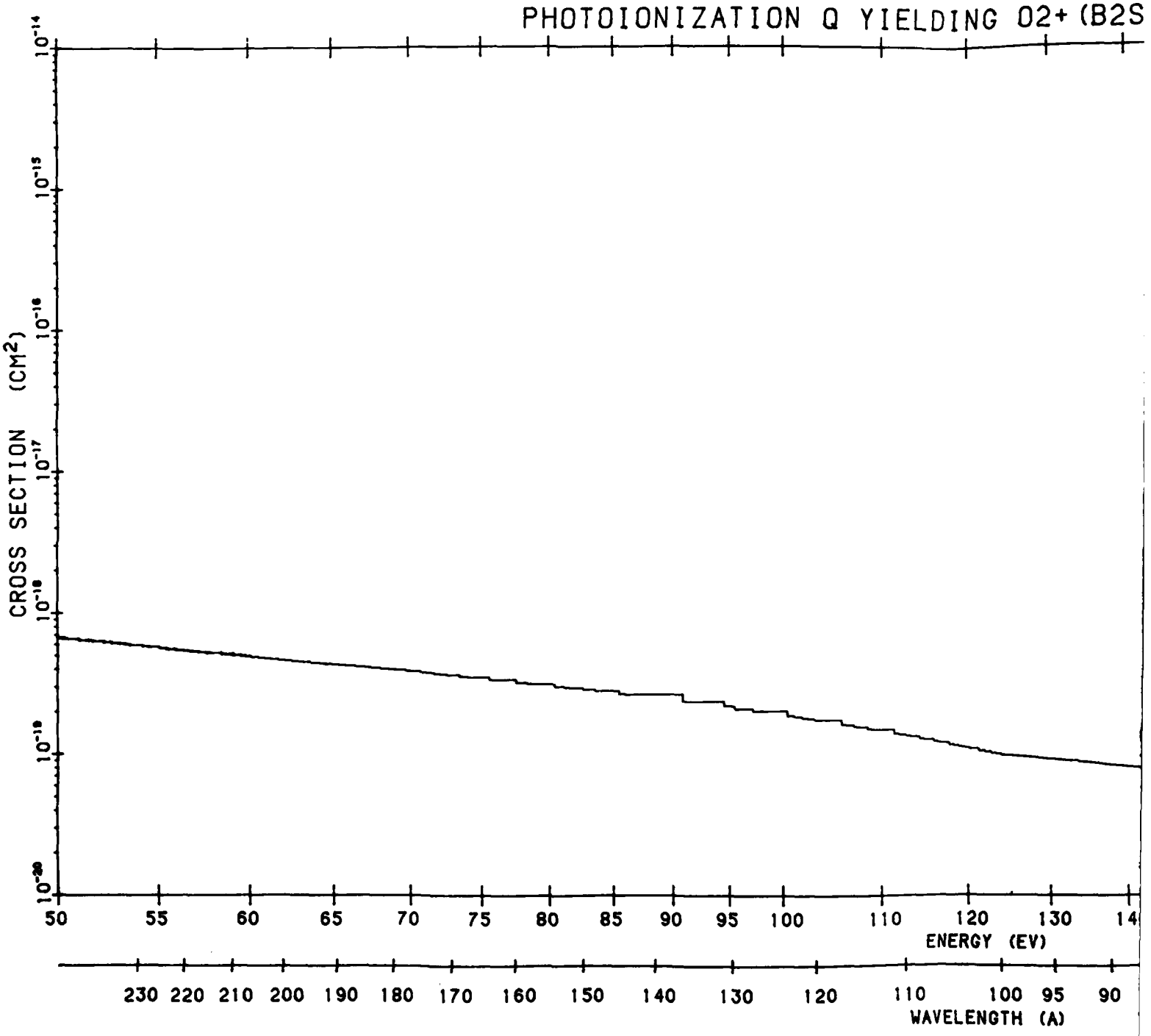
PHOTOIONIZATION Q YIELDING O2+ (B2S
CROSS SECTION (CM2)
10-14
10-15
10-16
10-17
10-18
10-19
10-20
50 55 60 65 70 75 80 85 90 95 100 110 120 130 14
ENERGY (EV)
230 220 210 200 190 180 170 160 150 140 130 120 110 100 95 90
WAVELENGTH (A)

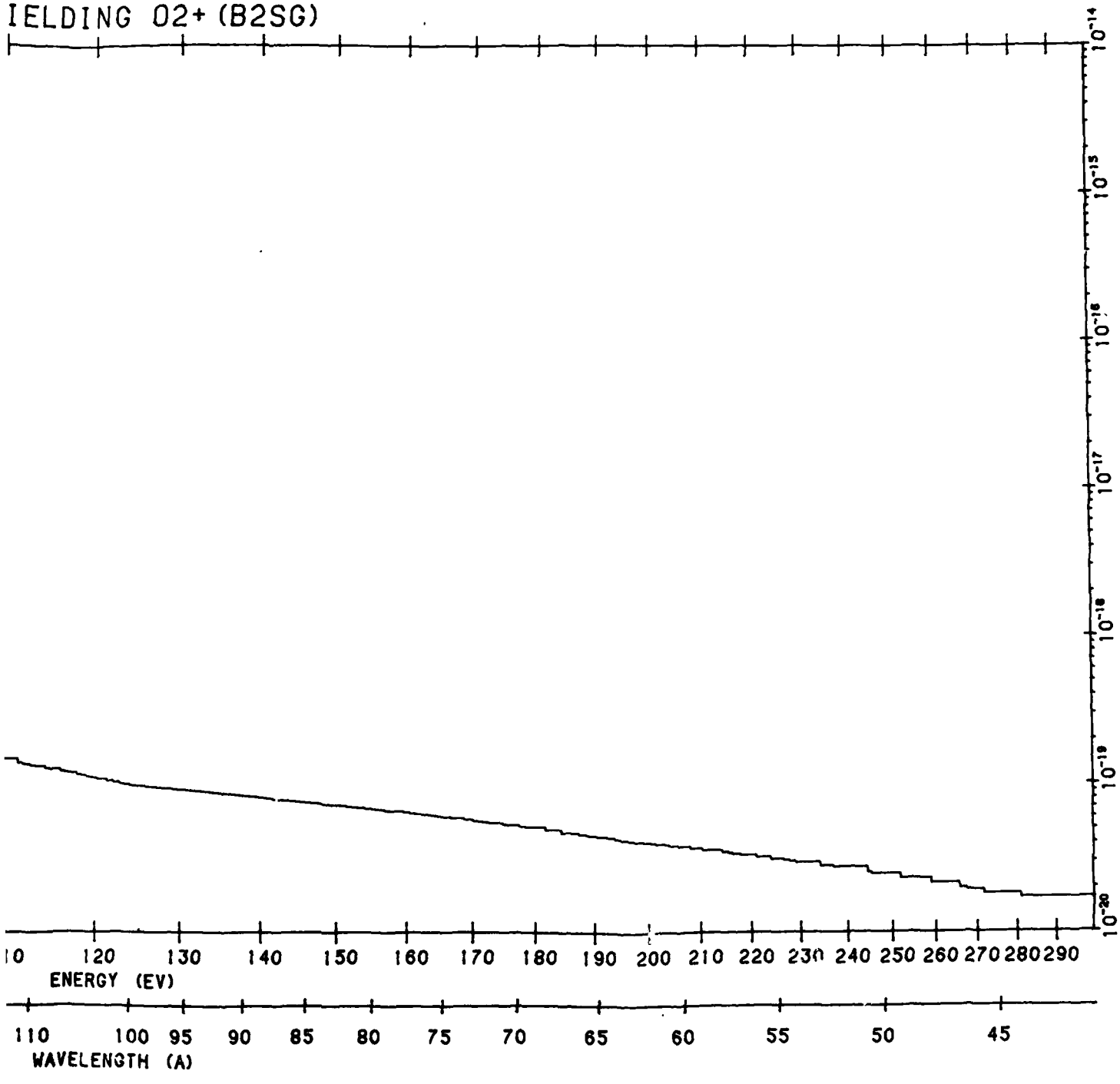


Figure B171. $O_2$ Photoionization Cross Section to $B\ ^2\Sigma_g^-$. The data source is the same as that of Figure B157 (Cont.)

2

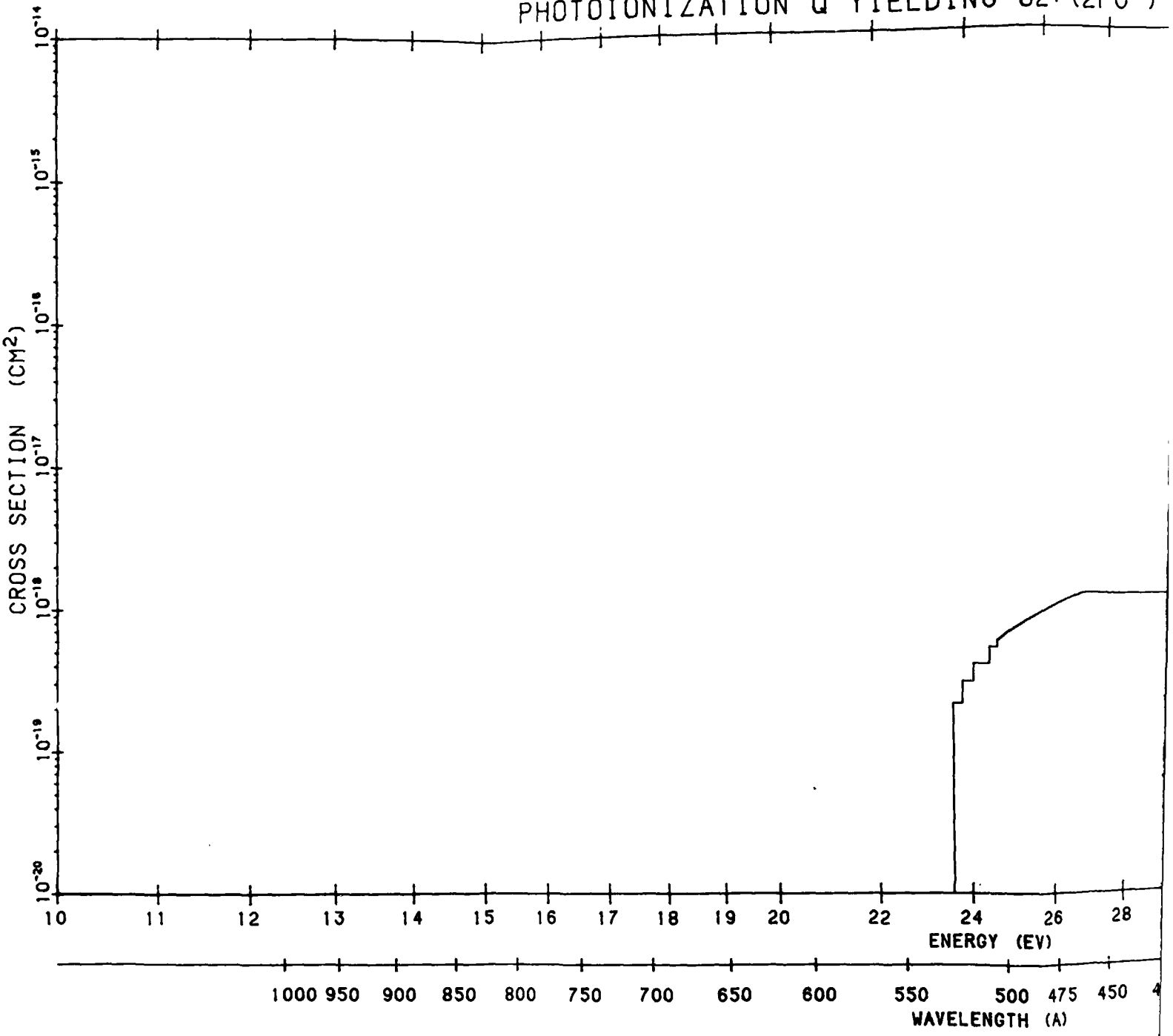
PHOTOIONIZATION Q YIELDING O2+ (2PU )
CROSS SECTION (CM2)
10-14
10-15
10-16
10-17
10-18
10-19
10-20
10 11 12 13 14 15 16 17 18 19 20 22 24 26 28
ENERGY (EV)
1000 950 900 850 800 750 700 650 600 550 500 475 450
WAVELENGTH (A)

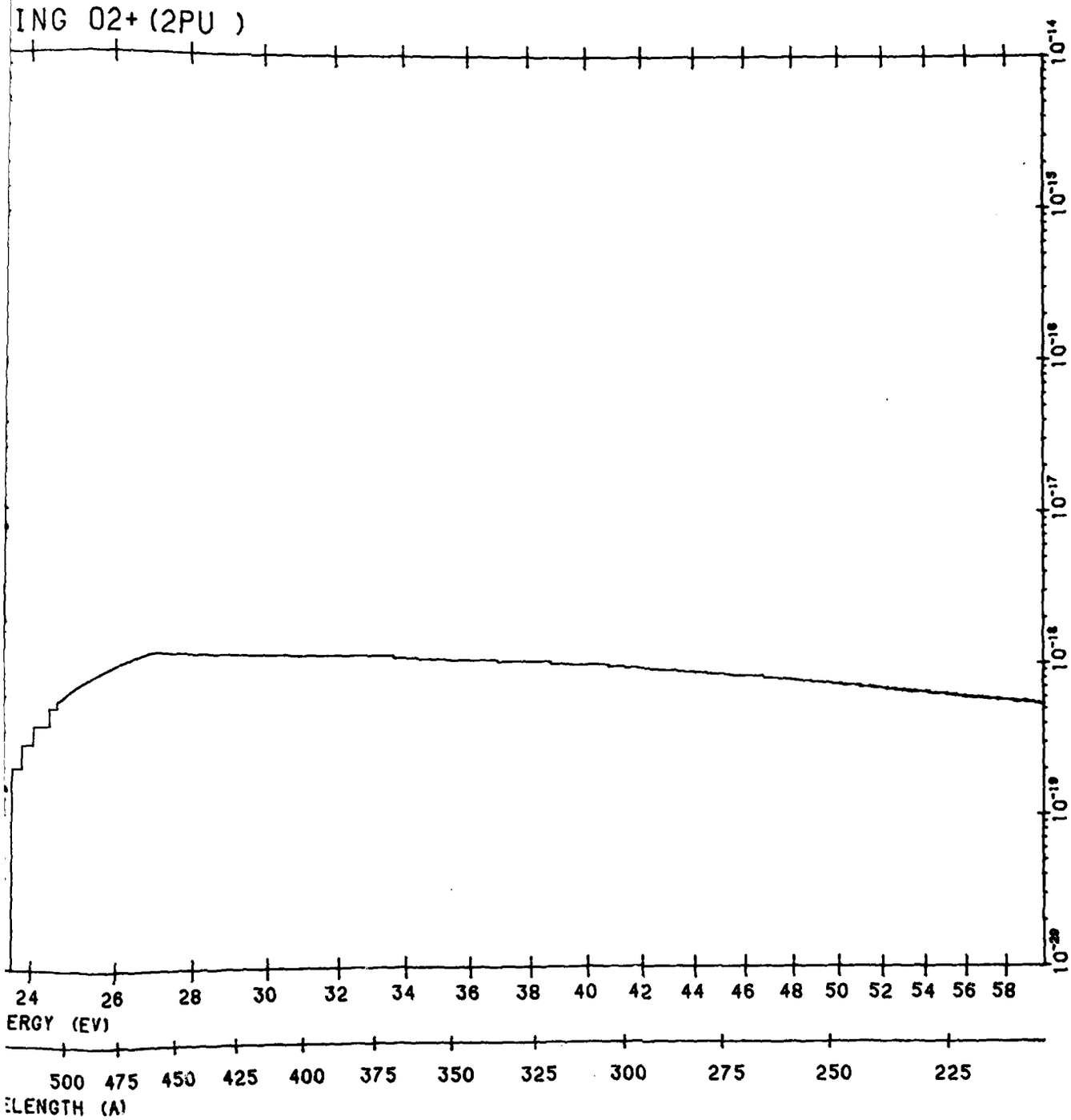


Figure B172. $O_2$ Photoionization Cross Section to $^2\Pi_u$. The data source is the same as that of Figure B157

2

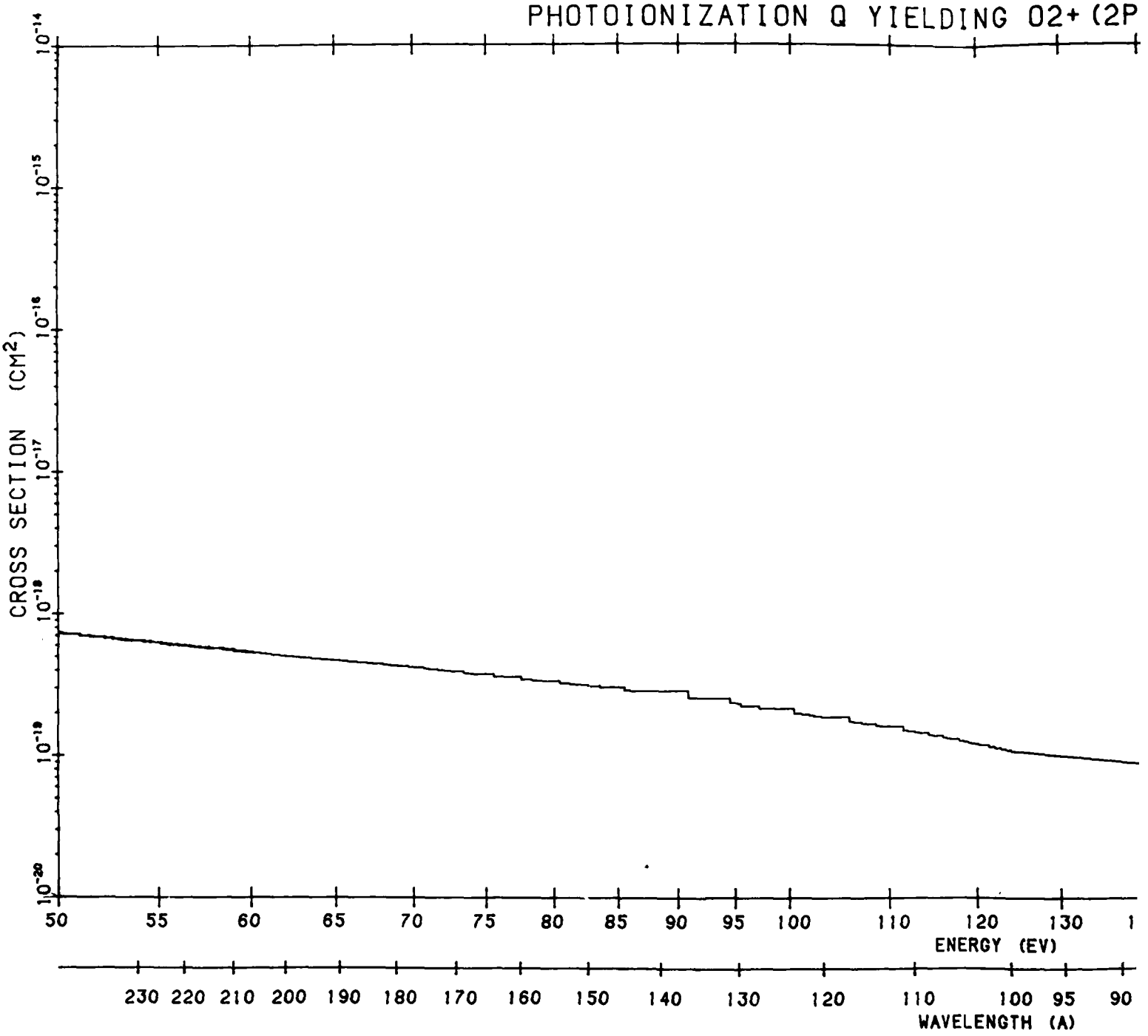
PHOTOIONIZATION Q YIELDING O2+ (2P
CROSS SECTION (CM2)
10-14
10-15
10-16
10-17
10-18
10-19
10-20
50 55 60 65 70 75 80 85 90 95 100 110 120 130 1
ENERGY (EV)
230 220 210 200 190 180 170 160 150 140 130 120 110 100 95 90
WAVELENGTH (A)

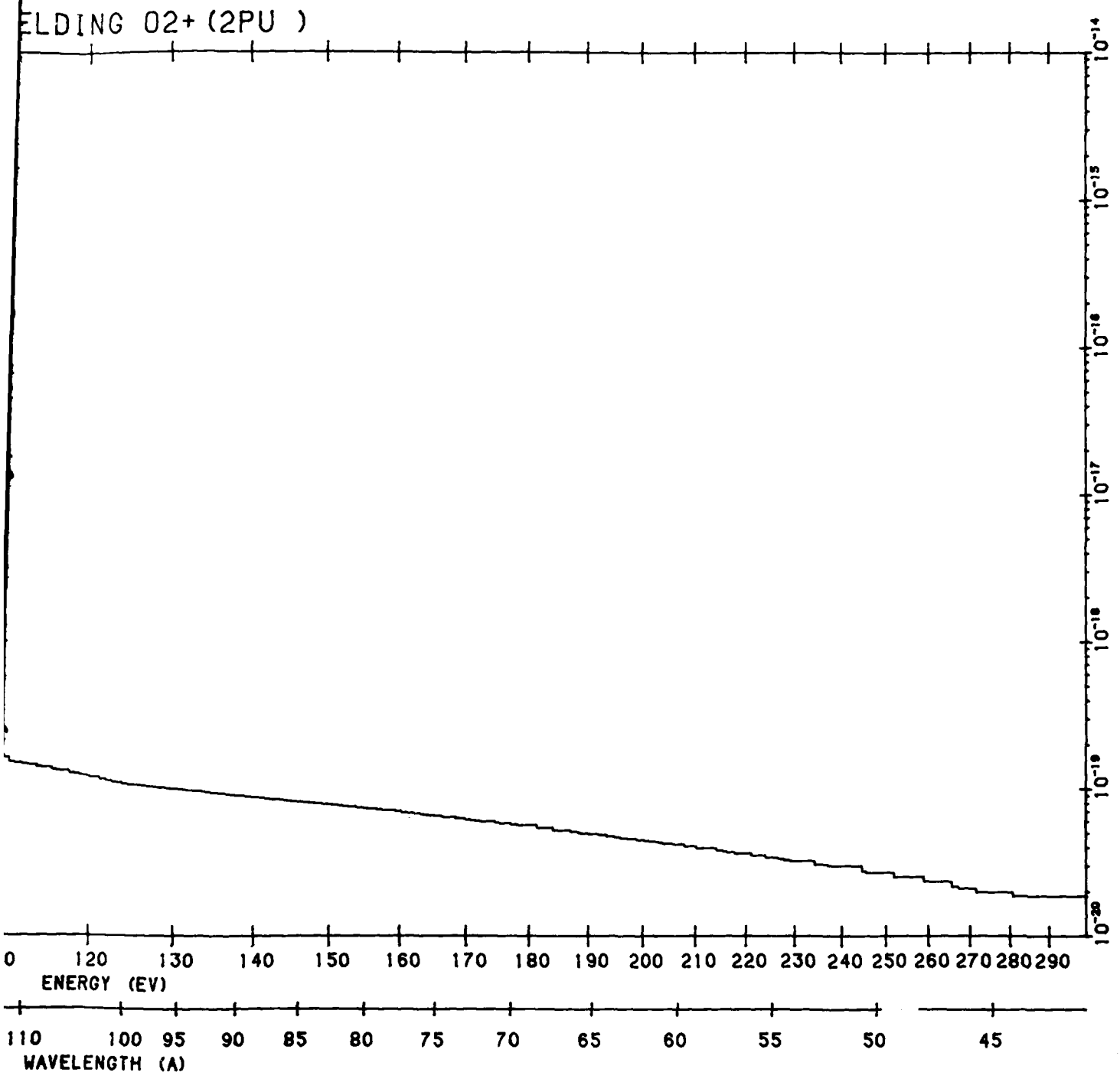


Figure B172. $O_2$ Photoionization Cross Section to $^2\Pi_u$. The data source is the same as that of Figure B157 (Cont.)

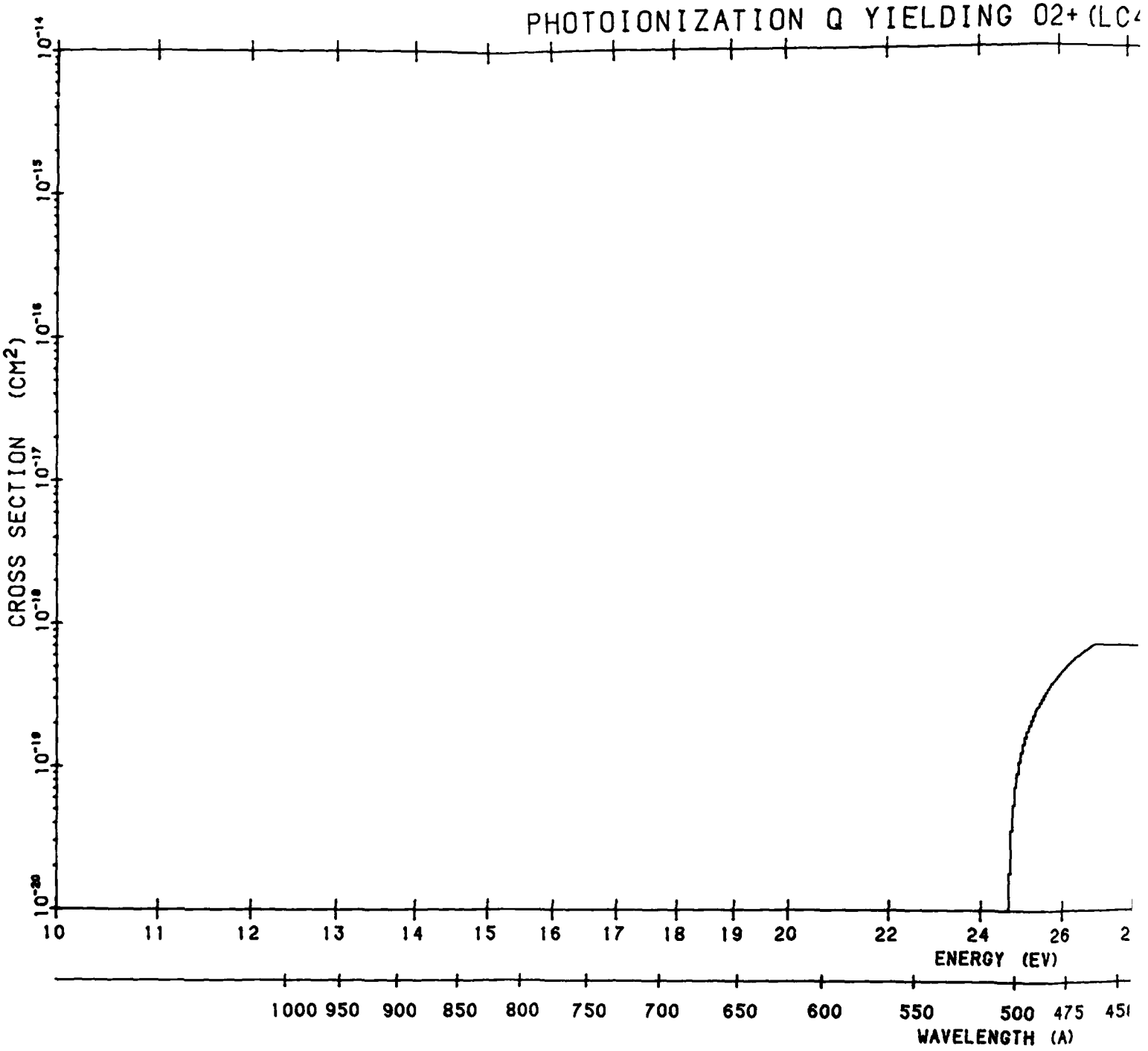
PHOTOIONIZATION Q YIELDING O2+ (LC
CROSS SECTION (CM2)
10-14
10-15
10-16
10-17
10-18
10-19
10-20
10 11 12 13 14 15 16 17 18 19 20 22 24 26 2
ENERGY (EV)
1000 950 900 850 800 750 700 650 600 550 500 475 45
WAVELENGTH (A)

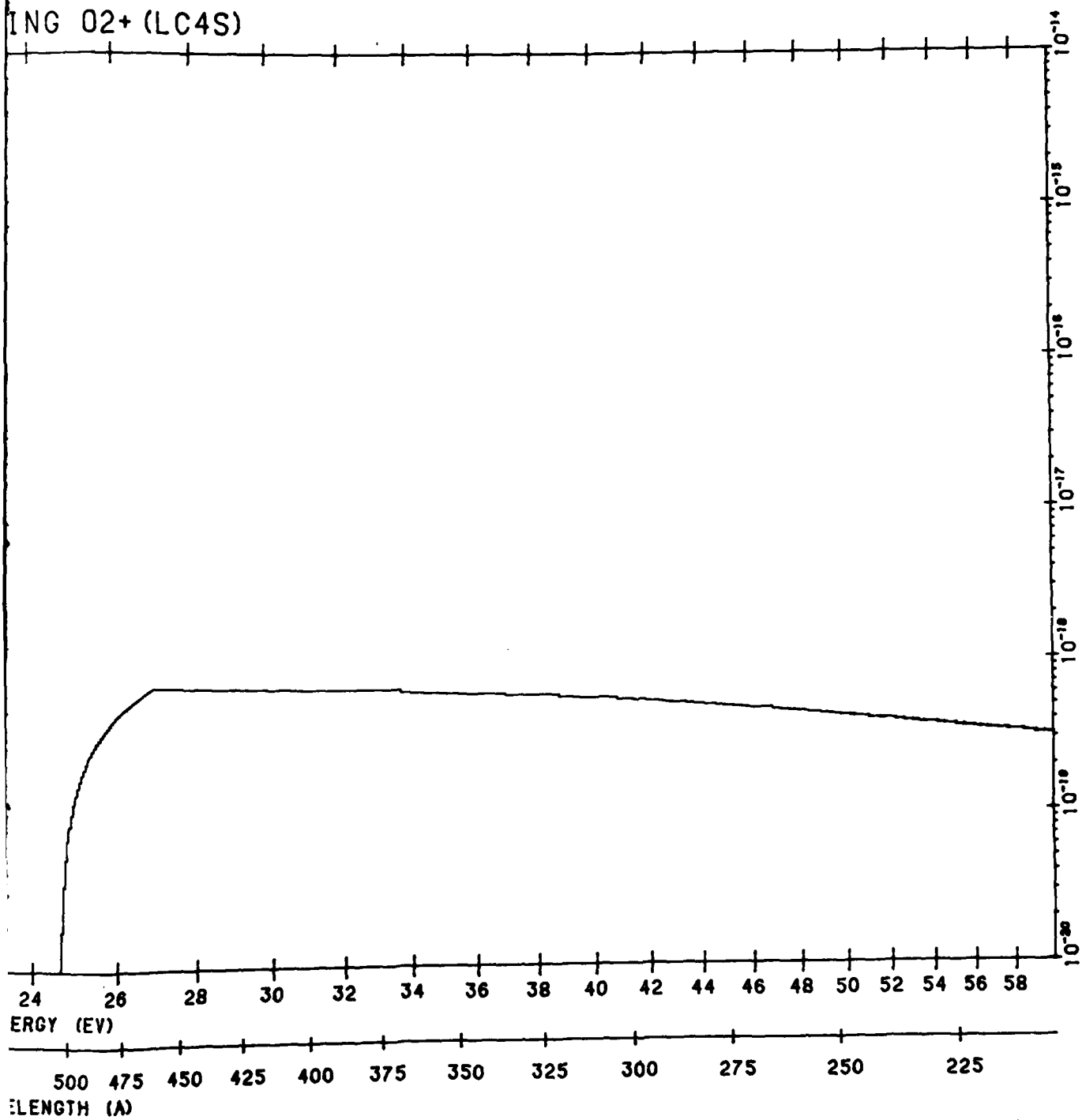


Figure B173. $O_2$ Photoionization Cross Section to c $^4\Sigma_u^-$. The data source is the same as that of Figure B157

2

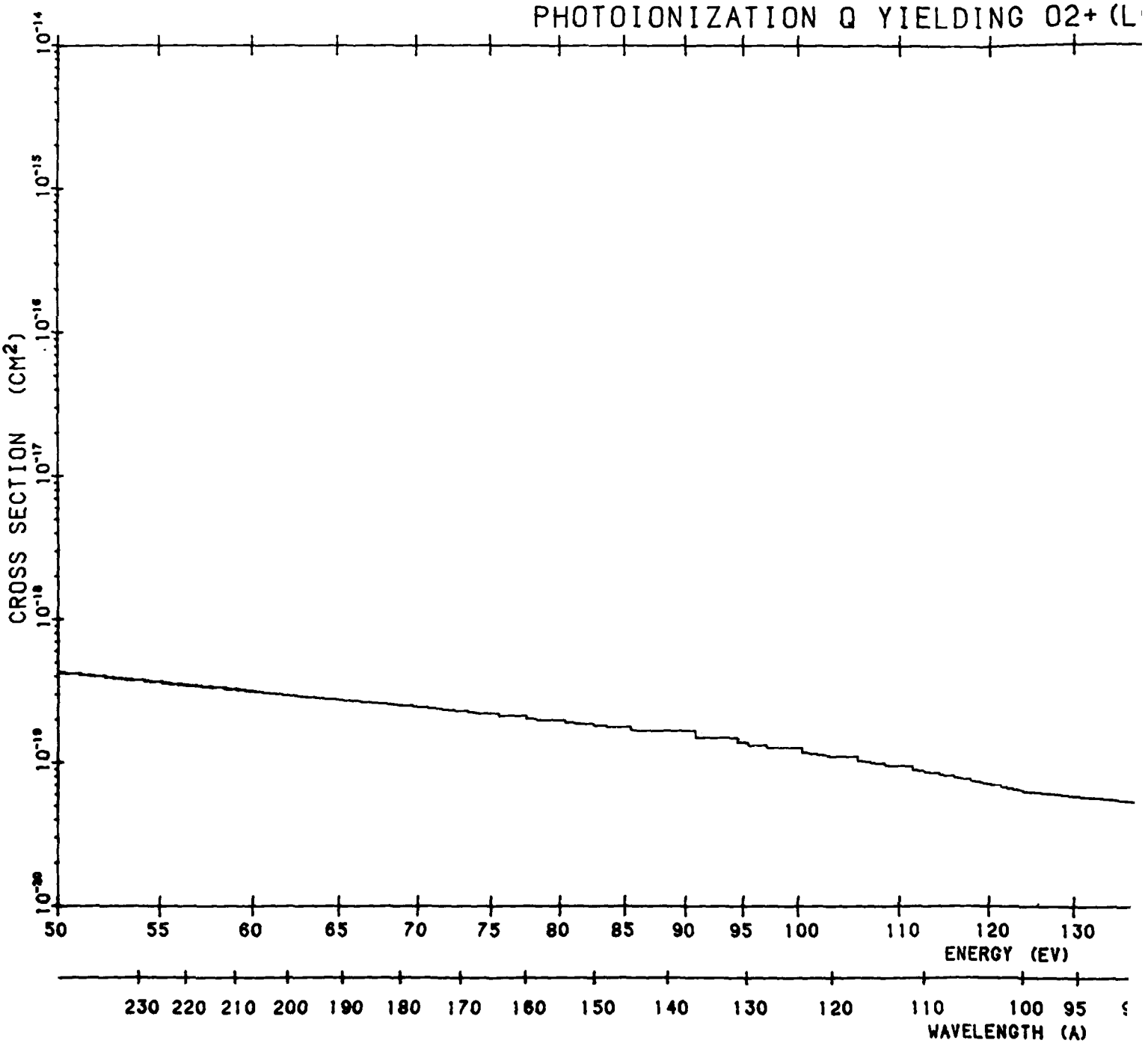
PHOTOIONIZATION Q YIELDING O2+ (L
CROSS SECTION (CM2)
10-14
10-15
10-16
10-17
10-18
10-19
10-20
50 55 60 65 70 75 80 85 90 95 100 110 120 130
ENERGY (EV)
230 220 210 200 190 180 170 160 150 140 130 120 110 100 95
WAVELENGTH (A)

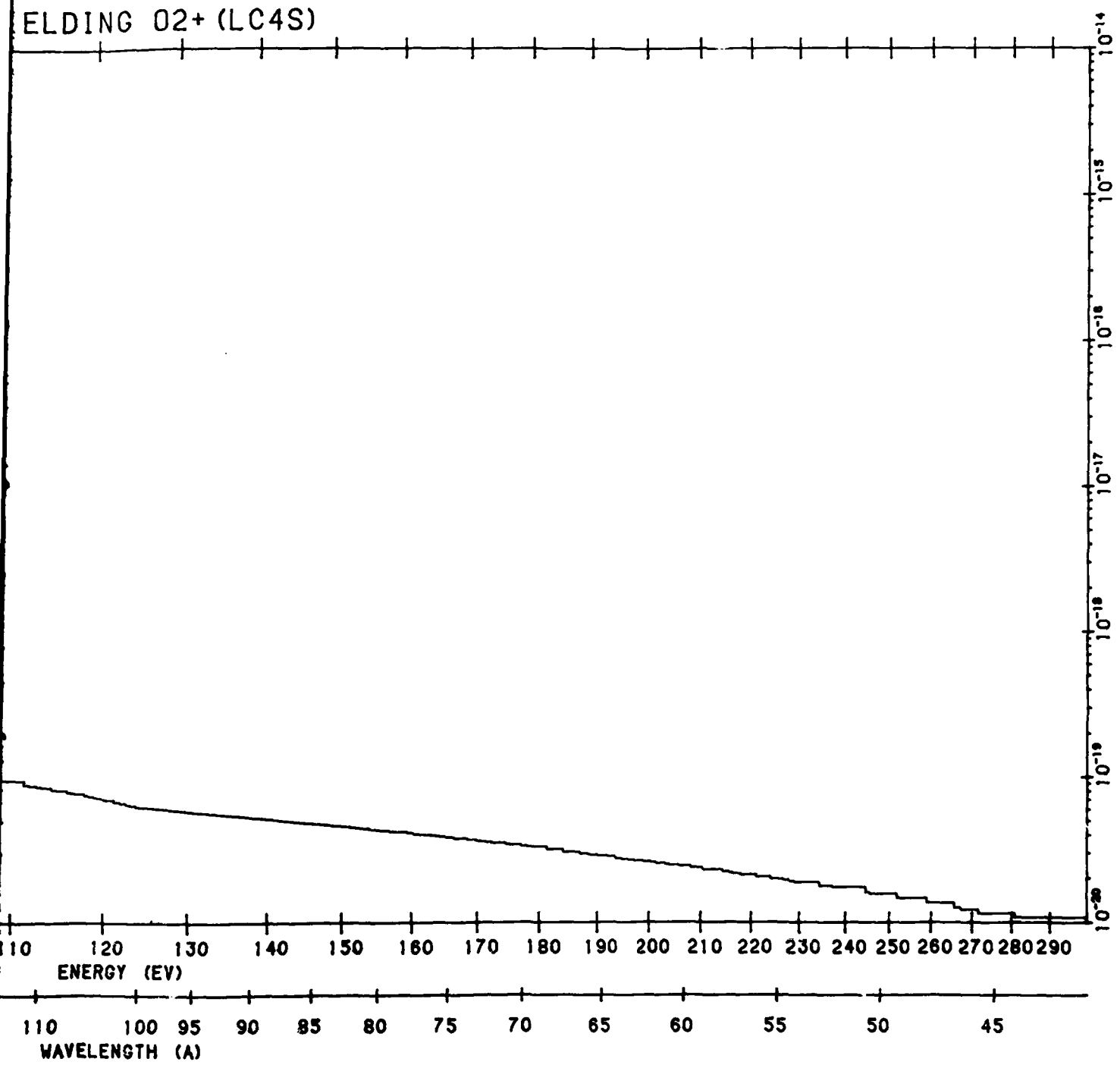


Figure B173. $O_2$ Photoionization Cross Section to c $^4\Sigma_u^-$. The data source is the same as that of Figure B157 (Cont.)

2

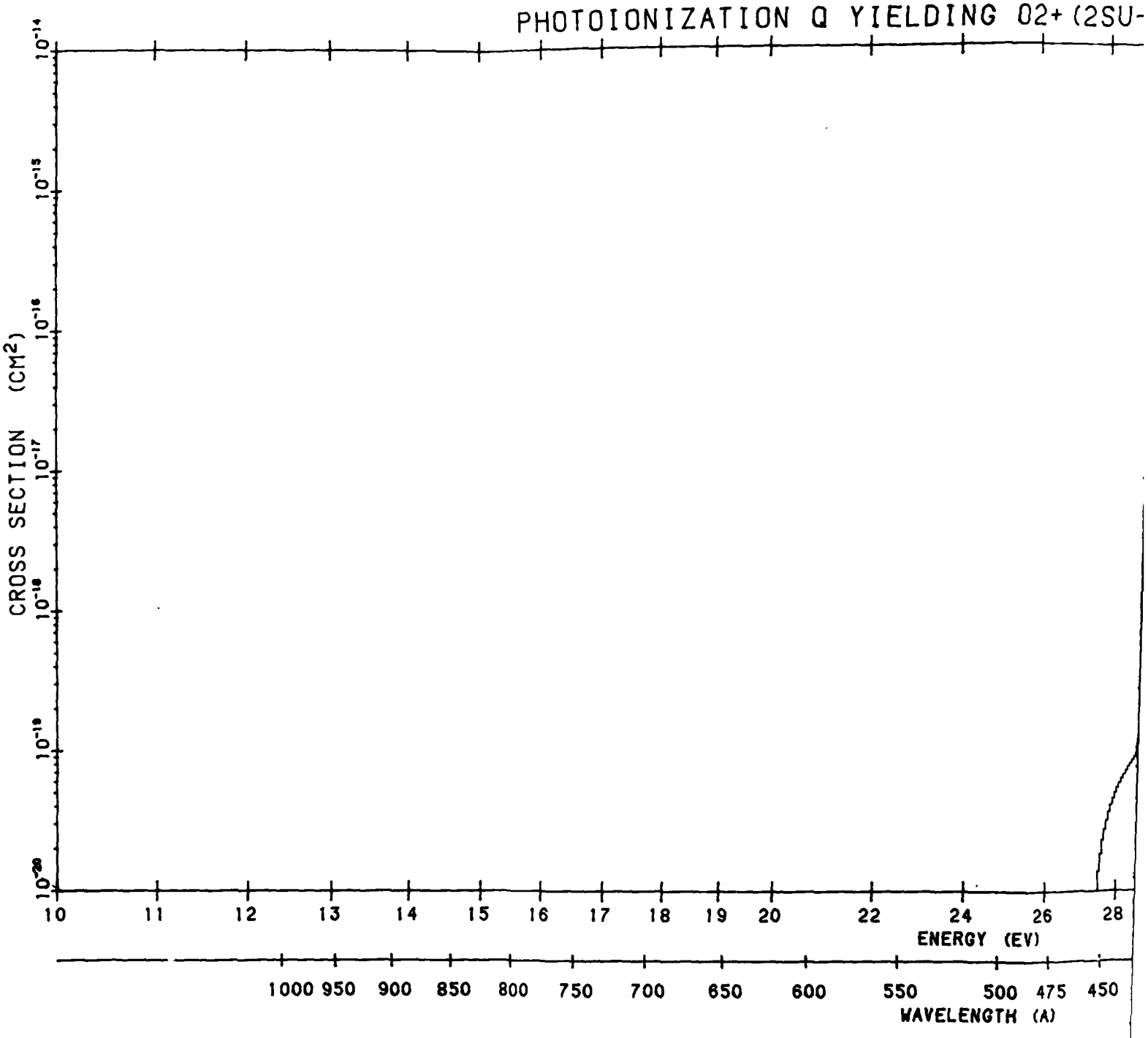
PHOTOIONIZATION Q YIELDING O2+ (2SU-
CROSS SECTION (CM2)
10-14
10-15
10-16
10-17
10-18
10-19
10-20
10 11 12 13 14 15 16 17 18 19 20 22 24 26 28
ENERGY (EV)
1000 950 900 850 800 750 700 650 600 550 500 475 450
WAVELENGTH (A)

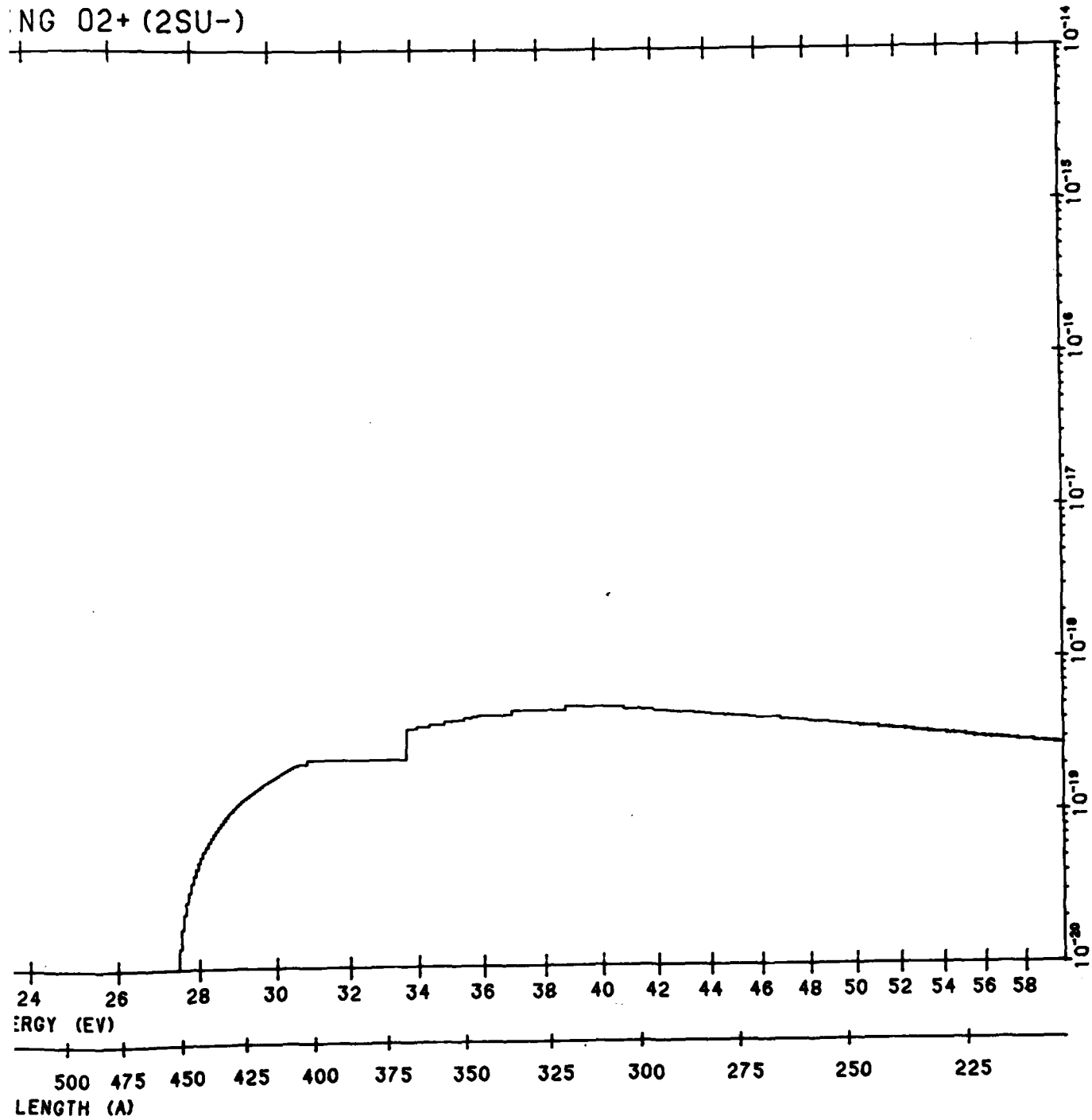


Figure B174. $O_2$ Photoionization Cross Section to $^2\Sigma_u^-$. The data source is the same as that of Figure B157

2

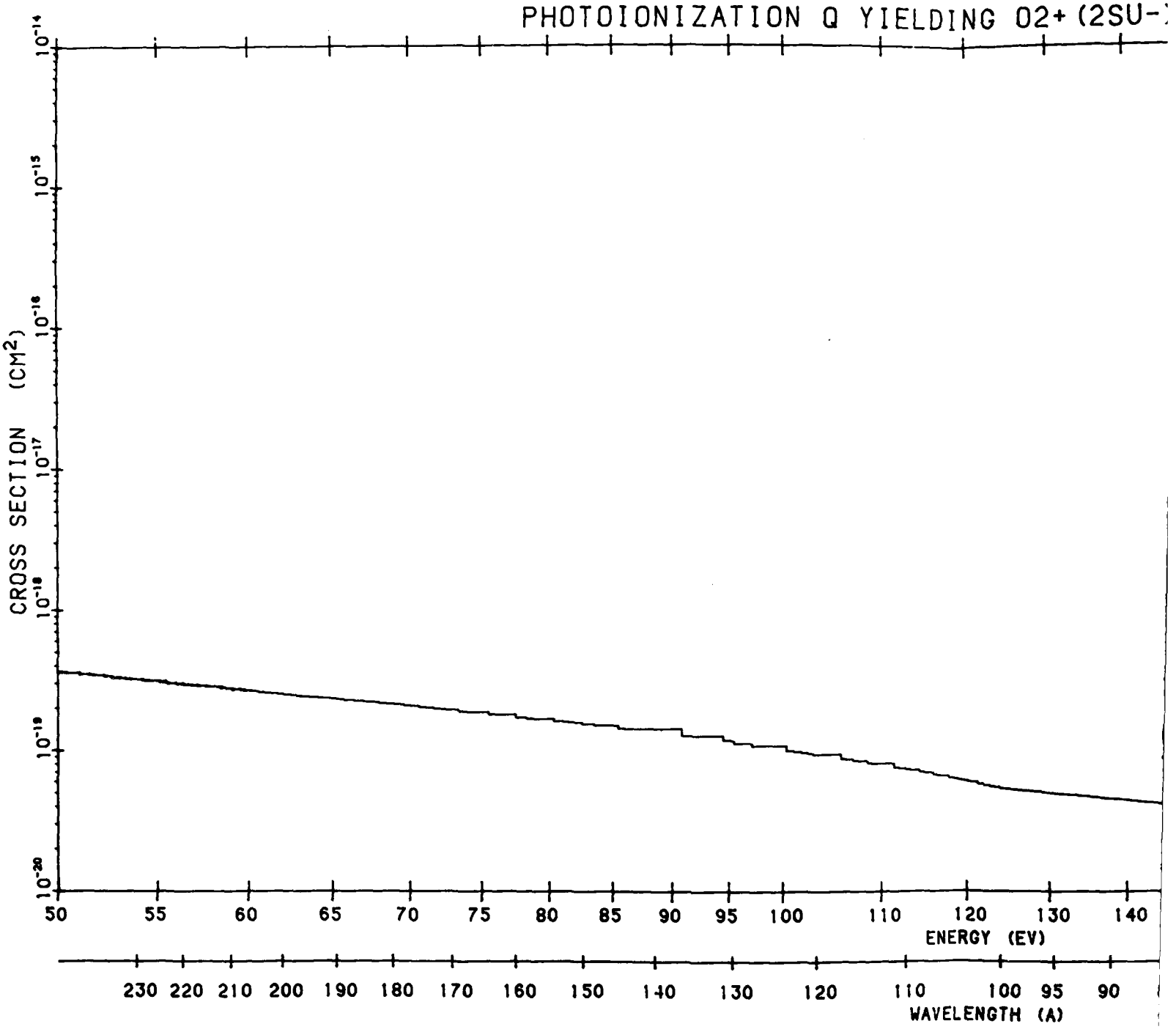
PHOTOIONIZATION Q YIELDING O2+ (2SU-)
CROSS SECTION (CM2)
10-14
10-15
10-16
10-17
10-18
10-19
10-20
50 55 60 65 70 75 80 85 90 95 100 110 120 130 140
ENERGY (EV)
230 220 210 200 190 180 170 160 150 140 130 120 110 100 95 90
WAVELENGTH (A)

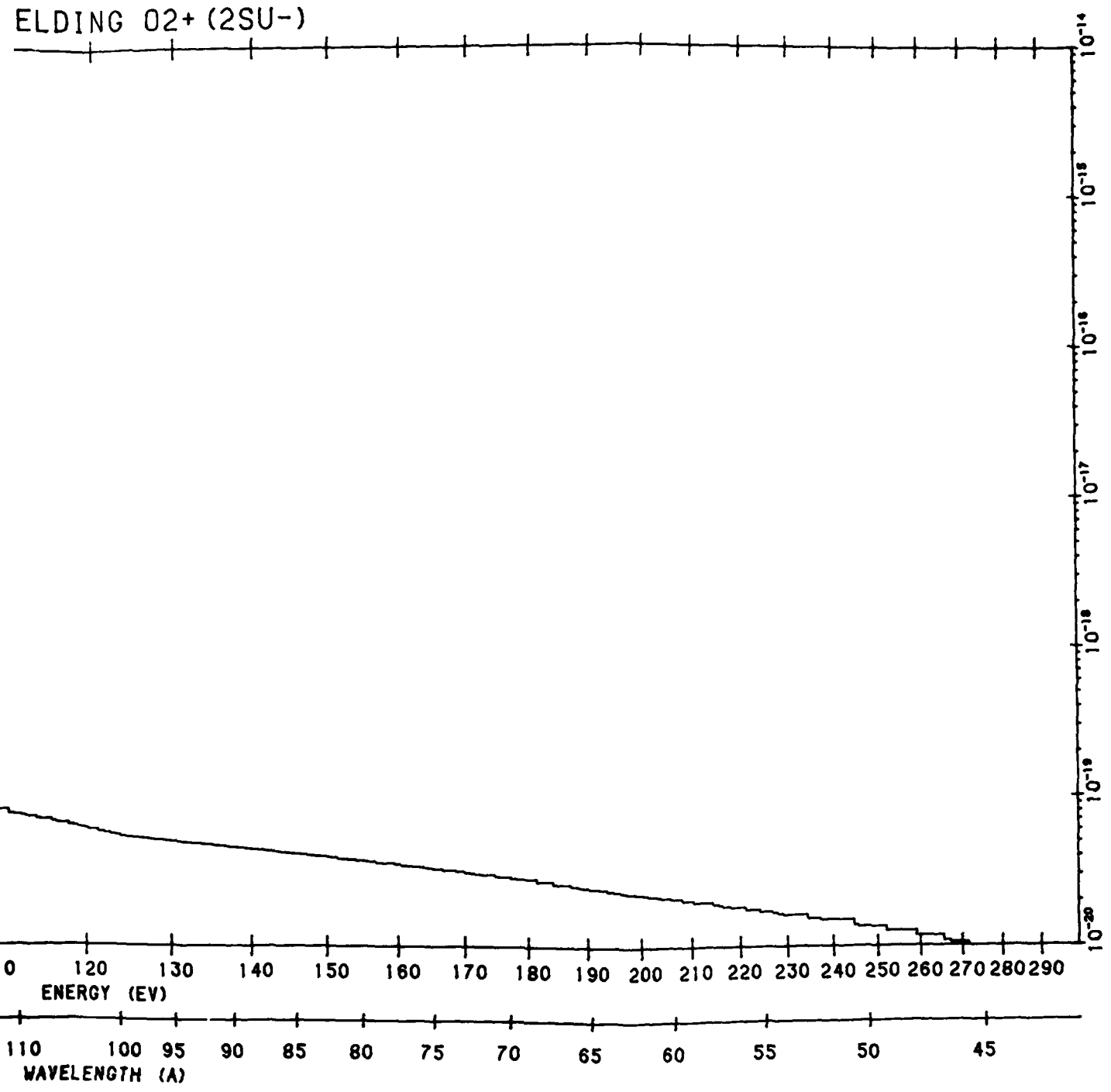


Figure B174. $O_2$ Photoionization Cross Section to $^2\Sigma_u^-$. The data source is the same as that of Figure B157 (Cont.)

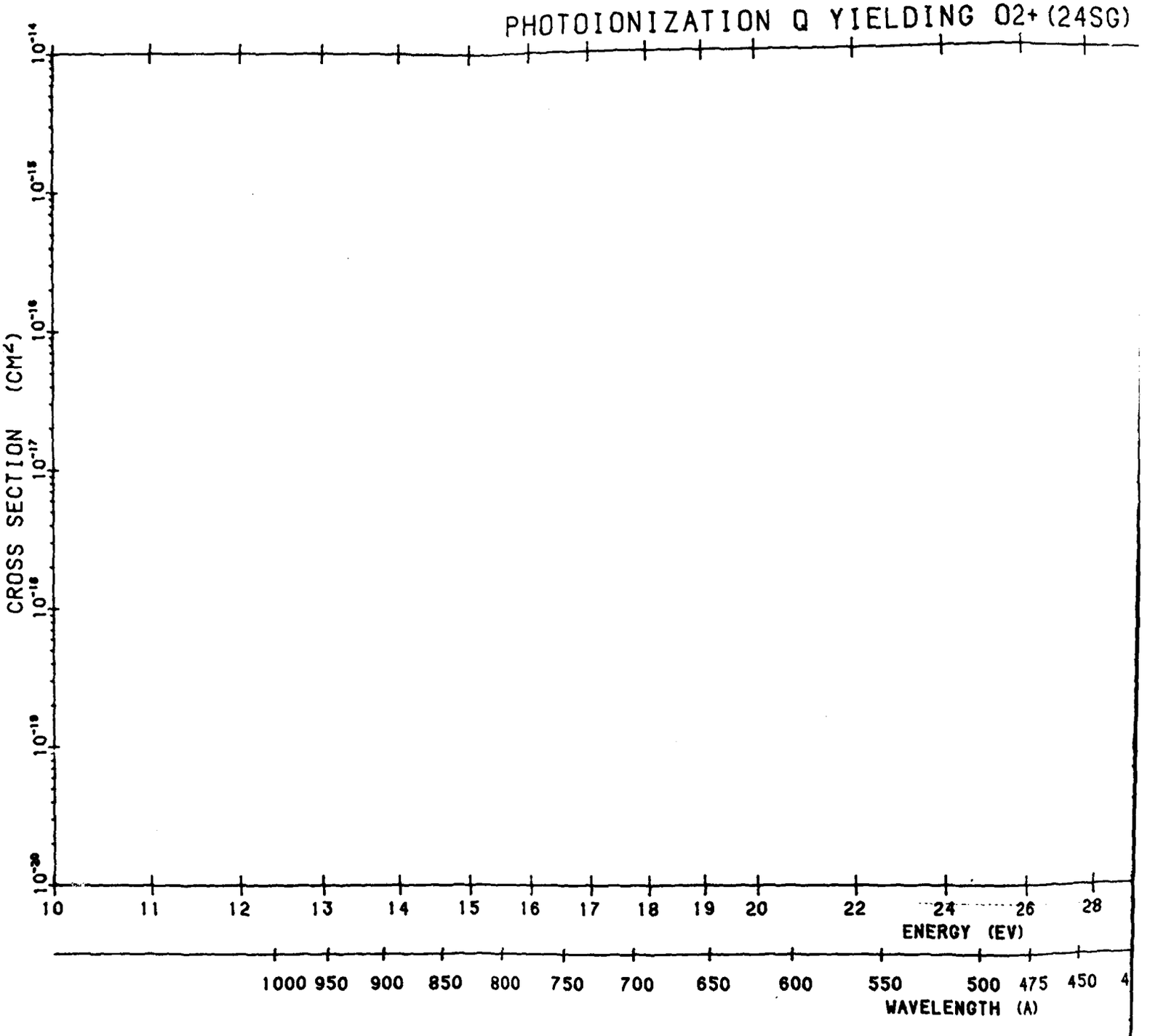
PHOTOIONIZATION Q YIELDING O2+ (2⁴SG)
CROSS SECTION (CM²)
10⁻¹⁴
10⁻¹⁵
10⁻¹⁶
10⁻¹⁷
10⁻¹⁸
10⁻¹⁹
10⁻²⁰
10 11 12 13 14 15 16 17 18 19 20 22 24 26 28
ENERGY (EV)
1000 950 900 850 800 750 700 650 600 550 500 475 450
WAVELENGTH (A)

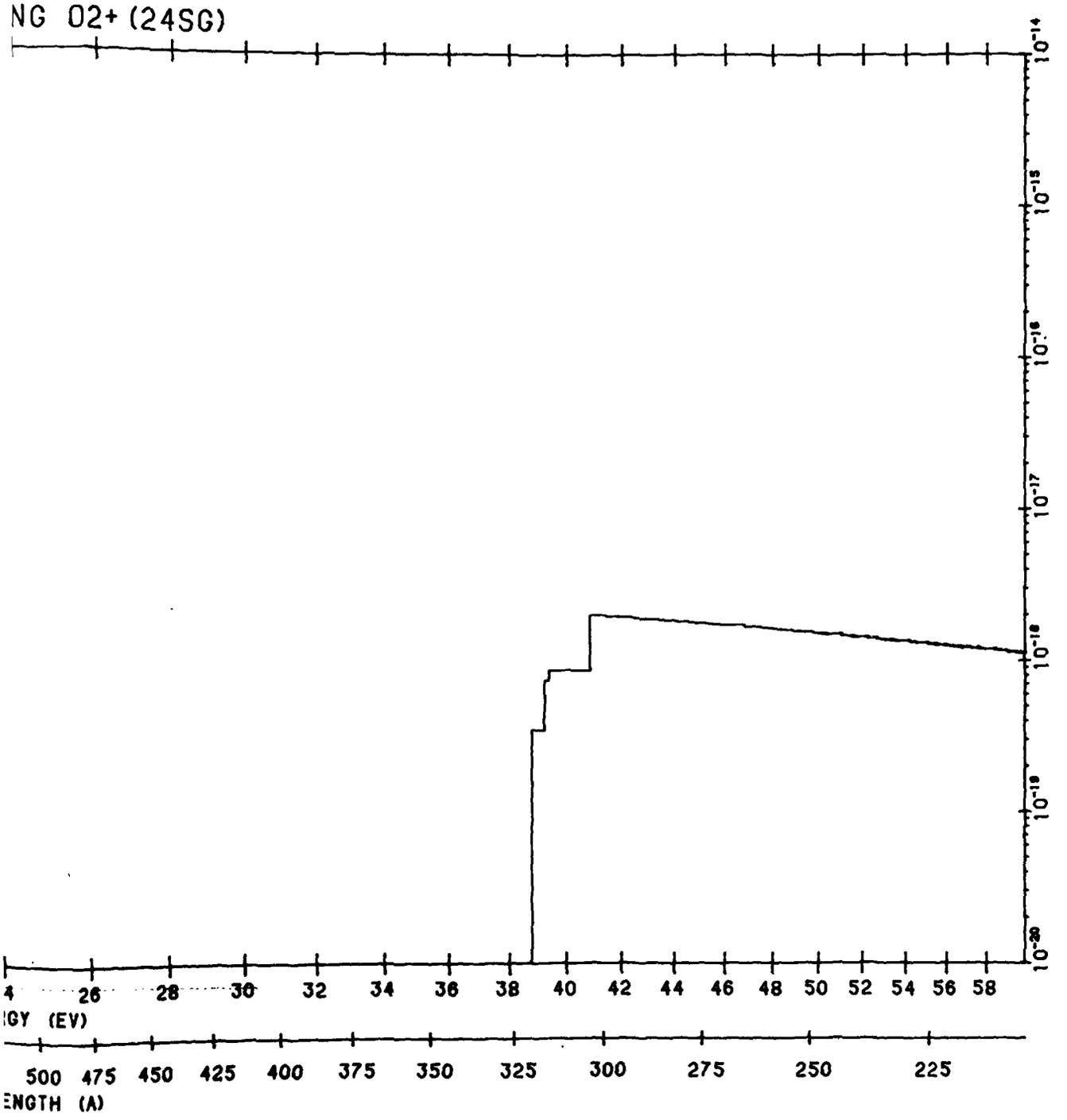


Figure B175. $O_2$ Photoionization Cross Section to $^{2,4}\Sigma_g^-$. The data source is the same as that of Figure B157

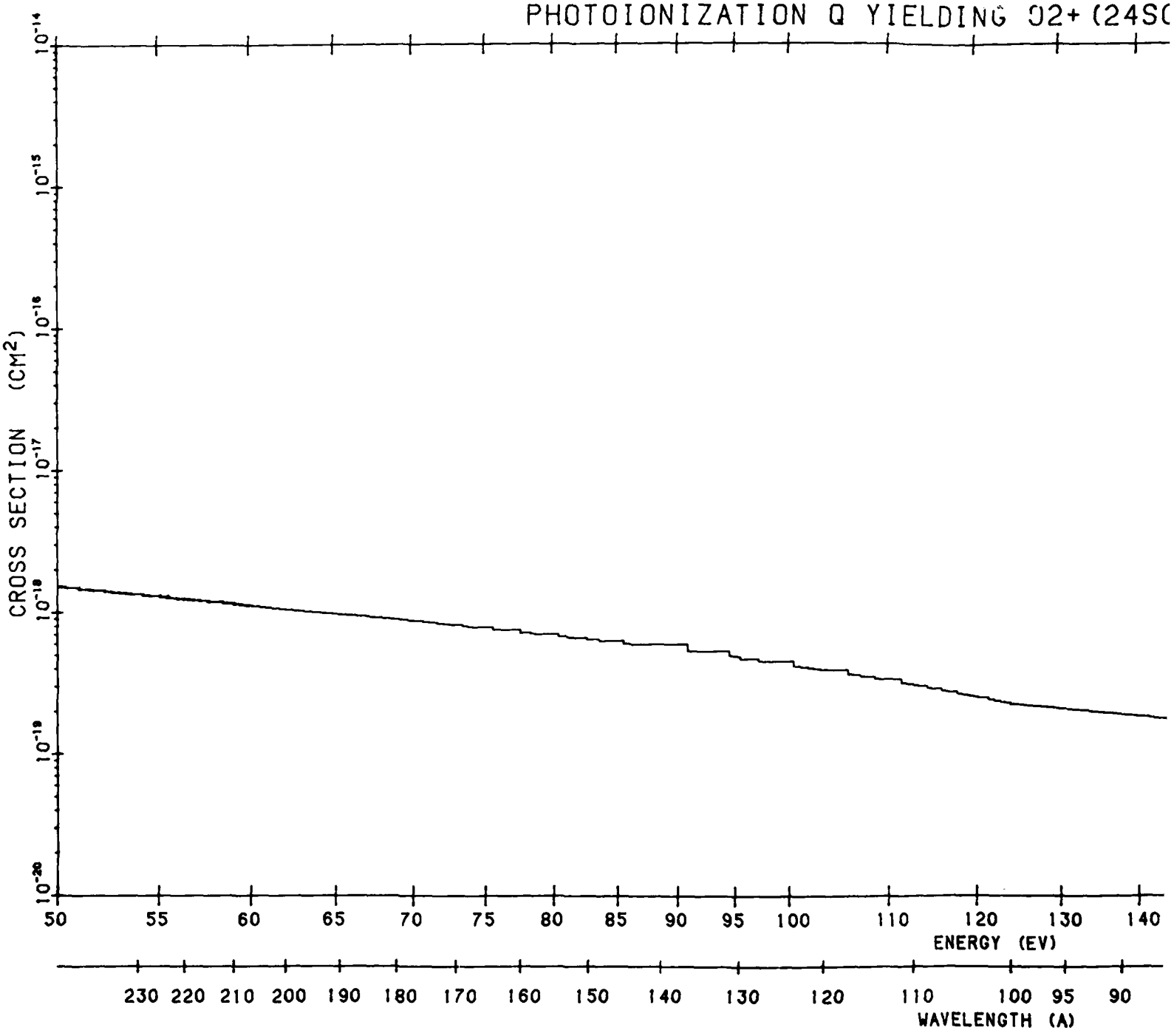
PHOTOIONIZATION Q YIELDING O2+ (24SC
CROSS SECTION (CM2)
10-14
10-15
10-16
10-17
10-18
10-19
10-20
50 55 60 65 70 75 80 85 90 95 100 110 120 130 140
ENERGY (EV)
230 220 210 200 190 180 170 160 150 140 130 120 110 100 95 90
WAVELENGTH (A)

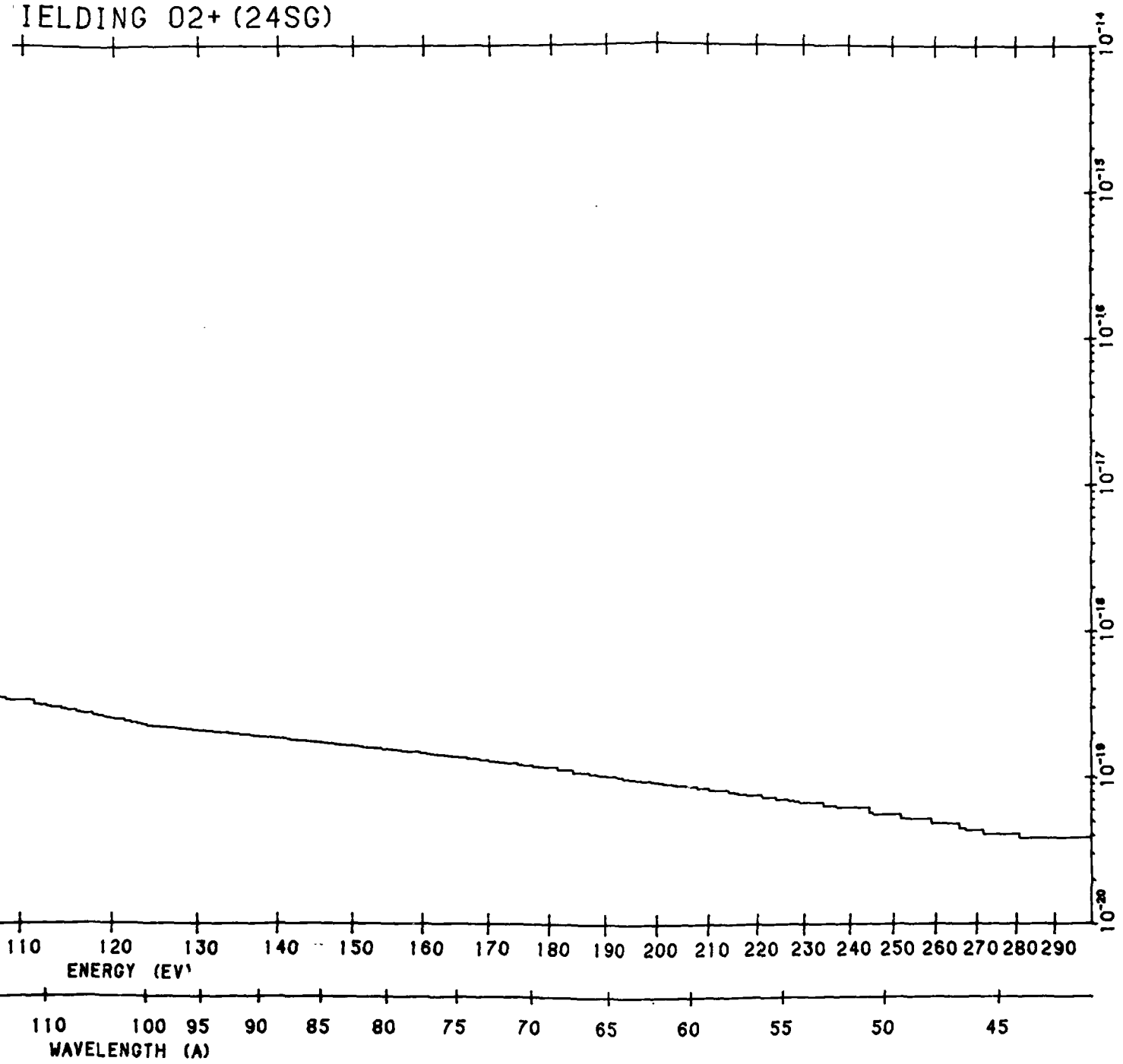


Figure B175. $O_2$ Photoionization Cross Section to $^{2,4}\Sigma_g^-$. The data source is the same as that of Figure B157 (Cont.)

2

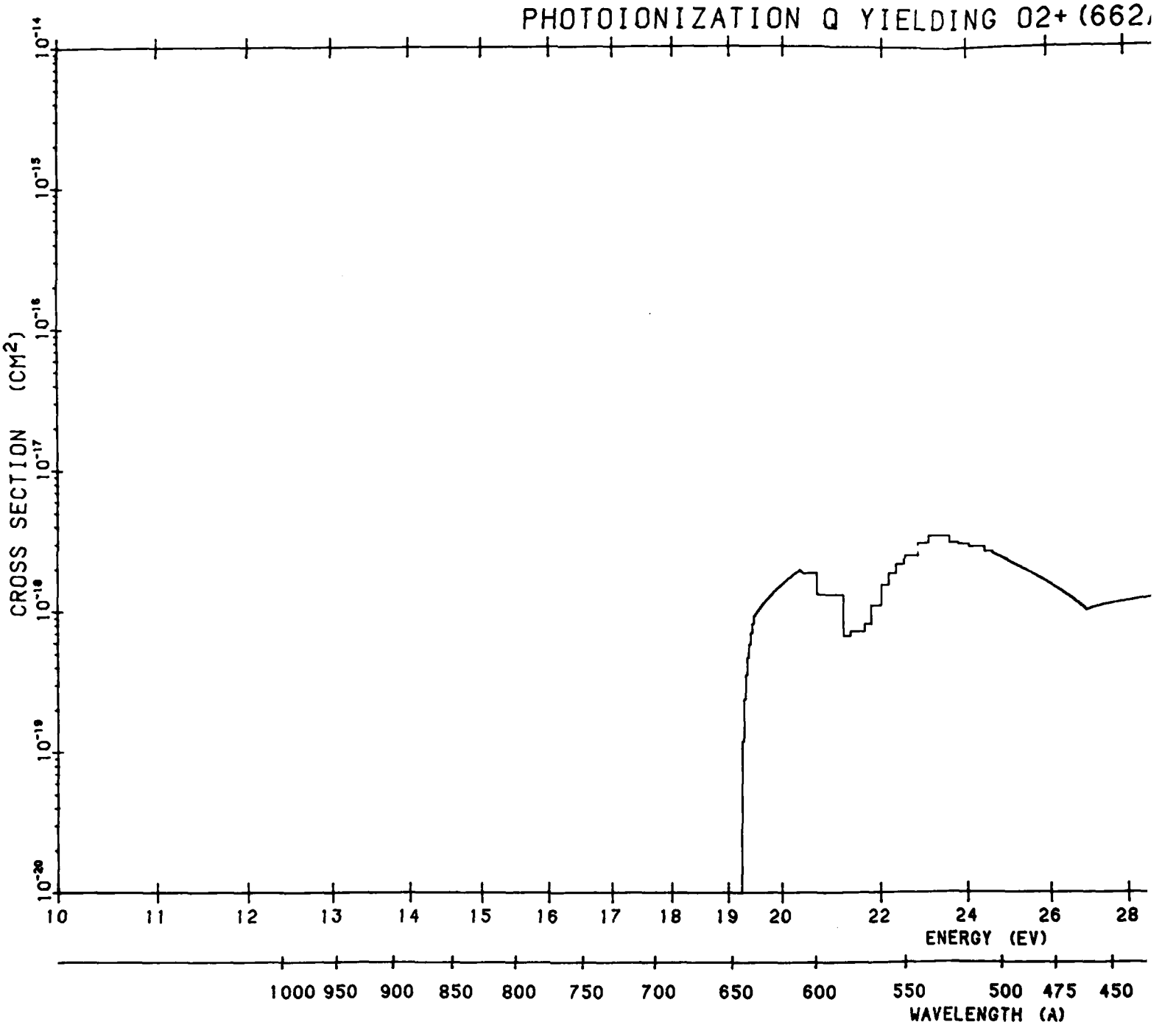
PHOTOIONIZATION Q YIELDING O2+ (662
CROSS SECTION (CM2)
10-14
10-15
10-16
10-17
10-18
10-19
10-20
10 11 12 13 14 15 16 17 18 19 20 22 24 26 28
ENERGY (EV)
1000 950 900 850 800 750 700 650 600 550 500 475 450
WAVELENGTH (A)

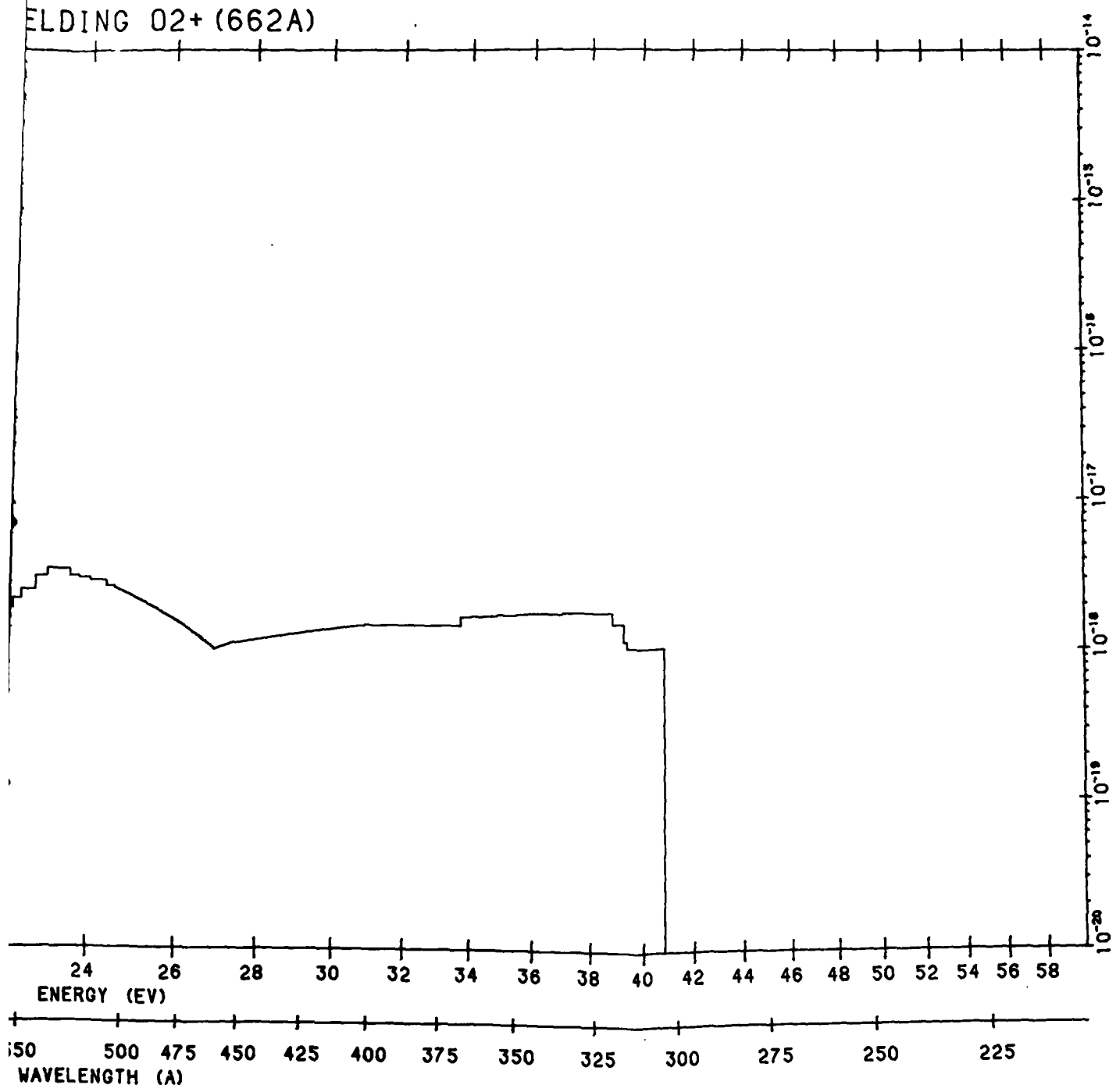


Figure B176. $O_2$ Dissociative Photoionization Cross Section. The data source is the same as that of Figure B157

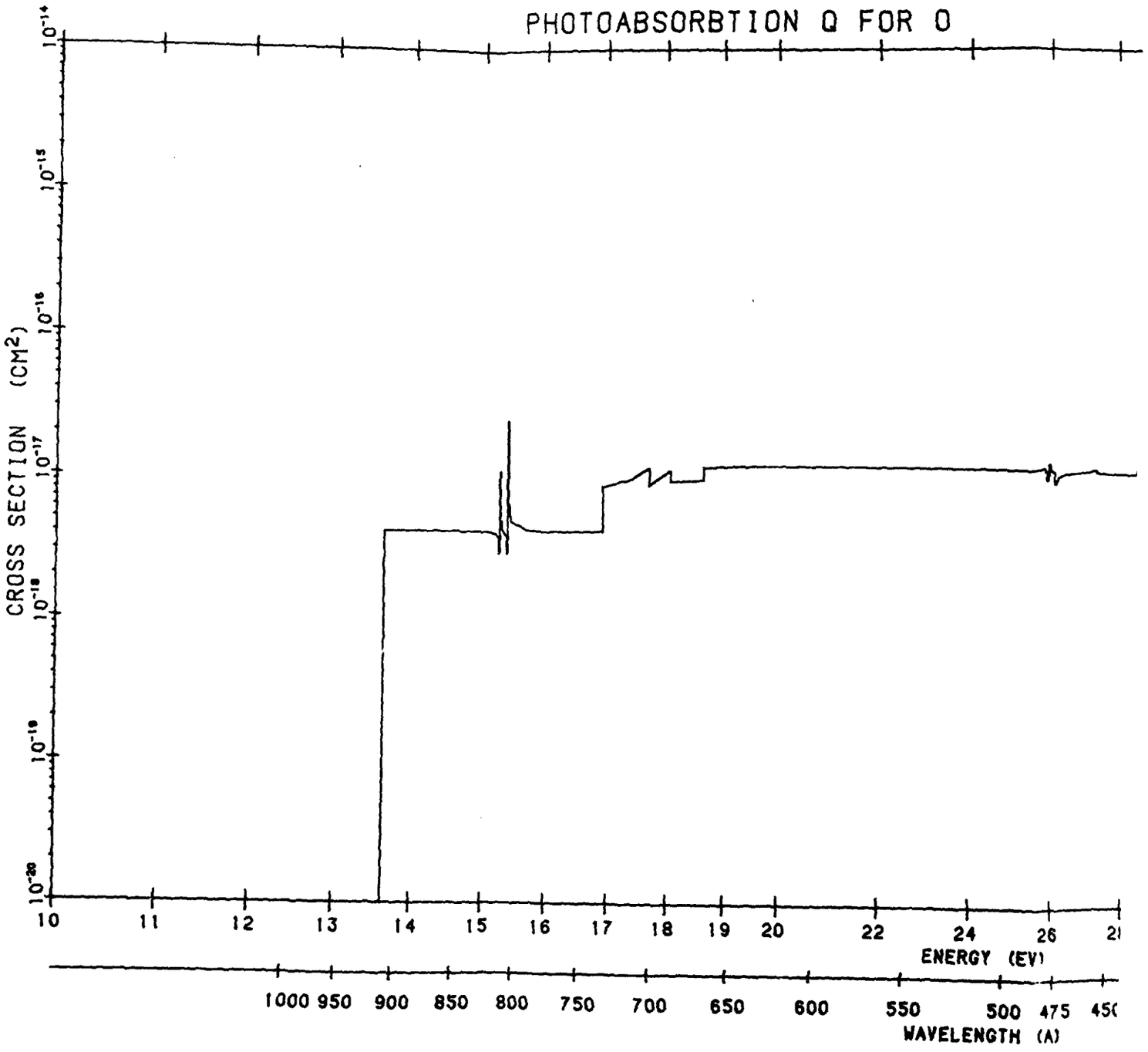
PHOTOABSORBTION Q FOR O
CROSS SECTION (CM2)
10-14
10-15
10-16
10-17
10-18
10-19
10-20
10 11 12 13 14 15 16 17 18 19 20 22 24 26
ENERGY (EV)
1000 950 900 850 800 750 700 650 600 550 500 475
WAVELENGTH (A)

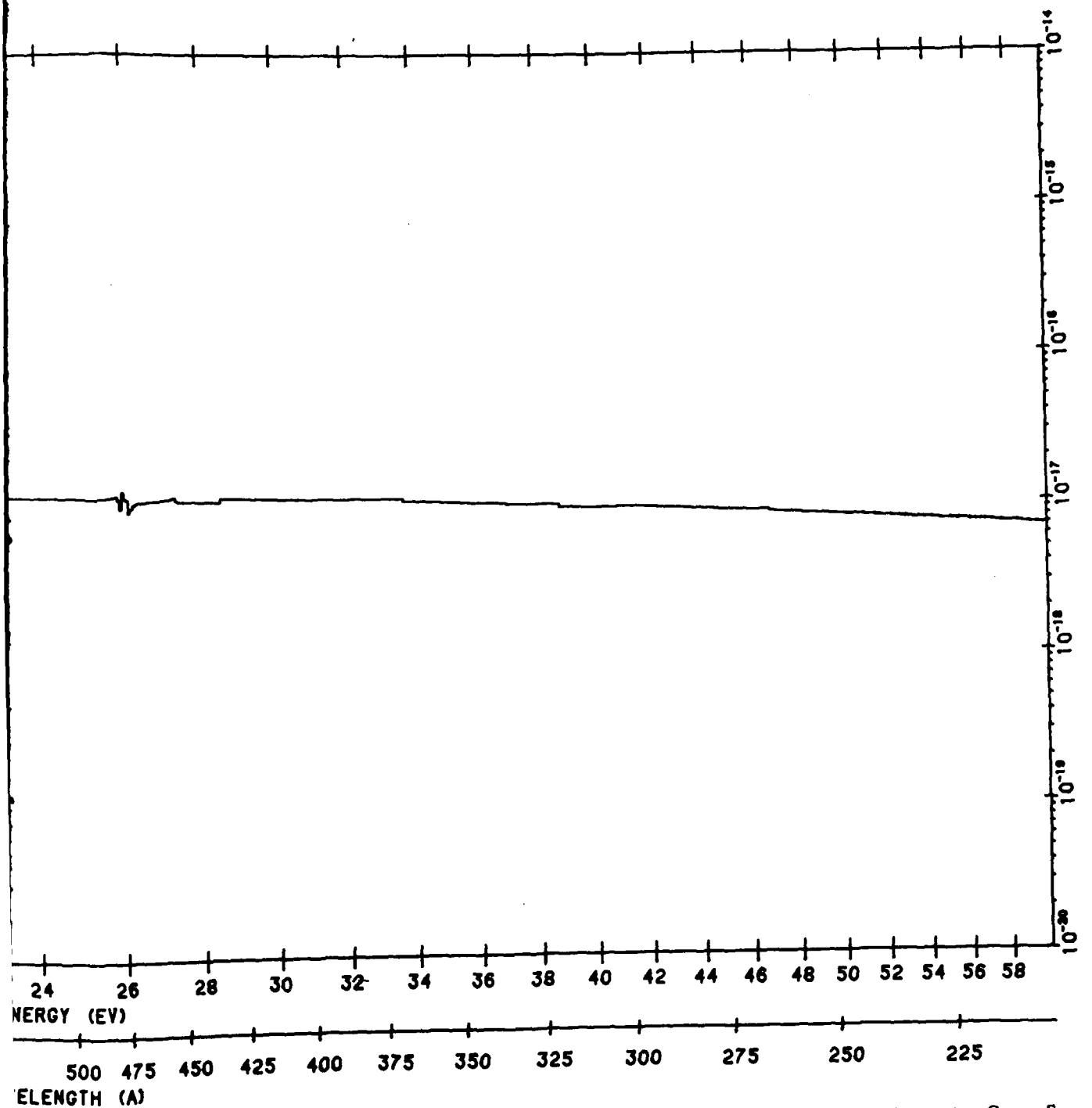


Figure B177. O Total Photoabsorption Cross Section. The data source is the same as that of Figure B157

2

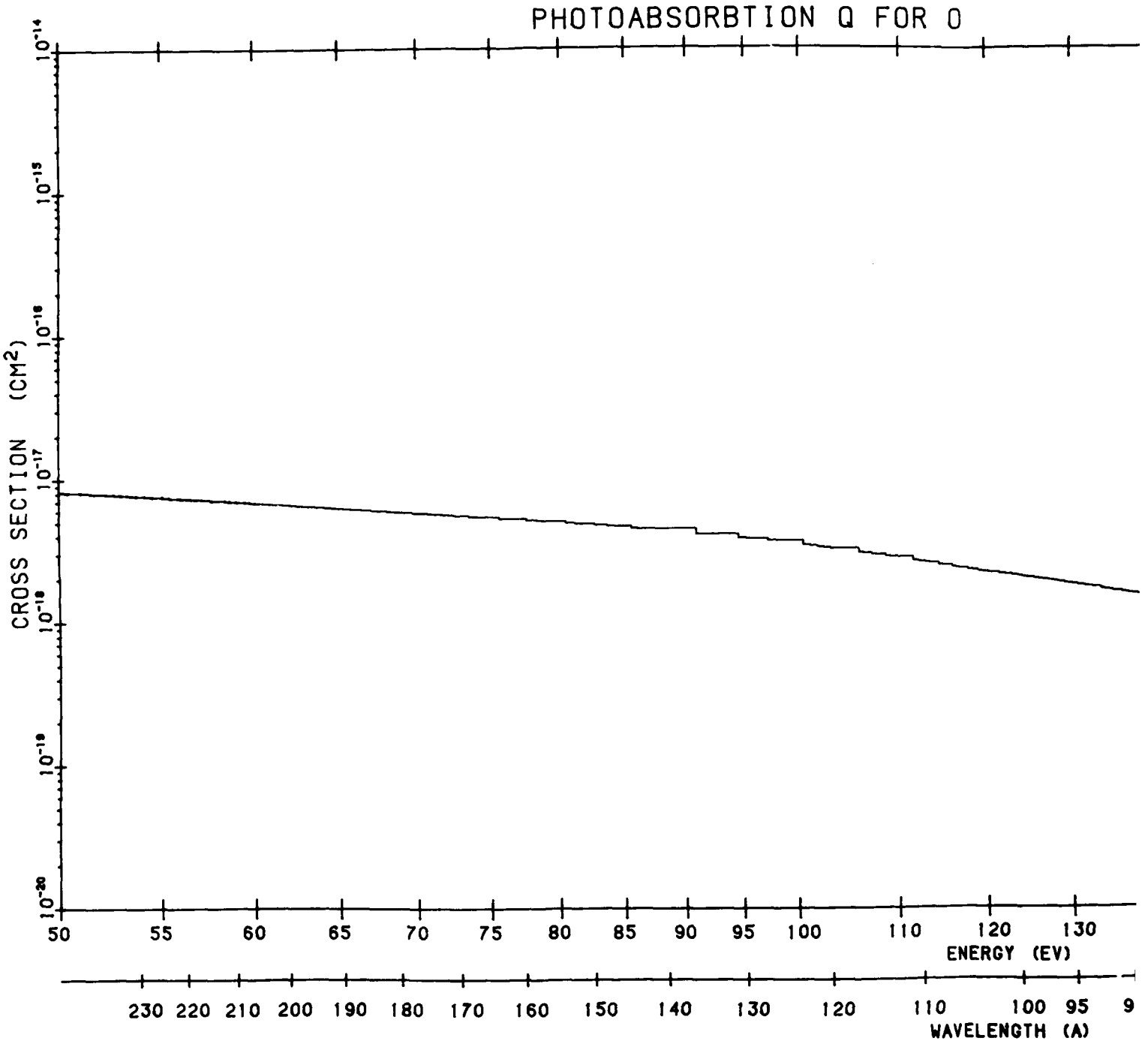
PHOTOABSORBTION Q FOR O
CROSS SECTION (CM2)
10-14
10-15
10-16
10-17
10-18
10-19
10-20
50 55 60 65 70 75 80 85 90 95 100 110 120 130
ENERGY (EV)
230 220 210 200 190 180 170 160 150 140 130 120 110 100 95 9
WAVELENGTH (A)

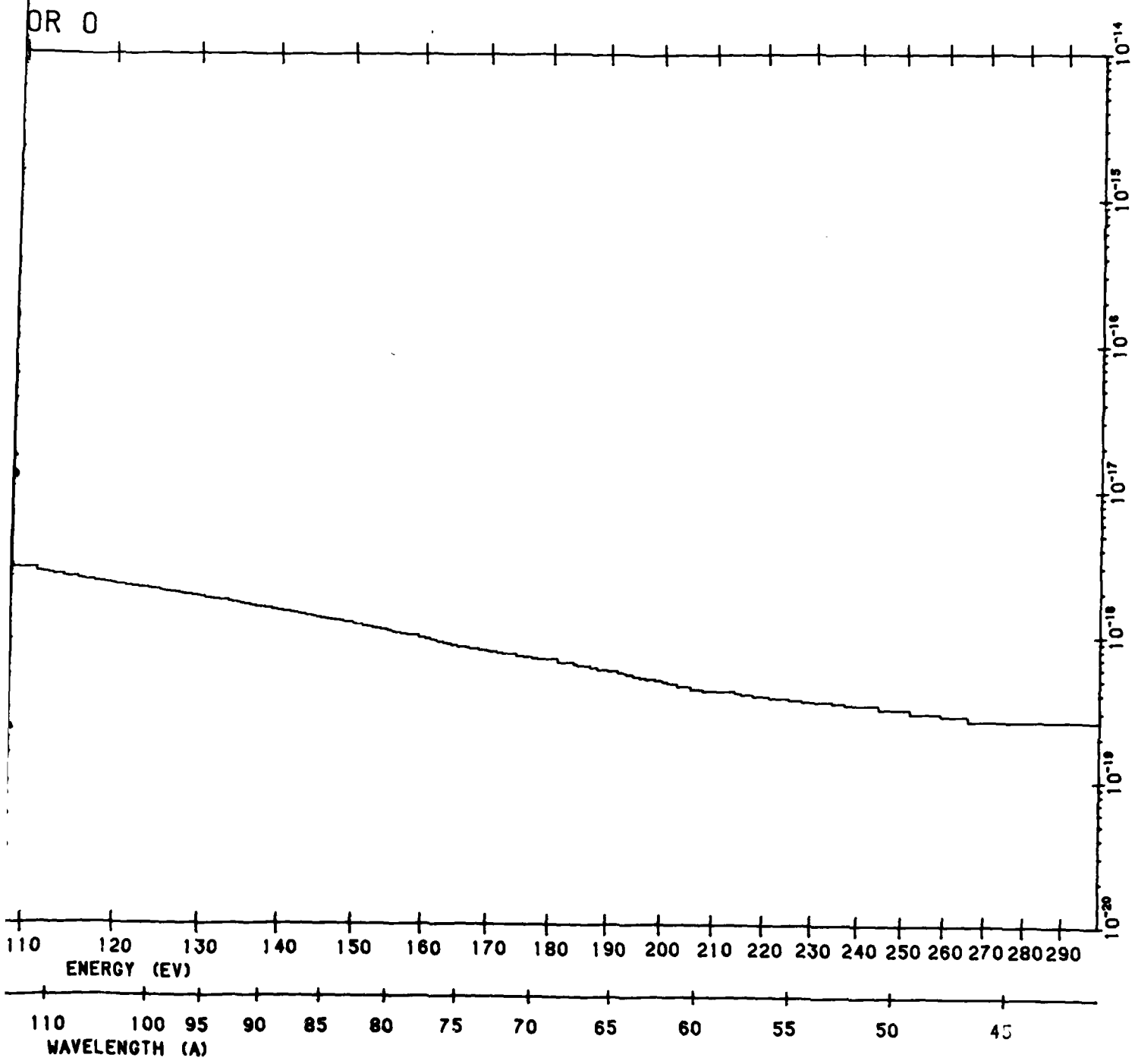


Figure B177. O Total Photoabsorption Cross Section. The data source is the same as that of Figure B157 (Cont.)

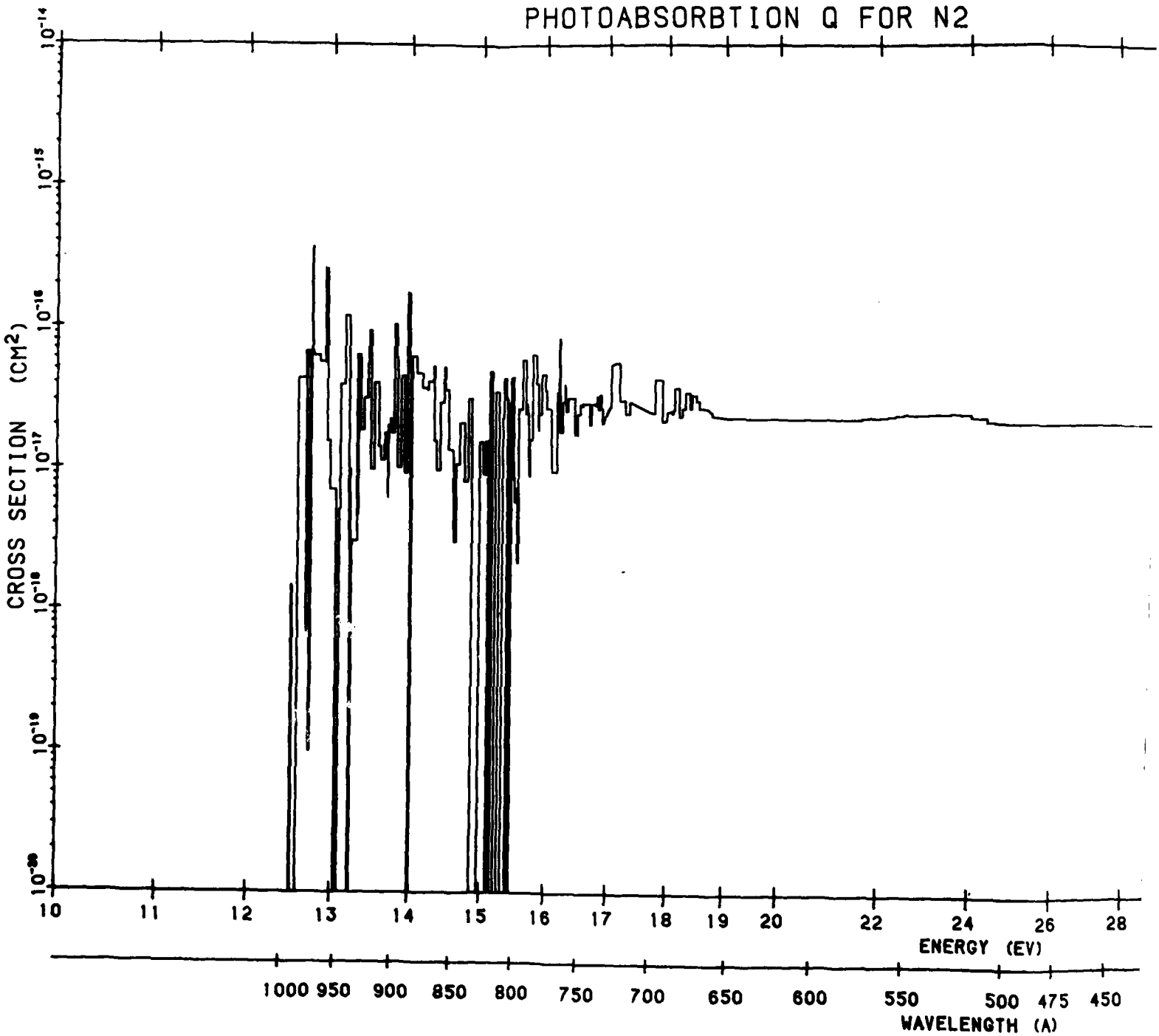
PHOTOABSORBTION Q FOR N2
CROSS SECTION (CM2)
10-14
10-15
10-16
10-17
10-18
10-19
10-20
10 11 12 13 14 15 16 17 18 19 20 22 24 26 28
ENERGY (EV)
1000 950 900 850 800 750 700 650 600 550 500 475 450
WAVELENGTH (A)

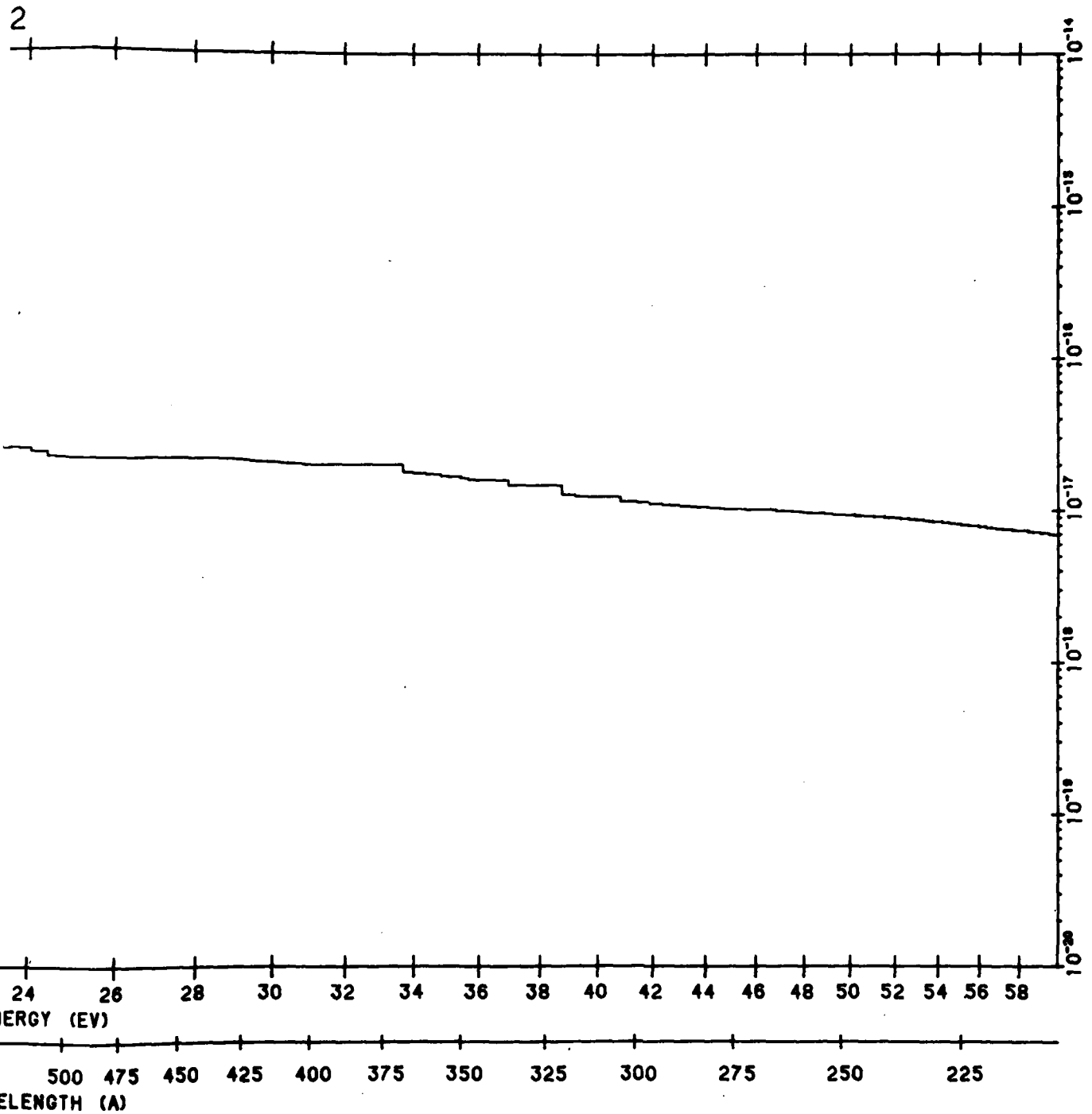


Figure B178. $N_2$ Total Photoabsorption Cross Section. The data source is the same as that of Figure B157

2

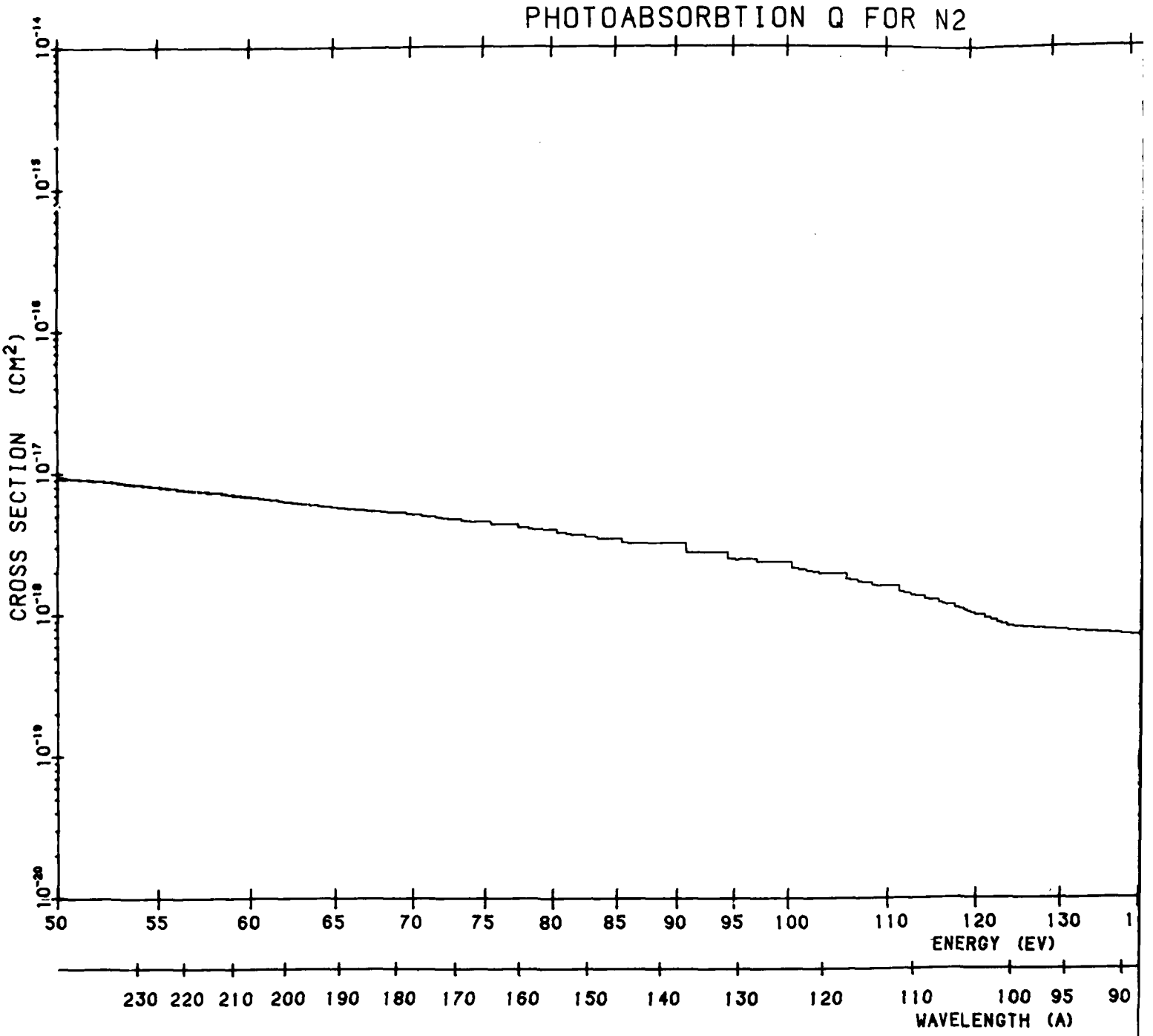
PHOTOABSORBTION Q FOR N2
CROSS SECTION (CM2)
10-14
10-15
10-16
10-17
10-18
10-19
10-20
50 55 60 65 70 75 80 85 90 95 100 110 120 130 1
ENERGY (EV)
230 220 210 200 190 180 170 160 150 140 130 120 110 100 95 90
WAVELENGTH (A)

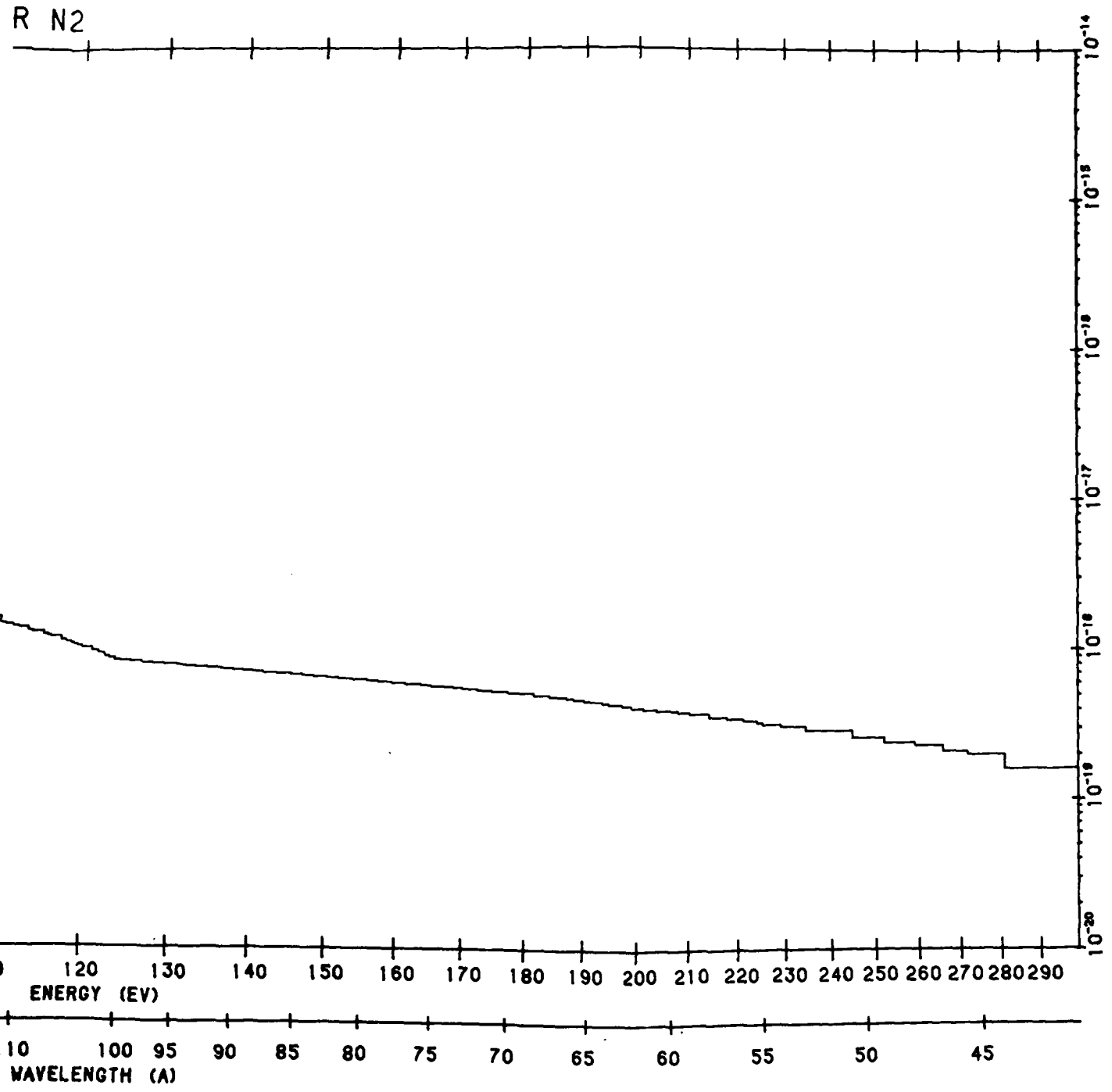


Figure B178. $N_2$ Total Photoabsorption Cross Section. The data source is the same as that of Figure B157 (Cont.)

2

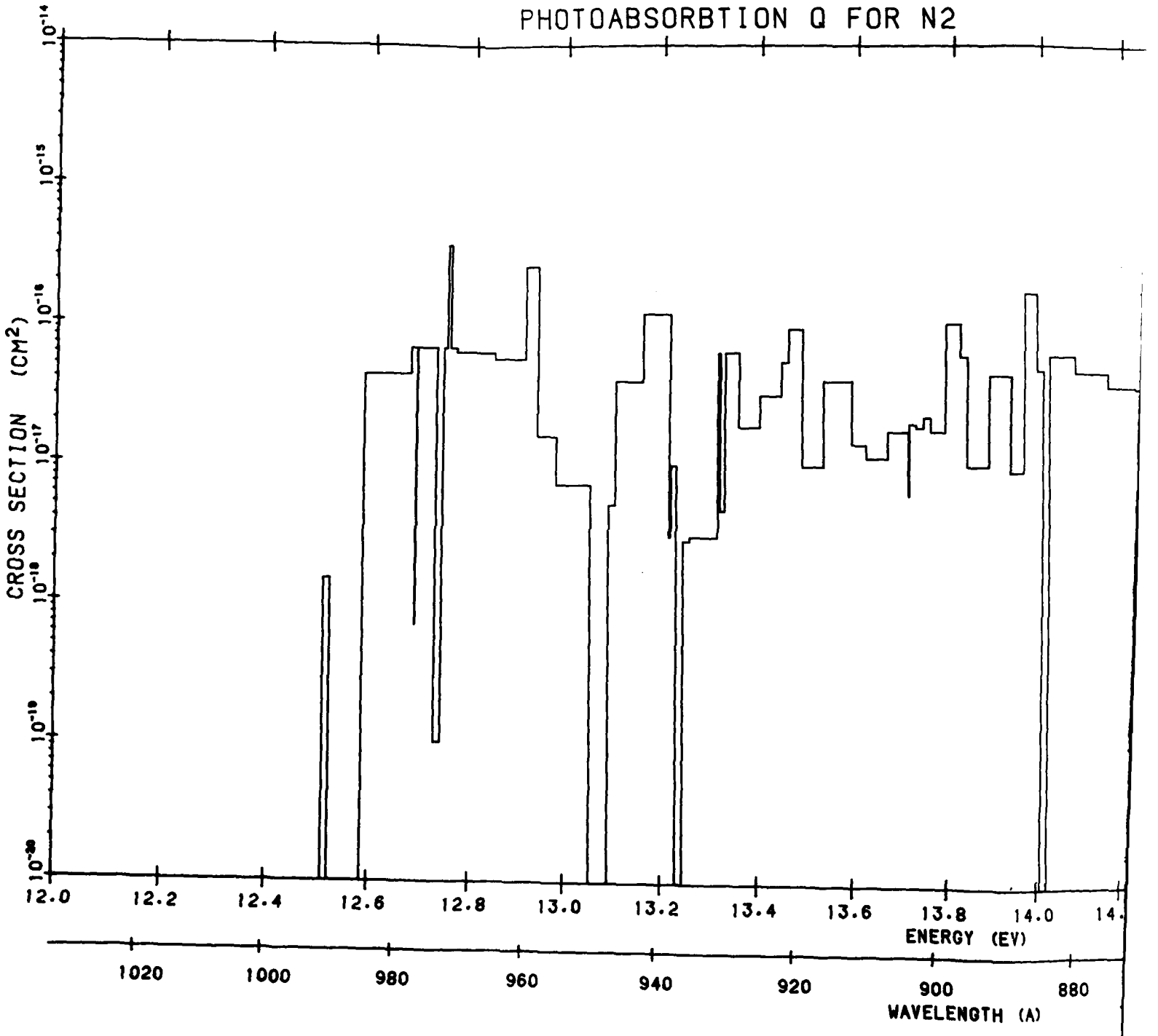
PHOTOABSORBTION Q FOR N2
CROSS SECTION (CM2)
10-14
10-15
10-16
10-17
10-18
10-19
10-20
12.0
12.2
12.4
12.6
12.8
13.0
13.2
13.4
13.6
13.8
14.0
14.
ENERGY (EV)
1020
1000
980
960
940
920
900
880
WAVELENGTH (A)

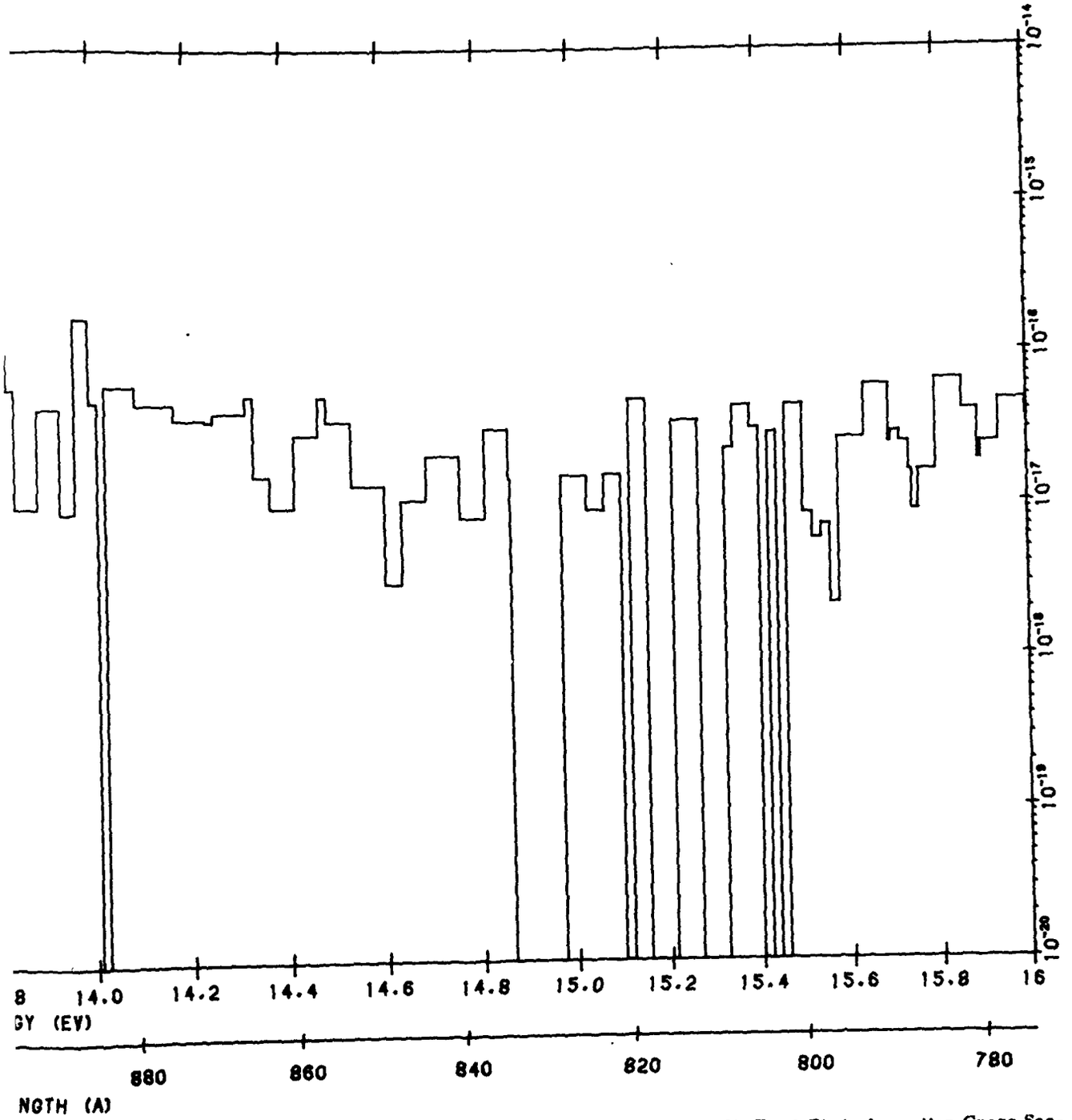


Figure B178. $N_2$ Total Photoabsorption Cross Section. The data source is the same as that of Figure B157 (Cont.)

2

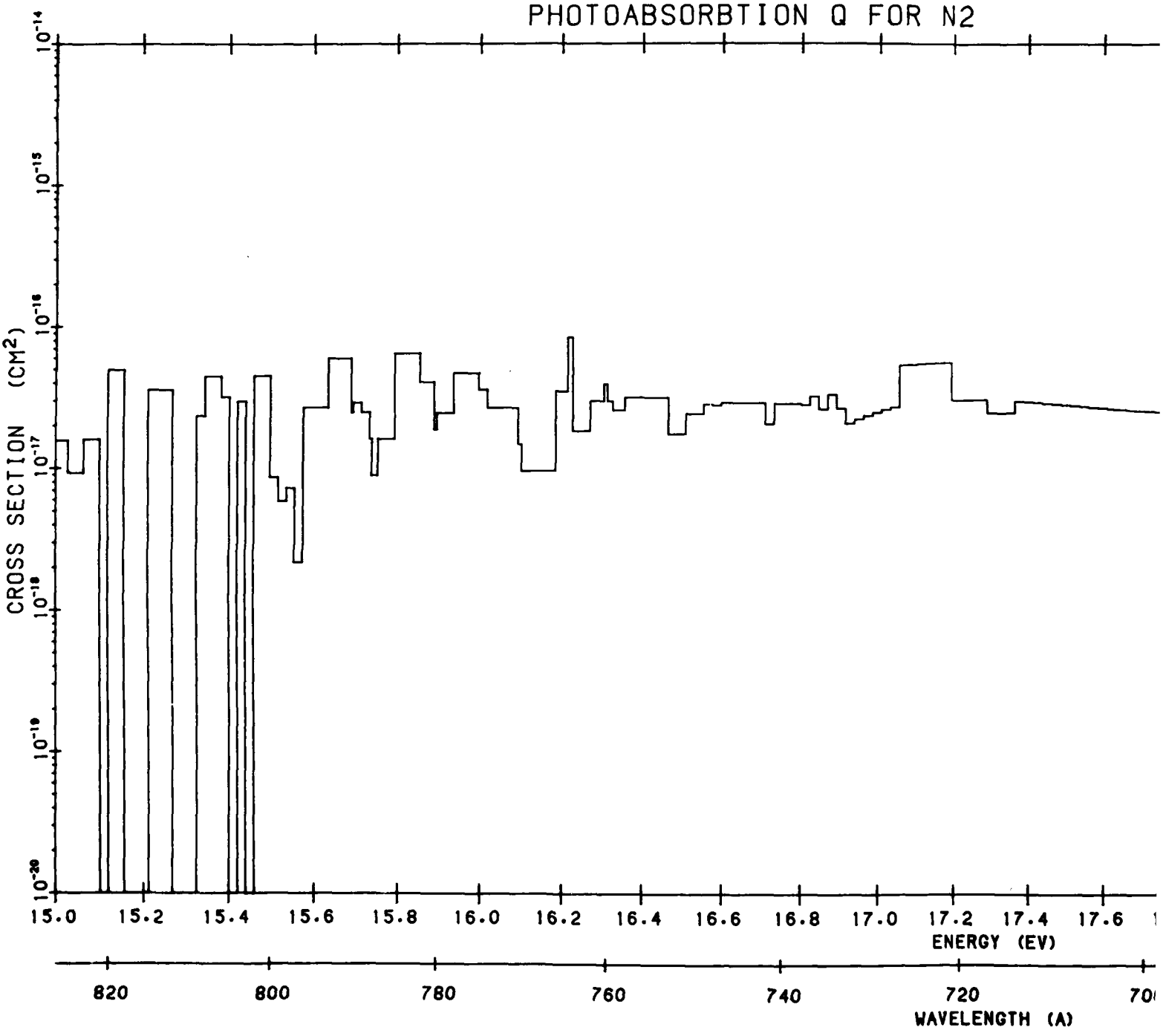
PHOTOABSORBTION Q FOR N2
CROSS SECTION (CM2)
10-14
10-15
10-16
10-17
10-18
10-19
10-20
15.0
15.2
15.4
15.6
15.8
16.0
16.2
16.4
16.6
16.8
17.0
17.2
17.4
17.6
ENERGY (EV)
820
800
780
760
740
720
WAVELENGTH (A)

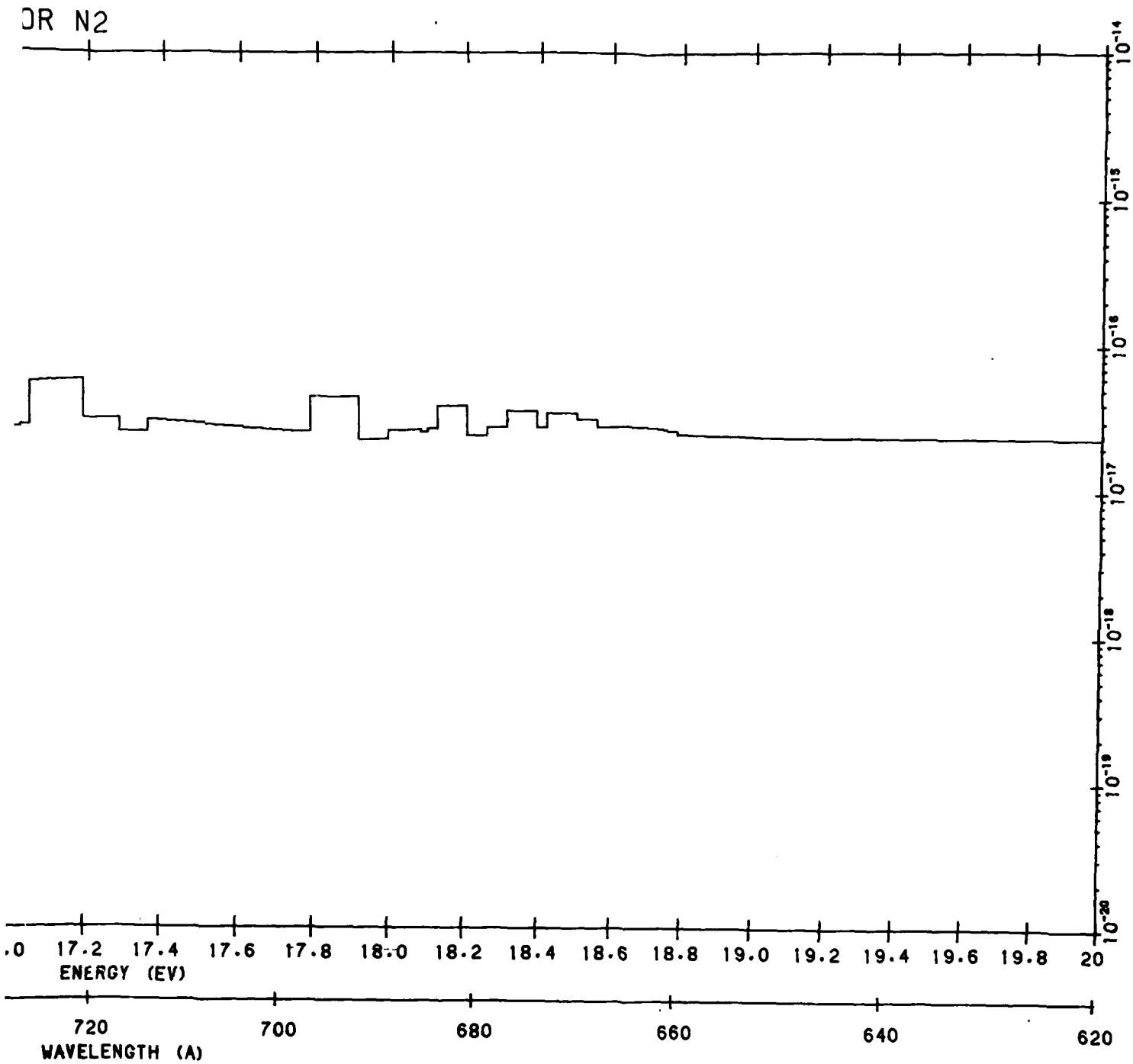


Figure B178. $N_2$ Total Photoabsorption Cross Section. The data source is the same as that of Figure B157 (Cont.)

2

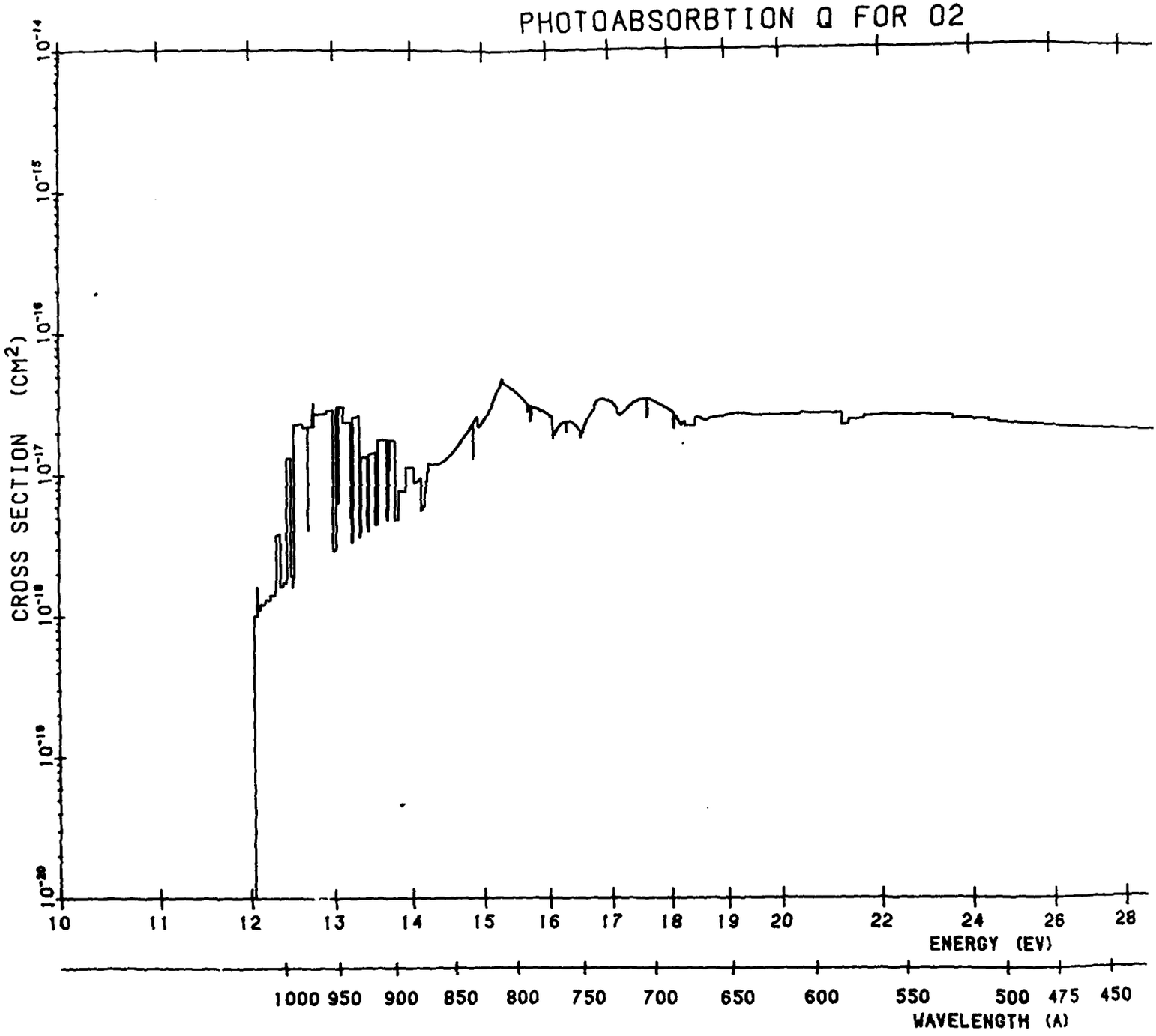
PHOTOABSORBTION Q FOR O2
CROSS SECTION (CM2)
10-14
10-15
10-16
10-17
10-18
10-19
10-20
10 11 12 13 14 15 16 17 18 19 20 22 24 26 28
ENERGY (EV)
1000 950 900 850 800 750 700 650 600 550 500 475 450
WAVELENGTH (A)

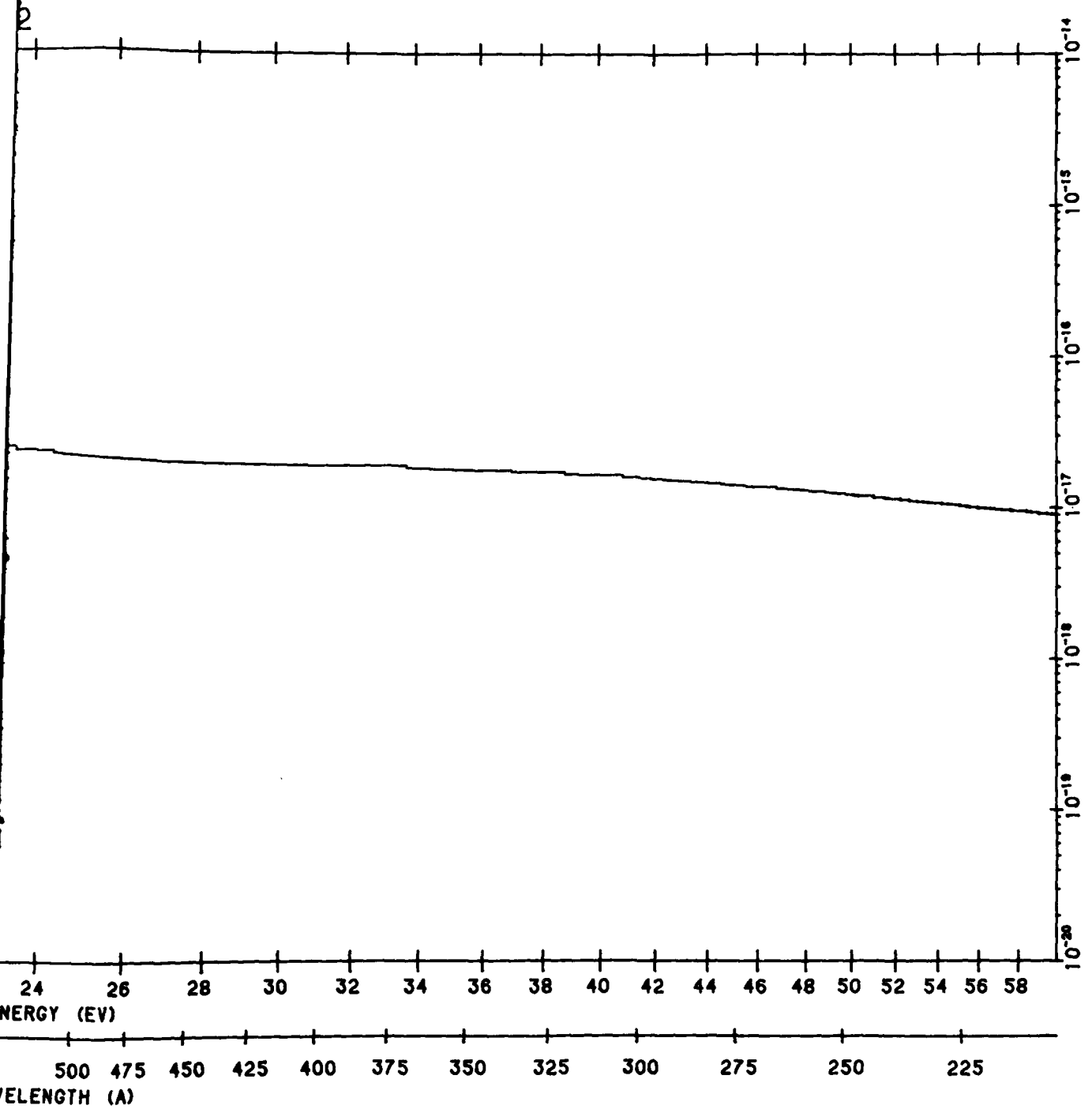


Figure B179. $O_2$ Total Photoabsorption Cross Section. The data source is the same as that of Figure B157

2

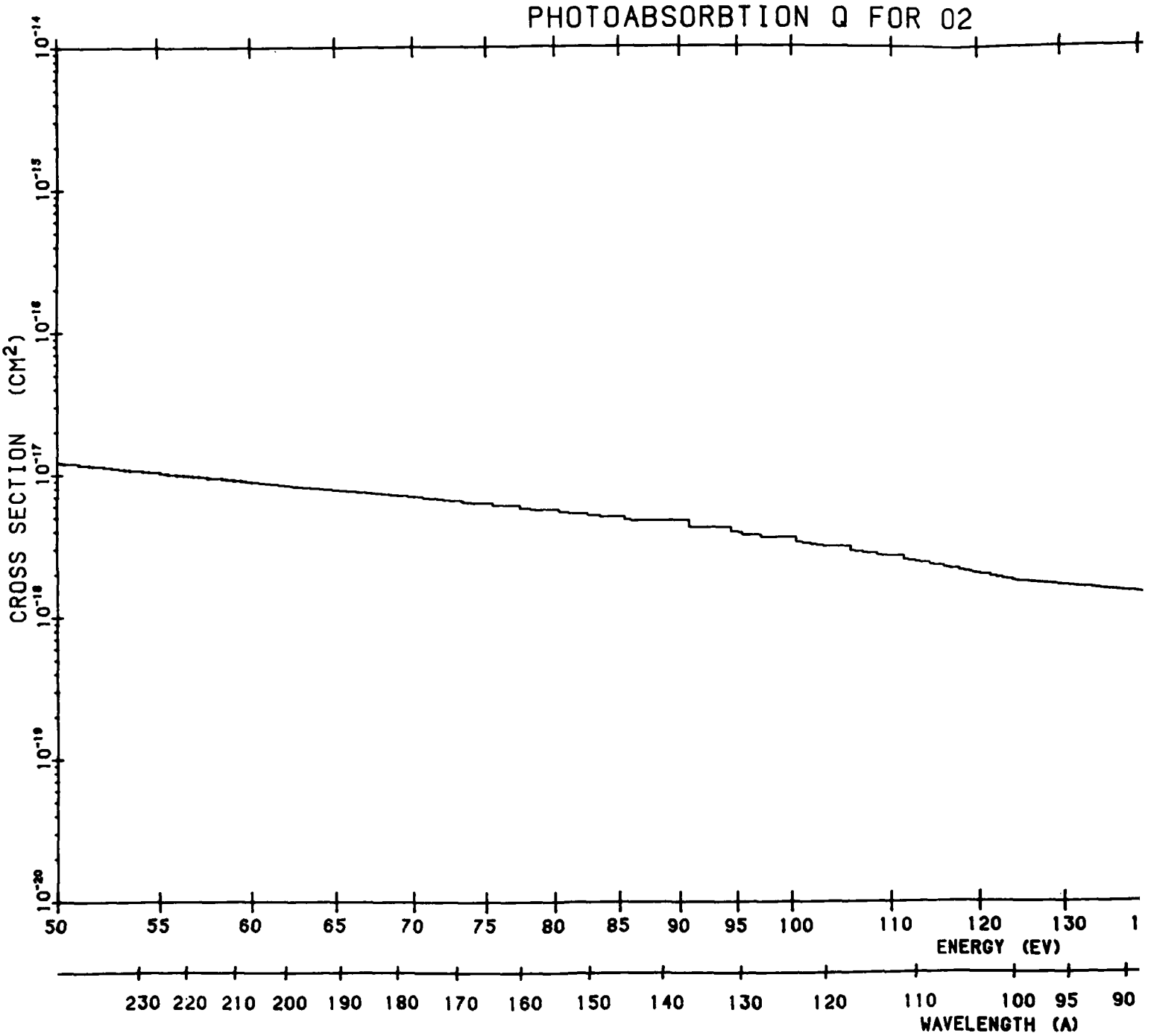
PHOTOABSORBTION Q FOR 02
CROSS SECTION (CM2)
10-14
10-15
10-16
10-17
10-18
10-19
10-20
50 55 60 65 70 75 80 85 90 95 100 110 120 130 1
ENERGY (EV)
230 220 210 200 190 180 170 160 150 140 130 120 110 100 95 90
WAVELENGTH (A)

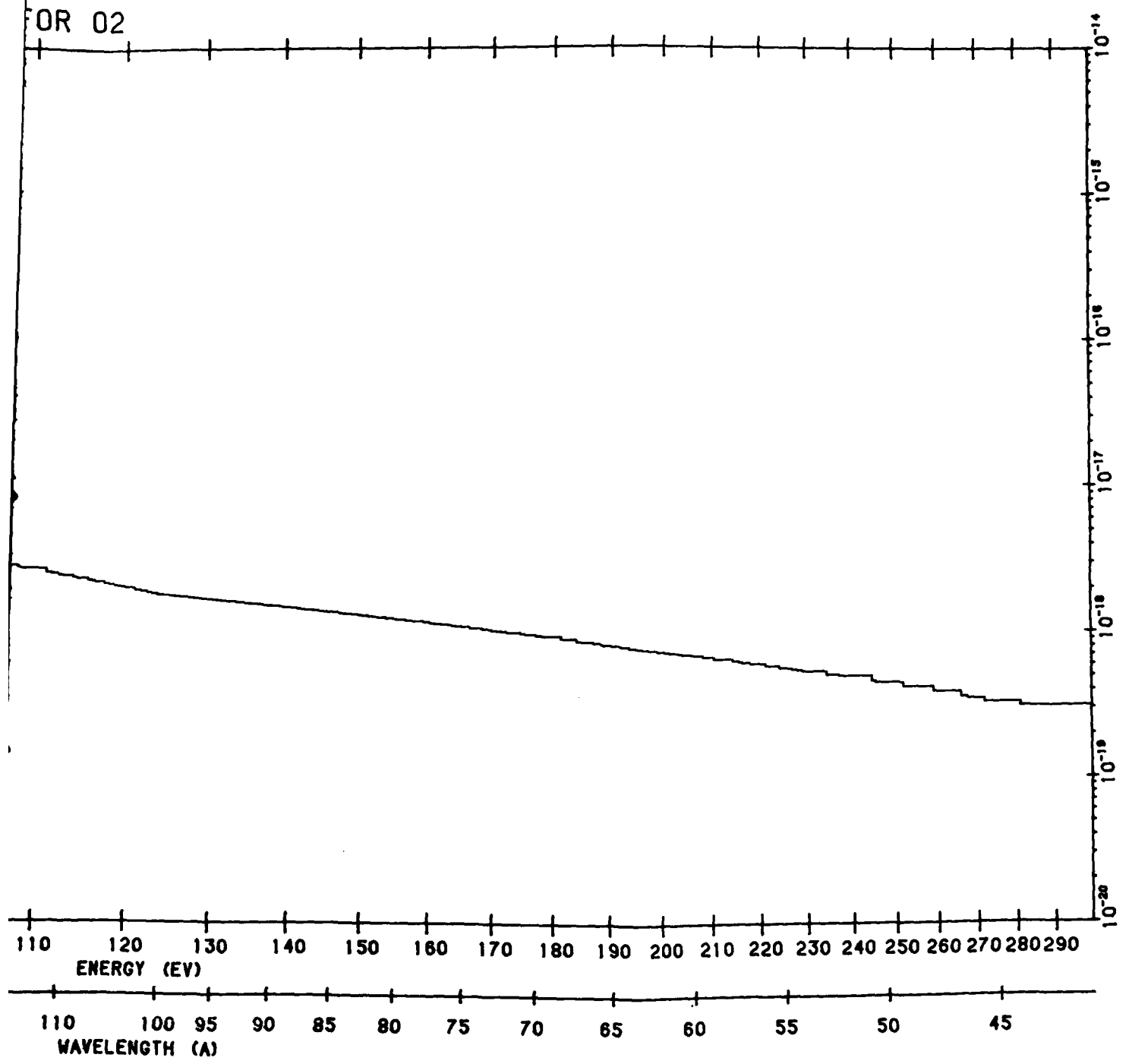


Figure B179. $O_2$ Total Photoabsorption Cross Section. The data source is the same as that of Figure B157 (Cont.)

2

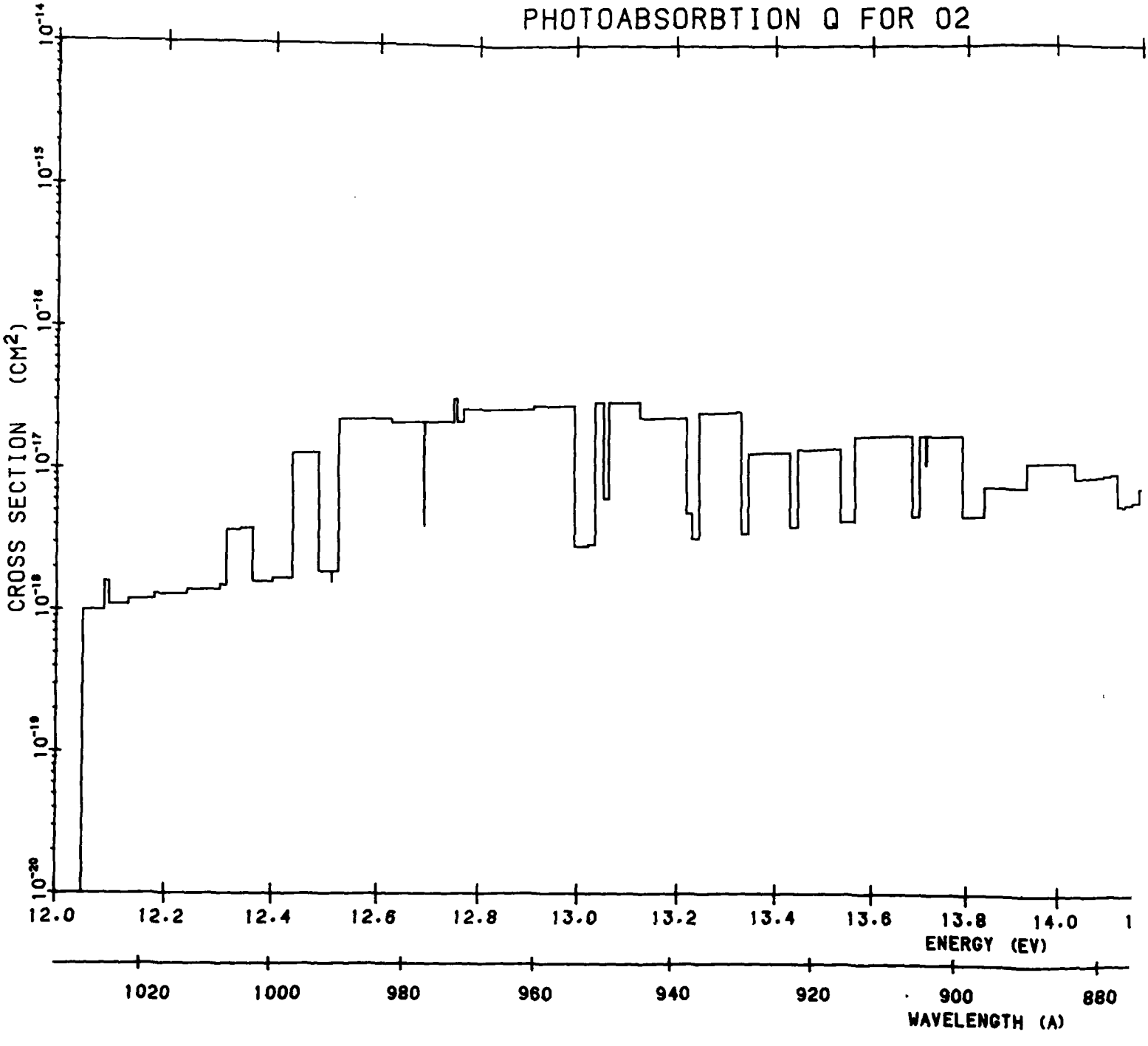
PHOTOABSORBTION Q FOR O2
CROSS SECTION (CM2)
10-14
10-15
10-16
10-17
10-18
10-19
10-20
12.0
12.2
12.4
12.6
12.8
13.0
13.2
13.4
13.6
13.8
14.0
ENERGY (EV)
1020
1000
980
960
940
920
900
880
WAVELENGTH (A)

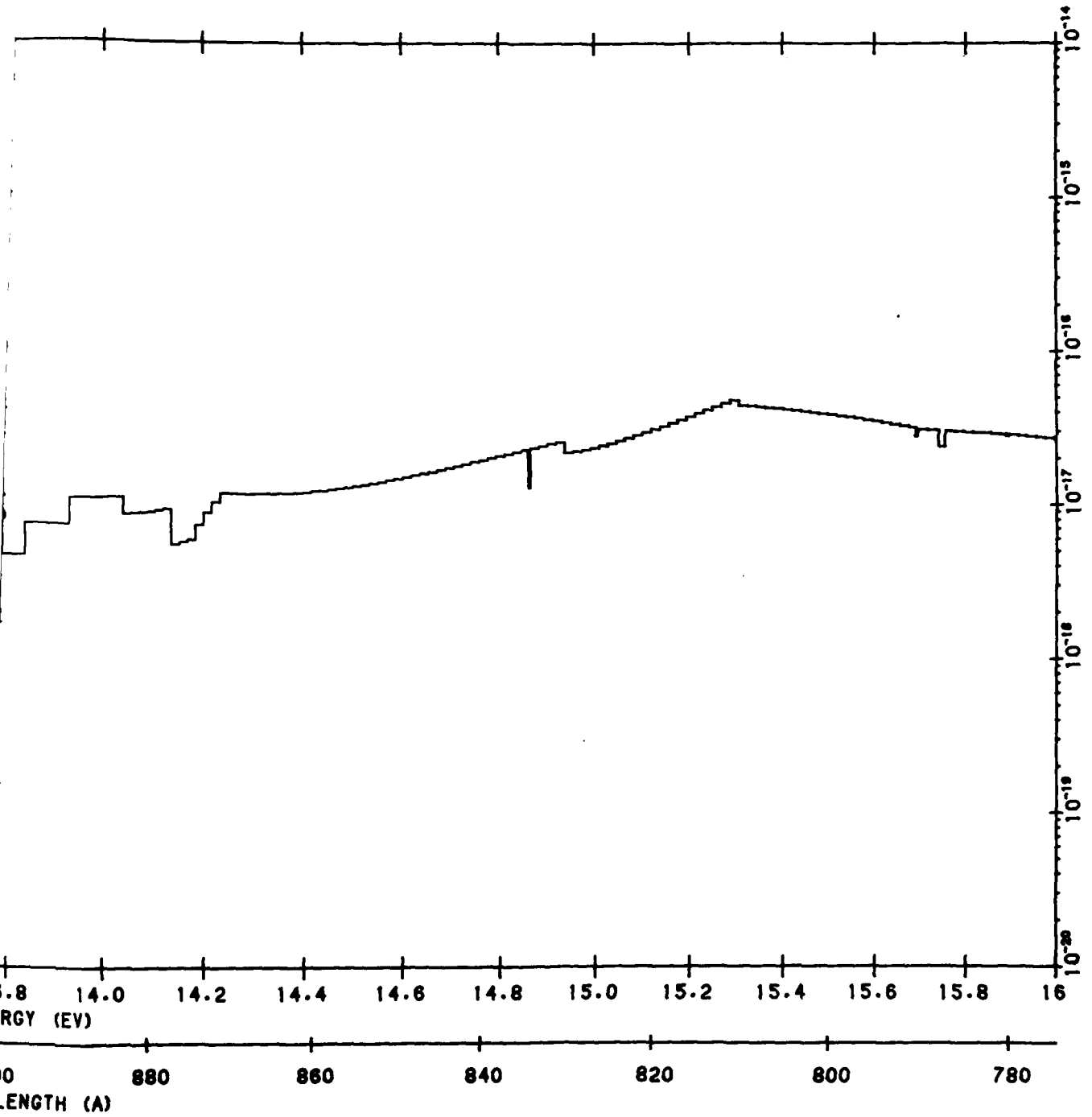


Figure B179. $O_2$ Total Photoabsorption Cross Section. The data source is the same as that of Figure B157 (Cont.)

2

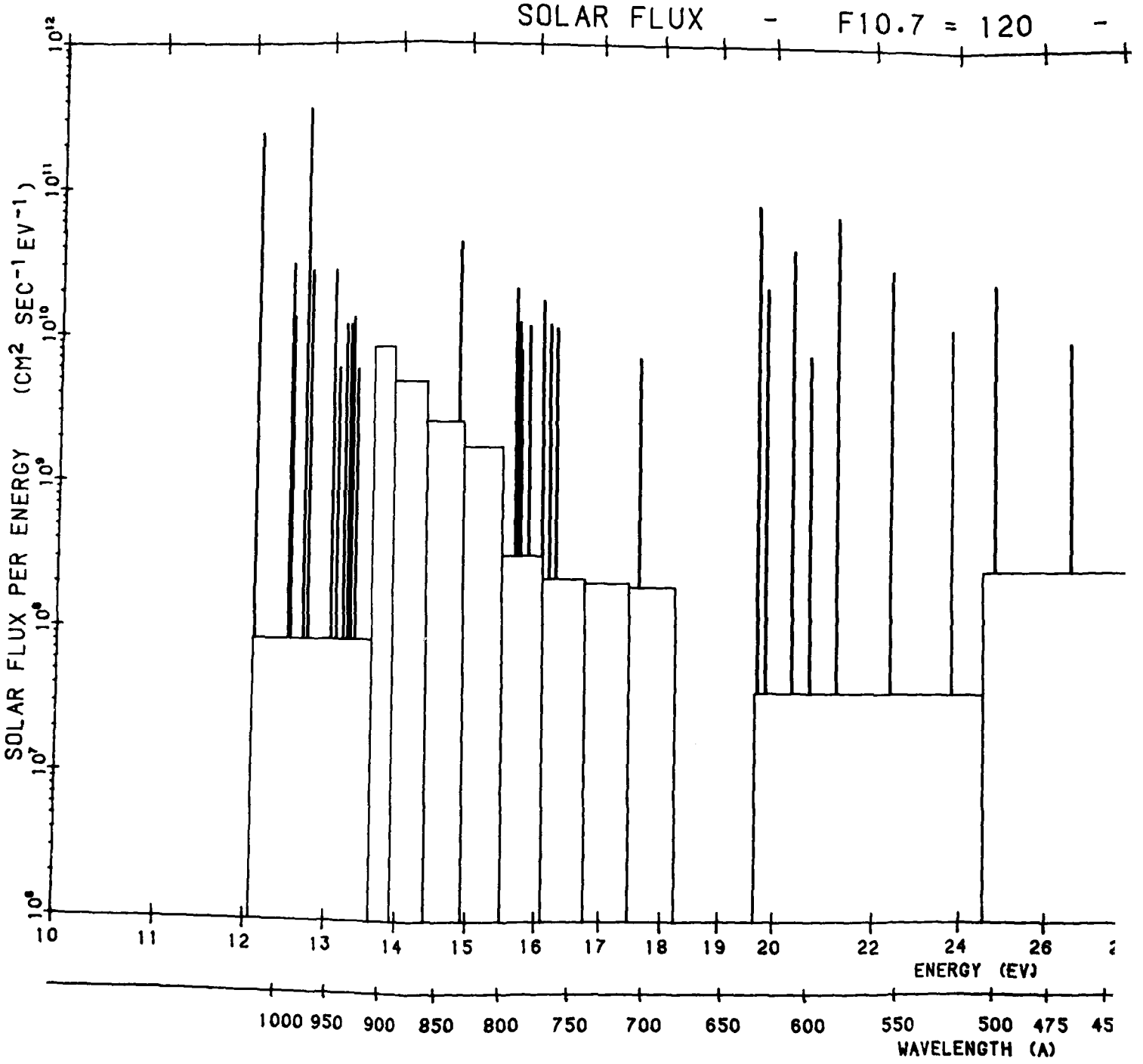
SOLAR FLUX - F10.7 = 120 -
SOLAR FLUX PER ENERGY (CM2 SEC-1 EV-1)
10^12
10^11
10^10
10^9
10^8
10^7
10^6
10 11 12 13 14 15 16 17 18 19 20 22 24 26
ENERGY (EV)
1000 950 900 850 800 750 700 650 600 550 500 475 45
WAVELENGTH (A)

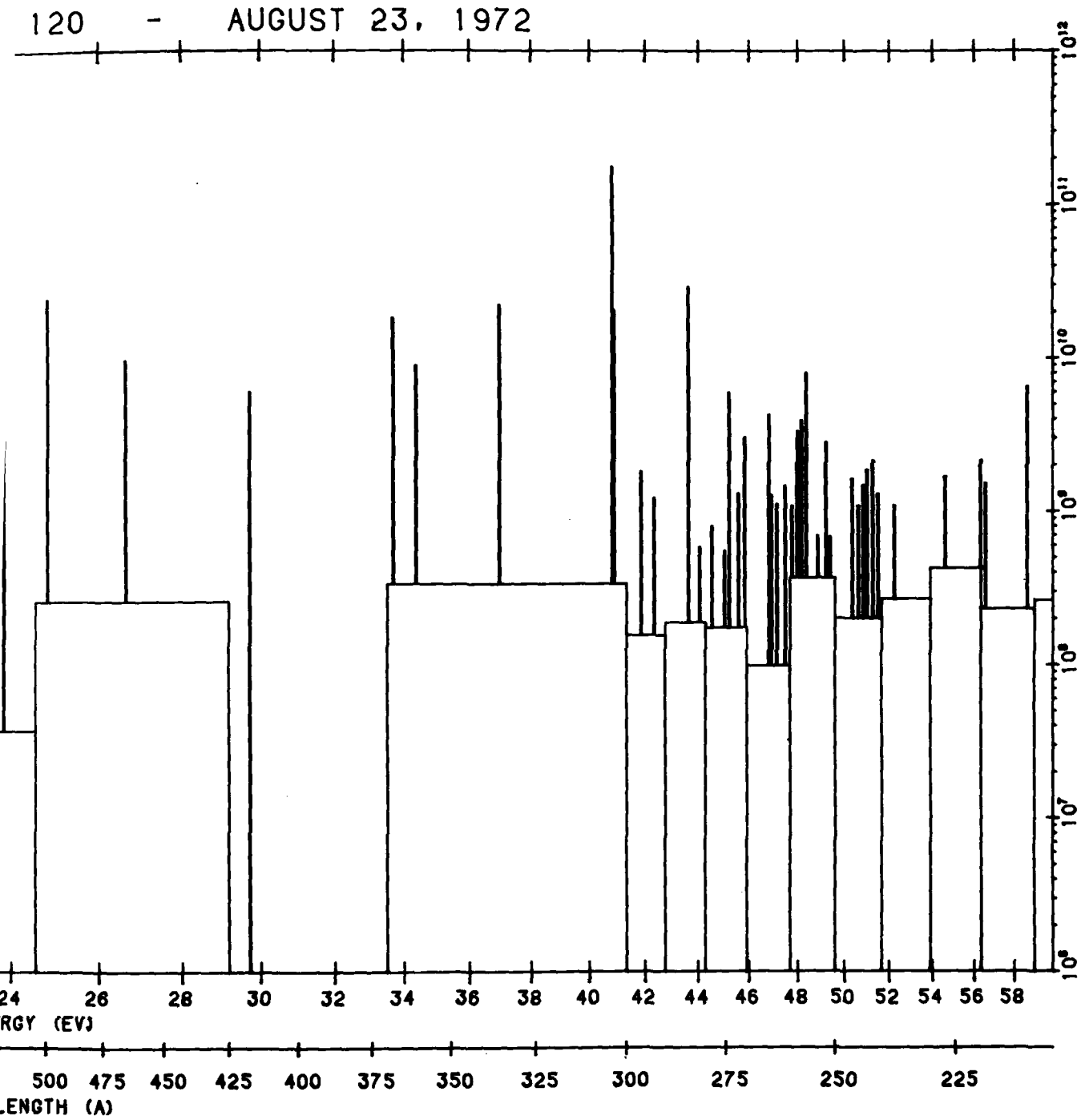


Figure B180. Solar Ultraviolet Flux for F10.7 near 120. The data from Heroux et al (1974)[B27] for 23 August 1972 are energy averaged over each interval to yield values which are constant over each interval and which give the correct total flux when integrated (Cont.)

B27. Heroux, L., Cohen, M., and Higgins, J. E. (1974) J. Geophys. Res. 79:5237, AFGL-TR-76-0031, AD A020775.

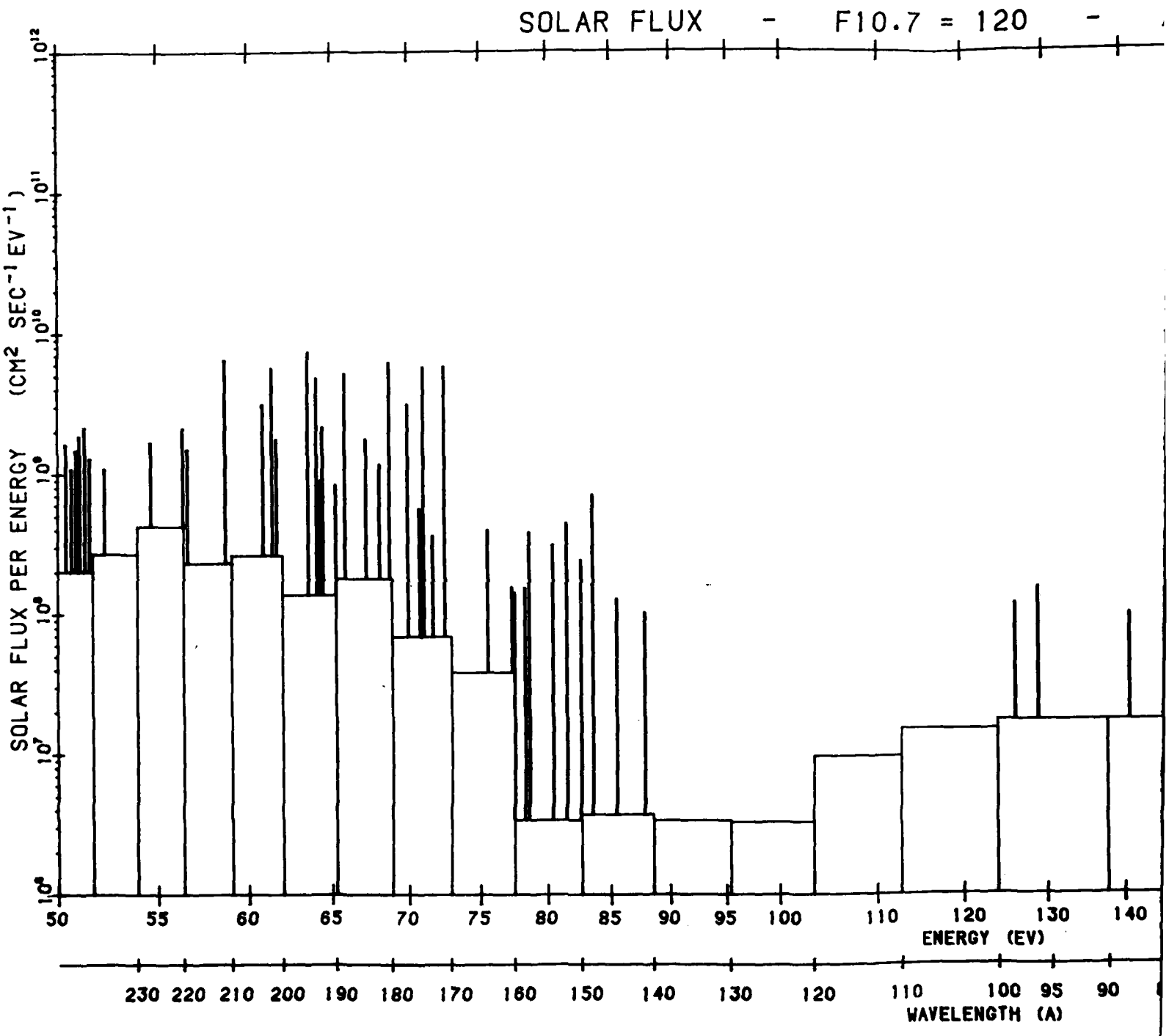
SOLAR FLUX - F10.7 = 120 -
SOLAR FLUX PER ENERGY (CM² SEC⁻¹ EV⁻¹)
10¹²
10¹¹
10¹⁰
10⁹
10⁸
10⁷
10⁶
50 55 60 65 70 75 80 85 90 95 100 110 120 130 140
ENERGY (EV)
230 220 210 200 190 180 170 160 150 140 130 120 110 100 95 90
WAVELENGTH (A)

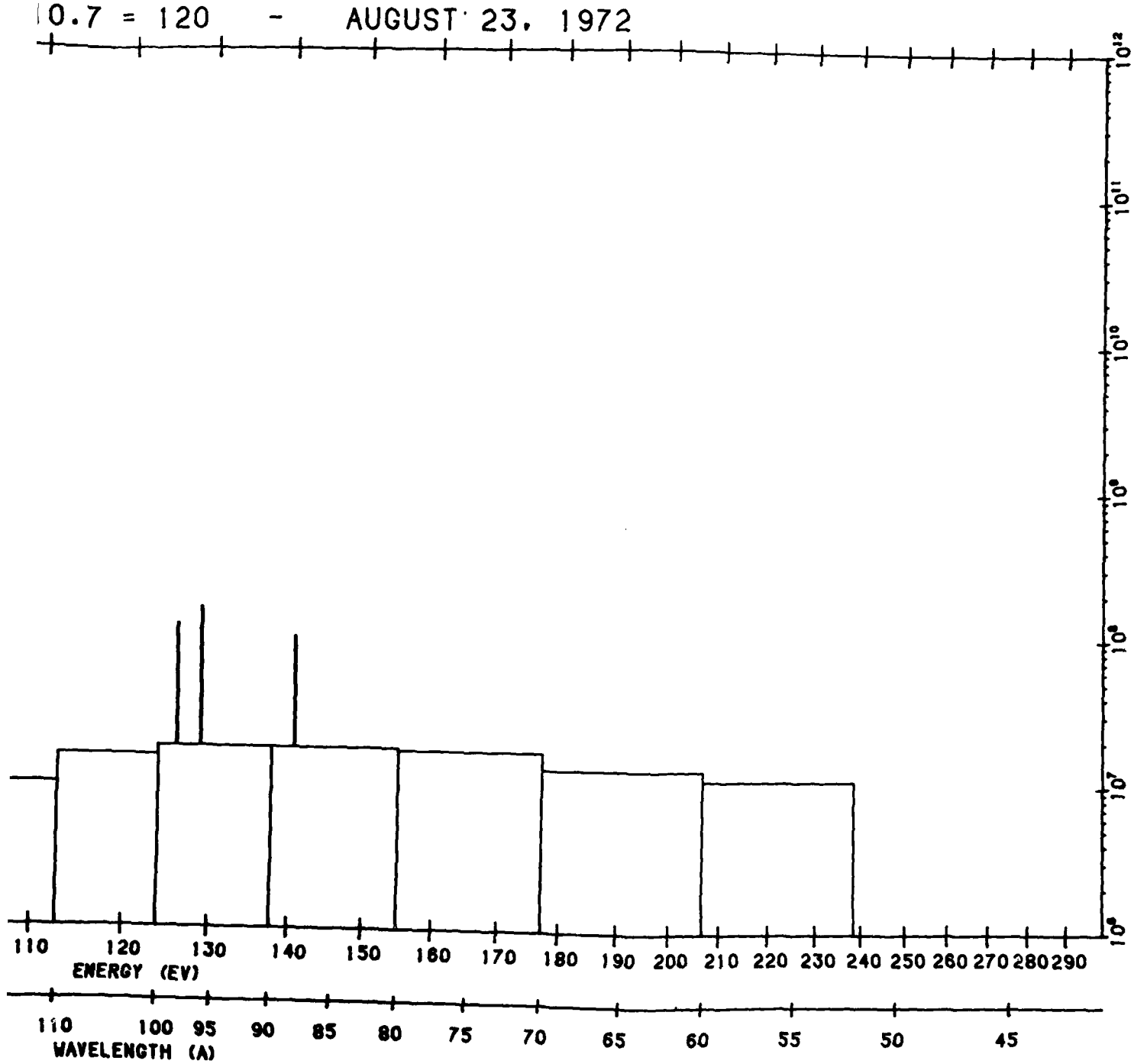


Figure B180. Solar Ultraviolet Flux for F10.7 near 120. The data from Heroux et al (1974) B27 for 23 August 1972 are *energy* averaged over each interval to yield values which are constant over each interval and which give the correct total flux when integrated (Cont.)

2

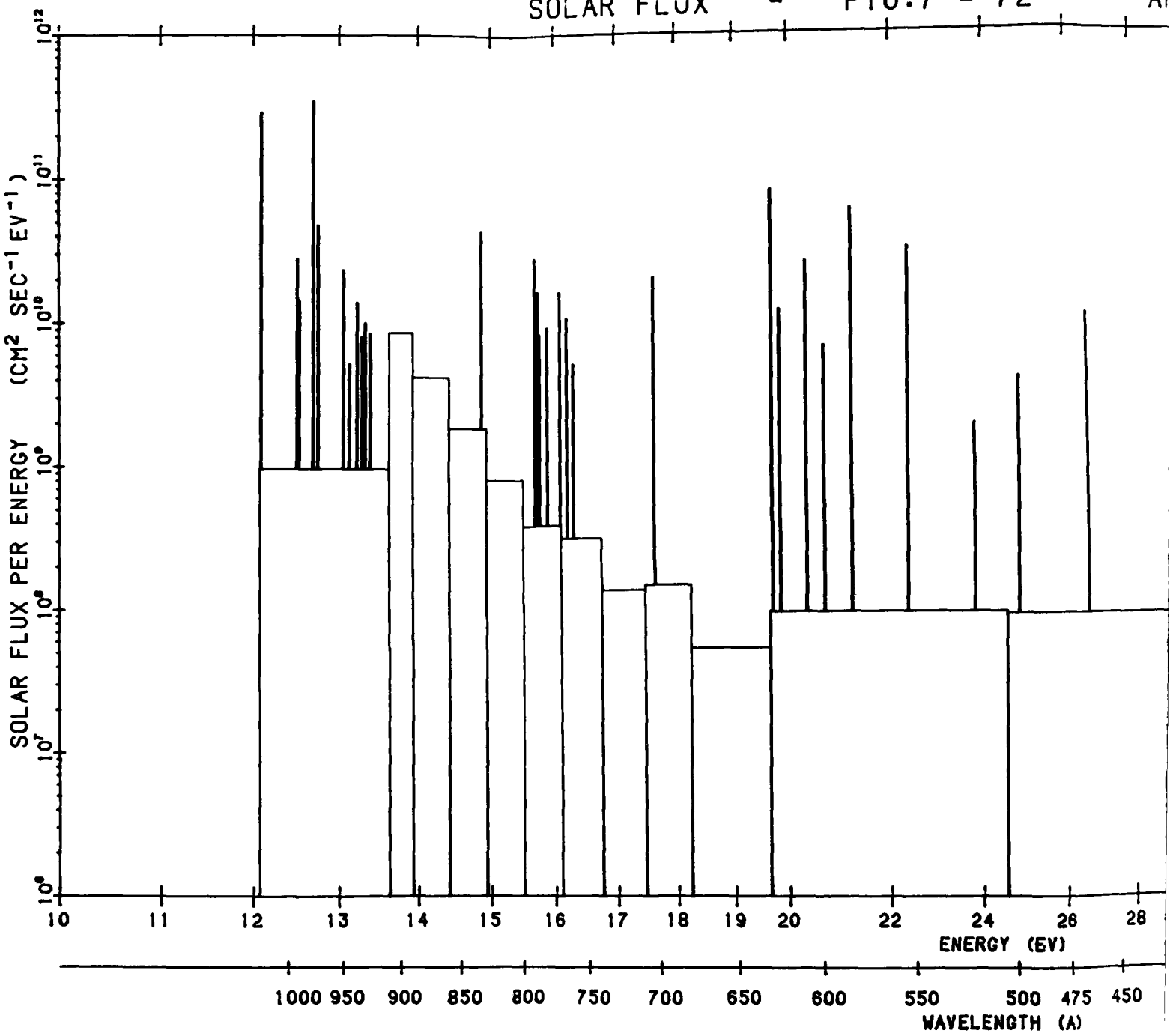



B28. Manson, J.E. (1976a) Satellite Measurements of Solar UV During 1974, AFCRL-TR-76-0006, AD A021490.

B29. Manson, J.E. (1976b) J. Geophys. Res. 81:1629, AFGL-TR-76-0103, AD A024617.

B30. Heroux, L., and Hinteregger, H.E. (1978) J. Geophys. Res. 83:5305, AFGL-TR-78-0297, AD A062634.

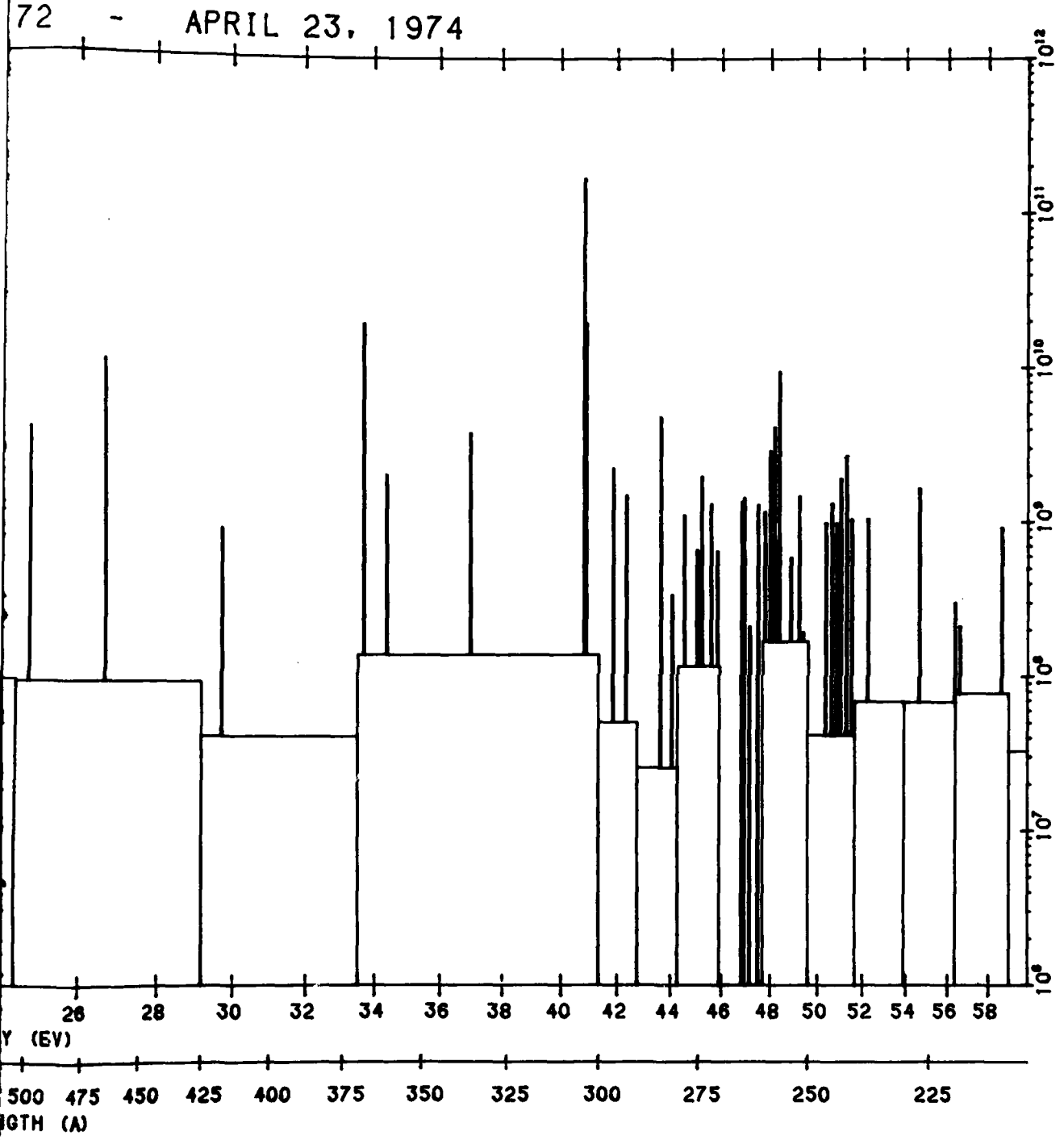


Figure B181. Solar Ultraviolet Flux for F10.7 near 70. The data from Manson (1976a, [B28] 1976b [B29]) and Heroux and Hinteregger (1978) [B30] for 23 April 1974 are energy averaged over each interval to yield values which are constant over each integral and which give the correct total flux when integrated

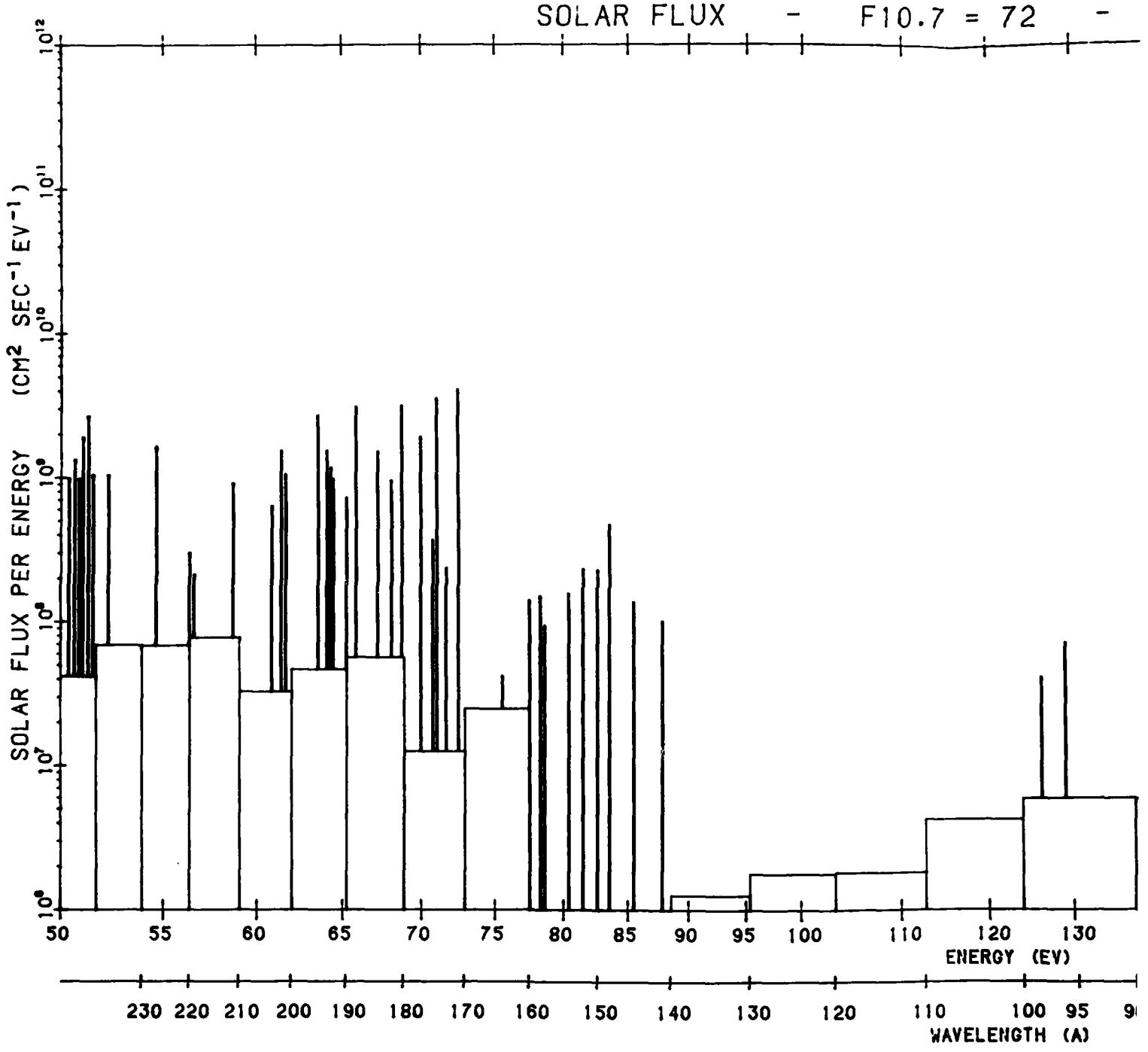
SOLAR FLUX - F10.7 = 72 -
SOLAR FLUX PER ENERGY (CM2 SEC-1 EV-1)
10^12
10^11
10^10
10^9
10^8
10^7
10^6
50 55 60 65 70 75 80 85 90 95 100 110 120 130
ENERGY (EV)
230 220 210 200 190 180 170 160 150 140 130 120 110 100 95
WAVELENGTH (A)

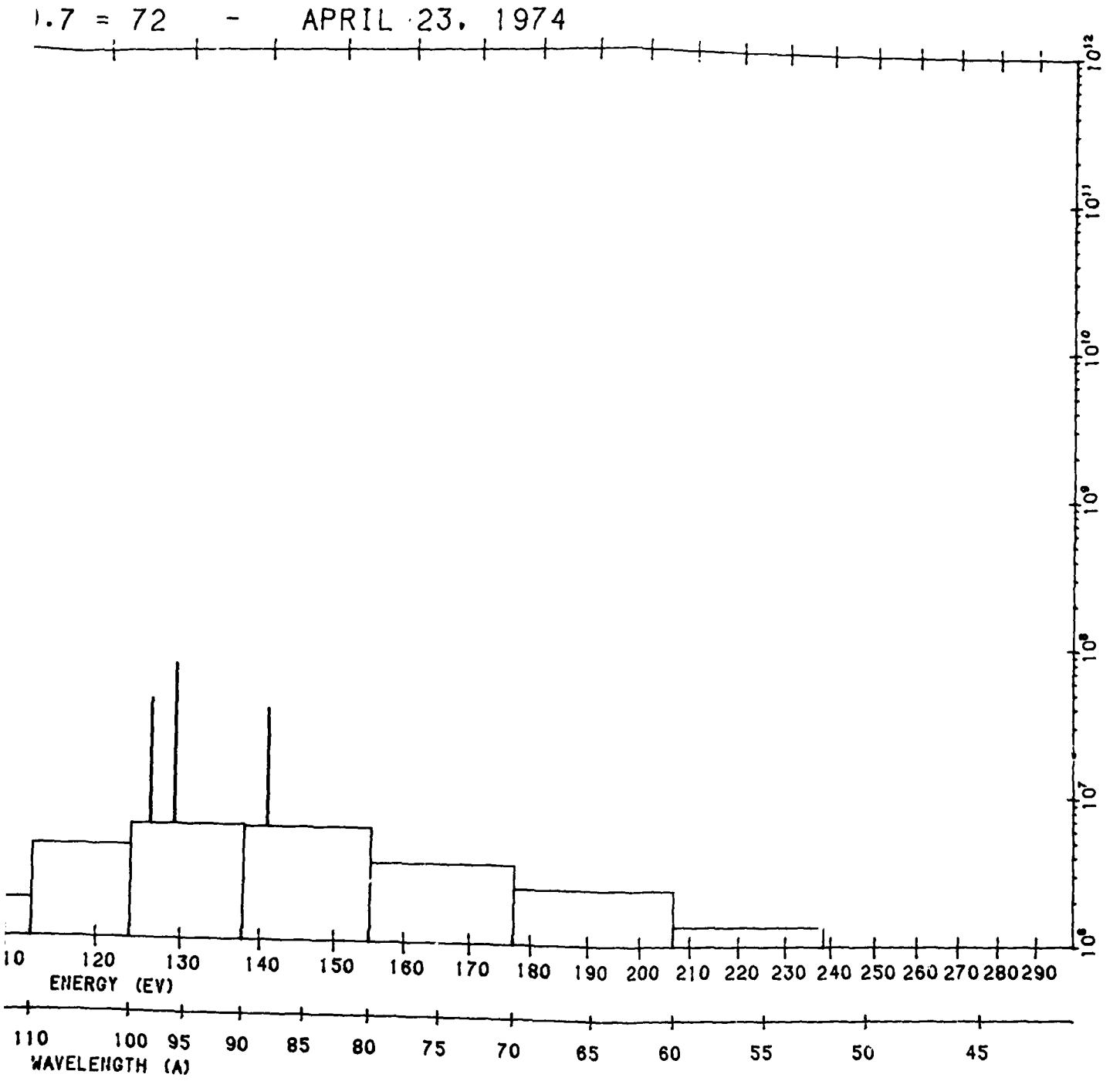


Figure B181. Solar Ultraviolet Flux for F10.7 near 70. The data from Manson (1976a, B28 1976b[B29]) and Heroux and Hinteregger (1978)[B30] for 23 April 1974 are energy averaged over each interval to yield values which are constant over each integral and which give the correct total flux when integrated (Cont.)

## References


B1. Thomas, L.D., and Nesbet, R.K. (1975) Phys. Rev. A11:170; addendum, Phys. Rev. A12:1279.

B2. Smith, K., Henry, R.J.W , and Burke, P.G. (1967) Phys. Rev. 157:51.

B3. Englehardt, A.G., Phelps, A.V., and Risk, C.G. (1964) Phys. Ref. 135:A1566.

B4. Srivastava, S.K., Chutjian, A., and Trajmar, S. (1976) J. Chem. Phys. 64:1340.

B5. Choi, B.H., Poe, R.T., Sun, J.G., and Shan, Y. (1979) Phys. Rev. A19:11[illegible].

B6. Lawton, S.A., and Phelps, A.V. (1978) J. Chem. Phys. 69:1055.

B7. Porter, H.S., and Jump, F.W. (1978) Computer Sciences Corporation/ TM-78/6017.

B8. Chandra, N., and Temkin, A. (1976) Phys. Rev. A13:188.

B9. Gerjuoy, E., and Stein, S. (1955) Phys. Rev. 97:1671.

B10. Lane, N.F. (1980) Rev. Mod. Phys. 52:29.

B11. LeDournef, M., and Nesbet, R.K. (1976) J. Phys. B9:L241.

B12. Tambe, B.R., and Henry, R.J.W. (1976) Phys. Rev. A13:224.

B13. Chen, J.C.Y. (1966a) Phys. Rev. 146:61.

B14. Chen, J.C.Y. (1966b) J. Chem. Phys. 45:2710.

B15. Schneider, B.I. (1980) Private communication.

B16. Truhlar, D.G., Brandt, M.A., Srivastava, S.K., Trajmar, S., and Chutjian, A. (1977) J. Chem. Phys. 66:655.

B17. Linder, F., and Schmidt, H. (1971) Z. Naturforsch 26:1617.

B18. Koike, F. (1973) J. Phys. Soc. Japan 35:1166.

B19. Wong, S.F., Boness, M.J.W., and Schulz, G.S. (1973) Phys. Rev. Lett. 31:699.

B20. Smith, E.R. (1976) Phys. Rev. 13:A65.

B21. Rountree, S.P., and Henry, R.J.W. (1972) Phys. Rev. A6:2106.

B22. Jackman, C.H., Garvey, R.H., and Green, A.E.S. (1980) Private communication.

B23. Vo Ky Lan, Feautrier, N., LeDournef, M., and Van Regemorter, H. (1972) J. Phys. B5:1506.

B24. Cartwright, D.C., Trajmar, S., Chutjian, A., and Williams, W. (1977) Phys. Rev. A16:1041.

B25. Trajmar, S., Cartwright, D.C., and Williams, W. (1971) Phys. Rev. A4:1462.

B26. Kirby, K., Constantinides, E.R., Babeu, S., Oppenheimer, M., and Victor, G.A. (1979) Atomic Data and Nuclear Data Tables 23:63.

B27. Heroux, L., Cohen, M., and Higgins, J.E. (1974) J. Geophys. Res. 79:5237, AFGL-TR-76-0031, AD A020775.

B28. Manson, J.E. (1976a) Satellite Measurements of Solar UV During 1974, AFCRL-TR-76-0006, AD A021490.

B29. Manson, J.E. (1976b) J. Geophys. Res. 81:1629, AFGL-TR-76-0103, AD A024617.

B30. Heroux, L., and Hinteregger, H.E. (1978) J. Geophys. Res. 83:5305, AFGL-TR-78-0297, AD A062634.

☆U. S. GOVERNMENT PRINTING OFFICE: 1982--500-000--55

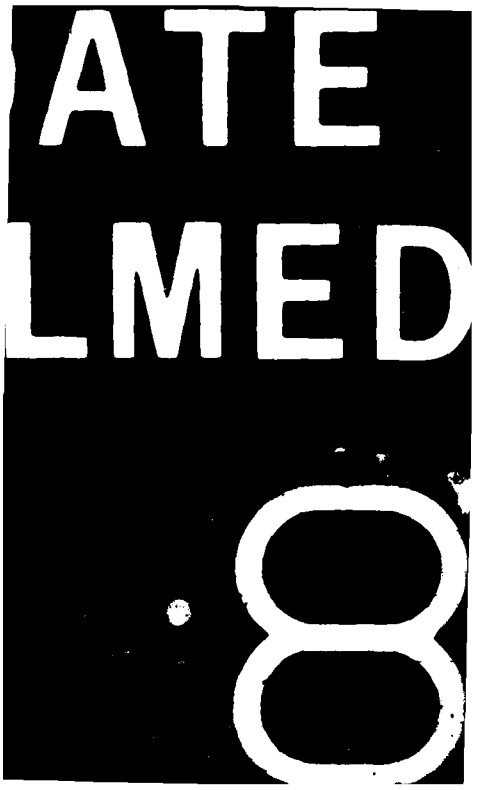
ATE
LMED
8